ANNUAL REPORT

East Texas and Western Louisiana Coastal Erosion Study

Year 4

Robert A. Morton, William A. White,
James C. Gibeaut, Roberto Gutierrez, and Jeffrey G. Paine
Assisted by Radu Boghici and Kami Norlin

Prepared for the U.S. Department of Interior
U.S. Geological Survey

Cooperative Agreement No. 14-08-0001-A0912

Bureau of Economic Geology
Noel Tyler, Director
The University of Texas at Austin
Austin, Texas 78713-8924

October 1995

BUREAU OF ECONOMIC GEOLOGY
THE UNIVERSITY OF TEXAS AT AUSTIN

University Station, Box X · Austin, Texas 78713-8924 · (512) 471-1534 or 471-7721 · FAX 471-0140
10100 Burnet Road, Bldg. 130 · Austin, Texas 78758-4497

October 24, 1995

Mr. Jack Kindinger
U. S. Geological Survey
600- 4th Street South
St. Petersburg, FL 33701

Reference: Cooperative Agreement No. 14-08-0001-A0912

Dear Mr. Kindinger:

Enclosed are two copies of the Annual Report for the referenced agreement for the period of September 16, 1994, through September 15, 1995.

Sincerely,

Bob Morton

Robert A. Morton
Senior Research Scientist

RAM:amm
Enclosures

cc: N. Samuels
D. Ratcliff

ANNUAL REPORT

East Texas and Western Louisiana Coastal Erosion Study

Year 4

Robert A. Morton, William A. White,
James C. Gibeaut, Roberto Gutierrez, and Jeffrey G. Paine
Assisted by Radu Boghici and Kami Norlin

Prepared for the U.S. Department of Interior
U.S. Geological Survey

Cooperative Agreement No. 14-08-0001-A0912

Bureau of Economic Geology
Noel Tyler, Director
The University of Texas at Austin
Austin, Texas 78713-8924

October 1995

CONTENTS

Addenda (attached)

Report Organization

The following report summarizes the major accomplishments achieved by the Bureau of Economic Geology during the fourth year study (FY 94-95) of coastal erosion and wetlands loss along the southeastern Texas coast. The report covers activities between September 1, 1994, and August 31, 1995. Major accomplishments are reported for each work element and task identified in the 5-year work plan of the cooperative agreement. Documents summarizing the major accomplishments and containing the important data sets and scientific conclusions are included as Addenda 1–12.

Work Element 1: Coastal Erosion Analysis

The coastal erosion work element is intended to (1) establish a computerized database of historical shoreline positions (1882–1982), (2) update the database using the most recent shoreline information (1990's), (3) analyze historical trends of shoreline movement in the context of the regional geologic framework and human modifications, (4) synthesize the physical and habitat characteristics of different shoreline types, (5) establish a network of field monitoring sites for surveying coastal changes, and (6) prepare documents of shoreline change suitable for coastal planning and resource management.

We continued examining relationships between wetland loss and accelerated relative sea-level rise resulting from human-induced subsidence and faulting along the southeastern Texas coast. Wetland loss in the vicinity of major oil and gas fields was analyzed. Marshes that have been converted to open water along active faults were identified and mapped to determine the extent of losses. Synthesis of data on wetland losses along the southeastern Texas coast shows that more than 11,700 ha of vegetated wetlands have been replaced by shallow subaqueous flats and open water. Salt, brackish, and fresh marshes and fluvial woodlands have been affected. Major losses have occurred in fluvial-deltaic areas along the Neches and Trinity rivers. Although many processes or activities may contribute to wetland loss, human-induced subsidence resulting from production of hydrocarbons and associated formation water is a major process affecting wetlands along the southeastern Texas coast. A paper on this analysis was completed for submission to the <u>Journal of Coastal Research</u>. The title of the paper by W. A. White and R. A. Morton is "Wetland Losses Related to Fault Movement and Hydrocarbon Production, Southeastern Texas Coast" **(Addendum 1)**.

<u>Task 2: Geomorphic Characterization.</u> During year 4, the geomorphic characteristics of Gulf beaches and dunes in Galveston County were classified in cooperation with the Texas General

Land Office. This work was jointly sponsored by the Texas Natural Resources Inventory Program, which is an effort to develop extensive databases of natural resources using a geographic information system (ARC/INFO). An ordinal ranking of dunes was prepared and a ranking of human impacts on foredunes was developed **(Addendum 2)**. Beach profiles were surveyed at 32 sites including the 8 sites that have been surveyed annually on Galveston Island and Follets Island **(Addendum 3)**.

SIGNIFICANT RESULTS. We prepared a report that summarizes and illustrates significant wetland losses associated with oil and gas production. The report concludes that most of these losses are caused by faults that were activated as a result of large-volume production of subsurface fluids (oil, gas, and formation water). Our GPS surveys and field observations were used by the Texas General Land Office to help establish the dune protection line in Galveston County.

Work Element 2: Regional Geologic Framework

Work element 2 investigated the geologic origin and evolution of the principal subenvironments that are present along the southeastern Texas coast. This is being accomplished by establishing a chronostratigraphic framework for the coastal systems and reconstructing the evolution of coastal environments during the post-glacial rising phase and highstand in sea level. This work element will also provide data on the physical characteristics and natural habitats of the various shoreline types in the context of shoreline stability.

Task 1: Stratigraphic Analysis. The study area encompasses a diverse assemblage of depositional environments ranging from non-marine fluvial systems and transitional coastal systems to the marine continental shelf. During year four, we used vibracores, faunal assemblages, isotopic dates, and seismic surveys to investigate the late Quaternary and Holocene stratigraphy of several of these environments.

Subtask 1: Data Inventory and Compilation. Dr. Martin Lagoe, micropaleontologist with the Department of Geological Sciences, The University of Texas at Austin, and Laura Stewart, graduate student, have completed the analyses of foraminifera from onshore cores CE-2, CE-4, CE-6, and CE-7 to help with the interpretation of depositional environments represented by homogeneous muds. Species identification and abundance were plotted against depth to establish changes in paleosalinity of coastal waters and the types of geological setting represented by the examined samples. Plots of foraminifera abundance and preliminary interpretations are presented in **Addendum 4**. Preliminary results indicate the interfluve sediments are mostly barren of forams. It is uncertain whether the absence of forams is related to the original depositional environment or diagenetic reactions since deposition. Agglutinated species are also largely absent from other samples and the reason for this is unknown. Recent discussions with Dr. Eric Collins (Dave Scott post-doctoral researcher at Dalhousie Univ.) indicate that drying of the cores may have resulted in loss of the forams. An experiment for taking cores from the modern environments is planned to address this question of original deposition versus preservation of forams.

Eighteen samples from 11 coastal plain and Sabine Lake cores were obtained for radiocarbon analyses. Materials sampled are whole valves and shell fragments (*Rangia*, *Crassostrea*, *Mulinea*, *Anadara*), peat, wood, and organic clay. The samples represent a wide range of environments including oyster reef, bayhead delta, shoreface, beach ridge, transgressive marsh, fluvial sand, and floodbasin swamp. Analyses conducted by The University of Texas at Austin Radiocarbon Lab are presented in **Addendum 5**.

Long topographic profiles were prepared for the Sabine, Neches and Trinity rivers showing the elevations and gradients of the Beaumont surface, Deweyville terraces, and modern floodplain. Differences in gradient are a function of the structural elements over which the streams flow as they enter the basin. A paper on the Deweyville Terraces (co-authored with Mike Blum) was accepted for publication in the 1995 Gulf Coast Association of Geological Societies Transactions. A preprint of the paper is attached as **Addendum 6**.

Subtask 2: Field Studies. During year 4, we prepared, photographed and described 8 cores in the entrenched valley fill of the Neches River, and 4 vibracores from the coastal wetland interfluve between the Sabine and Trinity River systems (McFaddin National Wildlife Refuge). The vibracore descriptions are presented in **Addendum 7**.

Also during year 4 we conducted experimental onshore seismic tests at interfluve (High Island), chenier plain (Sabine Pass) and incised valley (Neches River) sites using different sound sources (soil probe drop hammer, hammer and plate) and compressional wave geophones. Detailed meter-spacing of geophones allowed processing of data to detect noise (surf at High Island site and road traffic at other two sites) and filter the data so that the geological reflections could be evaluated. Preliminary results are encouraging and indicate that the methods warrant additional work. A summary report of the experiments entitled "Site Dependency of Shallow Seismic Data Quality in Saturated, Unconsolidated Coastal Sediments" is presented in **Addendum 8**.

SIGNIFICANT RESULTS. We now have enough seismic profiles, deep and shallow cores, foram data, and ^{14}C ages to begin a systematic stratigraphic analysis of the Sabine Lake–Sabine Bank region. Preliminary interpretations of depositional environments were made on the basis of detailed descriptions and stratigraphic cross sections prepared for the interfluve, chenier plain, and incised valley areas. A wood sample from the top of the fluvial sands (Deweyville) in the Neches entrenched valley near Sabine Pass yielded an age of about 8970 B.P. A peat sample just above the fluvial sand dated at 8770 BP indicates the time that the lower alluvial valley of the Sabine/Neches system was flooded. Apparently the wood was from a tree growing on the abandoned surface of the Deweyville and its age is not indicative of the time of Deweyville deposition.

Work Element 3: Coastal Processes

Understanding coastal processes is the key to understanding coastal erosion and predicting future coastal changes. Therefore, this work element involves numerous tasks that attempt to quantify basin energy, sediment motion, and the forcing functions that drive the coastal system. Objectives of this work element are to evaluate the magnitudes and rates of the relative rise in sea level during geological and historical time, to provide a basis for assessing wave and current energy as well as sediment transport, to assess climatic and meteorological influences on coastal processes, to evaluate the impacts of storms on shoreline stability and instantaneous erosion potential, and to begin quantifying the coastal sediment budget.

Task 2: Sediment Transport. In May 1995, another high-precision kinematic GPS survey was conducted at Galveston Island State Park to improve data collection techniques and to document actual beach changes. Preliminary results of the post-processed data indicate substantial changes in beach width and elevation. Sand was transferred from the forebeach to the backbeach probably as a result of beach cleaning operations routinely conducted after accumulations of Sargassum wash ashore.

Task 3: Sediment Budget. This task is evaluating the primary sediment sources (updrift erosion and fluvial sediment supply) and the principal sinks (beach accretion, onshore washover, dune construction, and offshore deposition). Some additional sediment losses occur at tidal inlets and some unknown quantity is trapped in the deep-draft navigation channels. Material periodically dredged from the ship channels deserves further evaluation as a potential source of beach nourishment material.

During the fourth year of study, we completed analysis of beach and offshore surveys along the northeastern end of Galveston Island encompassing the beach nourishment project in front of the seawall. These profiles were merged with additional offshore surveys conducted by T. L. James Co., the dredging contractor for the beach nourishment project. Combined beach and nearshore profiles at 22 sites are included in **Addendum 9**. We also interpreted the textural data for 70 sediment samples collected along the profiles and in the borrow site as part of their beach nourishment project. The beach and offshore profiling, which is a collaborative effort between the USGS study and the City of Galveston study, will provide baseline data before the dredging and pumping operations.

During year 4 we obtained the wave refraction model RCPWAVE provided by the U.S. Army Corps of Engineers' Coastal Engineering Research Center. Results from the model will be compared to large-scale (5 km) geomorphic features of the southeast Texas shoreline from East Matagorda Bay to Sabine Pass. Also we constructed a rectilinear bathymetric grid covering the study area, which is 300 km long and extends 100 km offshore to depths of 30 m. Grid cells measure 500 m alongshore and 125 m normal to shore forming a grid with 600 by 800 cells. Digital bathymetric data used to construct the grid were obtained from Mark Hanson of the U.S. Geological Survey in St. Petersburg, Florida. We used a combination of bathymetric data from surveys dating from the 1930's to the 1970's. Care was taken to use the latest available data for a particular area. Preliminary plots of the compiled bathymetry were printed to check for missing data and for quality control.

SIGNIFICANT RESULTS. Preliminary wave refraction analyses were conducted for the study area from Sabine Pass to Sargent Beach using a coarse grid. Results show constructive wave interference that is controlled by bathymetry and correlates well with the average long-term erosion rates on adjacent beaches.

Work Element 4: Prediction of Future Coastal Response

Task 1: Mathematical Analysis of Rates of Change. In year 4 development continued on the Shoreline Shape and Projection Program (SSAP) that will aid in determining future shoreline positions. The program will project future shoreline positions based on established methods that compute shoreline rates-of-change and a new method that involves comparing the shape of the projected shoreline with the expected shape. SSAP is being developed in FORTRAN for the Windows operating environment and is designed to easily accept historical shoreline data from a Geographic Information System (GIS) and to return projected shorelines to the GIS.

Work on SSAP in year 4 involved checking the algorithms that compute shoreline rates-of-change. Rate-of-change calculations from the literature and Bureau publications were compared with calculations from SSAP. Results from a computer program provided by Mike Fenster of the University of Virginia (UVA) were also compared. All comparisons have been favorable even though there were some slight differences with the UVA program and results published by Fenster et al., 1993, in the Journal of Coastal Research. The cause of these differences has been traced to variations in the methods of calculations and errors in the literature. A report providing detailed explanations of the methodology and test results is presented in **Addendum 10**.

SIGNIFICANT RESULTS. The program variables were documented to assist in subsequent program trouble shooting, additions, and upgrades. Variable names, types, uses, and occurrences have been traced through the program's subroutines and presented in a table.

Work Element 5: Sand Resources Investigations

This work is being conducted in cooperation with the Minerals Management Service as part of the sand assessment project. Textural analyses were completed for selected samples from 25 vibracores collected from Sabine Bank and Heald Bank. Core profiles for each of the 25 cores were prepared from visual descriptions and the sediment textures.

SIGNIFICANT RESULTS. We completed describing the 25 cores collected from the Sabine Bank–Heald Bank region and completed textural analyses for selected samples from the vibracores. Vibracore descriptions are presented in **Addendum 11** and sediment textures are presented in **Addendum 12**.

Work Element 6: Technology Transfer

The technology transfer work element provides for timely reporting of project results and makes the interpretations and conclusions available to users as needed. It also establishes a repository to preserve raw data and materials that would be a significant source of information for future studies.

SIGNIFICANT RESULTS. In year 4, four papers were presented at international conferences. A paper by R. A. Morton entitled "Global impact of mining and urbanization on earth surface processes and geomorphology in the coastal zone" was presented at the International Union of Geological Sciences Workshop that was held in Madrid, Spain. Results of the wetland-loss study were presented at the Society of Wetland Scientists annual meeting, held in Portland, Oregon, May 30–June 3, 1994. An abstract entitled "Marsh Loss in the Galveston Bay System, Texas," by W. A. White and R. A. Morton was published in the conference proceedings. Two papers were presented at the SEPM meeting in St. Petersburg, Fla. One paper by R. A. Morton and W. A. White was entitled "Evolution of incised coastal plain rivers, southeast Texas coast," the other by J. C. Gibeaut, J. A. Kyser, R. Gutierrez, and R. A. Morton was entitled "High-accuracy bathymetric surveys for coastal research."

Plans were initiated to hold an invited symposium on coastal research at the 1996 South-Central Section Meeting of the Geological Society of America. The meeting, which will be held in Austin, Texas, will highlight the USGS-BEG-LSU coastal cooperative research program.

Electronic files (ARC/INFO) containing all the shoreline positions for the southeastern Texas coast were transferred to the Minerals Management Service at the request of Melanie Stright, preservation officer. We also transferred ARC/INFO electronic files of shorelines of Galveston Island to a graduate student at TAMU College Station, and shorelines of South Padre Island to TAMU Corpus Christi, Conrad Blucher Institute.

Reprints of BEG articles documenting large-scale sedimentological and morphological changes in coastal environments related to hurricanes were sent to Chris Barton of the USGS in St. Petersburg.

Addendum 1. Wetland Losses Related to Fault Movement and Hydrocarbon Production, Southeastern Texas Coast

Wetland Losses Related to Fault Movement and Hydrocarbon Production, SoutheasternTexas Coast

William A. White and Robert A. Morton
Bureau of Economic Geology
The University of Texas at Austin
Austin, Texas 78713

ABSTRACT

Time series analyses of surface fault activity and nearby hydrocarbon production from the southeastern Texas coast show a high correlation among volume of produced fluids, timing of fault activation, rates of subsidence, and rates of wetland loss. Greater subsidence on the downthrown sides of faults contributes to more frequent flooding and generally wetter conditions, which are commonly reflected by changes in plant communities (e.g., Spartina patens to Spartina alterniflora) or progressive transformation of emergent vegetation to open water. Since the 1930s and 1950's, approximately 5,000 hectares of marsh habitat has been lost as a result of subsidence associated with faulting. Marshes have expanded locally along faults where hydrophytic vegetation has spread into former upland areas.

Fault traces are linear to curvilinear and are visible because elevation differences across faults alter soil hydrology and vegetation. Fault lengths range from 1 to 13.4 km and average 3.8 km. Seventy-five percent of the faults visible on recent aerial photographs are not visible on photographs taken in the 1930s indicating relatively recent fault movement. At least 80% of the surface faults correlate with extrapolated subsurface faults; the correlation increases to more than

90% when certain assumptions are made to compensate for mismatches in direction of displacement. Coastal wetlands loss in Texas associated with hydrocarbon extraction will likely increase where production in mature fields is prolonged without fluid reinjection.

INTRODUCTION

Along the northwestern Gulf of Mexico, significant oil and gas reserves coincide with the Nation's most extensive and productive coastal wetlands. Direct wetland losses caused by excavation of drilling sites, construction of canals, and installation of pipelines by the petroleum industry are easily observed and have been documented as a primary environmental impact (TURNER and CAHOON, 1988). Less obvious but equally destructive are wetland losses associated with subsidence and faulting induced by oil and gas production. This study extends the work of WHITE and TREMBLAY (1995) by examining in more detail changes in wetlands along faults and the histories of fault movement and fluid production.

Hundreds of faults offset Quaternary sediments and intersect the land surface along the southeast Texas Gulf Coast (VERBEEK, 1979). There is evidence that many faults have become active during the past few decades as a result of the withdrawal of water, oil and gas (VAN SICLEN, 1967; GUSTAVSON and KREITLER, 1976; VERBEEK and CLANTON, 1981). Wetland losses along surface faults have been documented (WHITE et al., 1985; MORTON and PAINE, 1990; WHITE and TREMBLAY, 1995; WHITE and MORTON, 1995), but the extent, timing, and probable causes of the fault activity have not been fully investigated. In this study, 40 faults that intersect coastal wetlands on the upper Texas coast were identified, mapped, and examined using aerial photographs (Figure 1). Primary objectives of this investigation were to document the locations and lengths of surface faults intersecting coastal wetlands, to determine historical activity of the faults, and to examine the relationship between fault movement, underground fluid production, and wetland changes.

METHODS

Most surface faults analyzed in this paper were initially identified as part of a wetlands mapping effort of the Texas Coastal Zone (WHITE et al., 1985 and 1987). Faults were identified primarily on photographs taken in 1979, from which the fault traces were optically transferred to USGS 7.5 minute topographic base maps.

Faults crossing wetlands are traceable on aerial photographs due to slightly lower elevations on the faults downthrown side creating contrasting moisture regimes and vegetation communities that highlight the fault trace (Figures 2 and 3) (CLANTON AND VERBEEK, 1981; WHITE et al., 1985). Sequential aerial photographs were used to determine when a fault first became visible and traceable at the land surface and to examine the subsequent progressive changes in vegetation and moisture conditions along the fault. The principal imagery examined to define fault traces and changes along the trace were aerial photographs taken in 1930, 1956, 1979, and 1989-1993. In selected areas, these photographs were supplemented with 1940s, early 1950s, and 1960s vintage photographs. The trace of each fault was classified as: (0) not visible , (1) faintly visible, or (2) distinctly visible. Faults that were distinctly visible and traceable on more recent photographs, but only partly traceable on older photographs were assigned two visibility classes, such as 0 to 1.

The distinctiveness of a fault trace can be influenced by soil moisture at the time the photographs were taken (VERBEEK and CLANTON, 1981). In general, we concluded that variations in moisture conditions during wetter periods should produce fault-normal variations in soils and vegetation that persist, making the faults visible on photographs even during drier periods. For example, faults traceable on 1930 photographs, which were taken during a period of higher than normal rainfall, were equally traceable on 1956 photographs, which were taken during a drought.

The link between surface faults and subsurface faults has been reported by many researchers (WEAVER and SHEETS, 1962; VAN SICLEN, 1967; REID, 1973; KREITLER, 1978; VERBEEK, 1979; VERBEEK and CLANTON, 1981). In this study, surface and subsurface faults were correlated by extrapolating subsurface faults shown on structure maps (from GEOMAP Co. and other sources) to the surface generally at angles between 45 and 80° (QUARLES, 1953; BRUCE, 1973; REID, 1973; GUSTAVSON and KREITLER, 1978).

Locations of surface faults and directions of throw were compared to the locations of oil and gas fields to determine the geographic relationship of the faults to the fields. A distance of 5,000 m was used as an estimate of geographic proximity between surface faults and producing fields. Faults may be activated greater distances than this from some fields if production from multiple fields causes regional depressurization and subsidence (EWING, 1985; GERMIAT and SHARP, 1990).

FAULT DISTRIBUTION, MOVEMENT, AND RELATION TO SUBSURFACE FAULTS

Distribution

Forty faults intersecting wetlands were identified and mapped between Sabine Lake and Matagorda Bay (Figure 1). Faults are scattered throughout this region and affect wetlands that have developed on Pleistocene deltaic and thin Holocene marsh deposits on the mainland, and Holocene barrier and flood-tidal delta deposits on the islands and peninsulas (FISHER et al. 1972). Four parallel faults forming a graben, which is defined at the surface by wetter conditions and lower marshes, were mapped on the inland margin of East Bay (Figure 1). VERBEEK and CLANTON (1981) mapped 5 faults in this area, one of which was identified in shallow high-resolution seismic reflection profiles. Inland from Follets Island, there are 9 faults, most of which have a NE strike. Several of these faults appear to be associated with the salt dome Hoskins Mound. In general, faults are linear to curvilinear, and their traceable lengths range from 1 to 13.4 km (Table 1).

Fault Movement

Most of the faults (about 75%) exhibited recent surface expression during the last 6 decades, with the majority appearing since the 1950s. Of the 40 faults mapped on recent aerial photographs, only 10 (25%), were visible on photographs taken in the 1930s (Table 1). By the early- to mid-1950s, 26, or approximately 65%, were identifiable on aerial photographs. Many of the faults identified on 1930s and 1950s photographs, however, were only faintly traceable and would not have been easily recognized without prior knowledge of the fault locations. By 1979, all but one of the 40 faults could be located and traced on aerial photographs. Distinctiveness of fault traces was due primarily to extensive replacement of emergent vegetation by open water along the downthrown side.

Surface and Subsurface Faults

Geological structures in the Gulf Coast Basin that influence near-surface coastal plain sediments formed as a result of gravity-driven tectonism involving tensional stresses and sediment mobilization. The dominant features are large expansion faults (growth faults), salt diapirs, and withdrawal basins. Late Cenozoic structural history of the region includes several stages of faulting and reactivation of older faults caused by episodic movement of salt and deep-water shale as well as shifting sites of diapirism. The regionally extensive expansion faults in the subsurface are aligned northeast-southwest, which is parallel to the present day coast.

Subsurface faults are high-angle normal faults that have increased throw with depth, and an angle that commonly steepens toward the earth's surface (VAN SICLEN, 1967; BRUCE, 1973, KREITLER, 1977; SHEETS, 1979; VERBEEK and CLANTON, 1981). Subsurface faults were extrapolated to the surface at angles generally ranging from about 45° to 80°. Most faults in this study had a best fit at angles of between 60° and 70° (Table 1).

Sixty percent of the mapped faults can be correlated with extrapolated faults shown on subsurface structure maps. The correlation of surface faults with subsurface faults increases to 80% if only those faults with adequate subsurface control for fault identification are considered. Sixteen surface faults have an excellent to good correlation with subsurface faults in terms of location, orientation, and direction of vertical displacement, and 8 exhibit at least some properties that correlate with subsurface faults. Four of the faults have reverse throws relative to nearby subsurface faults. Considering these as correlative brings the total out of the 30 with adequate subsurface control to 28, or 93% that can be correlated with subsurface faults .

Surface faults can have an apparent reverse throw relative to their subsurface equivalent for several reasons. First, the direction of movement along a fault at the surface can be locally opposite to the throw of the major fault plane at depth because of a rotational component associated with fault movement. This phenomenon commonly occurs along normal faults associated with salt domes and shale ridges in the Gulf Coast Basin (MARTIN JACKSON, 1995, Personnel Communication).

Second, movement at the surface across a fault can be in a reverse direction to the original displacement along the fault (BELL, 1991).

The relationship between subsurface and surface faults is exemplified on Bolivar Peninsula near the Caplen field, where two subsurface faults that intersect Lower Miocene strata at about 1,800 m have an excellent correlation with surface faults at extrapolated angles of approximately 65° (EWING, 1985).

CHANGES IN EMERGENT VEGETATION ACROSS FAULTS

Field observations and marsh transects indicate that vegetation communities change across faults as a result of elevation differences on the upthrown and downthrown sides. For example, along a topographic transect across a fault inland from Follets Island (Figure 1), plant communities on the upthrown side, which is about 25 cm higher than the downthrown side, change from an irregularly-flooded high marsh of Spartina spartinae and Spartina patens, to a more frequently-flooded low marsh of Spartina alterniflora, Distichlis spicata, and Salicornia sp. (Figure 4). Soils also vary from the upthrown to downthrown sides reflecting a change in the frequency of flooding and plant species composition (Table 2). Similar changes occur across faults in back-island salt marshes on Bolivar Peninsula. Field observations in May 1991 indicated that vegetation communities on the topographically higher upthrown sides of faults contained more Spartina patens and Distichlis spicata than the downthrown sides, which supported larger stands of Spartina alterniflora and patchy areas of Scirpus maritimus, Distichlis spicata, and Spartina patens.

Differences in plant communities across faults appear to be related to a successional change in vegetation as subsidence and associated relative sea-level rise increase the depth, frequency, and duration of flooding on the downthrown sides of faults. Because Spartina alterniflora can withstand more frequent flooding than Spartina patens and Distichlis spicata (ADAMS, 1963; CHABRECK, 1972; WEBB and DODD, 1978; GLEASON and ZIEMAN, 1981; MENDELSSOHN and MCKEE, 1988a; NAIDOO et al. 1992), a gradual replacement of these higher marsh species by Spartina alterniflora is expected. In a salt marsh in North Carolina, ADAMS (1963) attributed the replacement of portions of a maritime forest (Juniperus virginiana) by Spartina alterniflora to a relative rise in sea level. If fault-related subsidence and relative sea-level rise continue at rates that surpass rates of marsh sedimentation, eventually water depths and frequency of inundation will exceed even that which Spartina alterniflora can tolerate (MENDELSSOHN and MCKEE, 1988b) and all emergent vegetation will be replaced by open water.

These types of successional changes are occurring on the downthrown sides of faults crossing Bolivar Peninsula. Aerial photographs taken in the 1930s do not reveal the faults. Vegetation appears to be primarily that of a topographically high irregularly-flooded marsh characterized by Spartina patens and Distichlis spicata. By the 1950s, the faults are visible, and formerly high marshes on the faults downthrown sides had become partly replaced by low regularly-flooded Spartina alterniflora marsh, and open water. By 1979, there was additional local replacement of high marsh by low marsh, but the most significant and widespread change was that from marsh to open water.

Succession and loss of emergent vegetation in this area are attributed more to inundation than to increases in salinity. Estuarine salinities in East Bay, for example, average approximately 10-15 ppt (MARTINEZ 1973, 1974, 1975), which is within the tolerance range of salinities for most of the above listed species (PENFOUND AND HATHAWAY, 1938; CHABRECK,1972; MENDELSSOHN and MCKEE, 1988a). Salinity may play a roll in the succession, however, as Spartina patens is less tolerant of increasing salinities than Spartina alterniflora (PEZESHKI et al. 1987; MENDELSSOHN and MCKEE, 1988a; NAIDOO et al. 1992).

The progressive historical changes toward more extensive flooding, permanent inundation, and loss of wetlands on the downthrown sides of faults (Figure 5) is an indication of active fault movement. Approximately 5,000 hectares of emergent vegetation have been converted to open water as a result of fault-related subsidence from the 1930s and 1950s to the 1970s. About 70% of the loss has occurred in the Neches River Valley in association with two faults that cross the valley (Figure 6). Additional wetland losses totaling almost 900 hectares have occurred along faults in salt marshes on Bolivar Peninsula and in brackish marshes to the northeast (WHITE and TREMBLAY, 1995).

In some areas, differential subsidence along faults has resulted in an expansion of marshes rather than a loss of marshes. Marsh expansion is due to more frequent inundation and the spread of hydrophytes into areas previously characterized by prairie grasses. An example of this type of change occurred along an active fault that crosses Gordy Marsh near the eastern shore of Trinity Bay (Figure 7). This fault could not be clearly discerned on aerial photographs taken in 1930 nor in the 1950s, but by 1963, the fault had a distinct trace because of wetter conditions on the downthrown southeast side. By 1970 and 1979, the fault was even more distinct and wetlands, as interpreted on aerial photographs, had expanded. From the 1950s to 1989, marsh area increased by 275 hectares on the downthrown side of the fault (WHITE et al. 1993).

A scenario of vegetation succession similar to the irregularly to regularly flooded marshes can be envisioned for the prairie to marsh conversion as the frequency of flooding increases on the downthrown sides of faults. Prairie grasses near Gordy Marsh are dominated by Spartina spartinae, with other scattered species including Schizachyrium scoparium, Paspalum lividum, Setatia geniculata (CROUT

1976; HARCOMBE and NEAVILLE, 1977). Marshes are characterized by Spartina patens, Spartina spartinae, Distichlis spicata, Scirpus maritimus, Phragmites australis, and locally Spartina alterniflora, among other species (CROUT 1976; HARCOMBE and NEAVILLE, 1977; BENTON et al. 1979; and WHITE et al. 1985). As the area of prairie grasslands became more frequently inundated, there was a corresponding change in vegetation types from prairie species to marsh species. Vegetation and soil types are similar to those shown in Table 2.

SURFACE FAULTS AND OIL AND GAS PRODUCTION

Subsidence associated with the withdrawal of underground fluids such as ground water, oil, and gas, has been reported in many parts of the world (BELL, 1988) including the Gulf Coast Basin (GABRYSCH, 1969; POLAND and DAVIS, 1972; MARTIN and SERDENGECTI, 1984). Some early examples of subsidence and faulting associated with oil and gas production are the Goose Creek field in the Houston area, and the Saxet field in the Corpus Christi area (PRATT and JOHNSON, 1926; GUSTAVSON and KEITLER, 1976; HILLENBRAND, 1985). There is evidence that production from at least 18 oil and gas fields located on the Texas coastal plain has caused subsidence, some of which occurred along active faults (KREITLER, 1977; VERBEEK and CLANTON, 1981; EWING, 1985; KREITLER et al., 1988; HOLZER, 1990; WHITE and TREMBLAY, 1995).

Despite the widespread recognition of this phenomenon, the potential for significant wetland losses as a result of moderate to deep hydrocarbon production has generally been disregarded because in many old sedimentary basins, the magnitude of compaction strain associated with hydrocarbon production was small (GEERTSMA, 1973). This is not the case in relatively young sedimentary basins where large volumes of hydrocarbons and formation water are produced at moderate depths.

According to summaries presented in CHILINGARIAN et al. (1995), induced subsidence depends primarily on production depth, areal extent and thickness of reservoir, consolidation state of reservoir and overburden, heterogeneity of sediment column, and volume and rate of produced fluids. Tertiary reservoirs and overlying strata of the Gulf Coast basin where subsidence is pronounced are typically shallow to moderately deep, moderately thick (multiple pay zones) and areally extensive, unconsolidated, interbedded sandstones and mudstones with high in-situ porosities (MORTON and GALLOWAY, 1991). These sediments are highly compressible and subject to compaction as a result of fluid withdrawal.

Oil and gas reservoirs of the Gulf Coast are compartmentalized by sealing faults that create permeability boundaries and limit lateral flow of fluids. Because the reservoirs are confined by faults that prevent drainage from adjacent strata, large-volume fluid production results in greatly reduced pore pressures and increased shear stresses. In the absence of direct subsurface measurements, cumulative fluid production is a leading indicator of reduced pore pressures and increased shear stresses within the reservoir.

Previous studies in the Gulf Coast Basin demonstrate that land surface subsidence commonly occurs several kilometers away from producing wells rather than directly above the producing formation (GUSTAVSON and KREITLER, 1976; EWING, 1985; MORTON and PAINE, 1990). The locus of subsidence and wetland loss is controlled by the coupling between reservoir compaction and slip along the faults. The induced subsidence and wetland losses are concentrated along faults that become active when sufficiently large volumes of fluid (oil, gas, formation water) are removed from the subsurface. Fluid extraction causes a decline in pore pressure within the rocks and alters the state of stress near the faults. Thus, both the pattern of hydrocarbon production and the three-dimensional geometries of faults need to be considered in predicting the location and magnitude of wetland losses.

Geographic Association between Surface Faults and Oil and Gas Fields

In this study, 29 (about 70%) of the surface faults are within 5,000 m of an oil and gas field and have an orientation and direction of throw that suggests an association with the field. Only 21 fields (53%), however, have both a close geographic association with faults and production history (for example, year of discovery) that suggest that oil and gas production could be responsible for the faults initial appearance at the surface. Nevertheless, the progressive loss of wetlands along many of the faults indicates recent fault movement may be related to oil and gas production even though the faults were present before production began. In some cases fault movement may be related to regional extensional subsidence associated with large-volume regional fluid production from more distant fields.

VERBEEK and CLANTON (1981) and HOLZER and BLUNTZER (1984) concluded that differential subsidence and fault activation from hydrocarbon production in the Houston area is relatively minor compared to that associated with extensive volumes of groundwater withdrawal. Most of the faults analyzed in this study, however, are in areas that should not be significantly affected by groundwater pumpage.

Hydrocarbon Production, Fault Activity, and Associated Wetland Losses

To determine possible relationships between hydrocarbon production, and surface fault activity promoting wetland loss, we investigated production histories of three moderately large oil and gas fields that have a geographic association with surface faults. All three fields, Port Neches, Clam Lake, and Caplen (Figure 8), are associated with deep-seated salt domes (FISHER et al., 1972, 1973; MUSOLFF, 1962). Production histories of the three fields are somewhat similar in that each was discovered before 1940, production is from Miocene and Oligocene reservoirs, and cumulative oil production in each exceeds 19 million barrels. Surface faults correlate well with subsurface faults, and formerly extensive marshes have been converted to open water on the downthrown sides of the faults. Surface environments where the fields are located include the alluvial valley of a major river, an interfluvial coastal plain marsh and a barrier island (Figure 8).

Port Neches Field.

The Port Neches field is located in the Neches River valley near the head of Sabine Lake (Figure 8). Cumulative hydrocarbon production has exceeded 25 million barrels of oil and 40 billion ft^3 of gas since discovery of the field in 1929 (Figure 9). If associated fields (Port Neches, North, South, and West) are included, cumulative oil production exceeds 33 million barrels, and gas production 500 billion ft^3. Production in the Port Neches field is from average depths of about 1,800 m (TEXAS RAILROAD COMMISSION, 1994). Annual production records show rapid acceleration in gas production in the late 1950s, with production falling precipitously after 1959 (Figure 9). Oil production peaked in the early 1950s and gradually declined through the 1980s.

Traces of two surface faults mapped east of the Port Neches field (Figure 6) were not visible on photographs taken in the 1930s or mid 1950s, but were visible on photographs taken in the 1960s (Figure 5). Between 1956 and 1978, almost 3,500 hectares of wetlands in the Neches River valley were replaced by open water and shallow subaqueous flats (WHITE et al., 1987). These extensive losses occurred primarily on the downthrown side of the faults that border the field (Figure 5 and 6) indicating that differential subsidence over the field contributed to the loss of wetlands.

Complications arise in attributing all the wetland losses in the Neches River valley to subsidence because other processes can contribute to wetland loss. Among those processes are dredging and filling of wetlands, which can cause direct and indirect losses, and construction of upstream dams and reservoirs that can reduce the supply of fluvial sediments that nourish and maintain wetlands. The spatial and temporal relationships among oil and gas production, fault activation, and wetland loss are compelling evidence that there is a causal relationship between hydrocarbon production and differential subsidence across the mapped faults.

Clam Lake Field

The Clam Lake field, which is located in the interfluvial area between Sabine Lake and East (Galveston) Bay (Figure 8), was discovered in 1937. Since discovery, it has produced more than 21 million barrels of oil and 4 billion ft^3 of gas (Figure 10) at depths ranging from 700 m to 2000 m (WILLIAMS, 1962). The field is centered on a salt dome with complex subsurface faulting including a major north-south striking fault downthrown on the west side toward the field (WILLIAMS, 1962). Extrapolation of this fault to the surface at an angle of approximately 60° matches well with a surface fault that is traceable over a distance of about 6 km (Figure 11). The fault trace was not visible on aerial photographs in 1930 and 1956, but is distinctly visible on photographs taken in 1966 and later. The fault intersects brackish-water marshes and its visibility is accentuated because of ponded water and low marshes on the downthrown side of the fault (Figure 11). Between 1956 and

1987 approximately 275 hectares of marsh was converted to open water primarily on the downthrown side of the fault (WHITE and TREMBLAY, 1995).

Fault movement between 1956 and 1966 correlates well with annual oil production (Figure 10). Production gradually increased from 1937 to 1958, after which there was a rapid rise in production from 1958 to 1963 followed by a decline. Cumulative oil production through 1964 exceeded 10 million barrels (Figure 10). A second fault in this area was not clearly visible on 1978 photographs but is very distinct on 1989 photographs, indicating activation or accelerated movement during the past two decades.

Caplen Field

Production from the Caplen field is primarily from lower Miocene reservoirs at depths of 2,100 to 2,200 m (EWING, 1985). After its discovery in 1939, oil production reached a peak in the mid 1950s when annual production exceeded 600,000 barrels (TEXAS RAILROAD COMMISSION records). Between 1943 and 1979, annual production fluctuated between 300,000 and 600,000 barrels a year, declining at a relatively uniform rate after 1970. Gas production increased in the late 1950s and 1960s, with casinghead gas reaching a peak between 1968 and 1971, and non-associated gas reaching a peak in the early 1980s. Production of both oil and gas declined after 1980. Apparently most of the production comes from a strong water drive, and records from the Railroad Commission of Texas indicate a total fluid production, including formation water, of 30-40 million barrels to 1985 (EWING, 1985).

Two surface faults that cross the barrier island are not visible on aerial photographs taken in 1930, but portions of the faults are traceable on photographs taken in 1952. A benchmark releveling survey along Bolivar Peninsula indicates differential subsidence across a fault in this area from 1936 to 1954 (Figure 12). By 1950, cumulative production had reached about 3.7 million barrels of oil, and 647 million ft^3 of gas (Figure 13) . The faults are more pronounced on photographs taken in the 1970s and 1980s, as areas of open water expanded at the expense of marshes. Approximately 600 hectares of marsh were converted to open water between the 1950s and 1989 (WHITE and TREMBLAY, 1995). This wetland loss coincides with annual gas production that peaked in the late 1960s to early 1980s. As with the Port Neches and Clam Lake Fields, the spatial and temporal relationships between oil and gas production, faulting, and marsh loss support EWING'S (1985) conclusion of a causal relationship between fluid production and fault movement. Much larger fluid volumes produced from reservoirs at High Island salt dome (Figure 1), may have caused regional depressurization and subsidence, that contributed to reactivation of several faults along the northern margin of East Bay (EWING, 1985).

CONCLUSIONS

Recent artificially induced fault movement has resulted in the loss of large wetland areas on the southeastern Texas Gulf coast. Air photo analysis of 40 faults illustrate extensive replacement of emergent vegetation by open water along many of these faults. Upland and wetland response to fault movement is a time-dependent progression toward wetter conditions and eventually permanent inundation. Successional changes in wetlands may proceed from initial dense stands of topographically high marsh characterized by species such as Spartina patens and Spartina spartinae, to low, regularly-flooded marsh dominated by Spartina alterniflora. Continued subsidence and associated relative sea-level rise forms isolated ponds and shallow subaqueous flats, and eventually larger, coalescing ponds and open water. This expansion of open water on the downthrown sides of faults has contributed to the loss of approximately 5,000 hectares of wetland emergent vegetation since the 1930s and 1950s. Locally, however, differential subsidence along faults has resulted in an expansion of wetlands into areas previously mapped as uplands.

Land-surface subsidence and coastal wetland loss are not only caused by shallow groundwater extraction, but can also be caused by hydrocarbon production at depths of more than 2000 m. Subsidence in many areas is focused along surface faults.

Approximately 75% of the observed faults have been activated in recent decades. There is a close correlation between history of fluid production and history of fault movement. Production data from two fields indicate that fault movement was initiated during the first 10 to 20 years of production after about 5 million bbls of oil had been extracted. In a third field, large volumes of gas production appear to have triggered fault movement. Once faults are activated, wetland losses continue throughout the production period of the field. Documented wetland losses are greatest around moderately large fields that have produced more than 19 million bbls of liquids during a period of about 40 years.

Continued large-volume extraction of conventional energy resources as well as anticipated production of alternative energy resources (geopressured-geothermal fluids) and methane dissolved and entrained in formation water in the Gulf Coast region will only increase existing subsidence and wetland losses or cause inundation of areas that are currently stable unless techniques are developed to control the induced subsidence.

The long history of fluid production, subsidence, and wetland loss in the Gulf Coast region provides a basis for managing reservoirs in other coastal plain settings throughout the world where large oil and gas fields are being produced beneath valuable wetlands.

ACKNOWLEDGMENTS

Funding for this project was provided by the U.S. Geological Survey through a cooperative study on coastal erosion and land loss along the northern Gulf Coast.

LITERATURE CITED

ADAMS, D. A., 196. Factors influencing vascular plant zonation in North Carolina salt marshes. Ecology, 44, 445-455.

BELL, J. W. ,1991. Elevation changes associated with subsidence in Las Vegas Valley, Nevada. In: Johnson, A. I., (ed.), Land Subsidence, Proceedings of the Fourth International Symposium on Land Subsidence, Houston, Texas. Washington, DC, IAHS Publication No. 200, 473-481.

BELL, J. W., 1988. Subsidence associated with the abstraction of fluids. In: Bell, F. G.; Culshaw, M. G.; Cripps, J. C., and Lovell, M. A., (eds.), Engineering Geology of Underground Movements, Geological Society Engineering Geology Special Publication No. 5, 363-376.

BENTON, JR., A. R., SNELL, W. W., and CLARK, C. A., 1979. Monitoring and Mapping of Texas Coastal Wetlands, Galveston Bay and Sabine Lake Areas, 1978 Growing Season. College Station, Texas: Texas A&M University Remote Sensing Center, Technical Report RSC-102, variable pagination.

BRUCE, C. H., 1973. Pressured shale and related sediment deformation: mechanism for development of regional contemporaneous faults. American Association of Petroleum Geologists Bulletin, 57, 878-886.

CHABRECK, R. H., 1972. Vegetation, water and soil characteristics of the Louisiana Coastal region. Baton Rouge, Louisiana: Louisiana Agricultural and Experiment Station Bulletin No. 664, 72p.

CHILINGARIAN, G. V.; DONALDSON, E. C., and YEN, T. F., 1995. Subsidence due to fluid withdrawal: Developments in Petroleum Science 41, Elsevier, Amsterdam, 498p.

CLANTON, U. S. and VERBEEK, E. R., 1981. Phototgraphic portrait of active faults in the Houston Metropolitan area, Texas. In: ETTER, E. M, (ed.), Houston area Environmental Geology: Surface Faulting, Ground Subsidence, Hazard Liability. Houston, Texas: Houston Geological Society, 70-113.

CRENWELGE, G. W.; CROUT, J. D.; GRIFFIN, E. L; GOLDEN, M. L., and BAKER J. K., 1981. Soil Survey of Brazoria County, Texas. Washington, D. C.: U. S. Department of Agriculture, Soil Conservation Service, 140p.

CROUT, J. D., 1976. Soil Survey of Chambers County, Texas: U. S. Department of Agriculture Soil Conservation Service in cooperation with Texas Agricultural Experiment Station, 53p.

EWING, T.E., 1985. Subsidence and surface faulting in the Houston-Galveston area, Texas--related to deep fluid withdrawal?. In: DORFMAN, M.H., and MORTON, R.A. (eds.), Geopressured-Geothermal Energy: Proceedings of the 6th U.S. Gulf Coast Geopressured-Geothermal Energy Conference. New York: Pergamon Press, 289-298.

FISHER, W.L.; MCGOWEN, J.H.; BROWN, L.F., JR., and GROAT, C.G., 1972. Environmental Geologic Atlas of the Texas Coastal Zone--Galveston-Houston

Area. Austin, Texas: The University of Texas at Austin, Bureau of Economic Geology, 91p., 9 maps.

FISHER, W.L.; BROWN, L.F., JR.; MCGOWEN, J.H., and GROAT, C.G., 1973. Environmental Geologic Atlas of the Texas Coastal Zone--Beaumont-Port Arthur Area. Austin, Texas: The University of Texas at Austin, Bureau of Economic Geology, 93p., 9 maps.

GABRYSCH, R.K., 1969. Land-surface subsidence in the Houston-Galveston region, Texas. Tokyo, Japan: Proceedings, International Symposium on Land Subsidence, Publication No. 88, IAHS, 43-54.

GABRYSCH, R.K. and COPLIN, L.S., 1990. Land-surface subsidence resulting from ground-water withdrawals in the Houston-Galveston region, Texas, through 1987. Washington, D.C.: U.S. Geological Survey Report of Investigations No. 90-01, 53p.

GERMIAT, S. J. and SHARP, J. M., 1990. Assessment of future coastal land loss along the upper Texas Gulf Coast to the year 2050. Bulletin of the Association of Engineering Geologists, XXVII, 263-280.

GEERTSMA, J., 1973. Land subsidence above compacting oil and gas reservoirs. Journal of Petroleum Technology, 25, 734-744.

GLEASON, M. L. and ZIEMAN, J. C., 1981. Influence of tidal inundation on internal oxygen supply of Spartina alterniflora and Spartina patens. Estuarine, Coastal and Shelf Science, 13, 47-57.

GUSTAVSON, T. C. and KREITLER, C. W., 1976. Geothermal resources of the Texas Gulf Coast – environmental concerns arising from the production and disposal of geothermal waters. Austin Texas: The University of Texas at Austin, Bureau of Economic Geology Geological Circular 76-7, 35p.

HARCOMBE, P. A., and NEAVILLE, J. E., 1977, Vegetation types of Chambers County, Texas. The Texas Journal of Science, 39, 210-234.

HILLENBRAND, C. J., 1985. Subsidence and fault activation related to fluid extraction Saxet Field, Nueces County, Texas. Unpublished Masters Thesis. University of Houston, 144p.

HOLZER, T. L., 1990. Land subsidence caused by withdrawal of oil and gas in the Gulf Coastal Plain -- The Houston, Texas case history (abs.). Gulf Coast Association of Geological Societies Transactions, 40, 301.

HOLZER, T. L., and BLUNTZER, R. L., 1984. Land subsidence near oil and gas fields, Houston, Texas. Ground Water, 22, 450-459.

KREITLER, C.W., 1978. Faulting and land subsidence from ground-water and hydrocarbon production, Houston-Galveston, Texas. Austin, Texas: The University of Texas at Austin, Bureau of Economic Geology Research Note 8, 22 p.

KREITLER, C.W.; WHITE, W.A., and AKHTER, M.S., 1988. Land subsidence associated with hydrocarbon production, Texas Gulf Coast (abs.). American Association of Petroleum Geologists Bulletin, 72, 208.

MARTIN, J. C. and SERDENGECTI, S., 1984. Subsidence over oil and gas fields. In: Holzer, T. L., (ed.), Geological Society of America Reviews in Engineering Geology, VI, 23-34.

MARTINEZ, A. R., 1975. Coastal Hydrographic and Meteorological Study, Coastal Fisheries Project Report, Texas: Texas Parks and Wildlife Department, pp. 100-157.

MARTINEZ, A. R., 1974. Coastal Hydrographic and Meteorological Study, Coastal Fisheries Project Report, Texas: Texas Parks and Wildlife Department, pp. 61-108.

MARTINEZ, A. R., 1973. Coastal Hydrographic and Meteorological Study, Coastal Fisheries Project Report, Texas: Texas Parks and Wildlife Department, pp. 111-172.

MENDELSSOHN, I. A. and MCKEE, K. L., 1988a. Experimental field and greenhouse verification of the influence of saltwater intrusion and submergence on marsh deterioration: mechanisms of action. In: TURNER, R. E. and CAHOON D. R., eds., Causes of Wetland Loss in the Coastal Central Gulf of Mexico, Volume II: Technical Narrative: U.S. Department of the Interior, Minerals Management Service, MMS 87-0120, pp. 145-180.

MENDELSSOHN, I. A. and MCKEE, K. L., 1988b. Spartina alterniflora die-back in Louisiana: time-course investigation of soil waterlogging effects. Journal of Ecology, 76, 509-521.

MORTON, R. A. and GALLOWAY, W. E., 1991. Depositional, tectonic, and eustatic controls on hydrocarbon distribution in divergent margin basins: Cenozoic Gulf of Mexico case history. In: MEYER, A. W., DAVIES, T. A., and WISE, S. W., eds., Evolution of Mesozoic and Cenozoic continental margins: Marine Geology, 102, 239-263.

MORTON, R.A. and PAINE, J.G., 1990. Coastal land loss in Texas--an overview: Gulf Coast Association of Geological Societies Transactions, 40, 625-634.

MUSOLFF, N. C., 1962. Caplen Field, Galveston County, Texas. In: Denham, R. L., (ed.), Typical Oil and Gas Fields of Southeast Texas. Houston, Texas: Houston Geological Society, 30-33.

NAIDOO, G.; MCKEE, K. L.; and MENDELSSOHN, I. A., 1992, Anatomical and metabolic responses to waterlogging and salinity in Spartina alterniflora and S. Patens (Poaceae). American Journal of Botany, 79, 765-770.

PENFOUND, W. T., and HATHAWAY, E. S., 1938, Plant communities in the marshlands of southeastern Louisiana. Ecological Monographs, 8, 1-56.

PEZESHKI, S. R.; DELAUNE, R. D.; and PATRICK, JR., W. H., 1987, Response of Spartina patens to increasing levels of salinity in rapidly subsiding marshes of the Mississippi River Deltaic Plain. Estuarine, Coastal and Shelf Science, 24, 389-399.

POLAND, J. F. and DAVIS, G. H., 1972. Land subsidence due to withdrawal of fluids, In: Man and His Physical Enviroment, Readings in Environmental Geology. Minneapolis, Minnesota: Burgess Publishing Co., 77-90.

PRATT, W.E. and JOHNSON, D.W., 1926. Local subsidence of the Goose Creek oil field. Journal of Geology, 34, 577-590.

QUARLES, M., JR., 1953. Salt-ridge hypothesis on origin of Texas Gulf Coast type faulting. American Association of Petroleum Geologists Bulletin, 37, 489-508.

REID, W.M, 1973. Active faults in Houston, Texas. Austin, Texas: The University of Texas at Austin, Unpublished Ph.D. dissertation, 122p.

SHEETS, M. M., 1979. Oil fields, subsidence and surface faulting in the Houston area. Houston Geological Society Guidebook for AAPG/SEPM Convention, 20p.

TEXAS RAILROAD COMMISSION, 1994. Oil and Gas Division Annual Report, 1992, Volume 1. Austin, Texas: Railroad Commission of Texas, 440p.

TURNER, R.E. and CAHOON, D.R., (eds.), 1988. Causes of Wetland Loss in the Coastal Central Gulf of Mexico, Volume II: Technical Narrative. New Orleans, Louisiana: U.S. Department of the Interior, Minerals Management Service, OCS Study/MMS 87-0120, 400p.

VAN SICLEN, D., 1967. The Houston fault problem. Proceedings of the American Institute of Professional Geologists, 3rd Annual Meeting, Texas Section, Dallas, 9-31.

VERBEEK, E.R. and CLANTON, U.S., 1981. Historically active faults in the Houston metropolitan area. Texas. In: ETTER, E. M, (ed.), Houston area Environmental Geology: Surface Faulting, Ground Subsidence, Hazard Liability. Houston, Texas: Houston Geological Society, p. 28-68.

VERBEEK, E.R., 1979. Surface faults in the Gulf Coastal Plain between Victoria and Beaumont, Texas. Tectonophysics, 52, 373-375.

WEAVER, P. and SHEETS, M., 1962. Active faults, subsidence and foundation problems in the Houston, Texas, area. Houston, Texas: Geology of the Gulf Coast and Central Texas, Houston Geological Society Guidebook, 254-265.

WEBB, J. W., and DODD,J. D., 1978. Shoreline plant establishment and use of a wave-stilling device. U.S. Department of the Army Coastal Engineering Research Center Miscellaneous Report 78-1. Fort Belvoir, Virginia, 27p.

WHITE, W.A.; TREMBLAY, T.A.; WERMUND, E.G., JR., and HANDLEY, L.R., 1993. Trends and status of wetland and aquatic habitats in the Galveston Bay system, Texas. Webster, Texas: Galveston Bay National Estuary Program, GBNEP-31, 225p.

WHITE, W.A.; CALNAN, T.R.; MORTON, R.A.; KIMBLE, R.S.; LITTLETON, T.G.; MCGOWEN, J.H.; NANCE, H.S., and SCHMEDES, K.E., 1985. Submerged Lands of Texas, Galveston-Houston Area: Sediments, Geochemistry, Benthic Macroinvertebrates, and Associated Wetlands. Austin, Texas: The University of Texas at Austin, Bureau of Economic Geology, Special publication, 145 p.

WHITE, W.A., CALNAN, T.R., MORTON, R.A., KIMBLE, R.S., LITTLETON, T.G., MCGOWEN, J.H., and NANCE, H.S., 1987. Submerged Lands of Texas, Beaumont-Port Arthur Area: Sediments, Geochemistry, Benthic Macroinvertebrates, and Associated Wetlands. Austin, Texas: The University of Texas at Austin, Bureau Economic Geology Special Publication, 110 p.

WHITE, W.A. and PAINE, J.G., 1992. Wetland plant communities, Galveston Bay system. Webster, Texas: Galveston Bay National Estuary Program, GBNEP-16, 124p.

WHITE, W. A. and TREMBLAY, T. A., 1995. Submergence of wetlands as a result of human-induced subsidence and faulting along the upper Texas Gulf Coast. Journal of Coastal Research, 1, 788-807.

WHITE, W. A. and MORTON, R. A., 1995. Active faults and their effect of wetlands, upper Texas Gulf Coast (abs.). Boston, Massachusetts: Society of Wetland Scientists 16th Annual Meeting, 42-43.

WILLIAMS, K. O., 1962. Clam Lake Field, Jefferson County, Texas. In: Denham, R. L., (ed.), Typical Oil and Gas Fields of Southeast Texas. Houston, Texas: Houston Geological Society, 34-37.

YERKES, R.F. and CASTLE, R.O., 1969. Surface deformation associated with oil and gas field operations in the United States. Tokyo, Japan: Proceedings, International Symposium on Land Subsidence, Publication No. 88, AIHS, 1, 55-66.

Table 1. Length, historical development and angle of extrapolation of surface faults intersecting wetlands, upper Texas Coast.

Fault Number	Informal Fault Name	Fault Length (km)	Fault visibility 1930 Photo	Fault Visibility 1956 Photo	Fault Visibility 1979 Photo	Fault Visibility Late 1980s-1990s Photos	Approximate angle of extrapolation between surface and subsurface faults (degrees)
1	Orange	1.0		0 *	2	2	75
2	Neches Valley W	5.0	0	0	2	2	45
3	Neches Valley E	5.5	0	0	2	2	40
4	Texas Point E	1.6	0	0	2	2	
5	Texas Point C	1.8	0	0	0	2	
6	Texas Point W	3.7	0	1	2	2	
7	Blind Lake	10.8	0	0	2	2	
8	Clam Lake N	6.1	0	0	2	2	60
9	Clam Lake E	7.5	0	0	0-1	2	90
10	Star Lake	3.6	0	0	2	2	70
11	Mud Lake	2.9	0	1	2	2	68
12	High Island E	3.9	0	2	2	2	
13	High Island N	1.1	0	0	2	2	45
14	Robinson Lake E	3.0	0	0	2	2	69
15	Robinson Lake EC	5.0	0	0-1	2	2	68
16	Robinson Lake WC	1.0	0	0-1	2	2	64
17	Robinson Lake W	4.6	0	0	2	2	64
18	Bolivar Fan E-W	13.4	0	0-2	2	2	65
19	Bolivar Fan N	2.3	0	0-1	2	2	65
20	Flake	2.4	2	2	2	2	80
21	Point Bolivar	1.8	2	2	2	2	80
22	Gordy Marsh	2.5	0-1	0-1	2	2	75
23	Lost Lake	1.5	0	2	2	2	
24	Jones Bay	3.1	0	2	2	2	38
25	Hitchcock N	4.0	2	0-2	2	2	50
26	Hitchcock C	4.0	1	1	2	2	
27	Hitchcock S	2.6	0	1	2	2	70
28	Chocolate Bay N	3.2	0	0-1	2	2	64
29	Chocolate Bay C	6.6	1	1	2	2	79
30	Chocolate Bay S	5.1	0-1	2	2	2	54
31	Hoskins Mound	1.5	0	2	2	2	45
32	Mud Island N	1.2	0	0-1	2	2	45
33	Mud Island S	2.0	0-1	1	2	2	
34	Christmas Bay	2.7	2	2	2	2	
35	Salt Lake	12.5	2	1-2	2	2	83
36	Slop Bowl	4.2	0	1	2	2	
37	Bryan Mound	1.8	0	0-1	2	2	
38	Cedar Lakes	2.0	0	0	1-2	2	75
39	Dead Caney Lake	1.8	0	0-1	2	2	
40	Boggy Bayou	2.2	0	0	0-2	2	?

* Visibility on aerial photographs

Total length (km) 152.5 0= not visible

Average Length (km) 3.8 1= faintly visible

Mode = 1.8 2= distinctly visible

Table 2. Types and characteristics of soils located on the upthrown block and downthrown block of a fault crossing the Brazoria National Wildlife Refuge. From CRENWELGE et al. (1981).

UPTHROWN BLOCK:

Surfside Clay

Level saline soil-rarely flooded
Water table < 0.6 m during winter
Salty prairie vegetation
90% Spartina spartinae

DOWNTHROWN BLOCK:

Harris Clay

Level saline marsh soil
Water table < 0.5 m
Typically 50% Spartina patens
25% Disticlis spicata
10% Paspalum vaginatum
10% Scirpus americanus

Harris-Tracosa Complex

Broad tidal marsh areas
45% Harris Clay, 40% Tracosa Mucky Clay
Water table < 0.5 M
Depressions containing water
Tracosa Soils -- Ruppia maritima in depressions
Where vegetated-- 90% Spartina alterniflora

Figure Captions

Figure 1. Distribution of surface faults intersecting wetlands on the upper Texas Coast. Thirty-six of the forty faults are shown in this figure; the remaining four are to the southwest. Coastal deposition systems modified from FISHER et al. (1972; 1973).

Figure 2. Active coastal plain fault in the Brazoria National Wildlife Refuge inland from Follets Island (Figure 1). D = downthrown side, U = upthrown side. NASA photograph taken in 1979.

Figure 3. Field view of fault shown in Figure 2. Vegetation changes from Spartina patens on the upthrown side to Spartina alterniflora on the downthrown side. The change in vegetation is a result of lower elevations and more frequent flooding on the fault's downthrown side.

Figure 4. Topographic profile across an active fault (Figure 3) showing relative elevations and plant communities that occur on each side of the fault. Lower elevations of approximately 25 cm on the downthrown side of this fault are reflected in a topographically lower marsh community. From WHITE and PAINE (1992).

Figure 5. Neches River valley fault as shown on aerial photograph taken in 1966 by the U.S. Department of Agriculture. D = downthrown side, U = upthrown side. This is the westernmost fault shown in Figure 6.

Figure 6. Changes in the distribution of wetlands between 1956 and 1978 in the Neches River valley at the head of Sabine Lake. Differential subsidence along the

faults crossing the valley have contributed to the conversion of emergent vegetation to open water. D = downthrown side, U = upthrown side. Modified from WHITE et al. (1987).

Figure 7. Simplified illustration of fault that intersects Gordy Marsh on the southern margin of Trinity Bay (Figure 1). Marshes and ponded water characterize the downthrown side (D) of the fault. From WHITE et al. (1985).

Figure 8. Locations of Port Neches, Clam Lake, and Caplen oil and gas fields. Wetland loss around these fields has exceeded 4,500 ha since 1956.

Figure 9. Cumulative production of oil and gas from the Port Neches field located in the Neches River valley. Surface faults downthrown toward the field are not visible on aerial photographs taken in the mid-1950s but are visible by the mid-1960s after cumulative gas production had reached 40 billion ft^3. Production volumes are from the TEXAS RAILROAD COMMISSION.

Figure 10. Cumulative production of oil and gas from the Clam Lake field. A surface fault downthrown toward the field was not visible in 1956 but was distinctly visible in 1966 after broad areas of emergent vegetation were replaced by open water on the downthrown side of the fault. Cumulative oil production exceeded 12 million barrels in 1966. Production volumes are from the TEXAS RAILROAD COMMISSION.

Figure 11. Fault and associated marshes and water features near Clam Lake (Figure 8) in the McFaddin National Wildlife Refuge. From WHITE et al. (1987).

Figure 12. Aerial photograph and land-surface subsidence profile showing fault on Bolivar Peninsula near Caplen field (Figure 8). Land-surface subsidence profile is based on bench mark leveling surveys in 1936 and 1954 along State Highway 87. Projection to the southwest of the fault shown in the aerial photograph indicates it should cross the highway between bench marks R171 (shown in the photograph) and Q171 which is located out of the photograph to the southwest. Increased rates of subsidence at R171 indicates that it is on the downthrown side (D) of the fault and Q171 is on the upthrown side (U). Profile from CHARLES W. KREITLER, unpublished data.

Figure 13. Cumulative production of oil and gas from the Caplen field (Figure 8). Surface faults near the field were not visible in 1930 but were visible in the 1950s. Since the 1950s, there has been an expanding loss of wetland emergent vegetation on the faults downthrown sides. Production volumes are from the TEXAS RAILROAD COMMISSION.

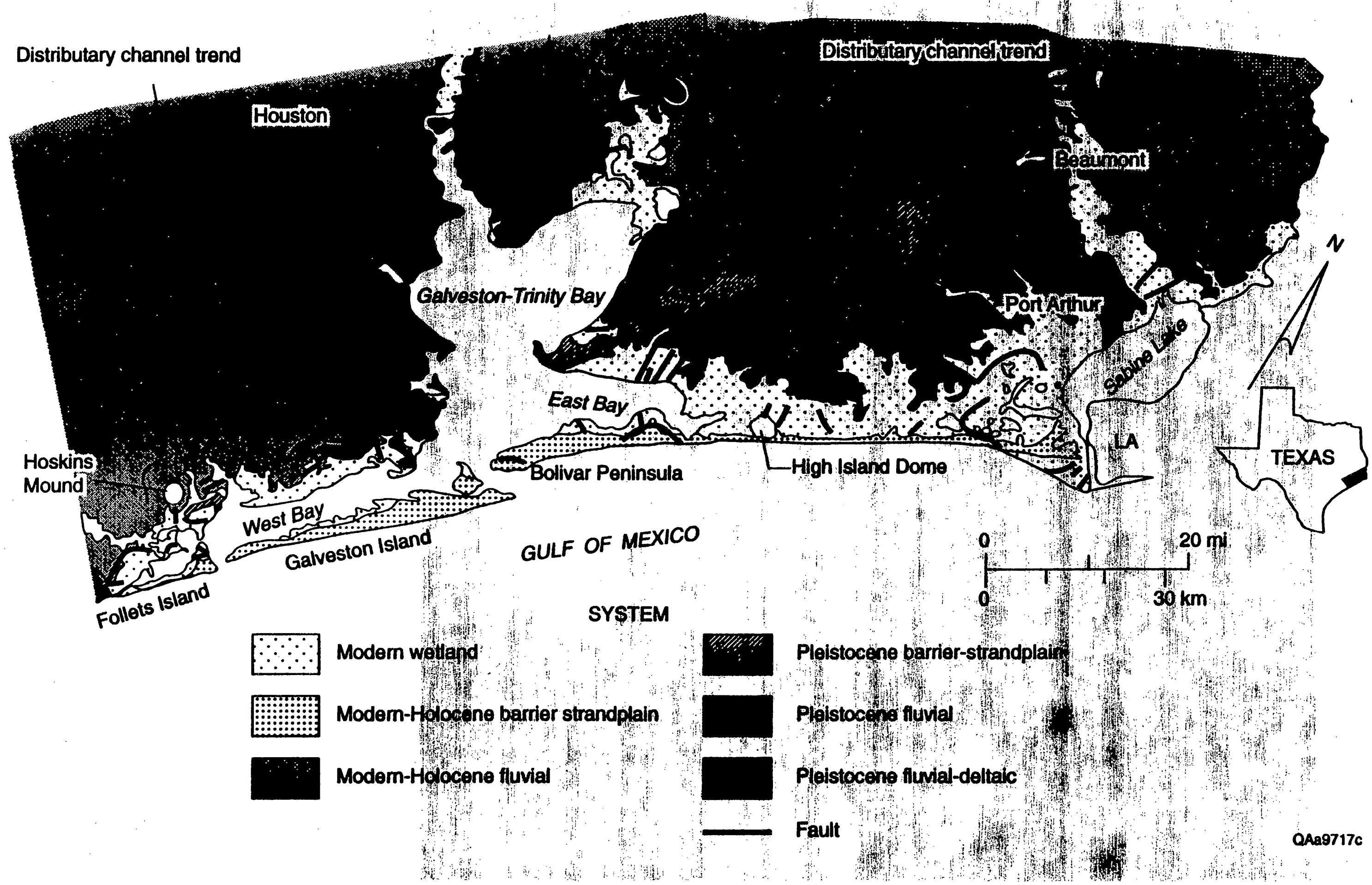
Distributary channel trend
Distributary channel trend
Houston
Beaumont
Galveston-Trinity Bay
Port Arthur
Sabine Lake
East Bay
LA
TEXAS
N
Hoskins Mound
Bolivar Peninsula
High Island Dome
West Bay
Galveston Island
Follets Island
GULF OF MEXICO
0
20 mi
0
30 km
SYSTEM
Modern wetland
Modern-Holocene barrier strandplain
Modern-Holocene fluvial
Pleistocene barrier-strandplain
Pleistocene fluvial
Pleistocene fluvial-deltaic
Fault
QAa9717c

Figure 1

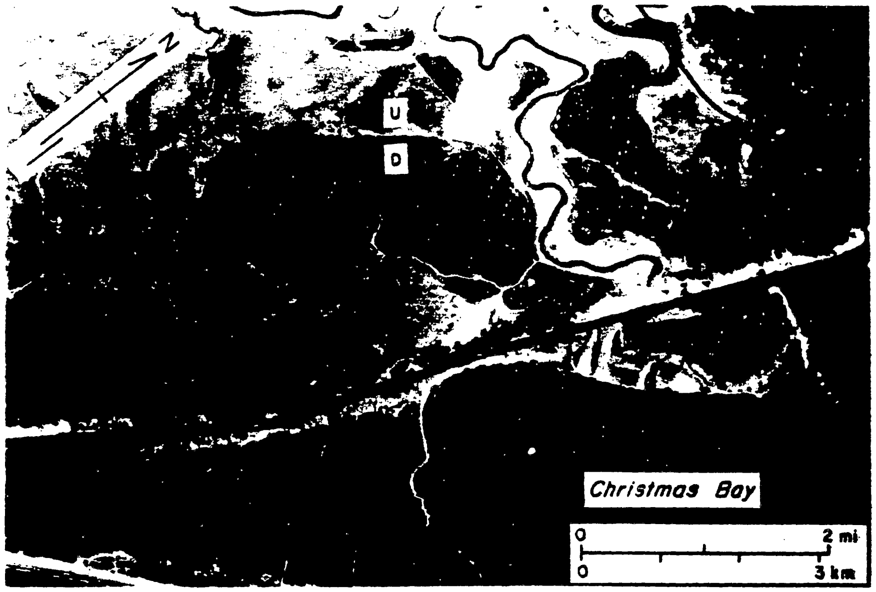

Figure 2

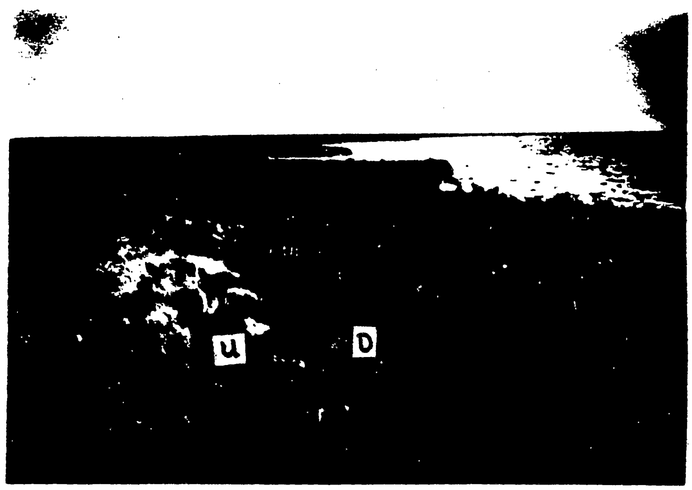

Figure 3

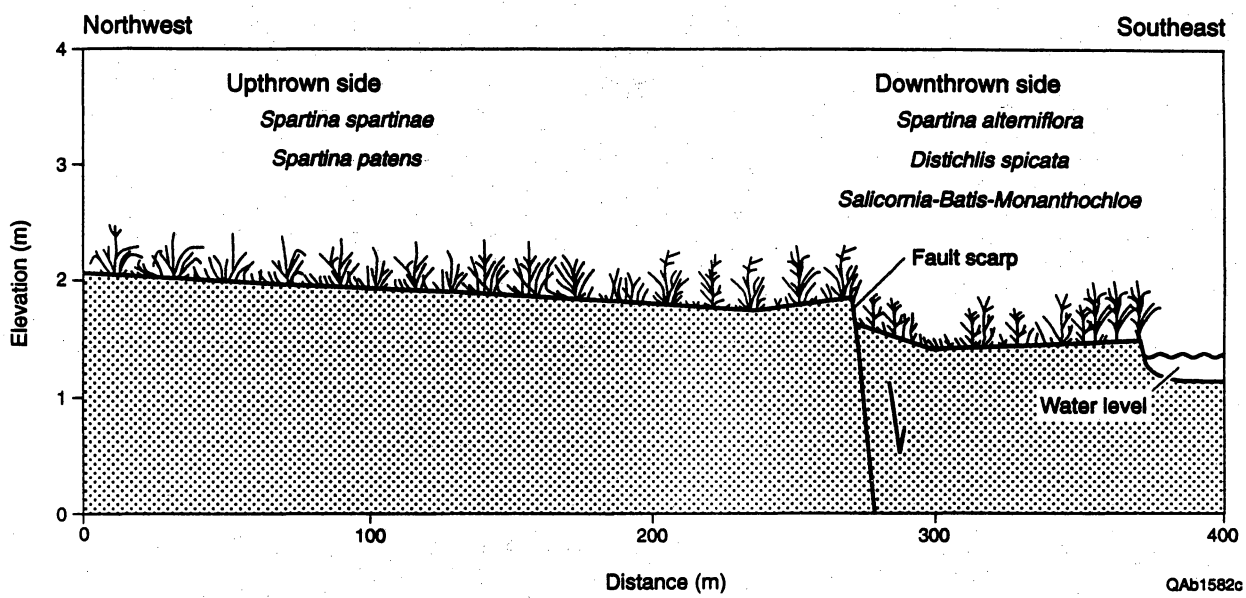

Northwest
Southeast
Upthrown side
Spartina spartinae
Spartina patens
Downthrown side
Spartina alterniflora
Distichlis spicata
Salicornia-Batis-Monanthochloe
Fault scarp
Water level
Elevation (m)
0
1
2
3
4
0
100
200
300
400
Distance (m)
QAb1582c

Figure 4

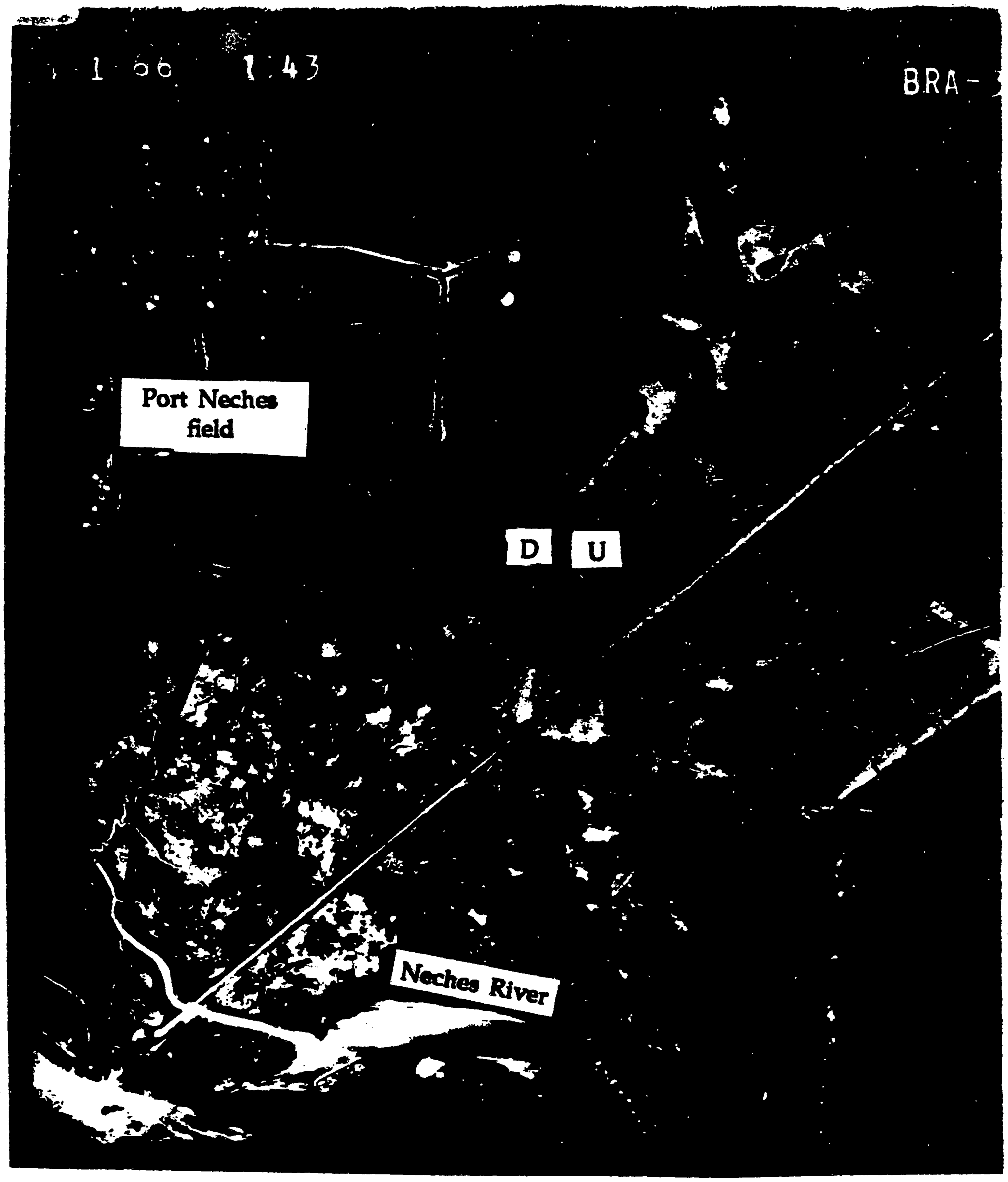

Figure 5

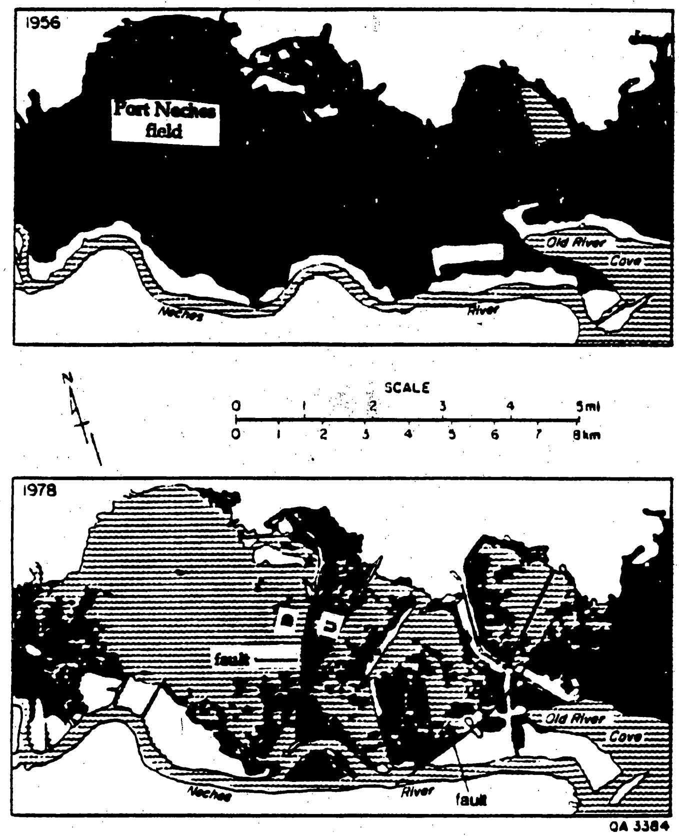

Map Unit	1956		1978		Net Change*	
	Acres	Hectares	Acres	Hectares	Acres	Hectares
Water	2,560	1,037	11,070	4,483	+8,510	+3,446
Marsh	15,740	6,375	6,330	2,564	−9,410	−3,811

* Loss of additional 900 acres (365 hectares) of marsh primarily due to spoil disposal.

Figure 6

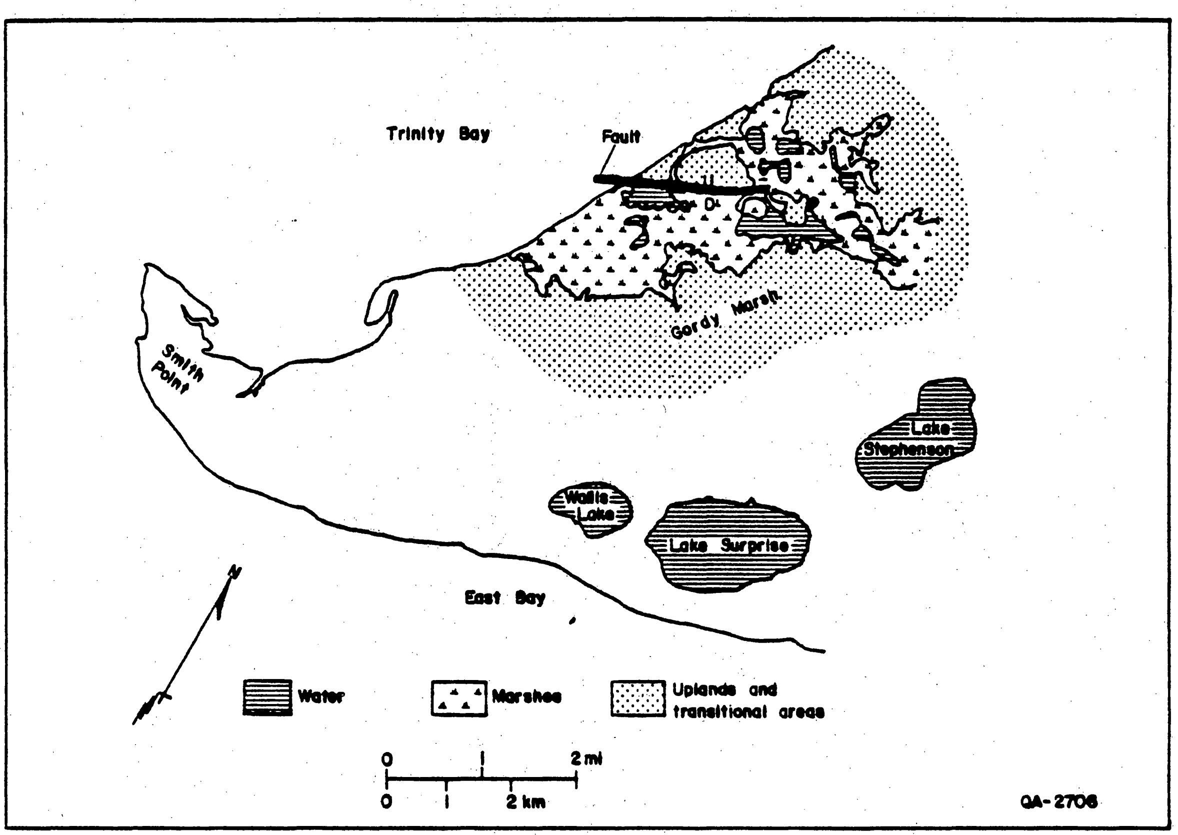
Trinity Bay
Fault
Gordy Marsh
Smith Point
Lake Stephenson
Wallis Lake
Lake Surprise
East Bay
N
Water
Marshes
Uplands and transitional areas
0
1
2 mi
0
1
2 km
QA-2706

Figure 7

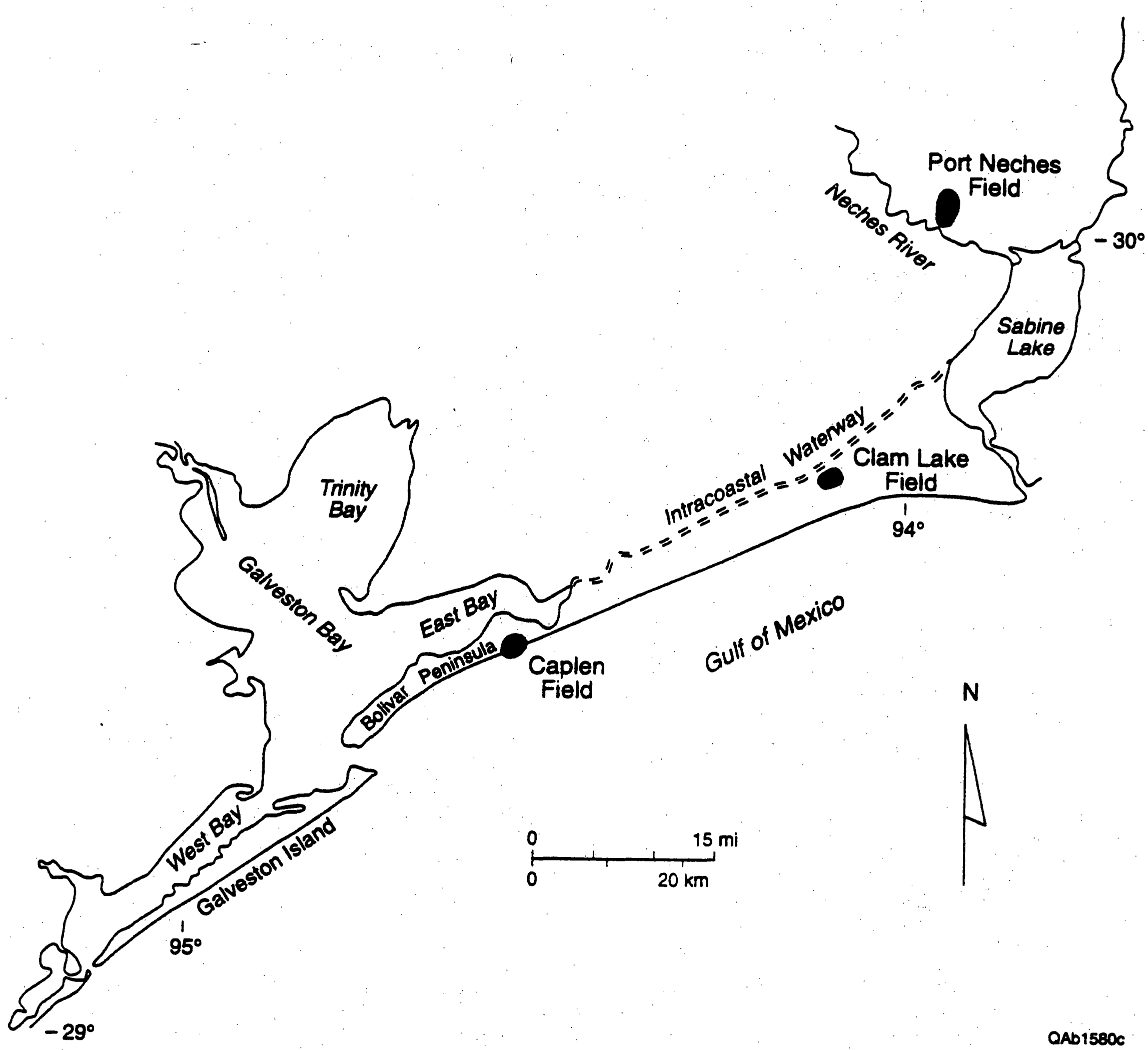
Port Neches Field
Neches River
30°
Sabine Lake
Intracoastal Waterway
Clam Lake Field
94°
Trinity Bay
Galveston Bay
East Bay
Bolivar Peninsula
Caplen Field
Gulf of Mexico
N
0
15 mi
0
20 km
West Bay
Galveston Island
95°
29°
QAb1580c

Figure 8

Port Neches Field Cumulative Production

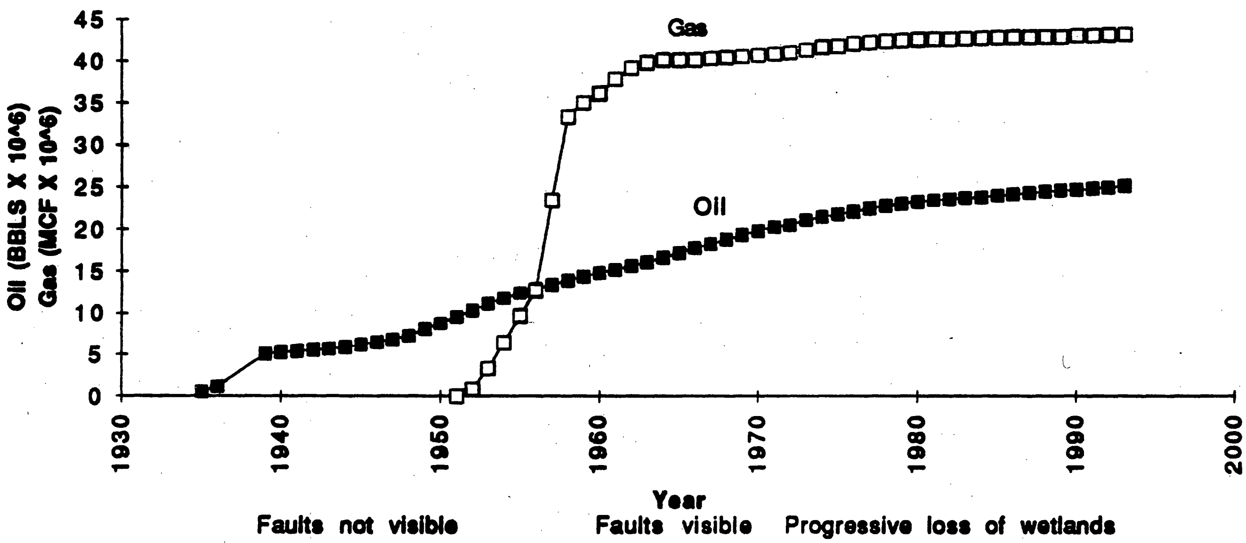

Figure 9

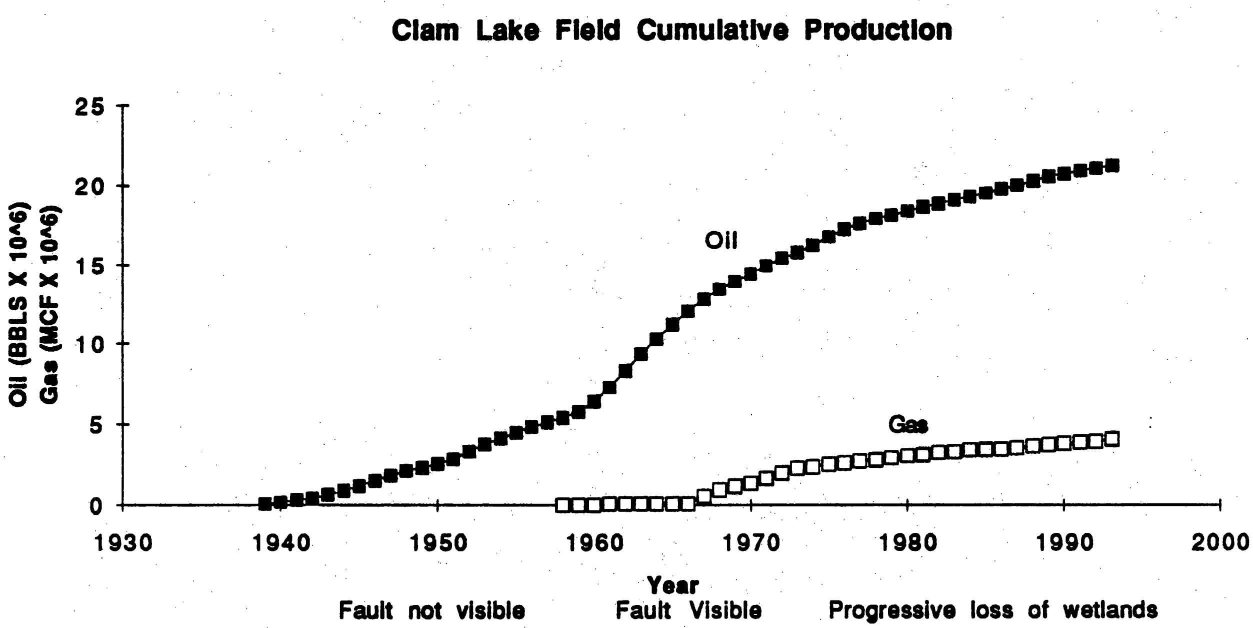
Clam Lake Field Cumulative Production
Oil (BBLS X 10^6)
Gas (MCF X 10^6)
25
20
15
10
5
0
Oil
Gas
1930
1940
1950
1960
1970
1980
1990
2000
Year
Fault not visible
Fault Visible
Progressive loss of wetlands

Figure 10

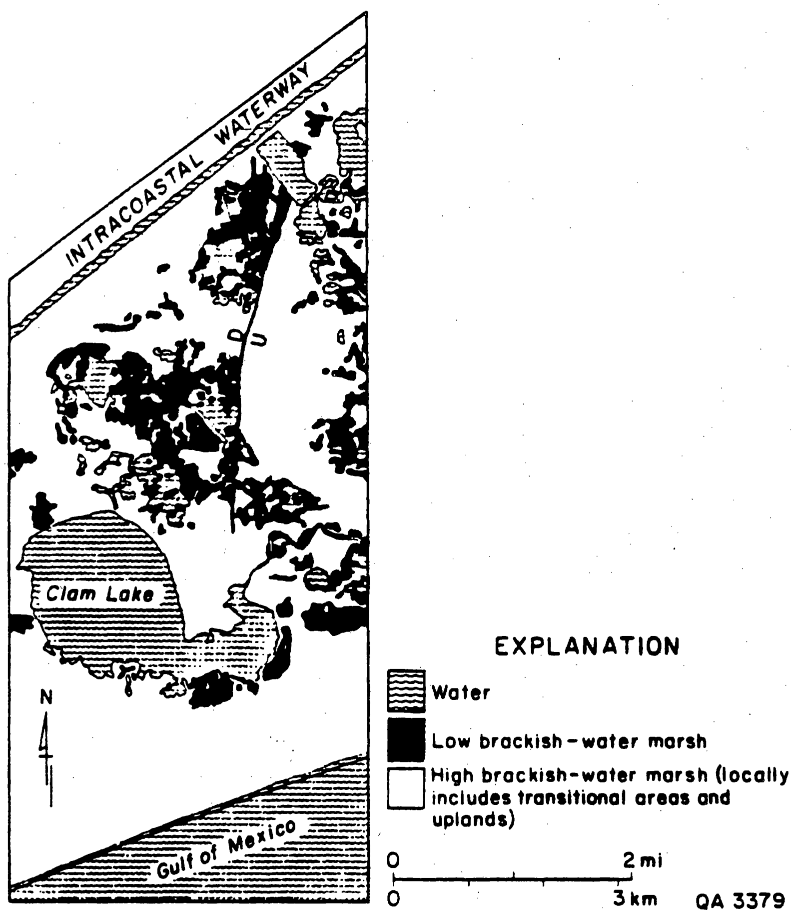
INTRACOASTAL WATERWAY
Clam Lake
N
Gulf of Mexico
EXPLANATION
Water
Low brackish-water marsh
High brackish-water marsh (locally includes transitional areas and uplands)
0
2 mi
0
3 km
QA 3379

Figure 11

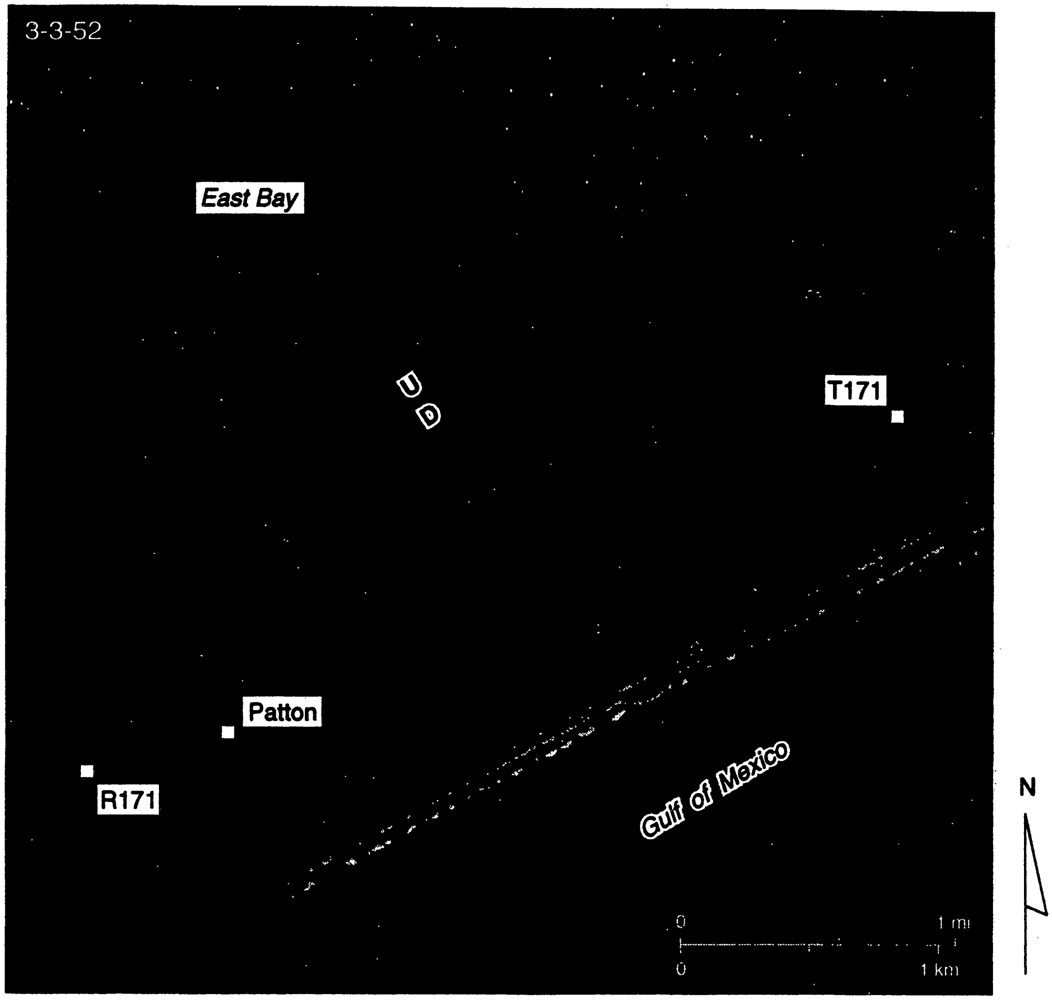
3-3-52
East Bay
U
D
T171
Patton
R171
Gulf of Mexico
N
0
1 mi
0
1 km

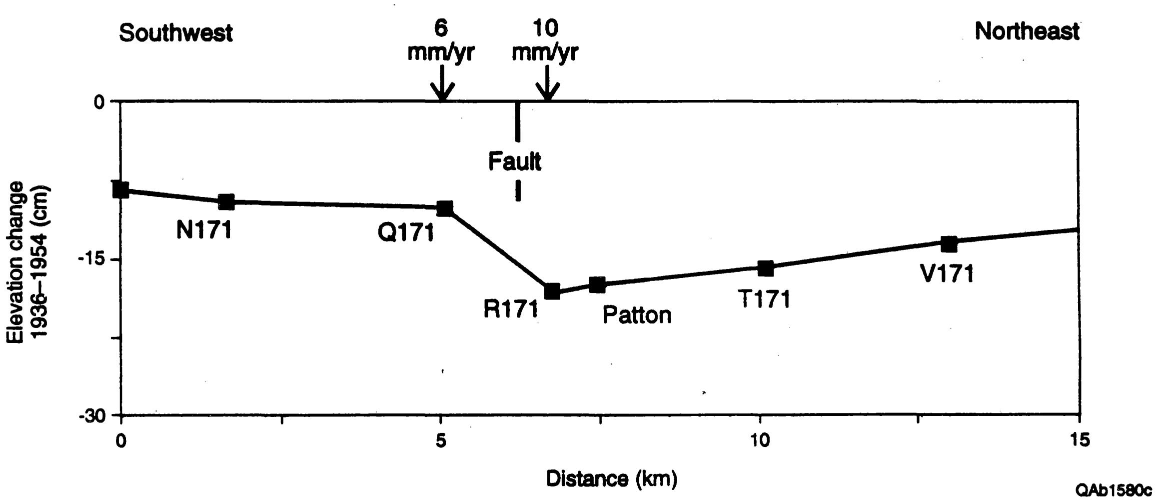
Southwest
6 mm/yr
10 mm/yr
Northeast
0
Fault
-15
-30
Elevation change 1936–1954 (cm)
N171
Q171
R171
Patton
T171
V171
0
5
10
15
Distance (km)
QAb1580c

Figure 12

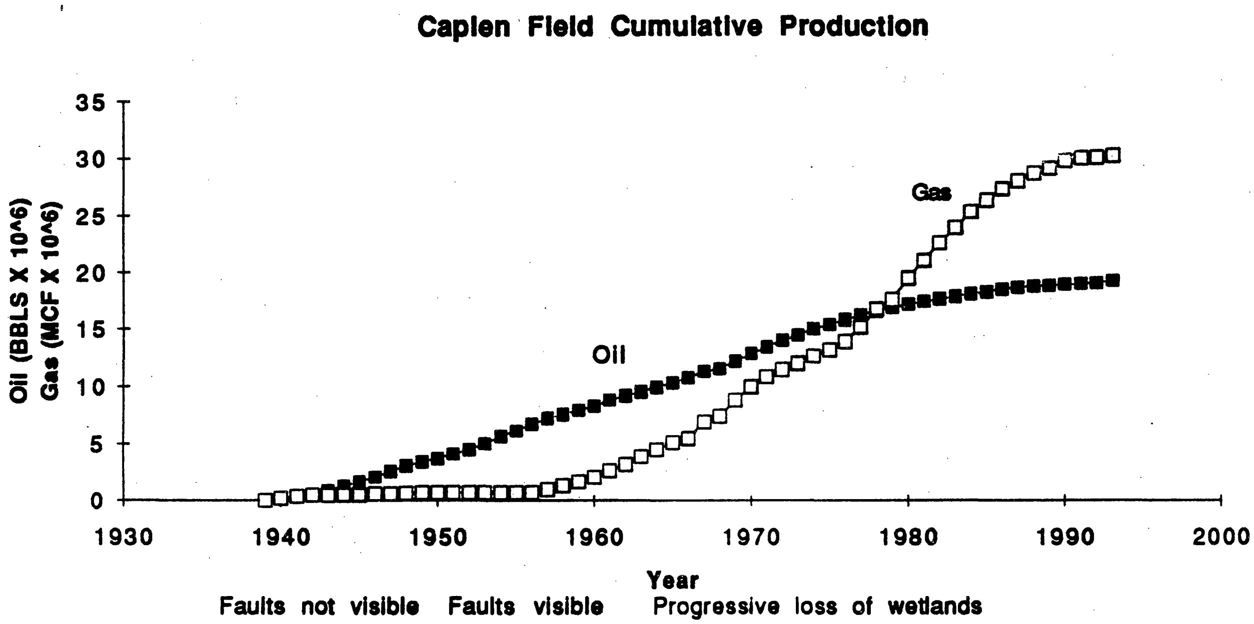
Caplen Field Cumulative Production
Oil (BBLS X 10^6)
Gas (MCF X 10^6)
35
30
25
20
15
10
5
0
Gas
Oil
1930
1940
1950
1960
1970
1980
1990
2000
Year
Faults not visible
Faults visible
Progressive loss of wetlands

Figure 13

Addendum 2. Index of Human Impact on Dunes and Vegetation

Index of Human Impact on Dunes and Vegetation

Index	Description
0	No visible impact of beach scraping or evidence of backbeach dumping. Dune morphologies and plant communities are natural. Essentially no modification of beach and dune profile.
1	Low, small-volume mounds of sand containing some minor beach trash such as *Sargassum*. Trash represents less than 20% of mound volume. Altered zone is narrow relative to the entire beach width.
2	Low, small-volume mounds of sand and some minor beach trash such as *Sargassum* and small pieces of wood. Trash represents less than 33% of mound volume. Altered zone is narrow relative to the entire beach width.
3	Moderately large mounds of sand at least 3 ft high. Mounds composed of approximately 33% trash including moderately large pieces of wood or other debris. Several rows (2-3) of modified dunes or sand mounds. Altered zone is moderately wide relative to the entire beach width.
4	Moderately large mounds of sand greater than 3 ft high. Mounds composed of more than 33% trash. Multiple rows of modified dunes or sand mounds forming moderately wide zone relative to the entire beach width. Modified area may include bypass zone(s) representing former backbeach road(s).
5	Large mounds of sand up to 6 ft high. Mounds composed of as much as 50% trash containing large logs, cut wood, tires, appliances, and concrete or other rubble. Multiple rows of modified dunes or sand mounds forming wide zone relative to the entire beach width. Modified area may include bypass zone(s) representing former backbeach road(s).

Addendum 3. Beach and Dune Profiles, Galveston County

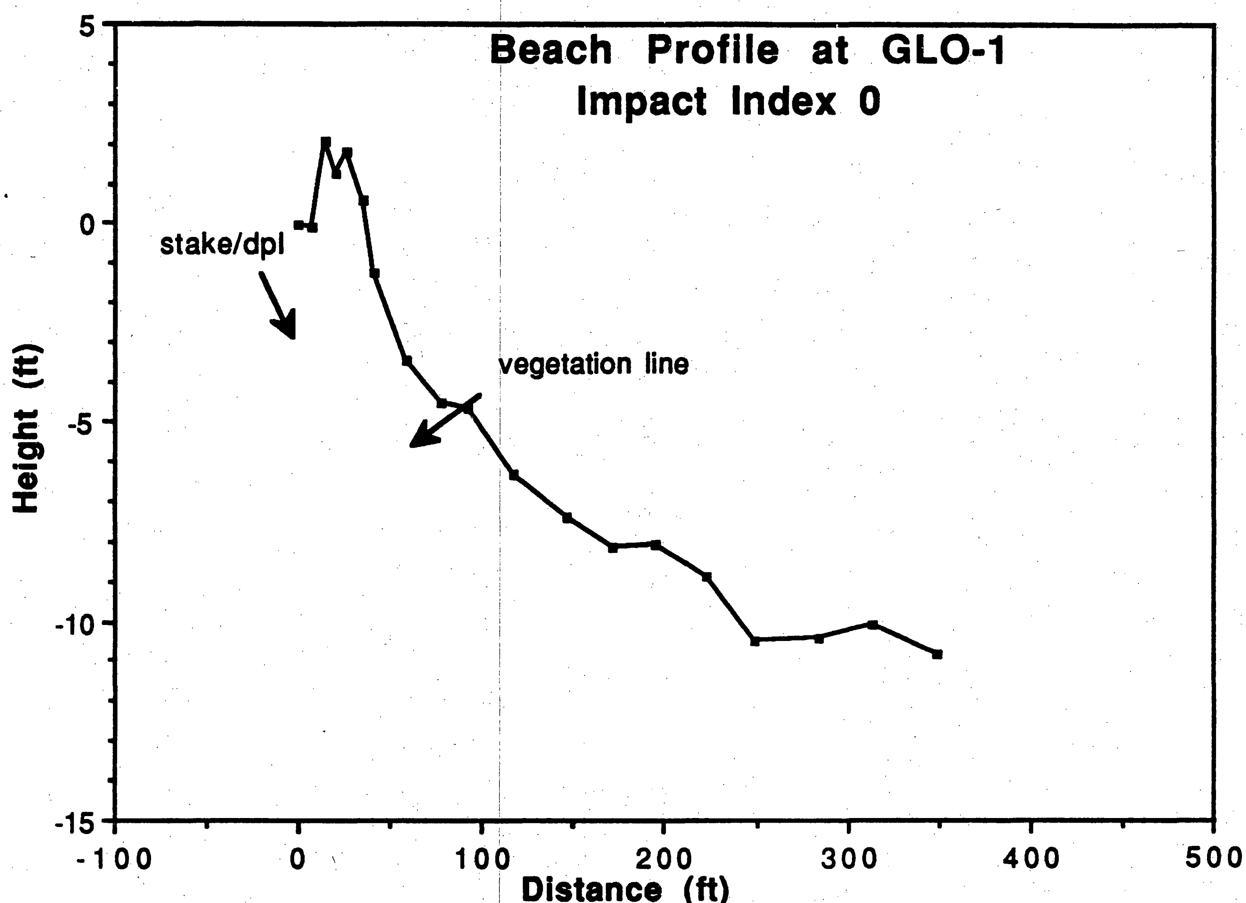

Beach Profile at GLO-1
Impact Index 0
stake/dpl
vegetation line
Height (ft)
Distance (ft)
5
0
-5
-10
-15
-100
0
100
200
300
400
500

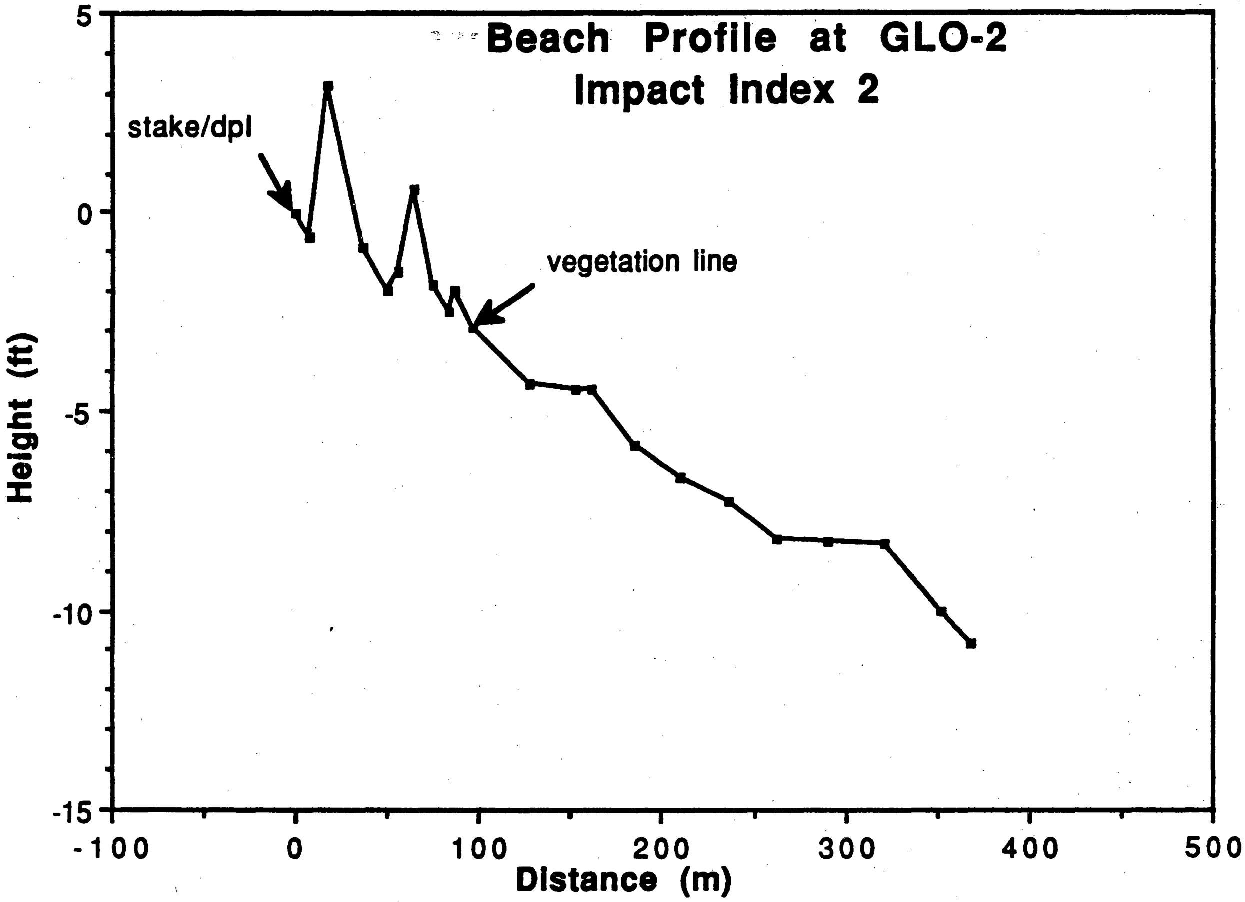

Beach Profile at GLO-2
Impact Index 2
stake/dpl
vegetation line
Height (ft)
Distance (m)
5
0
-5
-10
-15
-100
0
100
200
300
400
500

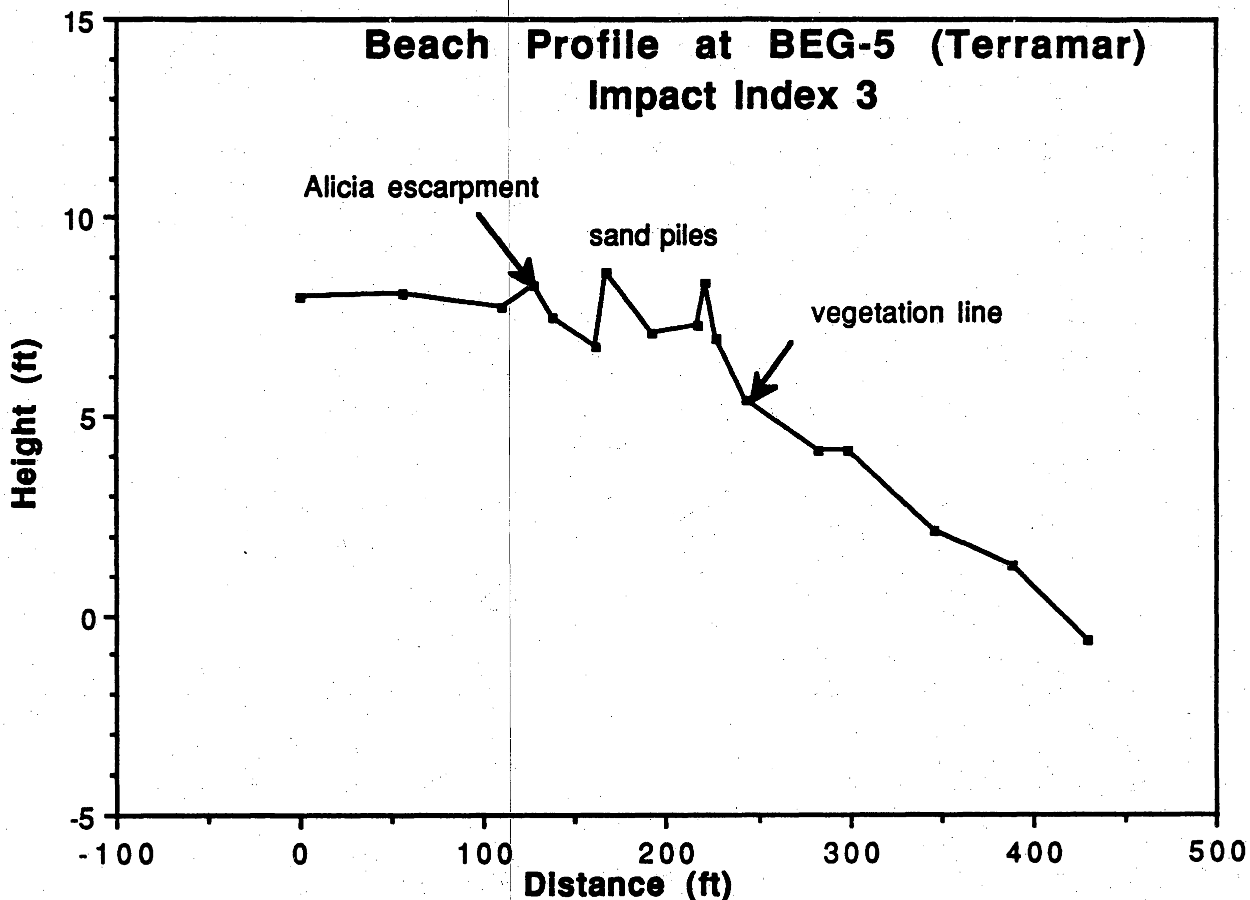
Beach Profile at BEG-5 (Terramar)
Impact Index 3
Alicia escarpment
sand piles
vegetation line
Height (ft)
Distance (ft)
15
10
5
0
-5
-100
0
100
200
300
400
500

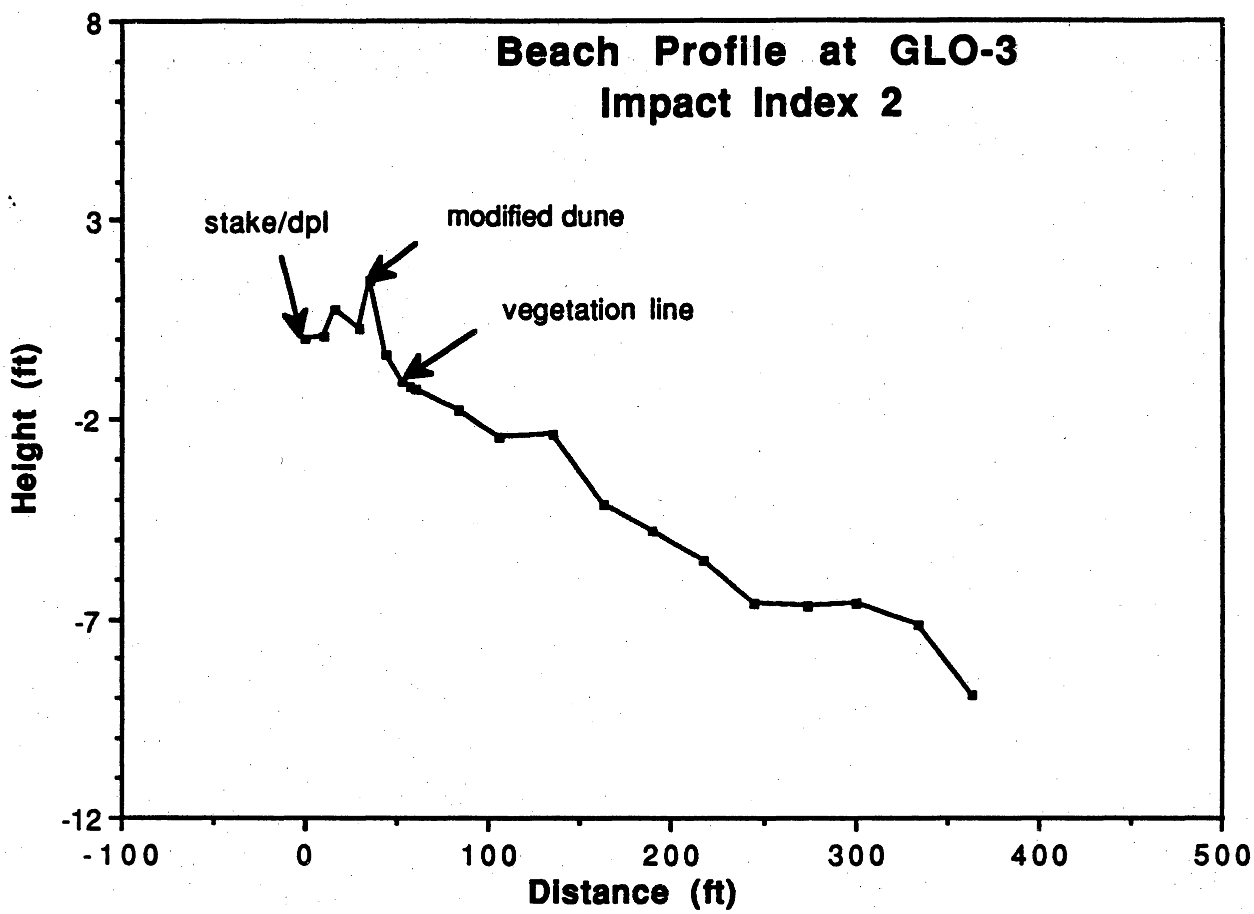

Beach Profile at GLO-3
Impact Index 2
stake/dpl
modified dune
vegetation line
Height (ft)
8
3
-2
-7
-12
-100
0
100
200
300
400
500
Distance (ft)

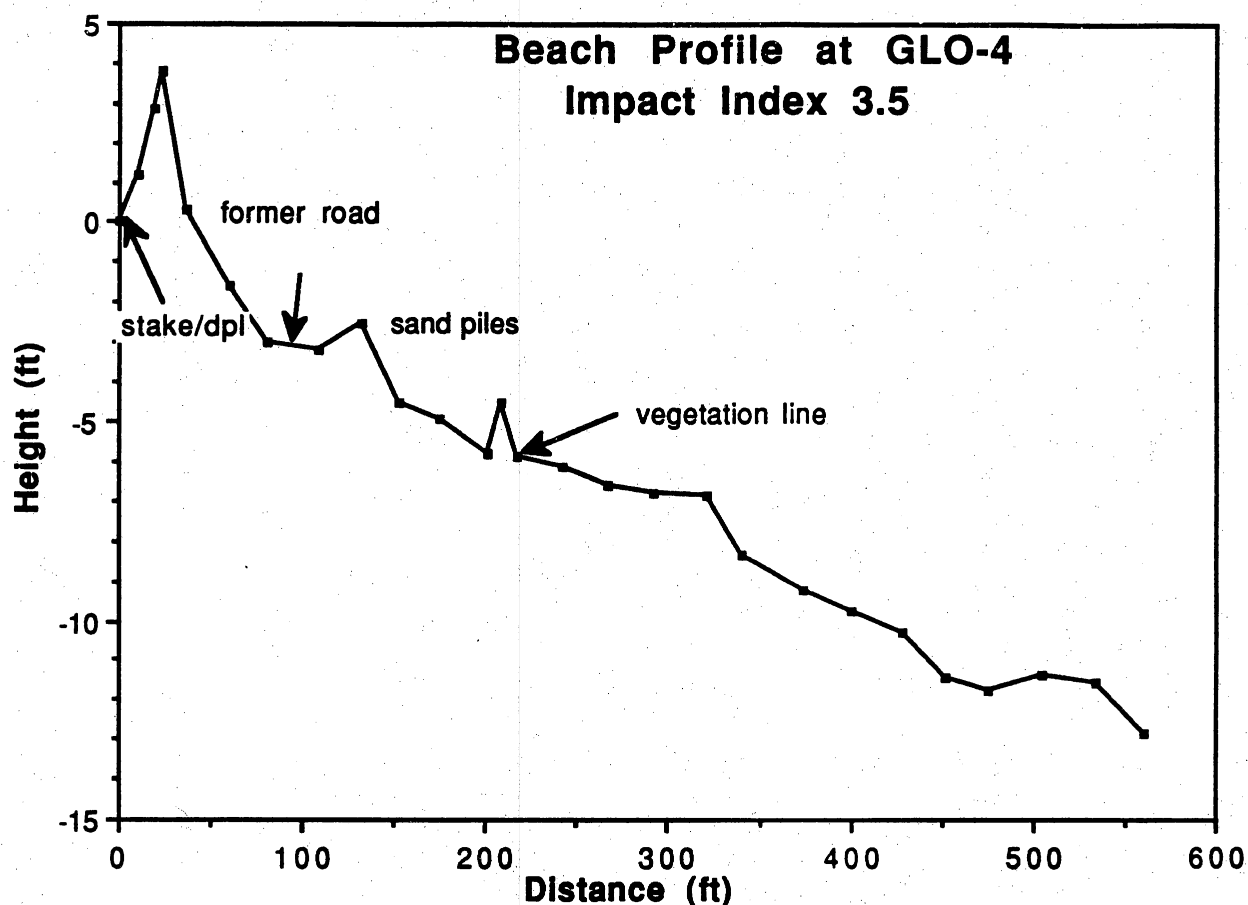

Beach Profile at GLO-4
Impact Index 3.5
former road
stake/dpl
sand piles
vegetation line
Height (ft)
Distance (ft)
5
0
-5
-10
-15
0
100
200
300
400
500
600

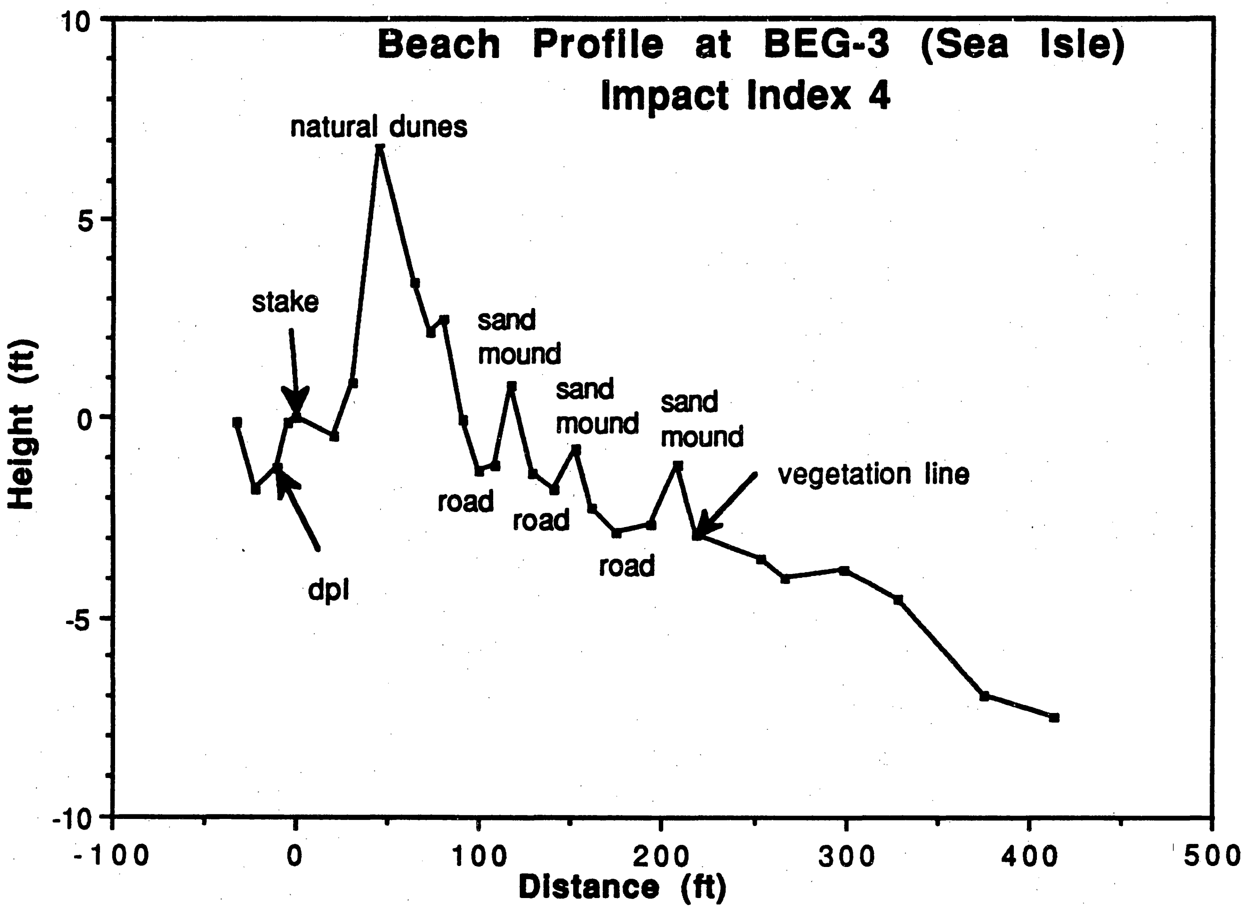
Beach Profile at BEG-3 (Sea Isle)
Impact Index 4
natural dunes
stake
sand mound
sand mound
sand mound
vegetation line
road
road
road
dpl
Height (ft)
10
5
0
-5
-10
-100
0
100
200
300
400
500
Distance (ft)

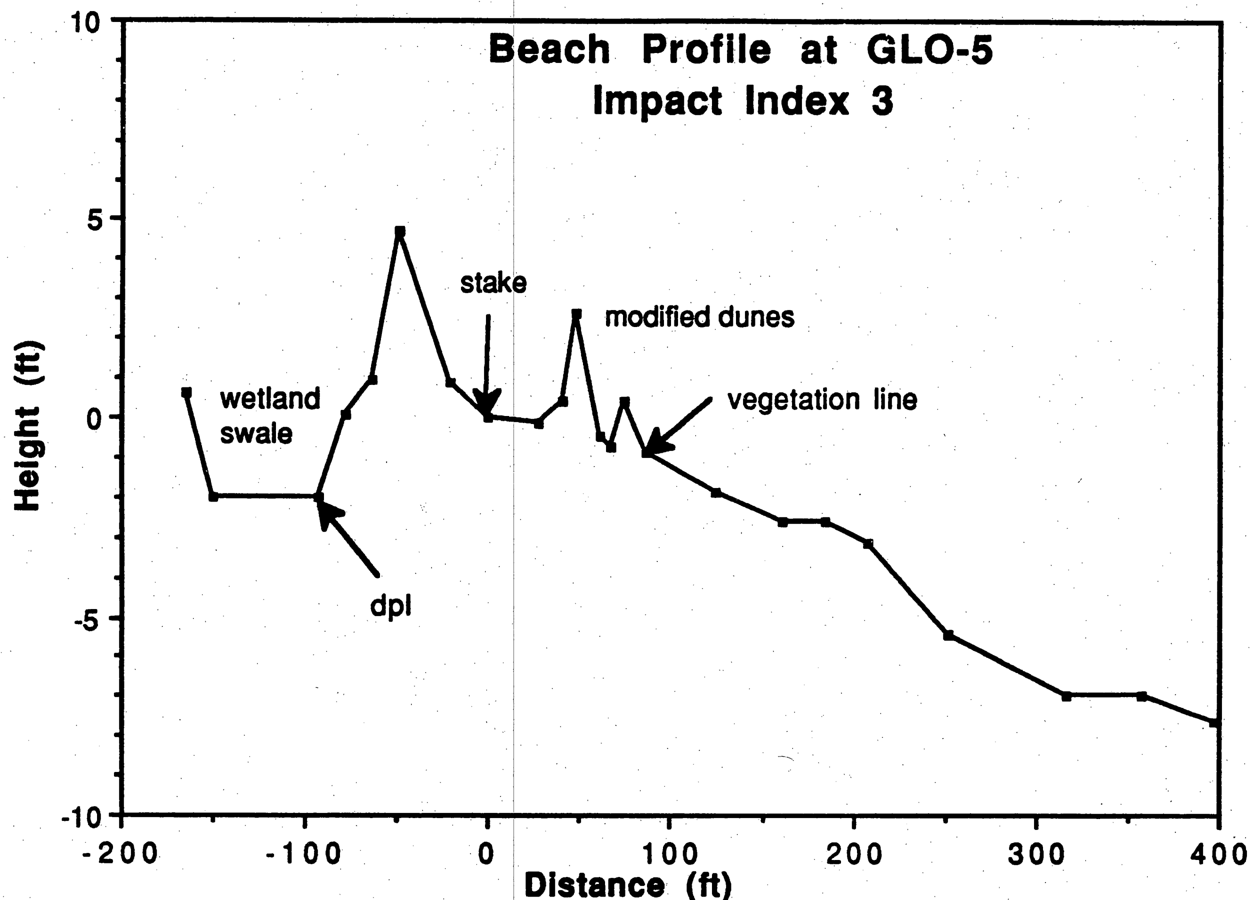

Beach Profile at GLO-5
Impact Index 3
10
5
0
-5
-10
Height (ft)
stake
modified dunes
wetland
swale
vegetation line
dpl
-200
-100
0
100
200
300
400
Distance (ft)

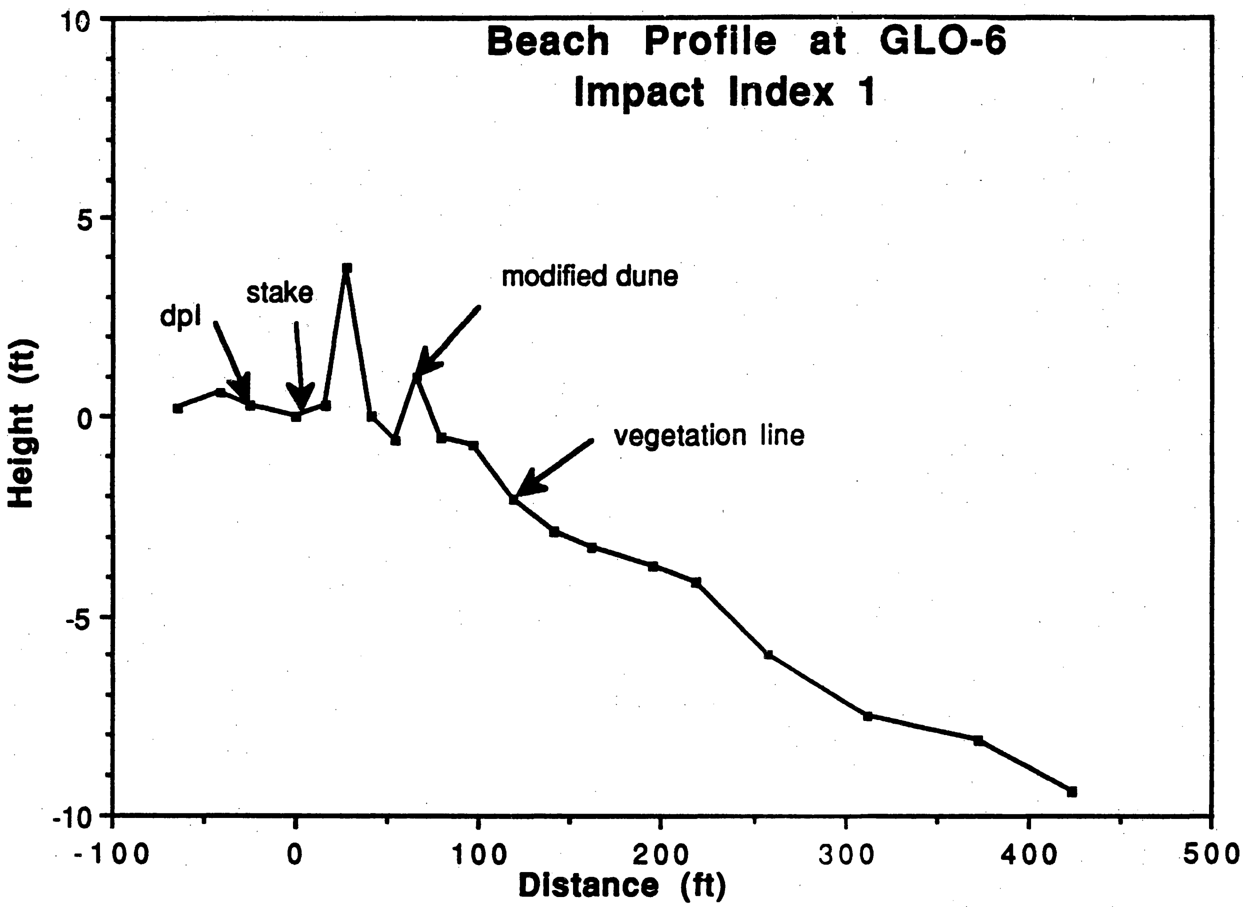
Beach Profile at GLO-6
Impact Index 1
Height (ft)
Distance (ft)
10
5
0
-5
-10
-100
0
100
200
300
400
500
dpl
stake
modified dune
vegetation line

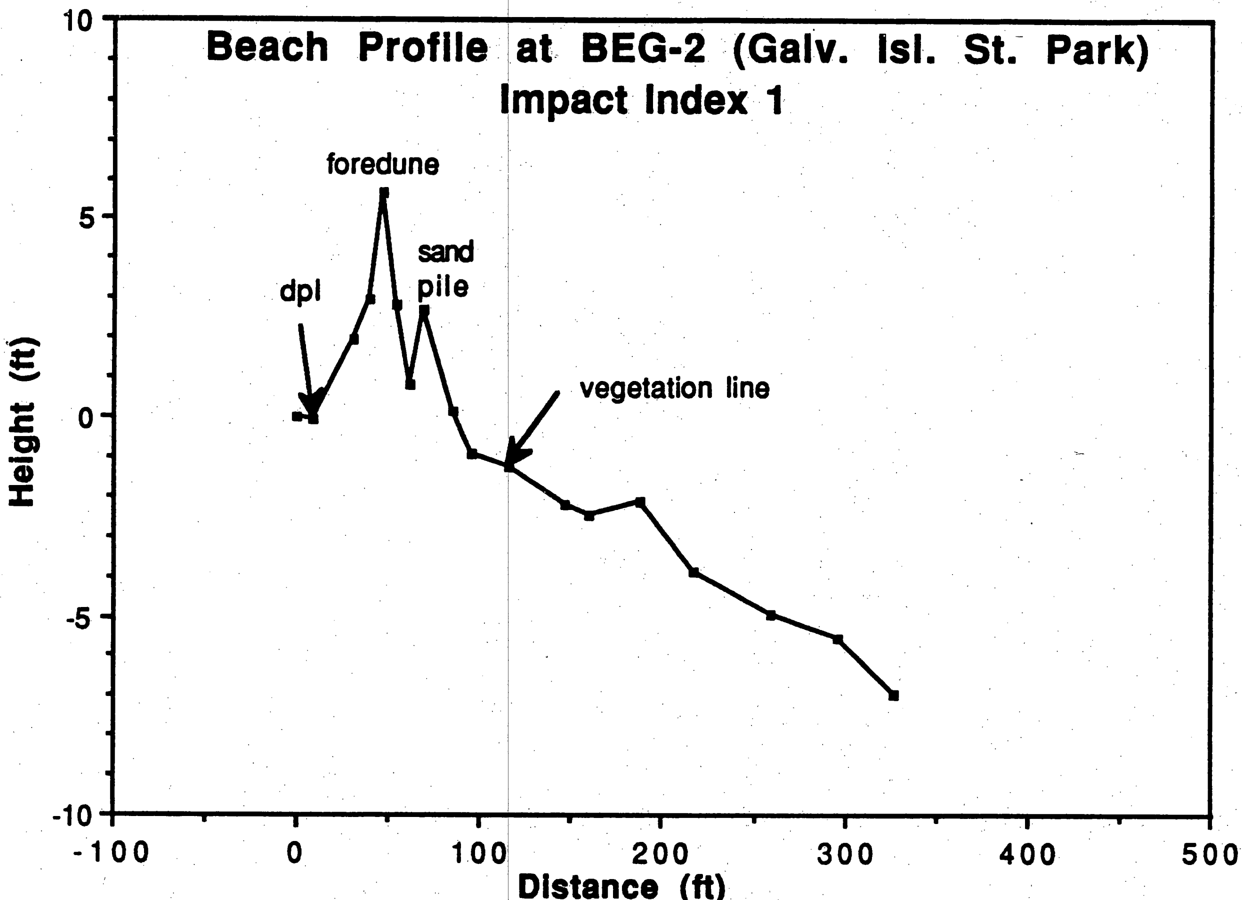

Beach Profile at BEG-2 (Galv. Isl. St. Park)
Impact Index 1
foredune
sand
pile
dpl
vegetation line
Height (ft)
Distance (ft)
10
5
0
-5
-10
-100
0
100
200
300
400
500

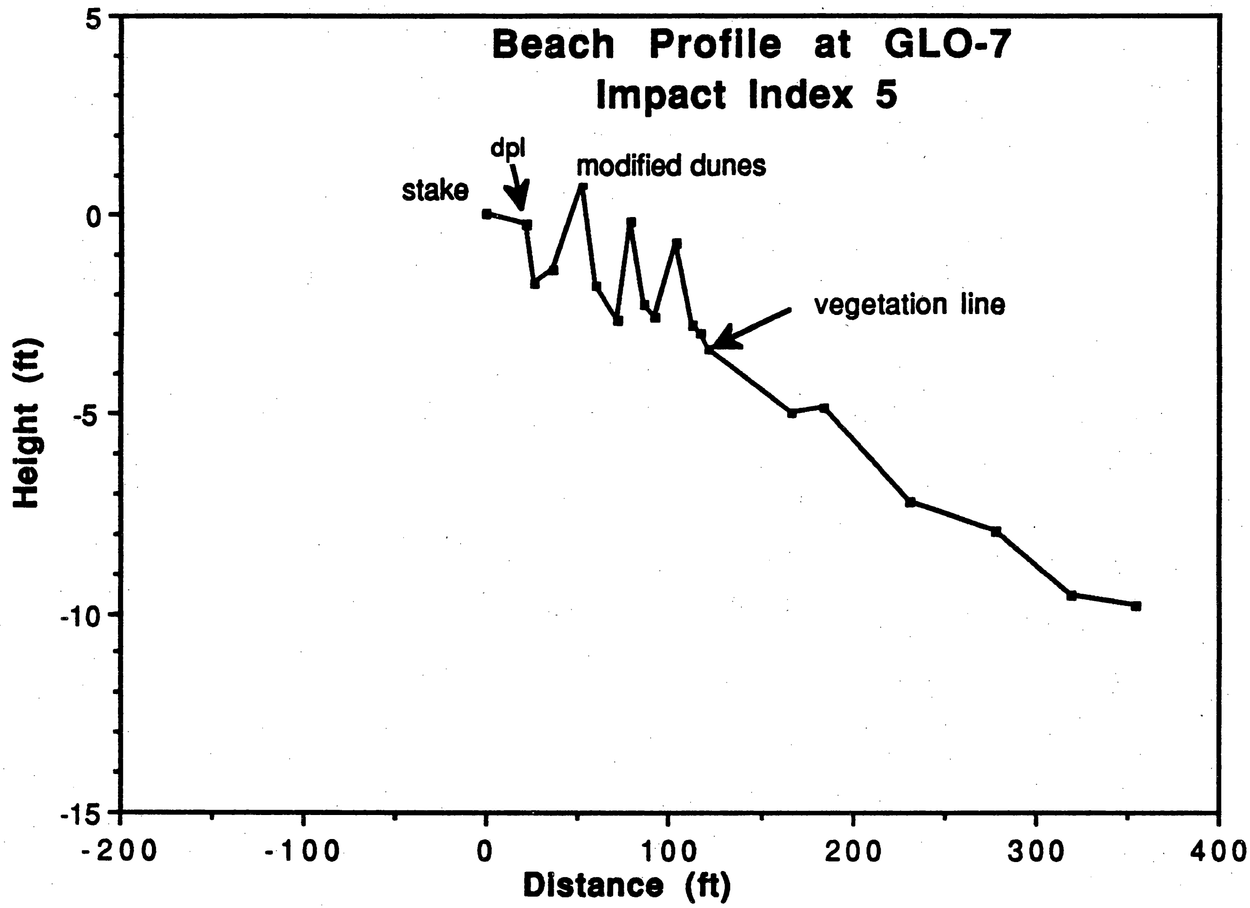

Beach Profile at GLO-7
Impact Index 5
stake
dpl
modified dunes
vegetation line
Height (ft)
Distance (ft)
5
0
-5
-10
-15
-200
-100
0
100
200
300
400

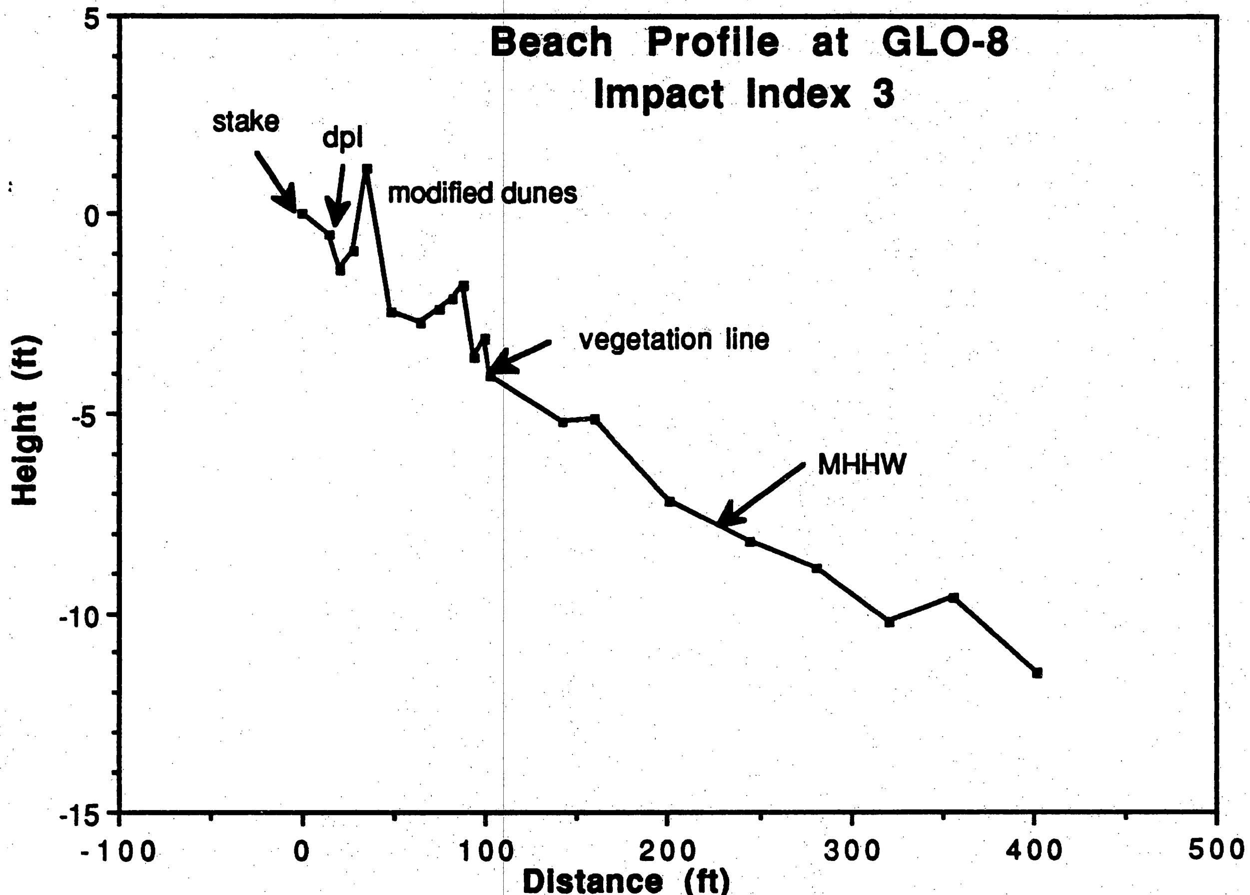

Beach Profile at GLO-8
Impact Index 3
stake
dpl
modified dunes
vegetation line
MHHW
Height (ft)
5
0
-5
-10
-15
-100
0
100
200
300
400
500
Distance (ft)

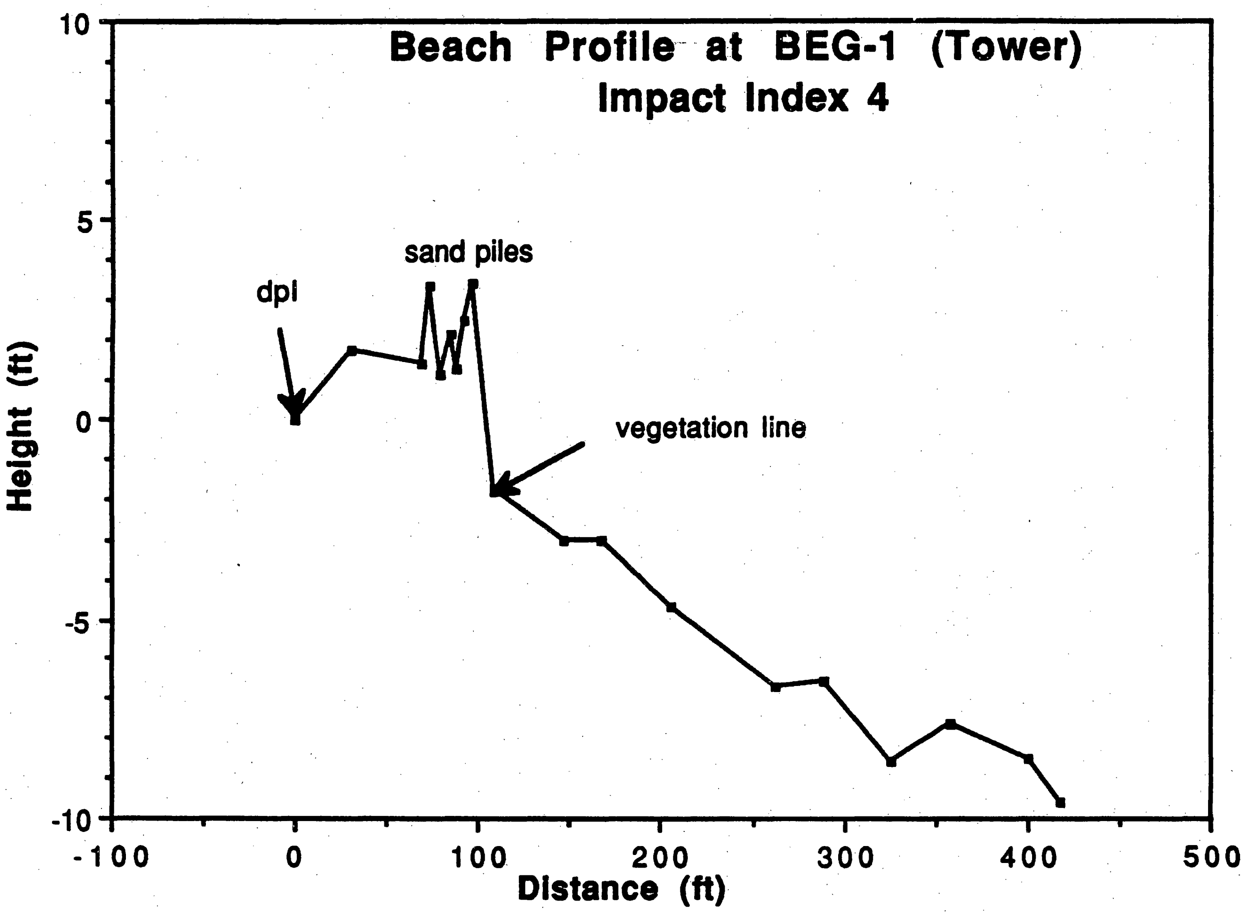

Beach Profile at BEG-1 (Tower)
Impact Index 4
sand piles
dpl
vegetation line
Height (ft)
Distance (ft)
10
5
0
-5
-10
-100
0
100
200
300
400
500

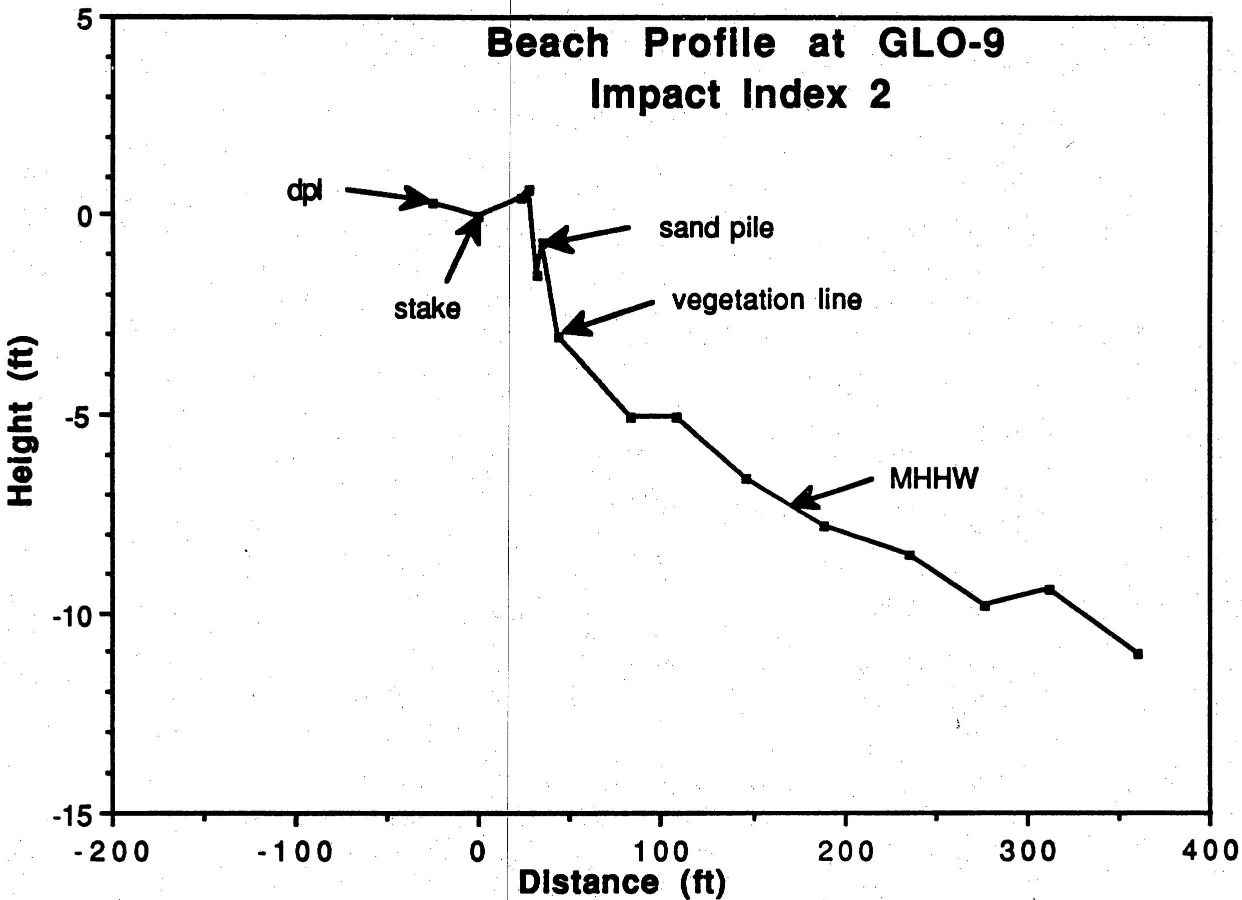

Beach Profile at GLO-9
Impact Index 2
dpl
stake
sand pile
vegetation line
MHHW
Height (ft)
Distance (ft)
5
0
-5
-10
-15
-200
-100
0
100
200
300
400

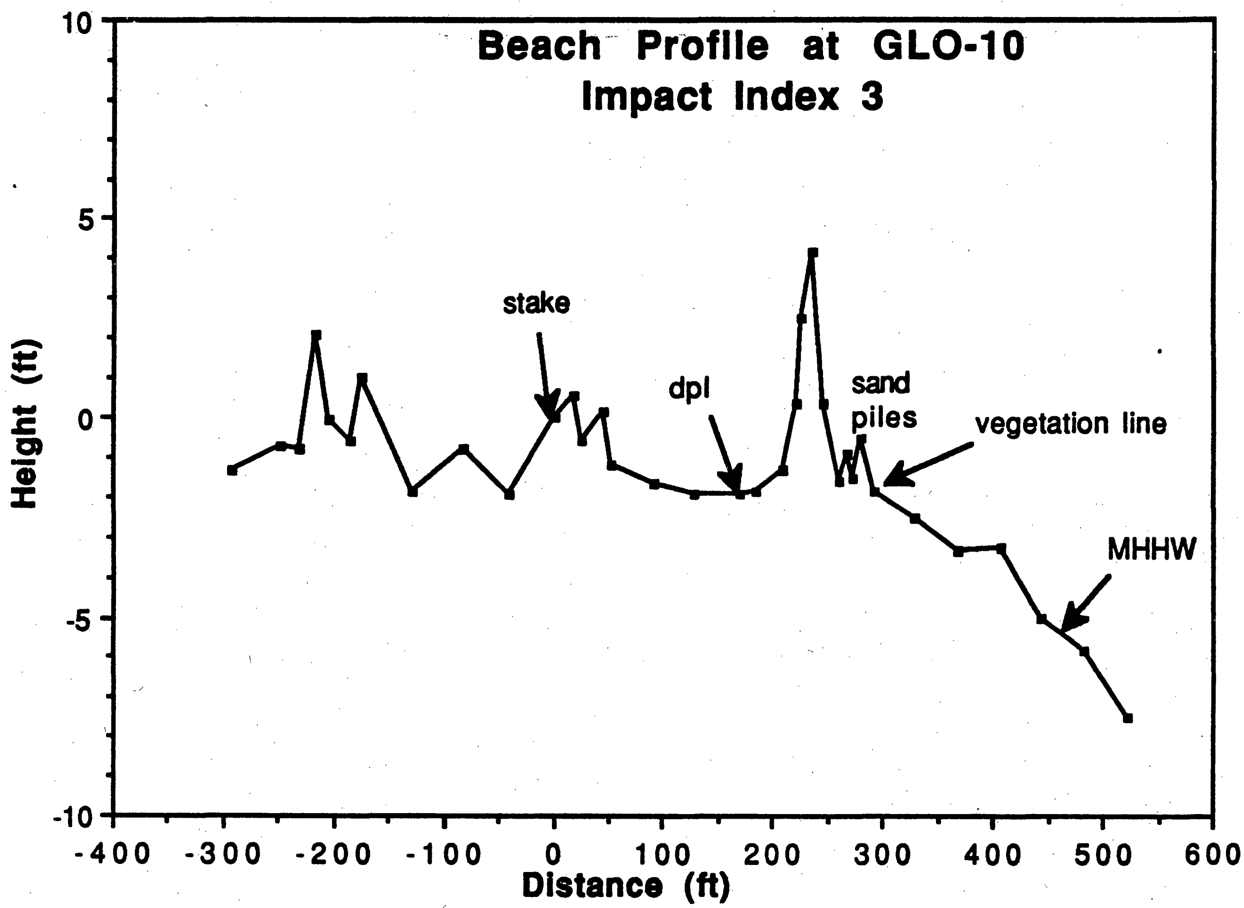
Beach Profile at GLO-10
Impact Index 3
Height (ft)
Distance (ft)
10
5
0
-5
-10
-400
-300
-200
-100
0
100
200
300
400
500
600
stake
dpl
sand
piles
vegetation line
MHHW

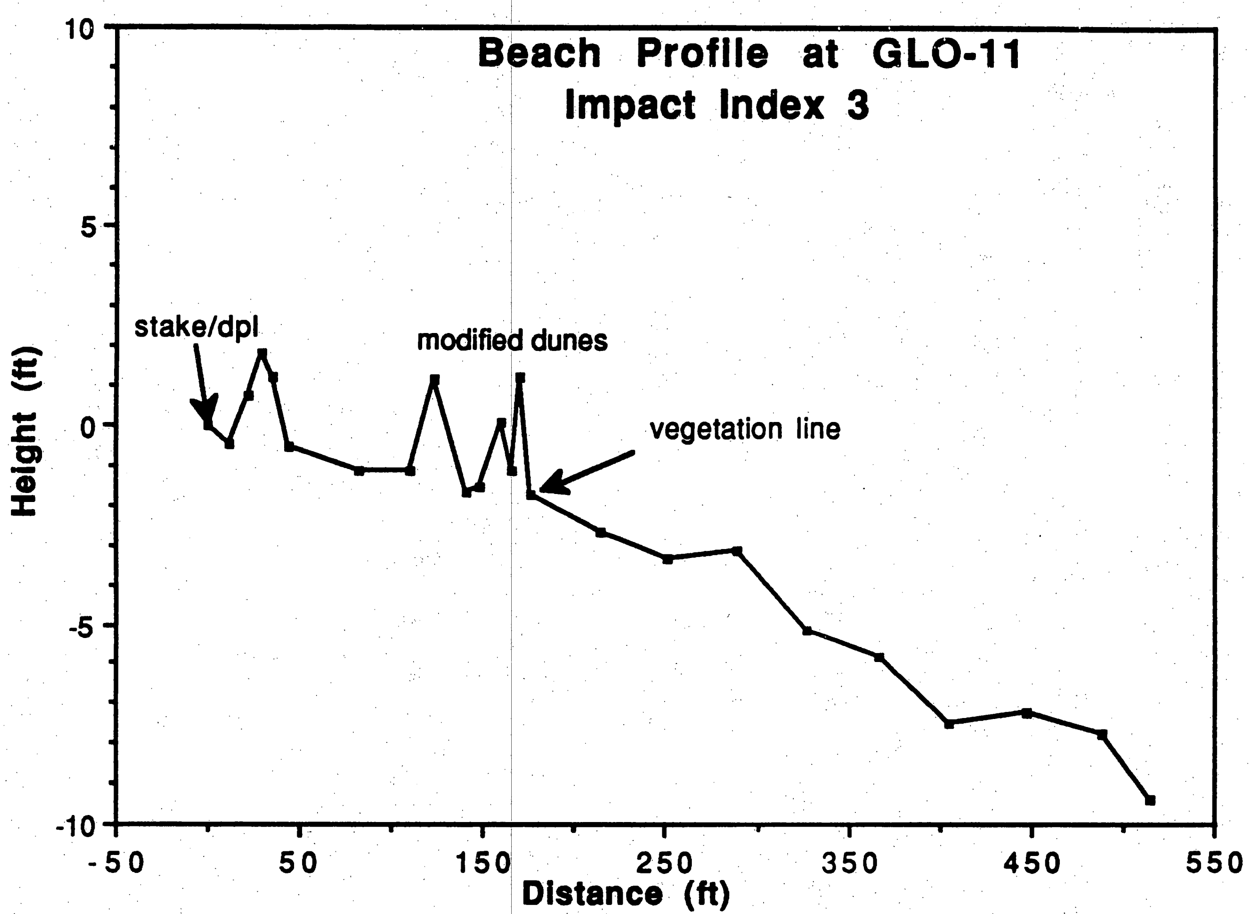

Beach Profile at GLO-11
Impact Index 3
stake/dpl
modified dunes
vegetation line
Height (ft)
10
5
0
-5
-10
-50
50
150
250
350
450
550
Distance (ft)

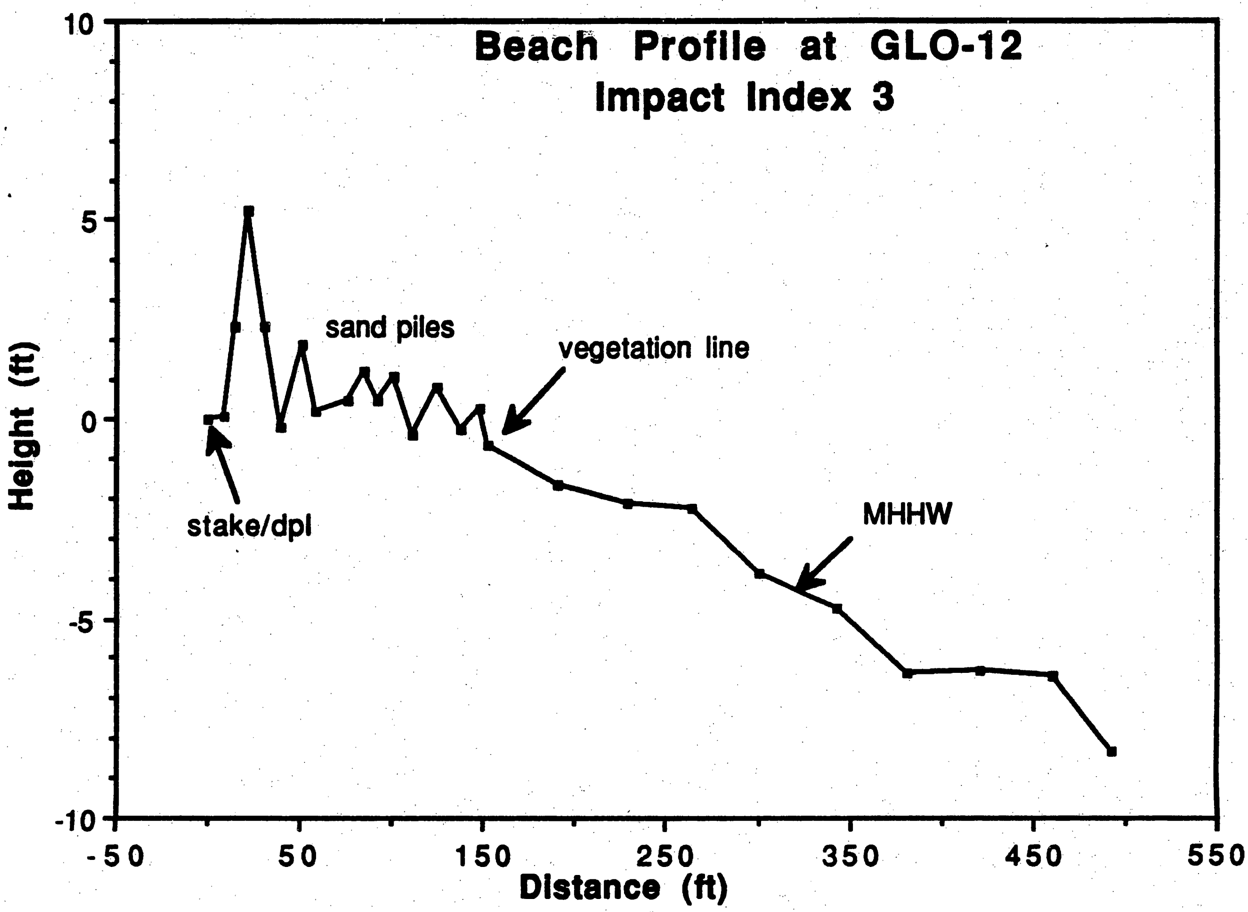

Beach Profile at GLO-12
Impact Index 3
10
5
0
-5
-10
Height (ft)
sand piles
vegetation line
stake/dpl
MHHW
-50
50
150
250
350
450
550
Distance (ft)

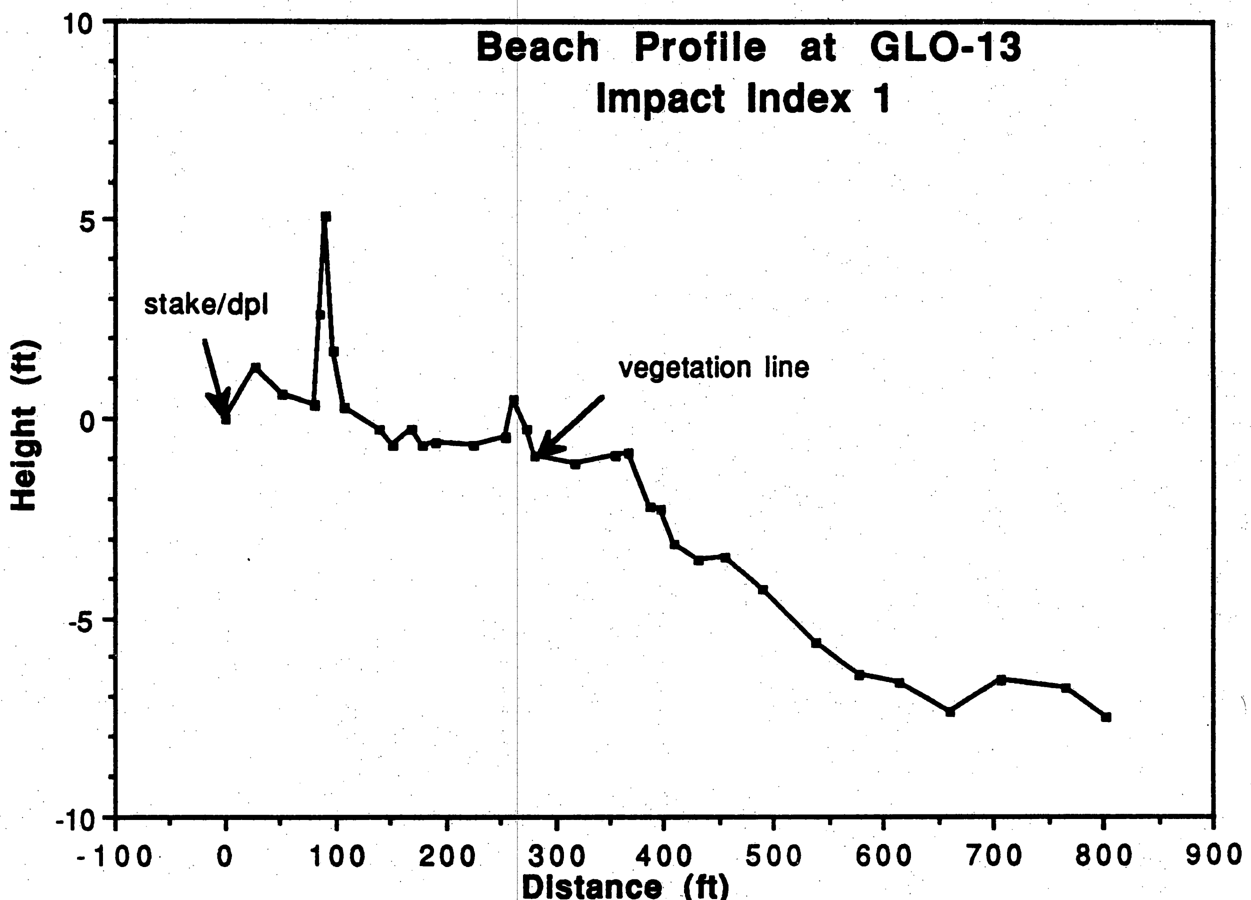
Beach Profile at GLO-13
Impact Index 1
stake/dpl
vegetation line
Height (ft)
Distance (ft)
10
5
0
-5
-10
-100
0
100
200
300
400
500
600
700
800
900

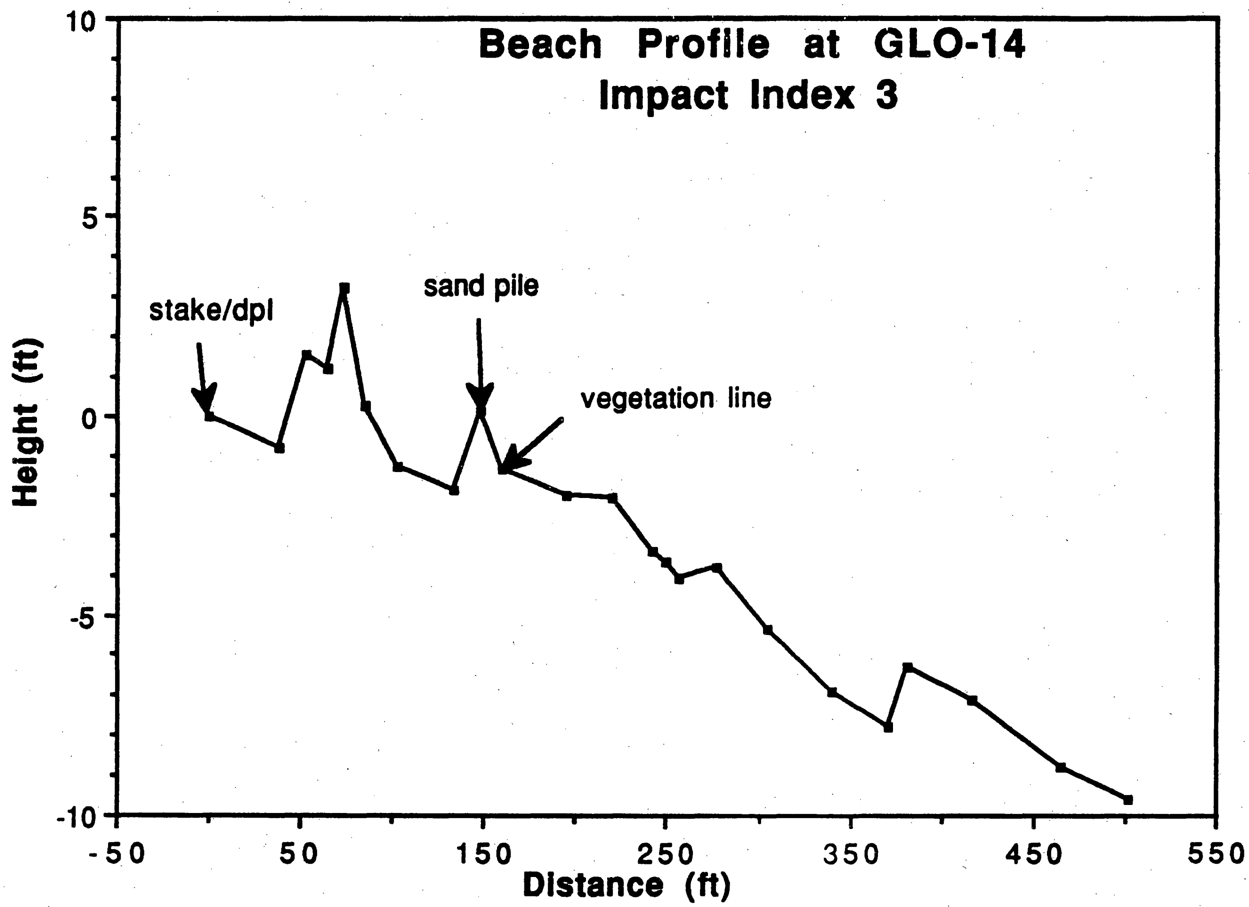
Beach Profile at GLO-14
Impact Index 3
stake/dpl
sand pile
vegetation line
10
5
0
-5
-10
Height (ft)
-50
50
150
250
350
450
550
Distance (ft)

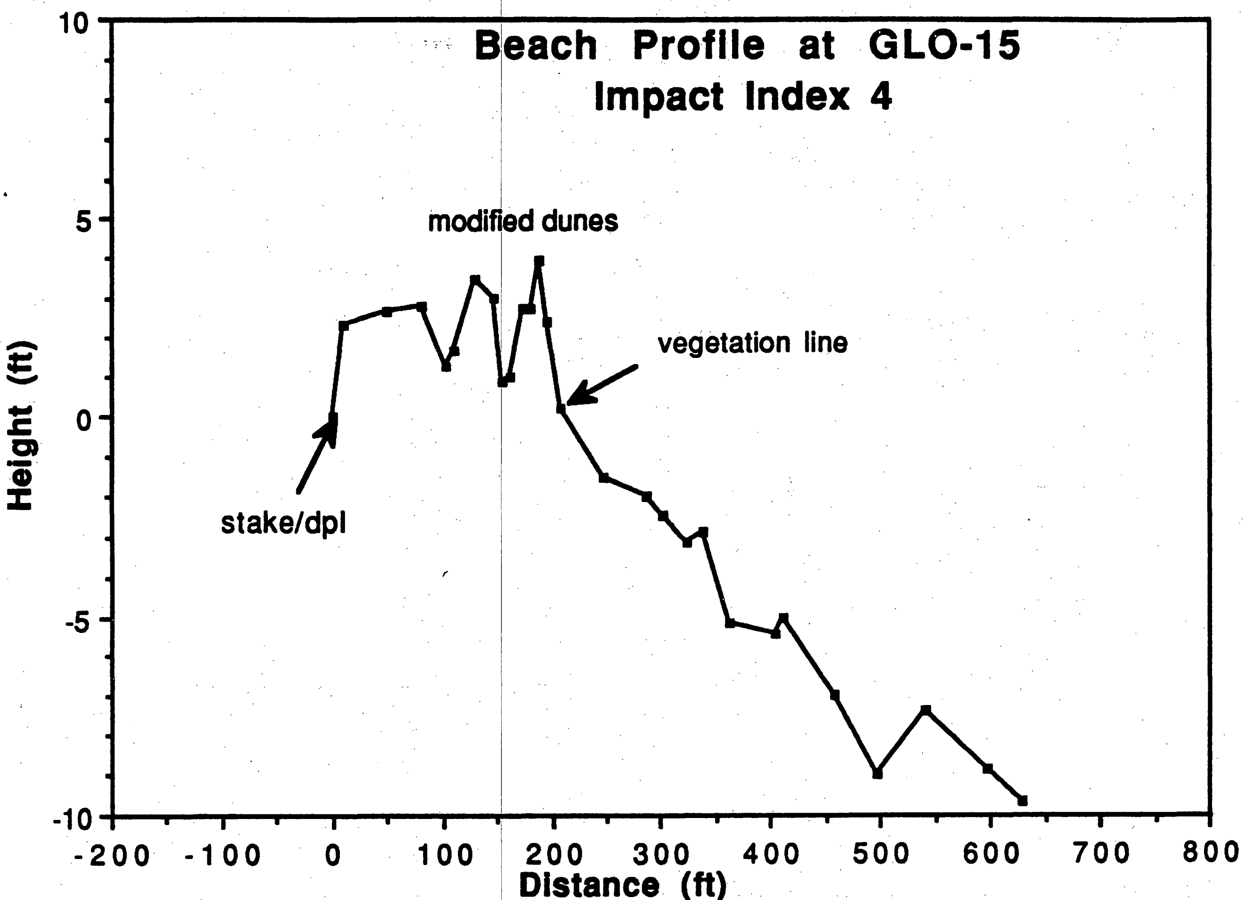

Beach Profile at GLO-15
Impact Index 4
modified dunes
vegetation line
stake/dpl
Height (ft)
Distance (ft)
10
5
0
-5
-10
-200
-100
0
100
200
300
400
500
600
700
800

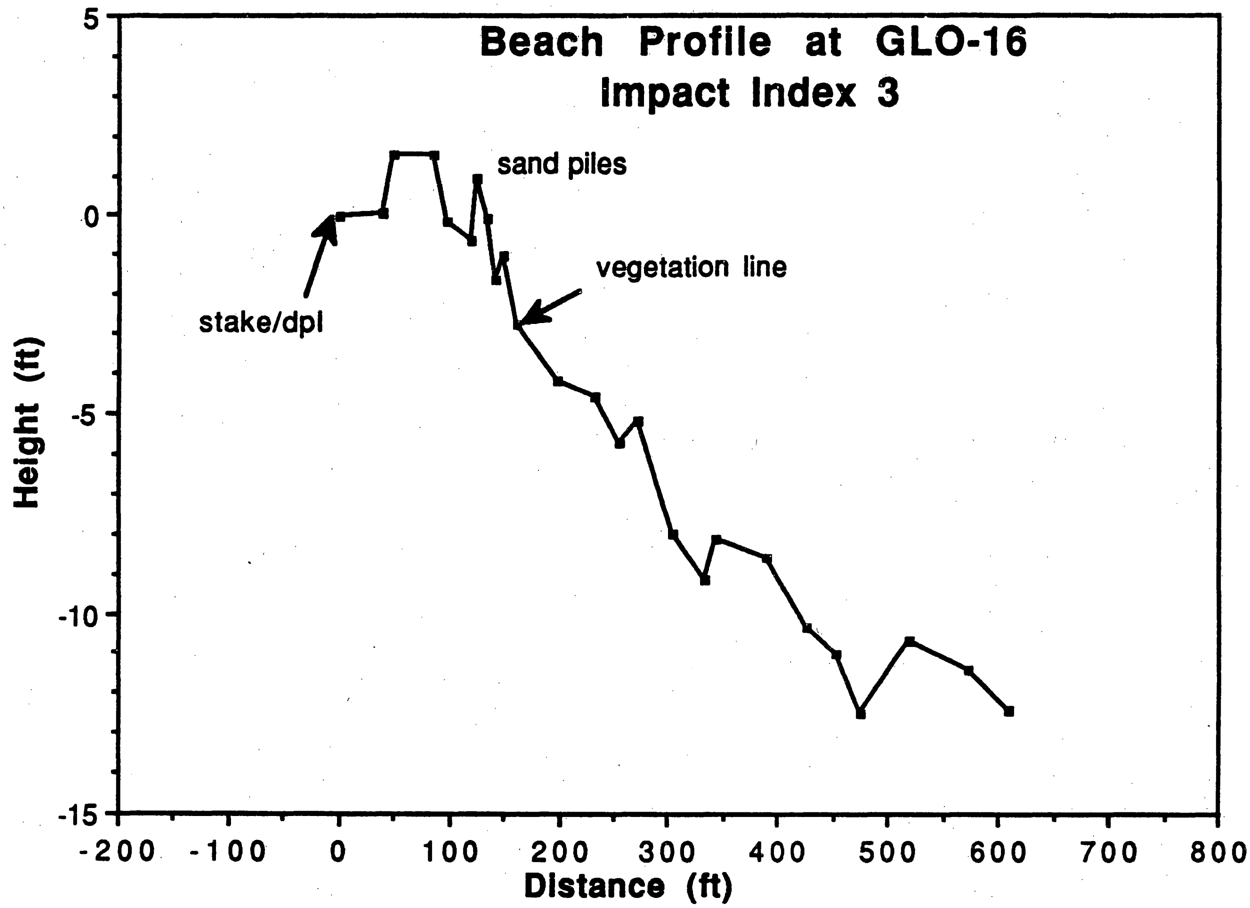

Beach Profile at GLO-16
Impact Index 3
sand piles
vegetation line
stake/dpl
Height (ft)
Distance (ft)
5
0
-5
-10
-15
-200
-100
0
100
200
300
400
500
600
700
800

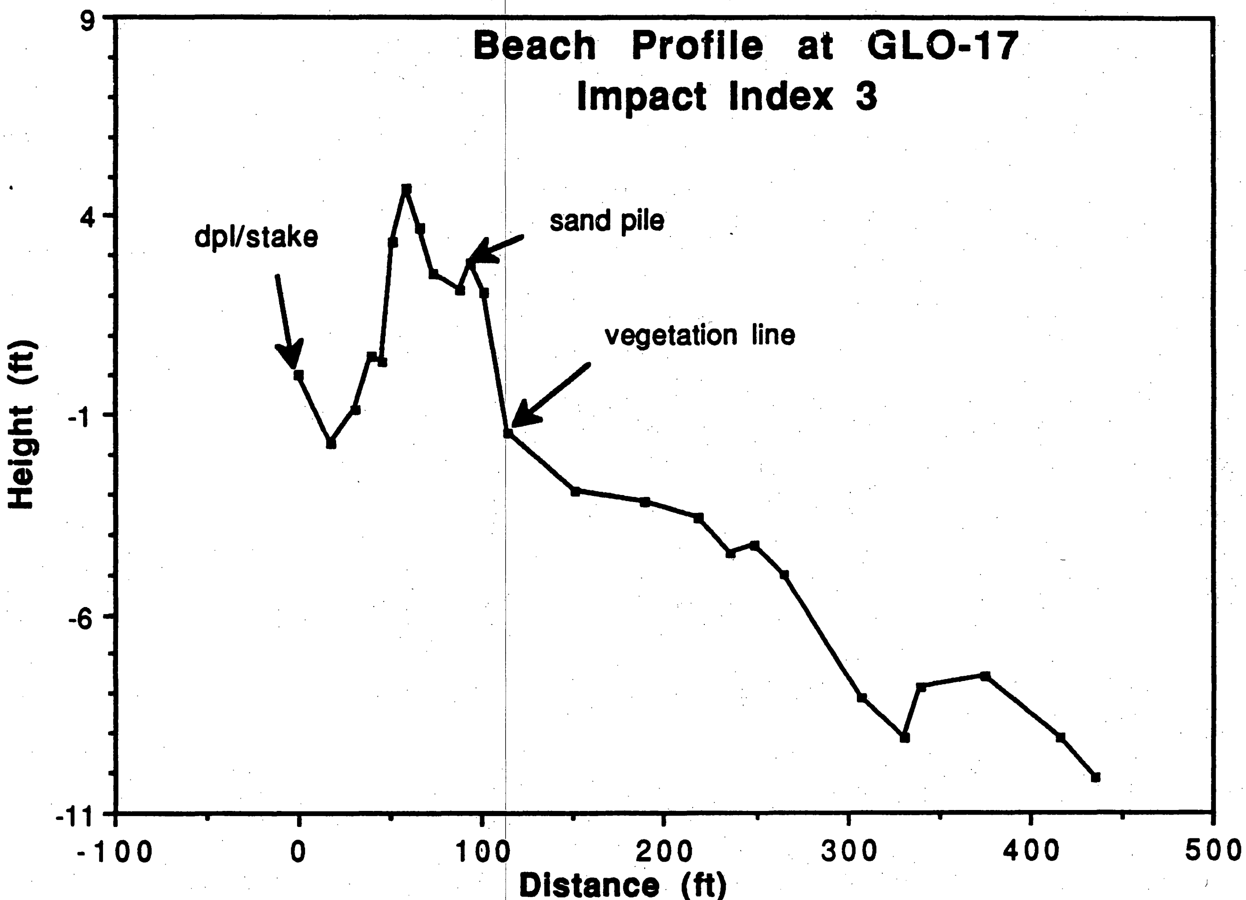

Beach Profile at GLO-17
Impact Index 3
dpl/stake
sand pile
vegetation line
Height (ft)
9
4
-1
-6
-11
-100
0
100
200
300
400
500
Distance (ft)

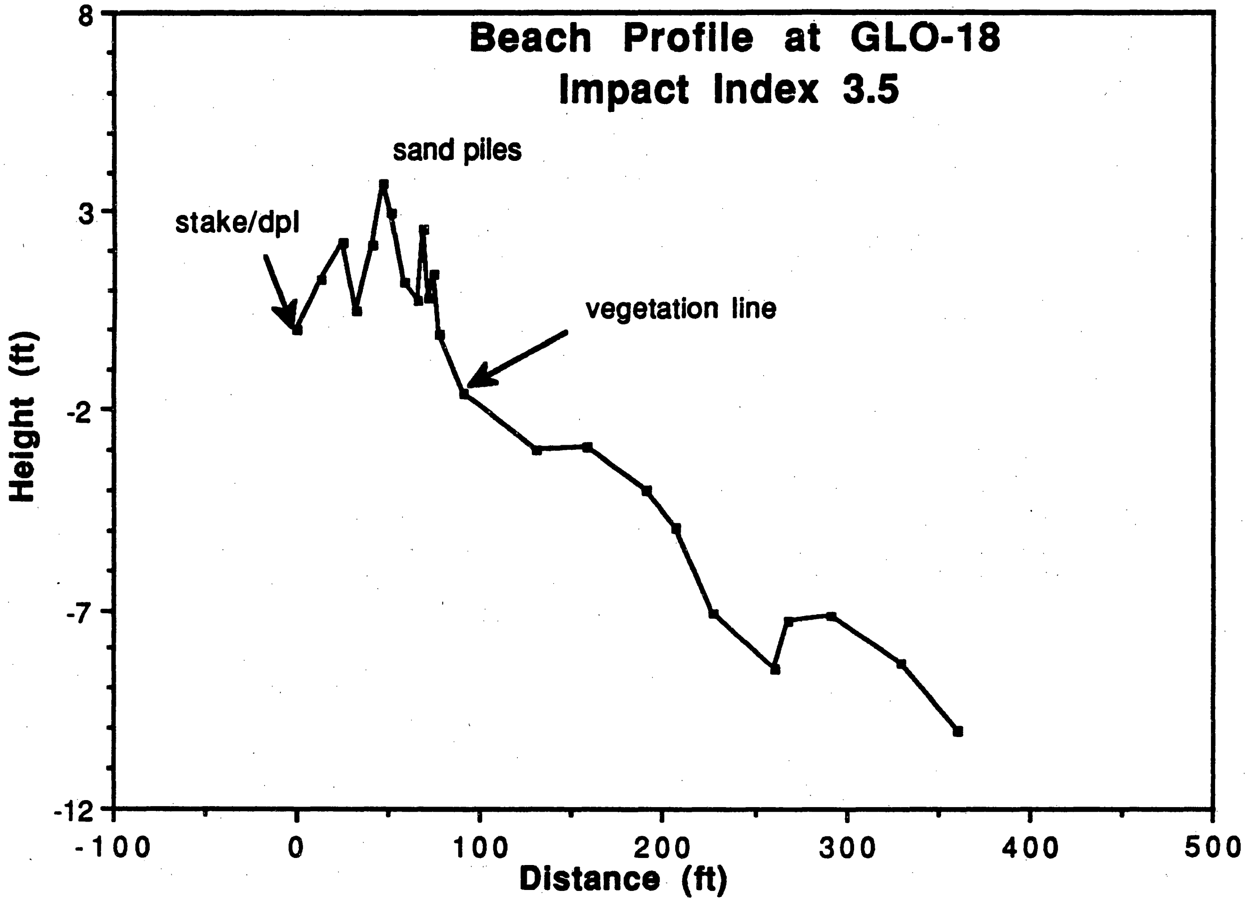
Beach Profile at GLO-18
Impact Index 3.5
sand piles
stake/dpl
vegetation line
8
3
-2
-7
-12
Height (ft)
-100
0
100
200
300
400
500
Distance (ft)

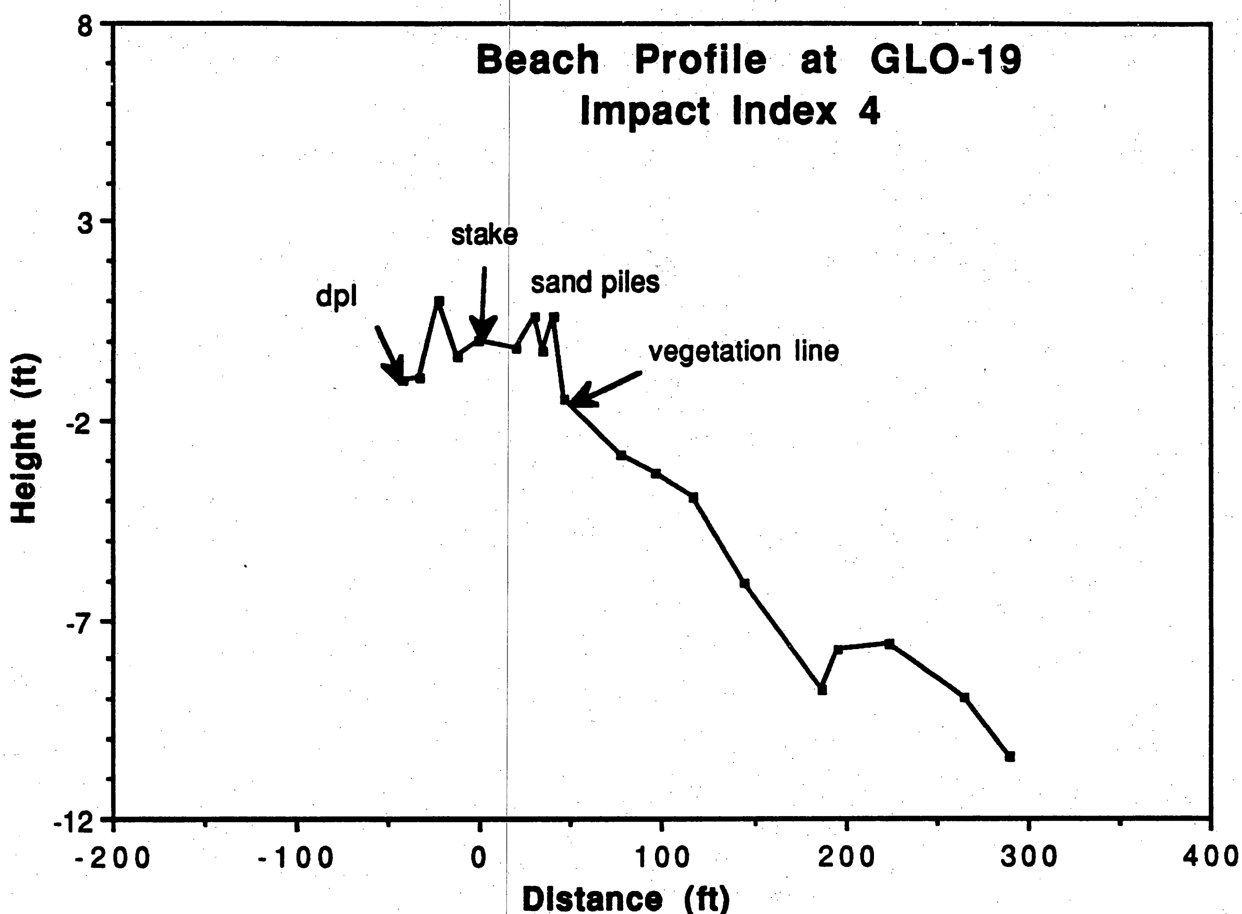

Beach Profile at GLO-19
Impact Index 4
stake
dpl
sand piles
vegetation line
8
3
-2
-7
-12
Height (ft)
-200
-100
0
100
200
300
400
Distance (ft)

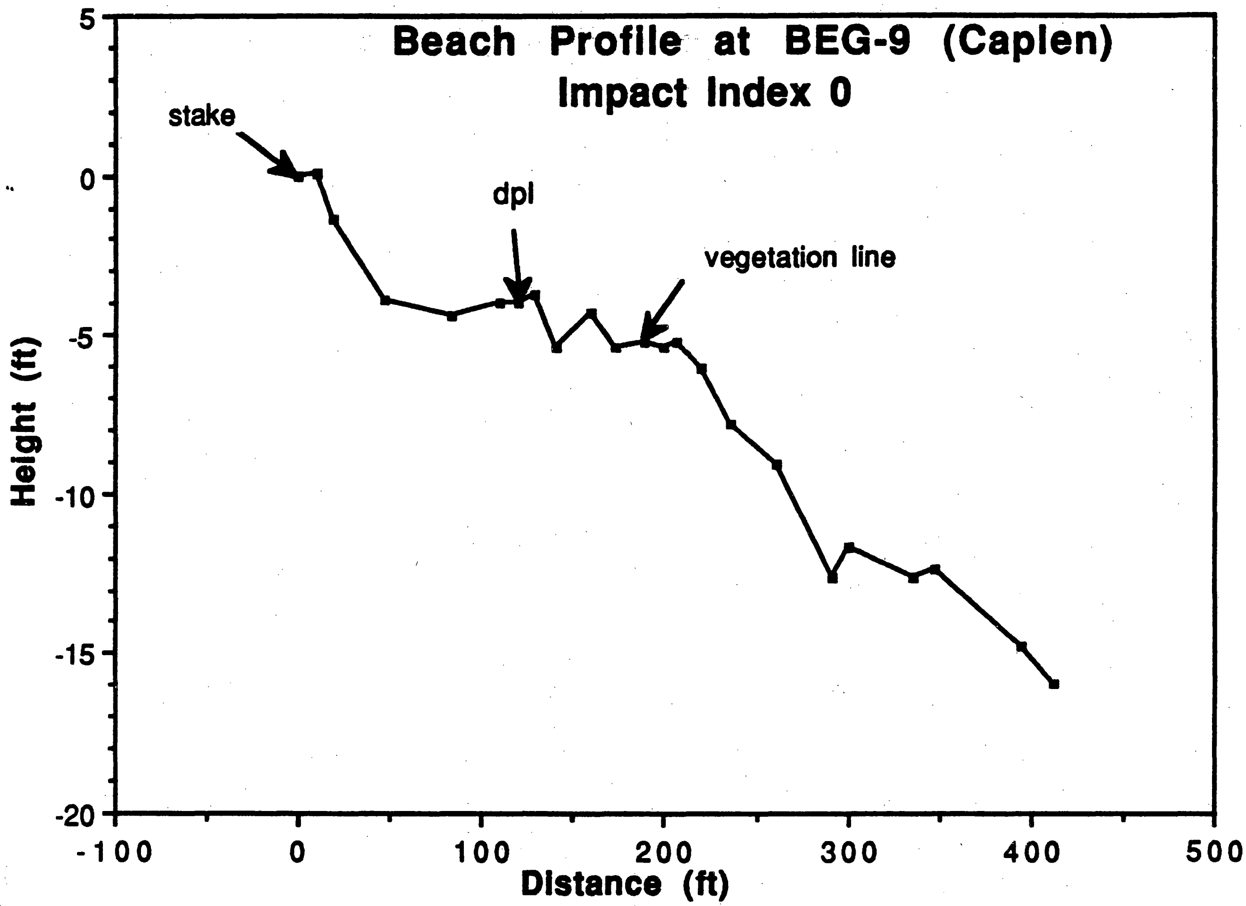

Beach Profile at BEG-9 (Caplen)
Impact Index 0
stake
dpl
vegetation line
Height (ft)
Distance (ft)
5
0
-5
-10
-15
-20
-100
0
100
200
300
400
500

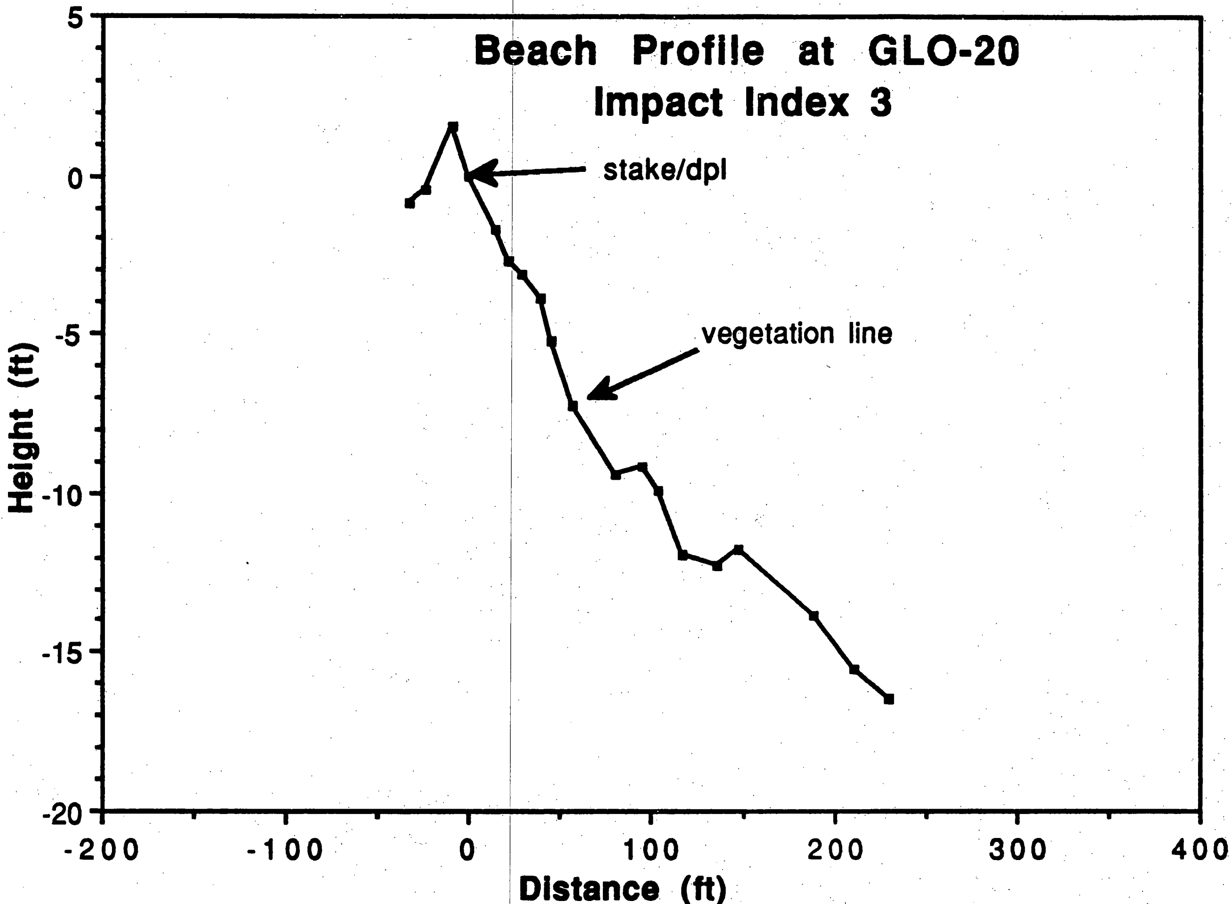

Beach Profile at GLO-20
Impact Index 3
stake/dpl
vegetation line
Height (ft)
Distance (ft)
5
0
-5
-10
-15
-20
-200
-100
0
100
200
300
400

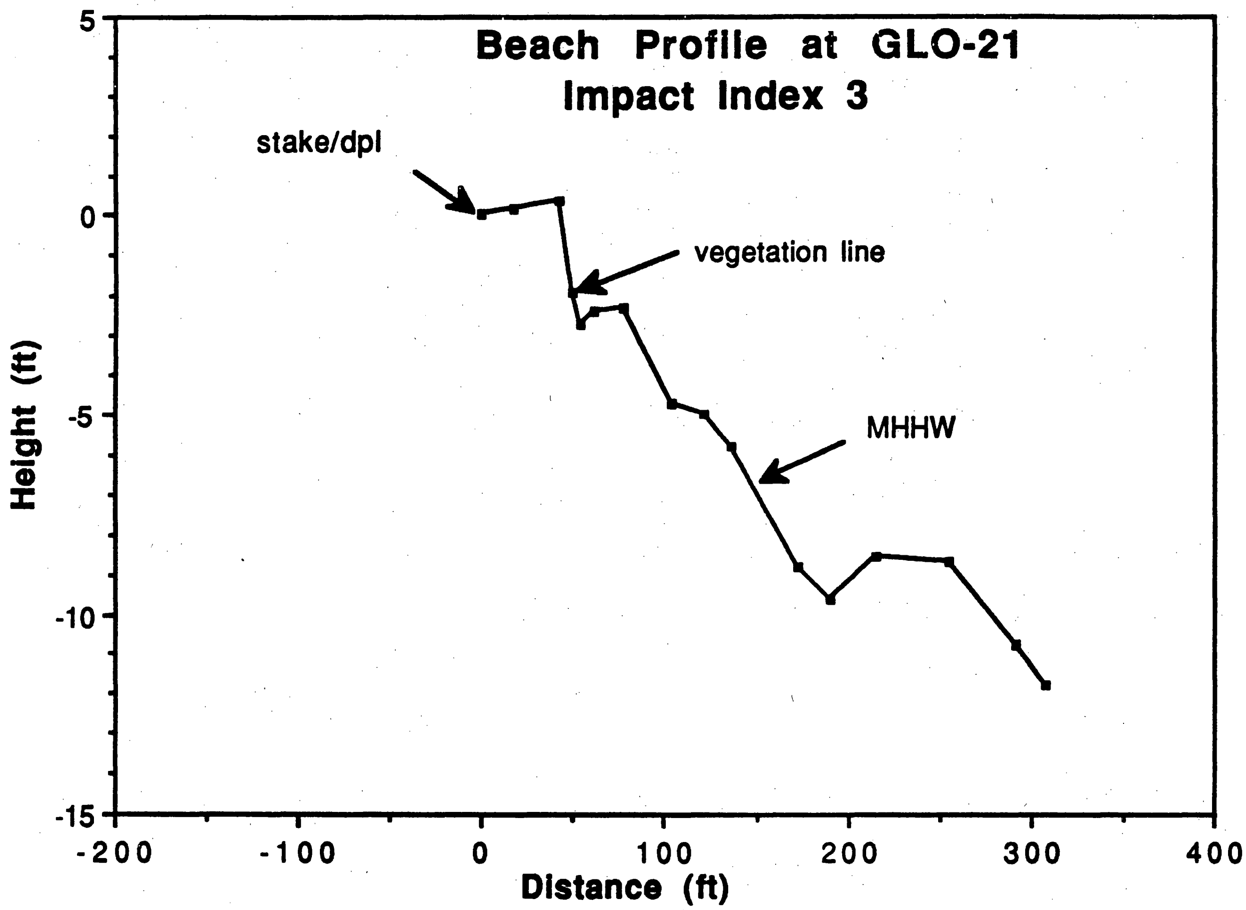

Beach Profile at GLO-21
Impact Index 3
stake/dpl
vegetation line
MHHW
Height (ft)
5
0
-5
-10
-15
-200
-100
0
100
200
300
400
Distance (ft)

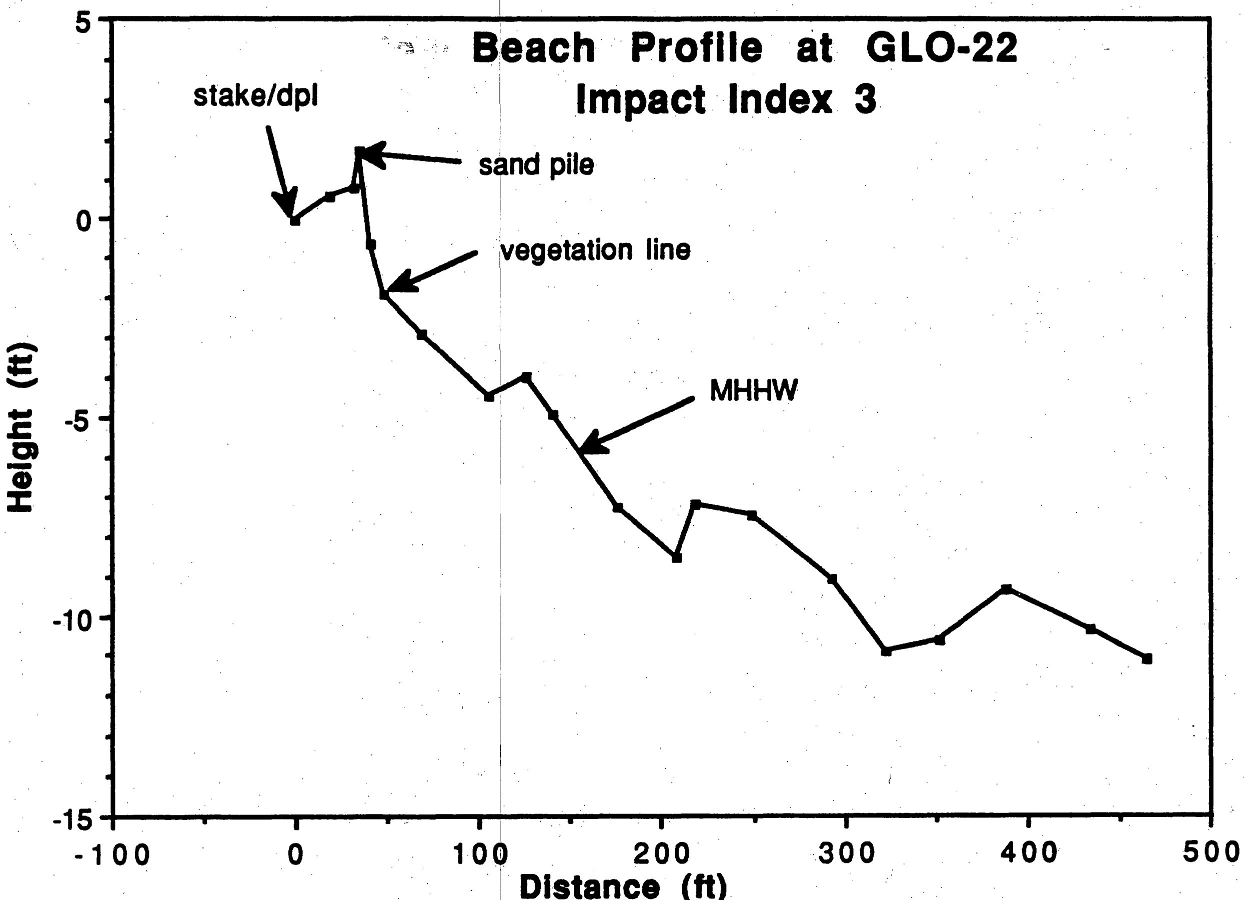
Beach Profile at GLO-22
Impact Index 3
stake/dpl
sand pile
vegetation line
MHHW
Height (ft)
Distance (ft)
5
0
-5
-10
-15
-100
0
100
200
300
400
500

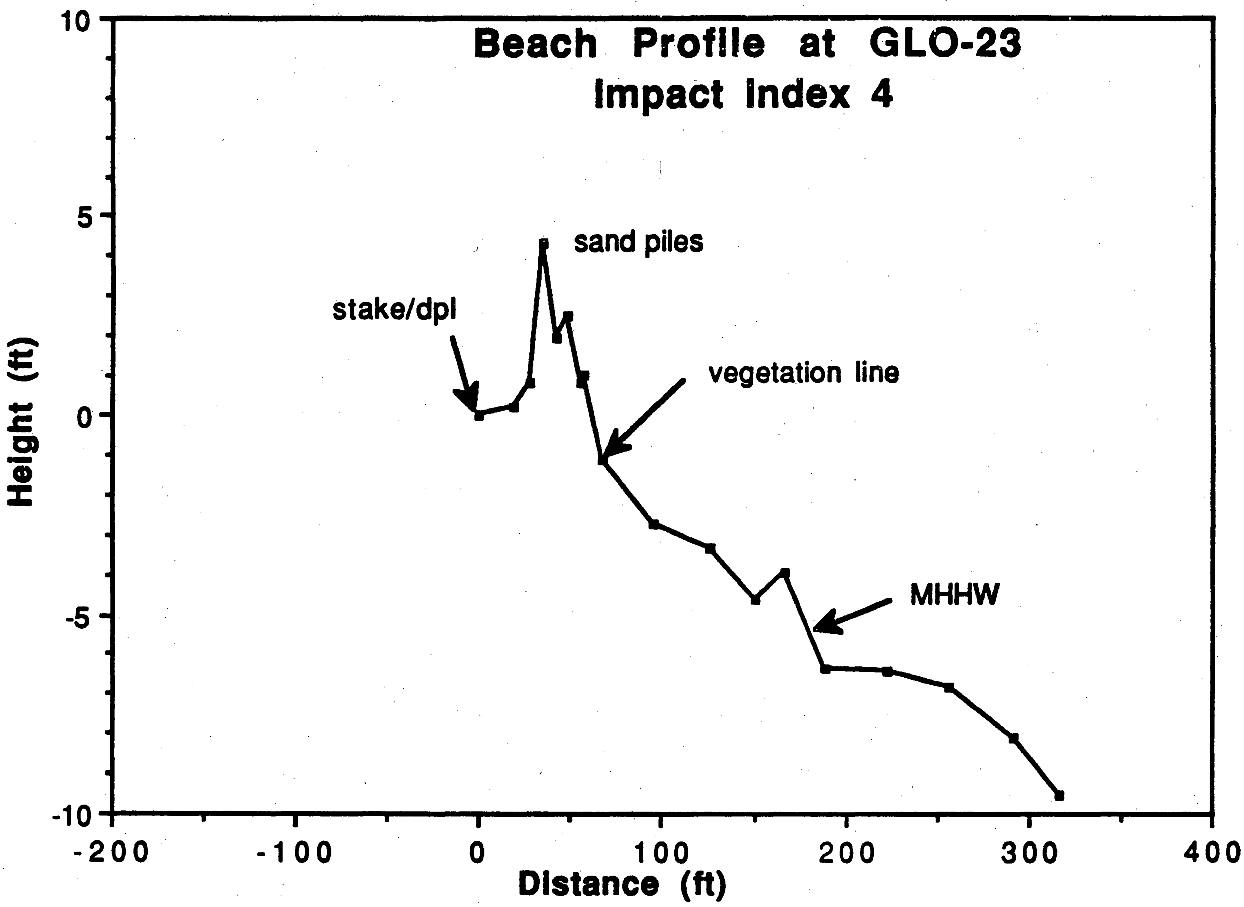

Beach Profile at GLO-23
Impact Index 4
sand piles
stake/dpl
vegetation line
MHHW
10
5
0
-5
-10
-200
-100
0
100
200
300
400
Height (ft)
Distance (ft)

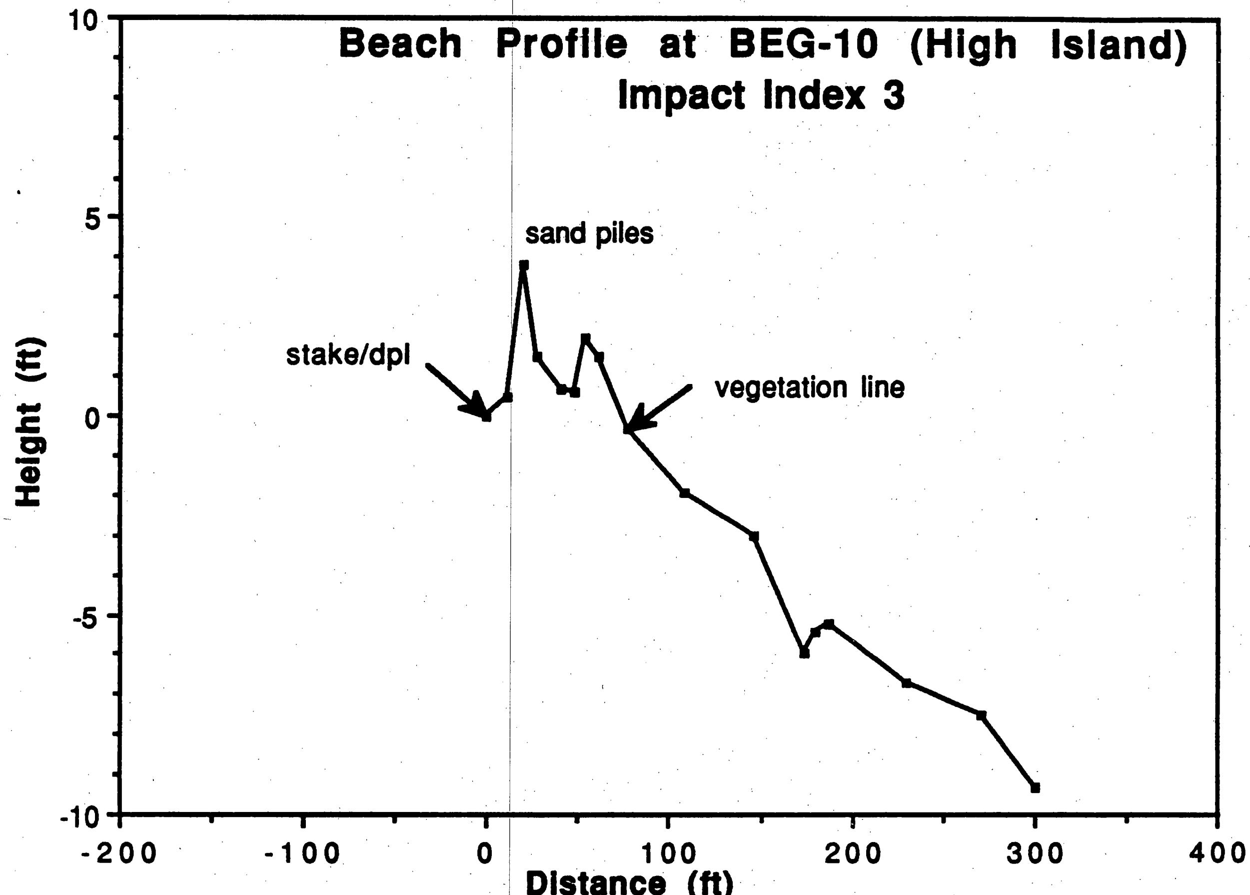

Beach Profile at BEG-10 (High Island)
Impact Index 3
sand piles
stake/dpl
vegetation line
Height (ft)
Distance (ft)
10
5
0
-5
-10
-200
-100
0
100
200
300
400

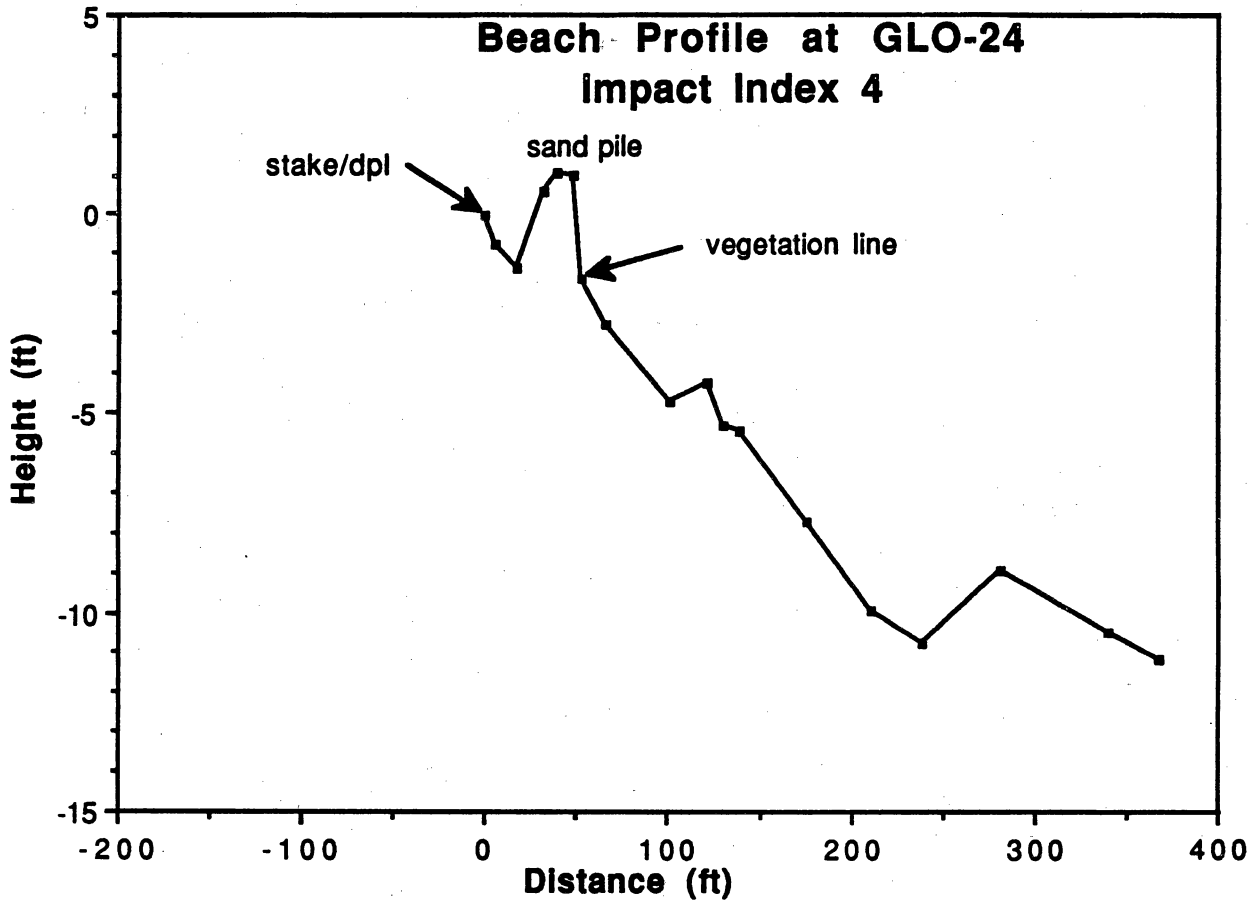

Beach Profile at GLO-24
Impact Index 4
stake/dpl
sand pile
vegetation line
Height (ft)
5
0
-5
-10
-15
-200
-100
0
100
200
300
400
Distance (ft)

Addendum 4. Foraminifera Analysis

Sample	misc. agglutinated	A. parkinsoniana	E. gunteri	E. discoidale	E. mexicanum	E. matagordanum	E. sp cf matagordanum	E. poeyanum	E. sp cf poeyanum	E. kugleri	juveniles	Elphidium spp.	rotalid fragments	Nonionella atlantica	Discorbis spp.	Hanzawaia concentrica	Palmerinella palmerae	Buccella hannai	Buliminella elegantissima	Brizalina lowmani	B. striatula	Fissurina sp.	total rare marine
CE7-132	0	92	144	37	11	2	0	1	0	0	0	1	7	0	0	0	5	0	0	0	0	0	0
CE7-292	0	87	187	5	2	1	0	0	2	0	0	0	11	0	0	0	5	1	0	0	0	0	0
CE7-445	2	75	170	31	14	0	0	0	1	0	0	0	2	0	0	0	11	0	0	0	0	0	0
CE7-465	0	104	195	22	25	0	0	0	0	0	0	0	9	0	0	0	0	0	0	0	0	0	0
CE7-498	0	125	199	34	9	0	0	0	0	0	0	5	8	0	0	0	18	0	0	0	0	0	0
CE7-528	0	111	191	24	11	0	0	0	5	0	0	0	18	0	0	0	4	2	0	0	0	0	0
CE7-602	0	104	134	22	33	0	0	1	0	0	0	0	3	0	0	0	2	2	0	0	0	0	0
CE7-629	0	128	103	37	5	0	0	0	1	0	0	2	4	0	0	0	2	0	0	0	0	0	0
CE7-640	0	95	199	51	42	2	0	0	0	0	0	11	5	0	0	0	3	1	0	0	0	0	0
CE7-671	1	108	211	8	0	0	0	0	24	0	0	1	17	0	0	0	0	4	1	1	0	0	2
CE7-693	0	77	237	0	0	2	0	1	26	0	0	0	18	0	0	0	8	1	0	0	0	0	0
CE7-726	0	0	37	0	0	0	0	2	0	0	0	2	0	0	0	0	5	0	0	0	0	0	0
CE7-757	0	131	260	8	1	0	0	0	5	0	0	0	3	0	0	0	1	1	0	0	0	0	0
CE7-787	0	13	2	0	0	0	0	0	0	0	0	0	0	0	0	0	0	0	0	0	0	0	0
CE7-813	0	4	2	0	0	0	0	0	0	0	0	0	0	0	0	0	0	0	0	0	0	0	0
CE10-146	6	38	179	0	0	0	0	1	1	0	0	0	103	0	0	0	0	1	1	0	1	0	2
CE10-267	1	139	113	7	2	0	1	0	1	0	0	0	20	0	0	0	0	0	0	0	0	0	0
CE10-295	1	142	113	3	1	0	0	0	0	0	0	0	18	0	0	0	0	0	0	0	0	0	0
CE10-330	0	36	51	5	0	0	5	0	4	0	5	0	55	0	0	0	0	0	0	1	1	0	2
CE10-368	1	77	156	6	4	1	3	0	1	0	6	0	46	0	0	0	0	0	0	1	0	0	1
CE10-394	0	57	206	5	0	2	1	0	0	0	3	0	29	1	0	0	1	0	0	0	0	0	1
CE10-439	0	88	177	12	0	1	4	0	23	0	7	0	36	1	0	0	2	4	2	0	1	0	4
CE10-483	0	81	164	4	1	2	6	2	21	1	8	0	33	0	0	0	2	4	0	1	1	0	2
CE10-525	1	82	143	2	1	2	0	0	7	0	4	0	32	0	0	0	2	1	2	0	2	0	4
CE10-561	0	73	165	4	1	0	3	0	6	0	1	0	47	0	0	0	2	0	0	0	0	0	0
CE10-593	0	80	158	11	6	0	3	0	3	0	4	2	19	0	0	0	4	0	0	0	0	0	0
CE10-625	0	67	87	3	0	1	103	0	9	0	12	0	20	0	0	0	2	3	2	1	1	0	4
CE10-658	0	73	122	6	0	4	31	0	17	0	28	6	25	0	0	0	15	6	2	0	2	4	8
CE10-688	0	58	114	0	4	0	65	1	5	1	36	0	13	0	0	0	28	7	1	1	1	0	3
CE10-716	1	68	131	4	1	4	47	0	6	4	25	0	13	1	0	0	6	4	1	1	2	0	5
CE10-753	0	131	159	15	4	0	0	4	0	0	0	0	5	0	0	0	0	0	0	0	0	0	0
CE10-793	0	104	158	19	2	2	0	3	2	0	0	0	10	0	0	0	4	1	0	0	0	0	0
CE10-826	1	119	126	11	6	0	0	1	4	0	0	0	9	0	0	0	0	1	0	0	0	0	0
CE10-839	2	127	176	15	5	4	5	9	10	0	5	0	21	0	0	0	0	2	0	0	1	0	1
CE10-876	0	109	160	11	2	8	0	1	9	4	1	3	20	0	0	0	2	5	1	0	1	0	2
CE10-917	0	107	182	15	0	4	0	0	7	8	3	0	12	0	0	0	2	4	0	1	2	0	3
CE10-950	1	80	182	6	2	1	5	3	4	3	5	0	11	0	2	0	2	2	1	1	4	1	9
CE10-987	0	105	138	6	0	1	8	0	14	7	1	0	14	1	0	0	0	2	1	1	1	0	4
CE101024	0	102	122	10	5	3	12	0	14	4	14	0	22	0	1	0	2	6	2	0	6	1	10
CE101086	0	80	141	2	1	0	9	2	17	4	18	0	13	0	0	0	0	10	1	1	1	2	5

Sample	Quinqueloculina compta	Q. seminuium	Q. funafutiensis	Q. lamarckiana	Quinqueloculina spp.	Massilina peruviana	Triloculina oblonga	Triloculina spp.	miliolid fragments	total miliolids	reworked forams	misc.	total forams	%misc. agglutinated	%A. parkinsoniana	%E. gunteri	%E. discoidale	%E. mexicanum	%E. matagordanum	%E. sp cf matagordanum	%E. poeyanum	%E. sp cf poeyanum	%E. kugleri	%juveniles
CE7-132	4	4	2	0	0	0	0	0	4	14	4	0	318	0	29	45	12	3	1	0	0	0	0	0
CE7-292	5	0	0	0	0	0	0	0	1	6	4	0	311	0	28	60	2	1	0	0	0	1	0	0
CE7-445	3	2	0	2	0	0	0	0	3	10	2	0	318	1	24	53	10	4	0	0	0	0	0	0
CE7-465	0	1	0	0	0	0	0	0	0	1	3	0	359	0	29	54	6	7	0	0	0	0	0	0
CE7-498	8	1	0	0	0	0	0	1	5	15	1	0	414	0	30	48	8	2	0	0	0	0	0	0
CE7-528	5	0	0	0	0	0	0	0	0	5	1	0	372	0	30	51	6	3	0	0	0	1	0	0
CE7-602	6	0	3	2	0	0	0	0	1	12	0	0	313	0	33	43	7	11	0	0	0	0	0	0
CE7-629	1	0	0	0	0	0	0	0	0	1	1	2	286	0	45	36	13	2	0	0	0	0	0	0
CE7-640	6	0	1	1	0	1	0	0	5	14	2	0	425	0	22	47	12	10	0	0	0	0	0	0
CE7-671	0	2	0	0	1	0	0	0	1	4	1	0	381	0	28	55	2	0	0	0	0	6	0	0
CE7-693	0	2	0	1	0	0	0	0	0	3	0	0	373	0	21	64	0	0	1	0	0	7	0	0
CE7-726	0	0	0	0	0	0	1	0	1	2	0	0	48	0	0	77	0	0	0	0	4	0	0	0
CE7-757	0	3	0	0	0	0	0	1	2	6	0	0	416	0	31	63	2	0	0	0	0	1	0	0
CE7-787	0	0	0	0	0	0	0	0	0	0	0	0	15	0	87	13	0	0	0	0	0	0	0	0
CE7-813	0	0	0	0	0	0	0	0	0	0	0	0	6	0	67	33	0	0	0	0	0	0	0	0
CE10-146	0	0	0	0	0	0	0	0	0	0	1	0	332	2	11	54	0	0	0	0	0	0	0	0
CE10-267	0	1	0	0	0	0	0	1	4	6	1	0	291	0	48	39	2	1	0	0	0	0	0	0
CE10-295	0	0	0	0	0	0	0	0	4	4	2	0	284	0	50	40	1	0	0	0	0	0	0	0
CE10-330	0	0	0	0	0	0	0	0	3	3	3	0	169	0	21	30	3	0	0	3	0	2	0	3
CE10-368	0	3	0	0	0	0	0	0	7	10	1	0	313	0	25	50	2	1	0	1	0	0	0	2
CE10-394	0	2	0	0	0	0	0	0	1	3	0	0	308	0	19	67	2	0	1	0	0	0	0	1
CE10-439	2	5	0	0	0	0	0	0	3	10	1	0	369	0	24	48	3	0	0	1	0	6	0	2
CE10-483	0	6	0	0	0	0	0	0	3	9	1	0	341	0	24	48	1	0	1	2	1	6	0	2
CE10-525	0	4	0	0	0	0	0	0	7	11	0	0	292	0	28	49	1	0	1	0	0	2	0	1
CE10-561	0	2	0	0	0	0	0	0	2	4	0	1	307	0	24	54	1	0	0	1	0	2	0	0
CE10-593	0	0	0	0	0	0	0	0	1	1	3	0	294	0	27	54	4	2	0	1	0	1	0	1
CE10-625	0	1	0	1	0	0	0	0	2	4	0	0	315	0	21	28	1	0	0	33	0	3	0	4
CE10-658	0	2	0	0	0	0	0	0	3	5	0	0	346	0	21	35	2	0	1	9	0	5	0	8
CE10-688	0	7	0	0	0	0	0	0	1	8	1	0	344	0	17	33	0	1	0	19	0	1	0	10
CE10-716	0	4	0	0	0	0	0	0	0	4	0	0	323	0	21	41	1	0	1	15	0	2	1	8
CE10-753	0	2	0	1	0	0	0	0	3	6	3	0	327	0	40	49	5	1	0	0	1	0	0	0
CE10-793	3	0	0	0	0	0	0	0	4	7	1	0	313	0	33	50	6	1	1	0	1	1	0	0
CE10-826	0	0	0	0	0	0	0	0	4	4	2	0	284	0	42	44	4	2	0	0	0	1	0	0
CE10-839	3	1	0	6	0	0	0	0	5	15	0	0	397	1	32	44	4	1	1	1	2	3	0	1
CE10-876	2	3	0	0	0	0	0	0	2	7	1	0	345	0	32	46	3	1	2	0	0	3	1	0
CE10-917	0	2	0	0	0	0	0	0	2	4	0	0	351	0	30	52	4	0	1	0	0	2	2	1
CE10-950	4	5	0	0	0	0	0	0	5	14	0	0	330	0	24	55	2	1	0	2	1	1	1	2
CE10-987	0	1	0	4	0	0	0	0	7	12	0	0	312	0	34	44	2	0	0	3	0	4	2	0
CE101024	1	2	0	0	0	0	1	0	2	6	0	0	332	0	31	37	3	2	1	4	0	4	1	4
CE101086	0	2	0	2	0	0	0	0	0	4	0	0	306	0	26	46	1	0	0	3	1	6	1	6

Sample	%Elphidium spp.	%rotalid fragments	%Nonionelia atlantica	%Discorbis spp.	%Hanzawaia concentrica	%Palmerinella palmerae	%Buccella hannai	%Buliminella elegantissima	%Brizalina lowmani	%B. striatula	%Fissurina sp.	%total rare marine	%Quinqueloculina compta	%Q. seminulum	%Q. funafutiensis	%Q. lamarckiana	%Quinqueloculina spp.	%Massilina peruviana	%Triloculina oblonga	%Triloculina spp.	%miliolid fragments	%total miliolids	%reworked forams	%misc.
CE7-132	0	2	0	0	0	2	0	0	0	0	0	0	1	1	1	0	0	0	0	0	1	4	1	0
CE7-292	0	4	0	0	0	2	0	0	0	0	0	0	2	0	0	0	0	0	0	0	0	2	1	0
CE7-445	0	1	0	0	0	3	0	0	0	0	0	0	1	1	0	1	0	0	0	0	1	3	1	0
CE7-465	0	3	0	0	0	0	0	0	0	0	0	0	0	0	0	0	0	0	0	0	0	0	1	0
CE7-498	1	2	0	0	0	4	0	0	0	0	0	0	2	0	0	0	0	0	0	0	1	4	0	0
CE7-528	0	5	0	0	0	1	1	0	0	0	0	0	1	0	0	0	0	0	0	0	0	1	0	0
CE7-602	0	1	0	0	0	1	1	0	0	0	0	0	2	0	1	1	0	0	0	0	0	4	0	0
CE7-629	1	1	0	0	0	1	0	0	0	0	0	0	0	0	0	0	0	0	0	0	0	0	0	1
CE7-640	3	1	0	0	0	1	0	0	0	0	0	0	1	0	0	0	0	0	0	0	1	3	0	0
CE7-671	0	4	0	0	0	0	1	0	0	0	0	1	0	1	0	0	0	0	0	0	0	1	0	0
CE7-693	0	5	0	0	0	2	0	0	0	0	0	0	0	1	0	0	0	0	0	0	0	1	0	0
CE7-726	4	0	0	0	0	10	0	0	0	0	0	0	0	0	0	0	0	0	2	0	2	4	0	0
CE7-757	0	1	0	0	0	0	0	0	0	0	0	0	0	1	0	0	0	0	0	0	0	1	0	0
CE7-787	0	0	0	0	0	0	0	0	0	0	0	0	0	0	0	0	0	0	0	0	0	0	0	0
CE7-813	0	0	0	0	0	0	0	0	0	0	0	0	0	0	0	0	0	0	0	0	0	0	0	0
CE10-146	0	31	0	0	0	0	0	0	0	0	0	1	0	0	0	0	0	0	0	0	0	0	0	0
CE10-267	0	7	0	0	0	0	0	0	0	0	0	0	0	0	0	0	0	0	0	0	1	2	0	0
CE10-295	0	6	0	0	0	0	0	0	0	0	0	0	0	0	0	0	0	0	0	0	1	1	1	0
CE10-330	0	33	0	0	0	0	0	0	1	1	0	1	0	0	0	0	0	0	0	0	2	2	2	0
CE10-368	0	15	0	0	0	0	0	0	0	0	0	0	0	1	0	0	0	0	0	0	2	3	0	0
CE10-394	0	9	0	0	0	0	0	0	0	0	0	0	0	1	0	0	0	0	0	0	0	1	0	0
CE10-439	0	10	0	0	0	1	1	1	0	0	0	1	1	1	0	0	0	0	0	0	1	3	0	0
CE10-483	0	10	0	0	0	1	1	0	0	0	0	1	0	2	0	0	0	0	0	0	1	3	0	0
CE10-525	0	11	0	0	0	1	0	1	0	1	0	1	0	1	0	0	0	0	0	0	2	4	0	0
CE10-561	0	15	0	0	0	1	0	0	0	0	0	0	0	1	0	0	0	0	0	0	1	1	0	0
CE10-593	1	6	0	0	0	1	0	0	0	0	0	0	0	0	0	0	0	0	0	0	0	0	1	0
CE10-625	0	6	0	0	0	1	1	1	0	0	0	1	0	0	0	0	0	0	0	0	1	1	0	0
CE10-658	2	7	0	0	0	4	2	1	0	1	1	2	0	1	0	0	0	0	0	0	1	1	0	0
CE10-688	0	4	0	0	0	8	2	0	0	0	0	1	0	2	0	0	0	0	0	0	0	2	0	0
CE10-716	0	4	0	0	0	2	1	0	0	1	0	2	0	1	0	0	0	0	0	0	0	1	0	0
CE10-753	0	2	0	0	0	0	0	0	0	0	0	0	0	1	0	0	0	0	0	0	1	2	1	0
CE10-793	0	3	0	0	0	1	0	0	0	0	0	0	1	0	0	0	0	0	0	0	1	2	0	0
CE10-826	0	3	0	0	0	0	0	0	0	0	0	0	0	0	0	0	0	0	0	0	1	1	1	0
CE10-839	0	5	0	0	0	0	1	0	0	0	0	0	1	0	0	2	0	0	0	0	1	4	0	0
CE10-876	1	6	0	0	0	1	1	0	0	0	0	1	1	1	0	0	0	0	0	0	1	2	0	0
CE10-917	0	3	0	0	0	1	1	0	0	1	0	1	0	1	0	0	0	0	0	0	1	1	0	0
CE10-950	0	3	0	1	0	1	1	0	0	1	0	3	1	2	0	0	0	0	0	0	2	4	0	0
CE10-987	0	4	0	0	0	0	1	0	0	0	0	1	0	0	0	1	0	0	0	0	2	4	0	0
CE101024	0	7	0	0	0	1	2	1	0	2	0	3	0	1	0	0	0	0	0	0	1	2	0	0
CE101086	0	4	0	0	0	0	3	0	0	0	1	2	0	1	0	1	0	0	0	0	0	1	0	0

Sample	total%
CE7-132	100
CE7-292	100
CE7-445	100
CE7-465	100
CE7-498	100
CE7-528	100
CE7-602	100
CE7-629	100
CE7-640	100
CE7-671	100
CE7-693	100
CE7-726	100
CE7-757	100
CE7-787	100
CE7-813	100
CE10-146	100
CE10-267	100
CE10-295	100
CE10-330	100
CE10-368	100
CE10-394	100
CE10-439	100
CE10-483	100
CE10-525	100
CE10-561	100
CE10-593	100
CE10-625	100
CE10-658	100
CE10-688	100
CE10-716	100
CE10-753	100
CE10-793	100
CE10-826	100
CE10-839	100
CE10-876	100
CE10-917	100
CE10-950	100
CE10-987	100
CE101024	100
CE101086	100

Sample	misc. agglutinated	A. parkinsoniana	E. gunteri	E. discoidale	E. mexicanum	E. matagordanum	E. sp cf matagordanum	E. poeyanum	E. sp cf poeyanum	E. kugleri	juveniles	Elphidium spp.	rotalid fragments	Nonionella atlantica	Discorbis spp.	Hanzawaia concentrica	Palmerinella palmerae	Buccella hannai	Buliminella elegantissima	Brizalina lowmani	B. striatula	Fissurina sp.	total rare marine
CE101123	0	89	114	0	3	7	4	0	27	6	3	0	20	0	0	0	0	1	2	0	2	1	5
CE101161	1	110	111	7	4	1	1	0	6	5	16	0	23	0	0	0	4	6	0	0	1	0	1
CE101191	0	82	157	7	4	0	24	0	8	0	4	0	12	0	0	0	3	4	0	2	1	0	3
CE101238	0	93	144	2	6	0	2	1	11	7	6	2	12	0	0	0	1	5	1	0	0	0	1
CE101270	0	98	130	5	3	2	2	3	13	2	1	0	16	0	0	1	0	3	1	0	0	0	2
CE101300	0	119	157	12	4	0	1	0	4	2	2	0	16	0	0	0	0	2	0	0	1	0	1
CE101334	0	128	183	9	4	1	2	0	2	8	0	0	15	0	0	0	0	2	0	0	3	0	3
CE101372	0	125	212	17	8	0	1	0	10	1	0	0	16	0	0	0	0	2	0	1	1	0	2
CE101412	0	116	183	12	1	0	3	1	7	0	0	0	20	0	0	0	1	2	1	0	2	1	4
CE101528	0	90	156	10	6	1	1	0	3	1	2	0	24	0	0	0	0	0	0	0	2	0	2
CE101650	0	185	124	4	0	0	3	0	4	0	5	0	13	0	0	0	1	1	0	0	0	0	0

Sample	Quinqueloculina compta	Q. seminulum	Q. funafutiensis	Q. lamarckiana	Quinqueloculina spp.	Massilina peruviana	Triloculina oblonga	Triloculina spp.	miliolid fragments	total miliolids	reworked forams	misc.	total forams	%misc. agglutinated	%A. parkinsoniana	%E. gunteri	%E. discoidale	%E. mexicanum	%E. matagordanum	%E. sp cf matagordanum	%E. poeyanum	%E. sp cf poeyanum	%E. kugleri	%juveniles
CE101123	1	5	0	2	0	0	0	0	4	12	0	1	292	0	30	39	0	1	2	1	0	9	2	1
CE101161	1	2	0	3	0	0	0	0	7	13	0	0	309	0	36	36	2	1	0	0	0	2	2	5
CE101191	0	6	0	0	0	0	0	0	6	12	0	0	320	0	26	49	2	1	0	8	0	3	0	1
CE101238	1	5	0	1	0	0	0	0	3	10	0	0	303	0	31	48	1	2	0	1	0	4	2	2
CE101270	0	7	0	0	0	0	0	0	8	15	1	0	296	0	33	44	2	1	1	1	1	4	1	0
CE101300	1	1	0	0	0	0	0	0	9	11	0	0	331	0	36	47	4	1	0	0	0	1	1	1
CE101334	0	0	0	0	0	0	0	0	4	4	0	0	361	0	35	51	2	1	0	1	0	1	2	0
CE101372	2	3	3	2	0	0	0	0	7	17	0	0	411	0	30	52	4	2	0	0	0	2	0	0
CE101412	0	0	0	0	0	0	0	0	0	0	0	0	350	0	33	52	3	0	0	1	0	2	0	0
CE101528	2	1	0	2	0	0	0	0	3	8	0	0	304	0	30	51	3	2	0	0	0	1	0	1
CE101650	0	0	0	0	0	0	0	0	2	2	0	0	342	0	54	36	1	0	0	1	0	1	0	1

Sample	%Elphidium spp.	%rotalid fragments	%Nonionella atlantica	%Discorbis spp.	%Hanzawaia concentrica	%Palmerinella palmerae	%Buccella hannai	%Buliminella elegantissima	%Brizalina lowmani	%B. striatula	%Fissurina sp.	%total rare marine	%Quinqueloculina compta	%Q. seminulum	%Q. funafutiensis	%Q. lamarckiana	%Quinqueloculina spp.	%Massilina peruviana	%Triloculina oblonga	%Triloculina spp.	%miliolid fragments	%total miliolids	%reworked forams	%misc.
CE101123	0	7	0	0	0	0	0	1	0	1	0	2	0	2	0	1	0	0	0	0	1	4	0	0
CE101161	0	7	0	0	0	1	2	0	0	0	0	0	0	1	0	1	0	0	0	0	2	4	0	0
CE101191	0	4	0	0	0	1	1	0	1	0	0	1	0	2	0	0	0	0	0	0	2	4	0	0
CE101238	1	4	0	0	0	0	2	0	0	0	0	0	0	2	0	0	0	0	0	0	1	3	0	0
CE101270	0	5	0	0	0	0	1	0	0	0	0	1	0	2	0	0	0	0	0	0	3	5	0	0
CE101300	0	5	0	0	0	0	1	0	0	0	0	0	0	0	0	0	0	0	0	0	3	3	0	0
CE101334	0	4	0	0	0	0	1	0	0	1	0	1	0	0	0	0	0	0	0	0	1	1	0	0
CE101372	0	4	0	0	0	0	0	0	0	0	0	0	0	1	1	0	0	0	0	0	2	4	0	0
CE101412	0	6	0	0	0	0	1	0	0	1	0	1	0	0	0	0	0	0	0	0	0	0	0	0
CE101528	0	8	0	0	0	0	0	0	0	1	0	1	1	0	0	1	0	0	0	0	1	3	0	0
CE101650	0	4	0	0	0	0	0	0	0	0	0	0	0	0	0	0	0	0	0	0	1	1	0	0

COASTAL EROSION PROJECT, CORE CE-2

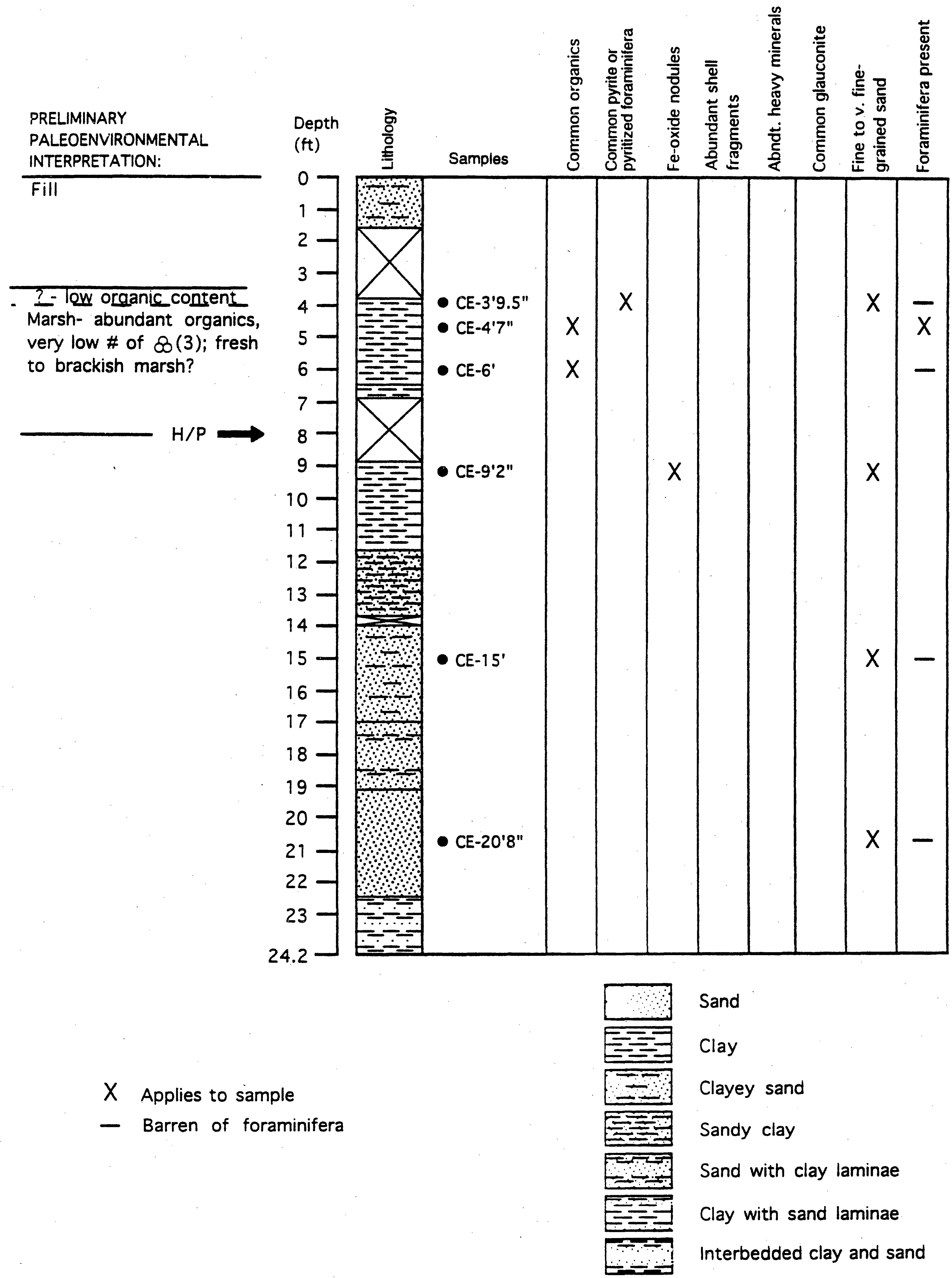

COASTAL EROSION PROJECT, CORE CE-4

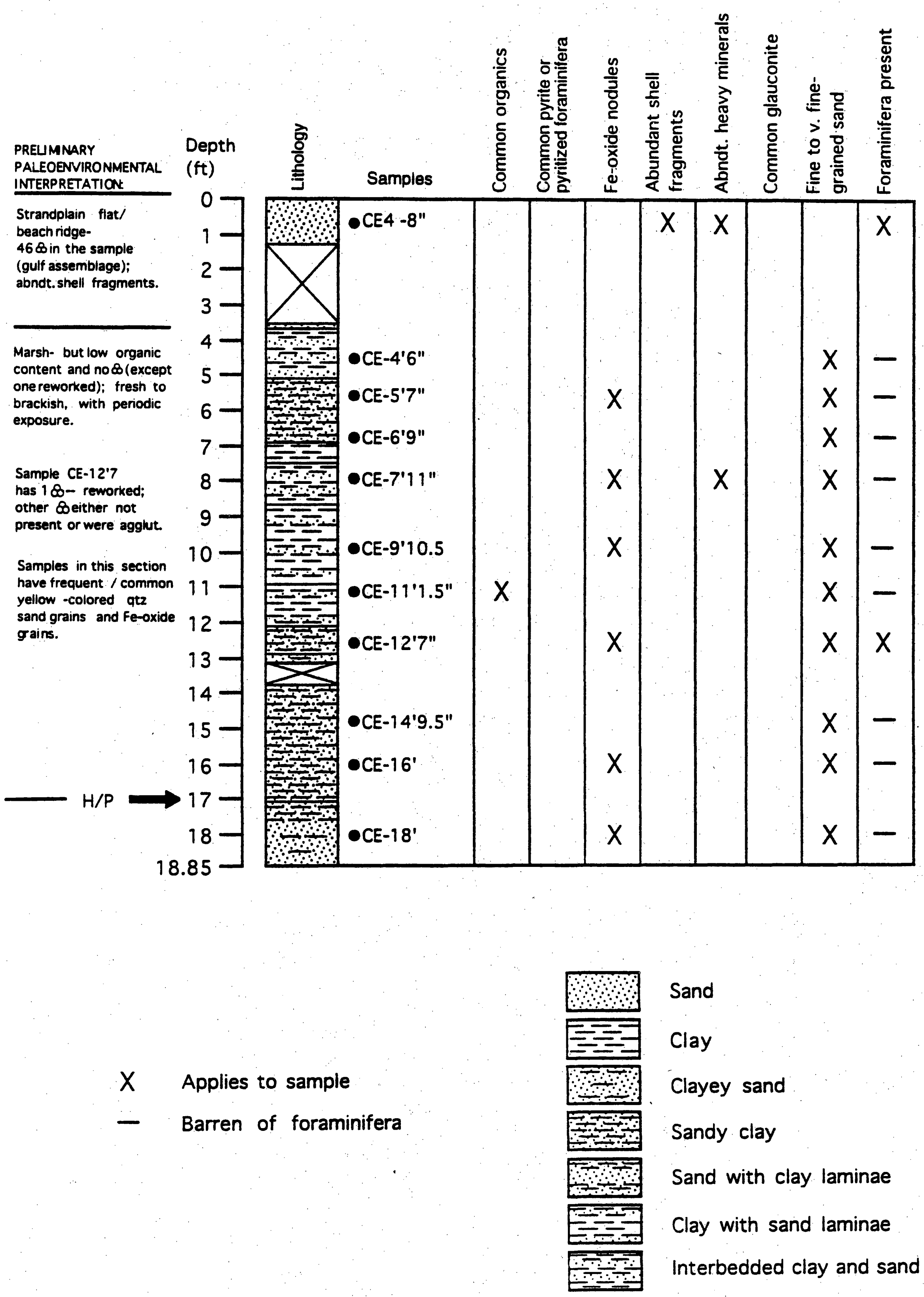

COASTAL EROSION PROJECT, CORE CE-6

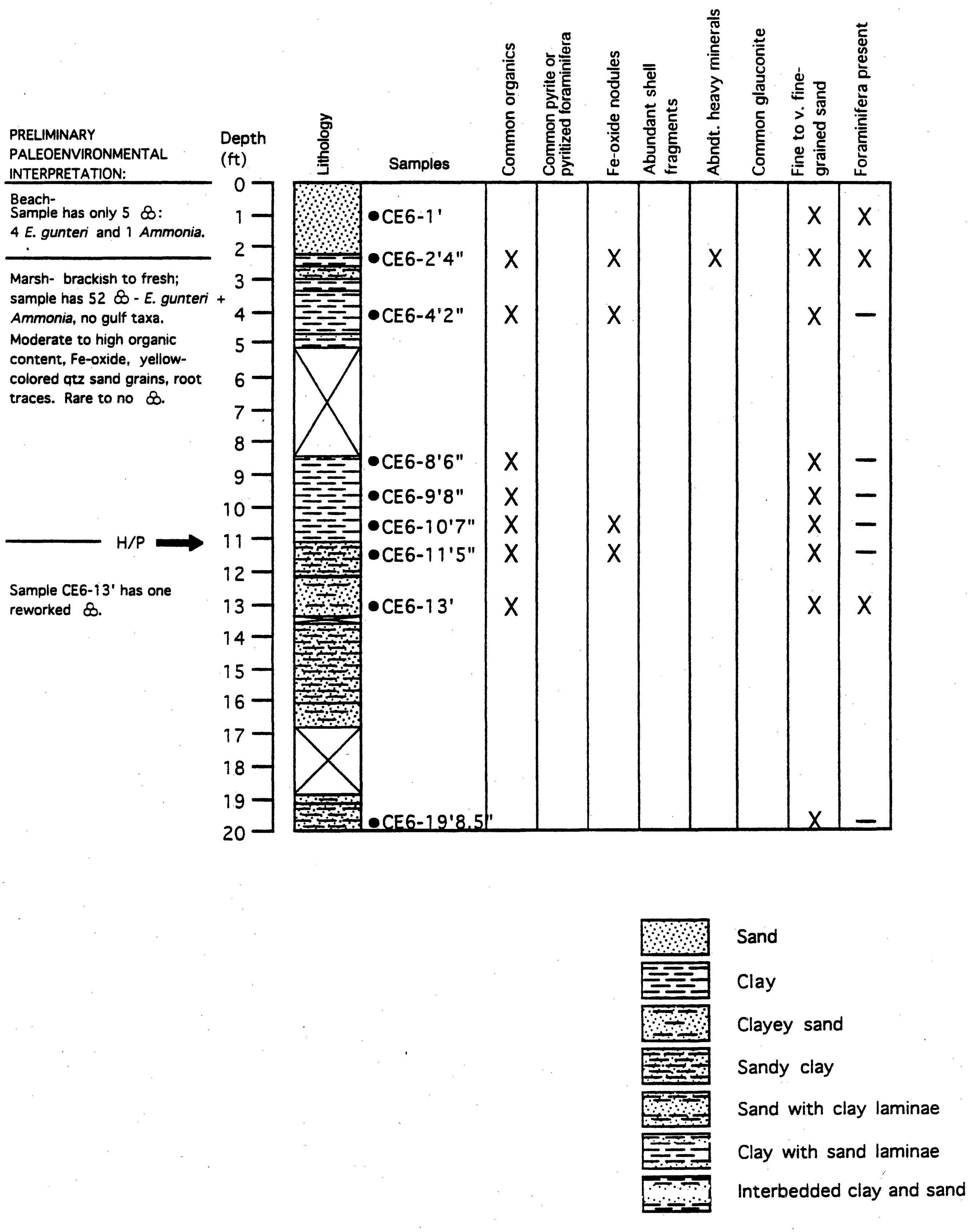

COASTAL EROSION PROJECT, CORE 7

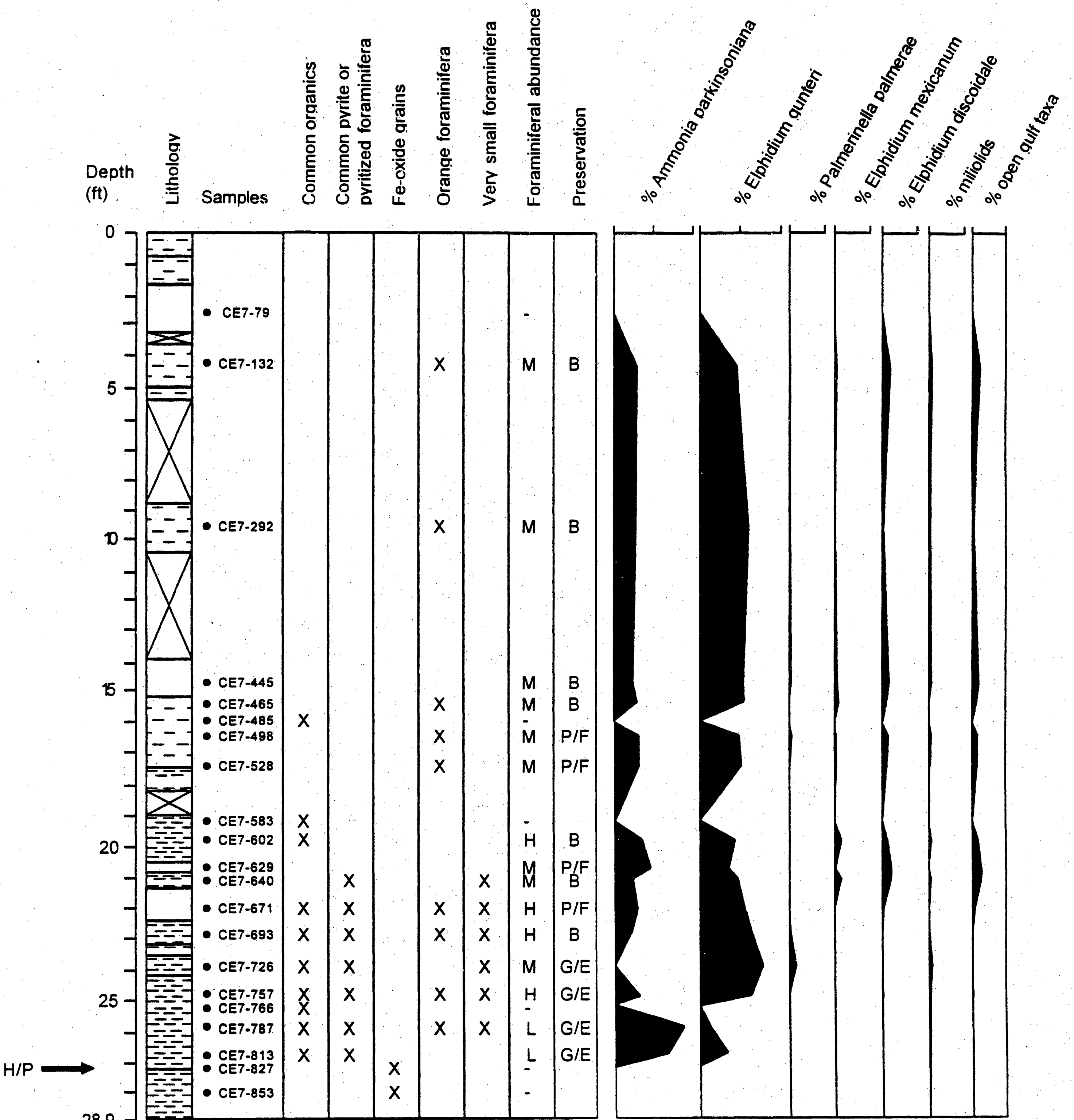

Samples	Common organics	Common pyrite or pyritized foraminifera	Fe-oxide grains	Orange foraminifera	Very small foraminifera	Foraminiferal abundance	Preservation
CE7-79						-	
CE7-132				X		M	B
CE7-292				X		M	B
CE7-445						M	B
CE7-465				X		M	B
CE7-485	X					-	
CE7-498				X		M	P/F
CE7-528				X		M	P/F
CE7-583	X					-	
CE7-602	X					H	B
CE7-629						M	P/F
CE7-640		X			X	M	B
CE7-671	X	X		X	X	H	P/F
CE7-693	X	X		X	X	H	B
CE7-726	X	X			X	M	G/E
CE7-757	X	X		X	X	H	G/E
CE7-766	X					-	
CE7-787	X	X		X	X	L	G/E
CE7-813	X	X				L	G/E
CE7-827			X			-	
CE7-853			X			-	

X = applies to sample
-- = barren of foraminifera
L = low
M = moderate
H = high
P/F = poor or fair
G/E = good or excellent
B = bimodal
All foraminiferal abundance graphs use the same scale.

Sand
Clay
Clayey sand
Sandy clay
Clay with sand laminae
Sand with clay laminae
Interbedded clay and sand

SAMPLE	DEPTH (ft/in)	COMMENTS	ENVIRONMENT
CE10-36	2'2"	Barren of all biotics except shell fragments.	[beach/chenier]
CE10-99	3'3"	"	"
CE10-125	4'1"	"	"
CE10-146	4'9.5"	Very poor preservation except 5 agglutinated forams. Mixed gulf and marsh taxa; probably indicates washover of wave-reworked gulf into marsh or mudflat. Or, could be marsh forms transported into nearshore gulf.	marsh/mudflat
CE10-267	8'9"	Appear reworked, except 1 agglutinated foram; Evidence of fluvial influence (Cretaceous foram and radiolarian due to erosion of upstream deposits).	"
CE10-295	9'8"	Orange, small, poorly preserved.	"
CE10-330	10'10"	" w/ many forams pyritized	"
CE10-368	12'1"	Very poor preservation and low abundance; 1 charophyte. Still mix of gulf fauna and fluvial indicators.	"
CE10-394	12'11"	Low to moderate diversity, but several "rare" gulf taxa. Orange w/ some very small forams.	"
CE10-439	14'5"	Very diverse, gulf assemblage but w/ strong fluvial influence (17 Cretaceous radiolarians plus one Cret. planktic foram).	gulf
CE10-483	15'10"	Small, sparse but quite diverse assemblage. Orange.	"
CE10-522	17'1.5"	Barren of all biotics. Possibly missing sandier of two samples?	[marsh?]
CE10-525	17'2.5"	Moderate diversity assemblage w/ a few gulf taxa. This could be the second sample (see CE10-522).	gulf
CE10-561	18'5"	Poor preservation. Reworked gulf or lower bay assemblage. Ten radiolarians.	gulf or lower bay
CE10-593	19'5.5"	Reworked, low diversity bay assemblage w/ 12 Cretaceous forms. Very sparse. Appears to be washover of well-worn bay fauna into non-marine environment (marsh, etc.).	marsh?
CE10-625	20'6"	High diversity. Small forams and many E. sp. cf. matagordanum. Reworked component in otherwise well preserved assemblage.	lower bay or gulf

		Probably stressed gulf environ.	
CE10-658	21'7"	As above, but w/-out the reworked component.	"
CE10-688	22'7"	"	"
CE10-716	23'6"	"	"
CE10-753	24'8.5"	Mod. to low diversity, low abundance. Fair preservation w/ some indication of reworking or high energy. Bay or "beach" assemblage.	bay or beach/inlet
CE10-793	26'	"	"
CE10-826	27'1"	"	"
CE10-839	27'6.5"	Moderate diversity, gulf assemblage, but w/ no "rare" gulf spp.	lower bay / gulf
CE10-876	28'9"	High diversity, gulf assemblage, but w/ no "rare" gulf spp. Good preservation.	"
CE10-917	30'1"	"	"
CE10-950	31'4"	Very high diversity (19). Several rare gulf spp.	gulf
CE10-987	32'4.5"	High diversity. Orange.	"
CE101024	33'7"	"	"
CE101086	35'7.5"	As above, but w/ many juveniles. Orange, but good preservation. Must be below wave-base.	"
CE101123	36'10"	"	"
CE101161	38'1"	High diversity. No rare gulf. One Ammotium.	lower bay / gulf
CE101191	39'1"	As above, but no agglut.	"
CE101238	40'7.5"	"	"
CE101270	41'8"	"	"
CE101300	42'8"	Bay assemblage plus a few miliolids. Mod. diversity.	bay
CE101334	43'9"	Bay assemblage. Sample has coarse fraction- bivalves.	bay
CE101372	45'	Bay assemblage plus oysters.	bay
CE101412	46'4"	Bay assemblage plus large bivalves (coarse fraction).	bay
CE101528	50'1.5"	Bay assemblage.	bay
CE101565	51'4"	Bay assemblage but no echinoids or bryozoans. Low abundance (< 100 forams picked). This suggests low marsh (washover of forams into nearby marshy area).	low marsh

CE101605	52'8"	As above, w/ common, pyritized diatoms. Very few forams.	"
CE101650	54'1.5"	Abundant, small forams. Very low diversity. Ammonia > Elphidium. Brackish assemblage w/ little gulf influence.	brackish bay or low marsh
CE101690	55'5.5"	Low abundance.	"
CE101728	56'8.5"	Barren of all biotics. Woody debris and absence of forams suggest brackish to fresh marsh.	[marsh]
CE101836	60'3"	Very few forams (~3). "Sandy" looking grains, very roughly resemble foram shapes. Could be gypsum-coated forams as mentioned in the Galveston Bay book. Need to see slide again.	marsh (low salinity)
CE101872	61'5"	"	"
CE101905	62'6"	Barren of forams. Frequent diatoms.	"
CE101939	63'7.5"	As above but rare diatoms.	"
CE101988	65'2.5"	Less than 20 forams.	"
CE102031	66'7.5"	One Ammonia parkinsoniana. Frequent diatoms	"
CE102066	67'9.5"	Barren of all biotics.	-
CE102093	68'8"	"	-
CE102126	69'9"	"	-
CE102159	70'10"	"	-
CE102210	72'6"	"	-

Note: samples with environmental interpretations given in [ ] are barren of foraminifera and other biotics; Interpretations of these samples are based only on lithology. Otherwise, interpretations given are based on fauna (taxa- forams and other; abundance; diversity; and preservation). Also, lower bay assemblage is very difficult to distinguish from "gulf" (due to proximity); Brackish marsh and brackish lake also have similar assemblages, as do saline marsh (low marsh) and tidal mudflat.

***** DENDROGRAM *****

DERIVED FROM COSINE THETA

Input file: coresb.txt (covers BEG Coastal Erosion cores CE7 & CE10).

<u>Variables:</u> *Ammonia parkinsoniana*; *Elphidium gunteri*; *E. discoidale*; *E. mexicanum*; *E.* sp. cf. *matagordanum*; *E.* sp. cf. *poeyanum*; juveniles (rotalids); *Palmerinella palmerae*; *Buccella hannai*; gulf taxa; total miliolids.

The "total miliolid" category includes: *Quinqueloculina compta*, *Q. seminulum*, *Q. funafutiensis*, *Q. lamarckiana*, *Quinqueloculina* spp., *Massilina peruviana*, *Triloculina oblonga*, *Triloculina* spp., misc. miliolids, and miliolid fragments. *Buliminella elegantissima*, *Brizalina lowmani*, *Brizalina stiatula*, *Fissurina* sp., *Nonionella atlantica*, *Discorbis* spp., and *Hanzawaia concentrica* are lumped in the "gulf taxa" category. Species with mean abundance < 1%, besides those in the "gulf taxa" or "miliolids" categories, are excluded from this run. All core samples containing foraminifera are included in this run.

NUMBER OF INDIVIDUALS = 51 NUMBER OF VARIABLES = 11

COPHENETIC CORRELATION COEFFICIENT = .805969

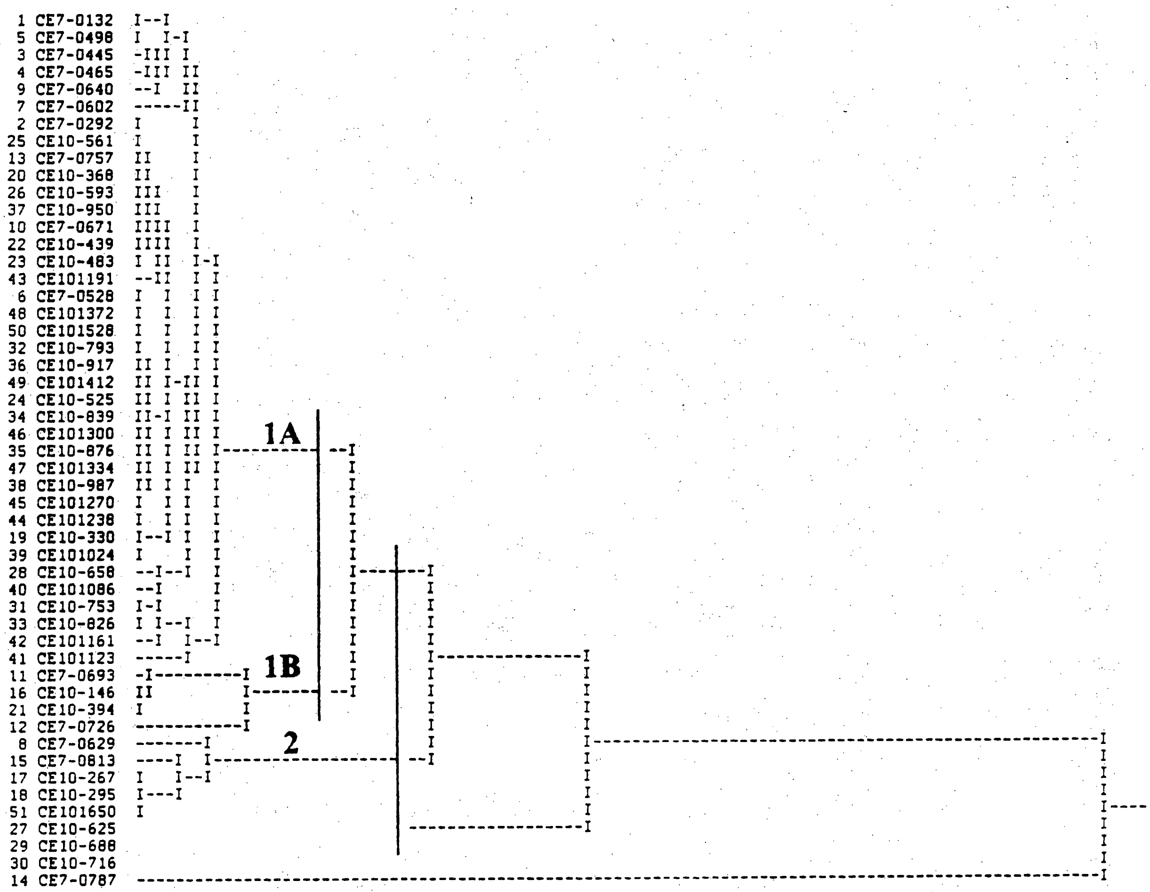

***** DENDROGRAM *****
DERIVED FROM COSINE THETA

Input file: coresa.txt (covers BEG Coastal Erosion cores CE7 & CE10). Excludes variables w/ mean abundance < 1%. All core samples containing foraminifera are included in this run.

Variables:
Ammonia parkinsoniana; *Elphidium gunteri*; *E. discoidale*; *E. mexicanum*; *E.* sp. cf. *matagordanum*; *E.* sp. cf. *poeyanum*; juveniles (rotalids); *Palmerinella palmerae*; *Buccella hannai*; *Quinqueloculina seminulum*.

NUMBER OF INDIVIDUALS = 51 NUMBER OF VARIABLES = 10
COPHENETIC CORRELATION COEFFICIENT = .805319

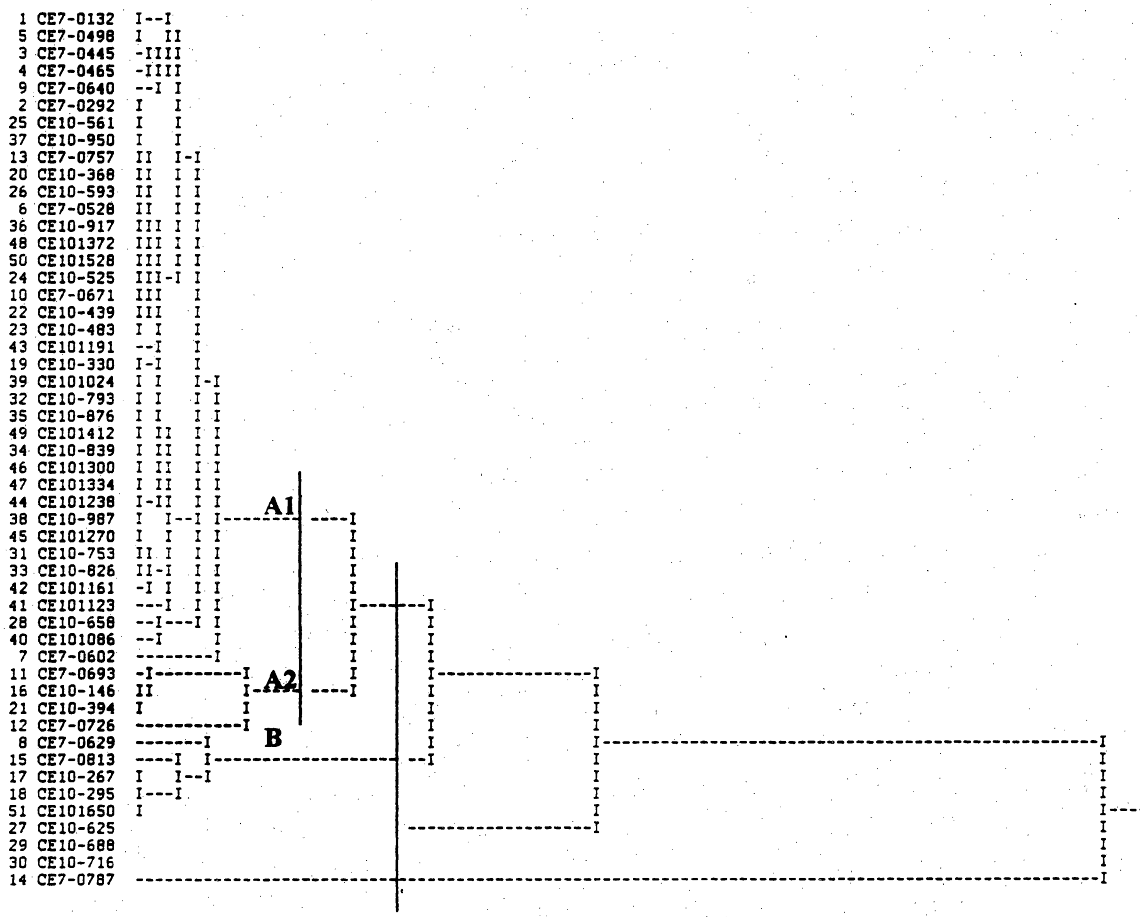

Comparison of Biofacies and Cluster Groups

Order: Compiled Biofacies / Sabine Lake Biofacies

I. Marsh #2 / Tidal-Mudflat / Agglutinated #1
Agglutinated spp., *Ammonia, E. gunteri* [*E. poeyanum, Palmerinella palmerae*]
Cluster Groups: B and 2

II. Marsh #3 / Brackish / Agglutinated #2
Agglutinated spp., *Ammonia, E. gunteri, E. discoidale, E. poeyanum, E. matagordanum, P. palmerae*
Cluster Groups: A2 and 1B

III. Middle Bay / Ammonia-Elphidium
Ammonia, E. gunteri, E. discoidale, E. poeyanum, E. matagordanum, Ephidium spp., *P. palmerae, Brizalina* spp., *B. elegantissima,* miliolids (mostly *Q. seminulum, Q. compta, Q. rhodiensis*), [*E. kugleri, Buccella hannai*]
Cluster Groups: C and 3

IV. Lower Bay-Bay Mouth / Beach-Tidal Inlet / Shoreface-Gulf / Miliolid
Ammonia, E. gunteri, E. discoidale, E. poeyanum, E. matagordanum, Ephidium spp., *Brizalina* spp., *B. elegantissima, Buccella hannai,* miliolids (*Q. lamarckiana, Q. compta, Q. seminulum, Q. funafutiensis*, etc.), [*E. mexicanum, Hanzawaia, Discorbis, Nonionella atlantica, Fissurina* sp.]
Cluster Groups: A1 and 1A

Addendum 5. Radiocarbon Analysis Report

RADIOCARBON ANALYSIS REPORT
Radiocarbon Laboratory
The University of Texas
Balcones Research Center, Austin, TX 78712

Sample: Tx- 8398

<u>Submitter</u>: Morton, Robert A.
Bureau of Economic Geology
University of Texas
J.J. Pickle Research Campus
Austin, TX 78712

<u>Bill to</u>: Morton, Robert A.
Bureau of Economic Geology
University of Texas
J.J. Pickle Research Campus
Austin, TX 78712

DATA FROM SAMPLE GREEN SHEET
PLEASE CHECK, AND CORRECT IF NECESSARY

1. **<u>Nature of sample</u>:** Wood fragments and clay

2. **<u>Submitter's catalogue number</u>:** BEG SLV-1 13.85-15.0

3. **<u>Name and number of site</u>:** Sabine Lake vibracore

4. **<u>Descriptive location of site</u>:**
   Mouth of Sabine River, East Pass of the Sabine delta

5. **<u>Latitude</u>:** 29°59.50'N **<u>Longitude</u>:** 093°45.92'W

   Country: USA **State/Province:** Texas **County:** Jefferson

6. **<u>Provenience of sample within site</u>:**
   Ca. 13.27-14.02 m below sea level

7. **<u>Collector and date</u>:** R. Morton, 7 Oct 1994

8. **<u>Context</u>:**
   Sample came from Holocene deposits

9. **<u>Previous radiocarbon dates</u>:**
   None

10. **<u>Variables affecting validity of date</u>:**
    Burrowing, sediment reworking

11. **<u>Significance of sample</u>:**
    Determine age of Sabine delta

12. **<u>Estimated sample age</u>:** < 15,000 BP

Radiocarbon Laboratory, The University of Texas at Austin
Analysis Results

TX- 8398   Run Number: II-581   Run Date: 08-23-1995

Submitter: Morton, Robert A.
Submitter's catalogue number: BEG SLV-1 13.85-15.0
Site name: Sabine Lake vibracore
Sample type: Wood
Submitter's age estimate: < 15,000 BP

Counting method: Liquid scillintilation, using one of four Beckman counters
Total counting time: 5644 minutes   Total counts: 49261
$\delta^{13}C$ determination: -26.9°/∘∘

$$\text{Rate of unknown} = \frac{\text{avg. counts/minute - background}}{\text{grams carbon in sample}}$$

$$= \frac{8.728 \pm 0.039 - 6.081 \pm 0.034}{0.678} = 3.904 \pm 0.076 \text{ c.p.m./gram C}$$

$$\text{Percent Modern Carbon} = \frac{\text{unknown rate}}{\text{NBS standard rate}} = \frac{3.904 \pm 0.076}{9.341 \pm 0.024} = 41.794 \pm 0.37\ \%$$

$$\text{Age} = 8033 \ln \frac{\text{std. rate}}{\text{unk. rate}} \pm 8033 \left[\left[\frac{\text{std. error}}{\text{std. rate}}\right]^2 + \left[\frac{\text{unk. error}}{\text{unk. rate}}\right]^2 \right]^{1/2}$$

$$= 8033 \ln \frac{9.341}{3.904} \pm 8033 \left[\left[\frac{0.024}{9.341}\right]^2 + \left[\frac{0.076}{3.904}\right]^2 \right]^{1/2}$$

= 7008 ± 158 years B.P. (rounded to nearest 10: 7010 ± 160)

$\delta^{14}C$ = -582.1 ± 3.7°/∘∘

Corrections for $\delta^{13}C$

Rate of unknown = 3.919 ± 0.076 c.p.m./gram C

Percent Modern Carbon = 41.955 ± 0.373%

Age = 6977 ± 157 years B.P. (rounded to nearest 10: 6980 ± 160)

$\delta^{14}C$ = -580.5 ± 3.7°/∘∘

RADIOCARBON ANALYSIS REPORT
Radiocarbon Laboratory
The University of Texas
Balcones Research Center, Austin, TX 78712

Sample: Tx- 8399

Submitter: Morton, Robert A.
Bureau of Economic Geology
University of Texas
J.J. Pickle Research Campus
Austin, TX 78712

Bill to: Morton, Robert A.
Bureau of Economic Geology
University of Texas
J.J. Pickle Research Campus
Austin, TX 78712

DATA FROM SAMPLE GREEN SHEET
PLEASE CHECK, AND CORRECT IF NECESSARY

1. **Nature of sample**: Peat

2. **Submitter's catalogue number**: BEG SLV-5 11.2-11.4

3. **Name and number of site**: Sabine Lake vibracore

4. **Descriptive location of site**:
Mouth of Sabine River, East Pass of the Sabine delta

5. **Latitude**: 29°59.50'N **Longitude**: 093°45.92'W

Country: USA **State/Province:** Texas **County:** Jefferson

6. **Provenience of sample within site**:
Ca. 7.98-8.04 m below sea level

7. **Collector and date**: R. Morton, 8 Oct 1994

8. **Context**:
Sample came from Holocene deposits

9. **Previous radiocarbon dates**:
None

10. **Variables affecting validity of date**:
Burrowing, sediment reworking

11. **Significance of sample**:
Determine age of Sabine delta

12. **Estimated sample age**: < 15,000 BP

Radiocarbon Laboratory, The University of Texas at Austin
Analysis Results

TX- 8399 Run Number: 1570 Run Date: 08-23-1995

Submitter: Morton, Robert A.
Submitter's catalogue number: BEG SLV-5 11.2-11.4
Site name: Sabine Lake vibracore
Sample type: Peat
Submitter's age estimate: < 15,000 BP

Counting method: Liquid scillintilation, using one of four Beckman counters
Total counting time: 5500 minutes Total counts: 63351
$\delta^{13}C$ determination: -27.3°/₀₀

$$\text{Rate of unknown} = \frac{\text{avg. counts/minute - background}}{\text{grams carbon in sample}}$$

$$= \frac{11.518 \pm 0.046 - 5.841 \pm 0.033}{1.826} = 3.109 \pm 0.031 \text{ c.p.m./gram}$$

$$\text{Percent Modern Carbon} = \frac{\text{unknown rate}}{\text{NBS standard rate}} = \frac{3.109 \pm 0.031}{7.220 \pm 0.021} = 43.061 \pm 0.18($$

$$\text{Age} = 8033 \ln \frac{\text{std. rate}}{\text{unk. rate}} \pm 8033 \left[\left[\frac{\text{std. error}}{\text{std. rate}}\right]^2 + \left[\frac{\text{unk. error}}{\text{unk. rate}}\right]^2 \right]^{1/2}$$

$$= 8033 \ln \frac{7.220}{3.109} \pm 8033 \left[\left[\frac{0.021}{7.220}\right]^2 + \left[\frac{0.031}{3.109}\right]^2 \right]^{1/2}$$

= 6768 ± 83 years B.P. (rounded to nearest 10: 6770 ± 80)

$\delta^{14}C$ = -569.4 ± 1.8°/₀₀

Corrections for $\delta^{13}C$

Rate of unknown = 3.123 ± 0.031 c.p.m./gram C

Percent Modern Carbon = 43.255 ± 0.180%

Age = 6732 ± 83 years B.P. (rounded to nearest 10: 6730 ± 80)

$\delta^{14}C$ = -567.5 ± 1.8°/₀₀

RADIOCARBON ANALYSIS REPORT
Radiocarbon Laboratory
The University of Texas
Balcones Research Center, Austin, TX 78712

Sample: Tx- 8400

Submitter: Morton, Robert A.
Bureau of Economic Geology
University of Texas
J.J. Pickle Research Campus
Austin, TX 78712

Bill to: Morton, Robert A.
Bureau of Economic Geology
University of Texas
J.J. Pickle Research Campus
Austin, TX 78712

DATA FROM SAMPLE GREEN SHEET
PLEASE CHECK, AND CORRECT IF NECESSARY

1. **Nature of sample:** Organic mud and peat

2. **Submitter's catalogue number:** BEG CE-6 10.3-11.0

3. **Name and number of site:** Auger core

4. **Descriptive location of site:**
   Beach at Sea Rim State Park

5. **Latitude:** 29°40'02"N **Longitude:** 094°04'23"W

   Country: USA **State/Province:** Texas **County:** Jefferson

6. **Provenience of sample within site:**
   Ca. 1.91-2.13 m below sea level

7. **Collector and date:** R. Morton, 4 Jun 1993

8. **Context:**
   Sample came from Holocene deposits

9. **Previous radiocarbon dates:**
   None

10. **Variables affecting validity of date:**
    Burrowing, sediment reworking

11. **Significance of sample:**
    Determine time of coastal plain aggradation

12. **Estimated sample age:** < 10,000 BP

Radiocarbon Laboratory, The University of Texas at Austin
Analysis Results

TX- 8400 Run Number: 1577 Run Date: 09-08-1995

Submitter: Morton, Robert A.
Submitter's catalogue number: BEG CE-6 10.3-11.0
Site name: Auger core
Sample type: Organic matter
Submitter's age estimate: < 10,000 BP

Counting method: Liquid scillintilation, using one of four Beckman counters
Total counting time: 3900 minutes Total counts: 47130
$\delta^{13}C$ determination: -18.0°/∘∘

$$\text{Rate of unknown} = \frac{\text{avg. counts/minute - background}}{\text{grams carbon in sample}}$$

$$= \frac{12.085 \pm 0.056 - 5.867 \pm 0.033}{1.400} = 4.441 \pm 0.046 \text{ c.p.m./gram}$$

$$\text{Percent Modern Carbon} = \frac{\text{unknown rate}}{\text{NBS standard rate}} = \frac{4.441 \pm 0.046}{7.229 \pm 0.021} = 61.433 \pm 0.25$$

$$\text{Age} = 8033 \ln \frac{\text{std. rate}}{\text{unk. rate}} \pm 8033 \left[\left[\frac{\text{std. error}}{\text{std. rate}}\right]^2 + \left[\frac{\text{unk. error}}{\text{unk. rate}}\right]^2 \right]^{1/2}$$

$$= 8033 \ln \frac{7.229}{4.441} \pm 8033 \left[\left[\frac{0.021}{7.229}\right]^2 + \left[\frac{0.046}{4.441}\right]^2 \right]^{1/2}$$

= 3914 ± 86 years B.P. (rounded to nearest 10: 3910 ± 90)

$\delta^{14}C$ = -385.7 ± 2.6°/∘∘

Corrections for $\delta^{13}C$

Rate of unknown = 4.379 ± 0.046 c.p.m./gram C

Percent Modern Carbon = 60.575 ± 0.252%

Age = 4027 ± 88 years B.P. (rounded to nearest 10: 4030 ± 90)

$\delta^{14}C$ = -394.2 ± 2.5°/∘∘

RADIOCARBON ANALYSIS REPORT
Radiocarbon Laboratory
The University of Texas
Balcones Research Center, Austin, TX 78712

Sample: Tx- 8401

Submitter: Morton, Robert A.
Bureau of Economic Geology
University of Texas
J.J. Pickle Research Campus
Austin, TX 78712

Bill to: Morton, Robert A.
Bureau of Economic Geology
University of Texas
J.J. Pickle Research Campus
Austin, TX 78712

DATA FROM SAMPLE GREEN SHEET
PLEASE CHECK, AND CORRECT IF NECESSARY

1. **Nature of sample**: Shell fragments

2. **Submitter's catalogue number**: BEG CE-8 10.9-11.3

3. **Name and number of site**: Auger core

4. **Descriptive location of site**:
   3.2 km W of Sabine Pass, Highway 87

5. **Latitude**: 29°42'47"N **Longitude**: 093°54'45"W

   Country: USA **State/Province:** Texas **County:** Jefferson

6. **Provenience of sample within site**:
   Ca. 1.18-1.31 m below sea level

7. **Collector and date**: R. Morton, 4 Jun 1993

8. **Context**:
   Sample came from Holocene deposits

9. **Previous radiocarbon dates**:
   See Gould & McFarlan, 1959, GCAGS, v. 9

10. **Variables affecting validity of date**:
    Burrowing, sediment reworking

11. **Significance of sample**:
    Determine time of beach ridge progradation

12. **Estimated sample age**: < 10,000 BP

Radiocarbon Laboratory, The University of Texas at Austin
Analysis Results

TX- 8401 Run Number: II-583 Run Date: 08-29-1995

Submitter: Morton, Robert A.
Submitter's catalogue number: BEG CE-8 10.9-11.3
Site name: Auger core
Sample type: Shell
Submitter's age estimate: < 10,000 BP

Counting method: Liquid scillintilation, using one of four Beckman counters
Total counting time: 2767 minutes Total counts: 43636
$\delta^{13}C$ determination: -0.8°/₀₀

$$\text{Rate of unknown} = \frac{\text{avg. counts/minute - background}}{\text{grams carbon in sample}}$$

$$= \frac{15.770 \pm 0.075 - 6.123 \pm 0.033}{1.465} = 6.585 \pm 0.056 \text{ c.p.m./gram}$$

$$\text{Percent Modern Carbon} = \frac{\text{unknown rate}}{\text{NBS standard rate}} = \frac{6.585 \pm 0.056}{9.350 \pm 0.024} = 70.428 \pm 0.43$$

$$\text{Age} = 8033 \ln \frac{\text{std. rate}}{\text{unk. rate}} \pm 8033 \left[\left[\frac{\text{std. error}}{\text{std. rate}}\right]^2 + \left[\frac{\text{unk. error}}{\text{unk. rate}}\right]^2 \right]^{1/2}$$

$$= 8033 \ln \frac{9.350}{6.585} \pm 8033 \left[\left[\frac{0.024}{9.350}\right]^2 + \left[\frac{0.056}{6.585}\right]^2 \right]^{1/2}$$

= 2816 ± 71 years B.P. (rounded to nearest 10: 2820 ± 70)

$\delta^{14}C$ = -295.7 ± 4.3°/₀₀

Corrections for $\delta^{13}C$

Rate of unknown = 6.266 ± 0.056 c.p.m./gram C

Percent Modern Carbon = 67.016 ± 0.417%

Age = 3215 ± 75 years B.P. (rounded to nearest 10: 3220 ± 80)

$\delta^{14}C$ = -329.8 ± 4.2°/₀₀

RADIOCARBON ANALYSIS REPORT
Radiocarbon Laboratory
The University of Texas
Balcones Research Center, Austin, TX 78712

Sample: Tx- 8402

Submitter: Morton, Robert A.
Bureau of Economic Geology
University of Texas
J.J. Pickle Research Campus
Austin, TX 78712

Bill to: Morton, Robert A.
Bureau of Economic Geology
University of Texas
J.J. Pickle Research Campus
Austin, TX 78712

DATA FROM SAMPLE GREEN SHEET
PLEASE CHECK, AND CORRECT IF NECESSARY

1. **Nature of sample**: Shell fragments (oysters, ^Mulinea^)
2. **Submitter's catalogue number**: BEG CE-~~8~~ 9 29.2-29.3
3. **Name and number of site**: Auger core
4. **Descriptive location of site**: Sabine Pass State Park
5. **Latitude**: 29°43'58"N **Longitude**: 093°52'34"W

   Country: USA **State/Province:** Texas **County:** Jefferson
6. **Provenience of sample within site**: Ca. 7.07-7.10 m below sea level
7. **Collector and date**: R. Morton, 4 Jun 1993
8. **Context**: Sample came from Holocene valley fill
9. **Previous radiocarbon dates**: None
10. **Variables affecting validity of date**: Burrowing, sediment reworking
11. **Significance of sample**: Determine age of Holocene fill
12. **Estimated sample age**: < 10,000 BP

Radiocarbon Laboratory, The University of Texas at Austin
Analysis Results

TX- 8402 Run Number: II-587 Run Date: 09-06-1995

Submitter: Morton, Robert A.
Submitter's catalogue number: BEG CE-8 29.2-29.3
Site name: Auger core
Sample type: Shell
Submitter's age estimate: < 10,000 BP

Counting method: Liquid scillintilation, using one of four Beckman counters
Total counting time: 2804 minutes Total counts: 53321
$\delta^{13}C$ determination: -1.6°/∘∘

$$\text{Rate of unknown} = \frac{\text{avg. counts/minute - background}}{\text{grams carbon in sample}}$$

$$= \frac{19.016 \pm 0.082 - 6.210 \pm 0.034}{2.411} = 5.311 \pm 0.037 \text{ c.p.m./gram C}$$

$$\text{Percent Modern Carbon} = \frac{\text{unknown rate}}{\text{NBS standard rate}} = \frac{5.311 \pm 0.037}{9.328 \pm 0.024} = 56.936 \pm 0.29\%$$

$$\text{Age} = 8033 \ln \frac{\text{std. rate}}{\text{unk. rate}} \pm 8033 \left[\left[\frac{\text{std. error}}{\text{std. rate}}\right]^2 + \left[\frac{\text{unk. error}}{\text{unk. rate}}\right]^2 \right]^{1/2}$$

$$= 8033 \ln \frac{9.328}{5.311} \pm 8033 \left[\left[\frac{0.024}{9.328}\right]^2 + \left[\frac{0.037}{5.311}\right]^2 \right]^{1/2}$$

= 4525 ± 60 years B.P. (rounded to nearest 10: 4530 ± 60)

$\delta^{14}C$ = -430.6 ± 3.0°/∘∘

Corrections for $\delta^{13}C$

Rate of unknown = 5.062 ± 0.037 c.p.m./gram C

Percent Modern Carbon = 54.267 ± 0.292%

Age = 4910 ± 62 years B.P. (rounded to nearest 10: 4910 ± 60)

$\delta^{14}C$ = -457.3 ± 2.9°/∘∘

RADIOCARBON ANALYSIS REPORT
Radiocarbon Laboratory
The University of Texas
Balcones Research Center, Austin, TX 78712

Sample: Tx- 8403

Submitter: Morton, Robert A.
Bureau of Economic Geology
University of Texas
J.J. Pickle Research Campus
Austin, TX 78712

Bill to: Morton, Robert A.
Bureau of Economic Geology
University of Texas
J.J. Pickle Research Campus
Austin, TX 78712

DATA FROM SAMPLE GREEN SHEET
PLEASE CHECK, AND CORRECT IF NECESSARY

1. **Nature of sample**: Oyster shell

2. **Submitter's catalogue number**: BEG CE-10 46.2-47.0

3. **Name and number of site**: Auger core

4. **Descriptive location of site**:
Highway 87, Sabine Pass

5. **Latitude**: 29°43'49"N **Longitude**: 093°53'02"W

Country: USA **State/Province:** Texas **County:** Jefferson

6. **Provenience of sample within site**:
Ca. 12.86-13.11 m below sea level

7. **Collector and date**: R. Morton, 5 Jun 1993

8. **Context**:
Sample came from Holocene valley fill

9. **Previous radiocarbon dates**:
None

10. **Variables affecting validity of date**:
Burrowing, sediment reworking

11. **Significance of sample**:
Determine age of valley fill

12. **Estimated sample age**: < 15,000 BP

Radiocarbon Laboratory, The University of Texas at Austin
Analysis Results

TX- 8403 Run Number: 1574 Run Date: 09-02-1995

Submitter: Morton, Robert A.
Submitter's catalogue number: BEG CE-10 46.2-47.0
Site name: Auger core
Sample type: Shell
Submitter's age estimate: < 15,000 BP

Counting method: Liquid scillintilation, using one of four Beckman counters
Total counting time: 2700 minutes Total counts: 45459
$\delta^{13}C$ determination: -1.2°/oo

$$\text{Rate of unknown} = \frac{\text{avg. counts/minute - background}}{\text{grams carbon in sample}}$$

$$= \frac{16.837 \pm 0.079 - 5.868 \pm 0.033}{2.347} = 4.674 \pm 0.036 \text{ c.p.m./gram}$$

$$\text{Percent Modern Carbon} = \frac{\text{unknown rate}}{\text{NBS standard rate}} = \frac{4.674 \pm 0.036}{7.230 \pm 0.021} = 64.647 \pm 0.227$$

$$\text{Age} = 8033 \ln \frac{\text{std. rate}}{\text{unk. rate}} \pm 8033 \left[\left[\frac{\text{std. error}}{\text{std. rate}}\right]^2 + \left[\frac{\text{unk. error}}{\text{unk. rate}}\right]^2 \right]^{1/2}$$

$$= 8033 \ln \frac{7.230}{4.674} \pm 8033 \left[\left[\frac{0.021}{7.230}\right]^2 + \left[\frac{0.036}{4.674}\right]^2 \right]^{1/2}$$

= 3504 ± 66 years B.P. (rounded to nearest 10: 3500 ± 70)

$\delta^{14}C$ = -353.5 ± 2.3°/oo

Corrections for $\delta^{13}C$

Rate of unknown = 4.452 ± 0.036 c.p.m./gram C

Percent Modern Carbon = 61.577 ± 0.221%

Age = 3895 ± 69 years B.P. (rounded to nearest 10: 3900 ± 70)

$\delta^{14}C$ = -384.2 ± 2.2°/oo

RADIOCARBON ANALYSIS REPORT
Radiocarbon Laboratory
The University of Texas
Balcones Research Center, Austin, TX 78712

Sample: Tx- 8404

Submitter: Morton, Robert A.
Bureau of Economic Geology
University of Texas
J.J. Pickle Research Campus
Austin, TX 78712

Bill to: Morton, Robert A.
Bureau of Economic Geology
University of Texas
J.J. Pickle Research Campus
Austin, TX 78712

DATA FROM SAMPLE GREEN SHEET
PLEASE CHECK, AND CORRECT IF NECESSARY

1. **Nature of sample**: Wood

2. **Submitter's catalogue number**: BEG CE-10 72.3-72.5

3. **Name and number of site**: Auger core

4. **Descriptive location of site**:
Highway 87, Sabine Pass

5. **Latitude**: 29°43'49"N **Longitude**: 093°53'02"W

   Country: USA **State/Province:** Texas **County:** Jefferson

6. **Provenience of sample within site**:
Ca. 20.82-20.88 m below sea level

7. **Collector and date**: R. Morton, 5 Jun 1993

8. **Context**:
Sample came from late Pleistocene or Holocene valley fill (Deweyville Formation?)

9. **Previous radiocarbon dates**:
None

10. **Variables affecting validity of date**:
Burrowing, sediment reworking

11. **Significance of sample**:
Determine age of valley fill and of a possible fluvial terrace

12. **Estimated sample age:** < 25,000 BP

Radiocarbon Laboratory, The University of Texas at Austin
Analysis Results

TX- 8404 Run Number: 972c Run Date: 08-23-1995

Submitter: Morton, Robert A.
Submitter's catalogue number: BEG CE-10 72.3-72.5
Site name: Auger core
Sample type: Wood
Submitter's age estimate: < 25,000 BP

Counting method: Liquid scillintilation, using one of four Beckman counters
Total counting time: 5500 minutes Total counts: 53198
$\delta^{13}C$ determination: -25.5°/∘∘

$$\text{Rate of unknown} = \frac{\text{avg. counts/minute - background}}{\text{grams carbon in sample}}$$

$$= \frac{9.672 \pm 0.042 - 6.957 \pm 0.036}{0.939} = 2.891 \pm 0.059 \text{ c.p.m./gram C}$$

$$\text{Percent Modern Carbon} = \frac{\text{unknown rate}}{\text{NBS standard rate}} = \frac{2.891 \pm 0.059}{8.834 \pm 0.021} = 32.726 \pm 0.252\%$$

$$\text{Age} = 8033 \ln \frac{\text{std. rate}}{\text{unk. rate}} \pm 8033 \left[\left[\frac{\text{std. error}}{\text{std. rate}}\right]^2 + \left[\frac{\text{unk. error}}{\text{unk. rate}}\right]^2 \right]^{1/2}$$

$$= 8033 \ln \frac{8.834}{2.891} \pm 8033 \left[\left[\frac{0.021}{8.834}\right]^2 + \left[\frac{0.059}{2.891}\right]^2 \right]^{1/2}$$

= 8973 ± 165 years B.P. (rounded to nearest 10: 8970 ± 170)

$\delta^{14}C$ = -672.7 ± 2.5°/∘∘

Corrections for $\delta^{13}C$

Rate of unknown = 2.894 ± 0.059 c.p.m./gram C

Percent Modern Carbon = 32.760 ± 0.252%

Age = 8965 ± 165 years B.P. (rounded to nearest 10: 8970 ± 170)

$\delta^{14}C$ = -672.4 ± 2.5°/∘∘

RADIOCARBON ANALYSIS REPORT
Radiocarbon Laboratory
The University of Texas
Balcones Research Center, Austin, TX 78712

Sample: Tx- 8415

<u>Submitter</u>: Morton, Robert A.
Bureau of Economic Geology
University of Texas
J.J. Pickle Research Campus
Austin, TX 78712

<u>Bill to</u>: Morton, Robert A.
Bureau of Economic Geology
University of Texas
J.J. Pickle Research Campus
Austin, TX 78712

DATA FROM SAMPLE GREEN SHEET
PLEASE CHECK, AND CORRECT IF NECESSARY

1. **Nature of sample:** Organic clay

2. **Submitter's catalogue number:** BEG CE-11 16.4-17.6

3. **Name and number of site:** Auger core

4. **Descriptive location of site:**
1.8 km N of Sabine Pass, Highway 87

5. **Latitude:** 29°44'21"N **Longitude:** 093°54'20"W

   Country: USA **State/Province:** Texas **County:** Jefferson

6. **Provenience of sample within site:**
Ca. 4.08-4.45 m below sea level

7. **Collector and date:** R. Morton, 8 Jun 1993

8. **Context:**
Sample came from Holocene valley fill

9. **Previous radiocarbon dates:**
None

10. **Variables affecting validity of date:**
Burrowing, sediment reworking

11. **Significance of sample:**
Determine age of valley fill

12. **Estimated sample age:** < 10,000 BP

Radiocarbon Laboratory, The University of Texas at Austin
Analysis Results

TX- 8415 Run Number: II-588 Run Date: 09-08-1995

Submitter: Morton, Robert A.
Submitter's catalogue number: BEG CE-11 16.4-17.6
Site name: Auger core
Sample type: Organic matter
Submitter's age estimate: < 10,000 BP

Counting method: Liquid scillintilation, using one of four Beckman counters
Total counting time: 4000 minutes Total counts: 60752
$\delta^{13}C$ determination: -25.1°/∘∘

$$\text{Rate of unknown} = \frac{\text{avg. counts/minute - background}}{\text{grams carbon in sample}}$$

$$= \frac{15.188 \pm 0.062 - 6.210 \pm 0.034}{1.661} = 5.405 \pm 0.043 \text{ c.p.m./gram C}$$

$$\text{Percent Modern Carbon} = \frac{\text{unknown rate}}{\text{NBS standard rate}} = \frac{5.405 \pm 0.043}{9.333 \pm 0.024} = 57.913 \pm 0.323\%$$

$$\text{Age} = 8033 \ln \frac{\text{std. rate}}{\text{unk. rate}} \pm 8033 \left[\left[\frac{\text{std. error}}{\text{std. rate}}\right]^2 + \left[\frac{\text{unk. error}}{\text{unk. rate}}\right]^2 \right]^{1/2}$$

$$= 8033 \ln \frac{9.333}{5.405} \pm 8033 \left[\left[\frac{0.024}{9.333}\right]^2 + \left[\frac{0.043}{5.405}\right]^2 \right]^{1/2}$$

= 4388 ± 67 years B.P. (rounded to nearest 10: 4390 ± 70)

$\delta^{14}C$ = -420.9 ± 3.2°/∘∘

Corrections for $\delta^{13}C$

Rate of unknown = 5.406 ± 0.043 c.p.m./gram C

Percent Modern Carbon = 57.923 ± 0.323%

Age = 4386 ± 67 years B.P. (rounded to nearest 10: 4390 ± 70)

$\delta^{14}C$ = -420.8 ± 3.2°/∘∘

Radiocarbon Laboratory, The University of Texas at Austin
Analysis Results

TX- 8415 Run Number: II-588 Run Date: 09-08-1995

Submitter: Morton, Robert A.
Submitter's catalogue number: BEG CE-11 16.4-17.6
Site name: Auger core
Sample type: Organic matter
Submitter's age estimate: < 10,000 BP

Counting method: Liquid scillintilation, using one of four Beckman counters
Total counting time: 4000 minutes Total counts: 60752
$\delta^{13}C$ determination: -25.1°/∘∘

$$\text{Rate of unknown} = \frac{\text{avg. counts/minute - background}}{\text{grams carbon in sample}}$$

$$= \frac{15.188 \pm 0.062 - 6.210 \pm 0.034}{1.661} = 5.405 \pm 0.043 \text{ c.p.m./gram}$$

$$\text{Percent Modern Carbon} = \frac{\text{unknown rate}}{\text{NBS standard rate}} = \frac{5.405 \pm 0.043}{9.333 \pm 0.024} = 57.913 \pm 0.32$$

$$\text{Age} = 8033 \ln \frac{\text{std. rate}}{\text{unk. rate}} \pm 8033 \left[\left[\frac{\text{std. error}}{\text{std. rate}}\right]^2 + \left[\frac{\text{unk. error}}{\text{unk. rate}}\right]^2 \right]^{1/2}$$

$$= 8033 \ln \frac{9.333}{5.405} \pm 8033 \left[\left[\frac{0.024}{9.333}\right]^2 + \left[\frac{0.043}{5.405}\right]^2 \right]^{1/2}$$

= 4388 ± 67 years B.P. (rounded to nearest 10: 4390 ± 70)

$\delta^{14}C$ = -420.9 ± 3.2°/∘∘

Corrections for $\delta^{13}C$

Rate of unknown = 5.406 ± 0.043 c.p.m./gram C

Percent Modern Carbon = 57.923 ± 0.323%

Age = 4386 ± 67 years B.P. (rounded to nearest 10: 4390 ± 70)

$\delta^{14}C$ = -420.8 ± 3.2°/∘∘

RADIOCARBON ANALYSIS REPORT
Radiocarbon Laboratory
The University of Texas
Balcones Research Center, Austin, TX 78712

Sample: Tx- 8405

Submitter: Morton, Robert A.
Bureau of Economic Geology
University of Texas
J.J. Pickle Research Campus
Austin, TX 78712

Bill to: Morton, Robert A.
Bureau of Economic Geology
University of Texas
J.J. Pickle Research Campus
Austin, TX 78712

DATA FROM SAMPLE GREEN SHEET
PLEASE CHECK, AND CORRECT IF NECESSARY

1. **Nature of sample**: Shell fragments (oysters, ^Mulinea^)
2. **Submitter's catalogue number**: BEG CE-11 24.0-25.5
3. **Name and number of site**: Auger core
4. **Descriptive location of site**:
   1.8 km N of Sabine Pass, Highway 87
5. **Latitude**: 29°44'21"N **Longitude**: 093°54'20"W

   Country: USA **State/Province:** Texas **County:** Jefferson
6. **Provenience of sample within site**:
   Ca. 6.40-6.86 m below sea level
7. **Collector and date**: R. Morton, 6 Jun 1993
8. **Context**:
   Sample came from Holocene valley fill
9. **Previous radiocarbon dates**:
   None
10. **Variables affecting validity of date**:
    Burrowing, sediment reworking
11. **Significance of sample**:
    Determine age of valley fill
12. **Estimated sample age**: < 10,000 BP

Radiocarbon Laboratory, The University of Texas at Austin
Analysis Results

TX- 8405 Run Number: 978c Run Date: 09-06-1995

Submitter: Morton, Robert A.
Submitter's catalogue number: BEG CE-11 24.0-25.5
Site name: Auger core
Sample type: Shell
Submitter's age estimate: < 10,000 BP

Counting method: Liquid scillintilation, using one of four Beckman counters
Total counting time: 2700 minutes Total counts: 50098
$\delta^{13}C$ determination: -1.4°/∘∘

$$\text{Rate of unknown} = \frac{\text{avg. counts/minute - background}}{\text{grams carbon in sample}}$$

$$= \frac{18.555 \pm 0.083 - 6.899 \pm 0.036}{2.400} = 4.857 \pm 0.038 \text{ c.p.m./gram C}$$

$$\text{Percent Modern Carbon} = \frac{\text{unknown rate}}{\text{NBS standard rate}} = \frac{4.857 \pm 0.038}{8.837 \pm 0.021} = 54.962 \pm 0.26$$

$$\text{Age} = 8033 \ln \frac{\text{std. rate}}{\text{unk. rate}} \pm 8033 \left[\left[\frac{\text{std. error}}{\text{std. rate}}\right]^2 + \left[\frac{\text{unk. error}}{\text{unk. rate}}\right]^2 \right]^{1/2}$$

$$= 8033 \ln \frac{8.837}{4.857} \pm 8033 \left[\left[\frac{0.021}{8.837}\right]^2 + \left[\frac{0.038}{4.857}\right]^2 \right]^{1/2}$$

= 4808 ± 66 years B.P. (rounded to nearest 10: 4810 ± 70)

$\delta^{14}C$ = -450.4 ± 2.6°/∘∘

Corrections for $\delta^{13}C$

Rate of unknown = 4.628 ± 0.038 c.p.m./gram C

Percent Modern Carbon = 52.371 ± 0.256%

Age = 5196 ± 69 years B.P. (rounded to nearest 10: 5200 ± 70)

$\delta^{14}C$ = -476.3 ± 2.6°/∘∘

RADIOCARBON ANALYSIS REPORT
Radiocarbon Laboratory
The University of Texas
Balcones Research Center, Austin, TX 78712

Sample: Tx- 8406

Submitter: Morton, Robert A.
Bureau of Economic Geology
University of Texas
J.J. Pickle Research Campus
Austin, TX 78712

Bill to: Morton, Robert A.
Bureau of Economic Geology
University of Texas
J.J. Pickle Research Campus
Austin, TX 78712

DATA FROM SAMPLE GREEN SHEET
PLEASE CHECK, AND CORRECT IF NECESSARY

1. **Nature of sample**: Marine shells (^Mulinea^)

2. **Submitter's catalogue number**: BEG CE-12A 12.4-12.7

3. **Name and number of site**: Auger core

4. **Descriptive location of site**:
 3.2 km N of Sabine Pass, Highway 87

5. **Latitude**: 29°44'52"N **Longitude**: 093°55'40"W

 Country: USA **State/Province:** Texas **County:** Jefferson

6. **Provenience of sample within site**:
 Ca. 2.25-2.34 m below sea level

7. **Collector and date**: R. Morton, 6 Jun 1993

8. **Context**:
 Sample came from Holocene valley fill

9. **Previous radiocarbon dates**:
 None

10. **Variables affecting validity of date**:
 Burrowing, sediment reworking

11. **Significance of sample**:
 Determine time of beach ridge progradation

12. **Estimated sample age**: < 10,000 BP

Radiocarbon Laboratory, The University of Texas at Austin
Analysis Results

TX- 8406 Run Number: 975c Run Date: 08-31-1995

Submitter: Morton, Robert A.
Submitter's catalogue number: BEG CE-12A 12.4-12.7
Site name: Auger core
Sample type: Shell
Submitter's age estimate: < 10,000 BP

Counting method: Liquid scillintilation, using one of four Beckman counters
Total counting time: 2700 minutes Total counts: 54958
$\delta^{13}C$ determination: -1.2°/∘∘

$$\text{Rate of unknown} = \frac{\text{avg. counts/minute - background}}{\text{grams carbon in sample}}$$

$$= \frac{20.355 \pm 0.087 - 6.875 \pm 0.036}{2.281} = 5.910 \pm 0.041 \text{ c.p.m./gram C}$$

$$\text{Percent Modern Carbon} = \frac{\text{unknown rate}}{\text{NBS standard rate}} = \frac{5.910 \pm 0.041}{8.839 \pm 0.021} = 66.863 \pm 0.30\%$$

$$\text{Age} = 8033 \ln \frac{\text{std. rate}}{\text{unk. rate}} \pm 8033 \left[\left[\frac{\text{std. error}}{\text{std. rate}}\right]^2 + \left[\frac{\text{unk. error}}{\text{unk. rate}}\right]^2 \right]^{1/2}$$

$$= 8033 \ln \frac{8.839}{5.910} \pm 8033 \left[\left[\frac{0.021}{8.839}\right]^2 + \left[\frac{0.041}{5.910}\right]^2 \right]^{1/2}$$

= 3234 ± 59 years B.P. (rounded to nearest 10: 3230 ± 60)

$\delta^{14}C$ = -331.4 ± 3.1°/∘∘

Corrections for $\delta^{13}C$

Rate of unknown = 5.629 ± 0.041 c.p.m./gram C

Percent Modern Carbon = 63.684 ± 0.296%

Age = 3625 ± 62 years B.P. (rounded to nearest 10: 3630 ± 60)

$\delta^{14}C$ = -363.2 ± 3.0°/∘∘

RADIOCARBON ANALYSIS REPORT
Radiocarbon Laboratory
The University of Texas
Balcones Research Center, Austin, TX 78712

Sample: Tx- 8407

Submitter: Morton, Robert A.
Bureau of Economic Geology
University of Texas
J.J. Pickle Research Campus
Austin, TX 78712

Bill to: Morton, Robert A.
Bureau of Economic Geology
University of Texas
J.J. Pickle Research Campus
Austin, TX 78712

DATA FROM SAMPLE GREEN SHEET
PLEASE CHECK, AND CORRECT IF NECESSARY

1. **Nature of sample:** Marine shell fragments (^Mulinea^)

2. **Submitter's catalogue number:** BEG CE-13 1.2-1.6

3. **Name and number of site:** Auger core

4. **Descriptive location of site:**
5.6 km N of Sabine Pass, Highway 87

5. **Latitude:** 29°45'58"N **Longitude:** 093°56'13"W

   Country: USA **State/Province:** Texas **County:** Jefferson

6. **Provenience of sample within site:**
Ca. 0.83-0.85 m below sea level

7. **Collector and date:** R. Morton, 7 Jun 1993

8. **Context:**
Sample came from the chenier ridge

9. **Previous radiocarbon dates:**
None

10. **Variables affecting validity of date:**
Burrowing, sediment reworking

11. **Significance of sample:**
Determine age of the chenier ridge

12. **Estimated sample age:** < 10,000 BP

Radiocarbon Laboratory, The University of Texas at Austin
Analysis Results

TX- 8407 Run Number: 979c Run Date: 09-08-1995

Submitter: Morton, Robert A.
Submitter's catalogue number: BEG CE-13 1.2-1.6
Site name: Auger core
Sample type: Shell
Submitter's age estimate: < 10,000 BP

Counting method: Liquid scillintilation, using one of four Beckman counters
Total counting time: 3900 minutes Total counts: 51378
$\delta^{13}C$ determination: $-1.8°/_{oo}$

$$\text{Rate of unknown} = \frac{\text{avg. counts/minute - background}}{\text{grams carbon in sample}}$$

$$= \frac{13.174 \pm 0.058 - 6.899 \pm 0.036}{1.054} = 5.954 \pm 0.065 \text{ c.p.m./gram C}$$

$$\text{Percent Modern Carbon} = \frac{\text{unknown rate}}{\text{NBS standard rate}} = \frac{5.954 \pm 0.065}{8.838 \pm 0.021} = 67.368 \pm 0.42$$

$$\text{Age} = 8033 \ln \frac{\text{std. rate}}{\text{unk. rate}} \pm 8033 \left[\left[\frac{\text{std. error}}{\text{std. rate}}\right]^2 + \left[\frac{\text{unk. error}}{\text{unk. rate}}\right]^2 \right]^{1/2}$$

$$= 8033 \ln \frac{8.838}{5.954} \pm 8033 \left[\left[\frac{0.021}{8.838}\right]^2 + \left[\frac{0.065}{5.954}\right]^2 \right]^{1/2}$$

= 3173 ± 90 years B.P. (rounded to nearest 10: 3170 ± 90)

$\delta^{14}C = -326.3 \pm 4.3°/_{oo}$

Corrections for $\delta^{13}C$

Rate of unknown = 5.678 ± 0.065 c.p.m./gram C

Percent Modern Carbon = 64.245 ± 0.413%

Age = 3554 ± 94 years B.P. (rounded to nearest 10: 3550 ± 90)

$\delta^{14}C = -357.5 \pm 4.1°/_{oo}$

RADIOCARBON ANALYSIS REPORT
Radiocarbon Laboratory
The University of Texas
Balcones Research Center, Austin, TX 78712

Sample: Tx- 8408

Submitter: Morton, Robert A.
Bureau of Economic Geology
University of Texas
J.J. Pickle Research Campus
Austin, TX 78712

Bill to: Morton, Robert A.
Bureau of Economic Geology
University of Texas
J.J. Pickle Research Campus
Austin, TX 78712

DATA FROM SAMPLE GREEN SHEET
PLEASE CHECK, AND CORRECT IF NECESSARY

1. **Nature of sample**: Oyster shell fragments

2. **Submitter's catalogue number**: BEG CE-13 20.7-20.9

3. **Name and number of site**: Auger core

4. **Descriptive location of site**:
   5.6 km N of Sabine Pass, Highway 87

5. **Latitude**: 29°45'58"N **Longitude**: 093°56'13"W

   Country: USA **State/Province:** Texas **County:** Jefferson

6. **Provenience of sample within site**:
   Ca. 5.09-5.15 m below sea level

7. **Collector and date**: R. Morton, 7 Jun 1993

8. **Context**:
   Sample came from Holocene valley fill

9. **Previous radiocarbon dates**:
   None

10. **Variables affecting validity of date**:
    Burrowing, sediment reworking

11. **Significance of sample**:
    Determine age of valley fill

12. **Estimated sample age**: < 15,000 BP

Radiocarbon Laboratory, The University of Texas at Austin
Analysis Results

TX- 8408 Run Number: 1573 Run Date: 08-31-1995

Submitter: Morton, Robert A.
Submitter's catalogue number: BEG CE-13 20.7-20.9
Site name: Auger core
Sample type: Shell
Submitter's age estimate: < 15,000 BP

Counting method: Liquid scillintilation, using one of four Beckman counters
Total counting time: 2700 minutes Total counts: 47588
$\delta^{13}C$ determination: -1.7°/∘∘

$$\text{Rate of unknown} = \frac{\text{avg. counts/minute - background}}{\text{grams carbon in sample}}$$

$$= \frac{17.625 \pm 0.081 - 5.868 \pm 0.033}{2.422} = 4.854 \pm 0.036 \text{ c.p.m./gram C}$$

$$\text{Percent Modern Carbon} = \frac{\text{unknown rate}}{\text{NBS standard rate}} = \frac{4.854 \pm 0.036}{7.230 \pm 0.021} = 67.137 \pm 0.23$$

$$\text{Age} = 8033 \ln \frac{\text{std. rate}}{\text{unk. rate}} \pm 8033 \left[\left[\frac{\text{std. error}}{\text{std. rate}}\right]^2 + \left[\frac{\text{unk. error}}{\text{unk. rate}}\right]^2 \right]^{1/2}$$

$$= 8033 \ln \frac{7.230}{4.854} \pm 8033 \left[\left[\frac{0.021}{7.230}\right]^2 + \left[\frac{0.036}{4.854}\right]^2 \right]^{1/2}$$

= 3201 ± 64 years B.P. (rounded to nearest 10: 3200 ± 60)

$\delta^{14}C$ = -328.6 ± 2.3°/∘∘

Corrections for $\delta^{13}C$

Rate of unknown = 4.628 ± 0.036 c.p.m./gram C

Percent Modern Carbon = 64.011 ± 0.225%

Age = 3584 ± 67 years B.P. (rounded to nearest 10: 3580 ± 70)

$\delta^{14}C$ = -359.9 ± 2.3°/∘∘

RADIOCARBON ANALYSIS REPORT
Radiocarbon Laboratory
The University of Texas
Balcones Research Center, Austin, TX 78712

Sample: Tx- 8409

Submitter: Morton, Robert A.
Bureau of Economic Geology
University of Texas
J.J. Pickle Research Campus
Austin, TX 78712

Bill to: Morton, Robert A.
Bureau of Economic Geology
University of Texas
J.J. Pickle Research Campus
Austin, TX 78712

DATA FROM SAMPLE GREEN SHEET
PLEASE CHECK, AND CORRECT IF NECESSARY

1. **Nature of sample:** Oyster shell fragments

2. **Submitter's catalogue number:** BEG CE-13 38.0-38.5

3. **Name and number of site:** Auger core

4. **Descriptive location of site:**
5.6 km N of Sabine Pass, Highway 87

5. **Latitude:** 29°45'58"N **Longitude:** 093°56'13"W

Country: USA **State/Province:** Texas **County:** Jefferson

6. **Provenience of sample within site:**
Ca. 10.36-10.51 m below sea level

7. **Collector and date:** R. Morton, 7 Jun 1993

8. **Context:**
Sample came from Holocene valley fill

9. **Previous radiocarbon dates:**
None

10. **Variables affecting validity of date:**
Burrowing, sediment reworking

11. **Significance of sample:**
Determine age of valley fill

12. **Estimated sample age:** < 15,000 BP

Radiocarbon Laboratory, The University of Texas at Austin
Analysis Results

TX- 8409 Run Number: II-585 Run Date: 09-02-1995

Submitter: Morton, Robert A.
Submitter's catalogue number: BEG CE-13 38.0-38.5
Site name: Auger core
Sample type: Shell
Submitter's age estimate: < 15,000 BP

Counting method: Liquid scillintilation, using one of four Beckman counters
Total counting time: 2757 minutes Total counts: 47645
$\delta^{13}C$ determination: -2.1°/∘∘

$$\text{Rate of unknown} = \frac{\text{avg. counts/minute - background}}{\text{grams carbon in sample}}$$

$$= \frac{17.281 \pm 0.079 - 6.123 \pm 0.033}{2.415} = 4.620 \pm 0.035 \text{ c.p.m./gram}$$

$$\text{Percent Modern Carbon} = \frac{\text{unknown rate}}{\text{NBS standard rate}} = \frac{4.620 \pm 0.035}{9.336 \pm 0.024} = 49.486 \pm 0.27$$

$$\text{Age} = 8033 \ln \frac{\text{std. rate}}{\text{unk. rate}} \pm 8033 \left[\left[\frac{\text{std. error}}{\text{std. rate}}\right]^2 + \left[\frac{\text{unk. error}}{\text{unk. rate}}\right]^2 \right]^{1/2}$$

$$= 8033 \ln \frac{9.336}{4.620} \pm 8033 \left[\left[\frac{0.024}{9.336}\right]^2 + \left[\frac{0.035}{4.620}\right]^2 \right]^{1/2}$$

= 5651 ± 64 years B.P. (rounded to nearest 10: 5650 ± 60)

$\delta^{14}C$ = -505.1 ± 2.8°/∘∘

Corrections for $\delta^{13}C$

Rate of unknown = 4.408 ± 0.035 c.p.m./gram C

Percent Modern Carbon = 47.215 ± 0.272%

Age = 6028 ± 67 years B.P. (rounded to nearest 10: 6030 ± 70)

$\delta^{14}C$ = -527.8 ± 2.7°/∘∘

RADIOCARBON ANALYSIS REPORT
Radiocarbon Laboratory
The University of Texas
Balcones Research Center, Austin, TX 78712

Sample: Tx- 8410

Submitter: Morton, Robert A.
Bureau of Economic Geology
University of Texas
J.J. Pickle Research Campus
Austin, TX 78712

Bill to: Morton, Robert A.
Bureau of Economic Geology
University of Texas
J.J. Pickle Research Campus
Austin, TX 78712

DATA FROM SAMPLE GREEN SHEET
PLEASE CHECK, AND CORRECT IF NECESSARY

1. **Nature of sample**: ^Rangia^ shell fragments

2. **Submitter's catalogue number**: BEG CE-13 82.8-83.0

3. **Name and number of site**: Auger core

4. **Descriptive location of site**:
   5.6 km N of Sabine Pass, Highway 87

5. **Latitude**: 29°45'58"N **Longitude**: 093°56'13"W

   Country: USA **State/Province:** Texas **County:** Jefferson

6. **Provenience of sample within site**:
   Ca. 24.01-24.08 m below sea level

7. **Collector and date**: R. Morton, 7 Jun 1993

8. **Context**:
   Sample came from Holocene valley fill

9. **Previous radiocarbon dates**:
   None

10. **Variables affecting validity of date**:
    Burrowing, sediment reworking

11. **Significance of sample**:
    Determine age of valley fill

12. **Estimated sample age**: < 15,000 BP

Radiocarbon Laboratory, The University of Texas at Austin
Analysis Results

TX- 8410 Run Number: 1572 Run Date: 08-29-1995

Submitter: Morton, Robert A.
Submitter's catalogue number: BEG CE-13 82.8-83.0
Site name: Auger core
Sample type: Shell
Submitter's age estimate: < 15,000 BP

Counting method: Liquid scillintilation, using one of four Beckman counters
Total counting time: 2700 minutes Total counts: 25305
$\delta^{13}C$ determination: -7.3°/∘∘

$$\text{Rate of unknown} = \frac{\text{avg. counts/minute - background}}{\text{grams carbon in sample}}$$

$$= \frac{9.372 \pm 0.059 - 5.868 \pm 0.033}{1.306} = 2.683 \pm 0.052 \text{ c.p.m./gram}$$

$$\text{Percent Modern Carbon} = \frac{\text{unknown rate}}{\text{NBS standard rate}} = \frac{2.683 \pm 0.052}{7.231 \pm 0.021} = 37.104 \pm 0.206$$

$$\text{Age} = 8033 \ln \frac{\text{std. rate}}{\text{unk. rate}} \pm 8033 \left[\left[\frac{\text{std. error}}{\text{std. rate}}\right]^2 + \left[\frac{\text{unk. error}}{\text{unk. rate}}\right]^2 \right]^{1/2}$$

$$= 8033 \ln \frac{7.231}{2.683} \pm 8033 \left[\left[\frac{0.021}{7.231}\right]^2 + \left[\frac{0.052}{2.683}\right]^2 \right]^{1/2}$$

= 7964 ± 157 years B.P. (rounded to nearest 10: 7960 ± 160)

$\delta^{14}C$ = -629.0 ± 2.1°/∘∘

Corrections for $\delta^{13}C$

Rate of unknown = 2.588 ± 0.052 c.p.m./gram C

Percent Modern Carbon = 35.790 ± 0.203%

Age = 8254 ± 163 years B.P. (rounded to nearest 10: 8250 ± 160)

$\delta^{14}C$ = -642.1 ± 2.0°/∘∘

RADIOCARBON ANALYSIS REPORT
Radiocarbon Laboratory
The University of Texas
Balcones Research Center, Austin, TX 78712

Sample: Tx- 8414

Submitter: Morton, Robert A.
Bureau of Economic Geology
University of Texas
J.J. Pickle Research Campus
Austin, TX 78712

Bill to: Morton, Robert A.
Bureau of Economic Geology
University of Texas
J.J. Pickle Research Campus
Austin, TX 78712

DATA FROM SAMPLE GREEN SHEET
PLEASE CHECK, AND CORRECT IF NECESSARY

1. **Nature of sample**: Peat

2. **Submitter's catalogue number**: BEG CE-14 8.2-8.6

3. **Name and number of site**: Auger core

4. **Descriptive location of site**:
Neches floodplain N of Neches River, Highway 87

5. **Latitude**: 30°32'N **Longitude**: 092°51'30"W

   Country: USA **State/Province**: Texas **County**: Jefferson

6. **Provenience of sample within site**:
Ca. 1.58-1.70 m below sea level

7. **Collector and date**: R. Morton, 8 Jun 1993

8. **Context**:
Sample came from Holocene valley fill

9. **Previous radiocarbon dates**:
None

10. **Variables affecting validity of date**:
Burrowing, sediment reworking

11. **Significance of sample**:
Determine age of valley fill

12. **Estimated sample age**: < 10,000 BP

Radiocarbon Laboratory, The University of Texas at Austin
Analysis Results

TX- 8414 Run Number: 974c Run Date: 08-29-1995

Submitter: Morton, Robert A.
Submitter's catalogue number: BEG CE-14 8.2-8.6
Site name: Auger core
Sample type: Peat
Submitter's age estimate: < 10,000 BP

Counting method: Liquid scillintilation, using one of four Beckman counters
Total counting time: 2700 minutes Total counts: 73819
$\delta^{13}C$ determination: -28.2°/₀₀

$$\text{Rate of unknown} = \frac{\text{avg. counts/minute - background}}{\text{grams carbon in sample}}$$

$$= \frac{27.340 \pm 0.101 - 6.875 \pm 0.036}{2.416} = 8.471 \pm 0.044 \text{ c.p.m./gram C}$$

$$\text{Percent Modern Carbon} = \frac{\text{unknown rate}}{\text{NBS standard rate}} = \frac{8.471 \pm 0.044}{8.839 \pm 0.021} = 95.837 \pm 0.41$$

$$\text{Age} = 8033 \ln \frac{\text{std. rate}}{\text{unk. rate}} \pm 8033 \left[\left[\frac{\text{std. error}}{\text{std. rate}}\right]^2 + \left[\frac{\text{unk. error}}{\text{unk. rate}}\right]^2 \right]^{1/2}$$

$$= 8033 \ln \frac{8.839}{8.471} \pm 8033 \left[\left[\frac{0.021}{8.839}\right]^2 + \left[\frac{0.044}{8.471}\right]^2 \right]^{1/2}$$

= 342 ± 46 years B.P. (rounded to nearest 10: 340 ± 50)

$\delta^{14}C$ = -41.6 ± 4.2°/₀₀

Corrections for $\delta^{13}C$

Rate of unknown = 8.525 ± 0.044 c.p.m./gram C

Percent Modern Carbon = 96.448 ± 0.419%

Age = 291 ± 46 years B.P. (rounded to nearest 10: 290 ± 50)

$\delta^{14}C$ = -35.5 ± 4.2°/₀₀

RADIOCARBON ANALYSIS REPORT
Radiocarbon Laboratory
The University of Texas
Balcones Research Center, Austin, TX 78712

Sample: Tx- 8411

Submitter: Morton, Robert A.
Bureau of Economic Geology
University of Texas
J.J. Pickle Research Campus
Austin, TX 78712

Bill to: Morton, Robert A.
Bureau of Economic Geology
University of Texas
J.J. Pickle Research Campus
Austin, TX 78712

DATA FROM SAMPLE GREEN SHEET
PLEASE CHECK, AND CORRECT IF NECESSARY

1. **Nature of sample**: ^Rangia^ shell fragments

2. **Submitter's catalogue number**: BEG CE-14 23.0-23.5

3. **Name and number of site**: Auger core

4. **Descriptive location of site**:
Neches floodplain N of Neches River, Highway 87

5. **Latitude**: 30°32'N **Longitude**: 092°51'30"W

Country: USA **State/Province**: Texas **County**: Jefferson

6. **Provenience of sample within site**:
Ca. 6.10-6.25 m below sea level

7. **Collector and date**: R. Morton, 8 Jun 1993

8. **Context**:
Sample came from Holocene valley fill

9. **Previous radiocarbon dates**:
None

10. **Variables affecting validity of date**:
Burrowing, sediment reworking

11. **Significance of sample**:
Determine age of valley fill

12. **Estimated sample age**: < 10,000 BP

Radiocarbon Laboratory, The University of Texas at Austin
Analysis Results

TX- 8411 Run Number: 1576 Run Date: 09-06-1995

Submitter: Morton, Robert A.
Submitter's catalogue number: BEG CE-14 23.0-23.5
Site name: Auger core
Sample type: Shell
Submitter's age estimate: < 10,000 BP

Counting method: Liquid scillintilation, using one of four Beckman counters
Total counting time: 2700 minutes Total counts: 37582
$\delta^{13}C$ determination: -6.3°/∘∘

$$\text{Rate of unknown} = \frac{\text{avg. counts/minute - background}}{\text{grams carbon in sample}}$$

$$= \frac{13.919 \pm 0.072 - 5.867 \pm 0.033}{2.412} = 3.338 \pm 0.033 \text{ c.p.m./gram}$$

$$\text{Percent Modern Carbon} = \frac{\text{unknown rate}}{\text{NBS standard rate}} = \frac{3.338 \pm 0.033}{7.226 \pm 0.021} = 46.194 \pm 0.18$$

$$\text{Age} = 8033 \ln \frac{\text{std. rate}}{\text{unk. rate}} \pm 8033 \left[\left[\frac{\text{std. error}}{\text{std. rate}}\right]^2 + \left[\frac{\text{unk. error}}{\text{unk. rate}}\right]^2 \right]^{1/2}$$

$$= 8033 \ln \frac{7.226}{3.338} \pm 8033 \left[\left[\frac{0.021}{7.226}\right]^2 + \left[\frac{0.033}{3.338}\right]^2 \right]^{1/2}$$

= 6204 ± 83 years B.P. (rounded to nearest 10: 6200 ± 80)

$\delta^{14}C$ = -538.1 ± 1.9°/∘∘

Corrections for $\delta^{13}C$

Rate of unknown = 3.213 ± 0.033 c.p.m./gram C

Percent Modern Carbon = 44.464 ± 0.185%

Age = 6511 ± 86 years B.P. (rounded to nearest 10: 6510 ± 90)

$\delta^{14}C$ = -555.4 ± 1.9°/∘∘

RADIOCARBON ANALYSIS REPORT
Radiocarbon Laboratory
The University of Texas
Balcones Research Center, Austin, TX 78712

Sample: Tx- 8412

Submitter: Morton, Robert A.
Bureau of Economic Geology
University of Texas
J.J. Pickle Research Campus
Austin, TX 78712

Bill to: Morton, Robert A.
Bureau of Economic Geology
University of Texas
J.J. Pickle Research Campus
Austin, TX 78712

DATA FROM SAMPLE GREEN SHEET
PLEASE CHECK, AND CORRECT IF NECESSARY

1. **Nature of sample**: Peat

2. **Submitter's catalogue number**: BEG CE-15 14.5-15.5

3. **Name and number of site**: Auger core

4. **Descriptive location of site**:
Neches floodplain N of Neches River, Highway 87

5. **Latitude**: 30°00'11"N **Longitude**: 092°51'52"W

   Country: USA **State/Province:** Texas **County:** Jefferson

6. **Provenience of sample within site**:
Ca. 3.50-3.81 m below sea level

7. **Collector and date**: R. Morton, 8 Jun 1993

8. **Context**:
Sample came from Holocene valley fill

9. **Previous radiocarbon dates**:
None

10. **Variables affecting validity of date**:
Burrowing, sediment reworking

11. **Significance of sample**:
Determine age of the Holocene valley fill

12. **Estimated sample age**: < 10,000 BP

Radiocarbon Laboratory, The University of Texas at Austin
Analysis Results

TX- 8412 Run Number: II-584 Run Date: 08-31-1995

Submitter: Morton, Robert A.
Submitter's catalogue number: BEG CE-15 14.5-15.5
Site name: Auger core
Sample type: Peat
Submitter's age estimate: < 10,000 BP

Counting method: Liquid scillintilation, using one of four Beckman counters
Total counting time: 2771 minutes Total counts: 56180
$\delta^{13}C$ determination: -23.1°/∘∘

$$\text{Rate of unknown} = \frac{\text{avg. counts/minute - background}}{\text{grams carbon in sample}}$$

$$= \frac{20.274 \pm 0.086 - 6.123 \pm 0.033}{2.409} = 5.874 \pm 0.038 \text{ c.p.m./gram}$$

$$\text{Percent Modern Carbon} = \frac{\text{unknown rate}}{\text{NBS standard rate}} = \frac{5.874 \pm 0.038}{9.342 \pm 0.024} = 62.877 \pm 0.316$$

$$\text{Age} = 8033 \ln \frac{\text{std. rate}}{\text{unk. rate}} \pm 8033 \left[\left[\frac{\text{std. error}}{\text{std. rate}}\right]^2 + \left[\frac{\text{unk. error}}{\text{unk. rate}}\right]^2 \right]^{1/2}$$

$$= 8033 \ln \frac{9.342}{5.874} \pm 8033 \left[\left[\frac{0.024}{9.342}\right]^2 + \left[\frac{0.038}{5.874}\right]^2 \right]^{1/2}$$

= 3727 ± 56 years B.P. (rounded to nearest 10: 3730 ± 60)

$\delta^{14}C$ = -371.2 ± 3.2°/∘∘

Corrections for $\delta^{13}C$

Rate of unknown = 5.852 ± 0.038 c.p.m./gram C

Percent Modern Carbon = 62.642 ± 0.316%

Age = 3757 ± 56 years B.P. (rounded to nearest 10: 3760 ± 60)

$\delta^{14}C$ = -373.6 ± 3.2°/∘∘

RADIOCARBON ANALYSIS REPORT
Radiocarbon Laboratory
The University of Texas
Balcones Research Center, Austin, TX 78712

Sample: Tx- 8413

Submitter: Morton, Robert A.
Bureau of Economic Geology
University of Texas
J.J. Pickle Research Campus
Austin, TX 78712

Bill to: Morton, Robert A.
Bureau of Economic Geology
University of Texas
J.J. Pickle Research Campus
Austin, TX 78712

DATA FROM SAMPLE GREEN SHEET
PLEASE CHECK, AND CORRECT IF NECESSARY

1. **Nature of sample**: Peat

2. **Submitter's catalogue number**: BEG CE-15 33.0-33.5

3. **Name and number of site**: Auger core

4. **Descriptive location of site**:
   Neches floodplain N of Neches River, Highway 87

5. **Latitude**: 30°00'11"N **Longitude**: 092°51'52"W

   Country: USA **State/Province**: Texas **County**: Jefferson

6. **Provenience of sample within site**:
   Ca. 9.14-9.29 m below sea level

7. **Collector and date**: R. Morton, 8 Jun 1993

8. **Context**:
   Sample came from Holocene valley fill

9. **Previous radiocarbon dates**:
   None

10. **Variables affecting validity of date**:
    Burrowing, sediment reworking

11. **Significance of sample**:
    Determine age of the Holocene valley fill

12. **Estimated sample age**: < 10,000 BP

Radiocarbon Laboratory, The University of Texas at Austin
Analysis Results

TX- 8413 Run Number: 976c Run Date: 09-02-1995

Submitter: Morton, Robert A.
Submitter's catalogue number: BEG CE-15 33.0-33.5
Site name: Auger core
Sample type: Peat
Submitter's age estimate: < 10,000 BP

Counting method: Liquid scillintilation, using one of four Beckman counters
Total counting time: 2700 minutes Total counts: 42337
$\delta^{13}C$ determination: $-28.7°/_{\circ\circ}$

$$\text{Rate of unknown} = \frac{\text{avg. counts/minute - background}}{\text{grams carbon in sample}}$$

$$= \frac{15.680 \pm 0.076 - 6.875 \pm 0.036}{2.403} = 3.664 \pm 0.035 \text{ c.p.m./gram}$$

$$\text{Percent Modern Carbon} = \frac{\text{unknown rate}}{\text{NBS standard rate}} = \frac{3.664 \pm 0.035}{8.840 \pm 0.021} = 41.448 \pm 0.226$$

$$\text{Age} = 8033 \ln \frac{\text{std. rate}}{\text{unk. rate}} \pm 8033 \left[\left[\frac{\text{std. error}}{\text{std. rate}}\right]^2 + \left[\frac{\text{unk. error}}{\text{unk. rate}}\right]^2 \right]^{1/2}$$

$$= 8033 \ln \frac{8.840}{3.664} \pm 8033 \left[\left[\frac{0.021}{8.840}\right]^2 + \left[\frac{0.035}{3.664}\right]^2 \right]^{1/2}$$

= 7075 ± 79 years B.P. (rounded to nearest 10: 7080 ± 80)

$\delta^{14}C = -585.5 \pm 2.3°/_{\circ\circ}$

Corrections for $\delta^{13}C$

Rate of unknown = 3.691 ± 0.035 c.p.m./gram C

Percent Modern Carbon = 41.753 ± 0.226%

Age = 7016 ± 79 years B.P. (rounded to nearest 10: 7020 ± 80)

$\delta^{14}C = -582.5 \pm 2.3°/_{\circ\circ}$

Addendum 6. "Deweyville" Terraces and Deposits of the Texas Gulf Coastal Plain

"DEWEYVILLE" TERRACES AND DEPOSITS OF THE TEXAS GULF COASTAL PLAIN

Michael D. Blum[1], Robert A. Morton[2], James M. Durbin[1]
[1] Department of Geology, University of Nebraska - Lincoln, Lincoln, Nebraska 68588
[2] Bureau of Economic Geology, The University of Texas at Austin, Austin, Texas 78758

ABSTRACT

Bernard (1950) defined the Deweyville beds as underlying a terrace along Sabine River that is intermediate in elevation between Pleistocene Beaumont alluvial plain surfaces and Holocene floodplains, and which has abandoned meanders that are considerably larger than those of the Beaumont surface or modern highly sinuous Sabine channel. Subsequent workers identify 2 or 3 distinct terraces and/or suites of deposits that fit the original morphostratigraphic concept of the Deweyville along the Sabine and other rivers of the Texas Coastal Plain, but most commonly attribute oversized meanders to greater annual discharge and/or extreme high magnitude floods during the late Pleistocene glacial period. This paper builds on the idea of a broader stratigraphic concept for "Deweyville" terraces and deposits, and suggests a process model that emphasizes fluvial responses to interacting climatic and glacio-eustatic controls.

We suggest the multiple "Deweyville" terraces and underlying fills of the Texas Gulf Coast should be treated as a series of unconformity-bounded allostratigraphic units that record: (a) abandonment of Beaumont isotope stage 5 alluvial plains ca. 100 ka, which partitioned post-Beaumont incised valleys; and (b) multiple episodes of lateral migration, aggradation, and/or degradation within those valleys during the stage 4, 3, and 2 glacial cycle when channels were graded to shorelines at mid-shelf or farther basinward positions. "Deweyville" allostratigraphic units of the Sabine, Trinity, Guadalupe, and Nueces Rivers have steeper gradients than modern floodplains, and the youngest "Deweyville" surfaces are onlapped by Holocene strata at or near modern bay-head

deltas. Similar units are present in the Colorado and Brazos(?) valleys, but onlap by Holocene strata occurs 100 km or more inland from the present highstand shoreline.

"Deweyville" allostratigraphic units may represent a glacial period process regime with more annual runoff, but smaller peak discharges than present. The deep inland penetration of tropical moisture and/or tropical cyclones, responsible for most extreme floods on Coastal Plain rivers, was rare through the 80-90 ky of the glacial cycle when temperatures were cooler and the Gulf was smaller. "Deweyville" allostratigraphic units also lack clear evidence for high magnitude overbank floods, as they are sand-dominated, much like channel facies of late Holocene streams, but there is a paucity of vertical accretion floodplain facies which suggests most flood events remained within bankfull channel perimeters. The shorter wavelength, highly sinuous meanders typical of the present interglacial process regime may reflect adjustments to bank-stabilizing vertical accretion facies produced by deep overbank floods, and, in lowermost reaches of the Coastal Plain, to a forced flattening of gradients due to post-glacial sea level rise.

INTRODUCTION

The Texas Gulf Coastal Plain consists of a series of low-gradient, fan-shaped alluvial-deltaic plains that emanate from each major river valley (Fig. 1). Coastal plain deposits were initially subdivided into three "morphostratigraphic units" of presumed Pleistocene age, and designated the Willis (oldest), Lissie, and Beaumont (youngest) Formations (Hayes and Kennedy, 1903; Duessan, 1914; 1924; Doering, 1935; see Morton and Price, 1987; DuBar et al., 1991 for reviews). Bernard (1950) first differentiated post-Beaumont landforms and deposits when he described the Deweyville terrace and beds along east Texas rivers. Elsewhere, post-Beaumont strata went, for the most part unnamed and undifferentiated, but were assumed to be Holocene in age.

Most genetic interpretations for Texas Coastal Plain surfaces and deposits were developed when the Pleistocene was divided into four long glacials with sea level lowstand and three long interglacials characterized by sea level highstand. Following Fisk's (1944) model for the Mississippi River, valley entrenchment and sediment bypass was inferred for glacial periods, and large-scale depositional units were interpreted to represent alluvial terraces and deltaic plains constructed during transgression and highstand. Beaumont strata were assigned to the "Sangamon" interglacial (e.g. Doering, 1956; Winker, 1979), or to a subsequent shorter-lived "Peorian" interglacial (e.g. Bernard and LeBlanc, 1965), whereas post-Beaumont valleys were presumed to represent entrenchment during the "Wisconsin" glacial, and filling with post-glacial sea level rise.

This paper is part of a continuing reevaluation of the genetic stratigraphy of Texas Gulf Coastal Plain fluvial deposits. This type of reevaluation becomes necessary when the empirical foundations of previous models have been substantially revised. Such is the case for the simple linkage between coastal plain depositional units and glacio-eustasy, a satisfactory model when the concept of four long Pleistocene interglacials was accepted, but one that needs reevaluation today. Willis, Lissie, Beaumont, and post-Beaumont strata are, for example, now thought to represent the entire Plio-Pleistocene to Holocene (DuBar et al., 1991), but studies of oxygen isotopes in marine sediments show seven glacial-interglacial cycles during the last 700,000 years alone (Chappell and Shackleton, 1986; Williams et al., 1988). Blum and Price (1994; in press) present the first stages of this reevaluation, showing that Beaumont alluvial plains consist of cross-cutting incised valley fills deposited over the last 3-400 ky or more. This paper builds on previous work to suggest a "Deweyville allostratigraphic framework", as well as a genetic model that emphasizes fluvial response to interacting glacio-eustatic and climatic controls.

BACKGROUND TO DEWEYVILLE TERRACES AND DEPOSITS

Barton (1930) first discussed the large relict channels on terraces of east Texas Rivers as distinct from those on older Beaumont or younger floodplains. Some 20 years later, Bernard (1950) formally recognized the Deweyville beds as underlying a terrace along Sabine River that is intermediate in elevation between Pleistocene Beaumont surfaces and Holocene floodplains, and which has channel dimensions much larger than the modern Sabine. He also noted similar terraces along the Neches, Trinity, San Jacinto, and Nueces Rivers (Angelita terrace of Price, 1933), and suggested that large arcuate scars along valley walls in the Brazos and Colorado valleys were correlative to Deweyville meanders, but buried by younger deposits.

Following this early work, similar terraces were recognized and studied throughout the Gulf Coastal Plain in Arkansas, Louisiana, and Texas, and in most cases workers identify 2-3 terraces that fit Bernard's Deweyville concept (e.g. Gagliano and Thom, 1967; Saucier and Fleetwood, 1970; Aten, 1983; Alford and Holmes, 1985; Pearson et al., 1986; Blum and Valastro, 1994). Moreover, Environmental Geologic Atlas maps published by The University of Texas' Bureau of Economic Geology identify at least 2 "Deweyville" terraces in the lower reaches of coastal plain valleys, except those of the Rio Grande, Colorado, and Brazos Rivers (Fisher et al., 1972; Brown et al., 1976; McGowen et al., 1976). Finally, seismic reflection and core-based studies of recent strata of the now-submerged east Texas shelf interpret terraces within the incised valley of the Sabine and Trinity Rivers, and suggest they correlate with Deweyville terraces onshore (Pearson et al., 1986; Thomas, 1990; Anderson et al., 1992; Thomas and Anderson, 1994).

Few chronometric controls are available for Deweyville terraces. Bernard (1950) inferred a latest Pleistocene age, whereas Bernard and LeBlanc (1965), Gagliano and Thom (1967), and Saucier and Fleetwood (1970) cite unpublished radiocarbon ages of ca. 30-17 ka from Deweyville deposits. Saucier and Fleetwood (1970) also suggest Deweyville terraces in Arkansas can be traced to late Wisconsin valley trains of Mississippi River. More recent estimates range over an order of magnitude, as Alford and Holmes (1985) suggest an early to middle Holocene age for Deweyville terraces along Sabine River, based on associated archaeological materials, and Thomas (1990) places Deweyville terraces of the Trinity valley in isotope stage 5c, ca. 100 ka, based on correlations with the Trinity incised valley fill offshore, and ages for the offshore record from oxygen isotope curves.

Barton (1930) provided an initial explanation for large meanders on terraces of east Texas rivers, suggesting late Pleistocene streams were larger than modern channels, and rainfall must have been greater. Bernard (1950) reviewed a number of explanations, but clearly favored linking Deweyville deposition and terrace formation to a cycle of rising then falling sea level during the latest

Wisconsin. Subsequent workers (Gagliano and Thom, 1967; Saucier and Fleetwood, 1970; Alford and Holmes, 1985) favored climatic controls, using hydraulic geometry relations to suggest Deweyville meander scars represent mean annual discharges significantly greater than modern. Most recently, Saucier (in Autin et al., 1991) suggests changes in precipitation seasonality and intensity, and changes in vegetation, were more important than changes in mean annual discharge, whereas Thomas (1990) linked deposition to rising sea level during isotope stage 5c, and Gagliano (1992) suggests Deweyville terraces represent Pleistocene "superfloods".

"DEWEYVILLE" ALLOSTRATIGRAPHIC FRAMEWORK

Studies that followed Bernard (1950) illustrate the complexity of post-Beaumont alluvial deposits of the Texas Gulf Coastal Plain, but also muddy the "Deweyville" waters a bit, as it seems that different workers are talking about different things. Because of the regional significance of the "Deweyville" phenomenon, we outline a broader conceptual framework, one that future studies can test and refine.

We suggest the distribution and variability of the "Deweyville" phenomenon can best be understood within the context of the large-scale geomorphology of the Texas Coastal Plain. For example, Winker (1979) and Galloway (1981) differentiate extrabasinal from basin fringe and intrabasinal fluvial systems. Extrabasinal systems (Rio Grande, Colorado, and Brazos) drain tectonic hinterlands, have large sediment supplies, and construct laterally extensive alluvial-deltaic headlands. By contrast, basin fringe fluvial systems (Sabine, Trinity, Guadalupe, and Nueces) cannibalize basin margins, whereas intrabasinal streams (San Jacinto, Navidad, and Aransas) drain updip parts of the basin fill. Because of the small drainage areas and sediment loads of basin-fringe and intrabasinal streams, they commonly flow into the basin at interdeltaic bights that consist of alluvial, bay-head deltaic, estuarine, and barrier island/strandplain depositional systems. Complementary to the above, Morton and McGowen (1980) show that rivers entering the basin over deep-seated structural lows have gradients much less steep than those that enter the basin, or flow over, deep structural highs.

Examples of low gradient streams would be the Sabine, Neches, Trinity, and Brazos, which enter the basin over the Houston embayment, and the Rio Grande, which enters the basin over the Rio Grande embayment. High gradient streams like the Colorado, Guadalupe, and Nueces emerge from the high-relief Edwards Plateau and cross the San Marcos arch before discharging into the Gulf.

Within this larger context, our mapping and construction of long profiles shows multiple terraces with Deweyville characteristics within post-Beaumont valleys of basin fringe fluvial axes (Fig. 2). For low-gradient east Texas rivers, like the Trinity, Sabine, and Neches, two terraces occur below the Beaumont surface and above the level of modern floodplains, and project seaward beyond modern bay-head deltas until they are cut out by modern bays. In addition, large arcuate scars are ubiquitous along valley walls (i.e. Lake Anahuac in the Trinity valley), and have always been referred to as "Deweyville" (see Gagliano and Thom, 1967; Aten, 1983; Pearson et al., 1986); but their long profiles coincide with modern floodplains, and they have been buried by veneers of younger floodbasin and/or delta plain facies, hence they are no longer terraces in the classic sense. By contrast, for the steeper gradient basin fringe rivers like the Guadalupe and Nueces, three distinct terraces occur well above modern floodplains, at least down to the bay-head delta plain, where the lowest "Deweyville" surface is onlapped and buried.

For the extrabasinal Colorado and Brazos valleys, Bernard (1950) suggested similar terraces might have been present, but they are now buried by younger alluvial deposits. Indeed, Blum and Valastro (1994) show that terraces with "Deweyville" characteristics are present in the Colorado valley, but onlap by Holocene strata occurs 100 km updip from the modern shoreline (Fig. 3). Mapping and stratigraphic data remain unavailable for much of the Brazos system, but White and Weigand (1989) correlate a Brazos terrace near the confluence with Navasota River, with the Deweyville. Bernard et al. (1970) show that modern floodplain facies veneer the post-Beaumont Brazos valley through the lowermost 100 km. By inference, Deweyville deposits would be buried by Holocene strata through the lower part of the Brazos valley, as they are in the Colorado, but the updip limits of onlap might be considerably greater due to the lower valley gradient.

In summary, landforms and/or deposits that correspond to Bernard's (1950) concept appear to be present along all of the major Texas Coastal Plain rivers except perhaps Rio Grande(?). However, the presence of multiple "Deweyvilles" complicates the picture, as do morphologic and stratigraphic differences that correspond to large-scale geomorphological setting. Hence, following recent efforts in the Gulf Coast (Autin, 1992; Blum and Valastro, 1994), we suggest "Deweyville" landforms and deposits should be treated as unconformity-bounded allostratigraphic units (NACSN, 1983), since some deposits have a similar age, origin, and genetic significance, but no longer have surface expression as a terrace. Fundamental characteristics of a "Deweyville" allostratigraphic framework might be as follows (Fig. 4): (a) the entire post-Beaumont succession should be bounded by a composite basal unconformity that traces up and out of the valley to soils on Beaumont surfaces; (b) the oldest "Deweyville" allostratigraphic unit occurs at the highest elevations, with successively younger units at successively lower elevations; (c) each "Deweyville" unit should be bounded by unconformities that trace up, and laterally to, soils developed on older units, and the upper boundary to each "Deweyville" unit should be defined by a soil profile; (d) "Deweyville" units project seaward to shorelines lower in elevation and farther seaward than today; and (e) the updip limits of onlap and burial of "Deweyville" units by younger strata depends on sediment supply and valley gradient.

Lithological characteristics play no formal role in definition of allostratigraphic units, but a number of workers note that facies underlying Deweyville terraces are coarser than Beaumont or Holocene deposits (e.g. Gagliano and Thom, 1967; Saucier and Fleetwood, 1970; see also Autin et al., 1991). Blum and Valastro (1994) suggest that gravely or sandy channel facies extend to the top of most sections in "Deweyville" correlatives of the Colorado valley, and vertical accretion facies are rare, which contrasts with late Holocene deposits where vertical accretion facies are thick and volumetrically significant. Our observations in the Sabine, Neches, Trinity, and Nueces valleys supports the view of limited to non-existent vertical accretion facies in "Deweyville" units, and an abundance of such facies in Holocene deposits. We also note that gravel and sand quarries occur frequently on "Deweyville" surfaces because of the lack of fine-grained overburden.

A precise chronology for "Deweyville" allostratigraphic units awaits future work, but stratigraphic relations indicate they fall between deposition of Beaumont alluvial plain strata and development of modern floodplains. The Colorado River is the only fluvial system with chronological control on Beaumont or younger strata. The youngest Beaumont meanderbelts have, for example, produced thermoluminescence ages ranging from ca. 119 to 102 ka, suggesting alluvial plains were abandoned during late isotope stage 5 as the Colorado incised in response to sea level lowering (Blum and Price, 1994; in press). At the other end of the time window, the youngest deposits correlative to Deweyville have produced radiocarbon ages that fall within isotope stage 2, ca. 20-14 ka (Blum and Valastro, 1994). From this, we infer that "Deweyville" allostratigraphic units were deposited sometime within the isotope stage 4, 3, and 2 glacial period.

GENETIC MODEL FOR "DEWEYVILLE" ALLOSTRATIGRAPHIC UNITS

Although climate change and/or changes in base level undoubtedly played a significant role in determining "Deweyville" morphological and stratigraphic characteristics, two problems should be addressed. First, values of precipitation or discharge suggested by previous workers seem extreme, perhaps out of the range of possibilities for the climate system in this region. It seems unlikely, for example, that mean annual discharge could have been significantly more than present, or that the glacial period would have had larger peak discharges than the present interglacial. Second, the nature of base level influence needs reevaluation in light of present understanding of glacio-eustasy, which is very different from the model that prevailed when Bernard (1950) conducted his work. Here we present a revised genetic model that can be tested or refined in future investigations.

Glacial versus Interglacial Climate Systems

Our model draws on Porter's (1989) concept of "average Pleistocene conditions". Most discussions of Quaternary climate or sea-level change focus on end-members such as the full-glacial or interglacial. However, oxygen isotope curves (Chappell and Shackleton, 1986; Williams et al., 1988) show that 80% of any middle to late Pleistocene 100 ky glacial cycle was intermediate in character, with global temperatures cooler than full interglacial conditions, but not as cold as a full-glacial, and with eustatic sea level at -15 to -65 meters (Fig. 5a). For Texas Coastal Plain rivers, this would translate to cooler land temperatures, and a cooler and smaller Gulf precipitation source for the entire stage 4, 3, and 2 glacial cycle. Moreover, rivers were extended to shorelines in mid-shelf or farther basinward positions, and much of the shelf was a subaerial extension of the coastal plain (Fig. 5b). Such conditions represent the norm for the last 100 ky, and the Holocene interglacial should be regarded as unique, with a warm climate, a large and warm Gulf precipitation source, and rivers graded to updip shoreline positions.

At a more specific level, Toomey et al. (1993) reconstruct the isotope stage 2 glacial climate of the Edwards Plateau, source terrain for the Colorado, Guadalupe, and Nueces Rivers. Regional temperatures were significantly cooler, and there was more effective moisture, but perhaps more important were the types of precipitation events, and the nature of upland soil mantles. Tropical cyclones were probably rare to non-existent when sea level was low and the Gulf was cooler (e.g. Wendland, 1977; Hobgood and Cerveny, 1988), as were high-intensity convectional storms, and most precipitation would have been derived from midlatitude cyclonic storms. Several lines of evidence also converge to show that full-glacial precipitation fell on uplands that were covered by deep soil mantles no longer present in the area today.

Precipitation events characteristic of the full-glacial on the Edwards Plateau might have prevailed through earlier parts of the last glacial cycle, and throughout the southcentral United States. Given the relationship between tropical cyclone frequency and sea surface temperature, or convectional storm frequency and land temperature, such storms should have been infrequent at best during the entire stage 4, 3, and 2 glacial period. Moreover, deep soils present at full-glacial time on the Edwards Plateau should have been present through earlier parts of the last glacial cycle as well.

since soils on these limestone uplands would have required a long time to form, probably through some combination of eolian dust influx and in situ weathering of bedrock, and therefore reflect long-term landscape stability. Although details may have differed elsewhere in the southcentral United States, landscape stability may have been the norm for the entire glacial period, especially if convectional and tropical storms were insignificant, and most precipitation resulted from less intense but areally widespread midlatitude cyclones.

Global climate changes that led to wastage of isotope stage 2 ice sheets resulted in changes in climate and vegetation in the southcentral United States. Toomey et al. (1993) suggest that post-glacial sea level rise, coupled with increased surface temperatures, promoted frequent inland penetration of warm, moist tropical air, and corresponding increases in the frequency of tropical cyclones and convectional storms. On the Edwards Plateau, these changes triggered a period of landscape instability and soil erosion so that upland landscapes now consist of exposed bedrock. Again, although details may differ, Holocene landscape instability may have been widespread in the southcentral United States due to the shift from glacial to interglacial climates.

Glacial versus Interglacial Fluvial Systems

Fundamental differences between glacial and interglacial climates would have resulted in equally fundamental differences in fluvial process regimes. While glacial periods had more effective moisture, related mean annual discharge values are not critical to explaining "Deweyville" characteristics (see Saucier, in Autin et al., 1991), since the morphology and depositional style of alluvial channels depend on floods that are less frequent (recurrence intervals of 1-10 years), and 1-3 orders of magnitude greater, than mean annual discharge (Wolman and Miller, 1960; Wolman and Gerson, 1978; Knox, 1983). Hence glacial to interglacial changes in storm types and landscape stability, and their effects on floods, should have been the most important factors.

Most extreme floods on the larger coastal plain rivers result from the inland penetration of tropical cyclones, or El Nino phenomena, and the related extreme rainfalls. Most importantly, these would be the only historic floods comparable in magnitude to those needed to explain the large channels common to "Deweyville" surfaces on hydraulic geometry grounds alone. As outlined above, it seems unlikely that tropical flood-generating mechanisms would have been significant during the glacial period. By contrast, precipitation from midlatitude cyclones, common to Spring and Fall months during the late Holocene, produces frequent moderate magnitude floods. We suggest such storms were the dominant flood-producing mechanism during the glacial period, and frequent moderate magnitude floods dominated "Deweyville" discharge regimes.

Regardless of meteorological cause, flood peaks, as contrasted with flood volume, are conditioned by rates at which precipitation is converted to discharge, which in turn reflects vegetation cover, soil mantles, and other landscape characteristics. For the Edwards Plateau, source region for the Colorado, Guadalupe, and Nueces Rivers, rates at which runoff was transferred to stream channels would have been at a minimum through the glacial period when uplands were covered by deep soils and a good vegetation cover, and a maximum during the Holocene interglacial when the bedrock landscape was exposed. By comparison, holding flood volume constant, glacial period discharge hydrographs would have been less peaked and more broad-based than those characteristic of the Holocene. Hence, not only were extreme flood-generating mechanisms less likely during the glacial period, but rates of runoff and resultant flood hydrographs were conditioned by upland landscape stability, and flood peaks should have been smaller and more broad-based than today (less flashy).

Sedimentary facies typical of "Deweyville" allostratigraphic units also suggest extreme floods were unimportant during their formative period. The paucity of vertical accretion facies indicates that most floods remained within bankfull channel perimeters, overbank flooding was a rare to non-existent occurrence, and "Deweyville" floodplains were constructed by lateral accretion and migration of point bars and channels. This contrasts with the late Holocene, with flashy floods that exceed bankfull channels, floodplain construction by vertical accretion and avulsion, and thick successions of fine-grained vertical accretion facies (Blum and Valastro, 1994). Waters and Nordt (1995) suggest similar changes in processes of floodplain construction for the Brazos River near College Station.

The absence of vertical accretion facies, and the inferred absence of overbank floods, may help explain the enigmatic large Deweyville channels. Examination of curves that relate discharge characteristics to channel geometry, upon which many empirical hydraulic geometry equations are based (e.g. Carlston, 1965; Dury, 1965), shows considerable variability in meander geometry for a given discharge. This may reflect largely on the influence of bank-stabilizing muds (see Schumm, 1960; 1969), with higher than average meander wavelengths and radii of curvature reflecting a lack of muds in floodplain settings, and lower values reflecting muddy systems. More recent thinking on floodplain processes support these views, as Brackenridge (1988) argues the thickness of vertical accretion facies is related to flashiness of the discharge regime.

In sum, we suggest that channels on Deweyville terraces may reflect hydraulic adjustments to the absence of bank-stabilizing muds, which in turn reflects an absence of deep and flashy overbank floods through the isotope stage 4, 3, and 2 glacial. Smaller channel dimensions on Holocene floodplains may simply reflect the presence of bank-stabilizing muds, which in turn may result from the deep, flashy overbank floods characteristic of the present interglacial.

Role of Glacio-Eustasy and Base Level Change

"Deweyville" allostratigraphic units extend farther upstream than the influence of base level changes during the last glacio-eustatic cycle, so their fundamental characteristics must be attributed to other causes, perhaps those outlined above. Nevertheless, base level changes played a major role in shaping the geomorphic and stratigraphic framework in downstream reaches of valleys on the present-day coastal plain. Post-Beaumont valleys initially formed in response to sea level lowering below isotope stage 5 interglacial positions, when channels incised Beaumont alluvial plains, and extended across the newly subaerial shelf. Glacial period rivers then flowed through a series of laterally-confined valleys, with channels extended to shorelines in mid-shelf or farther basinward positions (see Suter and Berryhill, 1985; Suter, 1987; Anderson et al., 1992; Thomas, 1990; Thomas and Anderson, 1994). However, this long-term degradational mode was punctuated by multiple

"Deweyville" episodes of lateral migration and/or minor aggradation with sediment storage, followed by renewed valley incision with terrace formation. With post-glacial sea-level rise, the lower reaches of coastal plain rivers switched from degradational to aggradational modes, with progressive onlap of "Deweyville" profiles by Holocene deposits.

In upstream reaches of the coastal plain, differences between "Deweyville" and Holocene depositional systems may be a function of changes in the climate system. But the volumetric significance of vertical accretion facies in downstream reaches of Holocene floodplains is greatly enhanced by a forced shortening of channels, flattening of longitudinal gradients, and forced storage of sediments in response to post-glacial sea level rise and shoreline trangression. Indeed channel shortening, valley aggradation, and reductions in depositional slope during late transgression and highstand has promoted avulsion and development of the anastamosing or distributary channel patterns seen in the lowermost reaches of modern-day streams. Low sediment yield basin fringe and smaller systems have yet to fill post-Beaumont incised valleys, so avulsion remains confined within the boundaries of the valley itself. At the other end of the spectrum, the high sediment yield Colorado River has filled its incised valley, and avulsed to reoccupy a Beaumont isotope stage 5 channel course (Blum, 1994; Blum and Valastro, 1994; Blum and Price, in press).

ACKNOWLEDGMENTS

Blum's recent research on "Deweyville" and other Texas Gulf Coastal Plain fluvial deposits has been supported by the National Science Foundation, the donors to the Petroleum Research Fund of the American Chemical Society, Exxon Production Research Company, Union Pacific Resources, and the Office of Research Development and Administration of Southern Illinois University. Morton's recent research on fluvial systems of the Texas Gulf Coastal Plain has been partly supported by the U.S. Geological Survey Coastal Geology Program and the National Science Foundation. We thank Dave Amsbury, John Suter, and GCAGS reviewer Whitney Autin for discussions or comments that clarified ideas presented in this paper.

REFERENCES

Alford, J. J. and Holmes, J. C., 1985, Meander scars as evidence of major climate changes in southeast Louisiana: Association of American Geographers Annals, v. 75, p. 395-403.

Anderson, J. B., Thomas, M. A., Siringin, F. P., and Smyth, W. C., 1992, Quaternary evolution of the Texas Coast and Shelf, *in* C. H. Fletcher III and J. F. Wehmiller, eds., Quaternary Coasts of the United States: Marine and Lacustrine Systems: Special Publication 48, Society for Sedimentary Geology. Tulsa. p. 253-265.

Aten, L. E., 1983, Indians of the Upper Texas Coast: New York, Academic Press.

Autin, W. J., 1992, Use of alloformations for definition of Holocene meanderbelts in the middle Amite River, southeastern Louisiana: Geological Society of America Bulletin, v. 104, p. 233-241.

Autin, W. J., Burns, S. F., Miller, B. J., Saucier, R. T. and Snead, J. J. , 1991, Quaternary geology of the Lower Mississippi Valley, *in* R. B., Morrison, ed. Quaternary Non-Glacial Geology of the Conterminous United States, v. K-2, The Geology of North America: Geological Society of North America, Boulder, Colorado. p. 547-582.

Barton, D. C., 1930, Surface geology of coastal southeast Texas: American Association of Petroleum Geologists Bulletin, v. 14, p. 1301-1320.

Bernard, H. A., 1950, Quaternary Geology of Southeast Texas: Unpublished Ph.D. Dissertation, Louisiana State University, Baton Rouge, Louisiana.

Bernard, H. A. and LeBlanc, R. J., 1965, Resume of the Quaternary Geology of the Northwestern Gulf of Mexico Province, *in* H. E. Wright and D. G Frey, eds., The Quaternary of the United States: Princeton, New Jersey, Princeton University Press. p. 137-185.

Bernard, H. A., Major, C. F., Parrott, B. S., and LeBlanc, R. J. Sr., 1970, Recent Sediments of Southeast Texas: Field Guide to the Brazos Alluvial-Deltaic Plain and the Galveston Barrier Island Complex: Guidebook 11, Bureau of Economic Geology, The University of Texas at Austin. Austin, Tx.

Blum, M. D., 1994, Genesis and architecture of incised valley fill sequences: a Late Quaternary example from the Colorado River, Gulf Coastal Plain of Texas, *in* P. Weimer and H. W. Posamentier, eds., Siliciclastic Sequence Stratigraphy: Recent Developments and Applications: American Association of Petroleum Geologists Memoir 58. p. 259-283.

Blum, M. D. and Valastro, S. Jr., 1994, Late Quaternary sedimentation, Lower Colorado River, Gulf Coastal Plain of Texas: Geological Society of America Bulletin. v. 106, pp. 1002-1016.

Blum, M. D., Toomey, R. S. III, and Valastro, S. Jr. , 1994, Fluvial response to Late Quaternary climatic and environmental change, Edwards Plateau of Texas: Paleogeography, Paleoclimatology, and Paleoecology. v. 108, pp. 1-21.

Blum, M. D. and Price, D. M., 1994, Glacio-eustatic and climatic controls on Pleistocene alluvial plain deposition, Texas Coastal Plain: Gulf Coast Association of Geological Societies Transactions, v. 44, p. 85-92.

Blum, M. D. and Price, D. M., in press, Pleistocene alluvial plain deposition in response to interacting glacio-eustatic and climatic controls, Gulf Coastal Plain of Texas. *in* Shanley, K. and McCabe, P., eds., Relative Role of Eustasy, Climate, and Tectonism in Continental Rocks: SEPM Special Publication.

Brackenridge, G. R., 1988, River flood regime and floodplain stratigraphy: p. 139-165 in Baker, V. R., Kochel, R. C., and Patton, P. C., eds., Flood Geomorphology: New York, John Wiley and Sons.

Brown, L. F., Brewton, J. L., McGowen, J. H., Evans, T. J., Fisher, W. L., and Groat, C. G., 1976, Environmental Geologic Atlas of the Texas Coastal Zone: Corpus Christi Area: Bureau of Economic Geology, University of Texas at Austin.

Carlston, C. W., 1965, Relation of free meander geometry to discharge and its geomorphic implications: American Journal of Science, v. 263, p. 864-885.

Chappell, J. and Shackleton, N. J., 1986, Oxygen isotopes and sea level: Nature, v. 324, p. 137-140.

Doering, J. A., 1935, Post-Fleming surface formations of southeast Texas and south Louisiana: American Association of Petroleum Geologists Bulletin, v. 19, p. 651-688.

Doering, J. A., 1956, Review of Quaternary surface formations of the Gulf Coast Region: American Association of Petroleum Geologists Bulletin, v. 40, p. 1816-1862.

DuBar, J. R., Ewing, T. E., Lundelius, E. L., Otvos, E. G., and Winker, C. D., 1991, Quaternary geology of the Gulf of Mexico Coastal Plain, *in* R. B. Morrison, ed., Quaternary Non-Glacial Geology of the Conterminous United States: Boulder, Colorado, Geology of North America Volume K-2, Geological Society of America. p. 583-610.

Duessan, A., 1914, Geology and Underground Waters of the Southeastern Part of the Texas Coastal Plain, United States Geological Survey Water Supply Paper 335, Washington.

Duessan, A., 1924, Geology of the Coastal Plain of Texas west of Brazos River: United States Geological Survey Professional Paper 126, Washington.

Dury, G. H., 1965, Principles of Underfit Streams: Professional Paper 452-A, United States Geological Survey, Washington.

Fisher, W. L., McGowen, J. H., Brown, L. F. Jr., and Groat, C. G., 1972, Environmental Geologic Atlas of the Texas Coastal Zone: Galveston - Houston Area: Bureau of Economic Geology, University of Texas at Austin.

Fisk, H. N., 1944, Geological Investigations of the Alluvial Valley of the Lower Mississippi River: Mississippi River Commission, US Army Corps of Engineers, Vicksburg, Mississippi.

Gagliano, S. M and Thom, B. G., 1967, Deweyville terrace, Gulf and Atlantic coasts: Coastal Studies Bulletin 1, Louisiana State University, p. 23-41.

Gagliano, S. M., 1991, Late Quaternary Deweyville interval superfloods: Gulf Coasat Association of Geological Societies Transactions, v. 41, p. 298.

Galloway, W. E., 1981, Depositional architecture of Cenozoic Gulf Coastal Plain fluvial systems. pp. 127-156 *in* Ethridge, F. G. and Flores, R. M., eds., Recent and Ancient Non-Marine Depositional Environments: Special Publication 31, Society of Economic Paleontologists and Mineralogists. Tulsa, Oklahoma.

Hayes, C. W. and Kennedy, W., 1903, Oil Fields of the Texas-Louisiana Gulf Coastal Plain: United States Geological Survey Bulletin 213, Washington, D. C.

Hill, R. T. and Vaughn, T. W., 1897, Geology of the Edwards Plateau and Rio Grande Plain Adjacent to Austin and San Antonio, Texas, with Reference to the Occurrence of Groundwaters: Annual Report 18, United States Geological Survey, Washington, D. C.

Hill, R. T. and Vaughn, T. W., 1902, Description of the Austin Quadrangle: Atlas Folio 76, United States Geological Survey, Washington, D. C.

Hobgood, J. S. and Cerveny, R. S., 1988, Ice-age hurricanes and tropical storms: Nature, v. 333, p. 243-245.

Knox, J. C., 1983, Responses of river systems to Holocene climates. *in* H. E. Wright and S. C. Porter, eds., Late Quaternary Environments of the United States: Volume 2, The Holocene. Minneapolis. University of Minnesota Press. p. 26-41.

McGowen, J. H., Brown, L. F., Evans, T. J., Fisher, W. L., and Groat, C. G., 1975, Environmental Geologic Atlas of the Texas Coastal Zone: Bay City-Freeport Area: Bureau of Economic Geology, University of Texas at Austin.

McGowen, J. H., Proctor, C. V., Brown, L. F., Evans, T. J., Fisher, W. L., and Groat, C. G., 1976, Environmental Geologic Atlas of the Texas Coastal Zone: Port Lavaca Area: Bureau of Economic Geology, University of Texas at Austin.

Morton, R. A. and McGowen, J. H., 1980, Modern Depositional Environments of the Texas Coast: Guidebook 20, Bureau of Economic Geology, University of Texas at Austin.

Morton, R. A. and Price, W. A., 1987, Late Quaternary sea-level fluctuations and sedimentary phases of the Texas Coastal Plain and shelf, *in* D. Nummedal and O. H. Pilkey, eds., Sea Level Fluctuations and Coastal Evolution: SEPM Special Publication No. 15, p.181-198.

North American Commission on Stratigraphic Nomenclature, 1983, The North American Stratigraphic Code: American Association of Petroleum Geologists Bulletin, v. 67, p. 841-875.

Pearson, C. E., Kelley, D. B., Weinstein, R. A., and Gagliano, S. M., 1986, Archaeological Investigations on the Outer Continental Shelf: A Study within the Sabine River Valley, Offshore Louisiana and Texas: Coastal Environments Inc., Report to the Minerals Management Service, United States Department of the Interior.

Porter, S. C., 1989, Some geological implications of average Quaternary glacial conditions. Quaternary Research, v. 32, p. 245-262.

Price, W. A., 1933, Role of diastrophism in topography of Corpus Christi area, Texas: American Association of Petroleum Geologists Bulletin, v. 17, p. 205-250.

Price, W. A., 1958, Sedimentology and Quaternary geomorphology of South Texas: Gulf Coast Association of Geological Societies Transactions, v. 8, p. 43-75.

Saucier, R. T. and Fleetwood, A. R., 1970, Origin and chronologic significance of Late Quaternary terraces, Quachita River, Arkansas and Louisiana: Geological Society of America Bulletin, v. 81, p. 869-890.

Schumm, S. A., 1960, The Shape of Alluvial Channels in Relation to Sediment Type: Professional Paper 352-B, United States Geological Survey, Washington, D. C.

Schumm, S. A., 1969, River metamorphosis: Proceedings of the Journal of the Hydraulics Division, American Society of Civil Engineers, v. 95, p. 255-273.

Thomas, M. A., 1990, The Impact of Long-Term and Short-Term Sea Level Change on the Evolution of the Wisconsinan-Holocene Trinity/Sabine Incised Valley System, Texas Continental Shelf: Unpublished Ph.D. Dissertation, Rice University, Houston, TX.

Thomas, M. A. and Anderson, J. B., 1994, Sea level controls on the facies architecture of the Trinity/Sabine incised valley system, Texas Continental Shelf. *in* R. M. Dalrymple, R. Boyd, and B. A. Zaitlin, eds., Incised Valley Systems: Origins and Sedimentary Sequences: SEPM Special Publication 51, p. 63-82.

Toomey, R. S. III, Blum, M. D., and Valastro, S. Jr., 1993, Late Quaternary climates and environments of the Edwards Plateau, Texas: Global and Planetary Change, v. 7, p. 299-320.

Waters, M. R. and Nordt, L. C., 1995, Late Quaternary floodplain history of the Brazos River in east-central Texas: Quaternary Research, v. 43, p. 311-319.

Wendland, W. M., 1977, Tropical storm frequencies related to sea-surface temperatures: Journal of Applied Meteorology, v. 16, p. 477-481.

White, K. L. and Wiegand, K. C., 1989, Geomorphic analysis of floodplain sand mounds, Navasota River, Texas: Bulletin of the Association of Engineering Geologists, v. 26, p. 477-500.

Williams, D. F., Thunnell, R. C., Tappa, E., Rio, D., and Raffi, I., 1988, Chronology of the Pleistocene oxygen isotope record, 0-1.88 million years before present: Paleogeography, Paleoclimatology, and Paleoecology, v. 64, p. 221-240.

Winker, C. D., 1979, Late Pleistocene Fluvial-Deltaic Deposition on the Texas Coastal Plain and Shelf: Unpublished MA Thesis, University of Texas at Austin, Austin, Texas.

Wolman, M. G. and Miller, J. P., 1960, Magnitude and frequency of forces in geomorphic processes: Journal of Geology, v. 68, p. 54-74.

Wolman, M. G. and Gerson, R., 1978, Relative scales of time and effectiveness of climate in watershed geomorphology: Earth Surface Processes, v. 3, p. 189-208.

FIGURE CAPTIONS

Figure 1. Geologic map of the Texas Coastal Plain between Sabine and Nueces Rivers, illustrating principal fluvial axes, the distribution of Lissie and Beaumont alluvial plain strata, and post-Beaumont valleys (simplified from DuBar et al., 1991).

Figure 2. (a) Surficial geologic map of the lower Trinity valley. (b) Surficial geologic map of the lower Nueces valley. Maps illustrate distribution of high, intermediate, and low Deweyville terraces, plus low Deweyville channel scars (LD) now covered by thin veneers of Holocene floodplain or delta plain facies (Trinity valley). (c) Longitudinal profiles for the basin fringe Sabine, Neches, Trinity, and Nueces Rivers. B = Pleistocene Beaumont surface, HD = highest "Deweyville" terrace, ID = intermediate "Deweyville" terrace, LD = lowest "Deweyville" terrace, and HF = Holocene floodplain. For the Sabine, Neches, and Trinity, the lowest "Deweyville" profile coincides with, or dips below, the Holocene floodplain, and is not plotted separately.

Figure 3. (a) Surficial geologic map of the lower Colorado valley between Columbus and Garwood, TX., illustrating distribution of Beaumont, "Deweyville", and Holocene landforms and deposits. Note that different "Deweyville" terraces have not been differentiated. (b) Long profiles of depositional surfaces in Colorado valley between Ellinger and Wharton, TX., illustrating onlap of "Deweyville" surfaces by deposits of Holocene age between towns of Eagle Lake and Garwood. Adapted from Blum and Valastro (1994).

Figure 4. Schematic valley cross-sections contrasting "Deweyville allostratigraphy" in different geomorphic settings along the Texas Coastal Plain, at similar distances updip from modern highstand shorelines. (a) Low-gradient basin fringe fluvial axis, where high and intermediate Deweyville surfaces remain as terraces, but low Deweyville surfaces occur at the same elevation as modern floodplains, and are veneered by floodplain / delta plain strata. (b) Steep-gradient basin fringe fluvial

axis, where low Deweyville surfaces remain as a terrace above modern floodplains until onlapped at modern bay-head deltas. (c) Extrabasinal fluvial axes, where all "Deweyville" surfaces have been onlapped and buried by Holocene strata, and post-Beaumont valleys are nearly filled. Relative scale of valley fill sequences as indicated. "Deweyville" allostratigraphic units are shown occurring on one side of the valley for illustration purposes only.

Figure 5. (a) Eustatic sea level curve inferred from oxogen isotopes for last 125 ky (adapted from Chappell and Shackleton, 1986), with shaded area representing inferred depths of -15 to -65 m below present. (b) Schematic illustration of differences between interglacial highstand, intermediate glacial period, and full-glacial lowstand shoreline positions. As in Figure 5a, shaded area represent depths of -15 to -65 m below present. Based in part on J. R. Suter (pers. communication, 1995).

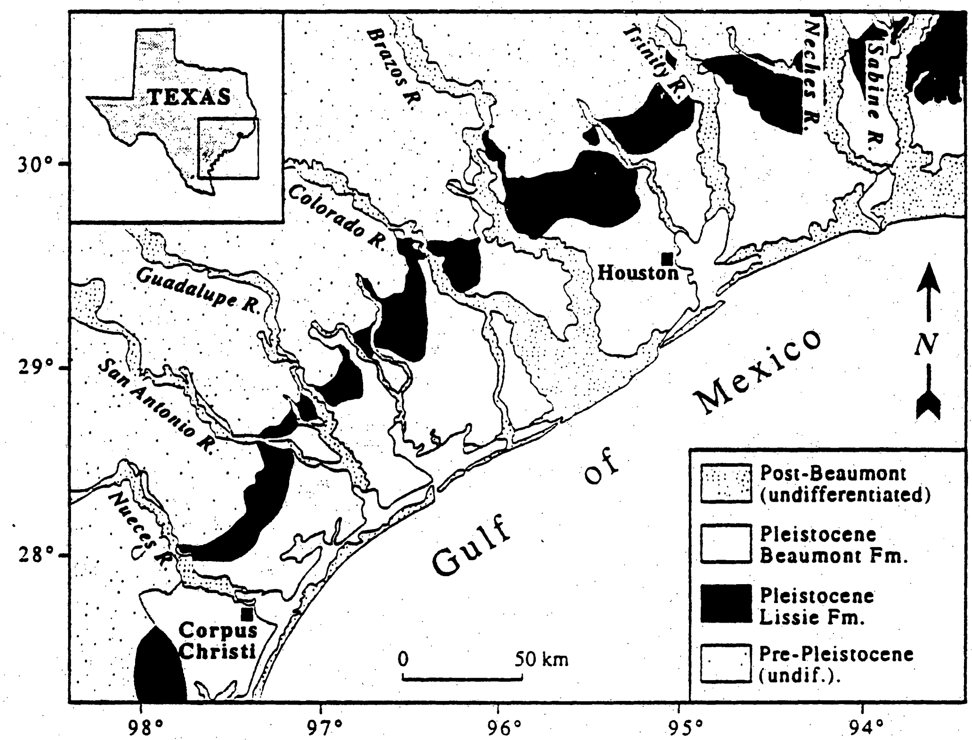

Blum et al. - Fig. 1

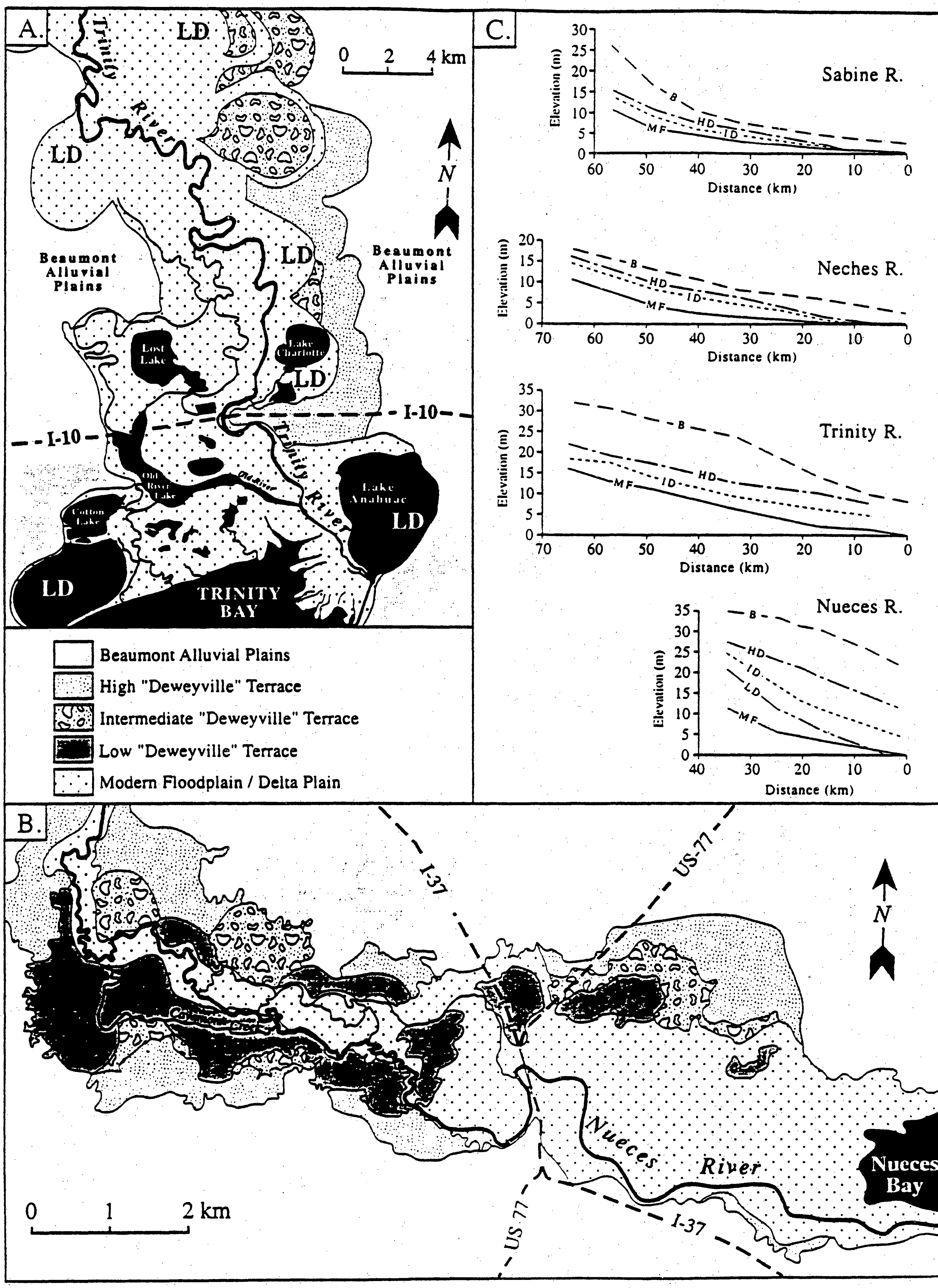

Blum et al. Fig. 2

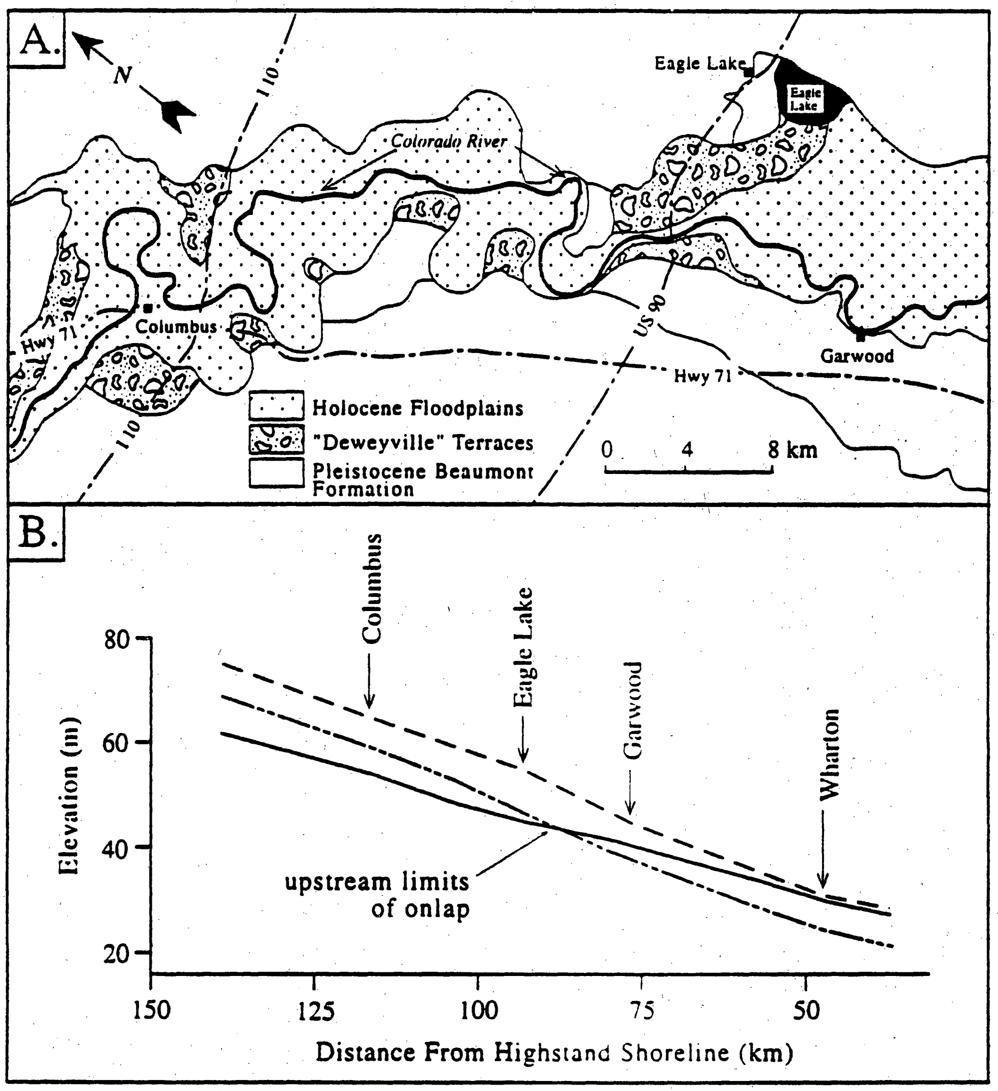

Blum et al. - Fig. 3

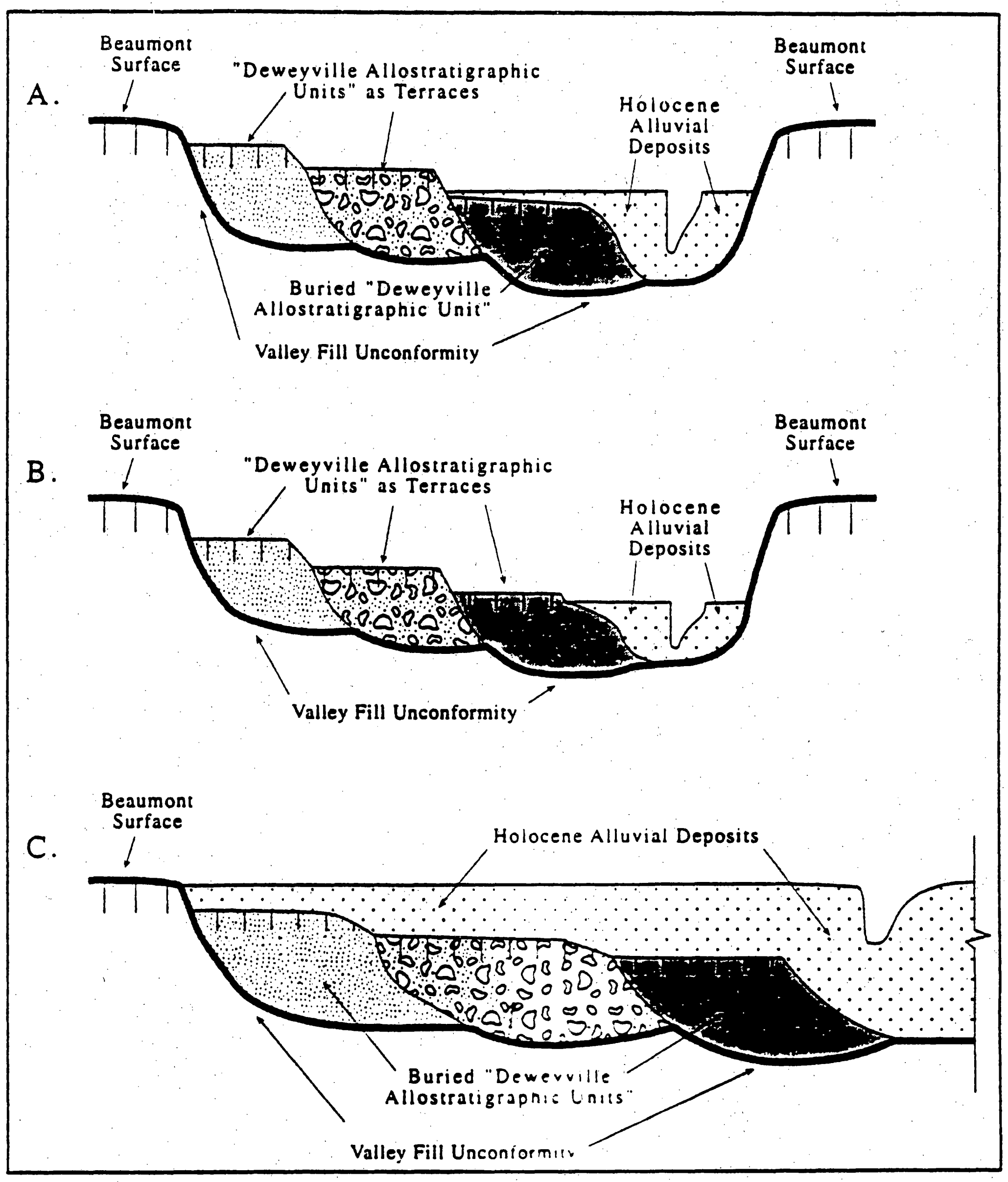

Blum et al. - Fig. 4

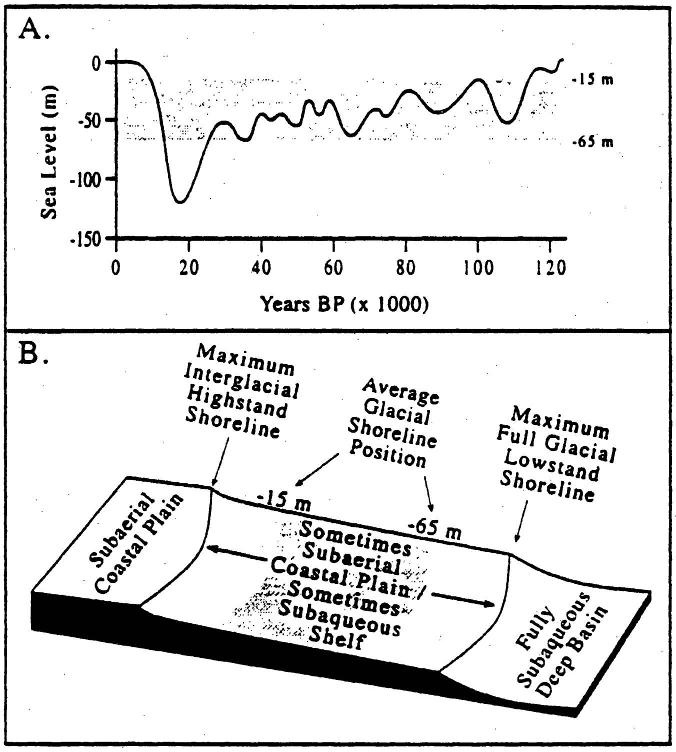

Blum et al. - Fig. 5

Addendum 7. Descriptions of Vibracores, Sabine Lake

CORE LOG

CORE # SLV-1(F) TYPE Vibracore LOCATION Sabine Lake - Fort Pass & Black Bayou
LATITUDE [illegible] LONGITUDE [illegible] SURFACE ELEVATION -5'
DEPTH PENETRATED ? LENGTH RECOVERED [illegible] %COMPACTION [illegible]

OBTAINED BY [illegible] Jones DATE 10-17-94
DESCRIBED BY [illegible] DATE [illegible]

DEPTH (ft, m)	SKETCH	LITHOLOGY	STRUCTURE	REMARKS

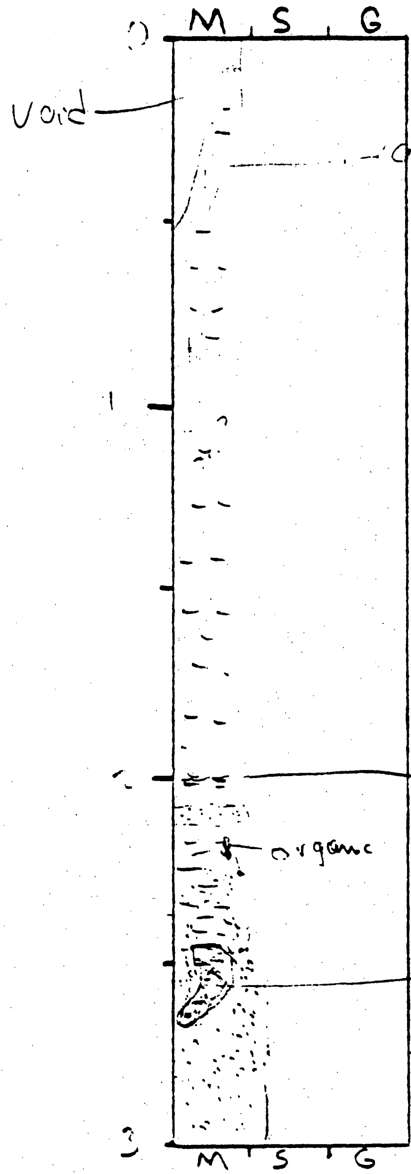

v soft mud, organic rich

organics (plant fragments)

alternating layers of Lt Olive gray and Olive gray with brownish black organics

organics more abundant above 1.2' and below 2'

v soft mud with scattered disseminated organics

organics

muddy sand

organics increase again below 2'

mud

sandy mud

large wood fragment

f. sand, possible slightly muddy, a few organics, no shells

General Comments:

CORE LOG

CORE # SLV-1 (B) TYPE ______ LOCATION ______
LATITUDE ______ LONGITUDE ______ SURFACE ELEVATION ______
DEPTH PENETRATED ______ LENGTH RECOVERED ______ %COMPACTION ______

OBTAINED BY ______ DATE ______
DESCRIBED BY ______ DATE ______

DEPTH (ft, m)	SKETCH	LITHOLOGY	STRUCTURE	REMARKS

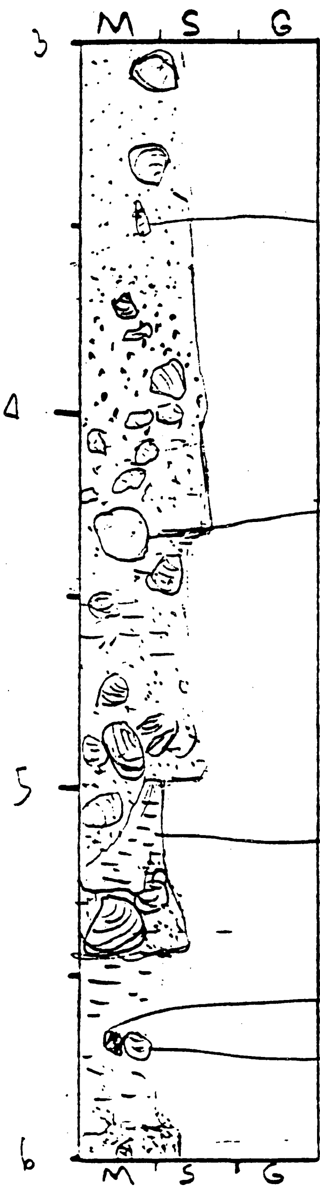

fine, slightly muddy, Sand — 2 Rangia shells — 3 ... gray 5Y/6 ...

wood fragment but exact original location uncertain

Coarse quartz sand, rangia shells from about 3.6 - 4.1' — Lt Olive gray ↑

This part of core was disturbed by splitter contents are difficult to pick.

fine sand and shells

large shell

organics associated with some shells

muddy, shelly, sand

muddy sandy shell, rangia (large) — Olive gray + Lt Olive

mud soft on right, muddy, sandy shell on left — 5Y 6/...

muddy sandy shell, rangia — Lt Olive gray to pale Olive gray to mud

soft mud, slightly sandy

wood chip

shell

muddy sand, one shell, scattered organics — Olive gray

General Comments:

CORE LOG

CORE # SLV-1 (C) TYPE ______ LOCATION ______
LATITUDE ______ LONGITUDE ______ SURFACE ELEVATION ______
DEPTH PENETRATED ______ LENGTH RECOVERED ______ %COMPACTION ______

OBTAINED BY ______ DATE ______
DESCRIBED BY ______ DATE ______

DEPTH (ft, m)	SKETCH	LITHOLOGY	STRUCTURE	REMARKS
6–9	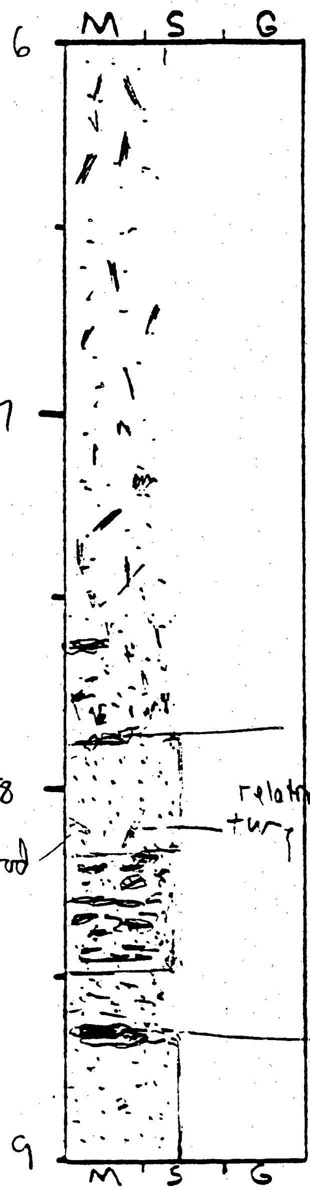	sand with abundant organics (wood chips) possibly slightly muddy		Lt Olive gray (5Y 6/1) with brownish black wood
				Detectable wood
		slightly muddy sd, abundant organics		
		wood		
		relatively clean med sand, few wood chips		yellowish gray
		turf		
		v. abundant organics (wood) woody sand		Lt Olive gray mottled with brownish black
		muddy sand wood fragments		
		sand, few organics		Lt Olive gray (5Y 6/1) to yellowish gray

General Comments:

CORE LOG

CORE # SLV-11D) TYPE ______ LOCATION ______
LATITUDE ______ LONGITUDE ______ SURFACE ELEVATION ______
DEPTH PENETRATED ______ LENGTH RECOVERED ______ %COMPACTION ______

OBTAINED BY ______ DATE ______
DESCRIBED BY ______ DATE ______

DEPTH (ft, m)	SKETCH	LITHOLOGY	STRUCTURE	REMARKS
9	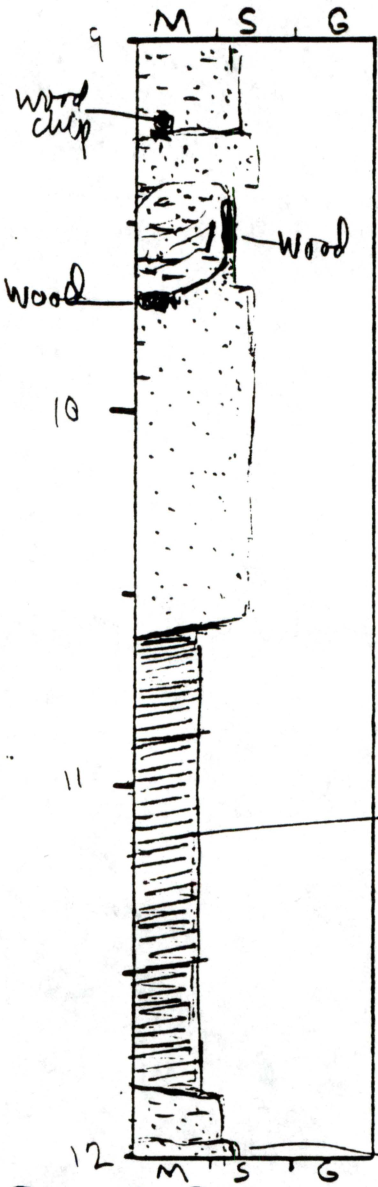	slightly muddy sand, a few organics		
		clean med sand yellowish gray		
		muddy sand		Dateable wood
10		med sand, clean, med. Lt gray to yellowish gray at top.		
11		all wood (Log cored)		W[illegible] moderate yellowish [illegible] brownish black at 11.15' to 11.25
		muddy sand Lt Olive gray		
12		slightly muddy sand		

General Comments:

CORE LOG

CORE # SLV-1 (E) TYPE ________ LOCATION ________________
LATITUDE ________ LONGITUDE ________ SURFACE ELEVATION ________
DEPTH PENETRATED ______ LENGTH RECOVERED ______ %COMPACTION ____

OBTAINED BY ______________________________ DATE ________
DESCRIBED BY ______________________________ DATE ________

DEPTH (ft, m)	SKETCH	LITHOLOGY	STRUCTURE	REMARKS

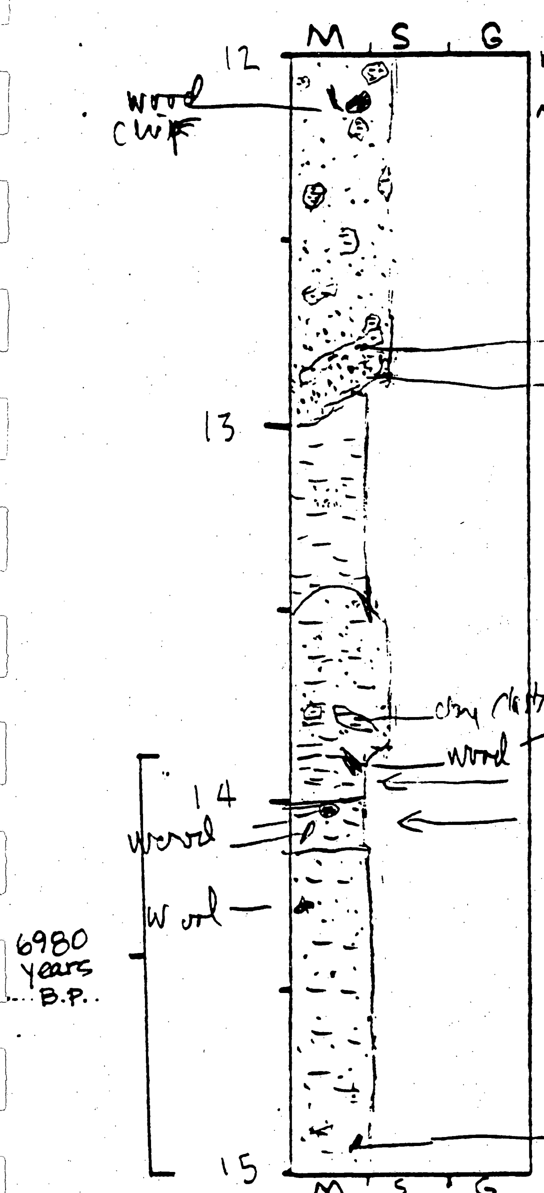

muddy sand, well sorted medium quartz grain — Lt gray to Lt Olive gray 5Y 6/1
clean except for occasional clay clast
some organics

clay clasts

coarse quartz sand, white to yellowish gray

clay — Lt Olive gray (5Y 6/1) to Pale Olive 10Y 6/2
— small amt of sand in pockets

clayey sand

datable

clay Lt Olive gray to Pale Olive (see above), some organics

clay medium gray, organics

sandy clay Lt greenish gray
occassional organics

wood

General Comments:

CORE LOG

CORE # SLV-1 (F) TYPE ________ LOCATION ________
LATITUDE ________ LONGITUDE ________ SURFACE ELEVATION ________
DEPTH PENETRATED ________ LENGTH RECOVERED ________ %COMPACTION ________

OBTAINED BY ________ DATE ________
DESCRIBED BY ________ DATE ________

DEPTH (ft. m)	SKETCH	LITHOLOGY	STRUCTURE	REMARKS
15–17	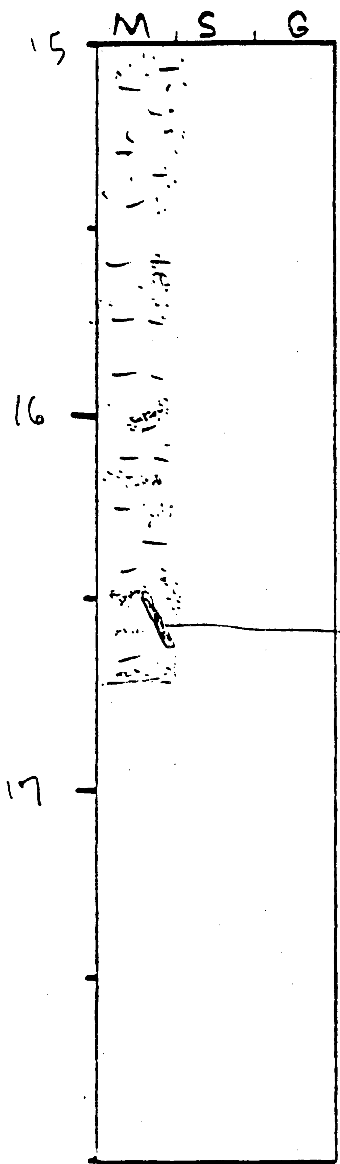	silty clay (or sandy) Clay with silt & sand in pockets plant fragment		Pale Olive to Lt Olive gray Lt Olive gray

General Comments:

CORE LOG

CORE # SLV-2(A) **TYPE** Vibracore **LOCATION** Sabine Lake
LATITUDE 29° 58.980 **LONGITUDE** 93° 46.700' **SURFACE ELEVATION** -19.5'
DEPTH PENETRATED ? **LENGTH RECOVERED** 17'0" **%COMPACTION** ?

OBTAINED BY Gibeaut - R/V Kit Jones **DATE** 10-8-94
DESCRIBED BY White **DATE**

DEPTH (ft, m)	SKETCH	LITHOLOGY	STRUCTURE	REMARKS
0		Soft mud or silty clay. Local organics disseminated w/ clay		Olive gray 5Y 4/1 mottled with Lt Olive gray 5Y 6/1
1				
2		darker brownish gray above sand zone		
		organic chip		
		F. sand (quartz ..., ... sorted, subrounded) Lt ... gray		
		muddy sand - ... and sand zones		Lt Olive gray
		wood chips (brownish ...)		
		F sand (99% quartz ... well sorted) Lt ... gray		
3				

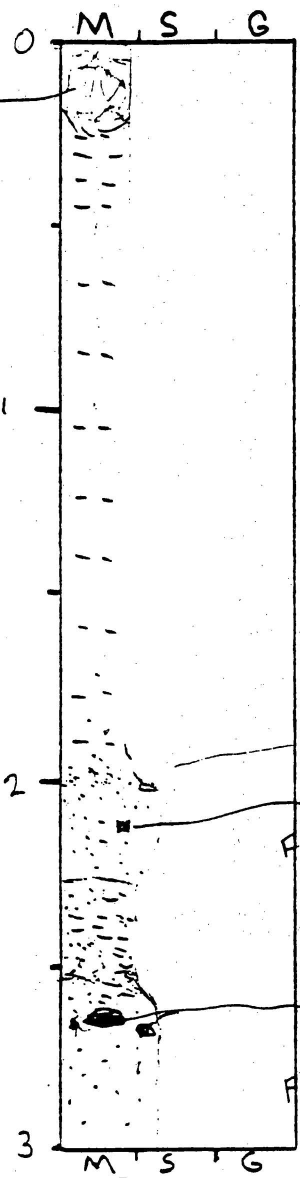

General Comments:

CORE LOG

CORE # SLV-2(B) TYPE ________ LOCATION ____________________
LATITUDE ________ LONGITUDE ________ SURFACE ELEVATION ________
DEPTH PENETRATED ______ LENGTH RECOVERED ______ %COMPACTION ____

OBTAINED BY ______________________________ DATE ________
DESCRIBED BY ______________________________ DATE ________

DEPTH (ft, m)	SKETCH	LITHOLOGY	STRUCTURE	REMARKS

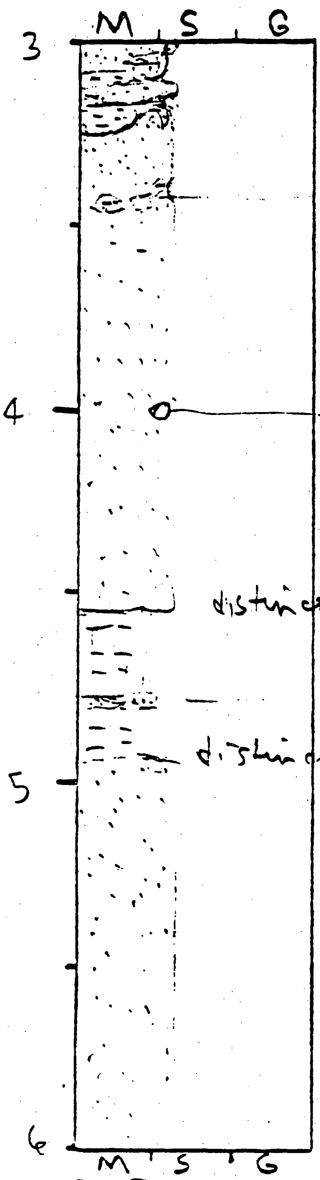

Interbedded sand & clay but possibly flattened clasts — Lt Olive gray 5Y 6/1 to yellowish gray in sand

Fine sand, quartz, well sorted, subrounded

— clay clasts

— shell (only one well worn (uncertain if this is proper depth because of disturbance of core along split margin)

distinct contact

clay Lt Olive gray with dark organic specks

— muddy sand layer

— distinct clay contact

Fine well sorted quartz sand
Lt Olive gray (5Y 6/1) to yellowish gray

General Comments:

CORE LOG

CORE # SLV-2(C) TYPE_____ LOCATION_____
LATITUDE_____ LONGITUDE_____ SURFACE ELEVATION_____
DEPTH PENETRATED_____ LENGTH RECOVERED_____ %COMPACTION_____

OBTAINED BY_____ DATE_____
DESCRIBED BY_____ DATE_____

DEPTH (ft, m)	SKETCH	LITHOLOGY	STRUCTURE	REMARKS

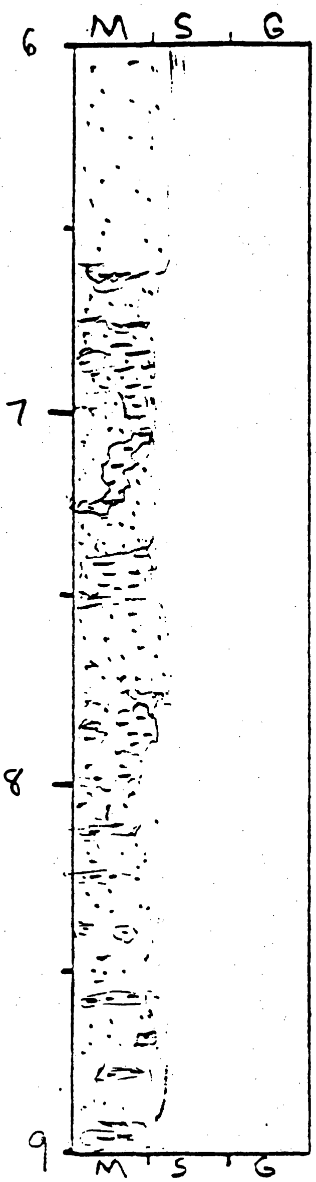

sand — Lt olive grey sand 5Y 6/1

some thin interbedding of clay & sand or possibly flattened clasts
clayey sand (common abundant than below)
clay clast, some questionable layers
Clay color is pale olive

Sand slightly muddy

muddy or clayey sand
discrete clay clasts — Lt Olive gray sand 5Y 6/1

Pale Olive Clay 10Y 6/2

General Comments:

CORE LOG

CORE # SLV-2(D) TYPE ________ LOCATION ________
LATITUDE ________ LONGITUDE ________ SURFACE ELEVATION ________
DEPTH PENETRATED ______ LENGTH RECOVERED ______ %COMPACTION ____

OBTAINED BY ________________________ DATE ________
DESCRIBED BY ________________________ DATE ________

DEPTH (ft, m)	SKETCH	LITHOLOGY	STRUCTURE	REMARKS
9	M S G	muddy or clayey sand (with distinct clasts of clay)		Lt Olive gray sand, clay slightly darker
10				
11		sandy clayey mud in muddy clayey sand		
12	M S G	sandy clayey mud		

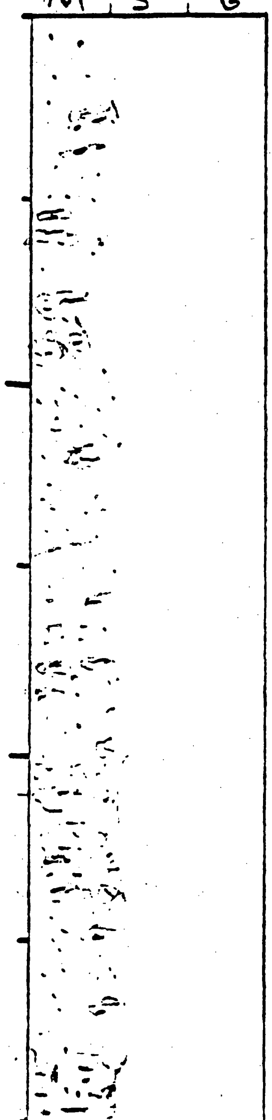

General Comments:

CORE LOG

CORE # SLV-2(E) TYPE ________ LOCATION ________
LATITUDE ________ LONGITUDE ________ SURFACE ELEVATION ________
DEPTH PENETRATED ________ LENGTH RECOVERED ________ %COMPACTION ________

OBTAINED BY ________ DATE ________
DESCRIBED BY ________ DATE ________

DEPTH (ft, m)	SKETCH	LITHOLOGY	STRUCTURE	REMARKS

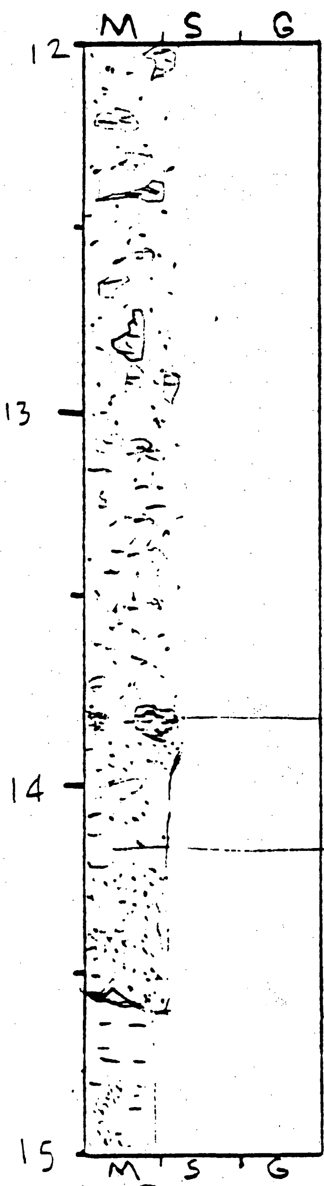

muddy (clayey) sand
scattered clay clasts

mottled with darker gray clay clasts in lt olive gray to yellowish gray sand

wood chips, (brownish black)

clay becoming more abundant below 14'

yellowish gray clay clasts from below

about equal amounts of sand & clay

sand? olive gray to lt olive gray

mottled color

sandy clay - yellowish gray clay splotchy with yellowish orange (Basement apparently)

General Comments:

CORE LOG

CORE # SLV-2(F) TYPE_____ LOCATION_____
LATITUDE_____ LONGITUDE_____ SURFACE ELEVATION_____
DEPTH PENETRATED_____ LENGTH RECOVERED_____ %COMPACTION_____

OBTAINED BY_____ DATE_____
DESCRIBED BY_____ DATE_____

DEPTH (ft, m)	SKETCH	LITHOLOGY	STRUCTURE	REMARKS

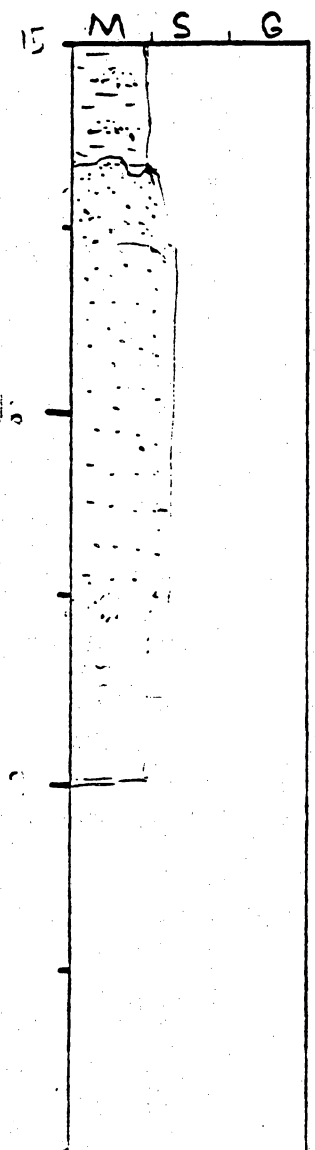

Sandy clay

Mottled Clay pale olive 10Y6/2 to yellowish green

darker olive gray sand pockets

Slightly muddy sand some darker organics

sand Lt Olive gray 5Y6/1) to Olive gray (5Y 4/1)

Medium sand, clean well sorted

yellowish grey (5Y 8/1

[illegible]

[illegible]

General Comments:

CORE LOG

CORE # SLV-3 (A) TYPE Vibracore LOCATION Sabine Lake
LATITUDE 29° 59.002' LONGITUDE 93° 46.617 SURFACE ELEVATION -6'
DEPTH PENETRATED ? LENGTH RECOVERED 17'9½" % COMPACTION ?

OBTAINED BY Gibeaut - R/V Kit Jones DATE 10-8-94
DESCRIBED BY White DATE 2-17-95

DEPTH (ft, m)	SKETCH	LITHOLOGY	STRUCTURE	REMARKS
0–3	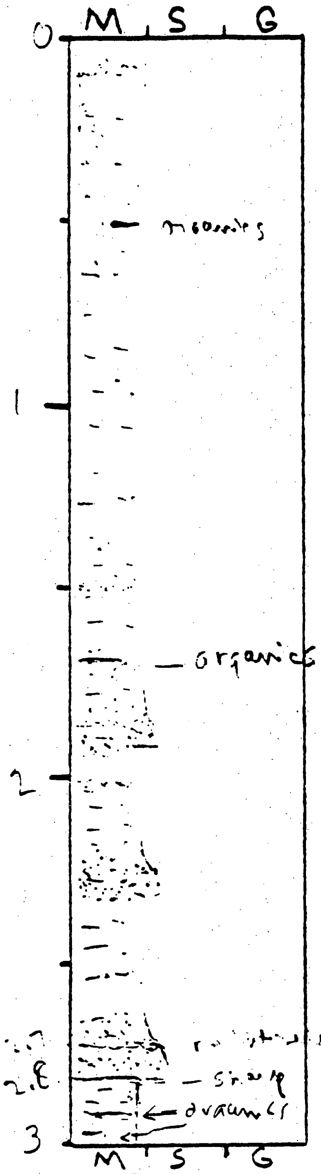	Primarily mud to sand, mud abundant organic flecks some thin discontinuous organic lenses	Distorted horizontal laminae	Alternating layers of Dark yellowish brown brownish gray and pale yellowish brown.
		Sand, muddy		
		Sand, muddy		
2.7		sharp contact at ... grading into muddy sand then		
2.8		Sand, clean, light gray in color		
		mud, organics		

General Comments:

CORE LOG

CORE # SLV-3(B) TYPE ______ LOCATION ______
LATITUDE ______ LONGITUDE ______ SURFACE ELEVATION ______
DEPTH PENETRATED ______ LENGTH RECOVERED ______ %COMPACTION ______

OBTAINED BY ______ DATE ______
DESCRIBED BY ______ DATE ______

DEPTH (ft, m)	SKETCH	LITHOLOGY	STRUCTURE	REMARKS

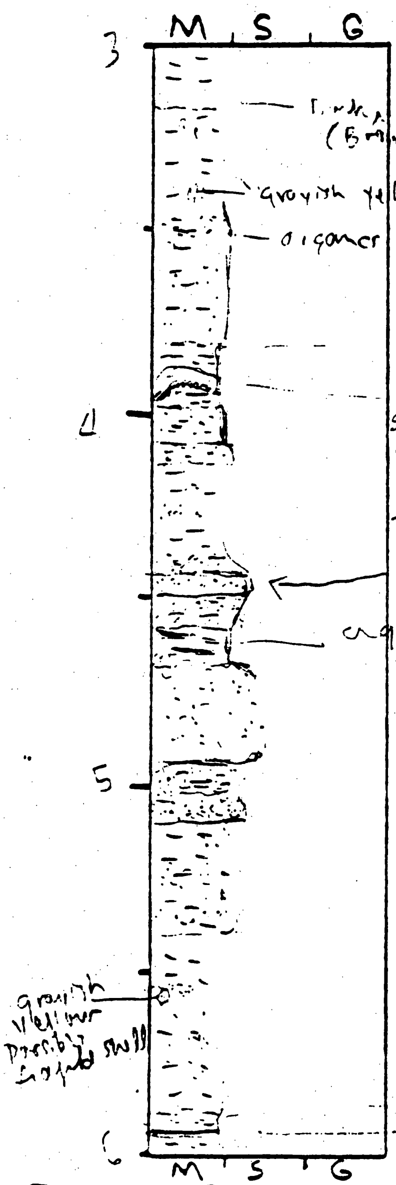

mud — Much of core Lt Olive gray in color (5Y 5/2) to Dark yellowish Brownish tint

Thin layer of mud (Brownish black), possibly organic rich, ~7mm in thickness

Grayish yellow objects, possibly fragile shell pieces.

organics — sandy mud

horizontal laminae apparent

mud — Dusky yellow to Lt Olive brown layer above thin brownish black layer

sandy mud

muddy sd

sandy mud

Relatively clean sand

muddy sand

organics — mud with organics some sand

clean sand

muddy sand

mud, slightly sandy

muddy sand — Lt Olive gray with dusky yellow mottling

mud, slightly sandy, Organic specks

Brownish black organic mud layer

General Comments:

CORE LOG

CORE # SLV-3(C) TYPE ______ LOCATION ______
LATITUDE ______ LONGITUDE ______ SURFACE ELEVATION ______
DEPTH PENETRATED ______ LENGTH RECOVERED ______ %COMPACTION ______

OBTAINED BY ______ DATE ______
DESCRIBED BY ______ DATE ______

DEPTH (ft, m)	SKETCH	LITHOLOGY	STRUCTURE	REMARKS

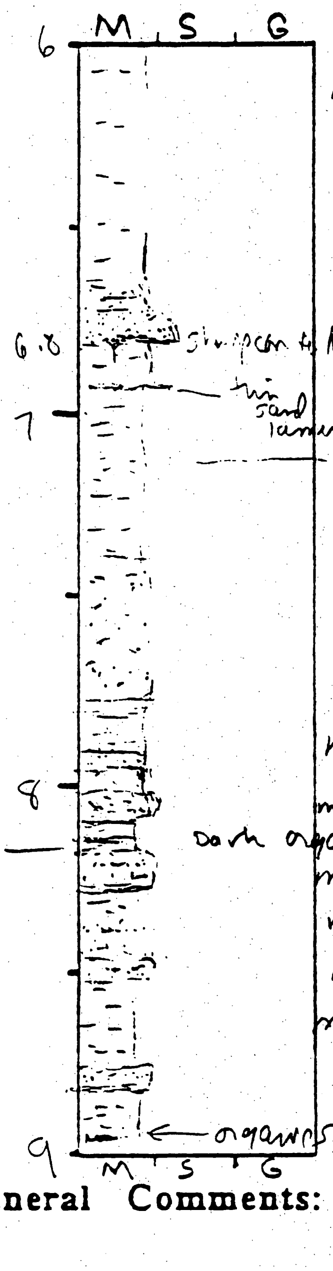

Lithology:

- mud with organics in horizontal lines
- sand grading upward into muddy sand; Brownish black organics at base of sand
- dusky yellow layer (mud)
- sandy mud to muddy sand
- mud slightly sandy alternate light olive gray & brownish black mud
- muddy sand
- Dark organic clay streak (mud)
- muddy sand
- mud with few horizontal sand layers
- muddy sand to sandy mud
- mostly mud
- sand layer
- mud

Structure: Obvious horizontal laminae

Remarks: Much of core Lt Olive gray 5Y 5/2 with alternating darker layers Olive gray (5Y 3/2) to Brownish black and locally Dusky yellow

General Comments:

CORE LOG

CORE # CLV-3(D) TYPE ______ LOCATION ______

LATITUDE ______ LONGITUDE ______ SURFACE ELEVATION ______

DEPTH PENETRATED ______ LENGTH RECOVERED ______ %COMPACTION ______

OBTAINED BY ______ DATE ______

DESCRIBED BY ______ DATE ______

DEPTH (ft, m)	SKETCH	LITHOLOGY	STRUCTURE	REMARKS
9		muddy sand		color mostly Lt Olive gray 5Y 5/2 with yellowish gray and brownish black alternating layers
		mud or clay organics		
	sharp contact			
	grayish yellow fragile material	F sand, well sorted, quartz, clean, yellowish gray		
	sharp contact			
		mud or clay, small silt or sand pocket	obvious horizontal lamina	
		muddy sand organics interlayered with clay		
10	organics	mud or clay, organics		sand layer yellowish gray
		dusky yellow clay layer		
	organics			
	relatively sharp contact			
		F sand, well sorted, clean	yellowish grey	
11	sharp contact	mud or clay		
		thin sandy layer		
	organics	mud or clay		
	sand pocket			
12				

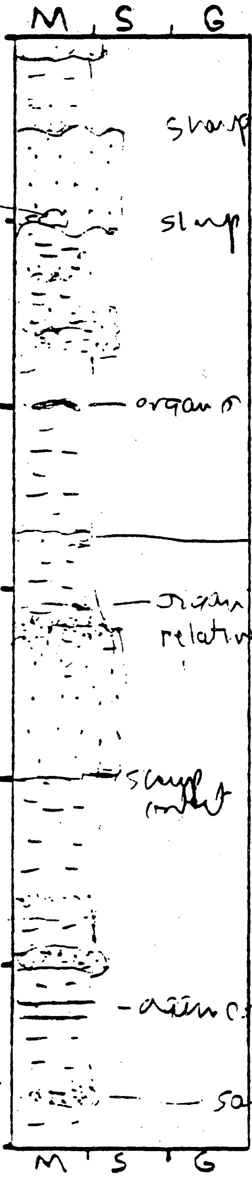

General Comments:

CORE LOG

CORE # SLV-3(E) TYPE______ LOCATION______
LATITUDE______ LONGITUDE______ SURFACE ELEVATION______
DEPTH PENETRATED______ LENGTH RECOVERED______ %COMPACTION______

OBTAINED BY______ DATE______
DESCRIBED BY______ DATE______

DEPTH (ft, m)	SKETCH	LITHOLOGY	STRUCTURE	REMARKS
12	M S G	mud or clay, organic lines & specks	horizontal laminae	alternating colors (horizontal) Lt olive gray to darker brownish black gray
		alternating thin layers of sand & mud		
13		sand		
		alternating thin layers of sand & mud		sand layers yellowish gray
		sand		
		mud with alternate layers with sand		
		F. sand, well sorted, clean quartz (yellowish gray); thin clay bars		
		mud or clay + some fragments; blue fragments		
14		F. sand, well sorted, clean (yellowish gray)		
		dusky yellow clay; streaks		
		mud or clay		
		muddy sand		
15	M S G	mud or clay		

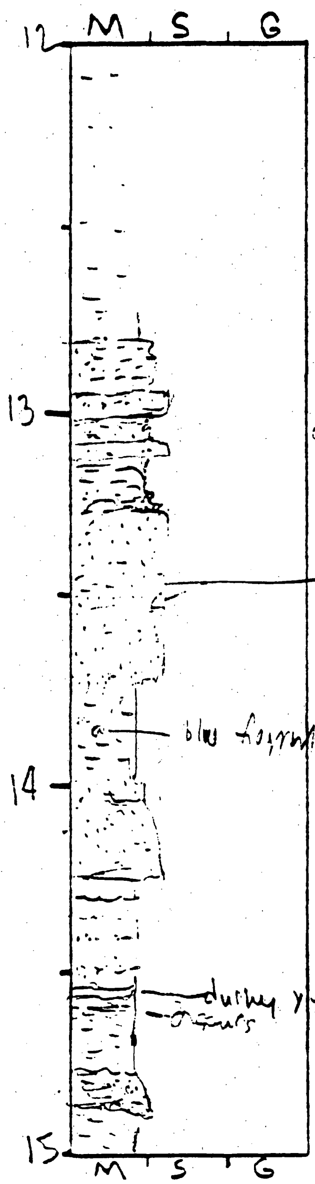

General Comments:

CORE LOG

CORE # SLV-3(F) TYPE ______ LOCATION ______
LATITUDE ______ LONGITUDE ______ SURFACE ELEVATION ______
DEPTH PENETRATED ______ LENGTH RECOVERED ______ %COMPACTION ______

OBTAINED BY ______ DATE ______
DESCRIBED BY ______ DATE ______

DEPTH (ft, m)	SKETCH	LITHOLOGY	STRUCTURE	REMARKS

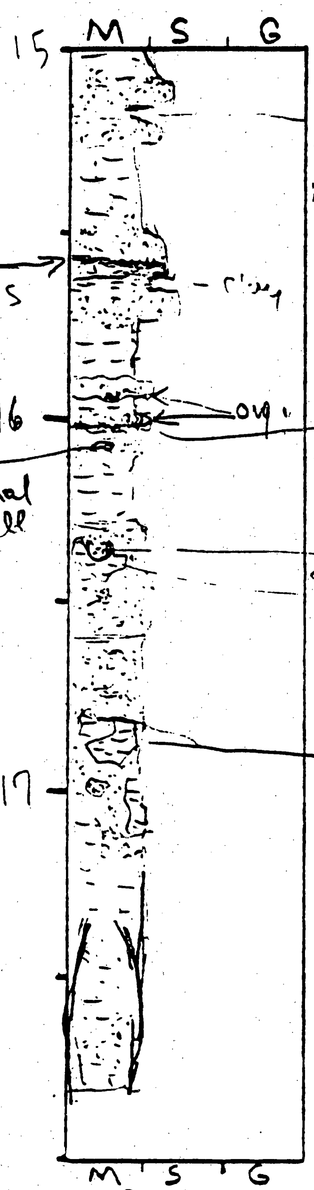

sandy mud
sand (gray)
mud layer
muddy sand
mud or fine slightly silty
muddy sand with organic material in layers alternating with clay
very clean fine sand, yellowish
mud or clay
muddy sand
mud
muddy organic sand
silty mud
mud or clay
clean yellowish sand in burrow
clay clast
muddy sand, gray clay clasts; olive gray sand
yellow clay clast from below (Beaumont)
Clay (Beaumont) yellowish gray to silty or sandy clay
becomes sandier near bottom

Lt olive gray with alternating lighter & darker layers

with mottled stains of dark yellowish orange.

General Comments:

CORE LOG

CORE # SLV-4(A) **TYPE** Vibracore **LOCATION** Sabine Lake - Power Plant channel
LATITUDE 29° 59.372' **LONGITUDE** 93° 53.990 **SURFACE ELEVATION** 5' 6"
DEPTH PENETRATED ? **LENGTH RECOVERED** 19' 1/2" **% COMPACTION** ?

OBTAINED BY Gibeaut - R/V Kit Jones **DATE** 10-8-94
DESCRIBED BY WB **DATE** 2-17-95

DEPTH (ft, m)	SKETCH	LITHOLOGY	STRUCTURE	REMARKS

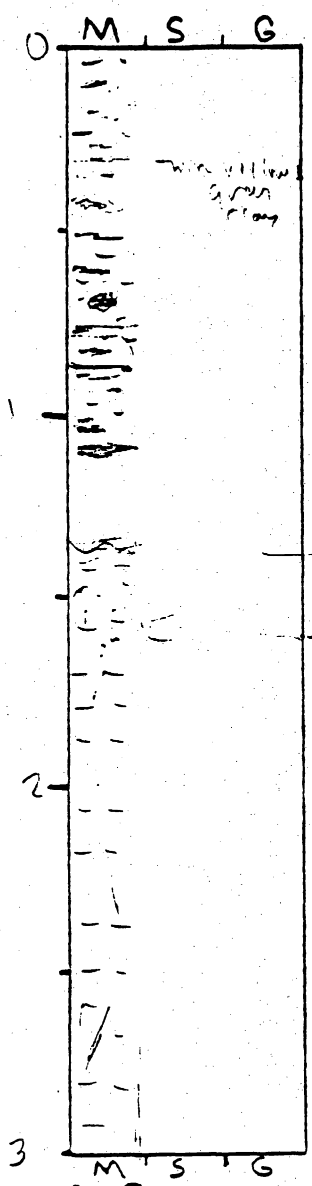

soft Organic rich mud and debris of various types

horizontal laminated

mottled Brownish Black except for isolated layers of yellowish gray clay

yellowish gray clay layer against

Near base of organic rich mud

Lt Olive gray clay becomes dominant

decreasing organic material

homogenous

Soft clay or mud scattered plant material (roots)

Lt Olive gray

sand yellowish gray

General Comments:

CORE LOG

CORE # SLV-4 (B) TYPE ________ LOCATION ________________________
LATITUDE ________ LONGITUDE ________ SURFACE ELEVATION ________
DEPTH PENETRATED ______ LENGTH RECOVERED ______ %COMPACTION ____

OBTAINED BY ______________________________ DATE ________
DESCRIBED BY ______________________________ DATE ________

DEPTH (ft, m)	SKETCH	LITHOLOGY	STRUCTURE	REMARKS

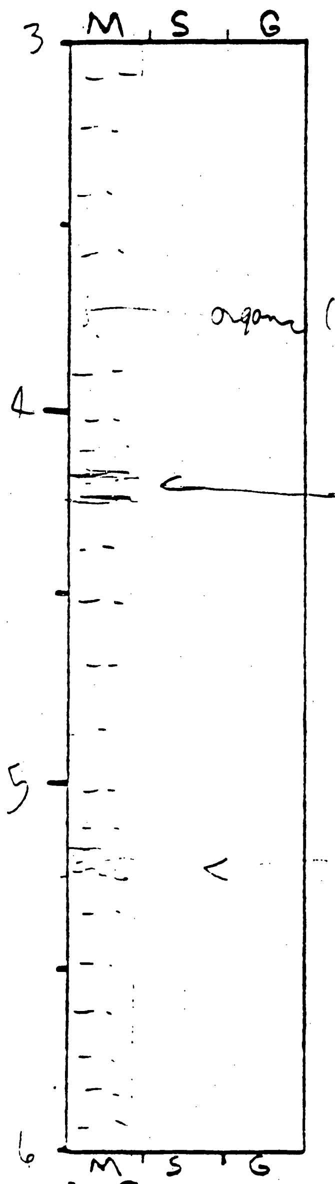

relatively homogeneous Lt Olive gray mud or silty clay

Lt Olive gray 5Y 6/1

Semi horizontal laminae

organic (plant frag)

yellowish gray clay layer thin silt laminae

yellowish gray clay layer (appear to have been offset by micro fault)

General Comments:

CORE LOG

CORE # SLV-4(C) TYPE______ LOCATION______
LATITUDE______ LONGITUDE______ SURFACE ELEVATION______
DEPTH PENETRATED______ LENGTH RECOVERED______ %COMPACTION______

OBTAINED BY______ DATE______
DESCRIBED BY______ DATE______

DEPTH (ft, m)	SKETCH	LITHOLOGY	STRUCTURE	REMARKS
6		soft Mud or Clay		Lt Olive gray 5Y 6/1 to 5Y 5/1
	organic (plant material)	thin silt laminas	faint horizontal laminae	
7		faint yellowish laminae		
	again this	faint yellowish laminae		
		Thin silt laminae interbedded with clay.		
8		thin silt laminae interbedded with clay		
9				

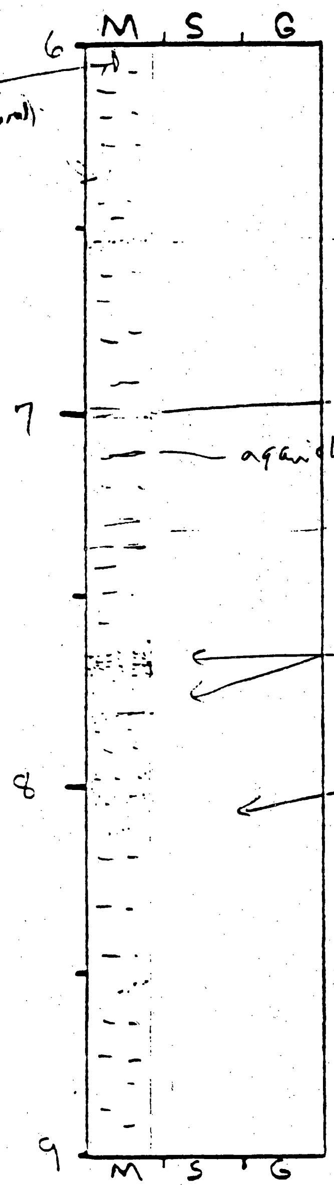

General Comments:

CORE LOG

CORE # SLV-4(D) TYPE______ LOCATION______
LATITUDE______ LONGITUDE______ SURFACE ELEVATION______
DEPTH PENETRATED______ LENGTH RECOVERED______ %COMPACTION______

OBTAINED BY______ DATE______
DESCRIBED BY______ DATE______

DEPTH (ft, m)	SKETCH	LITHOLOGY	STRUCTURE	REMARKS

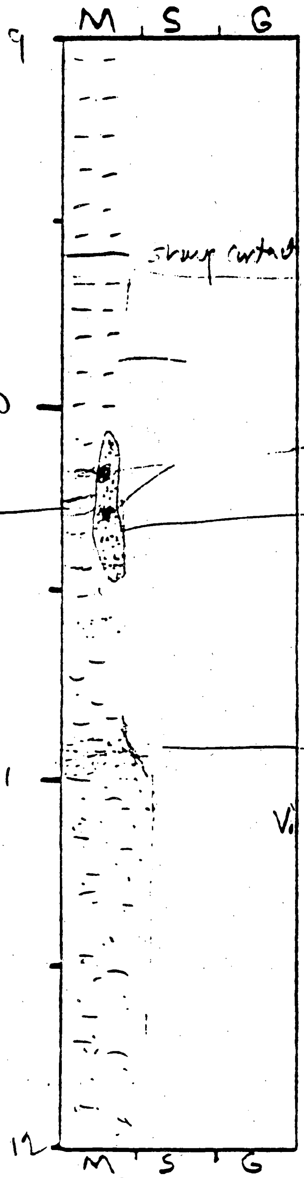

soft Lt olive gray mud, very homogeneous — Lt Olive Gray

sharp contact at top — yellowish gray layer (nodular clay)

— wood

(wood chips)
— sand & organics in burrow
small sorted clean yellowish sand
occasional thin silt laminae

yellowish grey clay layer

Clay Lt Olive gray

Sharp Color change → — organics abundant in base of clay & top of sand

V. muddy sand (dusky yellowish brown or olive black)

discrete sand & clay zones appears to be burrowed (No shells)

General Comments:

CORE LOG

CORE # SLV-4(E) TYPE ______ LOCATION ______
LATITUDE ______ LONGITUDE ______ SURFACE ELEVATION ______
DEPTH PENETRATED ______ LENGTH RECOVERED ______ %COMPACTION ______

OBTAINED BY ______ DATE ______
DESCRIBED BY ______ DATE ______

DEPTH (ft, m)	SKETCH	LITHOLOGY	STRUCTURE	REMARKS

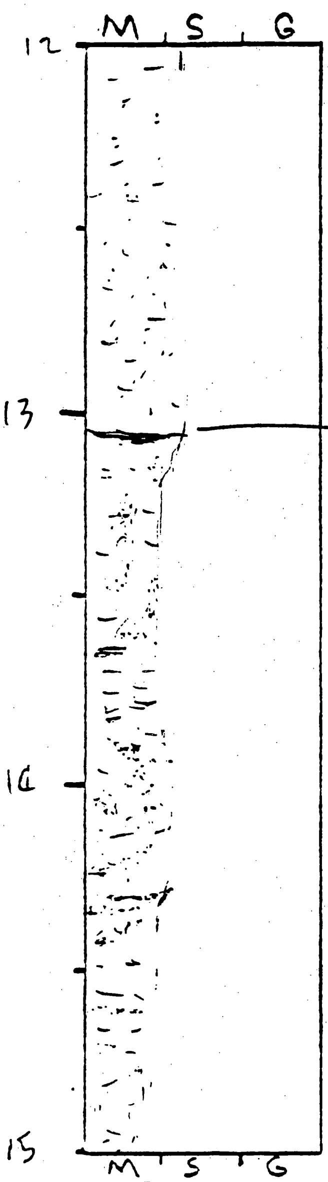

v. muddy sand — dusky yellowish brown to Olive black

organics

mud or clay
sand filled burrows in soft clay or mud

increase in disseminated black organics

abundant disseminated organics in soft mud with sand filled burrows. — Lt Olive grey (5Y 6/1) with dark mottling from organics

scattered organics

General Comments:

CORE LOG

CORE # SLV-4(F TYPE________ LOCATION____________________
LATITUDE________ LONGITUDE________ SURFACE ELEVATION________
DEPTH PENETRATED______ LENGTH RECOVERED______ %COMPACTION____

OBTAINED BY______________________________ DATE________
DESCRIBED BY______________________________ DATE________

DEPTH (ft, m)	SKETCH	LITHOLOGY	STRUCTURE	REMARKS

15

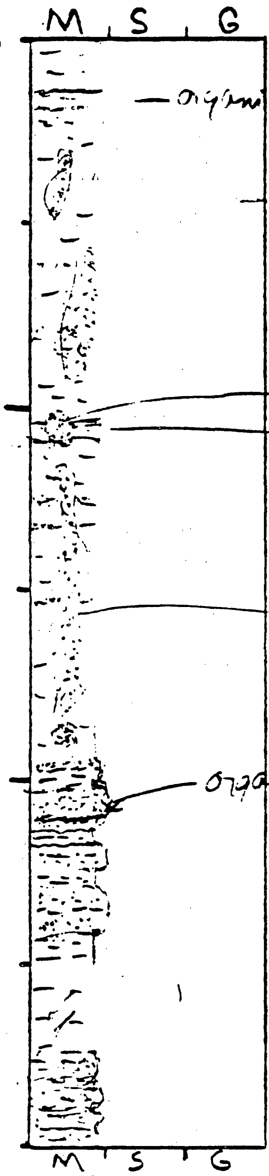

soft mud or clay organics — Lt olive grey

sand filled burrows

yellow sand in burrow

horizontal laminations, burrows

16

thin sand laminations

Lt olive grey

17

alternating layers of sand & clay — sand yellowish in color.

clay or mud, scattered organics — Lt olive grey

muddy sand (alternating layers of sand & clay) to sandy mud

18

General Comments:

CORE LOG

CORE # SLV-4 (G) TYPE______ LOCATION______
LATITUDE______ LONGITUDE______ SURFACE ELEVATION______
DEPTH PENETRATED______ LENGTH RECOVERED______ %COMPACTION______

OBTAINED BY______ DATE______
DESCRIBED BY______ DATE______

DEPTH (ft, m)	SKETCH	LITHOLOGY	STRUCTURE	REMARKS

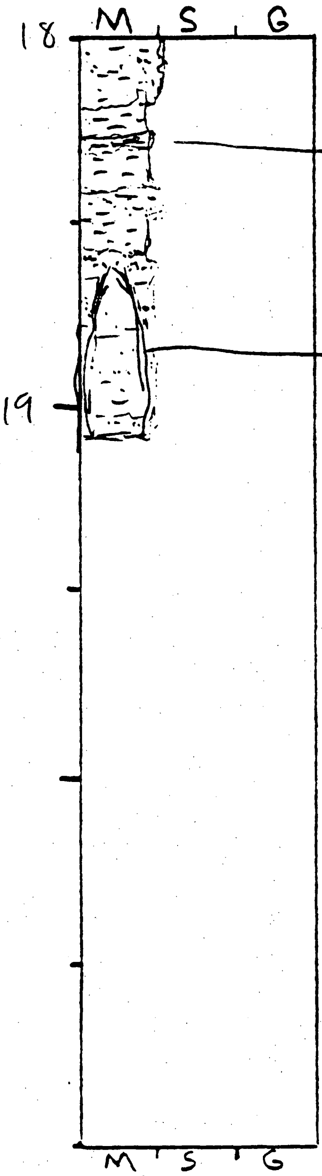

sandy mud — Olive gray

clay — possible ripple lamination — sand - - yellowish gray

organics, and thin silt layers in clay

clay

clayey sand

clay

clayey sand to sandy clay

core catcher — some oxidation stains Dark yellowish orange (possibly from core catcher)

General Comments:

CORE LOG

CORE # SLV-5 (A) **TYPE** Vibrocore **LOCATION** Sabine Lake - canal
LATITUDE 29° 59.957' **LONGITUDE** 93° 54.016' **SURFACE ELEVATION** -15'
DEPTH PENETRATED ? **LENGTH RECOVERED** 17' 3¾' **% COMPACTION** ?

OBTAINED BY Gibeaut - R/V Kit Jones **DATE** 10-8-94
DESCRIBED BY White **DATE** 2-20-94

DEPTH (ft, m)	SKETCH	LITHOLOGY	STRUCTURE	REMARKS
0	M S G	shelly muddy sand to shelly sandy mud with shell frags		moderate brown to dusky yellowish brown
	obscure contact	soft mud or clay scattered organics	burrowed in upper 1 ft.	
		sand filled burrow (dusky yellowish brown)		
1				Lt Olive gray 5Y6/1 with black organic inclusions (mottled)
		clay, abundant organic lines increasing with depth	distorted horizontal lamination of organic material in clay	
2		Darker clay with organics (med. dark gray) mottled with organics		
3	M S G	Lt Olive gray clay with blackish organics		

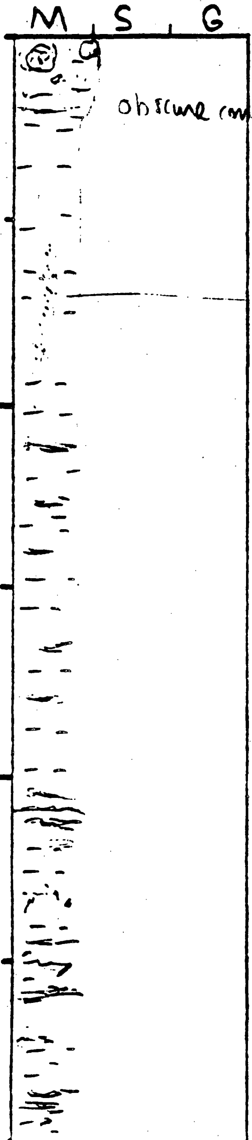

General Comments:

CORE LOG

CORE # SLV-5 (B) TYPE____ LOCATION____
LATITUDE____ LONGITUDE____ SURFACE ELEVATION____
DEPTH PENETRATED____ LENGTH RECOVERED____ %COMPACTION____

OBTAINED BY____ DATE____
DESCRIBED BY____ DATE____

DEPTH (ft, m)	SKETCH	LITHOLOGY	STRUCTURE	REMARKS

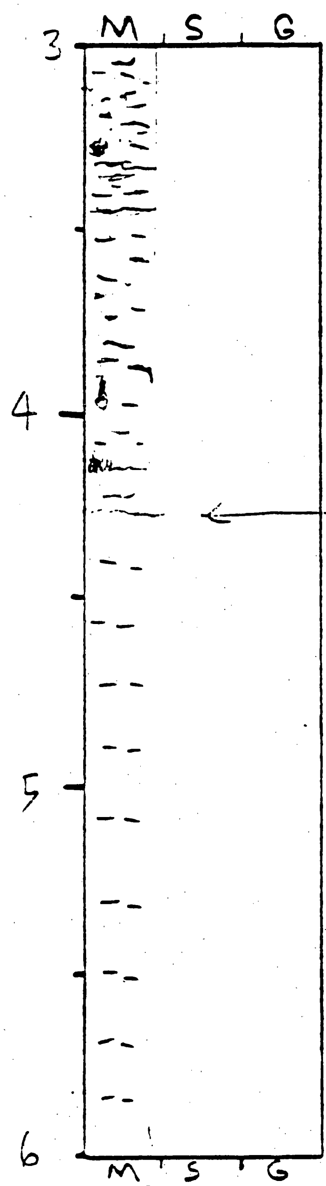

soft mud or clay with distorted laminations of black organics

5Y 6/1 Lt Olive gra with black org.

organics much less abundant below 4.3'

LT. olive gray clay (5Y 6/1) with scattered black organic specks

General Comments:

CORE LOG

CORE # SLV-5 (C) TYPE ______ LOCATION ______
LATITUDE ______ LONGITUDE ______ SURFACE ELEVATION ______
DEPTH PENETRATED ______ LENGTH RECOVERED ______ %COMPACTION ______

OBTAINED BY ______ DATE ______
DESCRIBED BY ______ DATE ______

DEPTH (ft, m)	SKETCH	LITHOLOGY	STRUCTURE	REMARKS

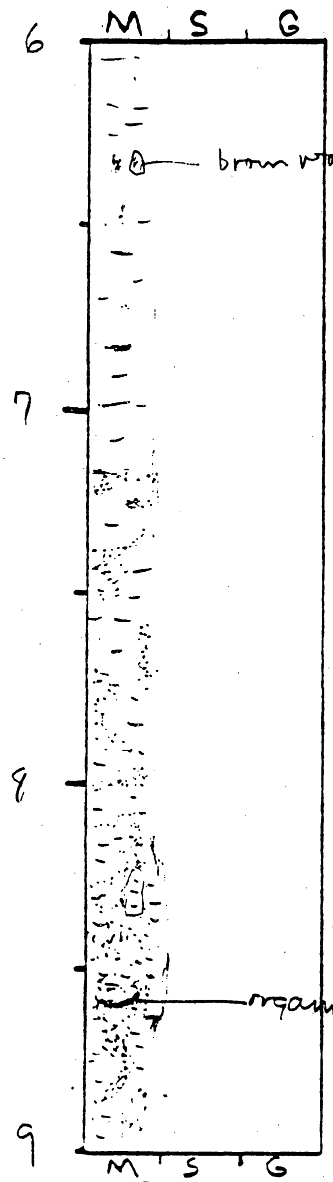

Lt Olive gray clay with scattered black organic specks

sandy mud (clay) — burrowed; sand filled burrows in soft clay — Lt Olive gray sand yellowish

(clayey) muddy sand

sandy clay — burrowed

General Comments:

CORE LOG

CORE # CLV-5(D) TYPE_____ LOCATION_____
LATITUDE_____ LONGITUDE_____ SURFACE ELEVATION_____
DEPTH PENETRATED_____ LENGTH RECOVERED_____ %COMPACTION_____

OBTAINED BY_____ DATE_____
DESCRIBED BY_____ DATE_____

DEPTH (ft, m)	SKETCH	LITHOLOGY	STRUCTURE	REMARKS

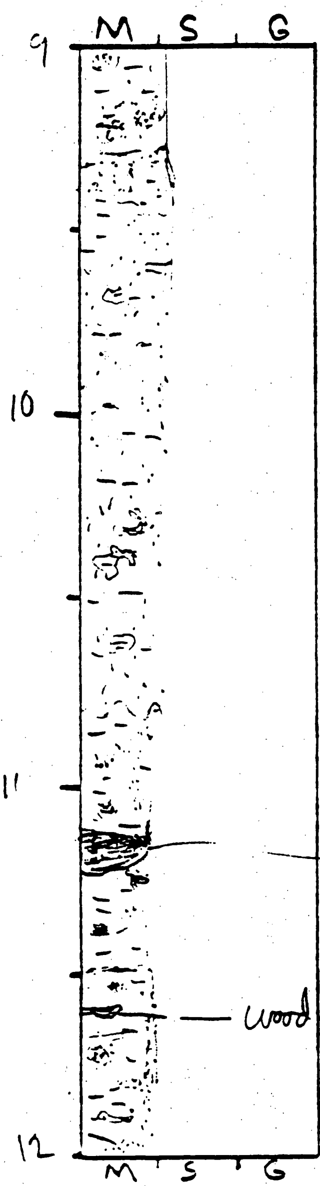

6730 years B.P.

sandy clay, burrowed — Lt Olive gray (5Y6/1)

clayey sand (mostly sand), discrete clay clasts, some scattered ? grains — Lt Olive gray (5Y 5/2)

burrowed

sandy clay

organic concentration brownish black,

slightly silty clay - Lt Olive gray (5Y 6/1)

wood chip — burrowed, organics

Dark gray sandy clay (sand in burrows, yellowish gray)

General Comments:

CORE LOG

CORE # SLV-5 (E) TYPE____ LOCATION____
LATITUDE____ LONGITUDE____ SURFACE ELEVATION____
DEPTH PENETRATED____ LENGTH RECOVERED____ %COMPACTION____

OBTAINED BY____ DATE____
DESCRIBED BY____ DATE____

DEPTH (ft, m)	SKETCH	LITHOLOGY	STRUCTURE	REMARKS

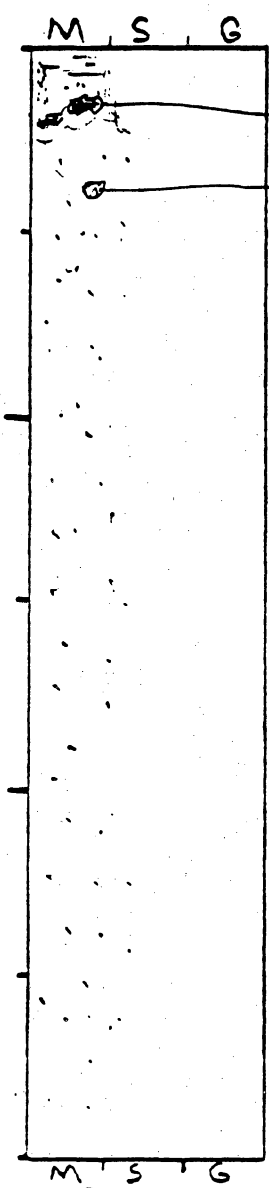

12 — Organic rich sandy clay — burrowed — Dark gray

wood

sand

wood chip, datable

13 — silty Sand, slightly clayey, Lt Olive gray to yellowish gray
some disseminated organics
Organics more abundant above 13'

14

Sand becomes lighter in color below. 14.8'

15

General Comments:

CORE LOG

CORE # SLV-5 (F) TYPE________ LOCATION____________
LATITUDE________ LONGITUDE________ SURFACE ELEVATION______
DEPTH PENETRATED______ LENGTH RECOVERED______ %COMPACTION____

OBTAINED BY____________________ DATE______
DESCRIBED BY____________________ DATE______

DEPTH (ft, m)	SKETCH	LITHOLOGY	STRUCTURE	REMARKS

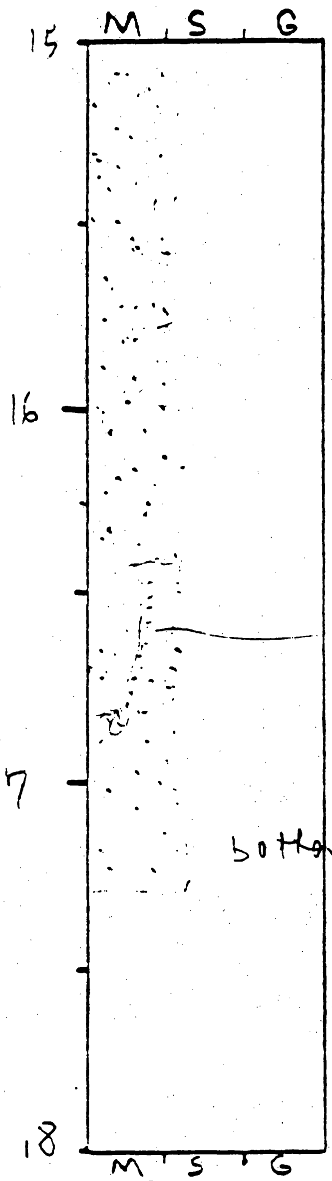

sand — some organic specks to about 15.5
mottled Lt Olive gray to yellowish gray sand

Med dark gray muddy sand filled burrow in Lt Olive brown sand
Some oxidation stain at 16.5'
mottled dark yellowish orange (oxidized) really begins approx 16.8'

bottom (no core catcher)

General Comments:

CORE LOG

CORE # SLV-6(A2) **TYPE** Vibrocore **LOCATION** Sabine Lake - Bessie Canal
LATITUDE 30° 01.076 **LONGITUDE** 93° 57.445 **SURFACE ELEVATION** -14.5'
DEPTH PENETRATED ? **LENGTH RECOVERED** 19'6.5" **% COMPACTION** ?

OBTAINED BY Gibeaut — R/V Kit Jones **DATE** 10-8-94
DESCRIBED BY White **DATE** 2-23-95

DEPTH (ft, m)	SKETCH	LITHOLOGY	STRUCTURE	REMARKS

*

I reversed the arrow pointing toward the top on this section, so it to make sense.

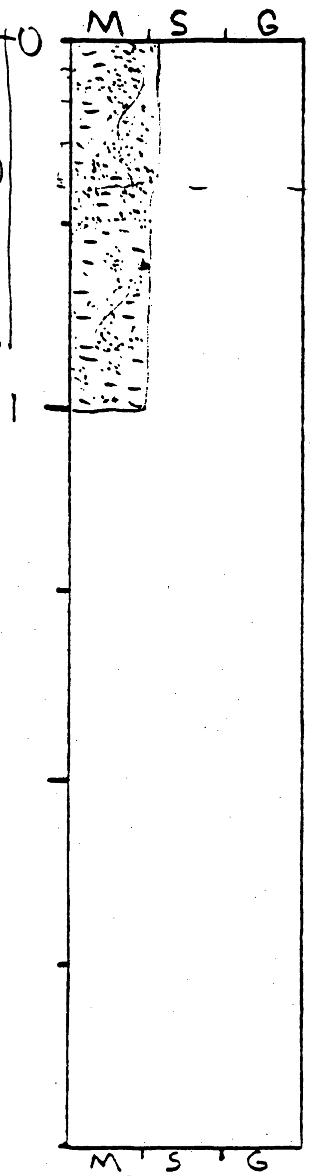

Bottom of A2 Section

med to fine sand filled burrows in mud or clay
enough sand to be called muddy sd

Burrowed

Dusky yellowish brown

clay or mud with organics & sand filled burrows
less sand than above 0.4'
Brownish black organics in clay.

medium gray to med dark gray clay with Dusky yellow sand & small chunks of yellowish gray clay (that becomes more common in next section)

General Comments:

CORE LOG

CORE # SLV-6(A1) TYPE______ LOCATION______
LATITUDE______ LONGITUDE______ SURFACE ELEVATION______
DEPTH PENETRATED______ LENGTH RECOVERED______ %COMPACTION______

OBTAINED BY______ DATE______
DESCRIBED BY______ DATE______

DEPTH (ft, m)	SKETCH	LITHOLOGY	STRUCTURE	REMARKS
1		mud or clay with sand filled burrows.	Burrowed	medium dark gray
				Mottling of medium dark gray clay with yellowish gray clay dominates color below 1.5'
2		clay or mud, organics - sand, yellowish gray		Sand in burrows - dusky yellowish brown to local spots of grayish orange
		clay or mud, organic rich; local silty pockets or thin layers	Distorted horizontal laminae of black organics	mottled layers of ~~brownish~~ black organics in yellowish gray [illegible] to medium gray clay
3				
4				

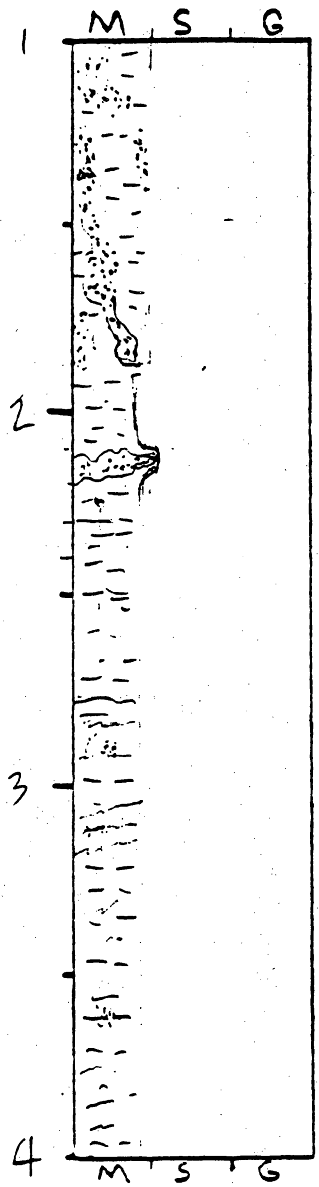

General Comments:

CORE LOG

CORE # SLV-6 (B1) TYPE ________ LOCATION ________
LATITUDE ________ LONGITUDE ________ SURFACE ELEVATION ________
DEPTH PENETRATED ________ LENGTH RECOVERED ________ %COMPACTION ________

OBTAINED BY ________ DATE ________
DESCRIBED BY ________ DATE ________

DEPTH (ft, m)	SKETCH	LITHOLOGY	STRUCTURE	REMARKS

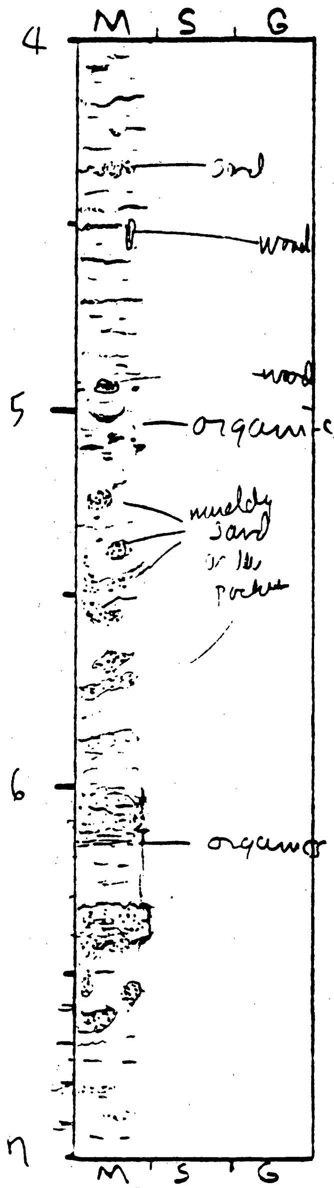

Clay, organic rich
local sand pocket

horizontal laminae of black organics

some local burrowing

(5 Y 6/1)
Lt Olive gray to yellowish gray with black organics

decreasing organics ↓

sandy mud

sand yellowish gray

sandy mud to muddy sd.

clay becoming a little darker in color

clay

Lt Olive gray 5Y 6/1

General Comments:

CORE LOG

CORE # SLV-6 (B2) **TYPE** ________ **LOCATION** ________
LATITUDE ________ **LONGITUDE** ________ **SURFACE ELEVATION** ________
DEPTH PENETRATED ______ **LENGTH RECOVERED** ______ **%COMPACTION** ____

OBTAINED BY ________________________ **DATE** ________
DESCRIBED BY ________________________ **DATE** ________

DEPTH (ft, m)	SKETCH	LITHOLOGY	STRUCTURE	REMARKS

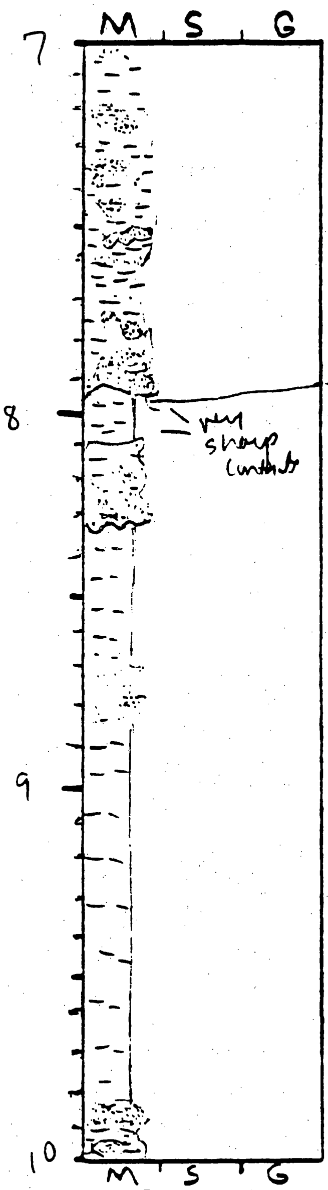

clay with sand pockets
some scattered organic inclusions
clay with sand filled mini troughs
and thin laminae
much of sand is very clean

Lt Olive gray to Olive gray with sand yellowish gray to very pale orange

scoured clay

clay

sandy clay, organics, [illegible]

clay with thin sand laminae

clay

mottled Lt Olive gray 5Y 5/2 with local yellowish gray

clay with thin sand laminae

sand yellowish gray to white

General Comments:

CORE LOG

CORE # SLV-6 (B3) TYPE ______ LOCATION ______
LATITUDE ______ LONGITUDE ______ SURFACE ELEVATION ______
DEPTH PENETRATED ______ LENGTH RECOVERED ______ %COMPACTION ______

OBTAINED BY ______ DATE ______
DESCRIBED BY ______ DATE ______

DEPTH (ft, m)	SKETCH	LITHOLOGY	STRUCTURE	REMARKS

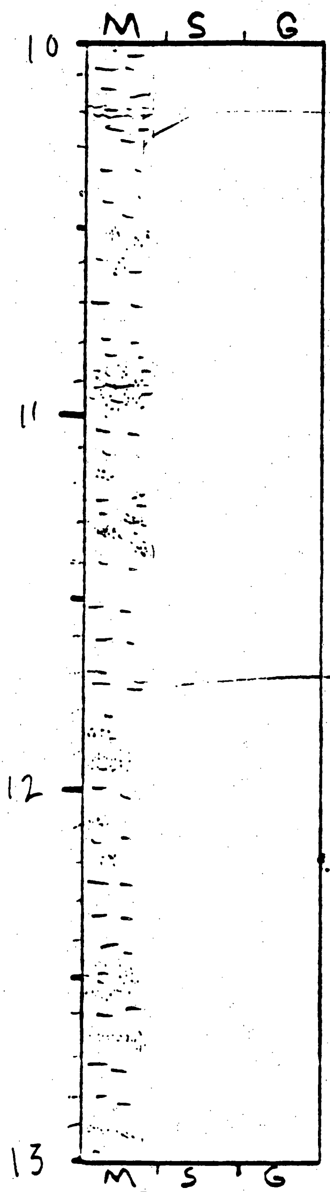

clay
dusky yellow clay layer
very scattered, small traces of organics
traces of sand in clay
traces of sand in clay
Dusky yellow. Clay horizon
traces of sand in clay
traces of sand in clay
very thin sand laminae in clay
traces of sand in clay

Remarks: mottled color in clay. Lt olive gray to olive gray 5Y 6/1 to 5Y 4/1

General Comments:

CORE LOG

CORE # SLV-6 (C1) TYPE____ LOCATION____
LATITUDE____ LONGITUDE____ SURFACE ELEVATION____
DEPTH PENETRATED____ LENGTH RECOVERED____ %COMPACTION____

OBTAINED BY____ DATE____
DESCRIBED BY____ DATE____

DEPTH (ft, m)	SKETCH	LITHOLOGY	STRUCTURE	REMARKS

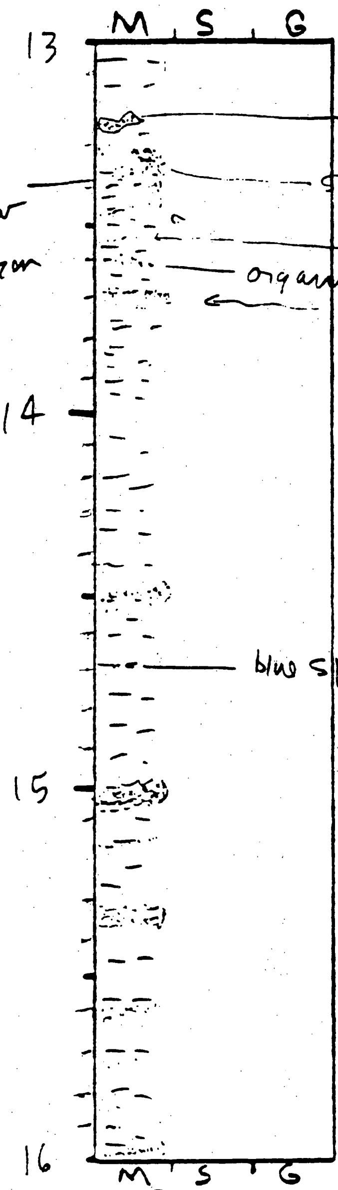

dusky yellow clay horizon

clay — Horizontal laminae — Alternating bands of Lt Olive gray, Olive gray & yellowish gray to grayish yellow

clean, well sorted sand yellowish gray to grayish orange

sand pocket in clay

very thin sand or silt laminae

organic specks

muddy sand laminae

thin alternating yellowish gray to olive gray clay laminae

clay with very thin organic lines

thin sand laminae sand yellowish gray to white

blue speck in organic line

thin sand ripple laminae, sand yellowish gray to white

thin sand laminae in clay

thin sand laminae in clay

General Comments:

CORE LOG

CORE # SLV-6 (C2) TYPE ________ LOCATION ________
LATITUDE ________ LONGITUDE ________ SURFACE ELEVATION ________
DEPTH PENETRATED ________ LENGTH RECOVERED ________ %COMPACTION ________

OBTAINED BY ________ DATE ________
DESCRIBED BY ________ DATE ________

DEPTH (ft, m)	SKETCH	LITHOLOGY	STRUCTURE	REMARKS

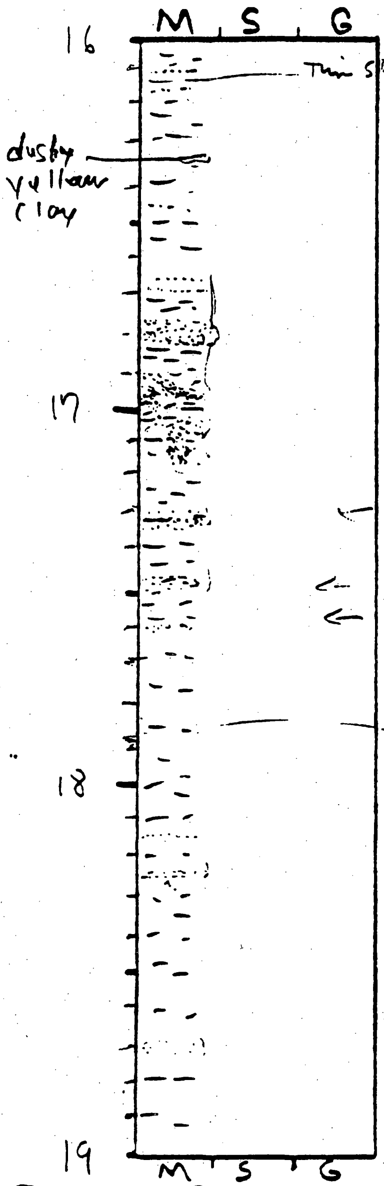

clay with occasional sand laminae and thin black organic lines — horizontal laminae — alternating bands of Lt olive gray, olive gray and yellowish gray clay with occasional thin black organic lines

very thin ripple sand laminae in clay

sand laminae and pockets yellowish gray to white

very thin sand laminae in clay

" "

dusky yellow clay (faint)

very thin sand layers in clay

very thin sand in clay layer

General Comments:

CORE LOG

CORE # SLV-6 (C3) TYPE ______ LOCATION ______
LATITUDE ______ LONGITUDE ______ SURFACE ELEVATION ______
DEPTH PENETRATED ______ LENGTH RECOVERED ______ % COMPACTION ______

OBTAINED BY ______ DATE ______
DESCRIBED BY ______ DATE ______

DEPTH (ft, m)	SKETCH	LITHOLOGY	STRUCTURE	REMARKS
19	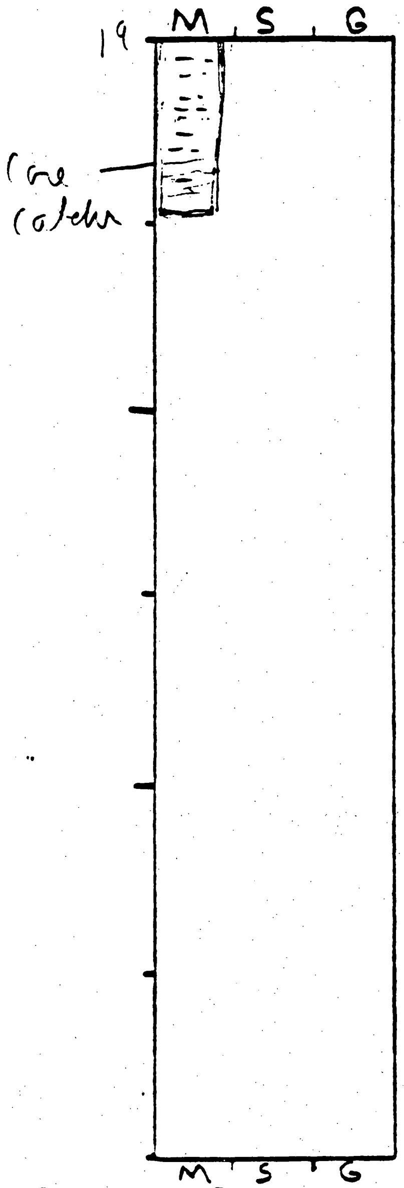	clay some small organic specks	horizontal	alternating layers of olive grey clay with bands of yellowish grey near bottom.

General Comments:

CORE LOG

Formerly SLV-1

CORE # SLV-7(A) **TYPE** Vibracore **LOCATION** Sabine Lake, near mouth
LATITUDE ______ **LONGITUDE** ______ **SURFACE ELEVATION** ______
DEPTH PENETRATED ? **LENGTH RECOVERED** 7.6 **%COMPACTION** ?

OBTAINED BY [illegible] / Gilbert **DATE** ______
DESCRIBED BY White **DATE** 2-28-95

DEPTH (ft, m)	SKETCH	LITHOLOGY	STRUCTURE	REMARKS

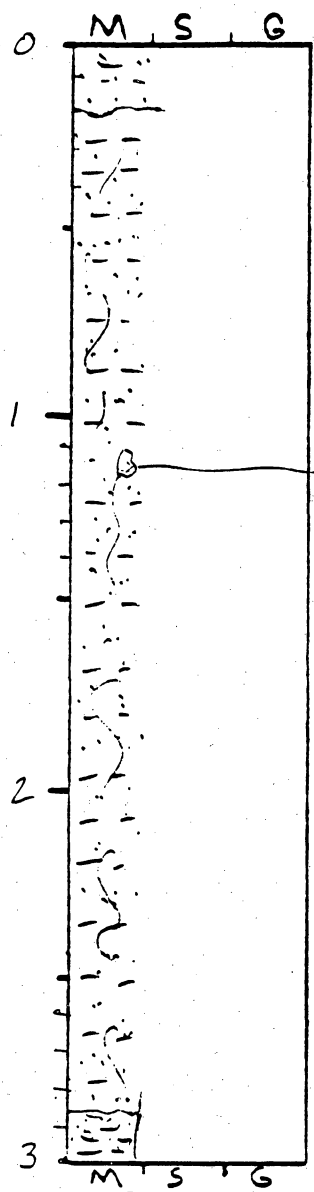

sandy mud to muddy sand — Olive gray with layer of moderate yellowish brown at about 0.2'

very muddy sand to sandy mud — Intensely burrowed — Olive gray (5Y 3/2)

discrete mud & sand components

Only shell frag in this section of core

mud appears more abundant transition above near base
sandy mud

General Comments:

CORE LOG

CORE # SLV-7 (B) TYPE ____ LOCATION ____
LATITUDE ____ LONGITUDE ____ SURFACE ELEVATION ____
DEPTH PENETRATED ____ LENGTH RECOVERED ____ %COMPACTION ____

OBTAINED BY ____ DATE ____
DESCRIBED BY ____ DATE ____

DEPTH (ft, m)	SKETCH	LITHOLOGY	STRUCTURE	REMARKS

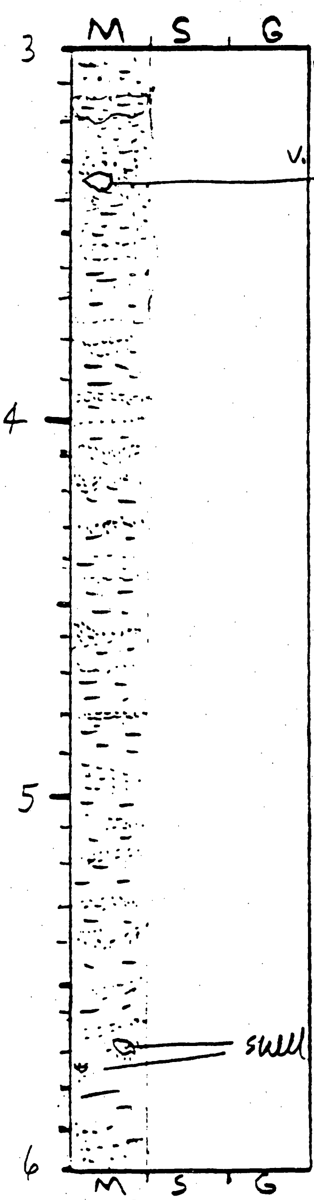

v. muddy sand
sandy mud
v. muddy sand
one of 3 shell frag in this section

near horizontal thin silt & sand laminae in mud

Olive gray (5Y3/2)

sandy mud

near horizontal thin silt & sand lamination in mud

Olive gray (5Y 3/2)

shell frags

General Comments:

CORE LOG

CORE # SLV-7 (C) TYPE ________ LOCATION ________
LATITUDE ________ LONGITUDE ________ SURFACE ELEVATION ________
DEPTH PENETRATED ______ LENGTH RECOVERED ______ %COMPACTION ____

OBTAINED BY ________________________ DATE ________
DESCRIBED BY ________________________ DATE ________

DEPTH (ft, m)	SKETCH	LITHOLOGY	STRUCTURE	REMARKS

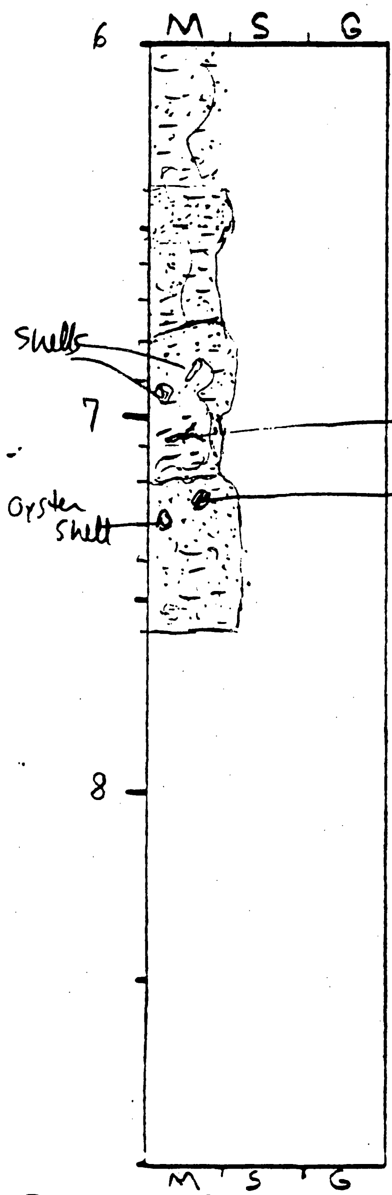

sandy mud, Olive gray

burrowed

muddy sand

sandy mud

muddy sand

wood fragments

datable wood chip (moderate brown)

muddy sand, but not as muddy as above muddy sands
scattered shell frags

General Comments:

Formerly SLV-2

CORE LOG

CORE # SLV-8 (A) TYPE Vibracore LOCATION Sabine Lake near mouth
LATITUDE ______ LONGITUDE ______ SURFACE ELEVATION ______
DEPTH PENETRATED ? LENGTH RECOVERED 11.3 ft %COMPACTION ?

OBTAINED BY Giburget / Gilbert DATE ______
DESCRIBED BY [illegible] DATE 2-28-95

DEPTH (ft, m)	SKETCH	LITHOLOGY	STRUCTURE	REMARKS

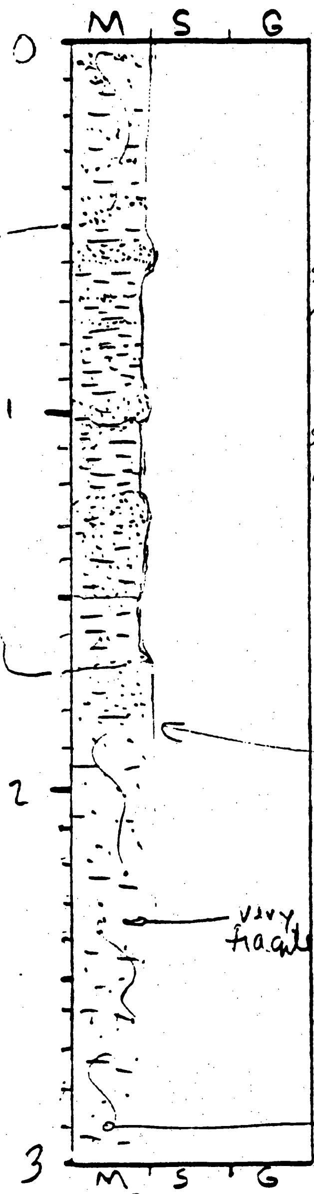

Primarily mud with thin silt & sand laminae with higher concentrations of silt & sand locally

Sandy mud to muddy sd — occassional burrows

Thin silt & sand horizontal laminae from 0.6-1.7 ft

Olive gray (5Y 4/1) with moderate brown oxidation halos in scattered sandy filled burrows down to 1.7 ft.

slightly sandy mud (thin sand laminae)

muddy sand — ripples

slightly sandy mud

muddy sand — ripples

Sandy mud to muddy sd

mostly clay a mud, slightly sandy

← traces of oxidation associated with burrows above 1.7 ft. No evidence of oxid. below

muddy sand (ripples)

Little evidence of horizontal laminae below here.

burrowed

Color becomes Olive gray (5Y 3/2) below 1.7'

very fragile shell? — discrete mud & sand components

Olive gray

shell frag.

General Comments:

CORE LOG

CORE # SLV-8 (B) TYPE ______ LOCATION ______
LATITUDE ______ LONGITUDE ______ SURFACE ELEVATION ______
DEPTH PENETRATED ______ LENGTH RECOVERED ______ % COMPACTION ______

OBTAINED BY ______ DATE ______
DESCRIBED BY ______ DATE ______

DEPTH (ft, m)	SKETCH	LITHOLOGY	STRUCTURE	REMARKS
3	M S G	very muddy sand	burrowed	Olive grey (5Y 3/2)
4		sandy mud	evidence of horizontal laminae	
		v muddy sand		
5			burrowed	
		sandy mud		
		v muddy sand to sandy mud		
		sandy mud		Olive gray (5Y 3/2)
6	M S G			

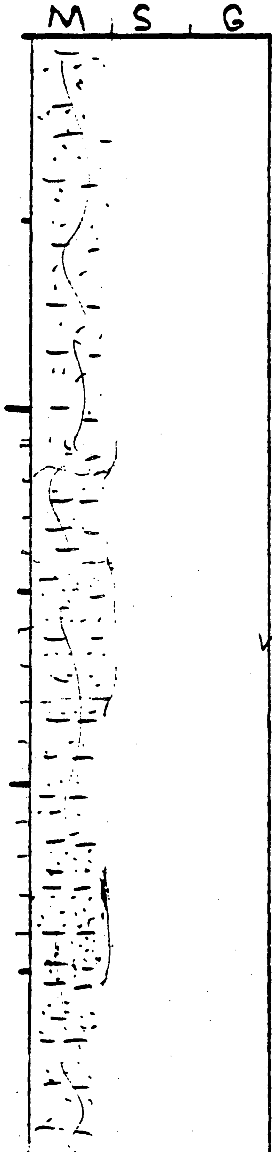

General Comments:

CORE LOG

CORE # SLV-8 (C) TYPE ________ LOCATION ________
LATITUDE ________ LONGITUDE ________ SURFACE ELEVATION ________
DEPTH PENETRATED ________ LENGTH RECOVERED ________ %COMPACTION ________

OBTAINED BY ________ DATE ________
DESCRIBED BY ________ DATE ________

DEPTH (ft, m)	SKETCH	LITHOLOGY	STRUCTURE	REMARKS
6		sandy mud	burrowed	Olive gray (5Y 3/2)
			occassional horizontal lamina & starved ripple lamina	
7		at 7.1' sand lamina dipping in opposite direction from those at 6.75'.	ripples & cross beds of thin sand lamina in mud	
		muddy sand, alternating thin layers of sand & mud.		
8		sandy mud		
		muddy sand		
		sandy mud		
		muddy sand		
		sandy mud		
contact distinct		muddy sand		
		muddy sandy shell to muddy shelly sand		
9		sand, muddy scattered shell		Olive gray (5Y 3/2) to (5Y 4/1)

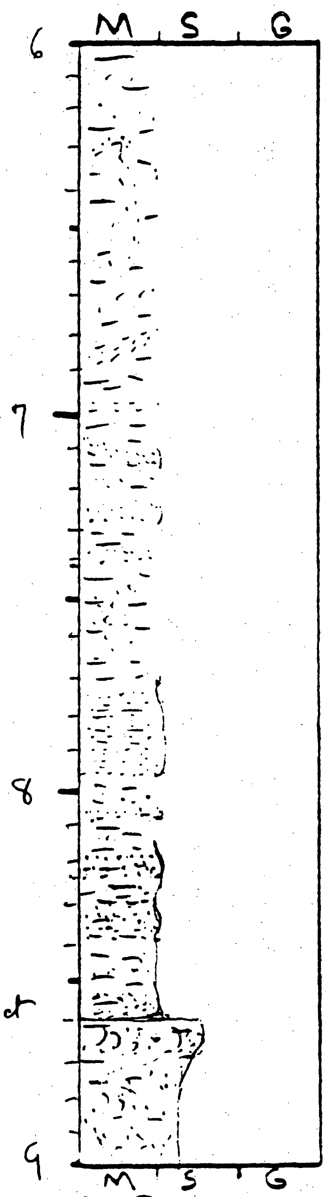

General Comments:

CORE LOG

CORE # SLV-8(D) **TYPE** ______ **LOCATION** ______
LATITUDE ______ **LONGITUDE** ______ **SURFACE ELEVATION** ______
DEPTH PENETRATED ______ **LENGTH RECOVERED** ______ **%COMPACTION** ______

OBTAINED BY ______ **DATE** ______
DESCRIBED BY ______ **DATE** ______

DEPTH (ft. m)	SKETCH	LITHOLOGY	STRUCTURE	REMARKS

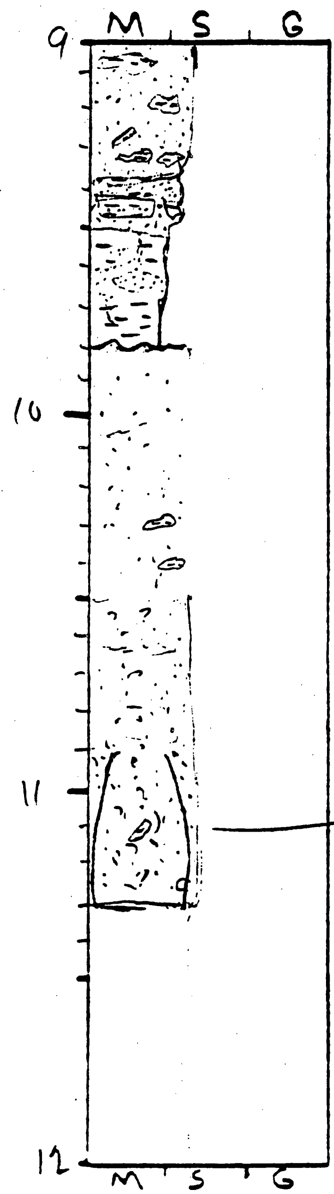

sand, isolated mud clasts — mottled Lt Olive to Olive gray, some spots of yellowish gray in sand.

interbedded sand & mud, thin

mud, some thin sand ripple lamina — Dark gray to Olive gray (5Y 3/2) mud

ripples at top of sand

sand, relatively clean
occassional small mud clast — (5Y 5/2) Lt Olive gray, spots of Olive gray (5Y 3/2)

sand, scattered shells, slightly muddy

↓ coarsening

sand, shell frags more abundant, some mud balls?
core catcher — dusky yellow sand

General Comments:

CORE LOG

Sea Rim State Park East of

CORE # Mc FV-2(A) TYPE Vibracore LOCATION Mc Faddin NWR
LATITUDE ______ LONGITUDE ______ SURFACE ELEVATION ______
DEPTH PENETRATED ? LENGTH RECOVERED 10.95' %COMPACTION ?

OBTAINED BY Morton / White DATE 5-5-92
DESCRIBED BY White DATE 2-28-95

DEPTH (ft, m)	SKETCH	LITHOLOGY	STRUCTURE	REMARKS

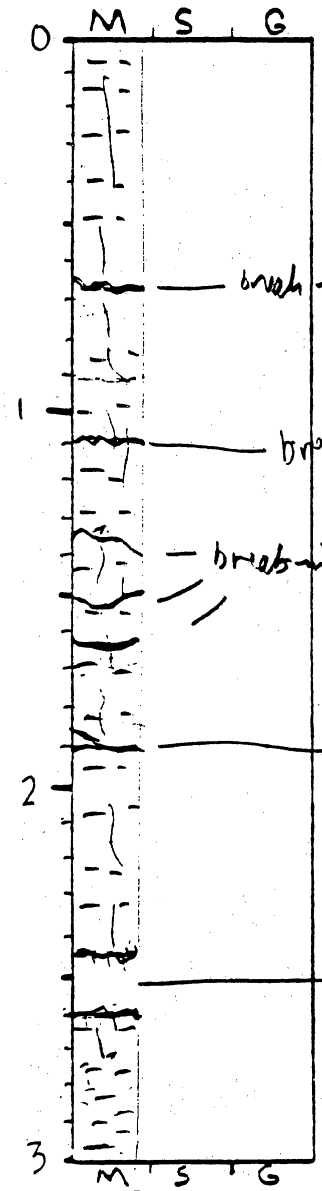

break in core

break in core

break in core

break in core & color change

dessication void

Organic rich mud or clay roots down to at least 2.7'

Mud or clay organics (roots) less abundant

brownish black organic inclusions

Core is dried out
Brownish black

Brownish black

Mottled Olive gray to Olive black

Brownish black

Mottled
Lt Olive gray
to dark gray

Some dark yellowish orange stain down center below 2.7'

General Comments:

CORE LOG

CORE # MCFV-2(B) TYPE________ LOCATION________
LATITUDE________ LONGITUDE________ SURFACE ELEVATION________
DEPTH PENETRATED______ LENGTH RECOVERED______ %COMPACTION____

OBTAINED BY________________________ DATE________
DESCRIBED BY________________________ DATE________

DEPTH (ft, m)	SKETCH	LITHOLOGY	STRUCTURE	REMARKS

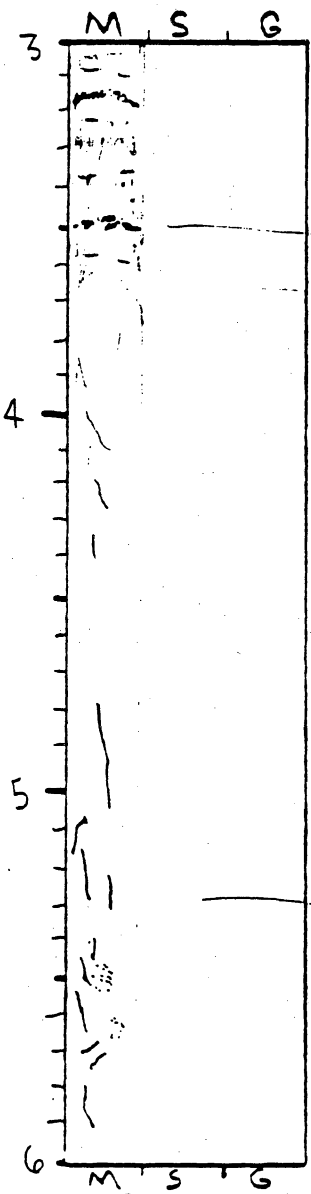

organic rich mud or clay

Dark gray to splotches of Lt gray

disseminated organics (brownish black)

color change

Yellowish gray to Lt Olive gray clay (5Y 6/1)
some mottling with darker color

scattered root traces with oxidation halos

core becomes darker in color with depth

mud, trace of sand
oxidized root traces

Medium dark gray

General Comments:

CORE LOG

CORE # McEV-2(C) TYPE____ LOCATION____
LATITUDE____ LONGITUDE____ SURFACE ELEVATION____
DEPTH PENETRATED____ LENGTH RECOVERED____ %COMPACTION____

OBTAINED BY____ DATE____
DESCRIBED BY____ DATE____

DEPTH (ft, m)	SKETCH	LITHOLOGY	STRUCTURE	REMARKS

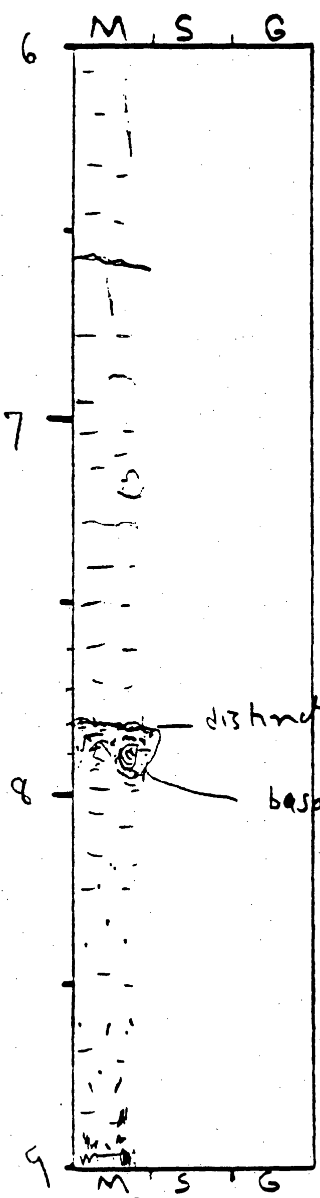

Mud medium gray
with occassional oxidation root traces

distinct contact
Gritty, shelly mud
some grayish brown coloration
shell frags & 1 almost whole shell 1.75cm

basal contact not clearly defined from splitting core

organic specks increase with depth

Olive black in color
with black organic inclusions

somewhat mottled near base
increase in organics

General Comments:

CORE LOG

CORE # MCEV-2(D) TYPE________ LOCATION____________
LATITUDE________ LONGITUDE________ SURFACE ELEVATION________
DEPTH PENETRATED______ LENGTH RECOVERED______ %COMPACTION____

OBTAINED BY______________________ DATE________
DESCRIBED BY______________________ DATE________

DEPTH (ft, m)	SKETCH	LITHOLOGY	STRUCTURE	REMARKS

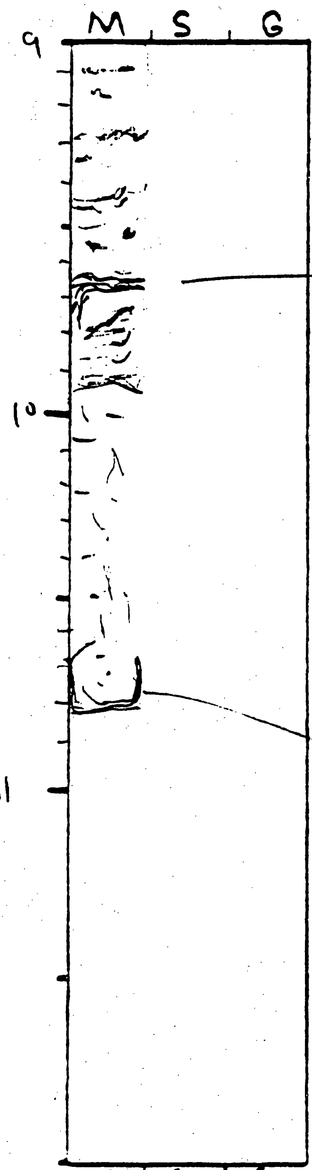

Organic rich clay or mud

mottled dusky yellowish brown or Olive black with lighter band of yellowish gray, brownish black organic inclu...

possibly enough organics for dating

Medium dark gray

core becomes lighter in color below 9.9'

Medium gray to Lt Olive gray with grayish yellow to pale yellowish orange spots along root traces

Olive gray (5Y 4/1) to brownish gray

roots apparently dragged down from surface

General Comments:

CORE LOG

CORE # McFV-3(A) TYPE Vibracore LOCATION McFaddin NWR, Near Exxon Office
LATITUDE ______ LONGITUDE ______ SURFACE ELEVATION ?
DEPTH PENETRATED ? LENGTH RECOVERED 7Ft %COMPACTION ?

OBTAINED BY Martin / White DATE 5-6-92
DESCRIBED BY White DATE 2-28-95

DEPTH (ft, m)	SKETCH	LITHOLOGY	STRUCTURE	REMARKS

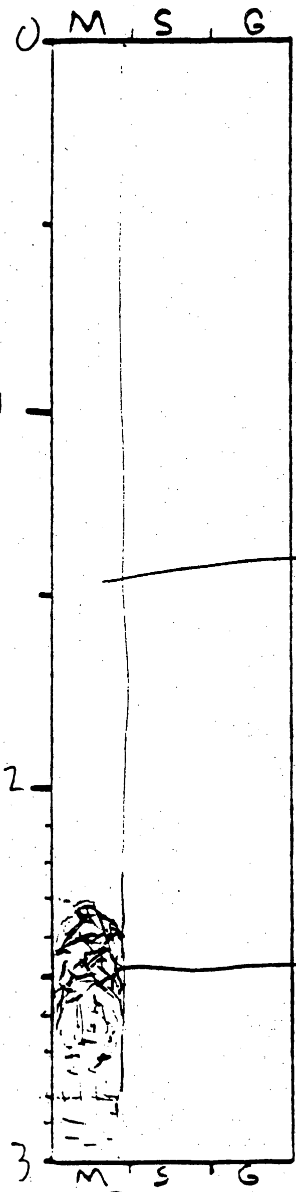

Empty core barrel

Organic roots, etc brownish black

loamy, scattered shells frags, organics Olive gray to brownish black

Organic mud or clay, Olive black

General Comments:

CORE LOG

CORE # McFV3(B) TYPE________ LOCATION________________________

LATITUDE________ LONGITUDE________ SURFACE ELEVATION________

DEPTH PENETRATED______ LENGTH RECOVERED______ %COMPACTION____

OBTAINED BY________________________ DATE________

DESCRIBED BY________________________ DATE________

DEPTH (ft, m)	SKETCH	LITHOLOGY	STRUCTURE	REMARKS

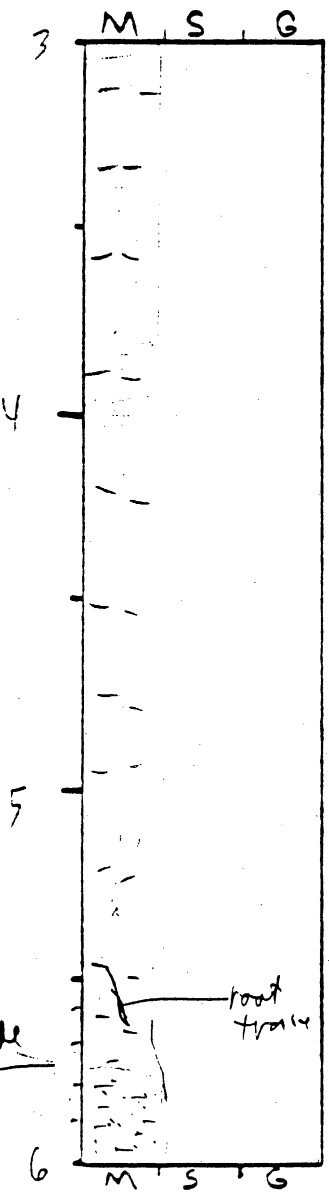

Organic rich mud or clay

mottled, Dark gray, with lighter colored areas of Light olive gray to Light greenish gray. Dark black organics. Spots of Dusky yellow some halos around root traces

mud or clay oxidation. ↓ mirrors? color becomes lighter

spots of dark yellowish orange in mottled areas of med dark and med light gray

Lt Olive gray with some oxidation

clayey sand → sandy clay yellowish gray with Drk yellowish orange stains

approximate cut foot with boundary

General Comments:

CORE LOG

CORE # Mr EV-3(C) TYPE ________ LOCATION ________
LATITUDE ________ LONGITUDE ________ SURFACE ELEVATION ________
DEPTH PENETRATED ________ LENGTH RECOVERED ________ %COMPACTION ________

OBTAINED BY ________ DATE ________
DESCRIBED BY ________ DATE ________

DEPTH (ft, m)	SKETCH	LITHOLOGY	STRUCTURE	REMARKS

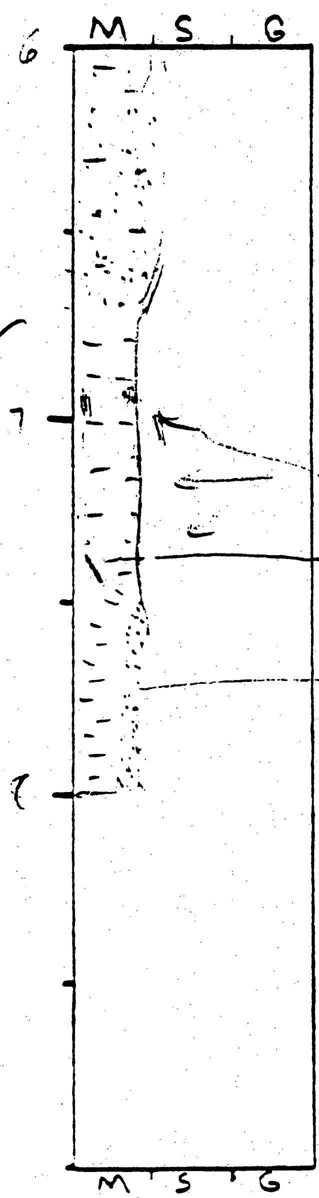

clayey sand

yellowish gray with striking Dark yellowish orange vertical mottling

obscure contact

Beaumont

mottled Lt Olive gray with Abundant Dark yellowish Orange & spots of Moderate red

clay

broken root

Lt Olive gray (5Y 6/1) clay

very pale orange to yellowish gray sand on right side of core

General Comments:

CORE LOG

CORE # McFV 5(A) TYPE Vibracore LOCATION McFaddin NWR
LATITUDE ____ LONGITUDE ____ SURFACE ELEVATION ____
DEPTH PENETRATED 12 FT LENGTH RECOVERED 9.2 Ft %COMPACTION ?

OBTAINED BY Morton & White DATE 5-6-02
DESCRIBED BY White DATE 2-23-95

DEPTH (ft, m)	SKETCH	LITHOLOGY	STRUCTURE	REMARKS

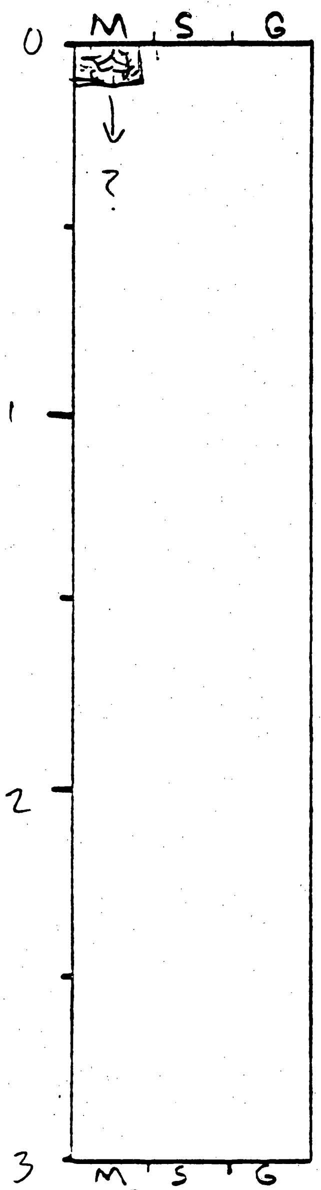

Blackish red organic plant mass only 0.2' recovered exact location unknown

General Comments:

CORE LOG

CORE # McEV-5(B) TYPE_______ LOCATION________
LATITUDE_______ LONGITUDE_______ SURFACE ELEVATION_______
DEPTH PENETRATED______ LENGTH RECOVERED______ %COMPACTION____

OBTAINED BY________________ DATE______
DESCRIBED BY________________ DATE______

DEPTH (ft, m)	SKETCH	LITHOLOGY	STRUCTURE	REMARKS

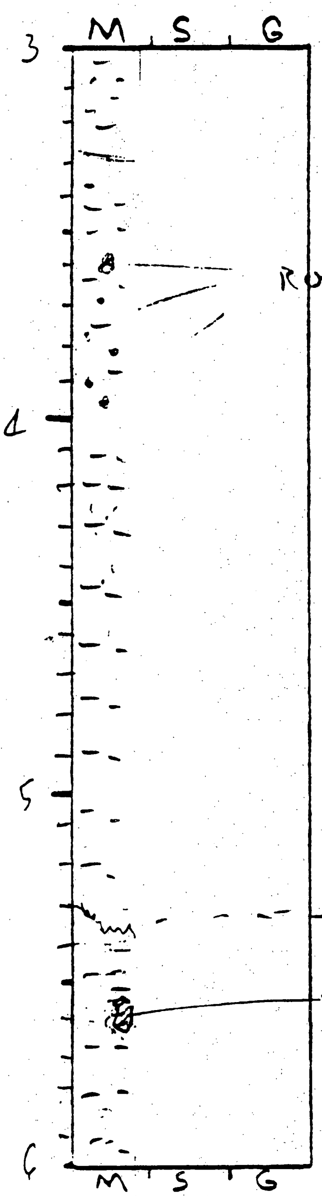

mud, organic rich

medium dark gray with moderate brown organic (plant roots)

mud n clay
scattered organics

Medium dark gray with mottling locally of moderate brown to Lt brown
black organic traces,

Stiffer clay — color change

fragment of friable material (Olive black)
Mud Lt gray to Lt gray clay

mottled with spots of blackish brown
Some Lt Brown oxidation traces

splotches of grayish olive green

General Comments:

CORE LOG

CORE # McFV-5C TYPE ______ LOCATION ______
LATITUDE ______ LONGITUDE ______ SURFACE ELEVATION ______
DEPTH PENETRATED ______ LENGTH RECOVERED ______ %COMPACTION ______

OBTAINED BY ______ DATE ______
DESCRIBED BY ______ DATE ______

DEPTH (ft, m)	SKETCH	LITHOLOGY	STRUCTURE	REMARKS

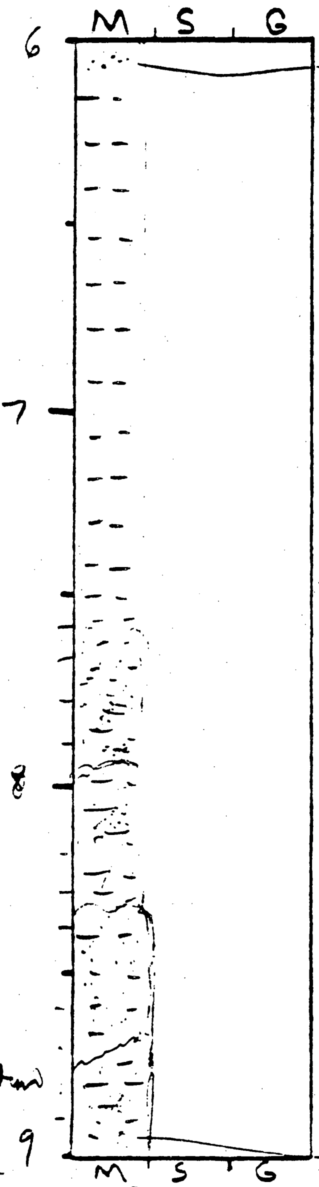

- splotches of grayish olive green
- clay, organic traces and thin layers, v. thin silty layers locally — medium gray with black organics
- silty clay (medium gray)
- Dark gray clay
- mottled clay, trace of sand & silt, lt gray & med dark gray
- Dark gray clay
- silty clay & v.f. sandy mottled light gray, to yellowish gray, to Med Light gray
- yellowish gray silty & v.f. sandy clay
- oxidation stain Dark yellowish orange

first indication Beaumont 9

General Comments:

CORE LOG

CORE # McFV-5(D) TYPE ________ LOCATION ________
LATITUDE ________ LONGITUDE ________ SURFACE ELEVATION ________
DEPTH PENETRATED ________ LENGTH RECOVERED ________ % COMPACTION ________

OBTAINED BY ________ DATE ________
DESCRIBED BY ________ DATE ________

DEPTH (ft, m)	SKETCH	LITHOLOGY	STRUCTURE	REMARKS
	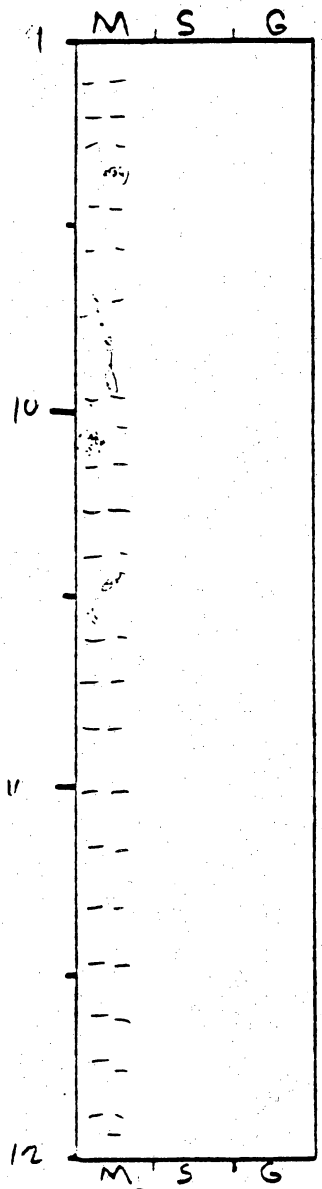	Beaumont Clay stiff Weakly Lt Olive gray silty and sandy clay pockets		Lt Gray to yellowish gray mottled with Dark yellowish orange splotches

General Comments:

CORE LOG

CORE # McFV-7(A) **TYPE** Vibracore **LOCATION** McFaddin NWR Gully Beach (Back b[illegible]
LATITUDE ________ **LONGITUDE** ________ **SURFACE ELEVATION** ?
DEPTH PENETRATED ? **LENGTH RECOVERED** 3.4ft **% COMPACTION** ?

OBTAINED BY Morton & White **DATE** 5-6-92
DESCRIBED BY White **DATE** 2-23-95

DEPTH (ft, m)	SKETCH	LITHOLOGY	STRUCTURE	REMARKS
0	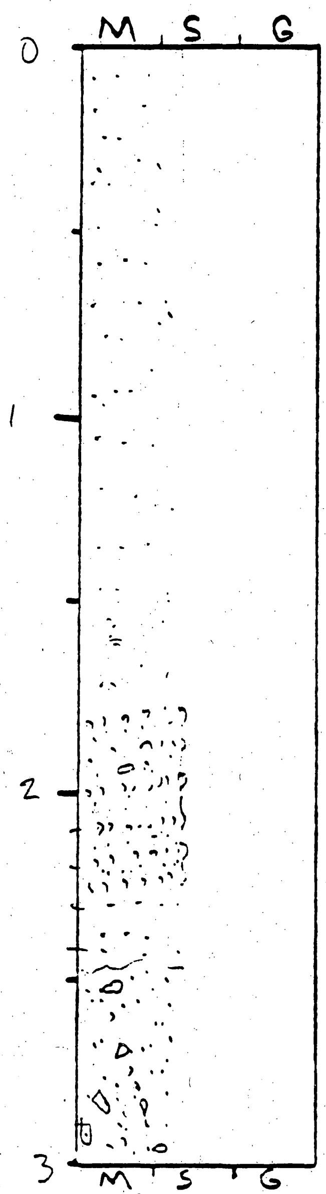	V. fine sand 99%, quartz, well sorted; v. scattered small shell frags		Grayish Orange
2		small granule shell frags in area in this area; faintly laminated and dipping gently 20-25°, shell frags in [illegible]		
		color change & increase in shell frags ≈ 20% shell locally		Grayish orange to areas of Dark yellowish brown

General Comments:

CORE LOG

CORE # McFv (7B) TYPE _____ LOCATION _____
LATITUDE _____ LONGITUDE _____ SURFACE ELEVATION _____
DEPTH PENETRATED _____ LENGTH RECOVERED _____ % COMPACTION _____

OBTAINED BY _____ DATE _____
DESCRIBED BY _____ DATE _____

DEPTH (ft, m)	SKETCH	LITHOLOGY	STRUCTURE	REMARKS

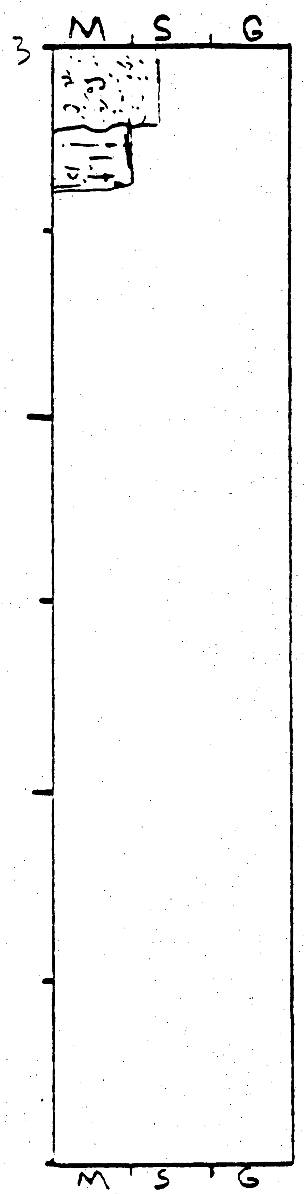

sand grayish orange splotches of Lt brown scattered small shell frags 10-20%

relatively stiff clay, organics near base some Moderate brown splotches.

Grayish brown to brownish gray. blackish spots near base.

General Comments:

Addendum 8. Site Dependency of Shallow Seismic Data Quality in Saturated, Unconsolidated Coastal Sediments

SITE DEPENDENCY OF SHALLOW SEISMIC DATA QUALITY IN SATURATED, UNCONSOLIDATED COASTAL SEDIMENTS

Paine, Jeffrey G., Morton, Robert A., and Garner, L. Edwin, Bureau of Economic Geology, The University of Texas at Austin, University Station, Box X, Austin, Texas 78713.

ABSTRACT

Shallow seismic reflection profiling using small sources is a viable method of imaging near-surface late Quaternary strata along the Texas coast. Seismic testing was completed at three representative coastal sites to determine the usefulness of land-based shallow seismic reflection profiling, to examine the dependence of data quality on environment, to evaluate compressional-wave sources for shallow profiling, and to determine the exploration depth range of shallow seismic reflection methods.

Tests in three environments, including unvegetated beach sands at High Island, Holocene marsh deposits at Sabine Pass, and a vegetated floodplain along the Neches River, show that near-surface sediment characteristics strongly influence data quality. A modified soil probe hammer, which is a low energy, broad frequency range seismic source, was used for the short reflection profiles at each site. Highest quality data were collected at the beach, where reflections were recorded as shallow as 7 m and as deep as 200 m. Data quality in the marsh at Sabine Pass and the vegetated floodplain along the Neches River was not as good. At these sites, surface wave velocities were higher, peak frequencies were lower, and exploration depths were limited.

Despite similar target depths and near-surface water tables at each site, optimum acquisition parameters varied. At High Island, one shot per shotpoint and a relatively low filter setting of 16 Hz produced good data. At the Sabine Pass marsh, where subsurface gases may have reduced data quality, a low-cut filter setting of 32 Hz improved data by reducing surface wave noise. At the Neches River site, a higher low-cut filter setting of 64 Hz diminished traffic noise, source-related surface waves, and bridge vibrations.

Similar shallow reflection surveys should be useful in a variety of coastal environments. Potential applications include studies of late Quaternary stratigraphy, reactivated near-surface faults, and buried archeological sites. On-land surveys can also augment borehole data, guide borehole placement, and extend offshore surveys across the shoreline and onto the coastal plain.

INTRODUCTION

Preliminary seismic tests were conducted along the upper Texas coast to (1) determine the usefulness of land-based shallow seismic reflection profiling of Pleistocene and Holocene strata in three representative environments, (2) examine the dependence of data quality on ground characteristics, (3) evaluate several compressional-wave seismic sources for ultra-shallow reflection profiling, and (4) determine the effective depth range of shallow seismic reflection methods in these environments.

Three sites were chosen for the tests between Galveston Bay and Sabine Pass (fig. 1). Tests at High Island were completed on the barren, sandy beach near the high tide line. Core from a nearby borehole drilled on the beach by the Bureau of Economic Geology (BEG) to a depth of 6 m shows that a 2-m thick veneer of Holocene beach and washover sand overlies Holocene marsh mud to a depth of 4 m, which in turn overlie upper Pleistocene fluvial and deltaic deposits of the Beaumont Formation at a depth of between 4 and 5.5 m.

The Sabine Pass site, located 4 km north of Sabine Pass (fig. 1), is in a muddy marsh environment between sandier Holocene chenier beach ridge deposits (Aronow and Barnes, 1982; Fisher and others, 1973). Two cores were acquired by BEG from boreholes located southeast and northwest of the test site to depths of 10 and 30 m, respectively. The interpreted erosional Holocene-Pleistocene contact deepens from 8 m southeast of the test site to 26 m northwest of the site into an erosional valley feeding into the ancestral Sabine River valley. Near-surface sediments (upper 6 to 8 m) are shelly sand

and sandy mud deposited in Holocene marsh and beach ridge and swale environments. A thick section (6 to 26 m depth) of estuarine and deltaic muds underlies the beach ridge and swale deposits in the northwestern core.

At the Neches River site (fig. 1), located along a bridge over the Neches River 2 km upstream from Sabine Lake, seismic tests were conducted on the vegetated Neches River floodplain within the modern Neches River valley (Aronow and Barnes, 1982; Fisher and others, 1973). BEG borehole samples and foundation boring descriptions from as deep as 35 m indicate that soft, organic-rich, clayey sediments, probably deposited in a floodplain environment, are present to a depth of about 10 m at the test site. These deposits are underlain by interpreted late Pleistocene or early Holocene Deweyville fluvial sands to a depth of about 17 m. Below 17 m are stiff upper Pleistocene clay and sandy clay of the Beaumont Formation.

METHODS

Seismic Tests

Seismic tests performed at the High Island, Sabine Pass, and Neches River sites included noise, filter, and source tests that were used to optimize acquisition geometry and recording settings for short reflection surveys. For these tests, the seismograph was connected to a spread of 48 high-frequency geophones spaced at 1 m intervals (table 1). For the noise test, the seismograph recorded background seismic noise with no source activated. This test and observations made during the surveys revealed that important sources of noise were wind (at each site), breaking waves (at the High Island site), vehicle noise (at the Sabine Pass and Neches River sites), and bridge vibrations (at the Neches River site). Wind noise was largely unavoidable, as was constant vehicle noise across Rainbow Bridge over the Neches River. Noise from breaking waves and bridge vibrations was reduced by using low-cut filters during data acquisition and vehicle noise was avoided at the Sabine Pass site by recording only when no vehicles were near the site.

Filter tests were conducted to determine the optimum setting for the analog low-cut filter. The intent was to raise the filter as high as possible to reduce low frequency surface wave noise, but keep it low enough to allow a wide frequency range and to allow the deepest events of interest to be recorded. Tests using the chosen acquisition geometry and low-cut filter settings of 4, 8, 16, 32, 64, 96, 128, and 192 Hz showed that the optimum filter setting was 16 Hz for the High Island site, 32 Hz for the Sabine Pass site, and 64 Hz for the Neches River site (table 2).

Compressional wave sources that were to be evaluated at the site included a sledgehammer, a modified soil probe hammer, and a Betsy Seisgun (table 1). The sledgehammer was struck on an aluminum plate resting on the ground. The soil probe hammer, originally manufactured to collect small diameter soil cores, consists of a sliding 3.6 kg weight mounted on a metal rod. The weight is driven downward by hand over a 45 cm stroke and strikes the top of a rod. A 225 cm^2 steel plate welded to the base of the rod delivers the seismic energy to the ground. This source produces less seismic energy than does the sledgehammer, but is easy to use and provides a consistent seismic pulse. Electronic switches mounted to the sources provided time breaks for the seismograph. We also planned to test a Betsy Seisgun using 0.410 gauge shotgun shells with 20 g shot and 12-gauge shells with 28 g slugs, but the unit was inoperable.

Stacking tests were conducted using the source-receiver geometry selected for the reflection lines. The soil probe hammer was fired repeatedly into the geophone spread in an attempt to increase the signal-to-noise ratio by partly canceling random noise. One shot per shotpoint was chosen to keep minor discrepancies in shot times from degrading the high frequency part of the source spectrum.

Other acquisition parameters chosen based on these tests included a seismograph sampling interval of 0.0005 to 0.001 s and a record length of 0.25 to 1 s (table 2). A Global Positioning System receiver was used to locate survey end points.

Acquisition Geometry

Three short seismic reflection lines were acquired at High Island, Sabine Pass, and the Neches River (fig. 1) in January 1995 using the common depth point method adapted to the shallow subsurface (Mayne, 1962; Steeples and Miller, 1990; Miller and others, 1990). Because we were interested in the shallowest reflections visible, the minimum source-receiver distance was 1 m (table 2). The farthest offset generally should be equal to or greater than the depth of the deepest target. Using 1-m shotpoint and geophone spacing, the maximum source-receiver offset was 24 m at the Neches River site and 48 m at the High Island and Sabine Pass sites (table 2). Source–receiver geometries were symmetric (split spread geometry with 24 geophones on each side of the shotpoint) at the Neches River site and were asymmetric (end-on geometry with the source trailing the geophone spread) at the High Island and Sabine Pass sites. One 40-Hz geophone was used at each geophone location for each line.

Processing

After the field work was completed, the seismic data were processed at BEG using the software SPW on a Macintosh computer. Processing procedures were those common to many types of reflection processing (Yilmaz, 1987).

The first processing step was to convert the data files to SPW format. Next, trace headers were created that combined the seismic data with acquisition geometry information. Dead or excessively noisy traces were then deleted from the data set. Automatic gain control was applied to amplify weak arrivals at late times or far offsets. A mute function was designed to delete the first arrivals from each shot gather to prevent them from stacking as a false reflector. Another mute function was designed to remove the air wave, or the sound of the source traveling through the air, from each shot gather. Bandpass filtering removed unwanted low- and high-frequency noise from Sabine Pass and Neches River data. Velocity analysis was conducted by fitting reflection hyperbolas to events on common midpoint (CMP) gathers (all traces that have the same source-receiver midpoint, but differing offsets). For 24-fold data, there are 24 traces in a CMP gather.

The velocity function derived from the CMP gathers was used to correct each trace in the gather for normal moveout (the delay in arrival time caused by increasing source-receiver offset) and to simulate zero offset for all traces. Each velocity-corrected trace in a CMP gather was summed to produce a single composite trace. A stacked seismic section is a display of these composite traces.

RESULTS

Gulf Beach at High Island

Of the three test sites, the highest quality data were recorded at the High Island test site. A sample field record (HIRL1003) from the short reflection survey at this site (fig. 2), recorded with one shot from the soil probe hammer and a 16-Hz low-cut filter, shows several types of seismic energy. Visible phases (fig. 2a) include (1) high amplitude, low frequency, and slowly propagating surface waves (lower left of field record, less than 80 m/s propagation velocity), (2) an air wave, or the sound of the hammer blow traveling in air (high frequency, 330 m/s propagation velocity), (3) a critically refracted arrival from the near-surface water table (1600 m/s propagation velocity), and (4) a few hyperbolic reflectors between 0 and 0.080 s two-way time. With automatic gain control applied (fig. 2b), later reflectors are visible (to 0.200 s), as is the hyperbolic signature of a Gulf of Mexico wave breaking on the shoreface at about 30 m offset.

The strongest events on these field records are the low frequency surface waves (figs. 2, 3a), which commonly obscure shallow reflectors in reflection surveys. At High Island, near-surface compressional velocities are about 20 times higher than surface wave propagation velocities (fig. 2c). This allows early reflections (0.010 s and later) to arrive at the geophones before the surface waves at near-source distances. Power spectra of individual traces at High Island show a power peak at about 30 Hz and a secondary peak at about 150 Hz (fig. 3a). After muting the surface-wave dominated part of the field record, the remainder of the seismic energy on the 10 m trace is mostly reflected and refracted energy and has a band of significant power between 100 and 200 Hz and a peak at about 150 Hz (fig. 3b). This peak is one to two orders of magnitude weaker than that for the surface waves.

Velocities picked for hyperbolic reflectors visible on CMP gathers show that velocities increase with two-way time (fig. 4). Velocities increase rapidly from about 1300 m/s to 1500 m/s between 0.020 and 0.050 s, then increase more slowly to about 2250 m/s at 0.200 s. A best-fit velocity function calculated from least-squares regression of two-way times and stacking velocities can be used to convert time to depth for the seismic data (fig. 4). This function is:

$$\text{velocity} = \text{two-way time} \times 4913 \text{ m/s}^2 + 1337 \text{ m/s}$$

which has a correlation coefficient of 0.987. Calculated depths for the reflectors visible on High Island field records range from as shallow as about 7 m to as deep as 200 m (fig. 4). Velocities calculated for these reflectors yield new information on seismic velocities within the upper Pleistocene and Holocene strata. They allow actual measured velocities to be used in depth calculations rather than theoretical relationships between two-way time and depth (Lehner, 1969).

Velocity picks were also used to correct traces of differing source-receiver offsets for delays caused by increasing source-receiver distance (normal moveout). After correcting and stacking traces with the same source-receiver midpoint, a seismic section was constructed (fig. 5a). Numerous major and minor reflectors are visible between about 0.010 and 0.250 s, the latest data processed. Major reflectors are visible near 0.050 s, 0.125 s, and 0.180 s. Though the section is only 70 m long, some geological information is present. There appears to be a narrow low in the 0.020 s reflector between CMP 32 and 38, a broad low in the 0.060 s reflector centered on CMP 30, and an increasing southwestward (leftward) apparent dip of reflectors later than 0.100 s. The earliest reflector has a calculated depth that is near that of the Pleistocene-Holocene contact in a nearby BEG borehole. Deeper reflectors arise from acoustic boundaries within upper Pleistocene and older strata.

Marsh at Sabine Pass

After source and noise tests at the chenier plain marsh at Sabine Pass, shallow reflection data were acquired employing one soil probe hammer pulse at each shotpoint (table 2). Data were acquired in an end-on configuration in both line directions, resulting in 96 traces per shotpoint. A relative amplitude display of a typical field record, in which the highest recorded amplitudes are equalized among the traces, reveals that low frequency surface waves, high frequency air waves, and random noise are all clearly recorded at the site (fig. 6). A few reflection hyperbolas are also visible, particularly at about 0.025 s, between 0.040 and 0.050 s, and at about 0.080 s. Other reflectors are either not present or are obscured by strong surface waves or noise. Data quality deteriorates with increasing offset and reflectors are difficult to see on the field record beyond about 35 m.

The propagation velocity of the surface waves is as high as 150 m/s, nearly twice as high as at the High Island site and stronger relative to the reflections. These faster surface waves increase the offset distance by which there is adequate separation between the arrival times of the reflected energy and the surface waves, which in turn increases the minimum exploration depth. Using a near-surface velocity of 1400 m/s and a zero offset two-way time of the earliest observed reflection of 0.020 s, the shallowest visible reflector corresponds to a depth of 14 m. The deepest reflector visible on the field record arrives at about 0.130 s, which represents a depth of about 120 m.

A power spectrum calculated for a trace with a 10 m source-receiver separation shows that most of the recorded seismic signal is below 100 Hz (fig. 7a). Power peaks at 30 and 50 Hz are removed when the surface-wave dominated part of the shot record is muted, and are replaced by a 70 Hz peak that is about 15 times weaker than the low frequency surface wave peaks (fig. 7b). This probably represents the dominant frequency of the reflected energy.

After velocity analysis, normal moveout correction, and CMP stacking, the stacked section shows a few strong reflectors between 0 and 0.1 s and a few weaker reflectors later than 0.1 s (fig. 5b). Reflection peaks are broader (lower frequency) than those in the High Island section and reflections are obscured in some parts of the Sabine pass section (between CMP 1050 and 1075, for example). The strong reflector at 0.020 s, calculated to be at a depth of 14 m, falls in the expected depth range for the Pleistocene-Holocene erosional contact. This contact deepens from 8 m in a borehole southeast of the site to 26 m in a borehole northwest of the site. Earlier arrivals in the stacked section may represent a weak reflection off the interface between chenier plain deposits and underlying bay and bayhead delta muds.

In general, the Sabine Pass section has a lower signal-to-noise ratio than the High Island section. Because much of the noise appears to be random wind-related noise and because there is little significant transmitted energy above 100 Hz, the signal-to-noise ratio might be improved by stacking several shots at each shotpoint.

Neches River Floodplain

At the Neches River site, seismic tests and a short seismic reflection survey were completed on the vegetated floodplain in the right-of-way of a heavily-trafficked bridge crossing the Neches River. Field records of low-cut filter tests using the soil probe hammer source show several types of recorded energy, including direct, critically refracted, and reflected compressional waves, surface waves, an air wave, bridge vibrations, and random wind-related noise (fig. 8). The direct wave, which travels from the source to the receiver without appreciable refraction, is visible as the first arrival at source-receiver offsets of 1 to 5 m. It propagates across the spread at 333 m/s, nearly the same speed as the air wave, and is distinguished from it by the direct wave's strong leftward (downward) deflection on the field record. Beyond 5 m offset, the first arrival is a compressional wave that propagates at 1565 m/s and is critically refracted at the shallow water table.

Bridge vibrations appear as low-frequency, high-amplitude, leftward-propagating waves on the field records (fig. 8a, b). With a dominant frequency of about 16 Hz, this noise source is diminished by applying a 16 Hz low-cut filter (fig. 8b) and almost completely removed by applying a 64 Hz filter (fig. 8c). Surface waves are also a low-frequency noise source that propagate at about 100 m/s at the Neches River site. The effect of increasing the low-cut filter is to remove progressively more of the low-frequency dominated surface waves. Surface wave strength is noticeably diminished as the filter was raised from 16 Hz to 64 Hz and finally 96 Hz (figs. 8b, c, and d). Along with the desirable reduction in surface wave strength is a reduction in reflected energy strength, which produces an undesirable decrease in signal-to-noise ratio, particularly at the 96 Hz low-cut filter setting (fig. 8d). A setting of 64 Hz was chosen for the reflection survey as a compromise that allowed enough reflected signal to be recorded while eliminating bridge noise and reducing surface wave strength.

The effect of the 64-Hz low-cut filter is shown on power spectra of 10-m offset traces from the Neches River reflection survey, recorded before (fig. 9a) and after (fig. 9b) muting the surface-wave dominated part of the record. Before muting, power peaks are centered at 31, 46, and 63 Hz (fig. 9a). After muting the surface-wave dominated part of the record, the 31 Hz and 46 Hz peaks are diminished and the 63 Hz peak remains nearly as strong as it was before the mute (fig. 9b). Unlike surveys at High Island and Sabine Pass, where lower low-cut filters were employed, the low frequency (less than 50 Hz) surface wave peaks are weaker at the Neches River site than the recorded compressional wave signal. Like at the Sabine Pass marsh site, little seismic energy above 100 Hz was recorded.

Processing steps to produce a stacked section (fig. 5c) included surface wave, air wave, and first-arrival mutes, bandpass filtering, velocity analysis, moveout correction, and CMP stacking. A weak reflector appears to be present as early as 0.015 s, which corresponds to a depth of about 8 m. This horizon may be an inadvertent stack of a weak refracted arrival, or it may correlate to the stratigraphic boundary between muddy Holocene floodplain deposits and underlying upper Pleistocene or lower Holocene Deweyville sands penetrated in nearby cores and foundation borings. A stronger reflector arrives at 0.025 s two-way time, which converts to 18 m depth. This is near the 17 m depth at which stiff upper Pleistocene clay and sandy clay of the Beaumont Formation are found in the borings. Several reflectors are visible as late as 0.130 s, which corresponds to a depth of 120 m. Overall data quality is better than that at the Sabine Pass marsh and not as good as that at the High Island beach.

DISCUSSION

Surface Wave and Compressional Wave Separation

A major limitation of compressional wave reflection surveys of the shallow subsurface is the interference of surface waves and reflected waves at near-source distances. Because the vertical component of surface waves is much stronger than that of typical reflected waves, geophone response is dominated by surface wave motion regardless of the dynamic range of the seismograph. This limitation is particularly severe where near-surface sediments are dry (air-filled pores) and unconsolidated;

compressional velocities can be less than 1000 m/s in these environments (Paine, 1994), not greatly higher than typical surface wave velocities of several hundred meters per second. Further, higher seismic frequencies are rapidly attenuated in dry sediments, making it difficult to filter low frequency surface waves without significantly degrading the overlapping frequency range of the reflected waves.

In wet, unconsolidated coastal environments represented by the three test sites and common in many parts of the world, adequate separation between surface waves and reflected compressional waves is attained much closer to the source due to the relatively low surface wave velocities (80 to 150 m/s at the coastal sites) and relatively high compressional wave velocities (about 1500 m/s). At High Island, for example, reflectors at two-way times as early as 0.010 s were recorded. While this is an early time, relatively high compressional velocities also mean that (1) the earliest observable reflector may be deeper than the near-surface zone of interest, and (2) seismic wavelengths are longer for a given frequency than in environments with lower compressional velocities, which reduces vertical resolution proportionately.

Shear-wave surveys offer promise if shallower depths are desired than those practical for a compressional wave survey. These surveys take advantage of lower shear wave velocities to increase resolution and use horizontally polarized shear waves to reduce the strength of the recorded surface wave.

Frequency Content

Frequency content is important because broader frequency ranges and higher frequencies increase seismic resolution and make it easier to filter surface wave noise. One issue is the frequency content of the source pulse, and another is the frequency content of the reflected wave at the geophone after subsurface attenuation. Hammer sources such as those used at the three coastal sites are considered to be low-frequency sources compared to explosive and projectile sources (Miller and others, 1986). Power spectra calculated after surface wave mutes show the highest frequency content at the High Island site, where peak signal power was recorded between 100 and 200 Hz. This implies that the soil probe hammer source produces significant seismic energy at least as high as 200 Hz. At seismic velocities of 1500 m/s, the wavelength at 200 Hz is 7.5 m. The theoretical limit of vertical resolution is between 1/4 and 1/8 wavelength (Widess, 1973), which is to 1 to 2 m.

Frequency content and vertical resolution is not as favorable at the Sabine Pass marsh and the Neches River floodplain. After surface wave mutes, peak seismic energy is found between 50 and 90 Hz at Sabine Pass and between 55 and 80 Hz at the Neches River. The same source was used at all three sites and there was little difference in coupling between the source and the land surface. Lower frequencies recorded at the Sabine Pass and Neches River sites are likely due to preferential subsurface attenuation of higher frequencies.

Exploration Depth

Determining both the minimum and maximum exploration depth was an objective of this study, but the minimum depth was more critical because the geological targets were within the Holocene and late Pleistocene units near the surface. For the compressional wave surveys, minimum exploration depth is highly dependent upon the velocity difference between surface waves and compressional waves, which was greatest at the High Island beach site. At this site, the earliest reflector visible over an adequate range of source-receiver offsets had an arrival time of about 0.010 s, which corresponds to a depth of about 7 m. This is at or below the contact between Holocene and Pleistocene sediments at the site, thus only Pleistocene reflectors are visible on the reflection line. The Sabine Pass and Neches River sites have similar near-surface compressional wave velocities but higher surface-wave velocities, which suggests that earliest detectable reflectors are later than 0.010 s and deeper than 7 m. The shallowest visible reflectors are calculated at 14 m for Sabine Pass and 8 m at the Neches River. These depths are sufficiently shallow to image some Holocene deposits at these sites

Maximum exploration depths are surprising for so small a source. Reflections were recorded as late as 0.200 s at High Island and 0.130 s at Sabine Pass and Neches River sites. Velocity analysis at these relatively late times is hindered by the acquisition geometry designed for shallower reflectors, but estimated depths to the deepest reflectors are 200 m at High Island and about 120 m at the Sabine Pass and Neches River sites. The soil probe hammer has a practical exploration depth range of 5 to more than 100 m at these coastal sites.

Potential Applications

Seismic reflection methods adapted for the shallow subsurface have several potential applications in coastal environments such as those represented in the upper Texas coast. The seismic tests carried out in this study demonstrate that reflection surveys can allow a better understanding of Holocene and late Pleistocene stratigraphy as shallow as a few meters below the land surface (perhaps shallower with shear-wave sources). Reflection surveys can provide a geological context for existing boreholes, both between and beneath the holes, and can guide placement of new boreholes. They can augment an abundance of existing high resolution inner shelf and estuarine seismic reflection data with needed shallow data landward of the shoreline. Finally, reflection surveys such as those carried out in this study can be used to determine offset on numerous reactivated coastal zone faults such as those mapped by White and Tremblay (1995).

CONCLUSIONS

Shallow seismic reflection profiling using small impulsive sources is a viable method of imaging near surface Holocene and late Pleistocene strata along the upper Texas coast. The modified soil probe hammer is a simple, low energy, broad frequency band seismic source that generates a consistent seismic pulse with frequencies to at least 200 Hz. Tests at three representative coastal environments, including unvegetated beach sands at High Island, Holocene marsh deposits at Sabine Pass, and a vegetated floodplain along the Neches River, show that near-surface sediment characteristics strongly influence data quality. Highest quality data were collected in the beach environment, where surface wave velocities were below 80 m/s, recorded peak frequencies were between 100 to 200 Hz, and reflections were recorded as shallow as 7 m and as deep as 200 m. Data quality in the marsh at Sabine Pass and the vegetated floodplain along the Neches River was not as good. At these sites, surface wave velocities were higher, peak frequencies were below 100 Hz, minimum exploration depths were deeper (8 to 10 m), and maximum exploration depths were shallower (about 120 m).

Despite similar target depths and near-surface water tables at each site, optimum acquisition parameters differed. At High Island, where the only major noise sources were wind and breaking waves, one shot per shotpoint and a relatively low filter setting of 16 Hz produced good data. At the Sabine Pass marsh, where data quality was poor perhaps because of trapped organic gases in pore space, a low-cut filter setting of 32 Hz diminished surface wave noise. More shots at each shotpoint might reduce random wind-related noise at this site. At the Neches River site, where data quality was moderate, a high filter setting of 64 Hz was required to diminish traffic noise, source-related surface waves, and bridge vibrations. Optimum processing steps and parameters also differ for each environment.

Similar shallow reflection surveys are relatively easy to perform and may prove useful in a variety of coastal environments. Potential applications of this technique include studies of late Quaternary stratigraphy, near-surface faulting, and buried archeological sites. On-land surveys can augment borehole data, guide placement of boreholes, and extend offshore and estuarine seismic surveys across the critical land-sea boundary.

ACKNOWLEDGMENTS

This study was funded by the U.S. Geological Survey under grant 14-08-0001-A0912, Robert A. Morton, Principal Investigator.

REFERENCES

Aronow, Saul, and Barnes, V. E., 1982, Geologic atlas of Texas, Houston sheet: The University of Texas at Austin, Bureau of Economic Geology, map scale 1:250,000.

Fisher, W. L., Brown, L. F., Jr., McGowen, J. H., and Groat, C. G., 1973, Environmental geologic atlas of the Texas coastal zone, Beaumont-Port Arthur area: The University of Texas at Austin, Bureau of Economic Geology, 93 p.

Lehner, Peter, 1969, Salt tectonics and Pleistocene stratigraphy on continental slope of northern Gulf of Mexico: American Association of Petroleum Geologists Bulletin, v. 53, p. 2431-2479.

Mayne, W. H., 1962, Common reflection point horizontal data stacking techniques: Geophysics, v. 27, p. 927–938.

Miller, R. D., Pullan, S. E., Waldner, J. S., and Haeni, F. P., 1986, Field comparison of shallow seismic sources: Geophysics, v. 51, p. 2067-2092.

Miller, R. D., Steeples, D. W., Hill, R. W., Jr., and Gaddis, B. L., 1990, Identifying intra-alluvial and bedrock structures shallower than 30 meters using seismic reflection techniques, *in* Ward, S. H., ed., Geotechnical and environmental geophysics:

Tulsa, Oklahoma, Society of Exploration Geophysicists, Investigations in Geophysics No. 5, v. 3, p. 89–97.

Paine, J. G., 1994, Subsidence beneath a playa basin on the Southern High Plains, U. S. A.: evidence from shallow seismic data: Geological Society of America Bulletin, v. 106, p. 233-242.

Steeples, D. W., and Miller, R. D., 1990, Seismic reflection methods applied to engineering, environmental, and groundwater problems, *in* Ward, S. H., ed., Geotechnical and environmental geophysics: Tulsa, Oklahoma, Society of Exploration Geophysicists, Investigations in Geophysics No. 5, v. 1, p. 1–30.

White, W. A., and Tremblay, T. A., 1995, Submergence of wetlands as a result of human-induced subsidence and faulting along the upper Texas Gulf Coast: Journal of Coastal Research, v. 11, p. 788-807.

Widess, M. B., 1973, How thin is a thin bed? Geophysics, v. 38, p. 1176-1180.

Yilmaz, Ozdogan, 1987, Seismic data processing: Tulsa, Oklahoma, Society of Exploration Geophysicists, Investigations in Geophysics No. 2, 526 p.

FIGURE CAPTIONS

Figure 1. Map of the upper Texas coast showing the location of three seismic testing sites: gulf beach at High Island (a), chenier plain marsh at Sabine Pass (b), and modern floodplain along the Neches River (c).

Figure 2. (a) Field record HIRL1003 from gulf beach at High Island with 36 dB display gain, (b) field record with automatic gain control (0.05 s window) applied, and (c) interpreted types of seismic energy.

Figure 3. High Island power spectrum at 10 m source-receiver offset, (a) before and (b) after surface wave mute.

Figure 4. Stacking velocity picks, best-fit velocity function, and time-to-depth conversion curve for seismic reflection line at High Island test site.

Figure 5. Processed seismic reflection sections from test sites at (a) High Island, (b) Sabine Pass, and (c) Neches River. Traces are 0.5 m apart and are displayed with automatic gain control (0.1 s window) applied.

Figure 6. Field record SPRL1127 from Sabine Pass site. Highest amplitudes in each trace have been equalized.

Figure 7. Sabine Pass power spectrum at 10 m source-receiver offset, (a) before and (b) after surface wave mute.

Figure 8. Field records from low-cut filter test at Neches River site. During the test, data were acquired with the low-cut filter at (a) 4 Hz, (b) 16 Hz, (c) 64 Hz, and (d) 96 Hz. Records displayed with highest amplitude equalized for each trace.

Figure 9. Neches River power spectrum at 10 m source-receiver offset, (a) before and (b) after surface wave mute.

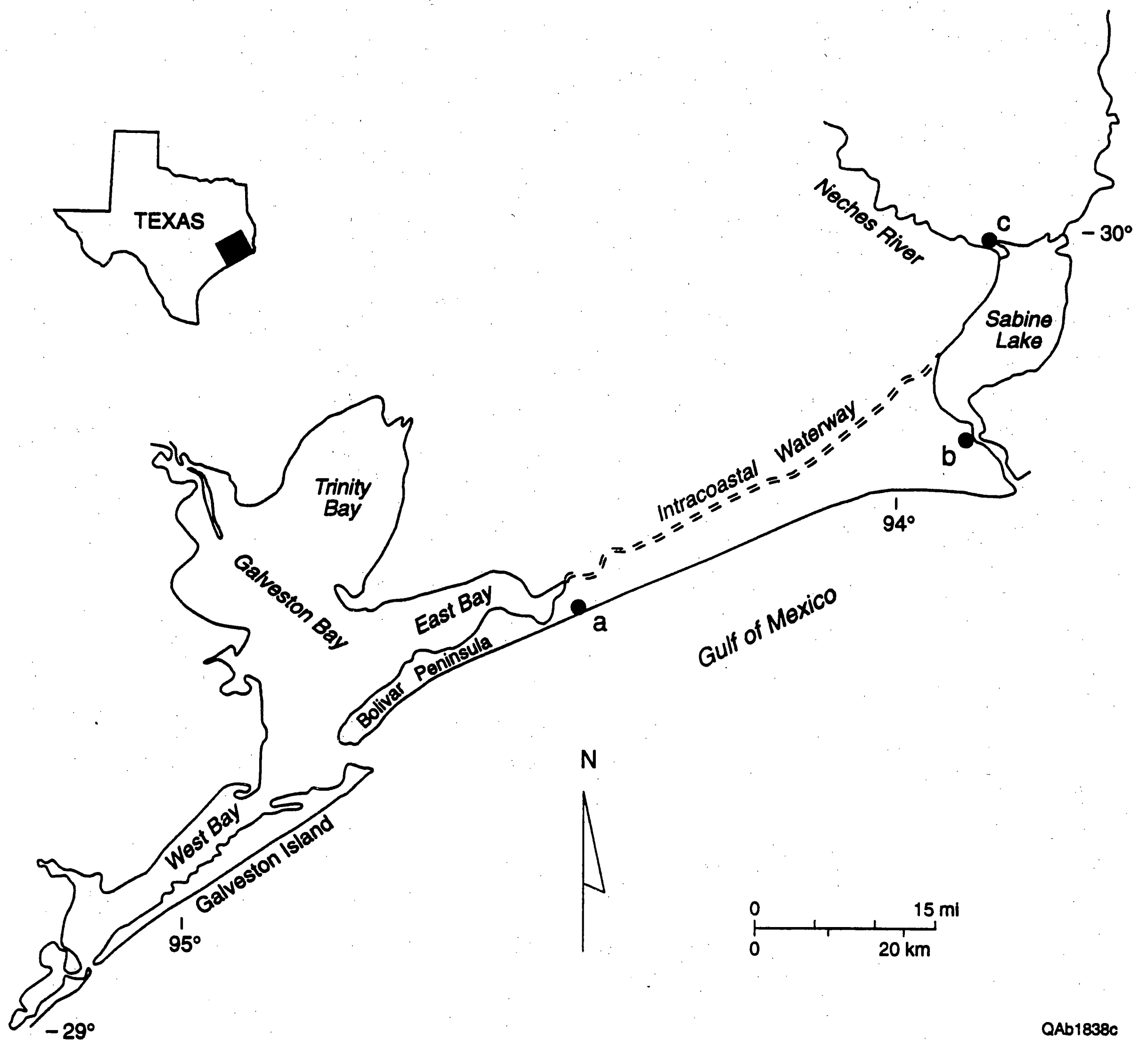
TEXAS
Neches River
c
– 30°
Sabine
Lake
Intracoastal Waterway
b
Trinity
Bay
94°
Galveston Bay
East Bay
a
Gulf of Mexico
Bolivar Peninsula
N
West Bay
Galveston Island
0
15 mi
0
20 km
95°
– 29°
QAb1838c

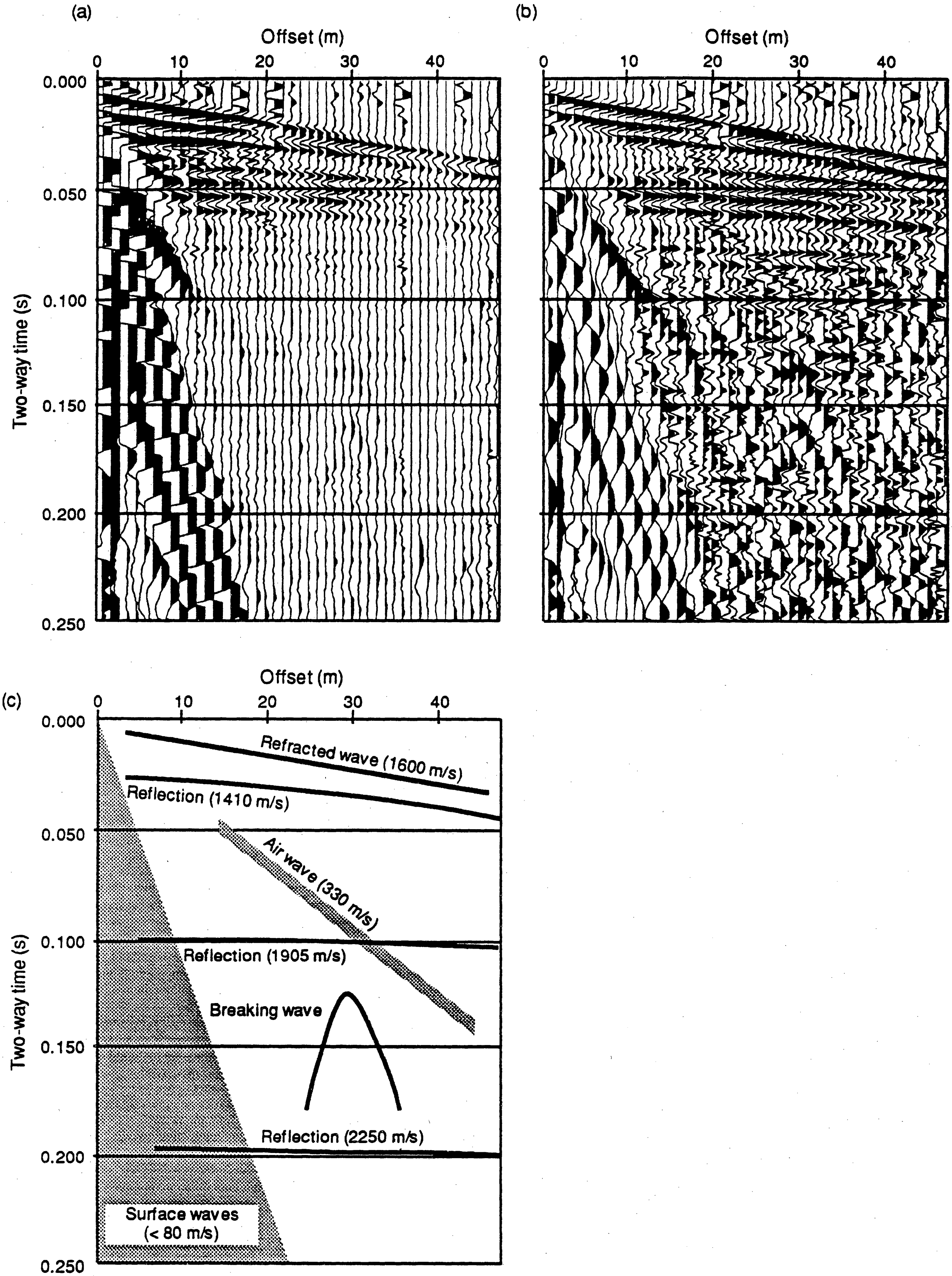
(a)
(b)
Offset (m)
0
10
20
30
40
Two-way time (s)
0.000
0.050
0.100
0.150
0.200
0.250
(c)
Refracted wave (1600 m/s)
Reflection (1410 m/s)
Air wave (330 m/s)
Reflection (1905 m/s)
Breaking wave
Reflection (2250 m/s)
Surface waves
(< 80 m/s)

(a)

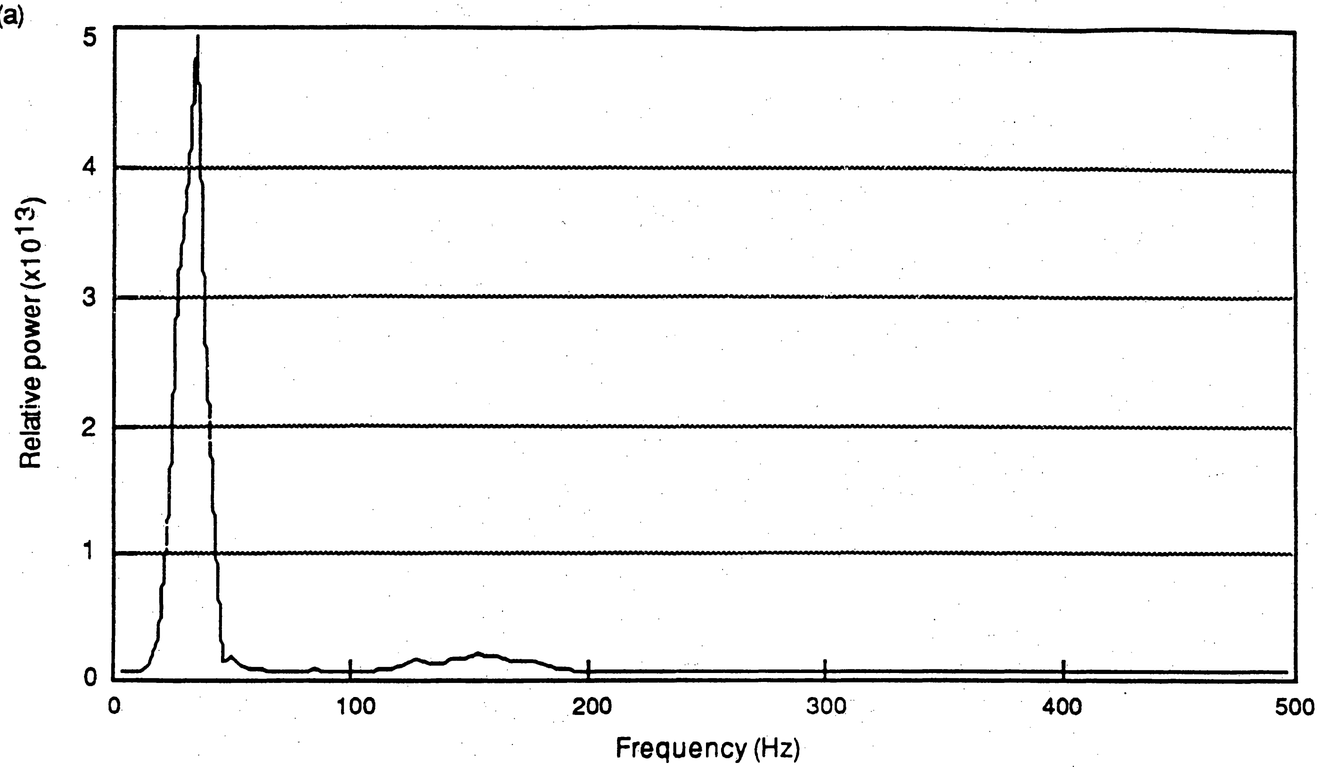

5
4
3
2
1
0
Relative power (x10^{13})
0
100
200
300
400
500
Frequency (Hz)

(b)

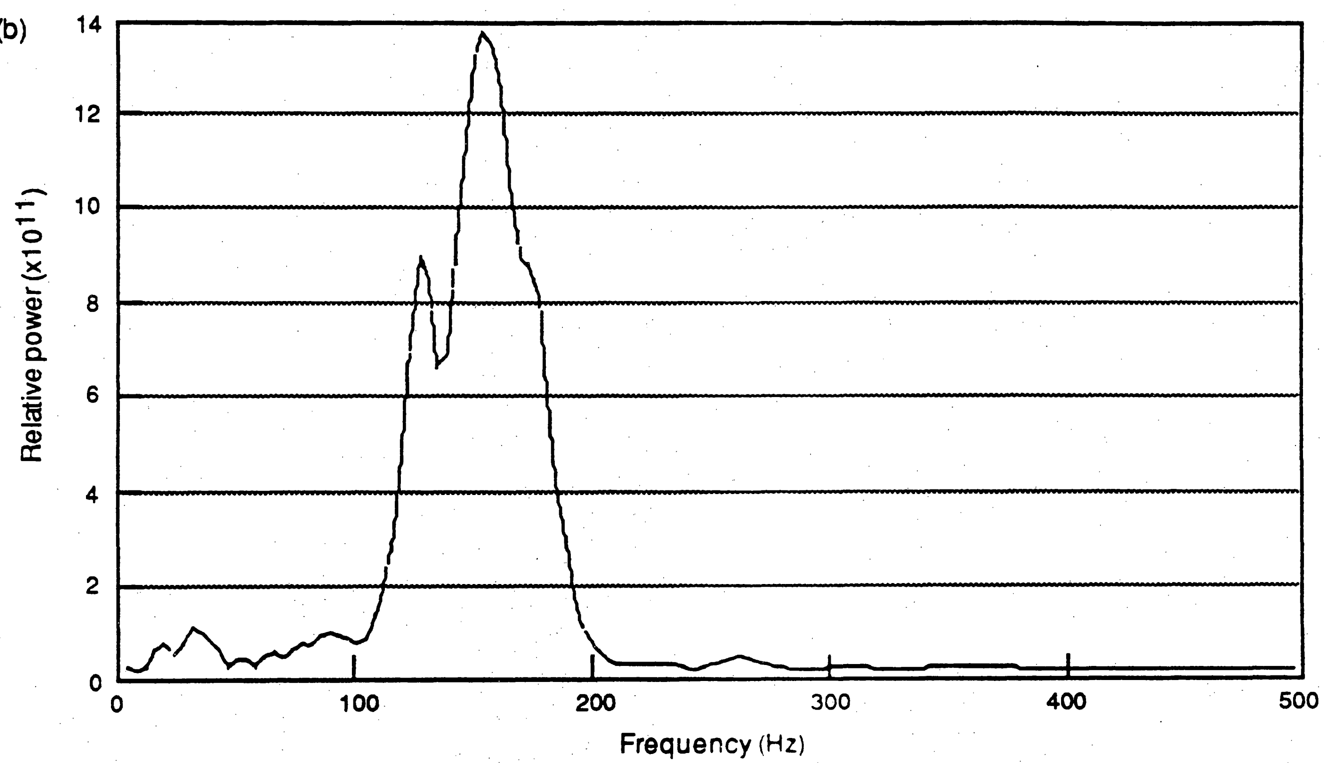

14
12
10
8
6
4
2
0
Relative power (x10^{11})
0
100
200
300
400
500
Frequency (Hz)

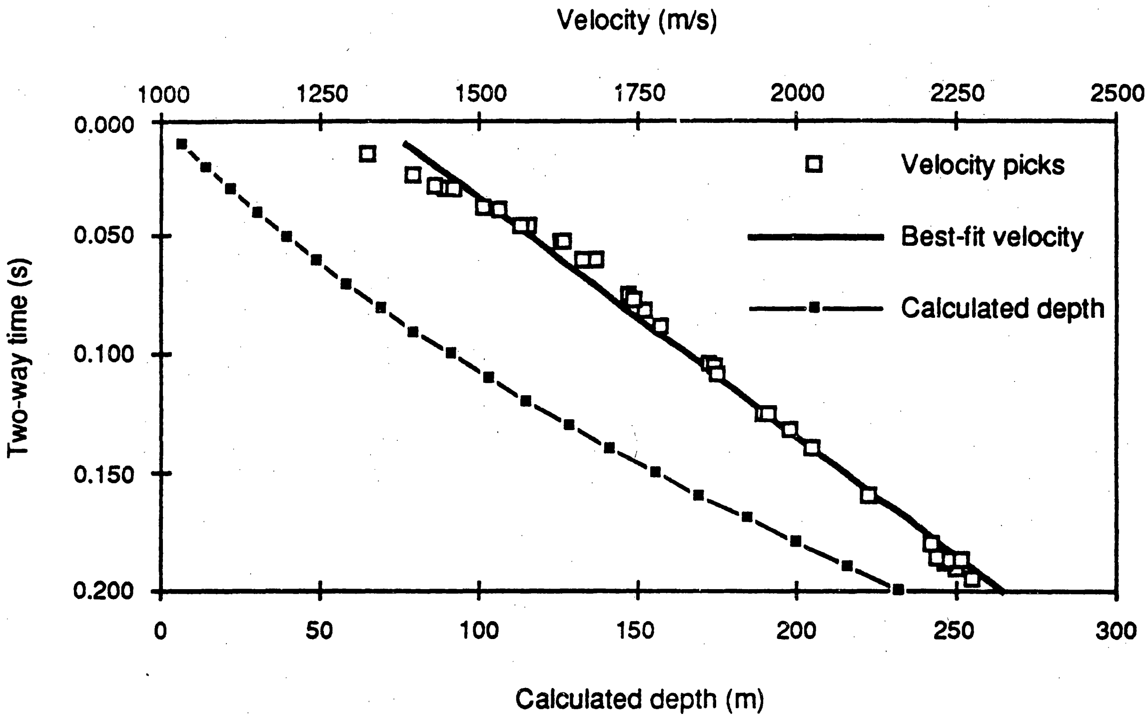

Velocity (m/s)
1000
1250
1500
1750
2000
2250
2500
0.000
0.050
0.100
0.150
0.200
Two-way time (s)
Velocity picks
Best-fit velocity
Calculated depth
0
50
100
150
200
250
300
Calculated depth (m)

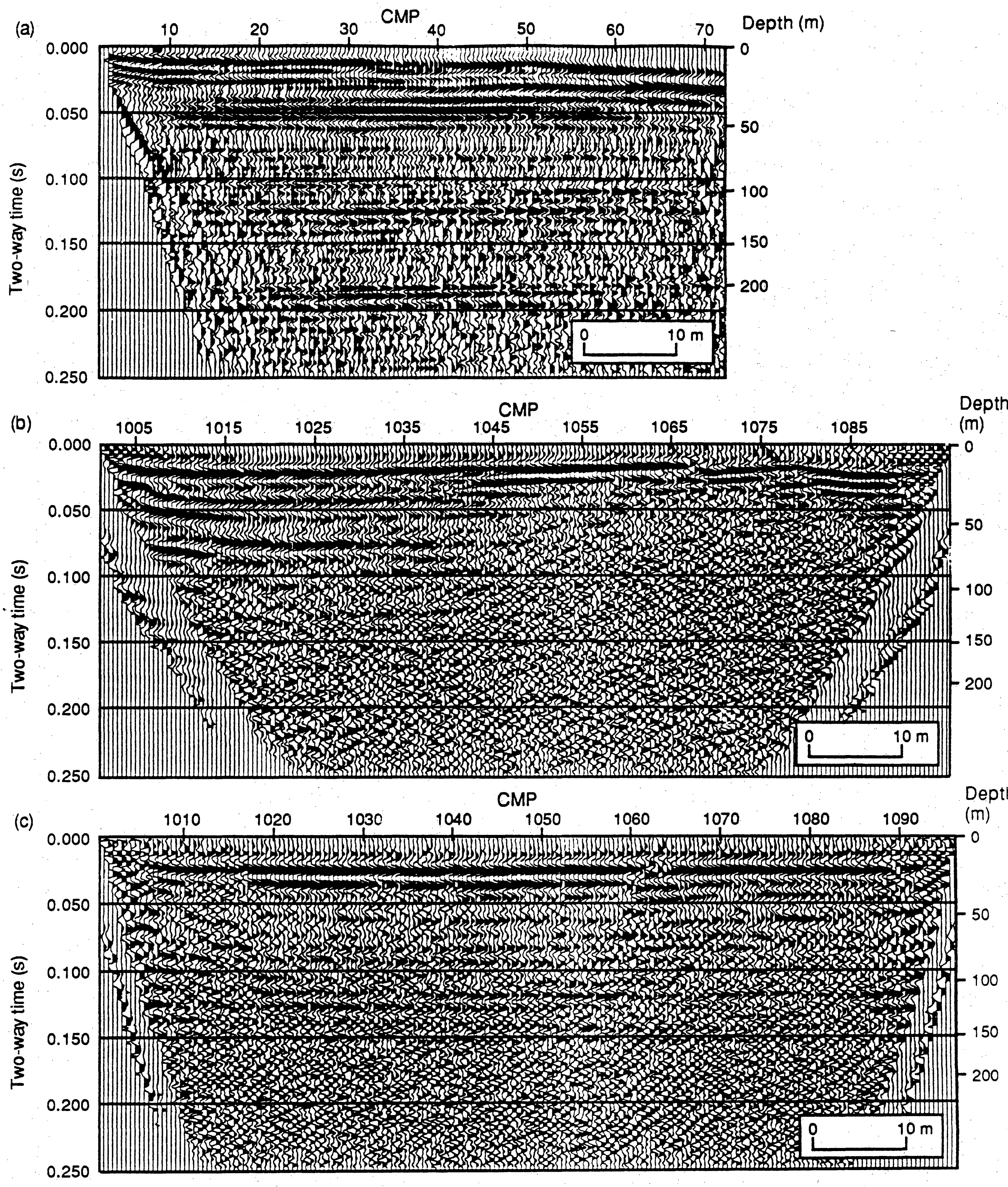

(a)
CMP
10 20 30 40 50 60 70
Depth (m)
Two-way time (s)
0.000 0.050 0.100 0.150 0.200 0.250
0 50 100 150 200
0 10 m
(b)
CMP
1005 1015 1025 1035 1045 1055 1065 1075 1085
Depth (m)
Two-way time (s)
0.000 0.050 0.100 0.150 0.200 0.250
0 50 100 150 200
0 10 m
(c)
CMP
1010 1020 1030 1040 1050 1060 1070 1080 1090
Depth (m)
Two-way time (s)
0.000 0.050 0.100 0.150 0.200 0.250
0 50 100 150 200
0 10 m

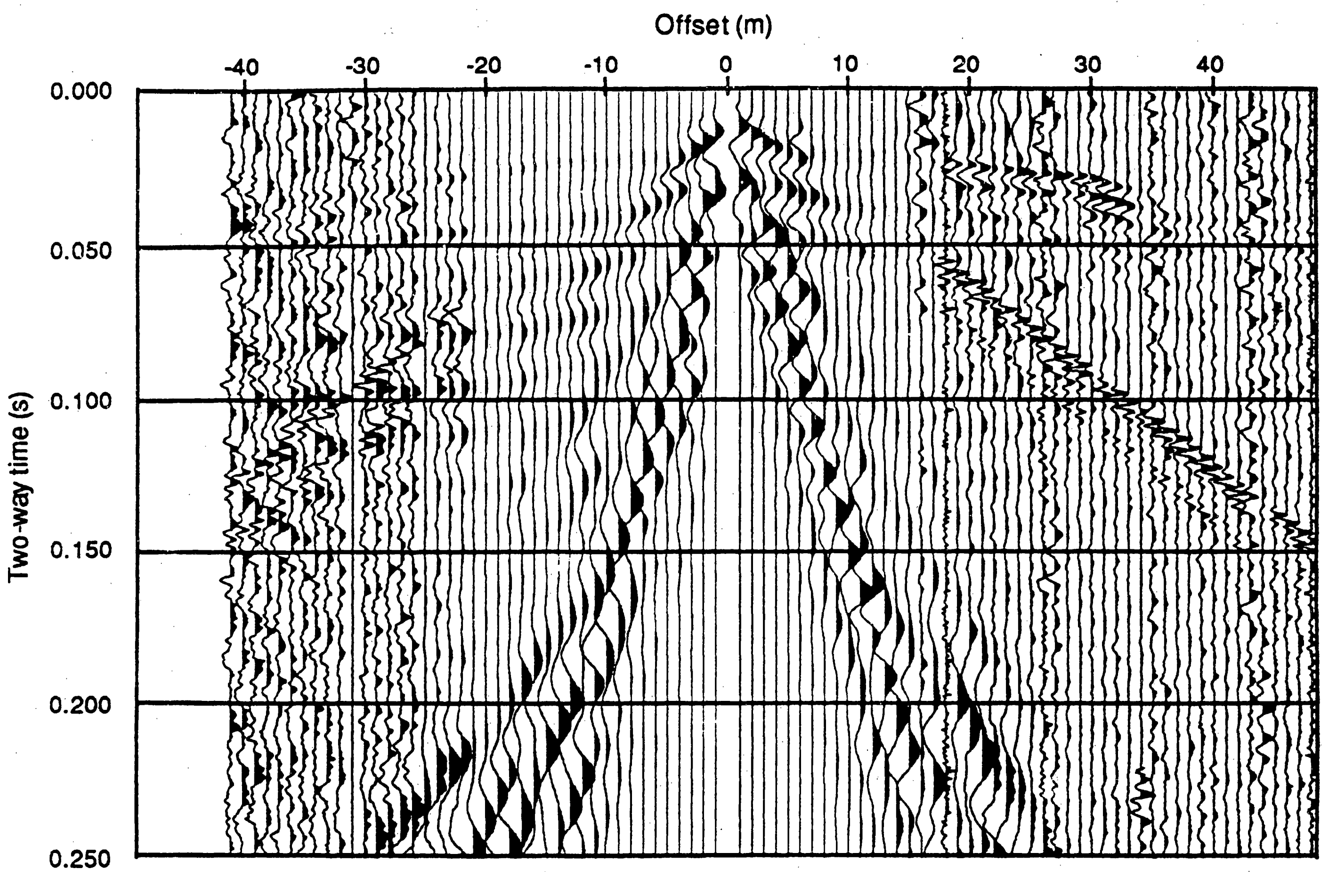
Offset (m)
-40
-30
-20
-10
0
10
20
30
40
Two-way time (s)
0.000
0.050
0.100
0.150
0.200
0.250

(a)

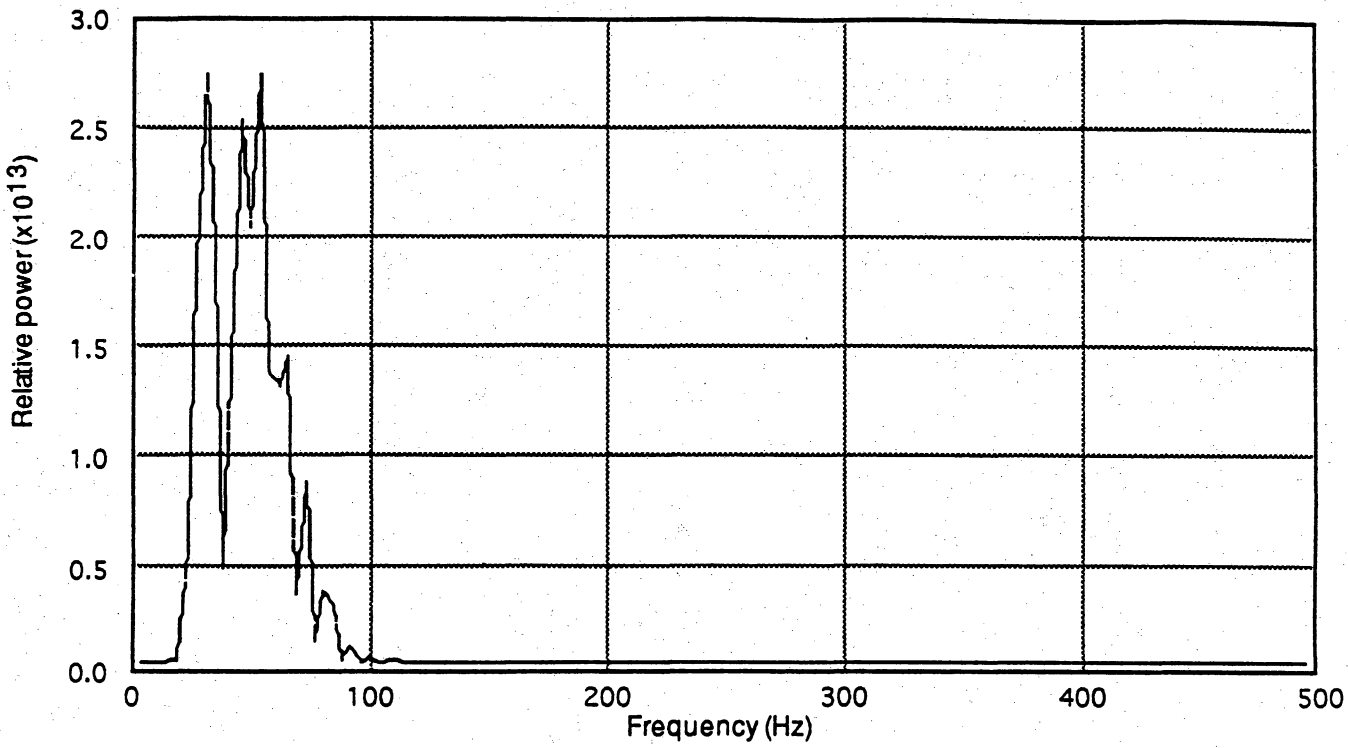
Relative power (x10^13)
3.0
2.5
2.0
1.5
1.0
0.5
0.0
0
100
200
300
400
500
Frequency (Hz)

(b)

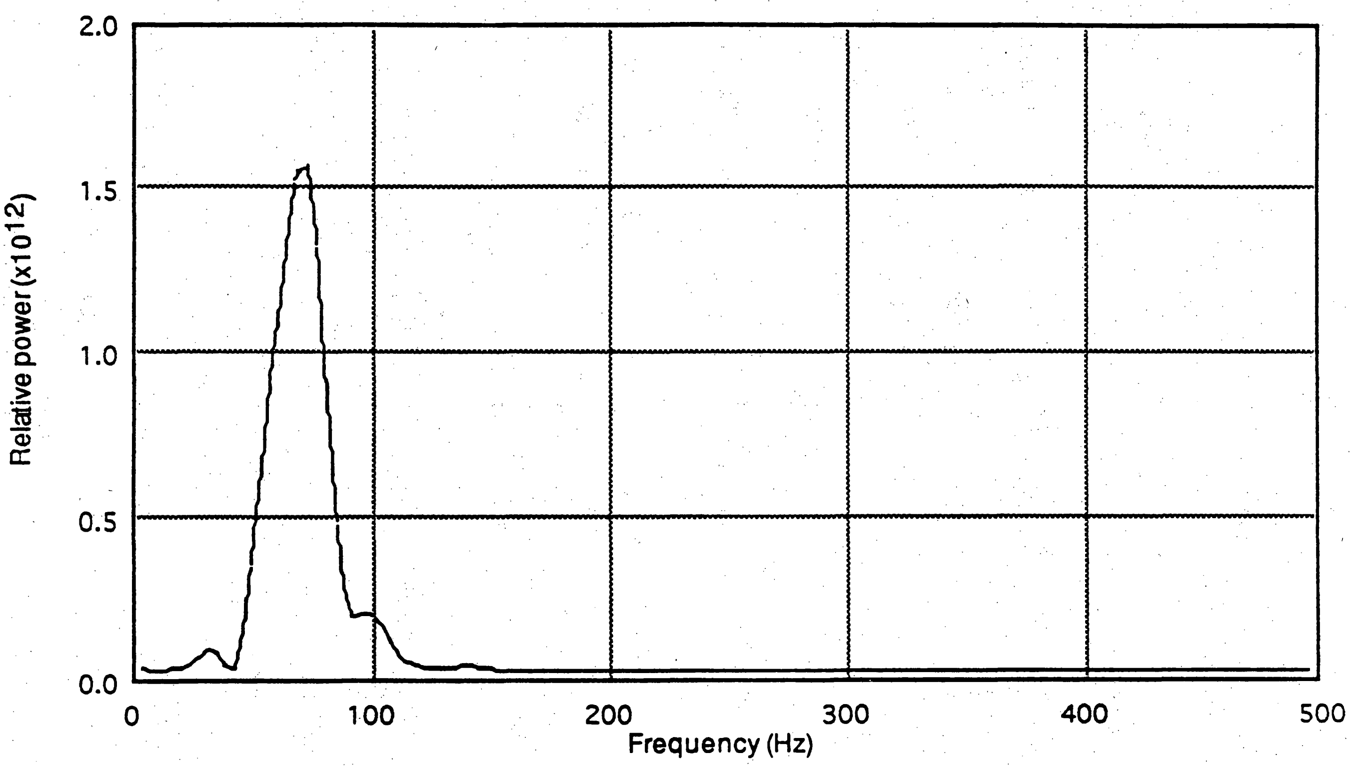
Relative power (x10^12)
2.0
1.5
1.0
0.5
0.0
0
100
200
300
400
500
Frequency (Hz)

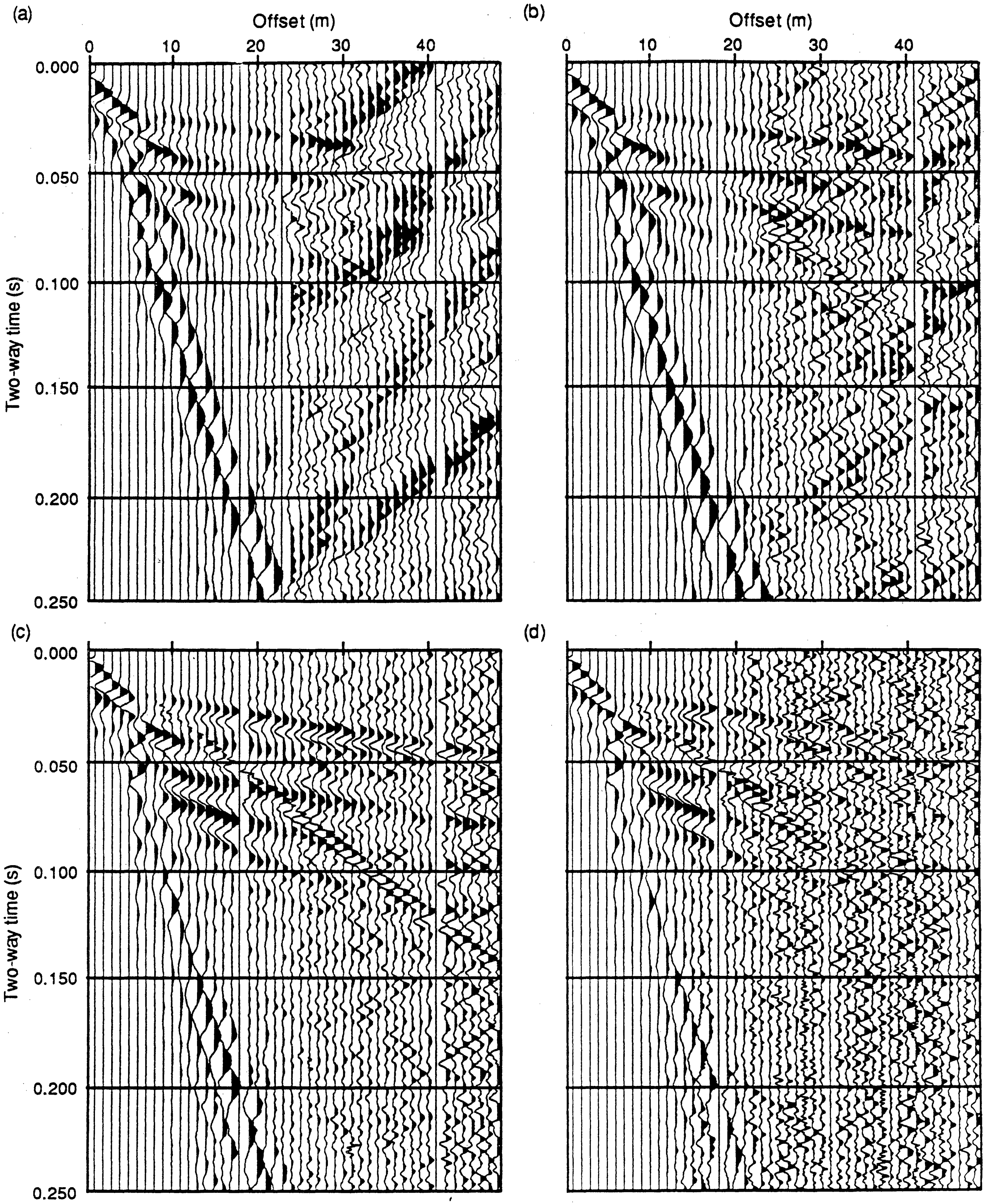

(a)
Offset (m)
0
10
20
30
40
0.000
0.050
0.100
0.150
0.200
0.250
Two-way time (s)
(b)
Offset (m)
0
10
20
30
40
(c)
0.000
0.050
0.100
0.150
0.200
0.250
Two-way time (s)
(d)

(a)

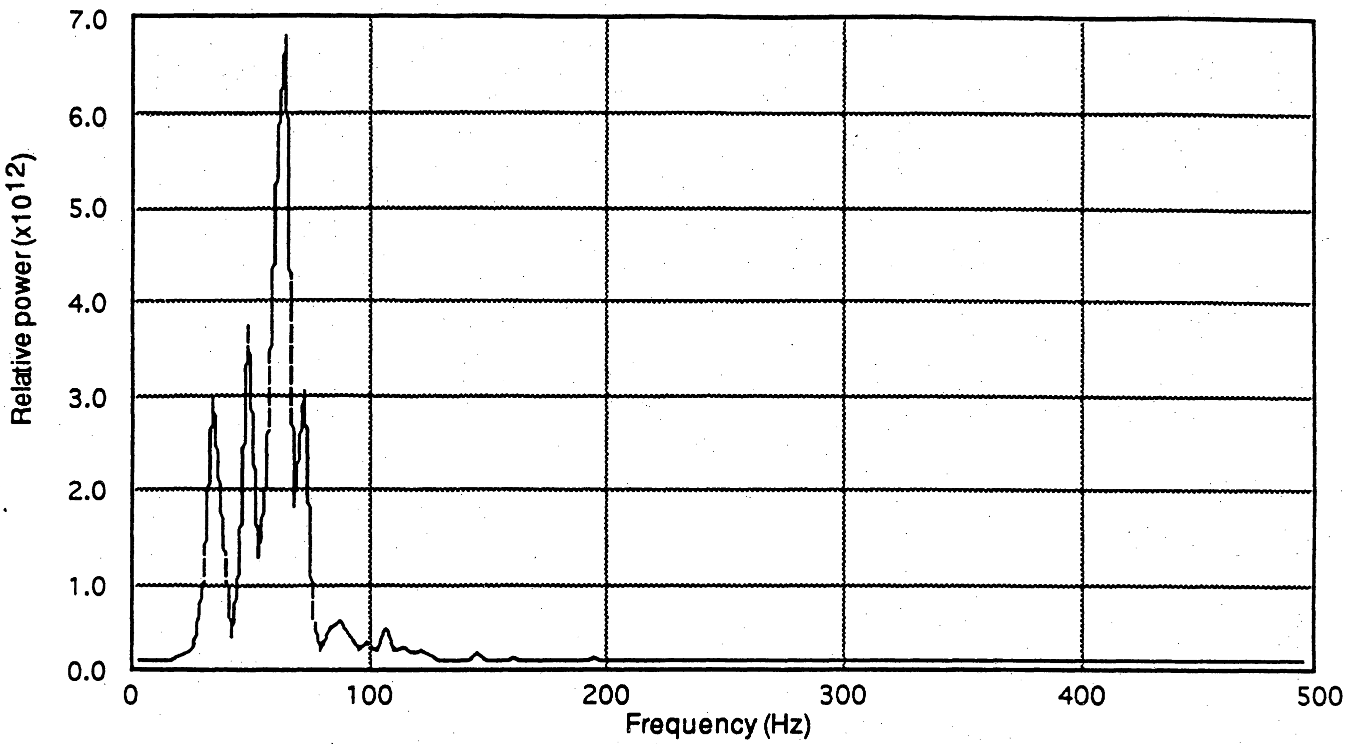
7.0
6.0
5.0
4.0
3.0
2.0
1.0
0.0
Relative power (x10^{12})
0
100
200
300
400
500
Frequency (Hz)

(b)

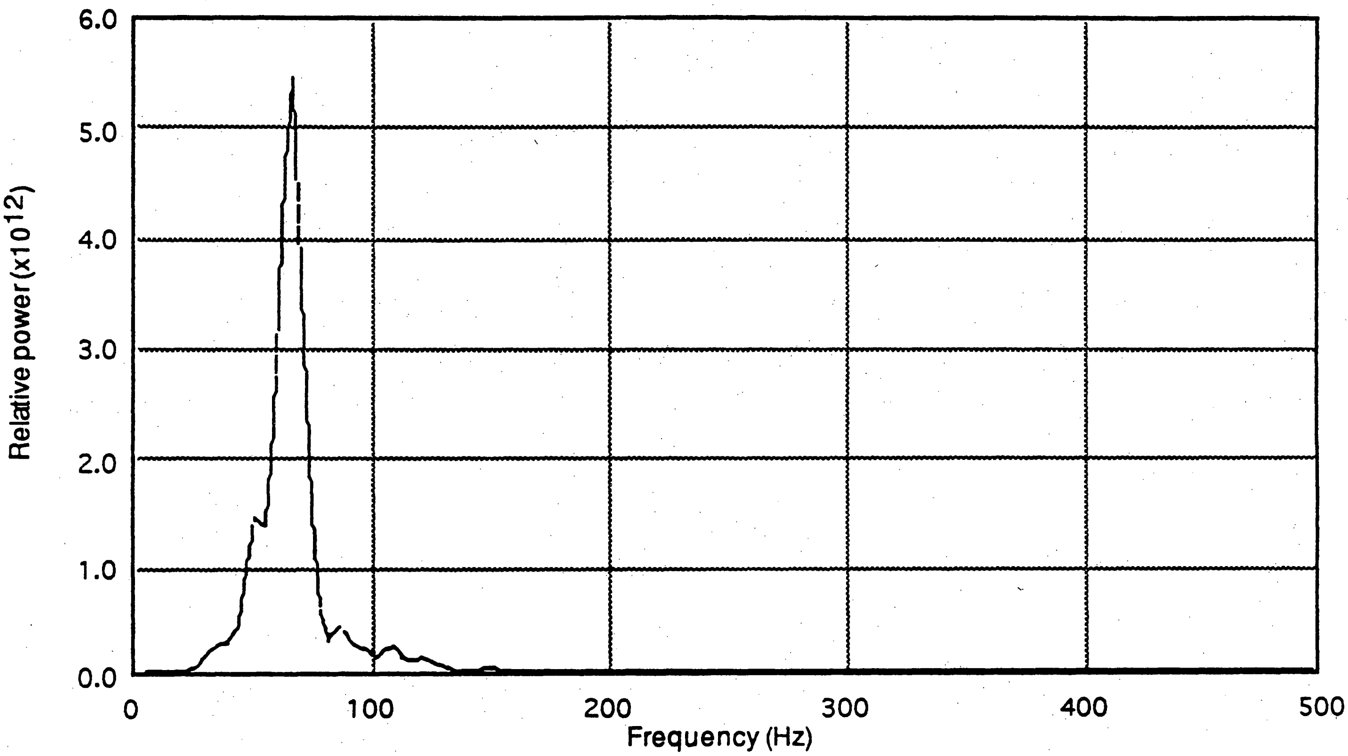
6.0
5.0
4.0
3.0
2.0
1.0
0.0
Relative power (x10^{12})
0
100
200
300
400
500
Frequency (Hz)

Table 1. Equipment used to collect shallow seismic data at High Island, Sabine Pass, and Neches River test sites.

Energy sources	3.6 kg modified soil probe hammer (reflection source) 5.4 kg sledge hammer on aluminum plate (refraction source)
Geophones	Mark Products L-40A (40 Hz, 515 ohm coil resistance, 13 cm spikes)
Seismograph	Bison 9048 (48 channel, 16 bit analog to digital conversion)

Table 2. Recording parameters and acquisition geometry used during seismic reflection surveys.

	High Island (January 3, 1995)	Sabine Pass (January 4, 1995)	Neches River (January 4, 1995)
Spread type	End-on	End-on	Split
Source to near trace offset (m):	1	1	1
Spread length (m)	47	47	23
Source stacks	1	1	1
Geophones in array	1	1	1
Geophone spacing (m)	1	1	1
Recording channels	48	48	48
Sample interval (ms)	1.0	0.5	0.5
Record length (s)	1.0	0.25	0.25
Analog low-cut filter (Hz)	16	32	64
Analog high-cut filter (Hz)	1000	1000	1000
Data fold	24	48	24

Addendum 9. Pre-project Profiles and Sediment Textures, Beach Nourishment Project

GPS UTM coordinates Galveston Surveys

Profile no.	UTM Coordinates	
S8	328128.648	3243216.188
SI	327928.186	3242984.517
S9	327728.354	3242750.516
9B	327485.247	3242532.448
11	327302.283	3242284.932
12	327118.571	3242129.948
15	326741.445	3241802.697
18	326385.299	3241497.489
20	326179.937	3241317.498
22	325864.794	3241076.027
23A	325745.854	3240991.415
26	325443.996	3240774.210
29	325089.773	3240521.363
31	324750.484	3240278.538
33	324473.180	3240098.352
36	324113.029	3239875.446
39	323744.028	3239624.768
42	323343.890	3239398.496
45	323007.686	3239174.865
48	322690.178	3238958.090
W0	322340.245	3238744.756
W1	322078.773	3238586.913
Sed. samples		
B1	330540.000	3242870.000
B2	331138.000	3243179.000
B3	330438.000	3242472.000
B4	329817.000	3243038.000
B5	329420.000	3242293.000
S8-2	328484.000	3242843.000
S8-3	328588.000	3242730.000
S8-4	328701.000	3242601.000
SI-2	328187.000	3242687.000
SI-3	328346.000	3242541.000
SI-4	328466.000	3242433.000
S9-4	328188.000	3242265.000
S9-3	328080.000	3242360.000
S9-2	327960.000	3242517.000
9B-4	327948.000	3242051.000
9B-3	327829.000	3242160.000
9B-2	327689.000	3242319.000
11-2	327429.000	3242074.000
11-3	327591.000	3241968.000
11-4	327716.000	3241830.000
12-4	327560.000	3241642.000
12-3	327418.000	3241829.000

12-2	327275.000	3241949.000
15-3	327016.000	3241482.000
15-4	327177.000	3241350.000
18-3	326689.000	3241199.000
18-2	326536.000	3241323.000
20-2	326350.000	3241145.000
20-3	326475.000	3241008.000
20-4	326595.000	3240877.000
22-3	326146.000	3240788.000
22-2	326041.000	3240917.000
23A-3	325968.000	3240681.000
23A-4	326114.000	3240514.000
26-4	325782.000	3240348.000
26-2	325584.000	3240619.000
29-2	325209.000	3240354.000
29-3	325321.000	3240234.000
29-4	325439.000	3240063.000
31-4	325108.000	3239786.000
31-3	324956.000	3239993.000
31-2	324884.000	3240135.000
33-3	324677.000	3239785.000
33-4	324789.000	3239601.000
36-2	324227.000	3239707.000
39-2	323858.000	3239466.000
39-4	324113.000	3239124.000
42-4	323611.000	3238864.000
42-3	323497.000	3239111.000
45-2	323091.000	3238984.000
45-3	323228.000	3238854.000
45-4	323368.000	3238666.000
48-3	322897.000	3238680.000
48-2	322819.000	3238776.000
W0-2	322463.000	3238508.000
W0-4	322567.000	3238266.000
W1-4	322291.000	3238094.000
W1-3	322225.000	3238261.000
W1-2	322193.000	3238357.000

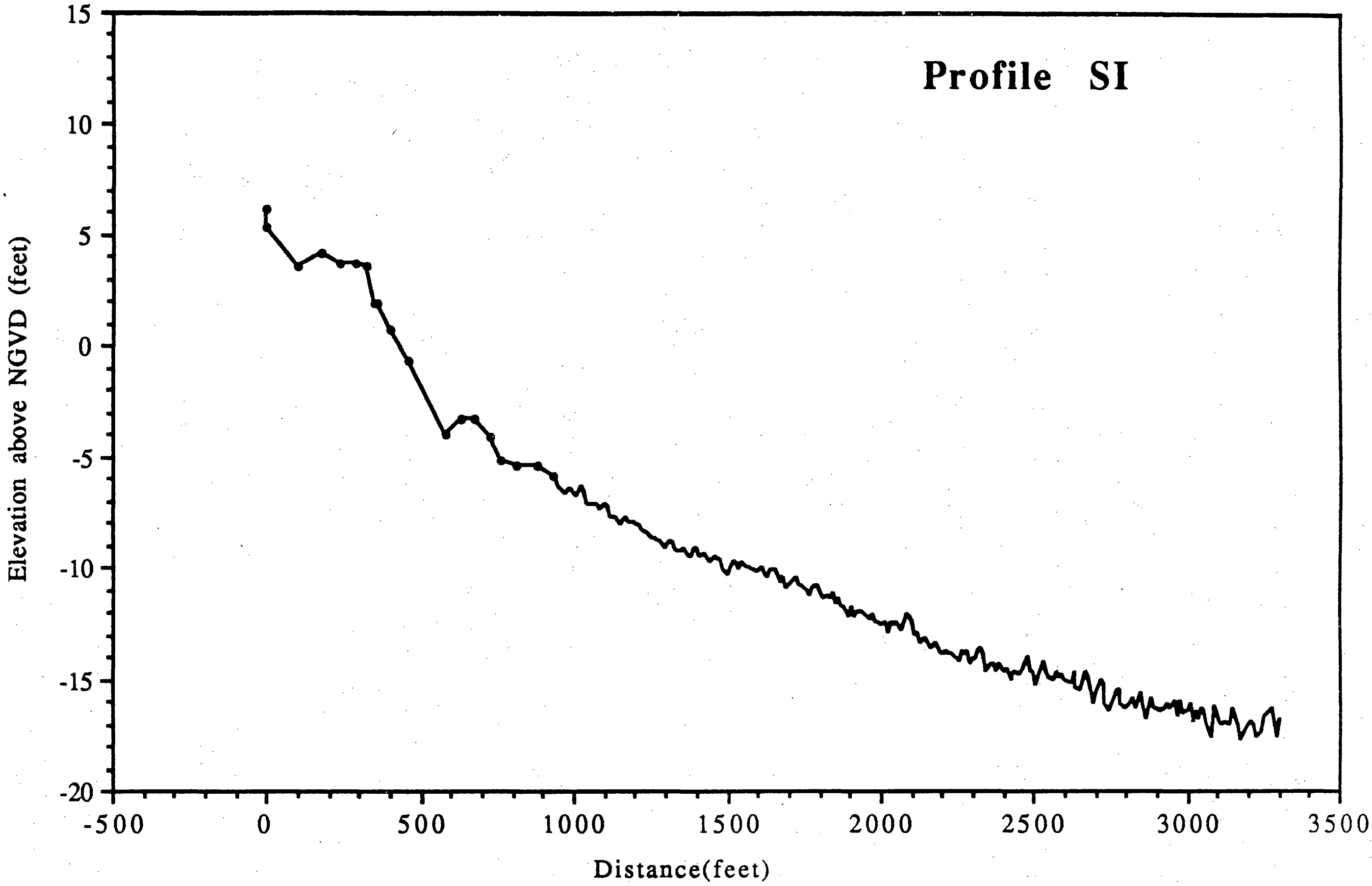
Profile SI
15
10
5
0
-5
-10
-15
-20
Elevation above NGVD (feet)
-500
0
500
1000
1500
2000
2500
3000
3500
Distance(feet)

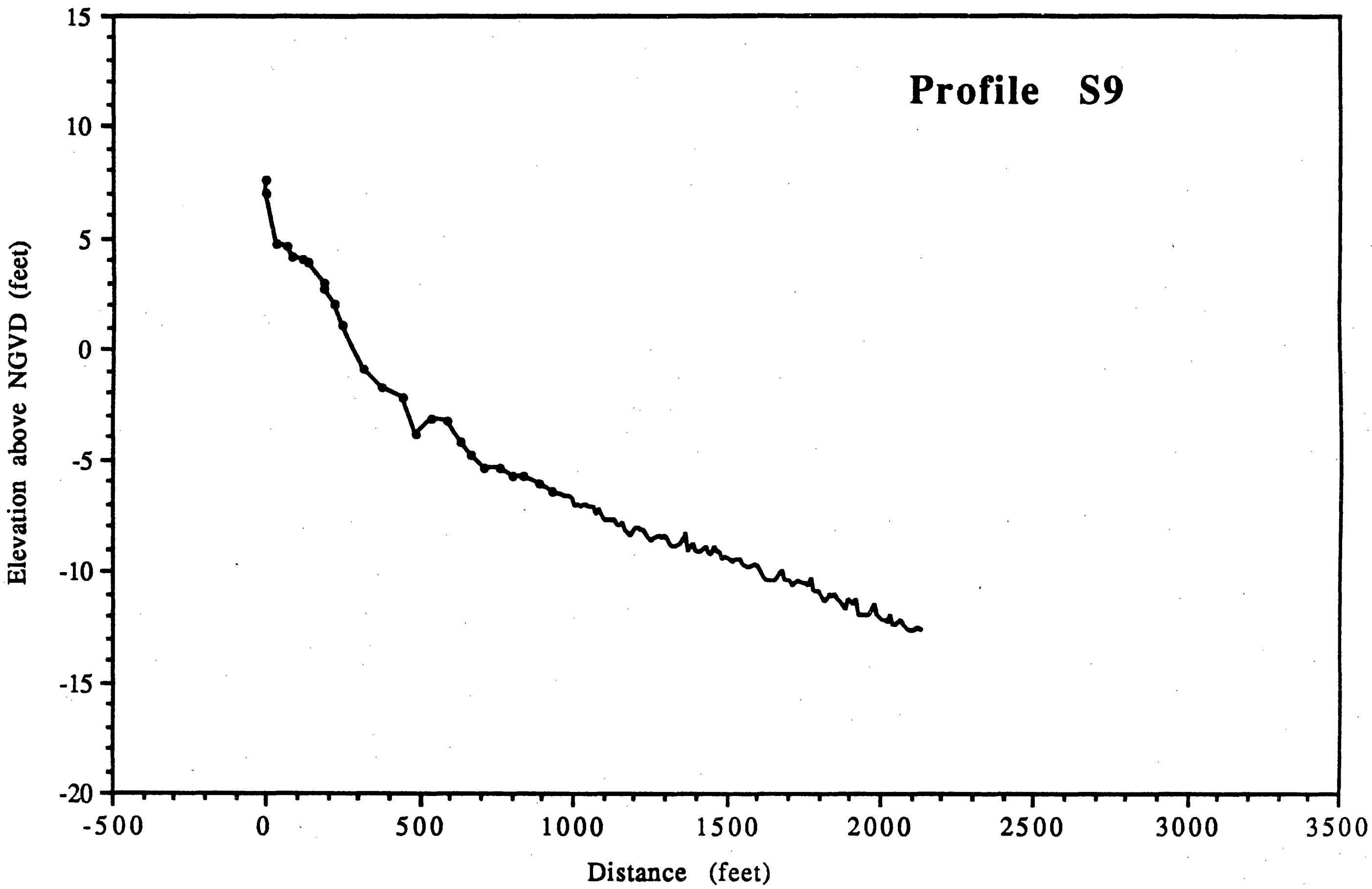

Profile S9
Elevation above NGVD (feet)
Distance (feet)
15
10
5
0
-5
-10
-15
-20
-500
0
500
1000
1500
2000
2500
3000
3500

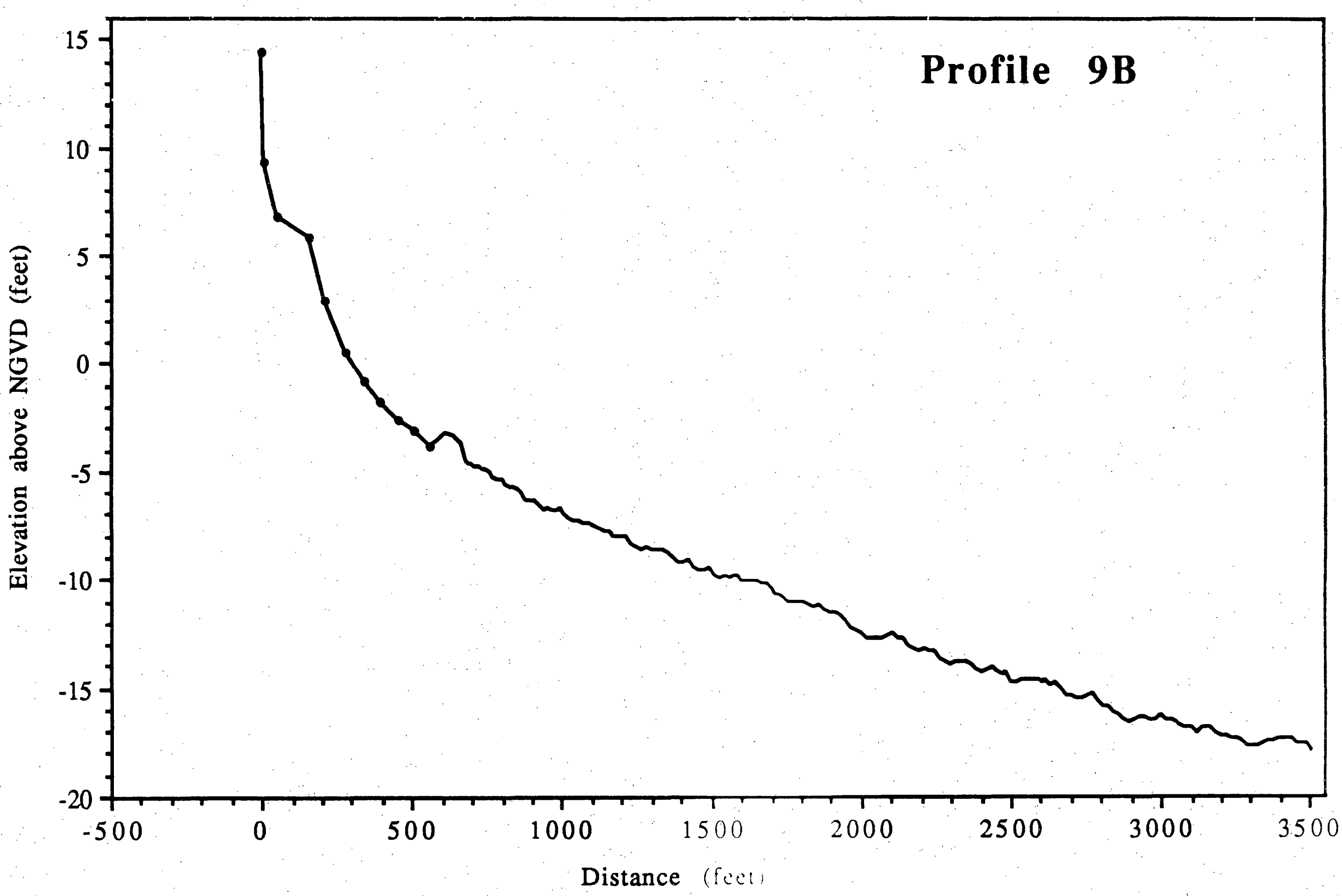

Profile 9B
Elevation above NGVD (feet)
15
10
5
0
-5
-10
-15
-20
-500
0
500
1000
1500
2000
2500
3000
3500
Distance (feet)

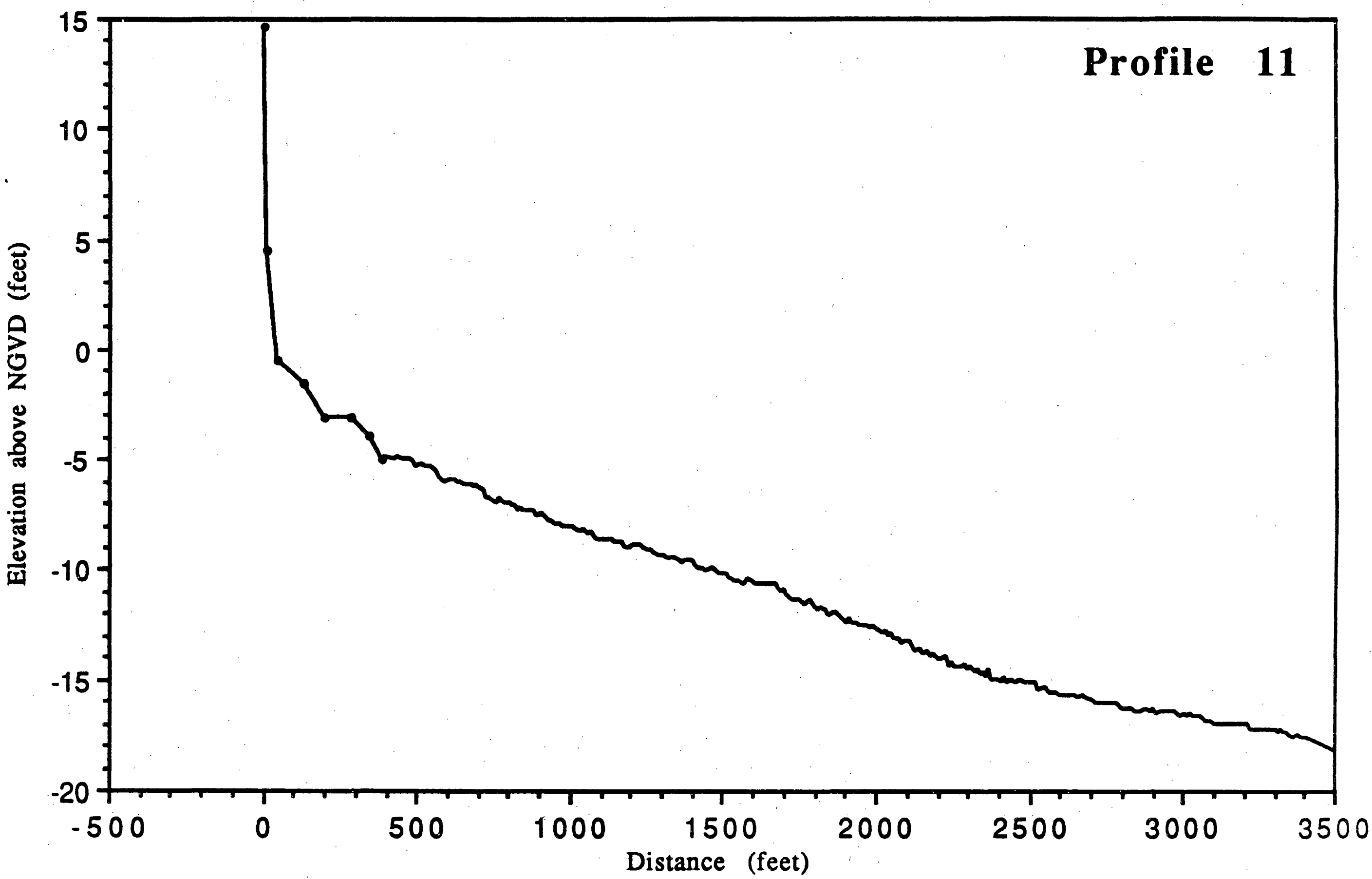
Profile 11
Elevation above NGVD (feet)
15
10
5
0
-5
-10
-15
-20
-500
0
500
1000
1500
2000
2500
3000
3500
Distance (feet)

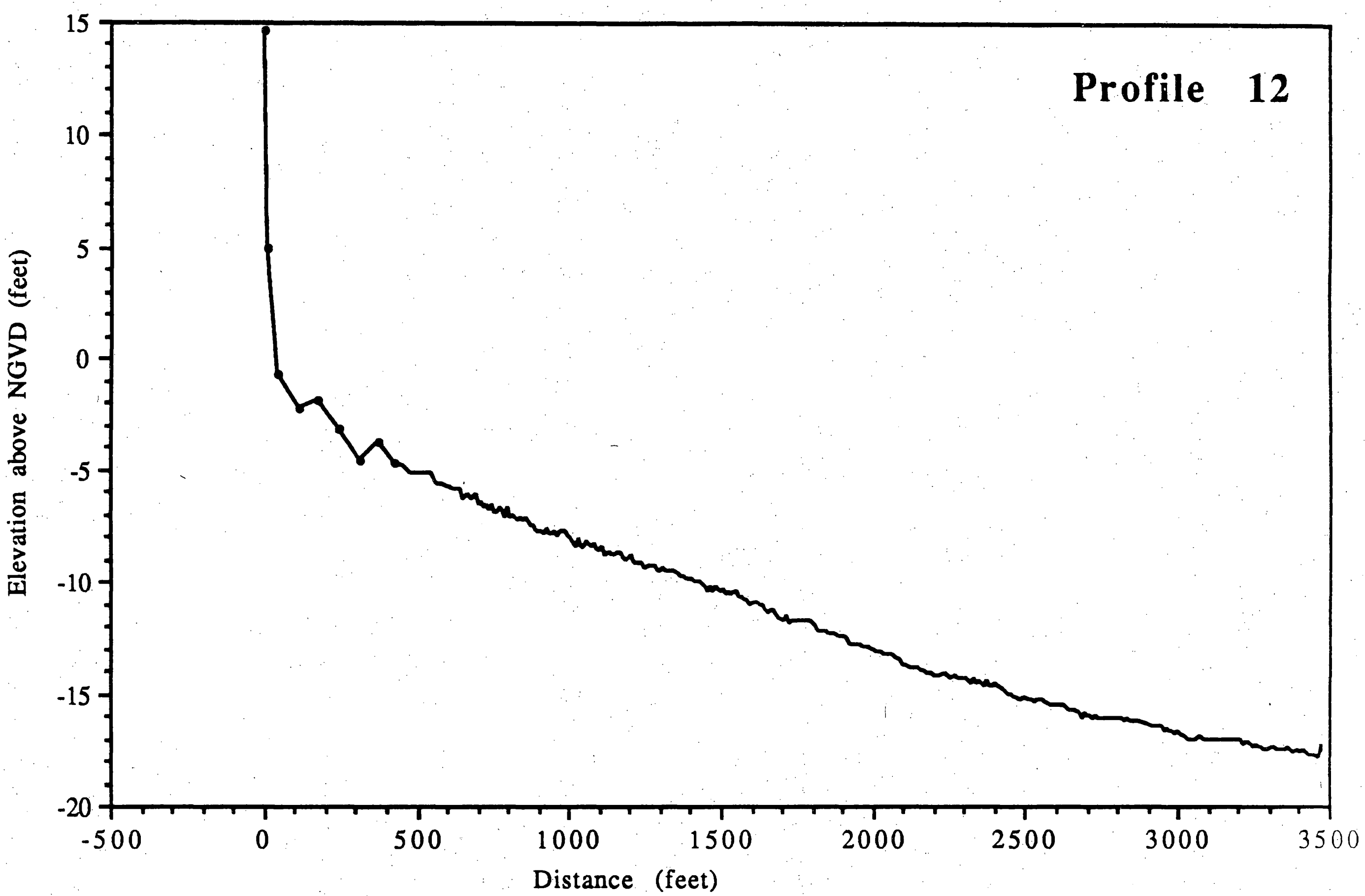

Profile 12
Elevation above NGVD (feet)
15
10
5
0
-5
-10
-15
-20
-500
0
500
1000
1500
2000
2500
3000
3500
Distance (feet)

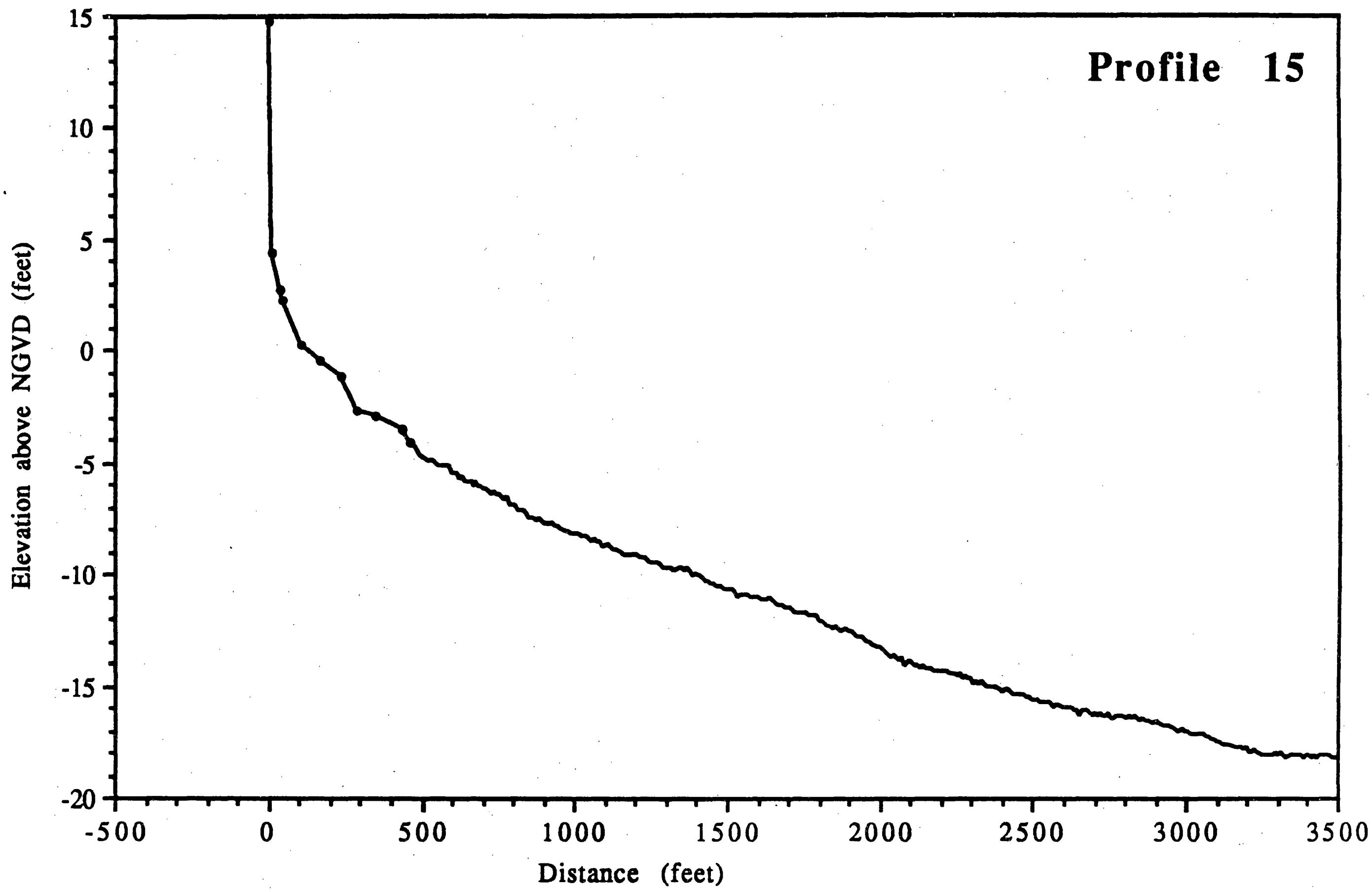

Profile 15
Elevation above NGVD (feet)
15
10
5
0
-5
-10
-15
-20
-500
0
500
1000
1500
2000
2500
3000
3500
Distance (feet)

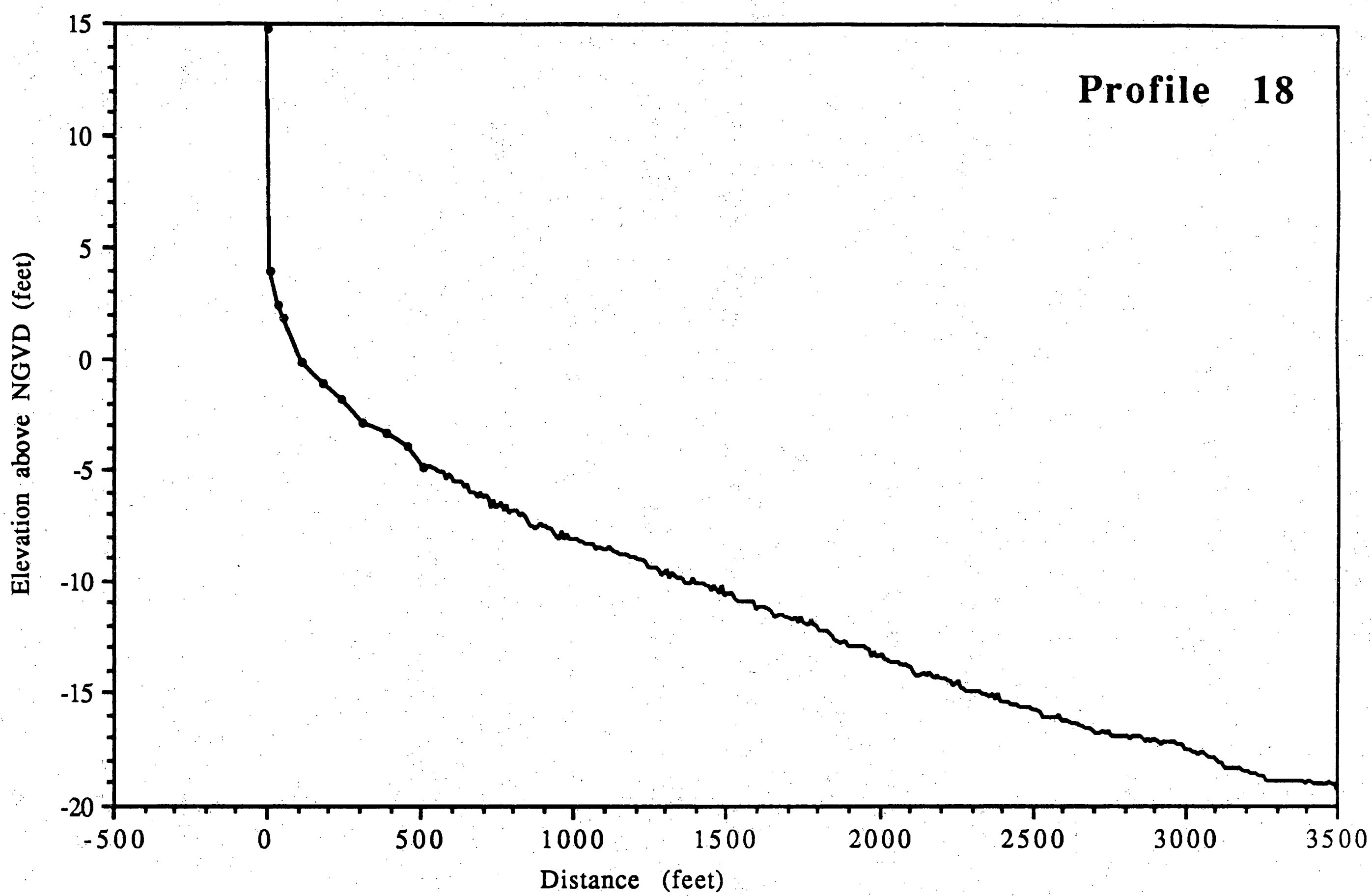

Profile 18
Elevation above NGVD (feet)
15
10
5
0
-5
-10
-15
-20
-500
0
500
1000
1500
2000
2500
3000
3500
Distance (feet)

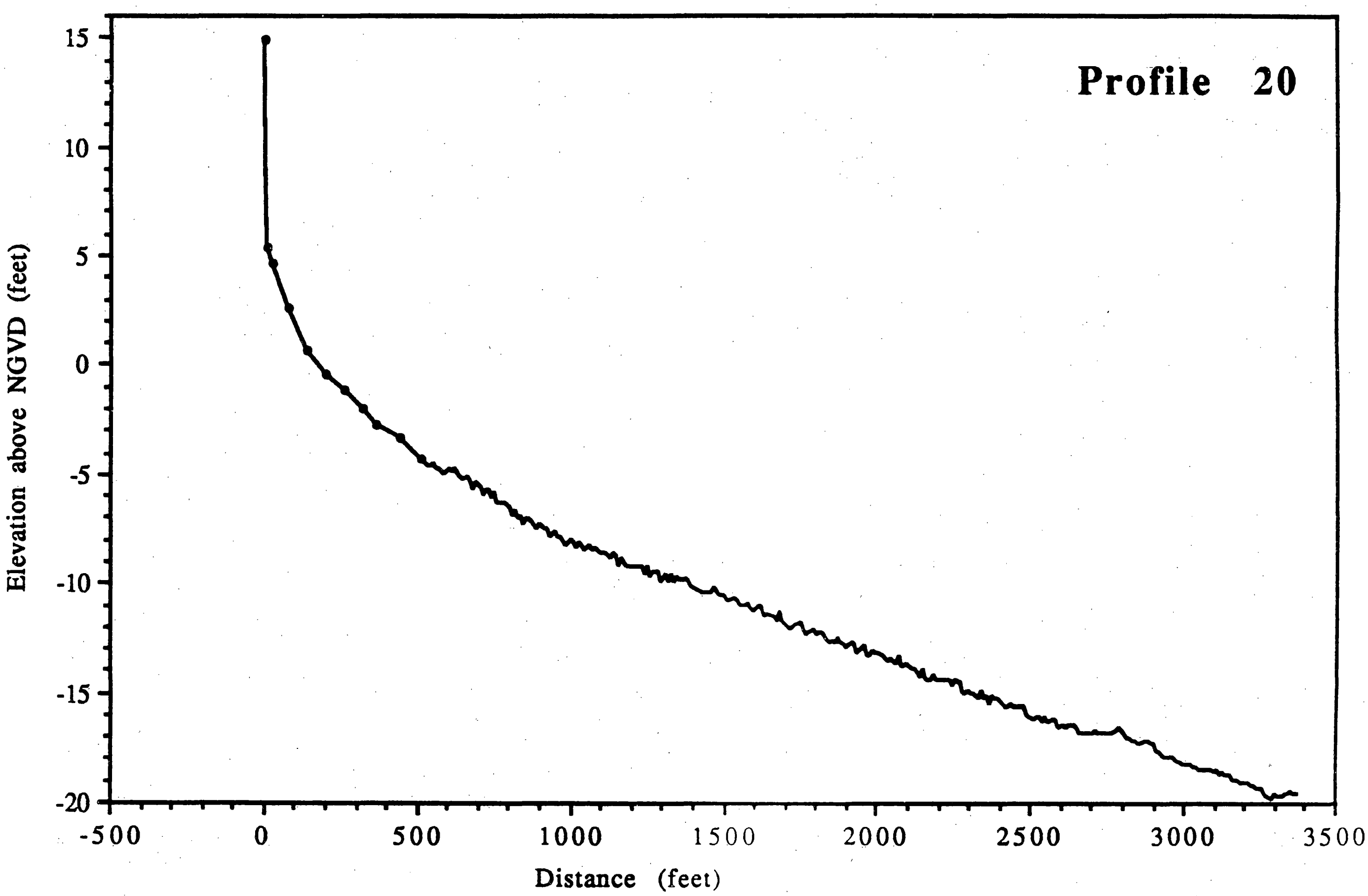

Profile 20
Elevation above NGVD (feet)
15
10
5
0
-5
-10
-15
-20
-500
0
500
1000
1500
2000
2500
3000
3500
Distance (feet)

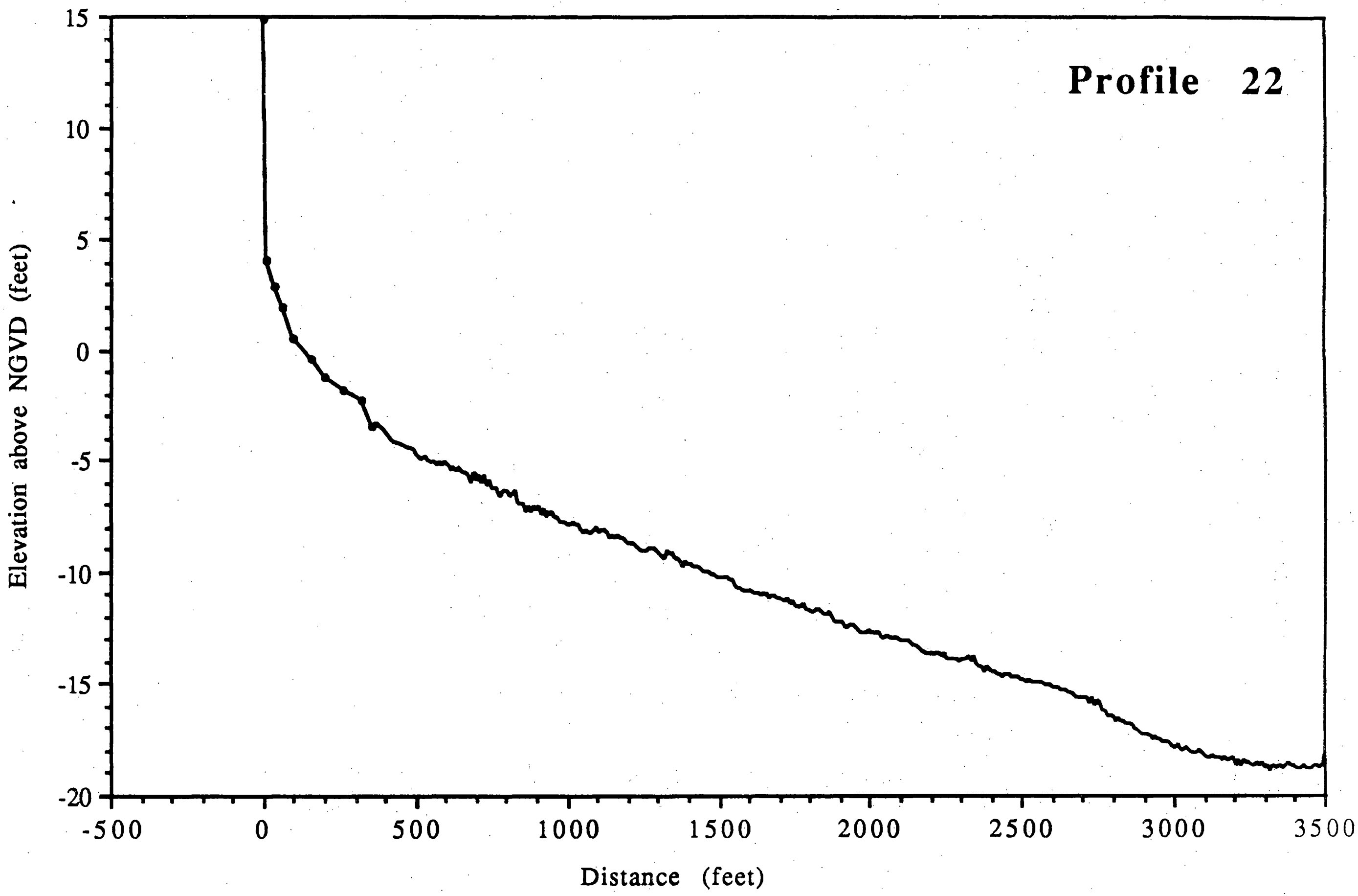
Profile 22
Elevation above NGVD (feet)
15
10
5
0
-5
-10
-15
-20
-500
0
500
1000
1500
2000
2500
3000
3500
Distance (feet)

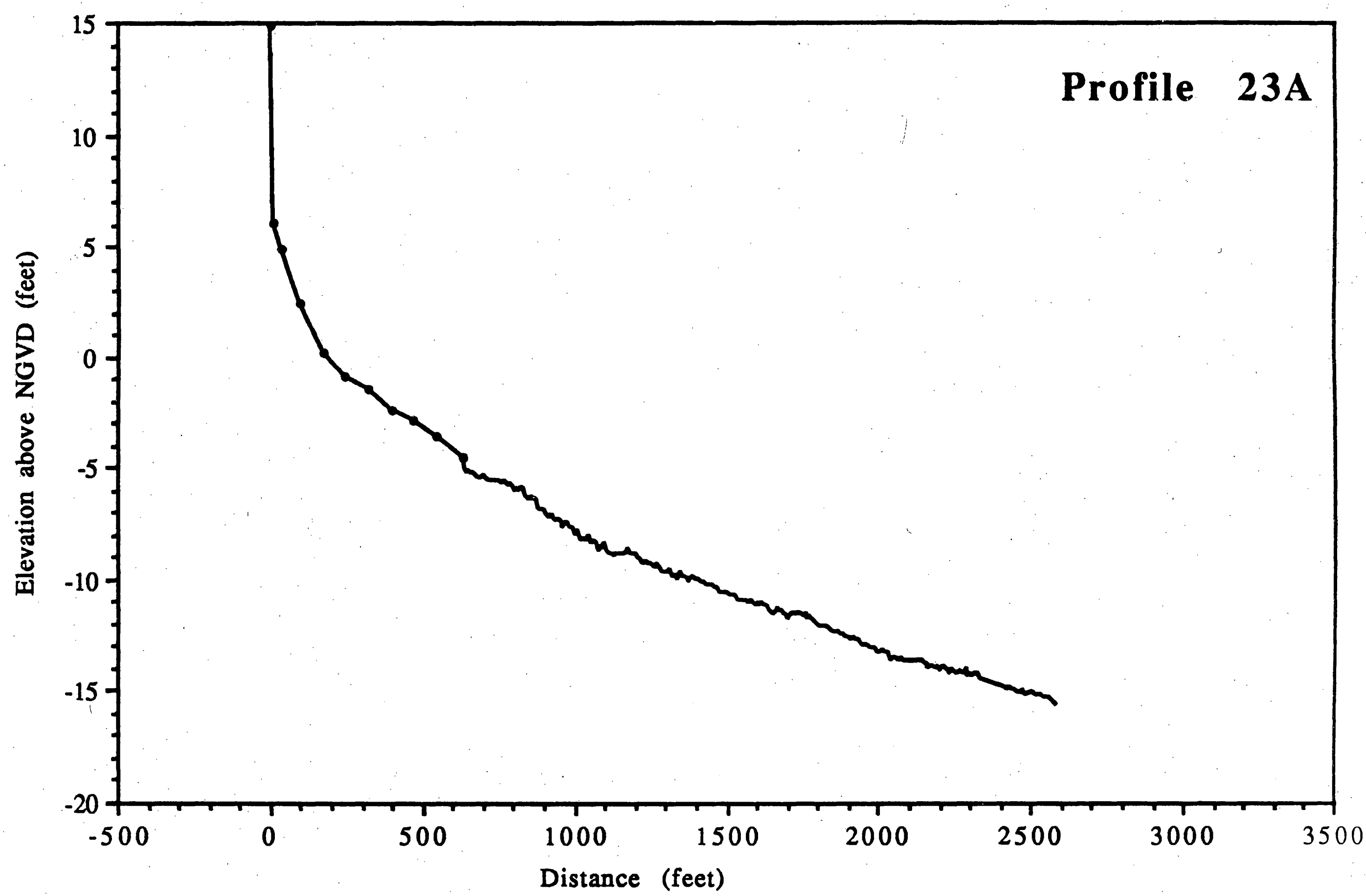

Profile 23A
Elevation above NGVD (feet)
15
10
5
0
-5
-10
-15
-20
-500
0
500
1000
1500
2000
2500
3000
3500
Distance (feet)

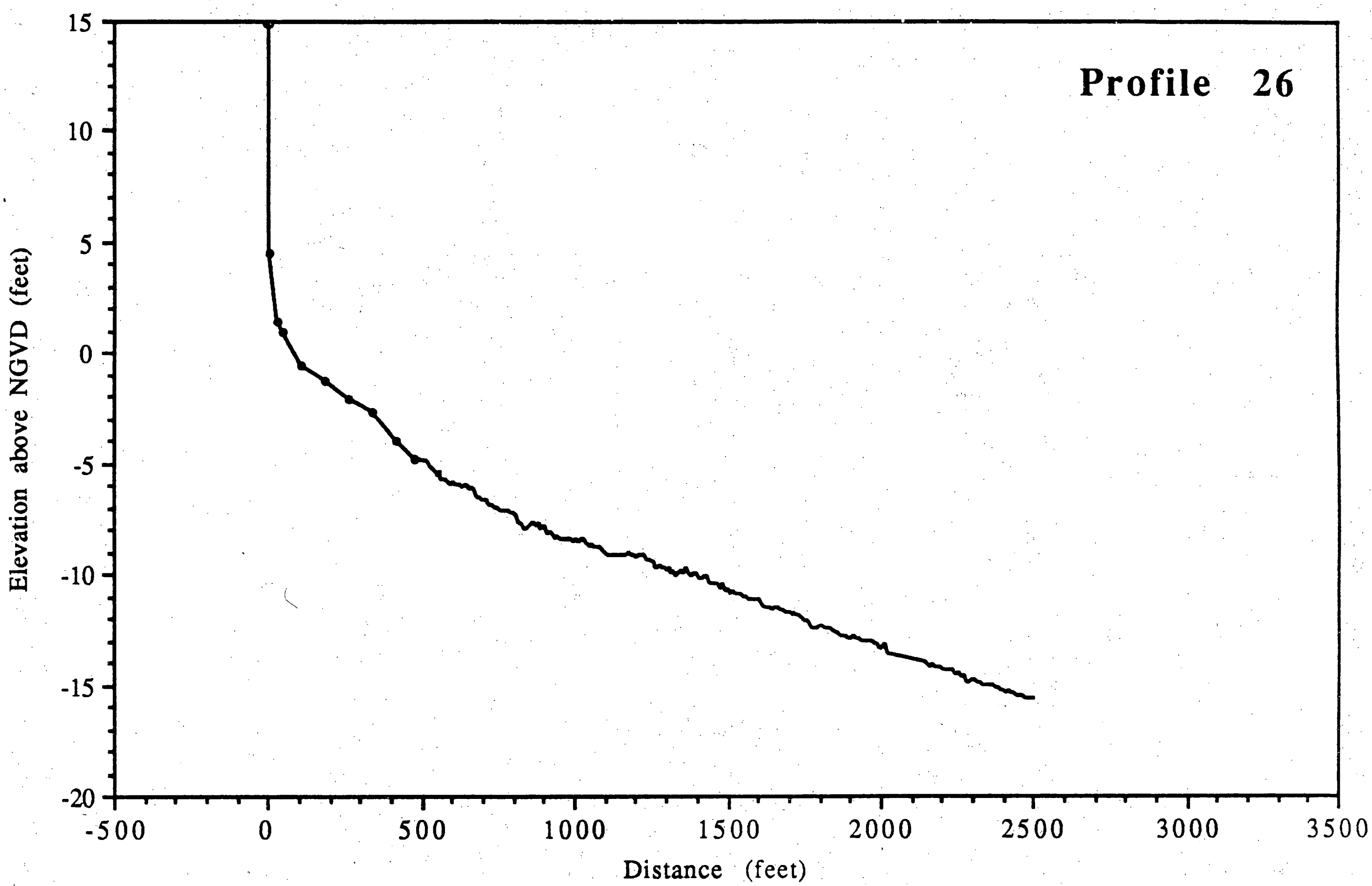

Profile 26
Elevation above NGVD (feet)
15
10
5
0
-5
-10
-15
-20
-500
0
500
1000
1500
2000
2500
3000
3500
Distance (feet)

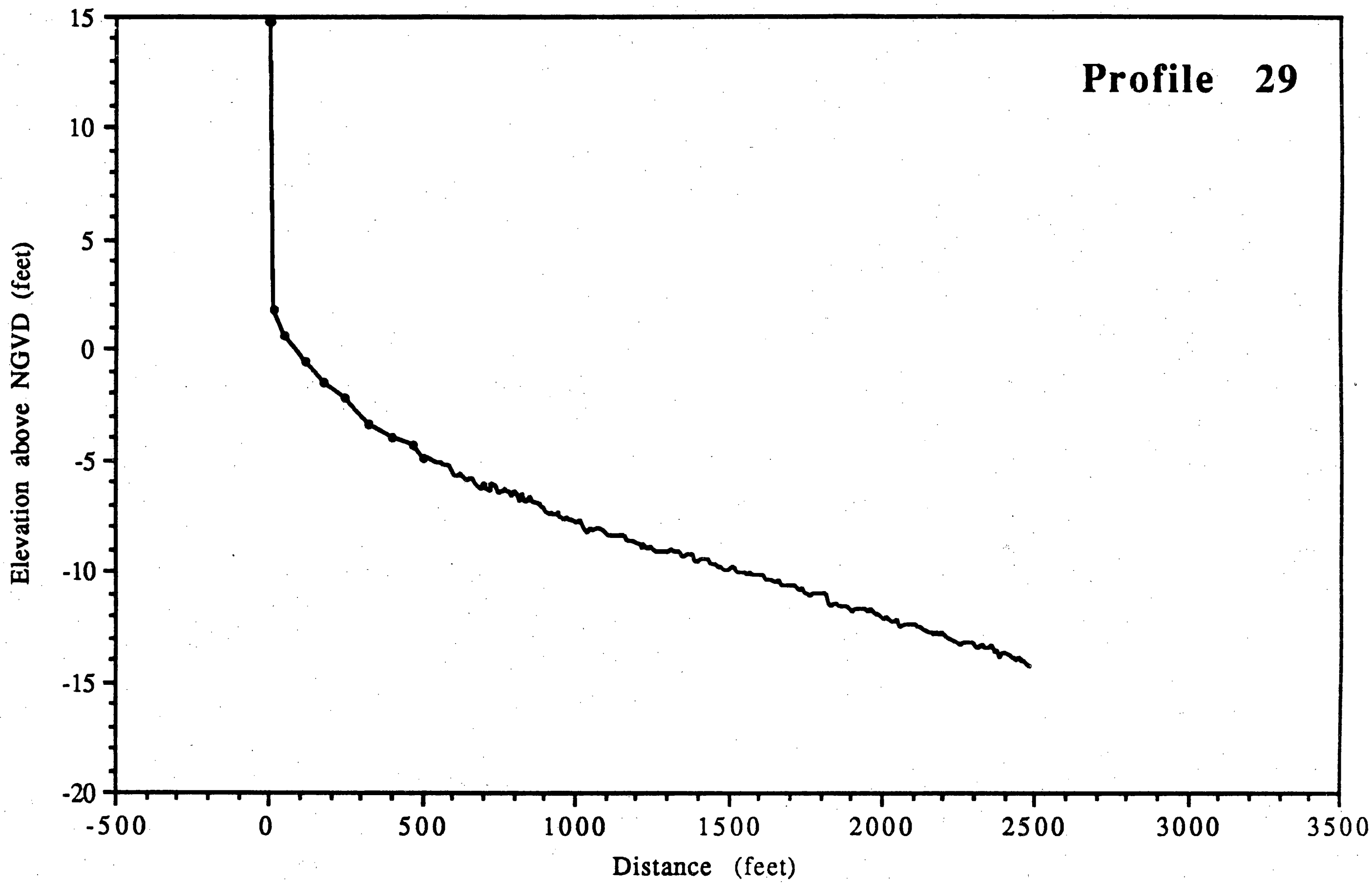
Profile 29
Elevation above NGVD (feet)
15
10
5
0
-5
-10
-15
-20
-500
0
500
1000
1500
2000
2500
3000
3500
Distance (feet)

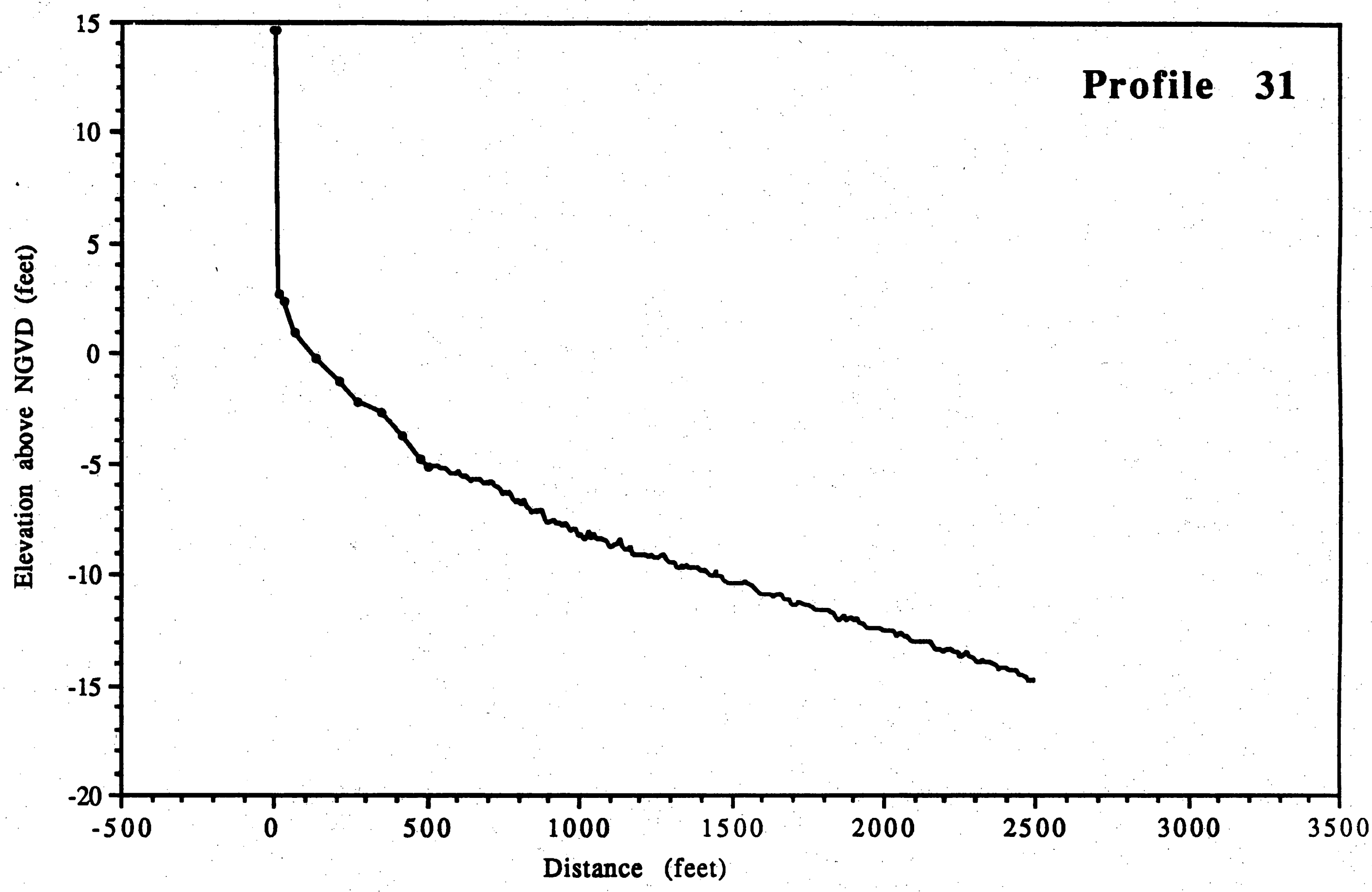

Profile 31
Elevation above NGVD (feet)
15
10
5
0
-5
-10
-15
-20
-500
0
500
1000
1500
2000
2500
3000
3500
Distance (feet)

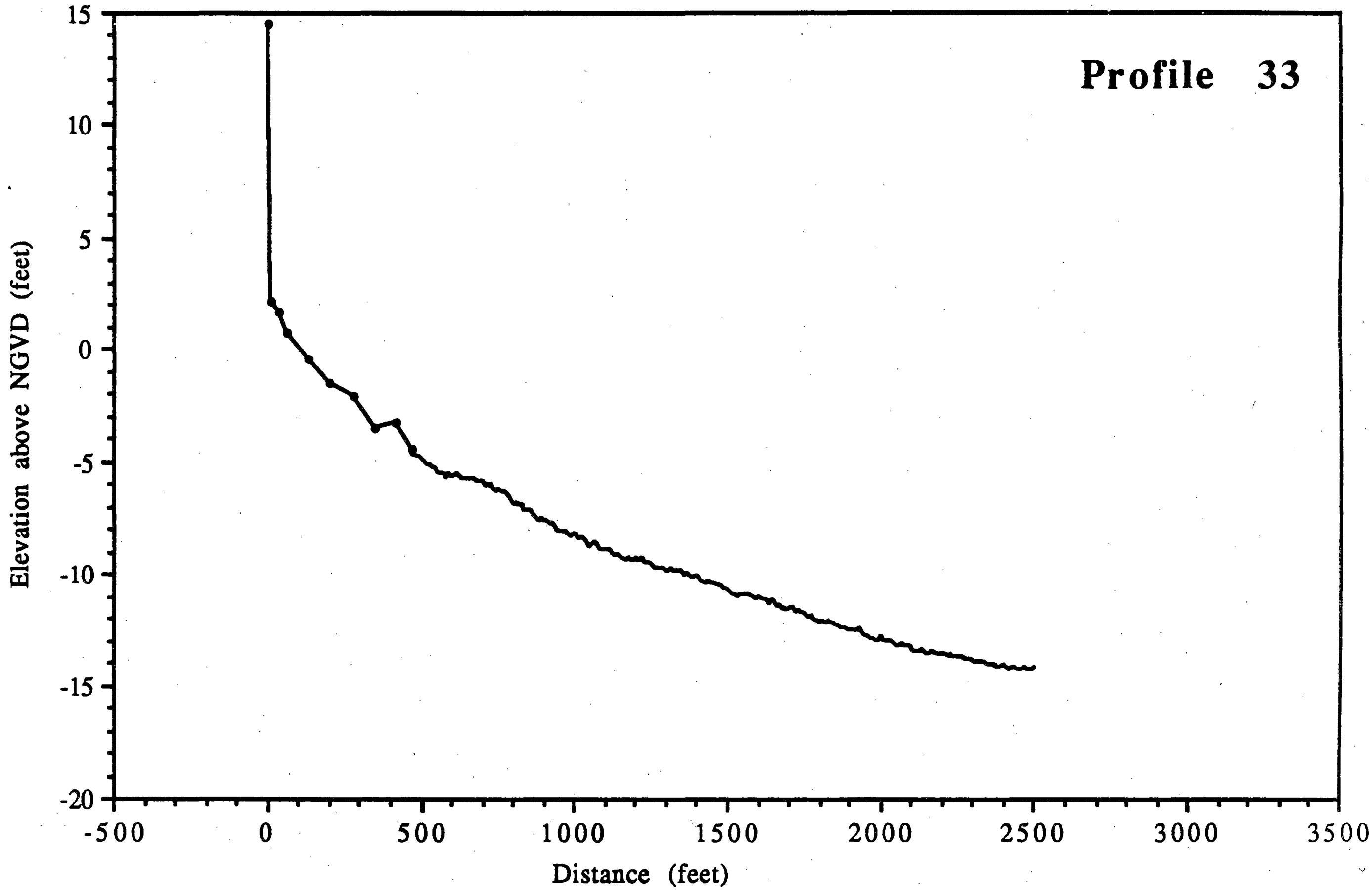
Profile 33
Elevation above NGVD (feet)
15
10
5
0
-5
-10
-15
-20
-500
0
500
1000
1500
2000
2500
3000
3500
Distance (feet)

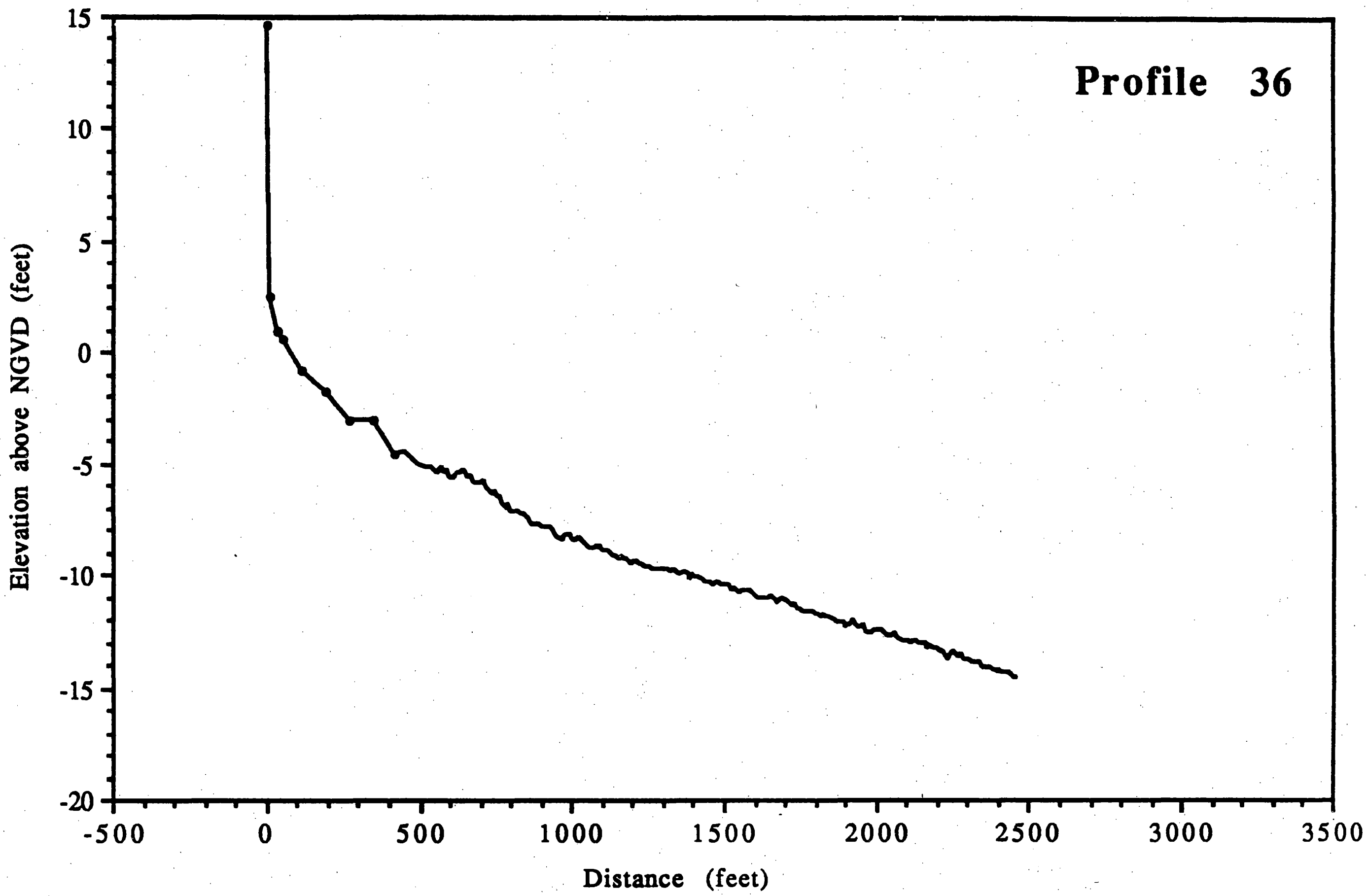
Profile 36
Elevation above NGVD (feet)
15
10
5
0
-5
-10
-15
-20
-500
0
500
1000
1500
2000
2500
3000
3500
Distance (feet)

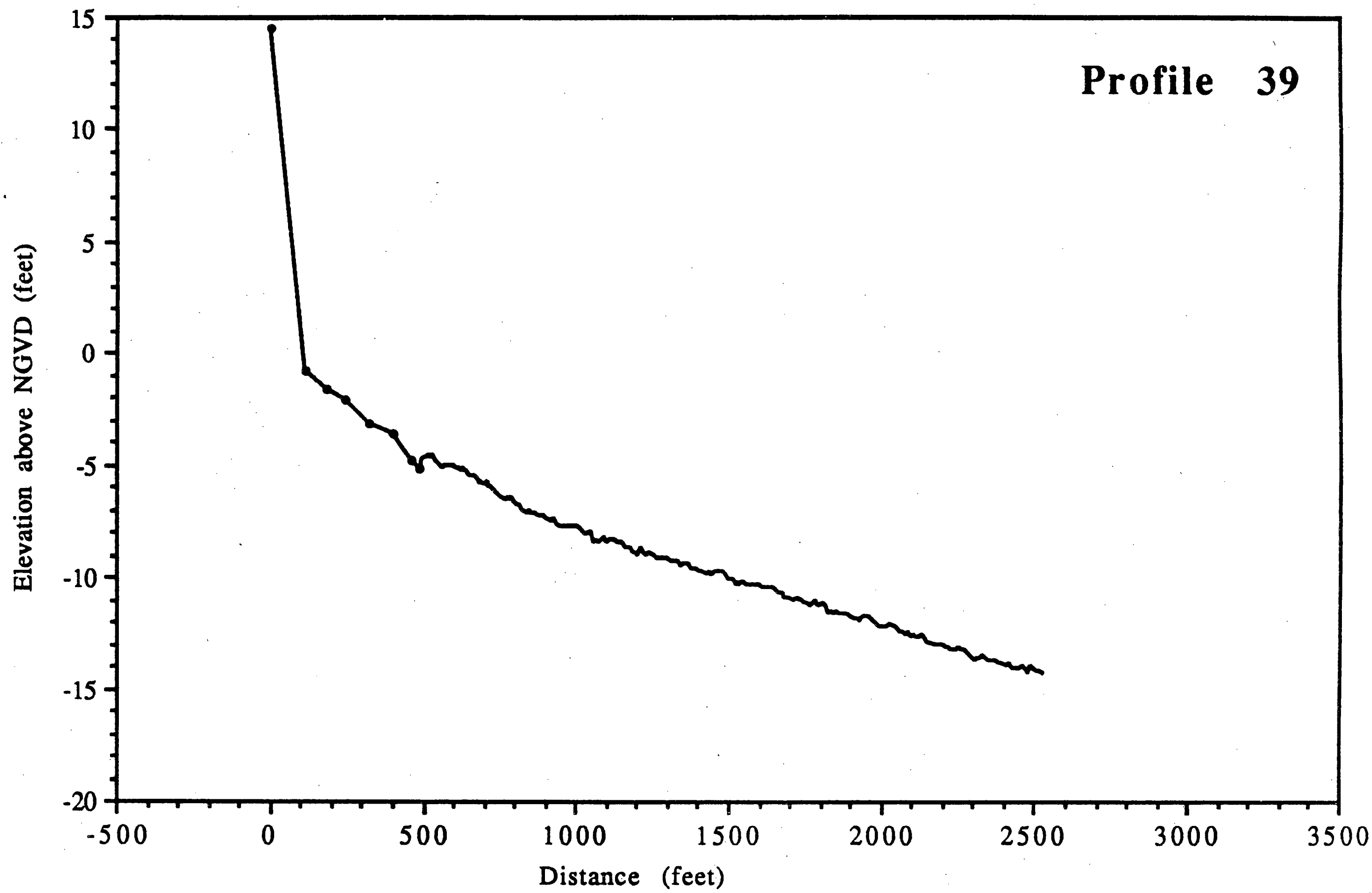

Profile 39
Elevation above NGVD (feet)
15
10
5
0
-5
-10
-15
-20
-500
0
500
1000
1500
2000
2500
3000
3500
Distance (feet)

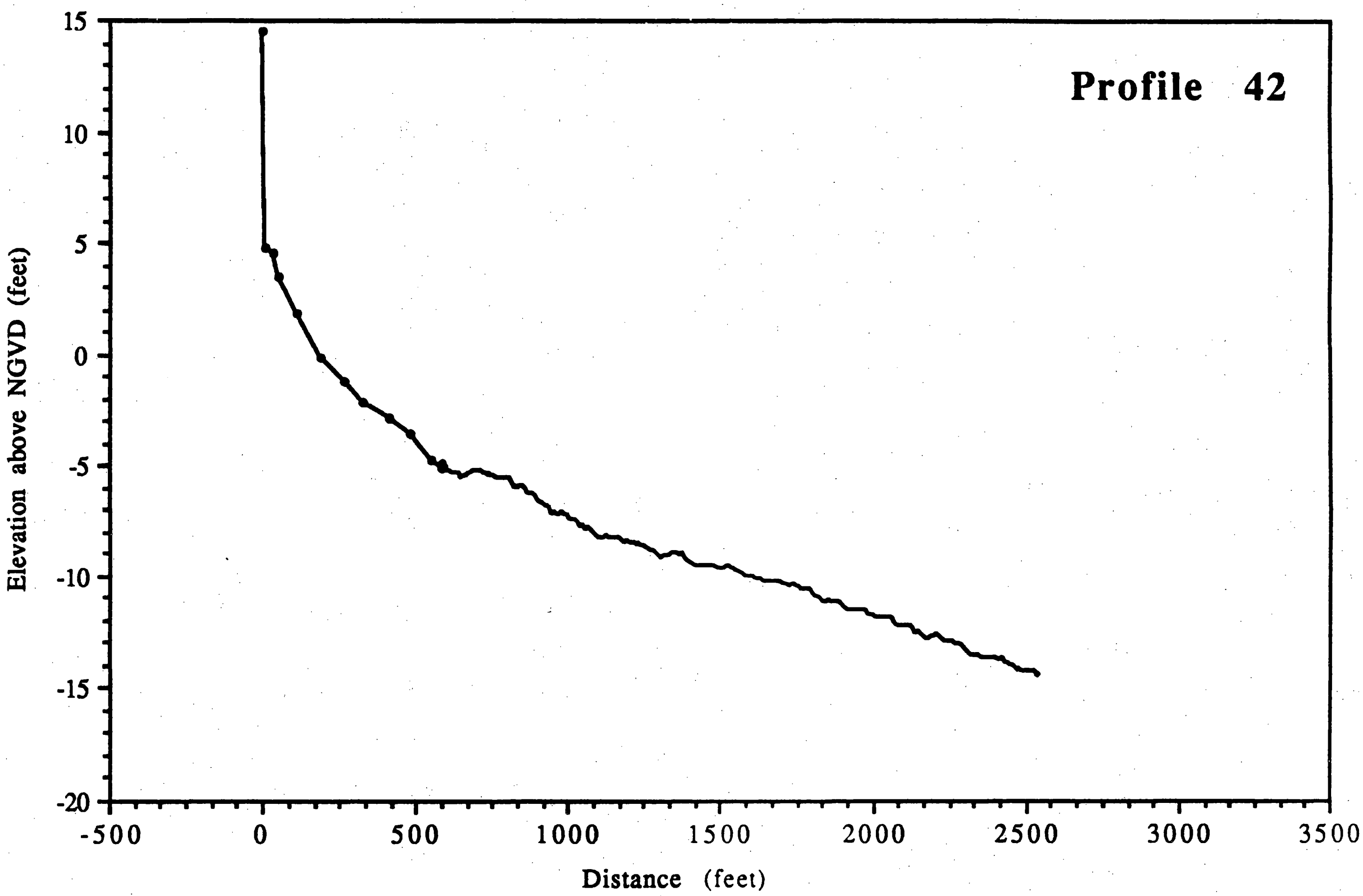

Profile 42
Elevation above NGVD (feet)
15
10
5
0
-5
-10
-15
-20
-500
0
500
1000
1500
2000
2500
3000
3500
Distance (feet)

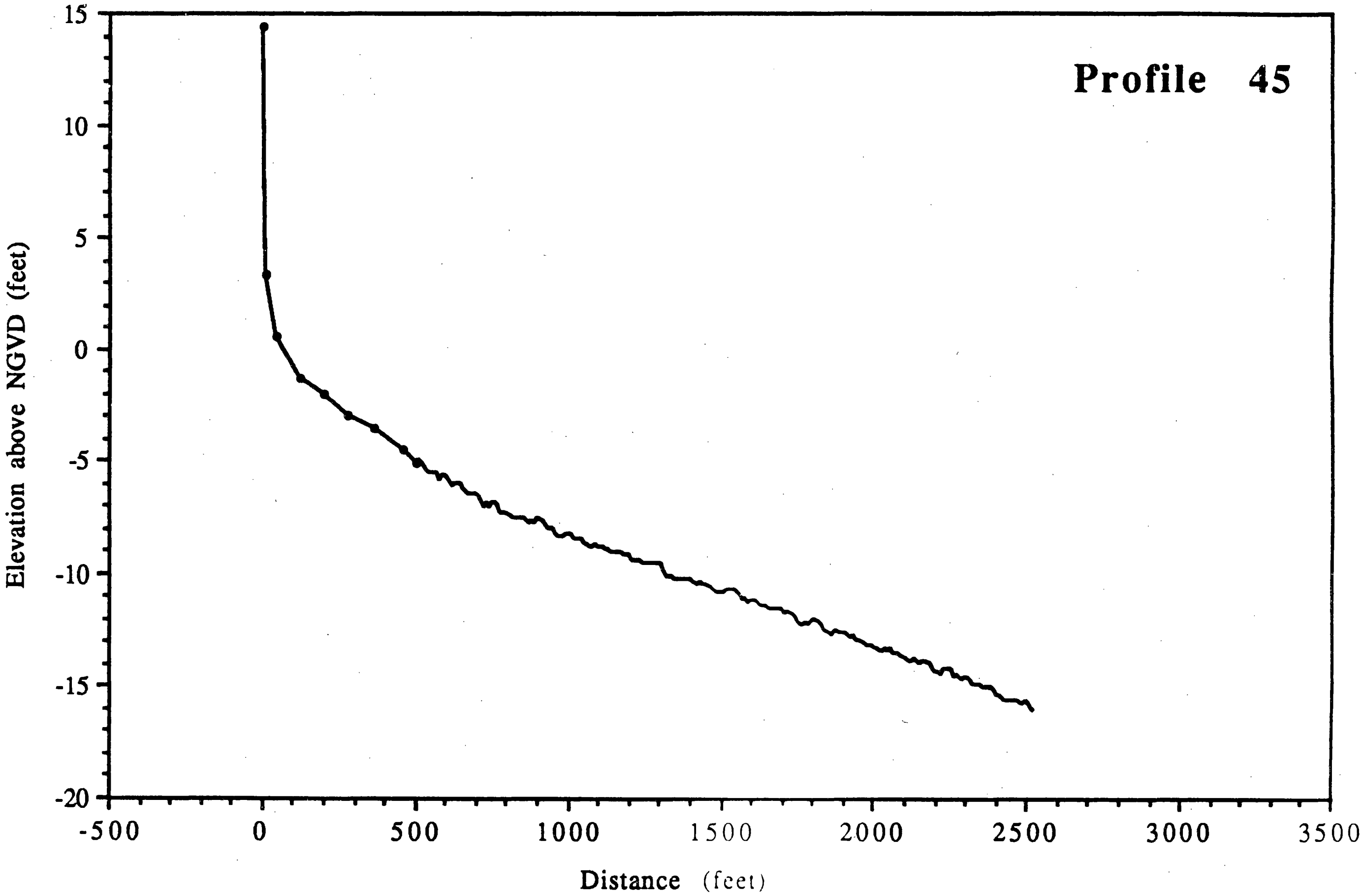

Profile 45
Elevation above NGVD (feet)
15
10
5
0
-5
-10
-15
-20
-500
0
500
1000
1500
2000
2500
3000
3500
Distance (feet)

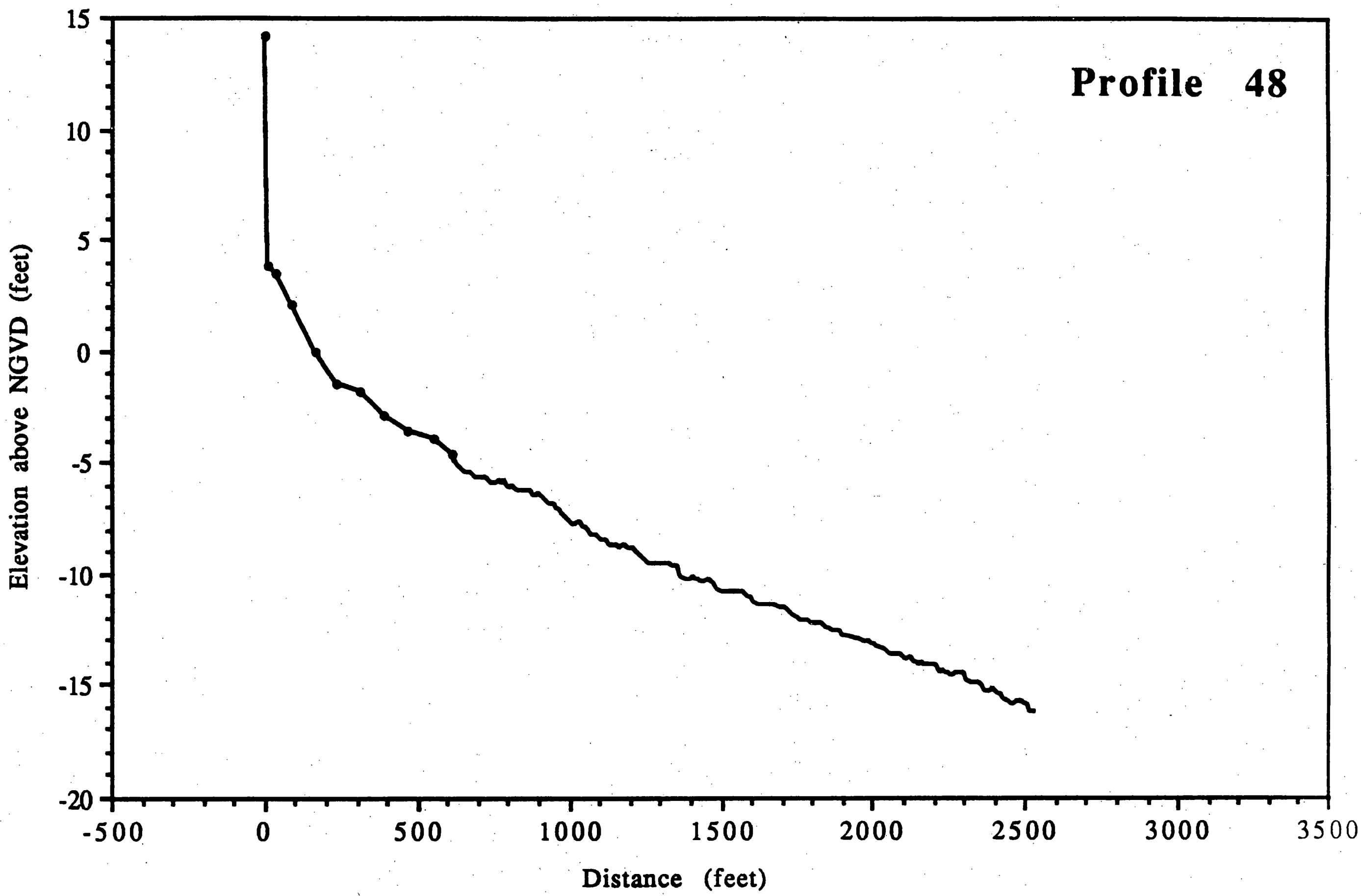

Profile 48
Elevation above NGVD (feet)
Distance (feet)
15
10
5
0
-5
-10
-15
-20
-500
0
500
1000
1500
2000
2500
3000
3500

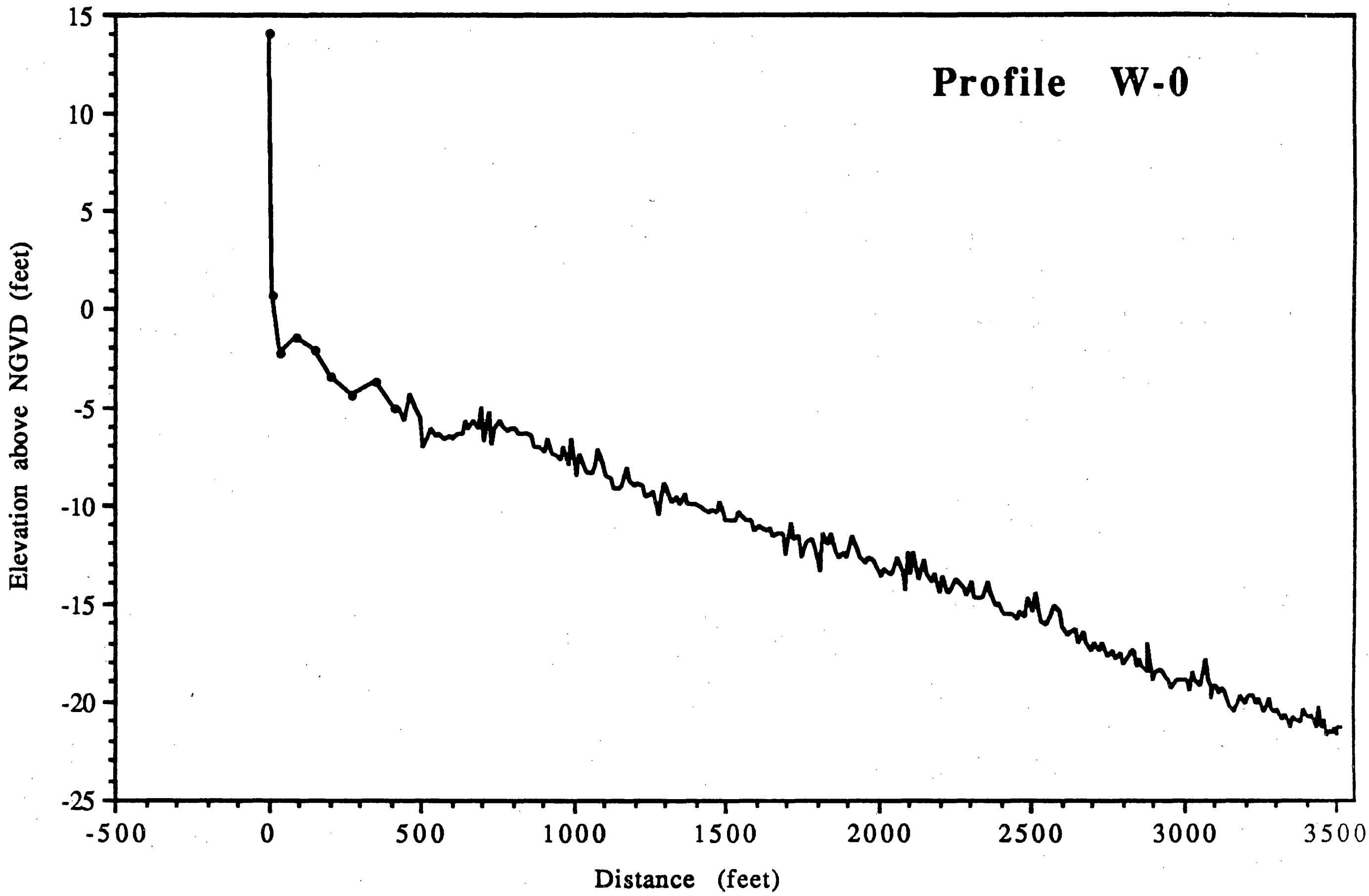
Profile W-0
Elevation above NGVD (feet)
15
10
5
0
-5
-10
-15
-20
-25
-500
0
500
1000
1500
2000
2500
3000
3500
Distance (feet)

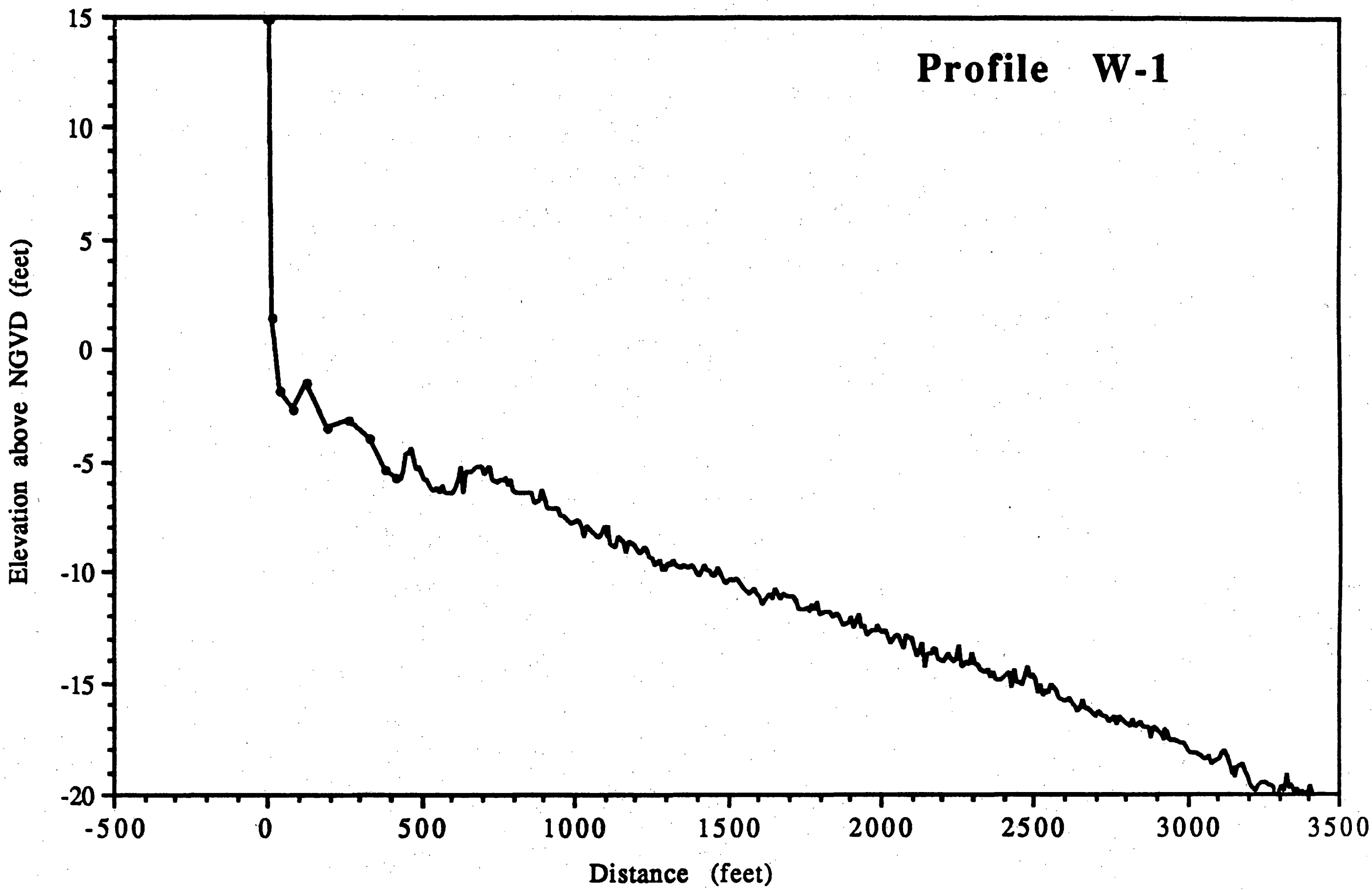

Profile W-1
Elevation above NGVD (feet)
15
10
5
0
-5
-10
-15
-20
-500
0
500
1000
1500
2000
2500
3000
3500
Distance (feet)

Particle Size Analyses - Sieve
Galveston Island area

cumulative %'s

Lab #	Sample ID	2.0ø %	2.5ø %	3ø %	3.5ø %	4.0ø %	pan %
1	W-0-2	0.0	0.1	2.5	77.1	99.3	100.0
2	W-0-4	0.1	0.2	2.4	50.3	98.0	100.0
3	W-1-2	0.1	0.1	2.2	75.8	99.0	100.0
4	W-1-4	0.1	0.2	2.6	67.7	99.5	100.0
5	48-2	0.3	0.4	2.4	54.3	96.7	100.0
6	48-3	0.0	0.1	8.0	82.6	99.5	100.0
7	48-A	0.2	0.7	37.0	96.9	99.9	100.0
8	45-2	0.1	0.1	2.2	71.0	98.7	100.0
9	45-4	0.8	0.9	3.5	51.4	95.4	100.0
10	45-A	1.1	2.8	39.2	97.2	99.8	100.0
11	42-3	0.1	0.1	1.9	68.4	98.1	100.0
12	42-4	1.0	1.2	3.7	48.7	95.0	100.0
13	42-A	0.3	1.6	30.8	96.0	99.9	100.0
14	39-2	0.1	0.2	2.3	72.7	98.8	100.0
15	39-4	0.8	1.0	3.7	49.3	93.6	100.0
16	39-A	1.1	2.9	34.7	97.7	100.0	100.0
17	36-2	0.2	0.3	5.8	79.1	99.2	100.0
18	36-A	0.6	2.0	36.8	97.6	100.0	100.0
19	33-4	0.4	0.6	3.8	50.8	96.1	100.0
20	33-A	1.2	2.3	25.1	94.7	99.9	100.0
21	31-2	0.0	0.0	3.0	78.5	99.7	100.0
22	31-4	0.4	0.5	3.0	48.5	95.3	100.0
23	31-A	0.4	1.0	20.1	94.3	99.9	100.0
24	29-2	0.0	0.2	6.2	78.0	98.6	100.0
25	29-3	0.0	0.0	2.0	74.5	99.0	100.0
26	29-4	0.5	0.7	2.7	44.6	98.3	100.0
27	29-A	1.6	3.4	30.8	95.2	99.9	100.0
28	26-2	0.1	0.2	3.7	68.5	99.4	100.0
29	26-A	1.2	2.7	27.3	95.7	99.8	100.0
30	12-2	0.2	0.3	4.2	67.4	99.6	100.0
31	23A-4	0.3	0.5	3.9	58.0	97.0	100.0
32	23A-A	0.7	2.1	32.5	94.8	99.9	100.0
33	22-3	0.0	0.1	1.6	67.5	99.0	100.0
34	22-A	0.1	0.9	35.1	97.4	100.0	100.0
35	20-2	0.2	0.2	8.4	86.1	99.5	100.0
36	20-3	0.0	0.1	2.1	68.2	98.7	100.0

37	20-4	0.0	0.1	3.7	61.6	96.8	100.0
38	20-A	0.0	0.9	32.0	96.4	99.8	100.0
39	18-2	0.1	0.2	5.3	81.5	99.3	100.0
40	18-A	1.0	3.2	43.4	97.6	99.9	100.0
41	15-4	0.8	1.0	8.1	70.2	97.0	100.0
42	15-A	1.4	8.4	59.0	98.4	99.9	100.0
43	12-3	0.1	0.2	4.1	65.5	98.4	100.0
44	12-4	0.6	0.8	8.9	75.7	97.3	100.0
45	12-A	4.9	8.3	50.7	98.3	99.9	100.0
46	11-2	0.1	0.2	3.3	72.0	98.4	100.0
47	11-3	0.0	0.2	3.8	66.5	98.4	100.0
48	11-4	0.9	1.2	9.0	73.2	97.8	100.0
49	11-A	4.1	10.4	56.1	98.6	99.9	100.0
50	9B-2	0.1	0.2	8.3	85.4	99.5	100.0
51	9B-3	0.2	0.4	5.2	71.0	98.4	100.0
52	9B-4	1.1	1.6	11.6	72.3	97.4	100.0
53	9B-A	0.5	6.3	56.6	98.2	100.0	100.0
54	S9-2	0.1	0.3	5.1	73.8	98.7	100.0
55	S9-3	0.2	0.4	4.3	63.2	98.1	100.0
56	S9-4	0.7	1.3	9.4	64.3	97.0	100.0
57	S9	0.9	3.6	39.3	96.8	99.9	100.0
58	SI-2	0.2	0.7	6.6	70.0	98.6	100.0
59	SI-3	0.7	1.0	5.8	58.7	97.7	100.0
60	SI-4	1.1	1.8	11.7	72.8	97.7	100.0
61	SI	1.0	5.1	35.2	94.9	99.9	100.0
62	S8-2	0.1	0.2	4.5	68.6	99.2	100.0
63	S8-3	0.0	0.3	4.1	56.4	98.1	100.0
64	S8-4	0.1	0.6	10.1	78.8	99.0	100.0
65	S8-A	0.2	1.2	19.2	91.4	99.7	100.0
66	B-1	0.1	0.4	14.0	84.7	99.3	100.0
67	B-2	0.1	0.6	14.8	82.7	98.0	100.0
68	B-3	0.1	0.3	11.8	80.2	99.3	100.0
69	B-4	0.2	0.6	10.0	82.0	98.8	100.0
70	B-5	0.2	0.6	14.8	83.2	99.5	100.0

Particle Size Analyses- Hydrometer
Galveston Island area

Lab #	Sample ID	Sand %	Silt %	Clay %
1	W-0-2	95	2	3
2	W-0-4	94	1	5
3	W-1-2	96	0	4
4	W-1-4	95	0	5
5	48-2	96	1	3
6	48-3	96	1	3
7	48-A	97	1	2
8	45-2	96	2	2
9	45-4	93	3	4
10	45-A	97	0	3
11	42-3	96	1	3
12	42-4	90	6	4
13	42-A	95	2	3
14	39-2	94	3	3
15	39-4	91	6	3
16	39-A	98	0	2
17	36-2	98	0	2
18	36-A	98	0	2
19	33-4	94	3	3
20	33-A	98	0	2
21	31-2	98	0	2
22	31-4	94	4	2
23	31-A	98	0	2
24	29-2	90	4	6
25	29-3	97	1	2
26	29-4	93	3	4
27	29-A	97	0	3
28	26-2	96	1	3
29	26-A	97	0	3
30	12-2	94	2	4
31	23A-4	94	3	3
32	23A-A	97	1	2
33	22-3	96	1	3
34	22-A	97	0	3
35	20-2	97	1	2
36	20-3	96	1	3

37	20-4	94	3	3
38	20-A	97	1	2
39	18-2	96	2	2
40	18-A	98	0	2
41	15-4	94	3	3
42	15-A	97	1	2
43	12-3	95	2	3
44	12-4	94	2	4
45	12-A	97	1	2
46	11-2	95	2	3
47	11-3	95	2	3
48	11-4	94	2	4
49	11-A	97	0	3
50	9B-2	96	1	3
51	9B-3	95	2	3
52	9B-4	95	1	4
53	9B-A	97	1	2
54	S9-2	96	1	3
55	S9-3	95	2	3
56	S9-4	92	3	5
57	S9	96	1	3
58	SI-2	95	2	3
59	SI-3	93	2	5
60	SI-4	93	2	5
61	SI	96	0	4
62	S8-2	95	0	5
63	S8-3	94	1	5
64	S8-4	94	1	5
65	S8-A	96	0	4
66	B-1	95	0	5
67	B-2	95	0	5
68	B-3	94	1	5
69	B-4	93	0	7
70	B-5	95	0	5

Addendum 10. Shoreline Shape and Projection Program (SSAP): Objectives, Techniques, and Initial Results

SHORELINE SHAPE AND PROJECTION PROGRAM (SSAP): OBJECTIVES, TECHNIQUES, AND INITIAL RESULTS

James C. Gibeaut and Robert A. Morton
Bureau of Economic Geology
The University of Texas at Austin

INTRODUCTION

Dolan et al. (1991) reviewed four statistical methods for calculating shoreline rates-of-change from time series of shoreline positions. These methods include the following: (1) end point rate; (2) average of rates (Foster and Savage, 1989); (3) linear regression; and (4) jackknife (Efron, 1982). Fenster et al. (1993) presented a new method that combines polynomial regression, weighted linear regression, and knowledge of site-specific coastal processes. Because of the various methods proposed for calculating shoreline change rates, the long stretches of shoreline for which rates are needed, and the wide-spread use of Geographic Information Systems (GIS) for shoreline mapping, the Bureau of Economic Geology developed a computer program that automates the calculation of rates-of-change, compares the different methods, and interacts with a GIS or a computer automated drafting program (CAD). A future development will involve morphological analysis of historical shorelines for use in modifying predicted shoreline shape and position.

The development of this computer program has been the first step in investigating the merits and detriments of the various statistical methods for determining shoreline rates-of-change from time series of historical shorelines. We can now quickly calculate shoreline rates-of-change and project future shoreline positions in a GIS or CAD program. This appendix describes the approach the program takes to this problem, the methods of rate-of-change analysis that are currently encoded, and some preliminary results from Galveston Island, Texas. With further application of this program, the overall best method or the need for a new method may be revealed.

COMPUTER PROGRAM

Objectives and Current Capabilities

Our overall computer programming goal is to automate the analysis of shoreline shape and change using time series of shoreline positions. The Shoreline Shape and Projection Program (SSAPP) is a modular FORTRAN program that uses subroutines to perform tasks required to compute shoreline rates-of-change and to project shorelines into the future based on those rates-of-change. It is written for the Windows 3.1 operating system and requires at least a 386 personal computer with 16 megabytes of random access memory. Specific objectives and characteristics of SSAPP include the following:

(1) SSAPP is able to use map data from and provide results to a GIS such as Arc/Info or CAD system such as AutoCad.

(2) As an alternative to mapped data, the program can use data where shoreline positions are provided as relative distances along a predetermined transect.

(3) When using map data, the baseline segments are automatically oriented by considering the orientations of mapped shorelines within a segment length.

(4) The user may select the length of baseline segments and the distance between transects where shoreline change rates are determined and along which future shoreline positions are projected.

(5) One can map predicted shoreline positions using selected future dates and rate-of-change method.

(6) Currently, the results of five methods of calculating shoreline rates-of-change are provided: (1) end point; (2) linear regression; (3) jackknife; (4) average of rates; and (5) weighted regression as presented by Fenster et al. (1993).

Automatic Baseline and Transect Determination

Baseline orientation can have a significant effect on calculated rates-of-change and on projecting future shoreline positions. If the baseline does not conform well to actual shoreline orientations, rates-of-change may be overestimated (Fig. 1). Nonconformal baselines also will not provide the correct frame of reference for determining the direction of shoreline change and may skew the shape of projected shorelines. Different baselines, therefore, may greatly alter the final results of a rate-of-change analysis. SSAPP overcomes this problem by objectively and rapidly determining baseline orientations.

SSAPP invokes a baseline and transect determination routine when input data consist of a time series of digitized shorelines, such as from a GIS. First, the linear trend of all combined shoreline data is calculated. All data are then rotated around the average northing and easting position so that the shoreline trend is zero (horizontal in an x,y plot). Using the value for baseline length provided by the user, the program then increments to the left of the average point (rotation point) and searches for all shoreline points lying within that increment (baseline segment) along the rotated trend line (x-axis). For each shoreline year within this segment, a linear regression is performed. The slopes and y-intercepts of each shoreline within the segment are then averaged. The end points of the initial baseline are determined by using this average line formula and the x-values bounding the increment. This baseline is subsequently adjusted and the rest of the baseline calculations proceed differently as described below.

To adjust the initial baseline and calculate the remaining baselines, SSAPP searches for points within an x-axis interval the length of the selected baseline length and centered on the x-value determined by adding the baseline length to the last endpoint of the previous baseline segment. When adjusting the initial baseline, the search is centered around the last end point of the current baseline segment. All y-values for shoreline positions within this interval are then averaged. The new baseline is now defined by the coordinates of the previous baseline endpoint and the x-value obtained by adding the baseline lenghth to the x-value of the previous endpoint and the average y-value. If the difference between the new y-value (average y-value) and the y-value of the previous baseline endpoint is greater than 0.1, then all shoreline data are rotated around the previous baseline endpoint by the amount of the angle formed by the juncture of the previous baseline and the newly determined baseline. Thus all shoreline data are realligned to the trend of the new baseline and a new search and endpoint calculation are made. This continues untill the 0.1 tolerance is met or ten itterations are made. When the end of the shoreline data is reached to the left, the routine begins again at the center of the data and proceeds to the right.

Transects are automatically placed along the baselines at user-selected intervals. Baseline length divided by desired transect interval must be a whole number. The first transect is placed at the beginning end point of a baseline and is oriented so that it bisects the angle formed between the adjacent baselines. Subsequent transects within a baseline are oriented perpendicualr to the baseline. If the selected baseline length and the transect interval are equal, then transects are placed in the middle of baselines and are oriented perpendicualar to the baselines. The transects are numbered with the center transect as zero and transects to the left as negative and to the right as positive numbers. Figure 2 is an example of baselines and transects automatically constructed by SSAPP.

Once each baseline is determined, SSAPP then proceeds to determine the distance from the baseline of each shoreline that crosses the transect. The program searches for points spanning the transect for each shoreline. Once the closest points on each side of the transect are found, a linear interpolation is made to determine the point where the transect crosses the shoreline. The distance from the baseline for each shoreline is then calculated.

Rate-of-Change Methods

Currently, SSAPP calculates rate-of-change values using five methods as described below.

End Point Rate-of-change

This is a simple routine that for each location determines the distance between the earliest and latest shoreline positions and divides by the number of years, thus providing an annual rate-of-change.

Linear Regression Rate-of-change

For this method, all the available data are used in a linear regression. The slope of the regression line is the shoreline rate-of-change. SSAPREG is actually a subroutine within SSAPP that computes the coefficients for any desired order of polynomial. When it is called to compute a linear regression rate-of-change, a polynomial order of one is passed to the routine.

Jackknife Rate-of-Change

This routine uses the Jackknife method as described by Efron (1982) to compute shoreline rates-of-change. A family of linear regression lines are computed by successively eliminating a single and different point. The slopes of these regression lines are then averaged to yield an annual rate-of-change.

Average of Rates Rate-of-Change

Foster and Savage (1989) developed this technique using data from Florida. It involves averaging the end point rates computed for all possible combinations of two points in a time series. Each combination of points must pass a minimum time criterion (T_{min}), however, to be included in the average.

$$T_{min} = [\sqrt{(E_1)^2 + (E_2)^2}\ ] / R_1$$

Where E_1 and E_2 are the assumed error ranges for shoreline position measurements 1 and 2, respectively, and R_1 is the end point rate for the longest time span in the time series. The end-point combinations with time spans greater than Tmin are considered "long-term" rates and their rates are averaged to yield the rate-of-change value.

Weighted Rate-of-Change (as presented by Fenster (1993))

This method of rate calculation is relatively complicated compared to the above methods. First an optimum polynomial is fitted to the time series based on the minimum description length criterion (MDL) as follows:

$$MDL_K = MSE_K + [\ln(N) \times K \times \sigma^2] / N$$

where MDL_K is the minimum description length for a model with K terms, MSE_K is the mean squared error of the model, K is the number of terms in the polynomial, N is the number of data points, and σ^2 is the noise variance. The model with the smallest MDL_K is selected for further analysis. In SSAPP the user selects the maximu K to be considered by the method.

Once the optimum polynomial is determined, points where the slope changes sign are found. These points indicate a change in the direction of shoreline movement at particular times. If there are no changes in the sign of the slope, then a linear regression is used as the rate-of-change. If changes of sign in the slope do occur, the most recent point when the slope changes is selected and all data prior to that time are weighted to zero. A new linear regression is calculated and is called the "zero-weight line." The user has the option to select the slope of this line as the best rate-of-change value. This would be the case if specific knowledge of a change in coastal processes suggest that the earlier data should be completely disregarded (weighted to zero).

Often specific knowledge of coastal processes is not available or it is not clear to what extent the earlier data should be considered. The Fenster method allows an objective means to value data that is available before a change in trend. This is accomplished by incrementally increasing the weights of the earlier data and recalculating the linear regression and MDL_K. The weights are increased until the MDL_K is equal to or just less than that of the MKL_K for the earlier determined optimum polynomial. Thus a nonlinear model is forced to be linear through a weighted linear regression technique.

Program Input

Shoreline data may be provided as digitized shorelines through a GIS such as Arc/Info or as an ASCII file in which data have been reduced to time series of shoreline distances from a baseline at particular locations along the shoreline. Often when digitizing or storing shoreline data within a GIS, sections of shoreline are digitized as separate polylines. For example, pieces of a shoreline on photographs or on topographical maps may be digitized separately and later merged to obtain continuous coverage. SSAPP recognizes these sections on input and does not require them to be in any particular geographical order. The user working within the GIS simply creates an ASCII output file of shoreline coordinates for input to SSAPP. Within ArcInfo, an ASCII dump of a shoreline coverage with the dates given as line indentifications or attributes will suffice. SSAPP is written to take advantage of double precision math, but double precision values are not required for input. The coordinate system for data input must be either State Plane or Universal Transverse Mercator (UTM). SSAPP does not perform any coordinate or map projection transformations.

The program queries the user for specific input parameters shown below. For this illustration, program questions are in all upper case, user responses are in italics, and program generated progress statements are in plain lower case text.

IN WHAT FORM ARE THE DATA?
1=TIME SERIES OF SHORELINE COORDINATES
2=TIME SERIES OF SHORELINE DISTANCES BY TRANSECT
1
SHORELINE FILE NAME? *galves.dat*

ARE DATA IN FEET (f) or METERS (m)? <m> *m*

ENTER DESIRED BASELINE LENGTH IN METERS: *200*

ENTER DISTANCE BETWEEN TRANSECTS DESIRED: *200*

ENTER THE MAP ERROR IN METERS <8.5> *8.5*

CONVERT RESULTS FROM METERS TO FEET? Y/N <N> *n*

OUTPUT FILE FOR SHORELINE CHANGE RATES? *change.out*

OUTPUT FILE FOR STATISTICAL PARAMETERS? *param.out*

OUTPUT FILE FOR PROJECTED SHORELINES? *proshore.out*

Reading and sorting data...

Calculating regression of all shoreline points...

Rotating shoreline points to linear trend...

Plotting rotated shorelines...

Determining baselines and transects...

Calculating end-point rate...finished.

Calculating long-term linear regression rate...finished.

Calculating jackknife rate...finished.

Calculating average-of-rates rate...finished.

Calculating Fenster et al. rate...

MAXIMUM ORDER FOR POLYNOMIAL (5 MAX)? *3*

finished.

Calculating projected shorelines...

HOW MANY PROJECTIONS? (5 MAX) *1*

LIST THE CALENDER YEARS FOR PROJECTION *2025*

finished.

During the above processing, graphics screens are opened and plots of shorelines, baselines, and transects are drawn as the program progresses.

Program Output

During execution, SSAPP first plots the shoreline data to the screen, then baselines and transects are overlain on the shorelines. After data processing, one may choose to view plots of relative shoreline distances along a transect versus the year for any given transect. Overlain on these plots are lines representing the fit of the various methods for calculating rates-of-change

The program creates two files. The first contains rate-of-change information for each transect and the coordinates of predicted shoreline positions (Table 1). The second file provides statistical parameters for each transect related to the results of the models (primarily Fenster's MDL model) (Table 2). Information in this second file may be used to evaluate the various rate-of-change calculations.

SSAPP provides an ASCII file of predicted shoreline positions in an Arc/Info line format for direct input to the GIS. SAPP also provides an ASCII DXF file of all shorelines, baselines, transects, and predicted shorelines. When the DXF file is imported into a CAD program, each shoreline is placed on separate layers. Baselines and transect lines are also placed on separate layers.

Tabel 1. - Sample of partial output file from SSAPP showing results of rate-of-change anlayses (TRAN= transect number, EPR= end point rate, LR= linear regression, JK= jacknife, AOR= average of rates, Wt.ed= weighted regression (Fenster method), 0-WT= zero-weight linear regression, Time Span= earliest and latest shoreline year that crosses the transect.

SHORELINE CHANGE RATES

shoreline file name: galves.dat

run date and time: 09/29/95 10:35

Baseline length= 200.0 m

Transect Spacing = 200.0 m Map Error= 8.5m

	METHODS							PREDICTED yr 2025 end point method UTM zone 15	
TRAN	EPR	LR	JK	AOR	Wt.ed	0-WT	Time Span	Easting	Northing
-117	0	0	******	0	0	0	.00- .00	312940.4	3232413
-116	1.13	1.75	1.52	1.9	1.12	-0.2	1850.00-1990.00	312769	3232310
-115	-0.74	-0.38	-0.75	-2.83	-10.6	-12.4	1850.00-1990.00	312598.3	3232205
-114	-1.34	-0.94	-1.37	-5.83	-10.73	-12.32	1850.00-1990.00	312428.7	3232098
-113	-1.46	-1.02	-1.46	-5.74	-10.58	-12.13	1850.00-1990.00	312257	3231995
-112	-1.54	-1.07	-1.49	-5.44	-10.08	-11.61	1850.00-1990.00	312086.9	3231889
-111	-1.57	-0.99	-1.34	-4.88	-9.51	-11.12	1850.00-1990.00	311919.2	3231779

Table 2. - Sample of partial output file from SSAPP showing statistical parameters from the results of rate-of-change analysis. TRAN= transect number, R2= linear regression correlation coefficient, MDL= mininum description length criterion, K= number of terms in optimum polynomial, LCP= latest critical point, WTS= weight applied to data earlier than the latest critical point, ANGLE= angle between the zero-weight line and the weighted line in the Fenster method.

SHORELINE CHANGE STATISTICS AND PARAMETERS

Shoreline file name: galves.dat

Run date and time: 9/29/95 10:35

Baseline length= 200.00m

Transect Spacing= 200.00m Map Error= 8.50m

PARAMETERS

TRAN	R2	MDL	K	LCP	WTS	ANGLE
-117	0	0	1	-999	0	-999
-116	0.26	12356.58	4	1963	0.3036	36.92
-115	0.01	17055.02	4	1953	0.0067	-0.78
-114	0.08	12295.14	4	1948	0.0062	-0.68
-113	0.1	10198.62	4	1948	0.0062	-0.69
-112	0.13	7528.09	4	1947	0.0065	-0.74
-111	0.13	5498.64	4	1951	0.0072	-0.86

PRELIMINARY RESULTS FROM GALVESTON ISLAND

Galveston Island, Texas (Fig. 3), a sandy barrier island, was used to demonstrate and evaluate the capabilities of SSAPP and to make an initial evaluation of the results of the various rates-of-change calculations. There is a variety of development along the shores of Galveston Island. On the northeast end, the Bolivar Roads south jetty has impounded sand, largely eroded from in front of the seawall to the west, causing the shoreline to accrete since the 1890's and forming East Beach (Morton 1974) (Fig. 3). The portion of the Galveston Seawall and associated groin system that backs the current beach streches for 11 km in front of the city of Galveston. Construction of the seawall occurred in phases from 1902 to 1952 and groins were added along this stretch of shoreline in 1885 and 1939 (Morton 1974) Currently, waves often reach the seawall except where a beach nourishment project was constructed in 1994. Development along the Gulf shoreline of Galveston Island southwest of the seawall consists of single family homes, and no beach nourishment projects or hard structures have been constructed. The southwest end of Galveston Island is bordered by San Luis Pass which is a natural tidal inlet and is where large shoreline changes have occurred in conjuction with island progradation and tidal channel and ebb-tidal delta interaction with the shoreline.

For this analysis, a baseline length of 200 m and a transect spacing of 200 m were used. A baseline spacing of 200 m appeared to adequately follow the shapes of the shorelines, particularly toward the southwest end of the island (Fig. 3). The transect spacing of 200 m provided a relatively smooth projected shoreline for the scale of this example. As described above, users have the option of changing baseline and transect spacing, and if one wishes to study the shoreline on a smaller or larger scale, this may be warranted. The map error range used was 8.5 m, and the maximum polynomial ordered to be considered by the weighted method was 3 (for a max K of 4).

Figure 4 shows a plot of the five calculated rates-of-change along the Galveston Island shoreline. The alongshore shapes of the rates-of-change curves computed using the end point, linear regression, jackknife, and average-of-rates methods are similar. East of the seawall along East Beach all methods reflect the accretion that has occurred from impoundment of sediment by the jetty. The effect of the seawall and groin field, which are to the west of East Beach, is expressed as erosion just east of the east end of the seawall at transect 90. Littoral drift along this portion of the island is to the east, and the seawall and groins have interupted littoral drift supply to the beach adjacent to the east end of the seawall causing local erosion. This section of shoreline (around transect 90) is apparently west of the direct influence of the sediment impoundment caused by the jetty.

In front of a relatively old part of the seawall between transects 55 and 80, the shoreline is nearly stable with rates-of-change of less than -0.5 m/yr. Farther to the west rates of erosion gradually increase and reach a maximum of almost -3.0 m/yr just west of the seawall at transect 25. Littoral drift here is to the west, and as was the case on the east end of the seawall, the seawall and groin field have interupted littoral drift supply causing erosion. From transect 20, about 2.5 km west of the seawall, to transect -10, a distance of 5 km, erosion rates gradually decrease for all methods except the weighted method. From transect -10 to -40, the shoreline is stable to slightly erosional (less than -0.5 m/yr) for all the methods except the weighted method. Although the average-of-rates method along this stretch generally conforms with the end point, linear regression, and jackknife methods, it is relatively erratic with several transects showing slight accretion.

From transect -40 to -80, erosion rates for all methods gradually increase. This increase, however, is more pronounced in the average-of-rates and weighted methods. From -80 southwest to San Luis Pass, erosion rates decrease then increase, and at the end of the island, the rates reflect accretion associated with island progradation. Variance in rates-of-change from transect -80 to the southwest end show the effects of San Luis Pass. Along this stretch, the linear regression method shows the least variance and the lowest rates-of-change. The Jackknife and end point methods show only slightly more variance, but the average-of-rates and weighted methods show large swings in rates-of-change.

As mentioned above, all methods except the weighted method have a similar alongshore shape in their rate-of-change curves. The average-of-rates method, however, shows more high- and low-frequency alongshore variance than the other methods. The weighted method also shows relatively large alongshore variance, and it departs dramatically from the other methods for about 16 km west of the seawall. Along this 16 km of shoreline, the weighted method computed erosion rates of 2 to 4 m/yr while the the other methods determined the shoreline to be nearly stable (Fig. 4).

DISCUSSION

At many sites along the Texas coast the trends of shoreline movement and rates of change have been greatly influenced by human activities. These activities have locally altered the littoral processes and sediment supply, causing either the trends of shoreline movement to abruptly reverse or to rapidly accelerate and decelerate. Therefore it is important to analyze shoreline movement in a historical context that recognizes the altered physical conditions and their impact on future shoreline movement.

The end point, linear regression, and jackknife methods yield similar results and usually the lowest erosion rates (Fig. 4). These methods also show low alongshore variance compared to the average-of-rates and weighted methods. The weighted method departs radically from the other methods west of the seawall. Inspection of the weights and critical points reveals that the weighted method completely discounted (applied zero weights to) data prior to 1915 along this stretch. Therefore, the weighted method automatically considered the change in littoral processes caused by the seawall. The weighted method holds promise for a relatively objective, unsupervised way of computing rates-of-change.

The alongshore variance in the average-of-rates and weighted methods is of concern when projecting predicted shorelines. This variability is cause by varying availability of shorelines through the years for adjacent transects and by actual variance in the shapes of the shorelines. Even if the rate-of-change variance does reflect actuall shoreline shape and change variablility over the time period of analysis, projecting a new shoreline using those rates will likely produce an unnatural shoreline shape. An example of this is shown in the inset in figure 3 where projected shorelines using the end point and weighted rates are mapped. The weighted method predicts landward shoreline movement of about 75 m, but there is a prominent bend in the shoreline that we have no reason to believe would actually form.

Over the next year we will devise a shoreline projection method that will consider shoreline shape. This method will perform various morphological analyses of actual and predicted shorelines. Such analyses may include fractal, fourier, and new hybrid techniques. Actual shorelines will be morphologically characterized, and using these characterizations, the "naturalness" of the predicted shorelines will be evaluated. Predicted shorelines that have unnatural shapes would suggest unreasonable rate-of-change values were used. This information may be used to go back and modify rate-of-change values for particular locations or to provide a limit on how far in the future one may reasonably project shorelines.

REFERENCES

Dolan, R., Fenster, M.S., and Holme, S.J., 1991, Temporal analysis of shoreline recession and accretion: Journal of Coastal Research, v. 7, no. 3, p. 723-744.

Efron, B., 1982, The Jackknife, the Bootstrap and Other Resampling Plans: Philadelphia, Pennsylvania: Society for Industrial and Applied Mathematics, 92p.

Fenster, M.S., Dolan, R., and Elder, J.F., 1993, A new method for predicting shoreline positions from historical data: Journal of Coastal Research, v. 9, no. 1, p. 147-171.

Foster, E.R. and Savage, R.J., 1989, Methods of historical shoreline analysis: in Magoon, O.T., Converse, H., Miner, D., Tobin, L.T., and Clark, D., (eds.), Coastal Zone '89, American Society of Civil Engineers, v. 5, p. 4434-4448.

Morton, R.A., 1974, Shoreline changes on Galveston Island (Bolivar Roads to San Luis Pass) An analysis of historical changes of the Texas Gulf shoreline: Geological Circular 74-2, Bureau of Economic Geology, The Universtity of Texas at Austin, Austion, Texas, 34pp.

FIGURE CAPTIONS

Figure 1. - Illustration of the effect of using a baseline obliquely oriented to shorelines on the computation of shoreline change rates and future shoreline projections. At transects one through eight, the distance between shorelines is greater for transects oriented perpendicular to a nonconformal baseline than it is for transects oriented perpendicular to the actual shoreline orientations (dashed lines). This may cause problems when projecting shorelines into the future based on historical erosion rates, because one must known in what direction to move the shoreline.

Figure 2. - Illustratration of how SSAPP automatically tracks the historical shorelines and constructs a series of baselines and transects that conform to the historical shoreline trends. Here the baseline length selected is 200 m and the transect spacing is 200 m. The user, however, may change these values.

Figure 3. - Map of Galveston Island with shoreline transects and future shoreline projections. The inset shows the results of projecting the shoreline 30 years into the future to the year 2025 in the Jamaica Beach area. The end point rate-of-change, which uses shorelines from the 1850's and 1990's in this area, predicts that the shoreline will move landward only about 6 m. The weighted linear regression method, which discounts shorelines prior to about 1915, predicts that the shoreline will move landward about 75 m.

Figure 4. - Plot of shoreline change rates along Galveston Island computed by various methods: EPR= end point rate; LR= linear regression; JK= jackknife; AOR= average of rates; and Wt.ed= weighted. See text for explanation of methods.

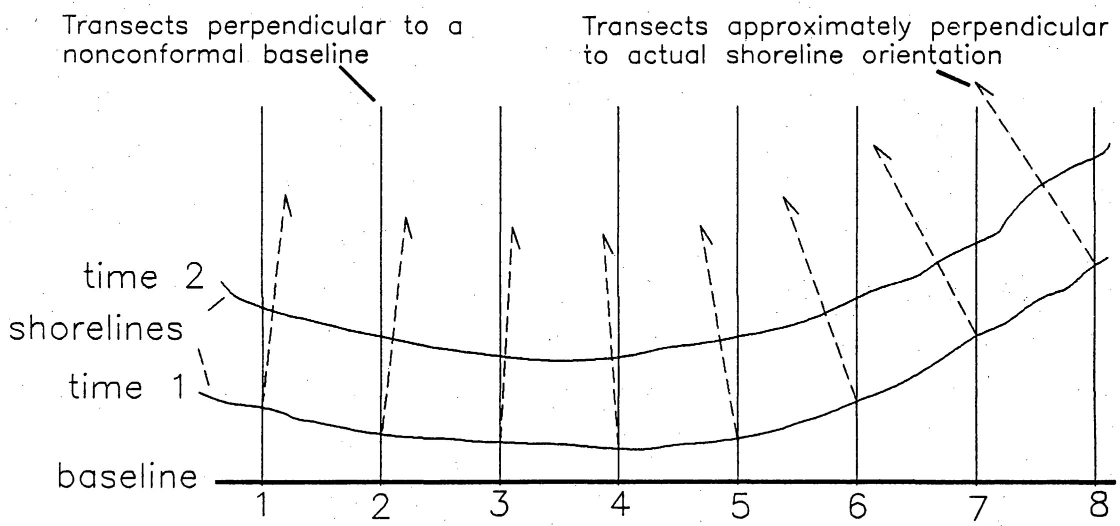
Transects perpendicular to a nonconformal baseline
Transects approximately perpendicular to actual shoreline orientation
time 2
shorelines
time 1
baseline
1
2
3
4
5
6
7
8

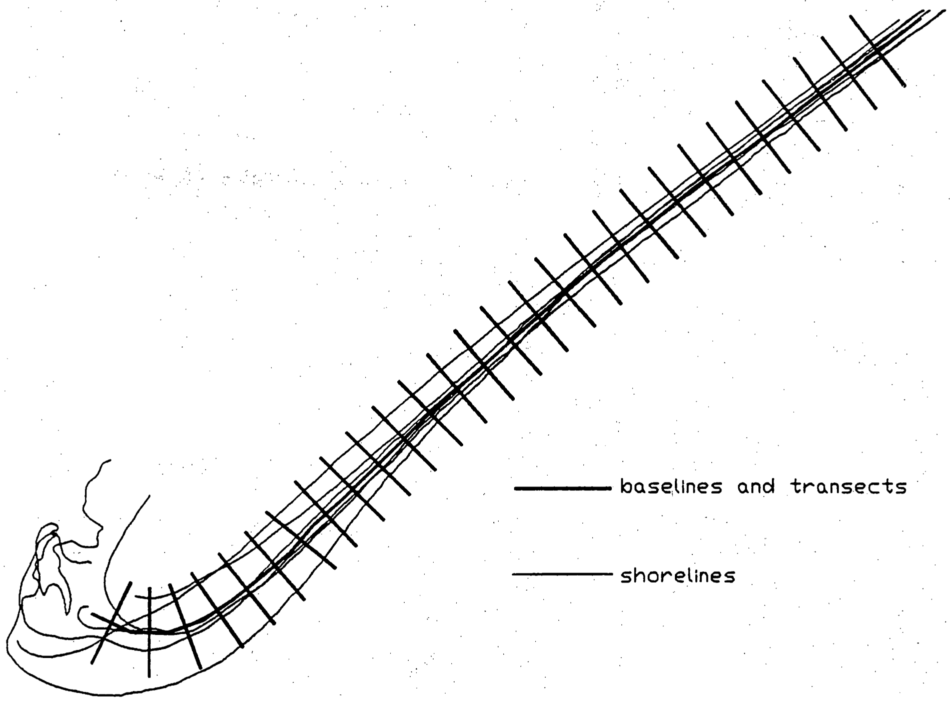
baselines and transects
shorelines

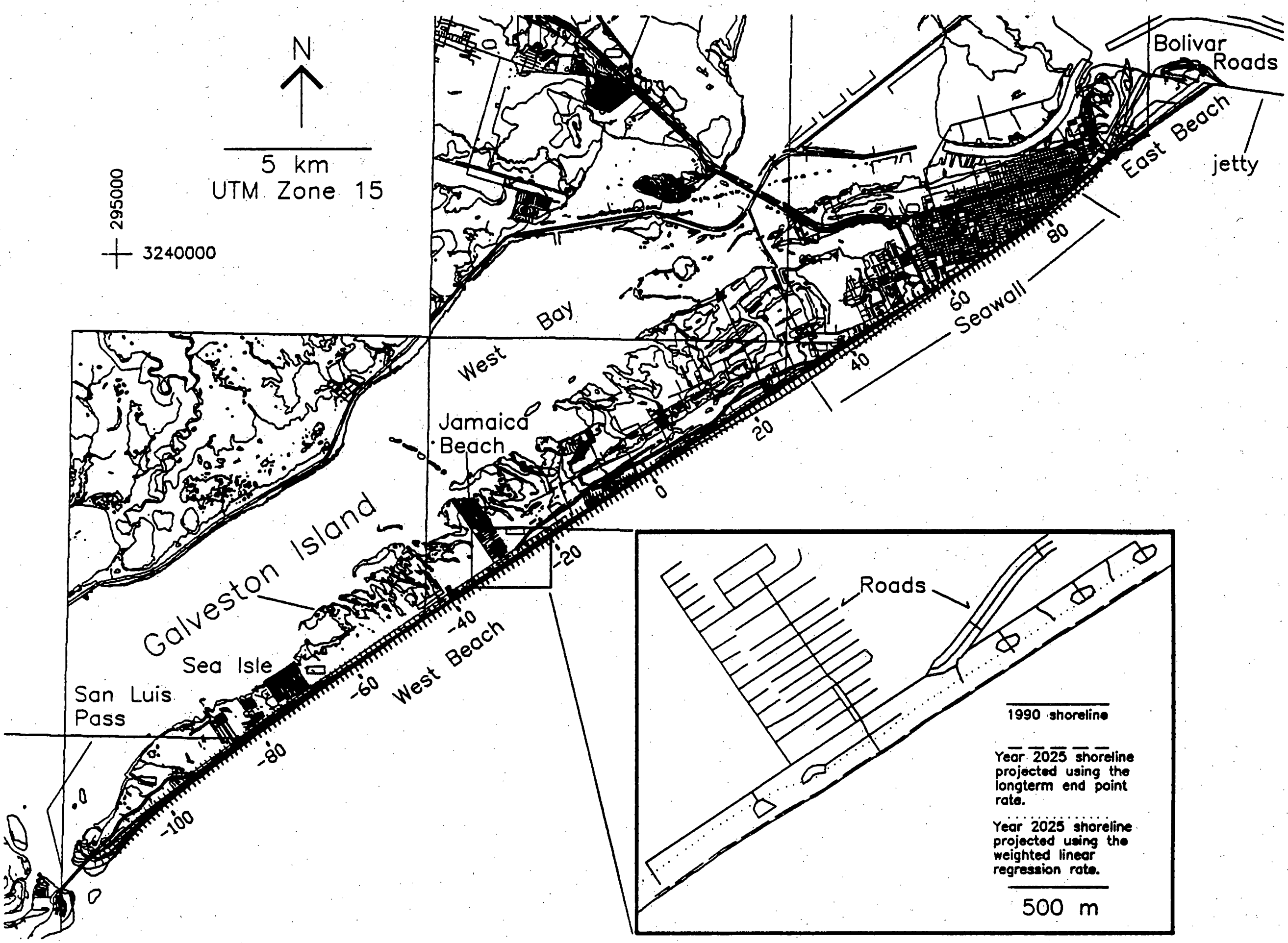

N
5 km
UTM Zone 15
295000
3240000
Bolivar
Roads
East Beach
jetty
80
60
Seawall
40
20
0
-20
-40
-60
-80
-100
West Bay
Jamaica
Beach
Galveston Island
Sea Isle
San Luis
Pass
West Beach
Roads
1990 shoreline
Year 2025 shoreline projected using the longterm end point rate.
Year 2025 shoreline projected using the weighted linear regression rate.
500 m

Fig. 3

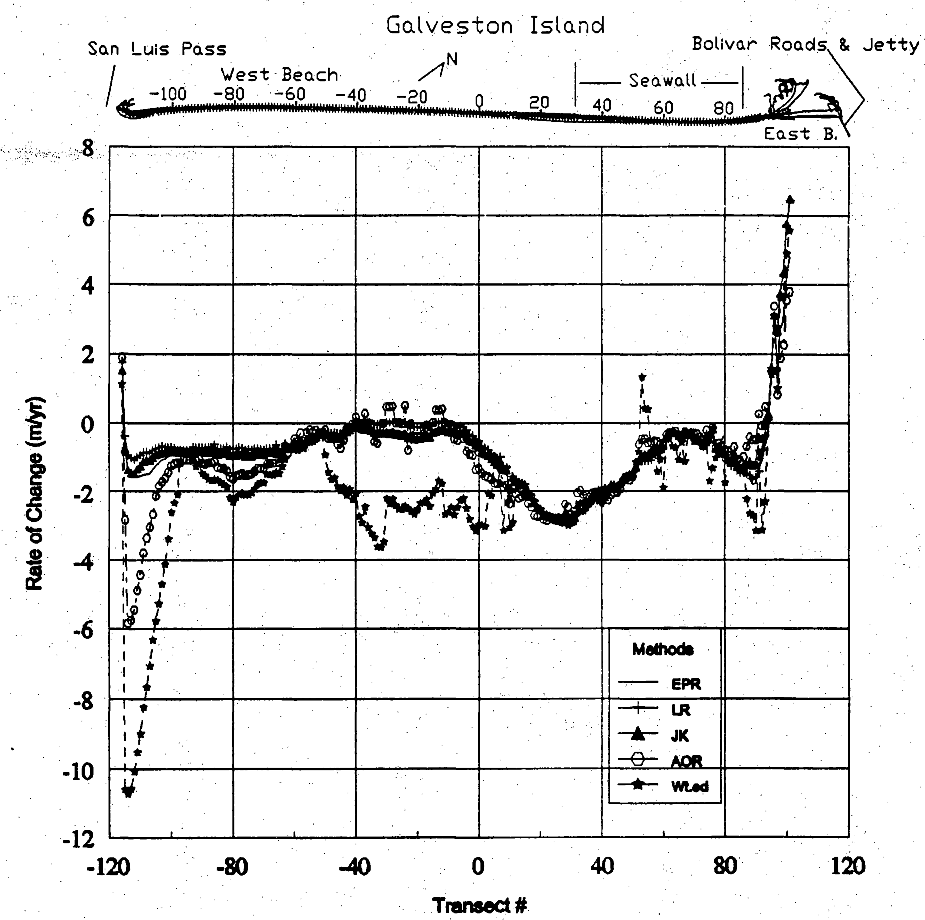

Galveston Island
San Luis Pass
West Beach
Seawall
Bolivar Roads & Jetty
East B.
N
-100
-80
-60
-40
-20
0
20
40
60
80
Rate of Change (m/yr)
Transect #
Methods
EPR
LR
JK
AOR
Wt.ed

Fig 4

Addendum 11. Descriptions of Vibracores, Sabine Bank and Heald Bank

CORE LOG

CORE # SBV-9 (A) TYPE Vibracore LOCATION Sabine Bank
LATITUDE 29° 38.090' LONGITUDE 94° 03.449' SURFACE ELEVATION 18'
DEPTH PENETRATED ? LENGTH RECOVERED 7' 2" (7.2') % COMPACTION ?

OBTAINED BY Gibeaut, R/V Kit Jones DATE 10-10-94
DESCRIBED BY WWt DATE 2-3-95

DEPTH (ft, m)	SKETCH	LITHOLOGY	STRUCTURE	REMARKS

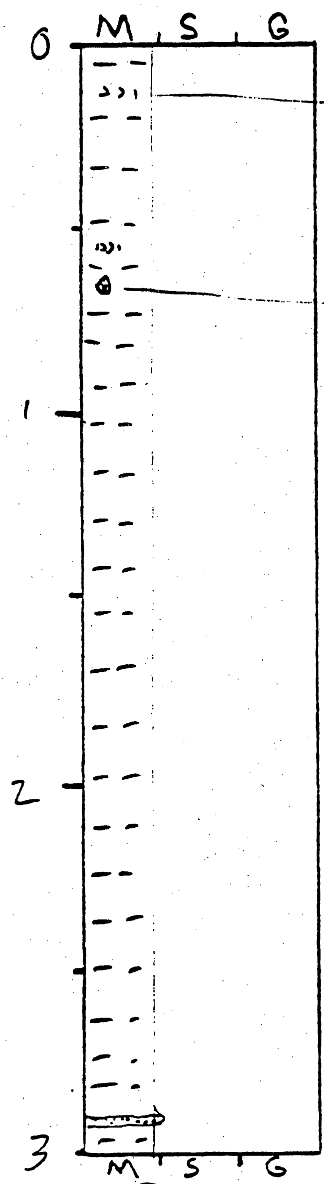

soft mud
a few small shells

Olive gray 5Y 4/1
hint of brown

a few scattered shells
whole shell

No shells

thin muddy sand layer

General Comments:

CORE LOG

CORE # SBV-9 (B) TYPE ________ LOCATION ________
LATITUDE ________ LONGITUDE ________ SURFACE ELEVATION ________
DEPTH PENETRATED ________ LENGTH RECOVERED ________ %COMPACTION ________

OBTAINED BY ________ DATE ________
DESCRIBED BY ________ DATE ________

DEPTH (ft, m)	SKETCH	LITHOLOGY	STRUCTURE	REMARKS
3	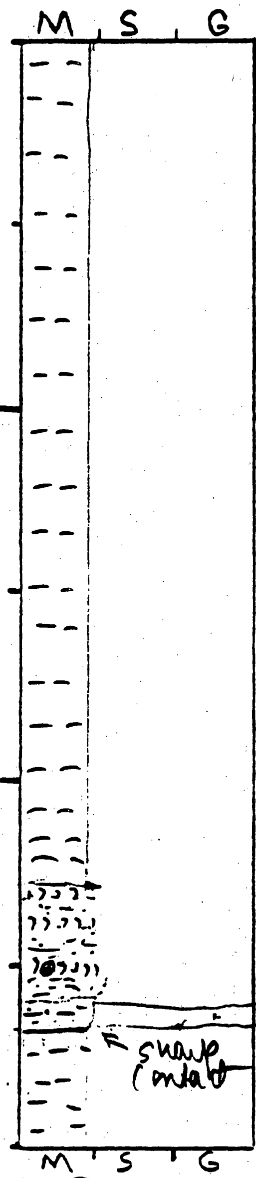	Soft mud		olive gray 5Y 4/1 hint of brown
4				
5				
shells decrease toward bottom		Shelly muddy sand (whole shells & frags up granule & small pebble)		medium dark gray to olive gray (5Y 3/2)
5.7'		muddy sand		
		stiff clay (Beaumont)		Lt gray with dark yellowish orange streaks
6				

General Comments:

CORE LOG

CORE # SBV-9(c) TYPE________ LOCATION____________________
LATITUDE__________ LONGITUDE__________ SURFACE ELEVATION__________
DEPTH PENETRATED______ LENGTH RECOVERED______ %COMPACTION___

OBTAINED BY______________________________ DATE________
DESCRIBED BY______________________________ DATE________

DEPTH (ft, m)	SKETCH	LITHOLOGY	STRUCTURE	REMARKS

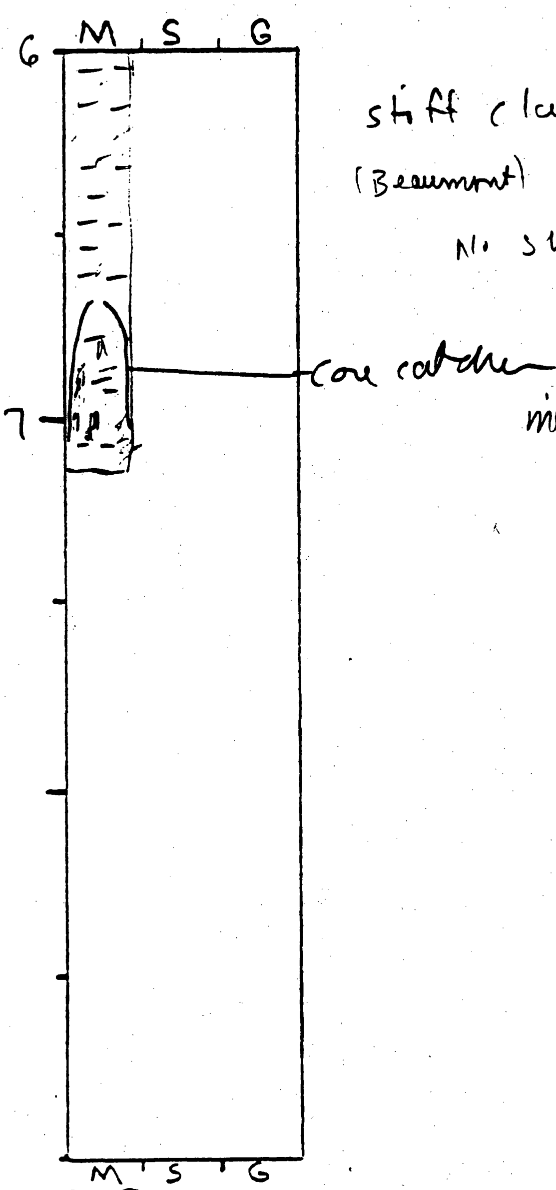

stiff clay (mottled)
(Beaumont)
No shells

light gray to pale olive with dark yellowish orange streaks (vertical)

mottled lt gray, dark yellowish orange, and small streaks of dark gray

General Comments:

CORE LOG

CORE # SBV-10(A) TYPE Vibracore LOCATION Sabine Bank
LATITUDE 29° 29.722' LONGITUDE 93°48.413' SURFACE ELEVATION -42'
DEPTH PENETRATED ? LENGTH RECOVERED 18.5' (18'6") %COMPACTION ?

OBTAINED BY Gibeaut & R/V Kit Jones DATE 10/11/94
DESCRIBED BY White DATE 2/3/95

DEPTH (ft, m)	SKETCH	LITHOLOGY	STRUCTURE	REMARKS

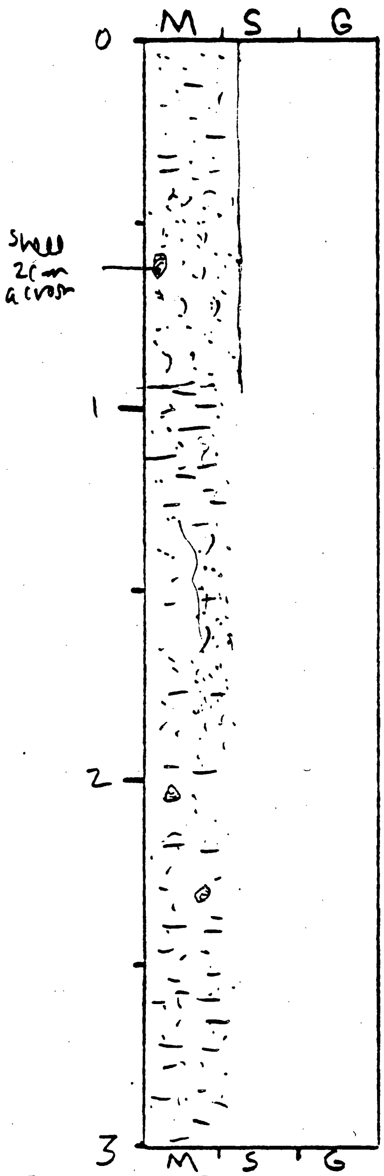

muddy sand (v. fine qtz sd) — Drk yellowish Brown

scattered shell frags & whole shells
granule & pebble in size
shells more concentrated (to 10%) from 0.4'–0.9' (higher conc. of sd at ?)
appears to be heavily burrowed
based on sand & mud relationships

(muddy sand)
muddier and more olive gray in color from 0.9'–1.4

burrows

Drk yellowish brown to olive gray

muddy sand but mud appears to be increasing at depth

color becoming more olive gray toward bottom (less brownish)

General Comments:

CORE LOG

CORE # SBV-40(B) TYPE ________ LOCATION ________
LATITUDE ________ LONGITUDE ________ SURFACE ELEVATION ________
DEPTH PENETRATED ________ LENGTH RECOVERED ________ %COMPACTION ________

OBTAINED BY ________ DATE ________
DESCRIBED BY ________ DATE ________

DEPTH (ft, m)	SKETCH	LITHOLOGY	STRUCTURE	REMARKS
3		muddy sand to sandy mud <u>few shells</u>	heavily burrowed	Olive gray (5Y 4/1) hint of brown
4		thin dark yellowish brown line (grayer below slightly brownish above) (fluid mud?)		
		muddy sand scattered small shell frag (few)	heavily burrowed	olive gray (5Y 3/2)
5		higher conc. of sand in this zone.		
		sandy mud	traces of organics	
		distinct contact (especially on sample half of core)		
		muddy sand		Olive gray (5Y 3/2)
6				

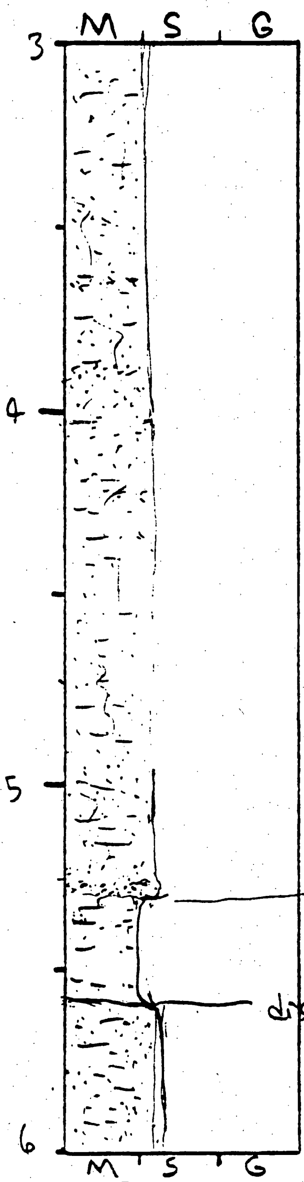

General Comments:

CORE LOG

CORE # SBV-10(9) TYPE ________ LOCATION ________
LATITUDE ________ LONGITUDE ________ SURFACE ELEVATION ________
DEPTH PENETRATED ________ LENGTH RECOVERED ________ %COMPACTION ________

OBTAINED BY ________ DATE ________
DESCRIBED BY ________ DATE ________

DEPTH (ft, m)	SKETCH	LITHOLOGY	STRUCTURE	REMARKS
6		muddy sand v. few shells	burrowed	Olive gray (5Y 3/2)
		sandy mud small sand pockets		
7				
		sand (slightly muddy)	burrowed	
		Sandy mud v. few shells		
8		sand (slightly muddy) a few small shells		
		Sandy mud (small sand pockets) (v. few shells)		Olive gray (5Y 3/2)
		muddy shelly sand (a couple of shell frag gravel size)	(burrowed)	
9				

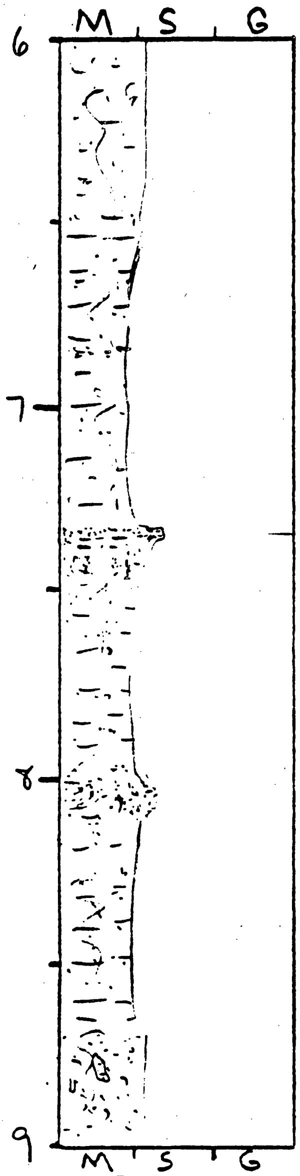

General Comments:

CORE LOG

CORE # SBV-10D' TYPE ________ LOCATION ________
LATITUDE ________ LONGITUDE ________ SURFACE ELEVATION ________
DEPTH PENETRATED ______ LENGTH RECOVERED ______ %COMPACTION ___

OBTAINED BY ________________________ DATE ________
DESCRIBED BY ________________________ DATE ________

DEPTH (ft, m)	SKETCH	LITHOLOGY	STRUCTURE	REMARKS

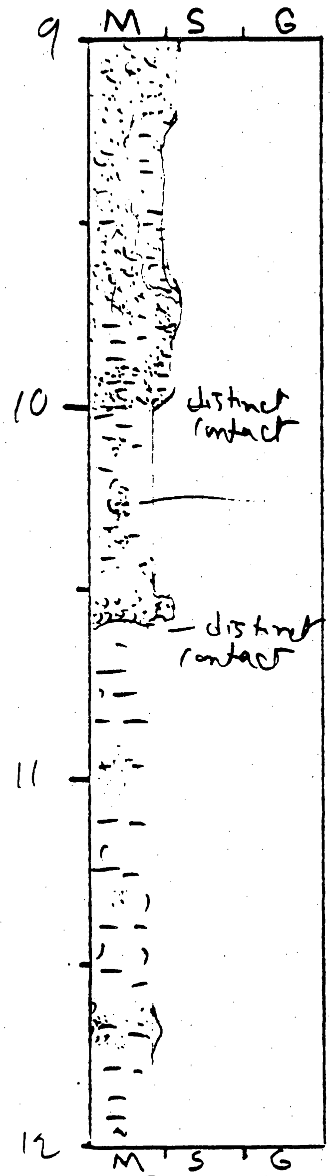

muddy sand (v. fine sand) — olive gray

slightly shelly < 10%

sand filled burrow — burrowed

discrete mud & sand zone

slightly sandy mud

sandy pockets; v. scattered shells in sand

muddy shelly sand (shell frags granule)

organic mud or clay traces of sand or silt (olive gray clay or mud with organic traces)

mud (traces of silt & sand in pockets)

scattered small shell frags (v. coarse to granule)

slightly more sand (sandy mud) (scattered small shell frags)

mud (organic traces) — olive gray

General Comments:

CORE LOG

CORE # SBV-10(E) TYPE________ LOCATION________________
LATITUDE________ LONGITUDE________ SURFACE ELEVATION________
DEPTH PENETRATED______ LENGTH RECOVERED______ %COMPACTION____

OBTAINED BY________________________ DATE________
DESCRIBED BY________________________ DATE________

DEPTH (ft, m)	SKETCH	LITHOLOGY	STRUCTURE	REMARKS

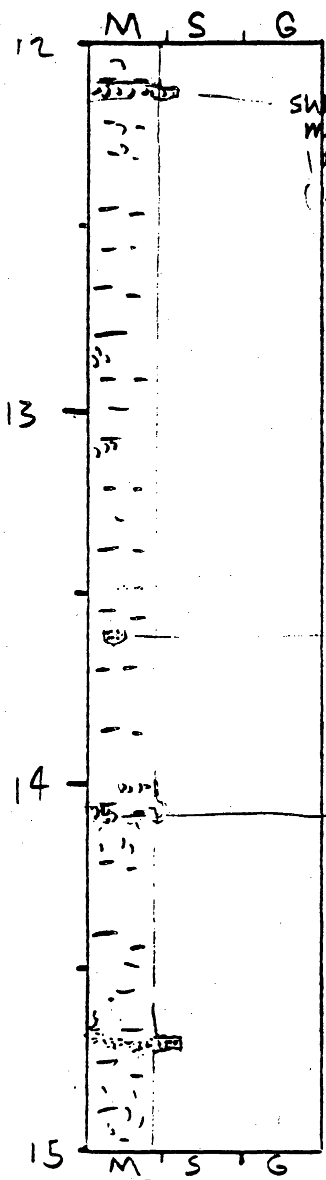

shelly mud layer (granule size frags) — mud traces of organics — very scattered small shell frags except in layers or pockets where more concentrated — Olive gray

mud (traces of sand in pockets)

sand pocket

muddy shell zone (granule to v. coarse sd size)

mud — Olive gray

thin sand layer (irregular)

General Comments:

CORE LOG

CORE # SBV-10 (F) TYPE ________ LOCATION ________
LATITUDE ________ LONGITUDE ________ SURFACE ELEVATION ________
DEPTH PENETRATED ______ LENGTH RECOVERED ______ %COMPACTION ___

OBTAINED BY ________ DATE ________
DESCRIBED BY ________ DATE ________

DEPTH (ft, m)	SKETCH	LITHOLOGY	STRUCTURE	REMARKS
15	M , S , G — few small shell frags	Organic clay or mud (traces of organics) shells absent except at very top and near bottom		Medium dark gray to olive gray
16		thin organic concentration — small wood fragment possibly 2mm x 1,2 cm		
		discrete although somewhat faint organic lines and possibly silt.		
		organics		
17		silty		
				medium gray
		pocket of small shell frags		
18	M S G			

General Comments:

CORE LOG

CORE # SBV-10(G) TYPE________ LOCATION________
LATITUDE________ LONGITUDE________ SURFACE ELEVATION________
DEPTH PENETRATED______ LENGTH RECOVERED______ %COMPACTION____

OBTAINED BY________ DATE________
DESCRIBED BY________ DATE________

DEPTH (ft, m)	SKETCH	LITHOLOGY	STRUCTURE	REMARKS

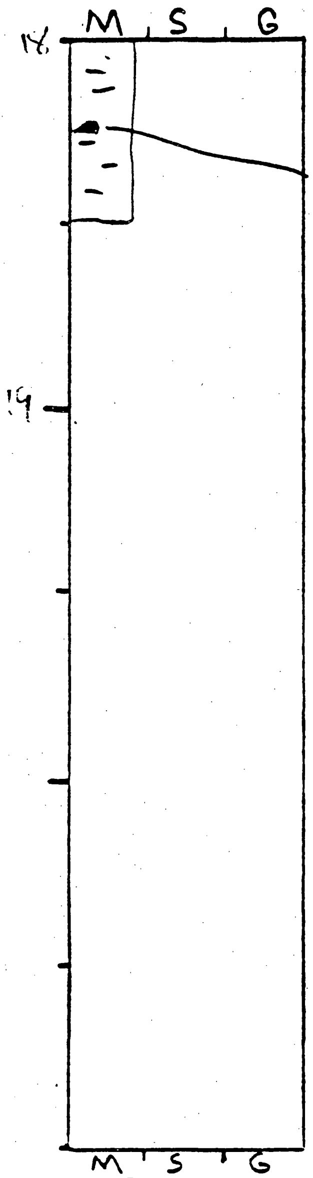

soft mud (no shells) medium gray

organic fragment (possibly could be dated)

General Comments:

CORE LOG

CORE # SBV-11(A) TYPE Vibracore LOCATION Sabine Bank
LATITUDE 29° 31.177' LONGITUDE 93° 35.649 SURFACE ELEVATION -37'
DEPTH PENETRATED ? LENGTH RECOVERED 11'3/4" % COMPACTION ?

OBTAINED BY Gibeaut - R/V Kit Jones DATE 10-13-94
DESCRIBED BY White DATE 3-6-95

DEPTH (ft, m)	SKETCH	LITHOLOGY	STRUCTURE	REMARKS
0	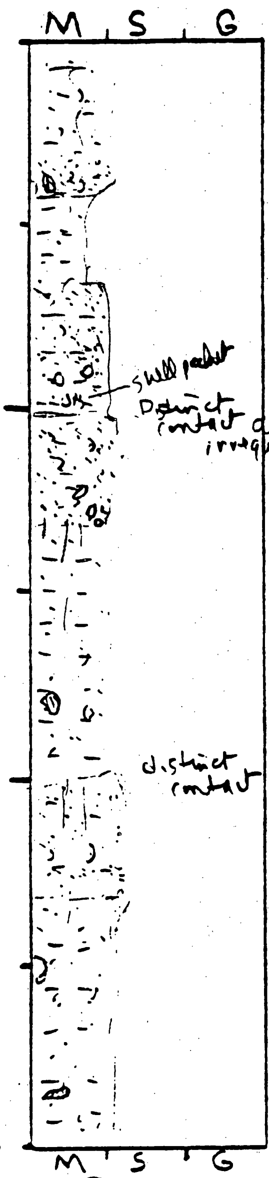	muddy sd, scattered shells near base	intensely burrowed	color - medium dark gray to olive gray
		sandy mud		
		muddy sd, occassional small (pebble) whole shells		
1		sd, slightly muddy, scattered shell frags (granule to pebble)		
		muddy sd, scattered shells		
2		sd, slightly muddy, scattered small shells		
		muddy sd, scattered shells		
3				

General Comments:

CORE LOG

CORE # SBV-11(B) TYPE ______ LOCATION ______
LATITUDE ______ LONGITUDE ______ SURFACE ELEVATION ______
DEPTH PENETRATED ______ LENGTH RECOVERED ______ %COMPACTION ______

OBTAINED BY ______ DATE ______
DESCRIBED BY ______ DATE ______

DEPTH (ft, m)	SKETCH	LITHOLOGY	STRUCTURE	REMARKS

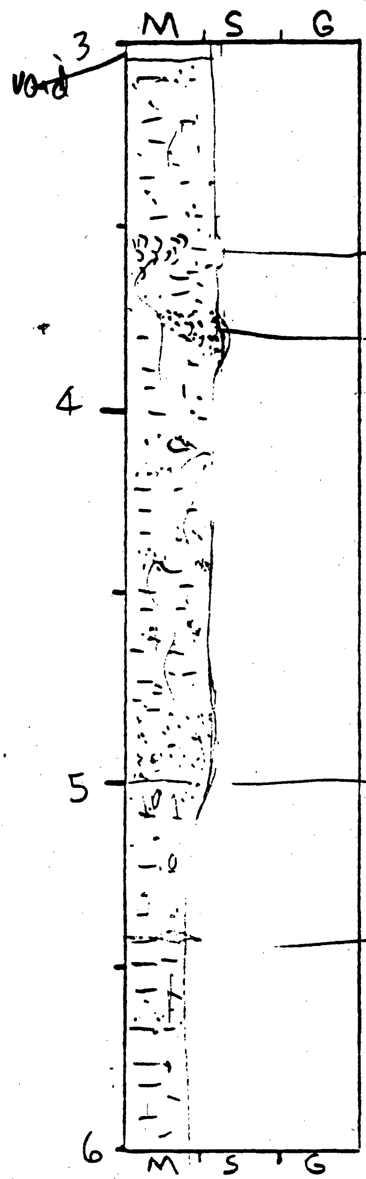

muddy sand — burrowed — Olive gray to med. drk gray (5 Y 3/2)

shell pocket shell frags & whole shells granule to pebble size

sand pocket & scattered small shells

appears to be muddy sand a few scattered shells (possibly sandy mud) — burrowed — Olive gray to med drk gray

discrete sand pockets -- possibly filled burrows

more sand in this zone

1st traces of Beaumont clay (mottled lt gray & Lt olive brown with dark gray muddy sand (clay clasts in muddy sand)

Beaumont clay become dominant below 5.4'

a little mixing of gray sand from above — mottled Lt olive gray & Lt olive brown

General Comments:

CORE LOG

CORE # SBV-11(C) **TYPE**________ **LOCATION**________
LATITUDE________ **LONGITUDE**________ **SURFACE ELEVATION**________
DEPTH PENETRATED______ **LENGTH RECOVERED**______ **%COMPACTION**____

OBTAINED BY________________ **DATE**________
DESCRIBED BY________________ **DATE**________

DEPTH (ft, m)	SKETCH	LITHOLOGY	STRUCTURE	REMARKS

M S G

6

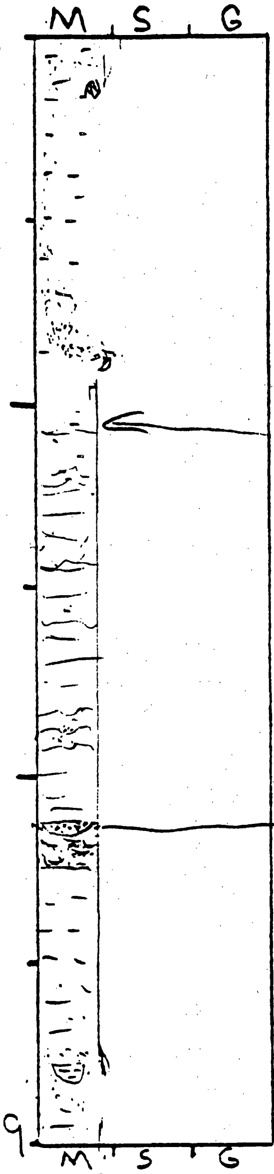

medium gray muddy sand at top
mixed below with - Lt olive brown
Beaumont clay with mod. yellowish brown ...

Burrow filled light to med. gray muddy sand
Lt gray with some brownish yellow layers

7

color becomes mottled & more brownish yellow below 7.1'
some organics slightly distorted
NO SHELLS horizontal laminae

Beaumont clay traces of sand in pockets
traces of organics

8

Lt gray sand lens at 8.2'
possible ripples

yellowish gray with yellowish orange mottling

clay

Silty clay to Clayey silt Lt gray to

9

M S G

General Comments:

CORE LOG

CORE # SBV 11 (D) TYPE________ LOCATION________________
LATITUDE________ LONGITUDE________ SURFACE ELEVATION________
DEPTH PENETRATED______ LENGTH RECOVERED______ %COMPACTION____

OBTAINED BY________________________ DATE________
DESCRIBED BY________________________ DATE________

DEPTH (ft, m)	SKETCH	LITHOLOGY	STRUCTURE	REMARKS

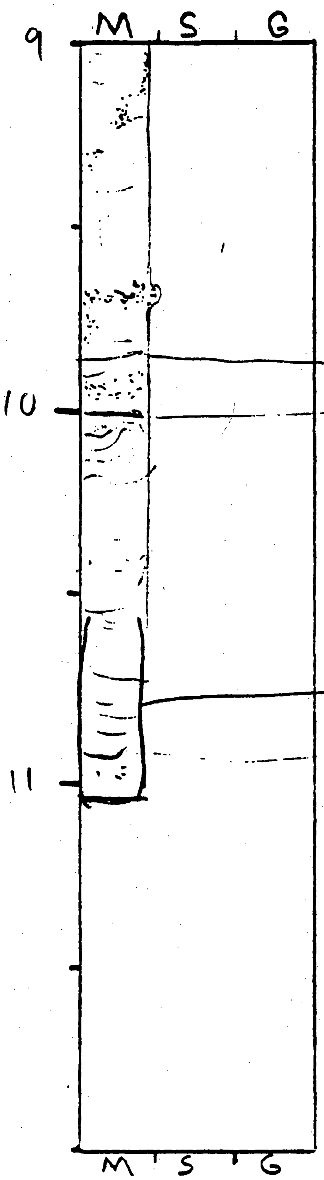

Beaumont clay
occassional thin v. fine sand or silt layers & organic layers

mottled colors from lt olive gray to drk yellow orange and grayish orange

organics — slightly distorted laminae

thin dark brown organic layer

core catcher

organics

General Comments:

CORE LOG

CORE # SBV-12(A) TYPE Vibracore LOCATION Sabine Bank
LATITUDE 29° 30.007 LONGITUDE 93° 35.397' SURFACE ELEVATION -25'
DEPTH PENETRATED ? LENGTH RECOVERED 16' 9" % COMPACTION ?

OBTAINED BY Gibeaut - R/V Kit Jones DATE 10-13-94
DESCRIBED BY White DATE

DEPTH (ft, m)	SKETCH	LITHOLOGY	STRUCTURE	REMARKS

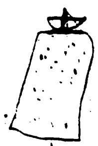

Bag of fine sand from top of Core 12

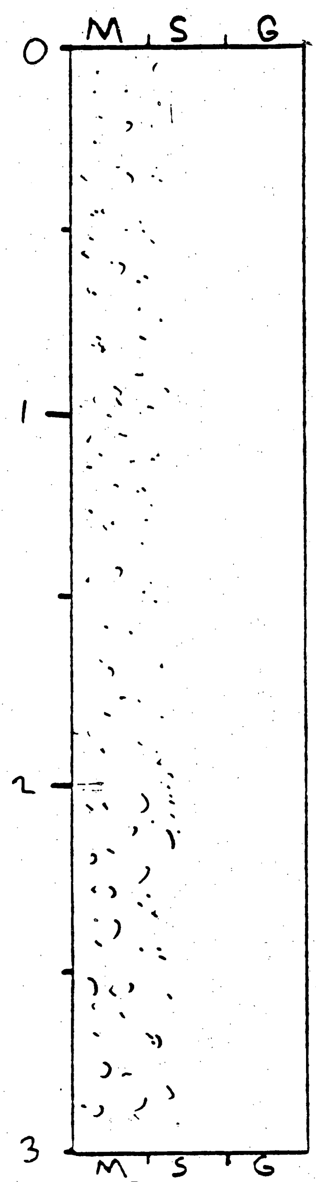

Fine quartz sand, subrounded, well sorted
5-10% shell frags - coarse to very coarse sand size

Lt olive gray (5Y 5/2) to olive gray hint of brown

Fining upward sequence

Fine quartz sand with increasing amounts of shell fragments, also coarsening of shell fragments -- granule in size
fragments approaching 25% below ≈ 2'

General Comments:

CORE LOG

CORE # SBV 12 (B) TYPE______ LOCATION______
LATITUDE______ LONGITUDE______ SURFACE ELEVATION______
DEPTH PENETRATED______ LENGTH RECOVERED______ %COMPACTION______

OBTAINED BY______ DATE______
DESCRIBED BY______ DATE______

DEPTH (ft, m)	SKETCH	LITHOLOGY	STRUCTURE	REMARKS
3		shelly sand		Lt Olive gray (5Y 5/2) to Olive gray (5Y 4/1)
		gradational increase in shell frags. quantity & size with depth		
		Fining upward		
4		sandy shell		
		coarsening of shells pebble size some whole shells		
5		shell pocket		
		Fine sand, scattered small shell frags.		Olive gray sd (5Y 5/2)
6				

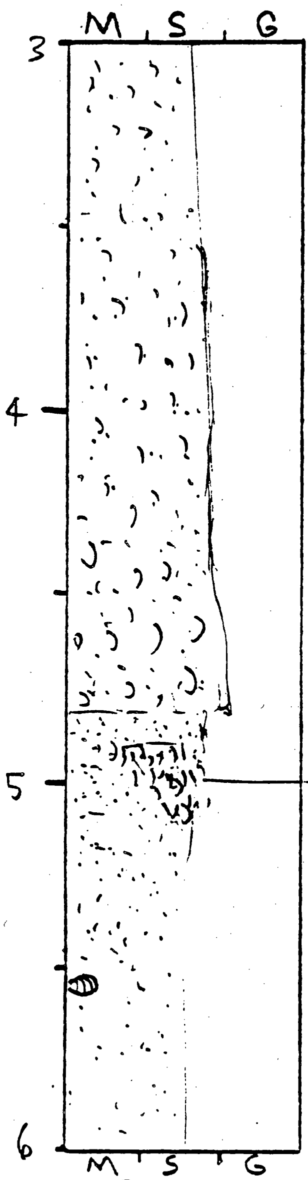

General Comments:

CORE LOG

CORE # SBV-12(C) TYPE ________ LOCATION ________
LATITUDE ________ LONGITUDE ________ SURFACE ELEVATION ________
DEPTH PENETRATED ______ LENGTH RECOVERED ______ %COMPACTION ___

OBTAINED BY ________ DATE ________
DESCRIBED BY ________ DATE ________

DEPTH (ft, m)	SKETCH	LITHOLOGY	STRUCTURE	REMARKS
6	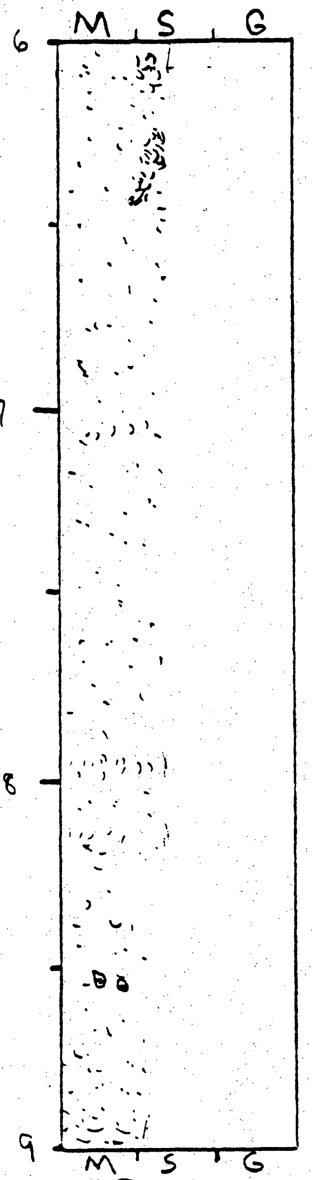	Fine quartz sand, sub rounded well sorted except for local shell pods, very coarse to granule shell frags		Olive gray 5Y 4/1 to 5Y 5/2
7		Fine quartz sand		
8		Local increase in shell frags mostly very coarse sand size <10% shell frags		
9		slightly muddy sand?		Olive gray 5Y 3/2

General Comments:

CORE LOG

CORE # SBV-12(D) TYPE ______ LOCATION ______
LATITUDE ______ LONGITUDE ______ SURFACE ELEVATION ______
DEPTH PENETRATED ______ LENGTH RECOVERED ______ %COMPACTION ______

OBTAINED BY ______ DATE ______
DESCRIBED BY ______ DATE ______

DEPTH (ft, m)	SKETCH	LITHOLOGY	STRUCTURE	REMARKS

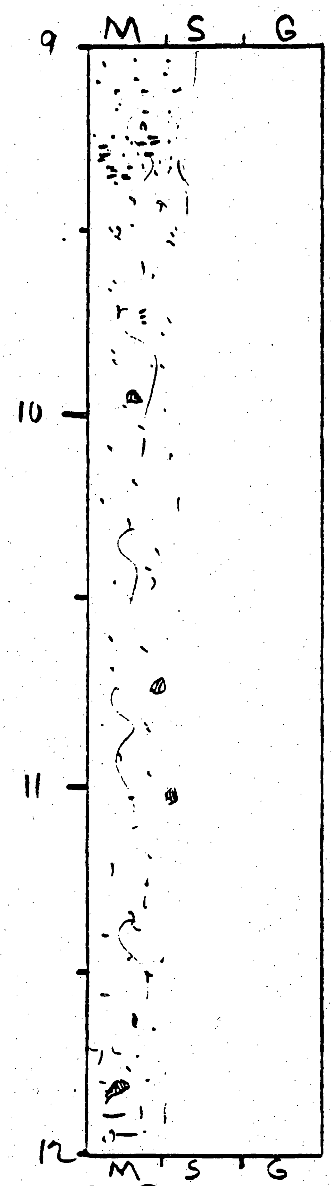

Fine to v. fine quartz sand — Olive gray (5Y 3/2)

muddy very fine sand (Burrowed)

discrete mud & sand — becoming dark gray than above sect.

slightly muddy sand

scattered shell fragments (small)

very coarse to granule size

mud clasts?

occasional whole (small) shell

Burrowed

v. fine sand, slightly muddy

mud clasts?

mud seems to increase near bottom

muddy sand — Olive gray (5Y 3/2

General Comments:

CORE LOG

CORE # SBV-12(E) TYPE ________ LOCATION ________
LATITUDE ________ LONGITUDE ________ SURFACE ELEVATION ________
DEPTH PENETRATED ______ LENGTH RECOVERED ______ %COMPACTION ___

OBTAINED BY ________________ DATE ________
DESCRIBED BY ________________ DATE ________

DEPTH (ft, m)	SKETCH	LITHOLOGY	STRUCTURE	REMARKS
12		muddy sand	intensely Burrowed	Olive gray (5Y 3/2)
		a few scattered shell frags ≤ 1 or 2%		becoming darker gray toward section
13		discrete sand and mud (clay) zones. slightly muddier from 13.1 – 13.6	Intensely Burrowed	
14		Lt Olive gray (brownish) sd layer & few larger shell (pebble size)		
		muddy sand occasional shell pocket		
15				Olive gray (5Y 3/2)

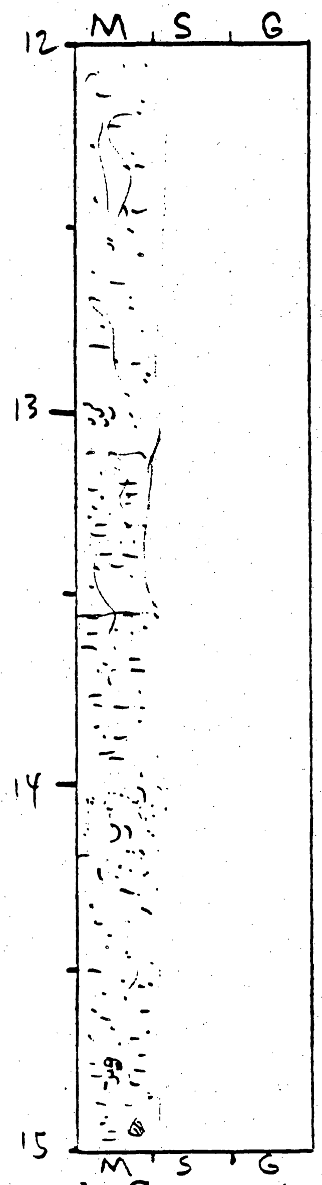

General Comments:

CORE LOG

CORE # SBV-12 F **TYPE** ______ **LOCATION** ______
LATITUDE ______ **LONGITUDE** ______ **SURFACE ELEVATION** ______
DEPTH PENETRATED ______ **LENGTH RECOVERED** ______ **%COMPACTION** ______

OBTAINED BY ______ **DATE** ______
DESCRIBED BY ______ **DATE** ______

DEPTH (ft, m)	SKETCH	LITHOLOGY	STRUCTURE	REMARKS
15		muddy sand to sandy mud whole shell ≈ 2 cm long < 1% shell frags discrete sand pockets & clay zone	Intensely burrowed	Olive gray (5 Y 3/2) darker than above
16		core catcher		

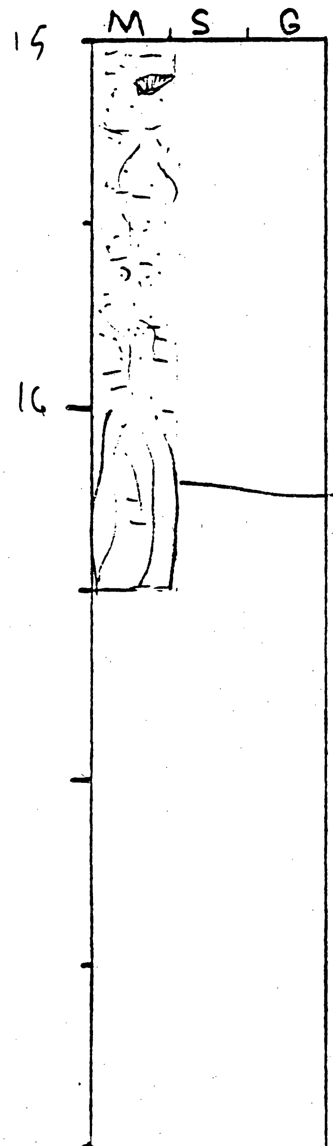

General Comments:

CORE LOG

CORE # SBY-13 (A) TYPE Vibracore LOCATION Sabine Bank
LATITUDE 29° 28.729 LONGITUDE 93° 34.872 SURFACE ELEVATION -37'
DEPTH PENETRATED ? LENGTH RECOVERED 19'4" % COMPACTION ?

OBTAINED BY Gibeaut - R/V Kit Jones DATE 10-13-94
DESCRIBED BY White DATE 2-7-95

DEPTH (ft, m)	SKETCH	LITHOLOGY	STRUCTURE	REMARKS

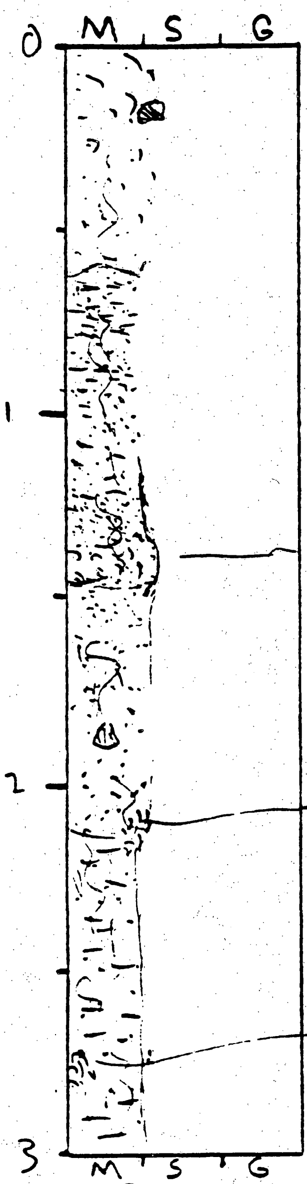

shelly fine sand, fragmented whole up to pebble size

Olive gray (5Y 3/2 to 5Y 4/1)

Larger shell fragments near top, decrease below

muddy sand to sandy mud

intensely burrowed

muddy shelly sand

sand, scattered shell frags, slightly muddy

shell pocket

becomes muddier

intensely burrowed

muddy sand

shell pocket

Olive gray (5Y 3/2)

General Comments:

CORE LOG

CORE # SBV-13(B) TYPE ________ LOCATION ________
LATITUDE ________ LONGITUDE ________ SURFACE ELEVATION ________
DEPTH PENETRATED ______ LENGTH RECOVERED ______ %COMPACTION ___

OBTAINED BY ________ DATE ________
DESCRIBED BY ________ DATE ________

DEPTH (ft, m)	SKETCH	LITHOLOGY	STRUCTURE	REMARKS
3	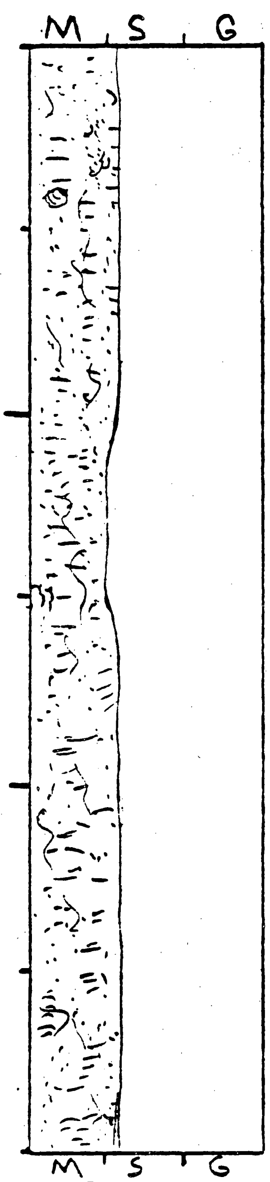	Muddy sand		Olive gray (5Y 3/2)
		Very scattered shells <1%	Intensely Burrowed	
4		muddier muddy sand to sandy mud	Intensely Burrowed	
5		Muddy sand; discrete mud & sand areas	Intensely Burrowed	
6				Olive gray (5Y 3/2)

General Comments:

CORE LOG

CORE # SBV-13(C) TYPE ______ LOCATION ______
LATITUDE ______ LONGITUDE ______ SURFACE ELEVATION ______
DEPTH PENETRATED ______ LENGTH RECOVERED ______ %COMPACTION ______

OBTAINED BY ______ DATE ______
DESCRIBED BY ______ DATE ______

DEPTH (ft, m)	SKETCH	LITHOLOGY	STRUCTURE	REMARKS

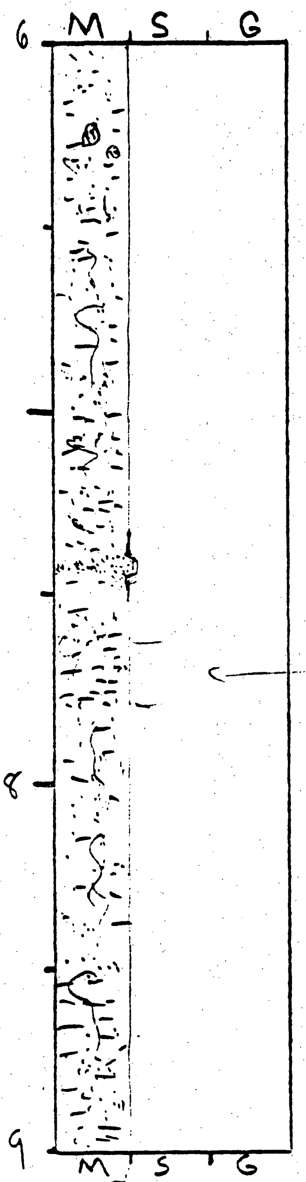

muddy sand to sandy mud
mud becomes more abundant in this section, still lots of fine sand

Olive gray 5Y 3/2

Intensely Burrowed

o few scattered shells

discrete sand and mud areas

discrete mud & sand zone

thin sand layer (light olive gray to Olive gray)

sandy mud

Intensely Burrowed

muddy sand to sandy mud

very scattered shell frags <1%

Olive gray (5Y 3/2)

General Comments:

CORE LOG

CORE # SBV-13(D) TYPE________ LOCATION__________
LATITUDE________ LONGITUDE________ SURFACE ELEVATION________
DEPTH PENETRATED______ LENGTH RECOVERED______ %COMPACTION____

OBTAINED BY____________________ DATE________
DESCRIBED BY____________________ DATE________

DEPTH (ft, m)	SKETCH	LITHOLOGY	STRUCTURE	REMARKS

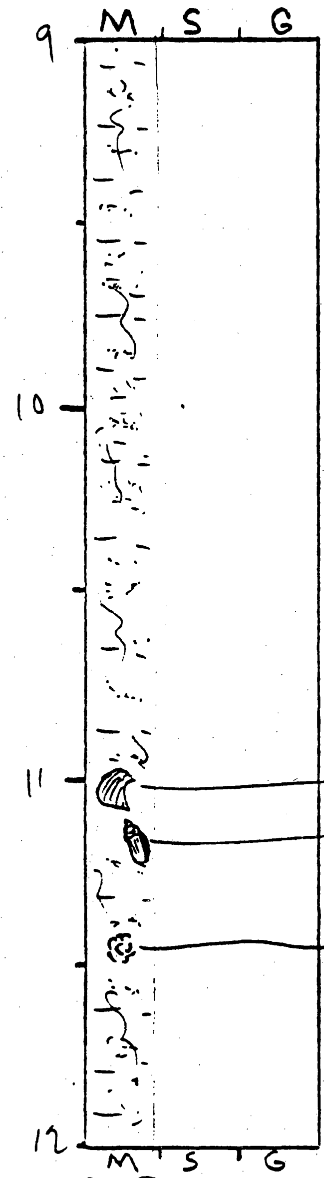

Sandy mud few shell — Intensely Burrowed — Olive gray (5Y 3/2)

small sand filled burrows?

Intensely burrowed

Dinocardium (Both halfs) (whole shell)

Large gastropod (whelk)

shell packet small whole shells

Olni gray 5Y(3/2)

General Comments:

CORE LOG

CORE # SBV-13(E) TYPE ________ LOCATION ________
LATITUDE ________ LONGITUDE ________ SURFACE ELEVATION ________
DEPTH PENETRATED ________ LENGTH RECOVERED ________ %COMPACTION ________

OBTAINED BY ________ DATE ________
DESCRIBED BY ________ DATE ________

DEPTH (ft, m)	SKETCH	LITHOLOGY	STRUCTURE	REMARKS

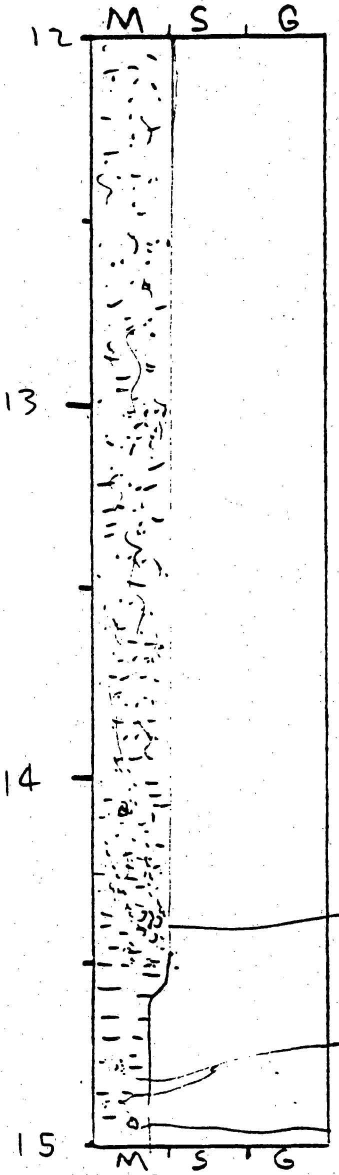

muddy sand to sandy mud
few shell fragments
<1%
except for
pockets near bottom

Intensely
burrowed

Olive gray
5Y 3/2

muddy sand to
sandy mud

discrete mud & sand

shell pocket (granule size shell frags)

sand filled burrows
Clay

few
burrows

medium gray

shell frag

General Comments:

CORE LOG

CORE # SBV-13(F) TYPE________ LOCATION________________
LATITUDE__________ LONGITUDE__________ SURFACE ELEVATION________
DEPTH PENETRATED______ LENGTH RECOVERED______ %COMPACTION___

OBTAINED BY______________________________ DATE__________
DESCRIBED BY______________________________ DATE__________

DEPTH (ft, m)	SKETCH	LITHOLOGY	STRUCTURE	REMARKS
15–18	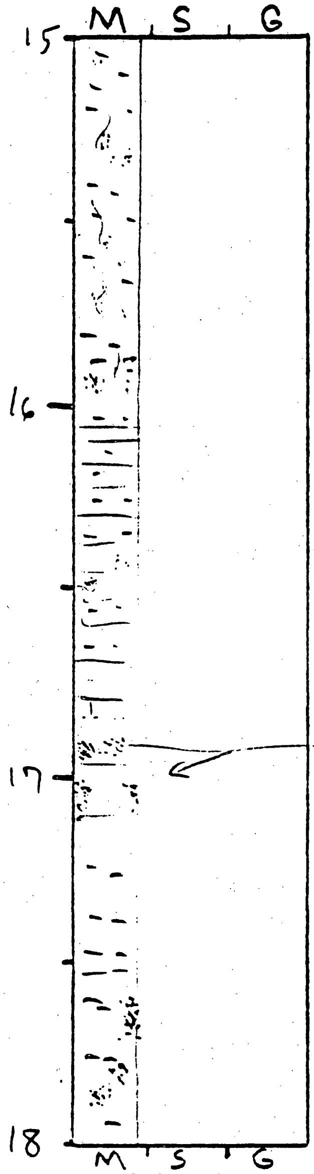	mud or silty clay; silt or fine sand pockets (burrows)	burrowed	medium dark gray to olive gray; medium gray below 19.6'
		silty clay	fine horizontal silty laminae	
		v. few shells - mostly restricted to sand pockets		
	sand pockets			
			some burrows	medium gray to olive gray (5Y 3/2)

General Comments:

CORE LOG

CORE # SBV13(G) TYPE ______ LOCATION ______
LATITUDE ______ LONGITUDE ______ SURFACE ELEVATION ______
DEPTH PENETRATED ______ LENGTH RECOVERED ______ %COMPACTION ______

OBTAINED BY ______ DATE ______
DESCRIBED BY ______ DATE ______

DEPTH (ft, m)	SKETCH	LITHOLOGY	STRUCTURE	REMARKS
18		silty clay or possibly sandy mud	burrowed	medium gray to Olive gray 5Y 3/2
		small silt or sand filled burrows		
19		core catcher		
		soft Olive gray slightly gritty mud in baggie from bottom of corer		

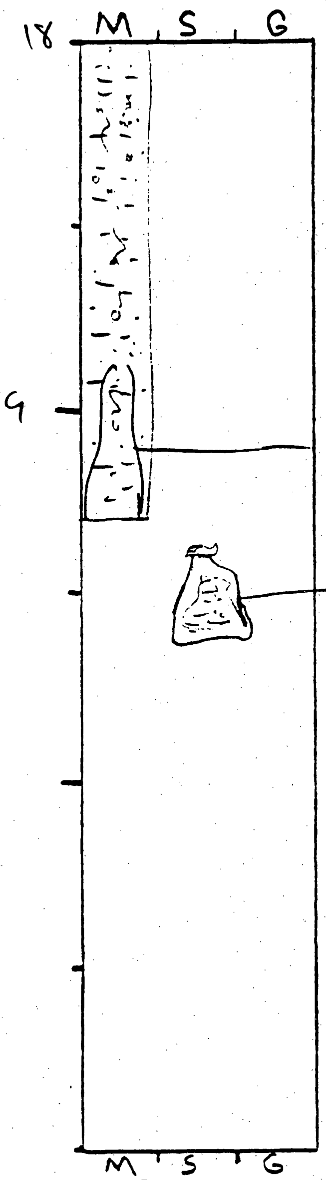

General Comments:

CORE LOG

CORE # SBV-14(A) **TYPE** Vibrocore **LOCATION** Sabine Bank
LATITUDE 29° 29.283 **LONGITUDE** 93° 38.052 **SURFACE ELEVATION** -32'
DEPTH PENETRATED ? **LENGTH RECOVERED** 19'9¼" **% COMPACTION** ?

OBTAINED BY Gibeaut - R/V Kit Jones **DATE** 10-13-94
DESCRIBED BY White **DATE** 2-7-95

DEPTH (ft, m)	SKETCH	LITHOLOGY	STRUCTURE	REMARKS

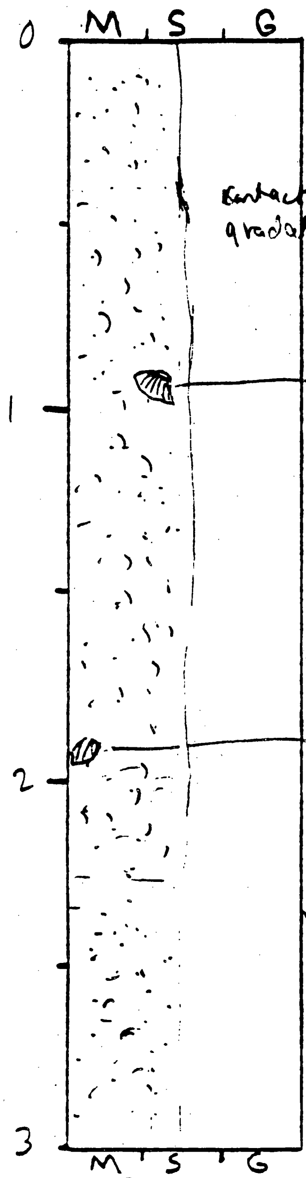

fine to v fine sand, some shells
shell fragments & whole shells
most granule or small
a few pebble size

contact gradational

shelly v. fine sand, slightly muddy

whole shell (3 cm across)

large shell fragment

v. fine sand; shells less abundant below about -2.3'.
slightly muddy

Olive gray 5Y 3/2

← core interrupted in this area leaving some void space

Olive gray 5Y 3/2

General Comments:

CORE LOG

CORE # SBV-14(B) TYPE______ LOCATION______
LATITUDE______ LONGITUDE______ SURFACE ELEVATION______
DEPTH PENETRATED______ LENGTH RECOVERED______ %COMPACTION______

OBTAINED BY______ DATE______
DESCRIBED BY______ DATE______

DEPTH (ft, m)	SKETCH	LITHOLOGY	STRUCTURE	REMARKS
3		sand slightly muddy shells ≃ 5% frags & whole local concentrations	burrowed	Olive gray
		becomes slightly more muddy below 3.6'		
4		possibly muddy sand		
		granule size shell concentration muddy shelly sandy		
5		shell pocket – muddy shelly sand		
		muddy sand v few shells		Olive gray
6				

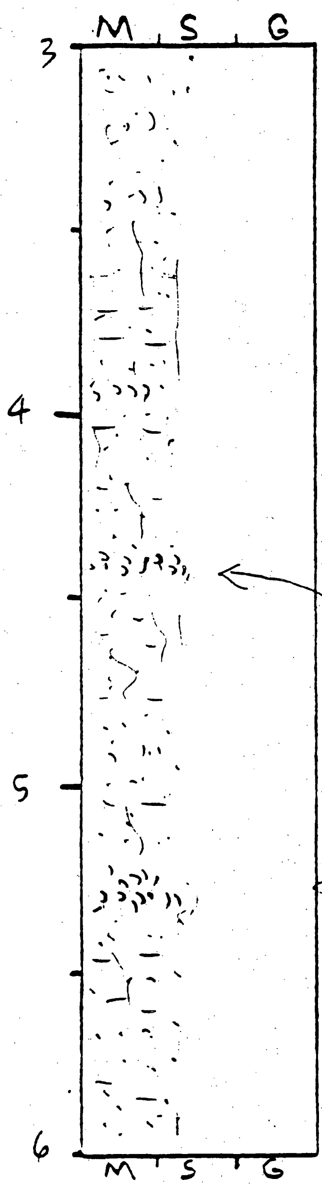

General Comments:

CORE LOG

CORE # SBV-14(C) TYPE ______ LOCATION ______
LATITUDE ______ LONGITUDE ______ SURFACE ELEVATION ______
DEPTH PENETRATED ______ LENGTH RECOVERED ______ %COMPACTION ______

OBTAINED BY ______ DATE ______
DESCRIBED BY ______ DATE ______

DEPTH (ft, m)	SKETCH	LITHOLOGY	STRUCTURE	REMARKS
6	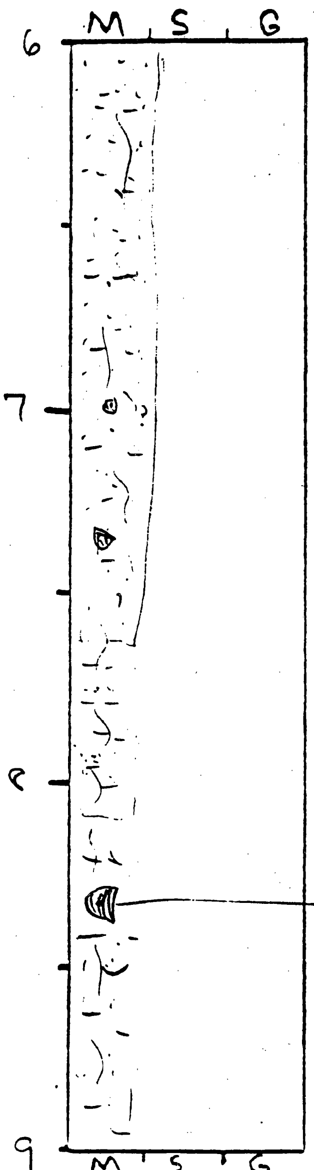	muddy sand a few shells & shell frag. to sandy mud	burrowed	Olive gray 5Y 3/2
7			burrowed	
8		mud some sand in burrows		
		large shell	Intensely burrowed	
9		sandy mud		Olive gray 5Y 3/2

General Comments:

CORE LOG

CORE # SBV-14(D) TYPE ________ LOCATION ________
LATITUDE ________ LONGITUDE ________ SURFACE ELEVATION ________
DEPTH PENETRATED ______ LENGTH RECOVERED ______ % COMPACTION ____

OBTAINED BY ________________________ DATE ________
DESCRIBED BY ________________________ DATE ________

DEPTH (ft, m)	SKETCH	LITHOLOGY	STRUCTURE	REMARKS
9		sandy mud	Intensely Burrowed	Olive grey (5Y 3/2)
		a few shells (very scattered < 1%)		
10		(slightly more sand from 10 - 11.2')		
		sandy mud		
		discrete sand & mud areas		
11				
		sandy mud		Olive gray (5Y 3/2)
		sandy unit not well defined		
		sand filled burrows		
12				

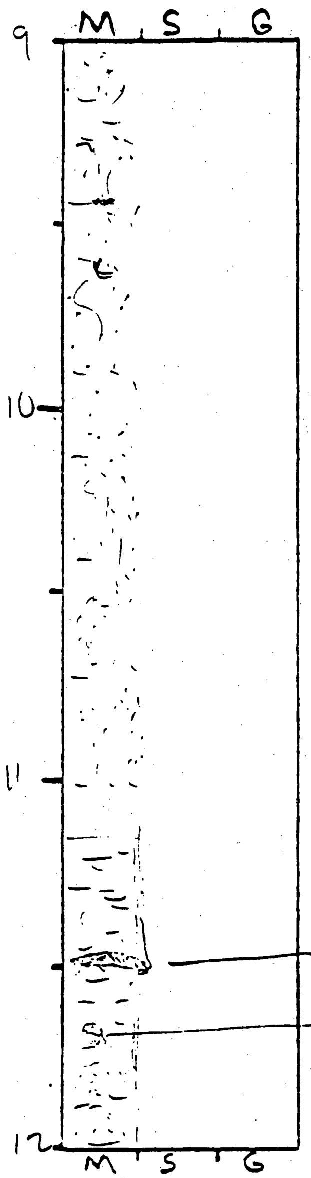

General Comments:

CORE LOG

CORE # SBV-14(E) TYPE______ LOCATION______
LATITUDE______ LONGITUDE______ SURFACE ELEVATION______
DEPTH PENETRATED______ LENGTH RECOVERED______ %COMPACTION______

OBTAINED BY______ DATE______
DESCRIBED BY______ DATE______

DEPTH (ft, m)	SKETCH	LITHOLOGY	STRUCTURE	REMARKS
12–15	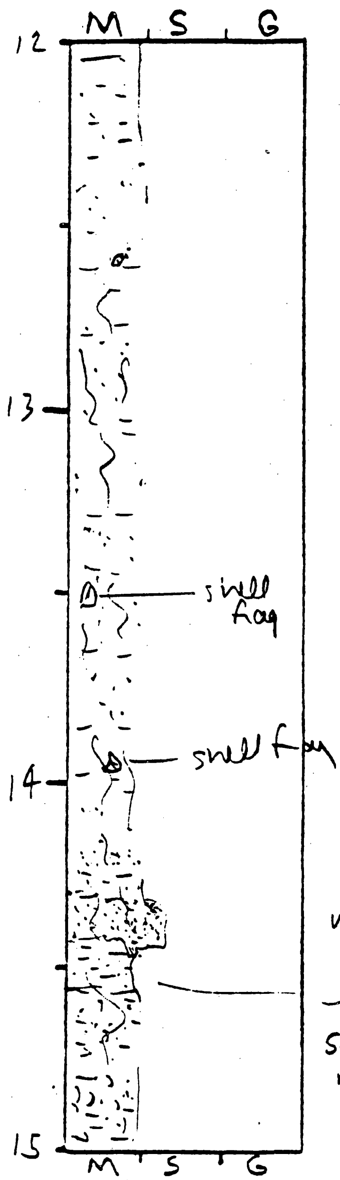	sandy mud v. scattered shell frags <1%		Olive gray (5Y 3/2)
		sand increases below ≃ 12.4'	Intensely burrowed	
		sandy mud to muddy sand		
		discrete pockets of sand in burrows		
			Intensely burrowed	
		v. fine sand horizon		
		Sandy mud		
		sandy mud to muddy sand more shell frags. ≥ 10% below 14.7' shells granule size		Olive grey (5Y 3/2)

General Comments:

CORE LOG

CORE # SBV-14F) TYPE ______ LOCATION ______
LATITUDE ______ LONGITUDE ______ SURFACE ELEVATION ______
DEPTH PENETRATED ______ LENGTH RECOVERED ______ %COMPACTION ______

OBTAINED BY ______ DATE ______
DESCRIBED BY ______ DATE ______

DEPTH (ft, m)	SKETCH	LITHOLOGY	STRUCTURE	REMARKS

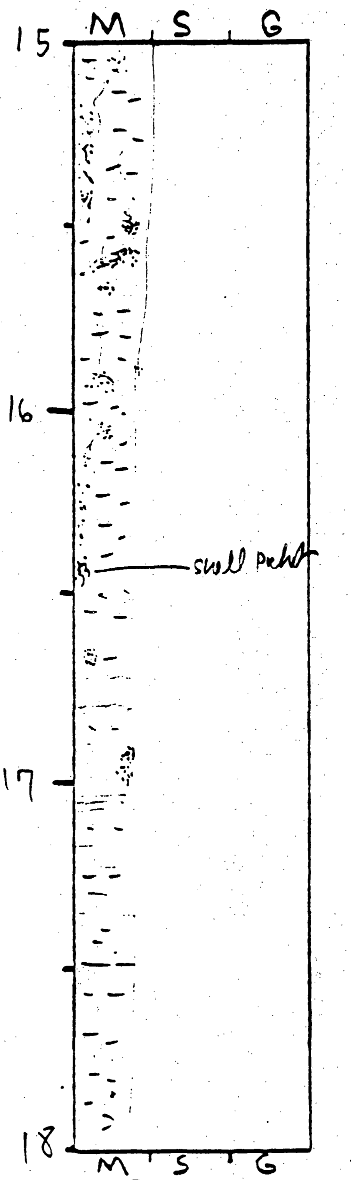

sandy mud (sand filled burrows)

Olive gray (5Y 3/2) to medium gray

discrete sand filled burrows
a few v. coarse shell frags
in sandy areas

Occasional burrows

clay

few burrows

medium gray

thin silty horizontal laminae
in clay

no burrows

medium gray

clay some organic specks

General Comments:

CORE LOG

CORE # SBV-14 (G) TYPE ________ LOCATION ________
LATITUDE ________ LONGITUDE ________ SURFACE ELEVATION ________
DEPTH PENETRATED ________ LENGTH RECOVERED ________ % COMPACTION ________

OBTAINED BY ________ DATE ________
DESCRIBED BY ________ DATE ________

DEPTH (ft, m)	SKETCH	LITHOLOGY	STRUCTURE	REMARKS
18		Clay some organic specks very scattered shell frags v coarse sand size		medium gray to olive gray

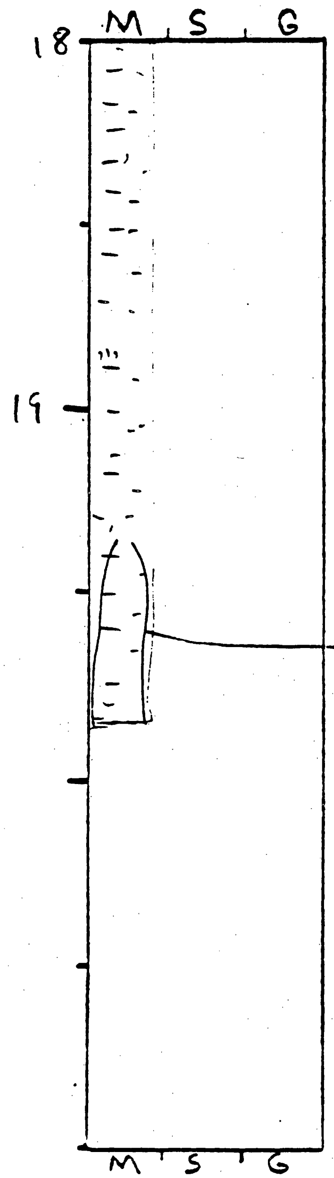

core catcher

General Comments:

CORE LOG

CORE # SBV-15(A) **TYPE** Vibracore **LOCATION** Sabine Bank
LATITUDE 29° 25.341 **LONGITUDE** 93° 44.381 **SURFACE ELEVATION** -42'
DEPTH PENETRATED ? **LENGTH RECOVERED** 5' 10 3/4" **% COMPACTION** ?

OBTAINED BY Gibeaut - R/V Kit Jones **DATE** 10-13-94
DESCRIBED BY White **DATE** 2-8-95

DEPTH (ft, m)	SKETCH	LITHOLOGY	STRUCTURE	REMARKS
0	M, S, G	muddy sand scattered shells < 5%		medium dark gray to olive gray (5Y 3/2)
1		Sand, scattered shell ≈ 5% up to granule size slightly muddy		
		clast of Beaumont clay		mottled Lt olive gray & Lt olive brn in medium gray sand
2		clayey sand v. scattered shell frags		mottled Greenish gray (5GY 6/1) to medium gray
3	M S G			

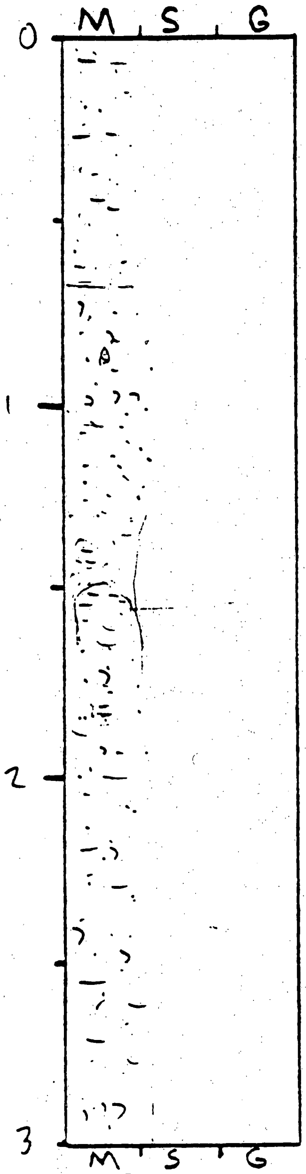

General Comments:

CORE LOG

CORE # SBV-15(B) TYPE ________ LOCATION ________
LATITUDE ________ LONGITUDE ________ SURFACE ELEVATION ________
DEPTH PENETRATED ________ LENGTH RECOVERED ________ %COMPACTION ________

OBTAINED BY ________ DATE ________
DESCRIBED BY ________ DATE ________

DEPTH (ft, m)	SKETCH	LITHOLOGY	STRUCTURE	REMARKS

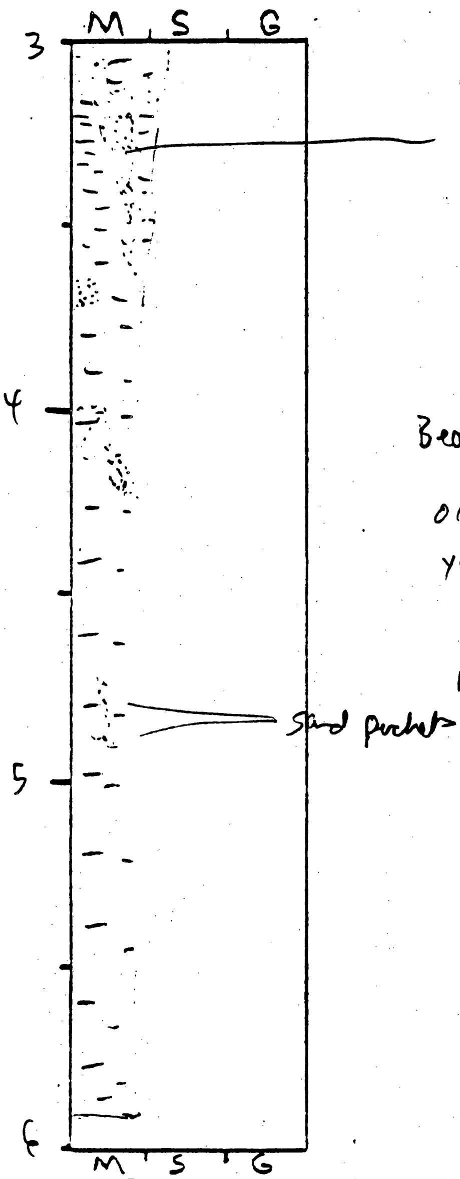

clayey sand
sand filled burrows
down into Beaumont clay

mottled greenish gray with some yellowish gray sand med grain
Beaumont clay Lt Olive brown to Drk yellowish orange

Beaumont Clay
occasional sand pocket mostly yellowish orange sand but some Lt gray sand in pockets
No shells

mottled greenish gray with oxidized sand pocket Lt brown to Drk yellow orange

Lt Olive gray with local Lt brown to Drk yellowish orange spots

General Comments:

CORE LOG

CORE # SBV-16(A) **TYPE** Vibrocore **LOCATION** Sabine Bank
LATITUDE 29° 26.13' **LONGITUDE** 93° 44.899 **SURFACE ELEVATION** -33'
DEPTH PENETRATED ? **LENGTH RECOVERED** 15' 3¾" **% COMPACTION** ?

OBTAINED BY Gibeaut - R/V Kit Jones **DATE** 10-13-94
DESCRIBED BY White **DATE** 2-8-95

DEPTH (ft, m)	SKETCH	LITHOLOGY	STRUCTURE	REMARKS

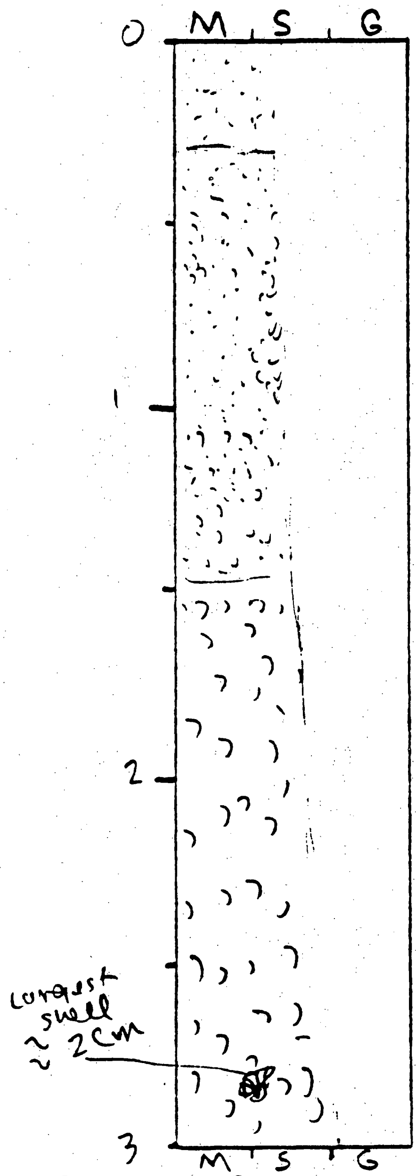

F quartz sand subrounded with ≈ 10% v. coarse sd size shell frags

Olive gray (5Y 4/1)

mixed quartz sand & v coarse to granule size shell frags.

F sd & shell (v. coarse) bimodal 25% shell

Excellent fining upward sequence

V. coarse sand (predominantly shell hash)

Noticeable increase in shell hash quantity & size at about 1.5'

Increase in size (gradual) shell grains

Dk yellowish brown to Pale yellowish brown very speckled in color

granules to pebbles size shell hash

General Comments:

CORE LOG

CORE # SB11-16 (B) TYPE______ LOCATION______
LATITUDE______ LONGITUDE______ SURFACE ELEVATION______
DEPTH PENETRATED______ LENGTH RECOVERED______ %COMPACTION______

OBTAINED BY______ DATE______
DESCRIBED BY______ DATE______

DEPTH (ft, m)	SKETCH	LITHOLOGY	STRUCTURE	REMARKS

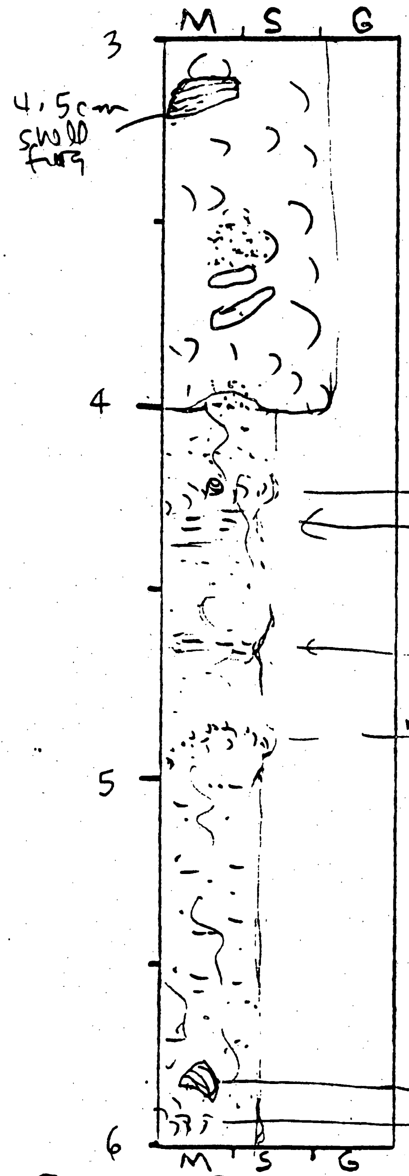

shell gravel

Brownish gray to Lt Olive gray

some sand mixing from below

slightly muddy sd.

shelly sand (granule size, some whole shells)

muddier

Olive g[illegible] to medium gray

slightly muddy sand

muddier — discrete mud "clasts"

Intensely burrowed

muddy shelly sand (granule size shells) some whole shells

muddy sand

Dinocardium (probably)

shell pocket

General Comments:

CORE LOG

CORE # SBV-16(C) TYPE________ LOCATION________
LATITUDE________ LONGITUDE________ SURFACE ELEVATION________
DEPTH PENETRATED______ LENGTH RECOVERED______ %COMPACTION____

OBTAINED BY________________________ DATE________
DESCRIBED BY________________________ DATE________

DEPTH (ft, m)	SKETCH	LITHOLOGY	STRUCTURE	REMARKS
6	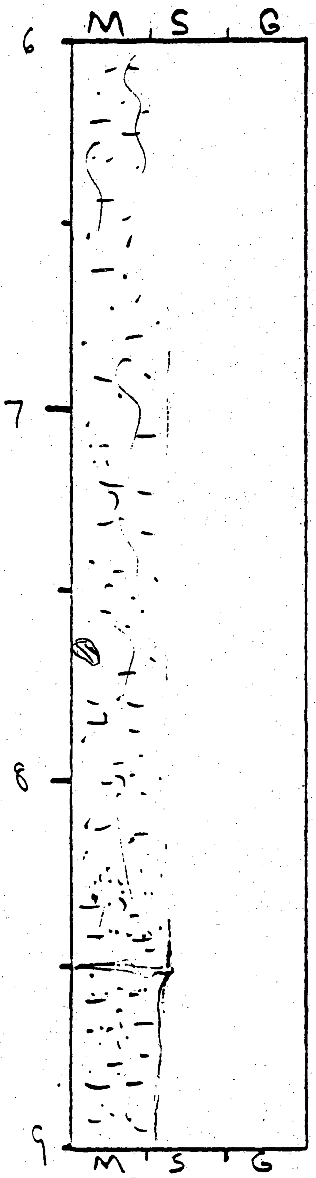	muddy sand (more mud than in previous section)	(Intensely burrowed)	
		v. scattered small shells occasional larger frag. (< 2%)		Olive gray
7		muddy sand		
		discrete mud clasts? in sand		
8				
		sandy mud		
9				

General Comments:

CORE LOG

CORE # SBV-16(D) TYPE ______ LOCATION ______
LATITUDE ______ LONGITUDE ______ SURFACE ELEVATION ______
DEPTH PENETRATED ______ LENGTH RECOVERED ______ %COMPACTION ______

OBTAINED BY ______ DATE ______
DESCRIBED BY ______ DATE ______

DEPTH (ft, m)	SKETCH	LITHOLOGY	STRUCTURE	REMARKS
9		sandy mud	intensely burrowed	Olive gray (5Y 3/2)
	shell pocket above shell	v. scattered shell frags. mostly in sand pockets		
10		Local whole shell (granule size)		Looks like Mulinia
		discrete sand pockets (filled burrows) in mud		
11				
		sandy mud		Olive gray
12				

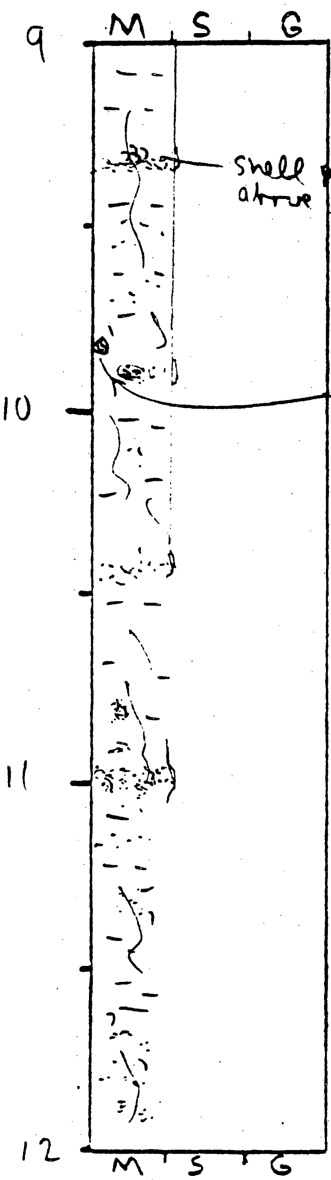

General Comments:

CORE LOG

CORE # SBV-16(E) TYPE ____ LOCATION ____
LATITUDE ____ LONGITUDE ____ SURFACE ELEVATION ____
DEPTH PENETRATED ____ LENGTH RECOVERED ____ %COMPACTION ____

OBTAINED BY ____ DATE ____
DESCRIBED BY ____ DATE ____

DEPTH (ft, m)	SKETCH	LITHOLOGY	STRUCTURE	REMARKS

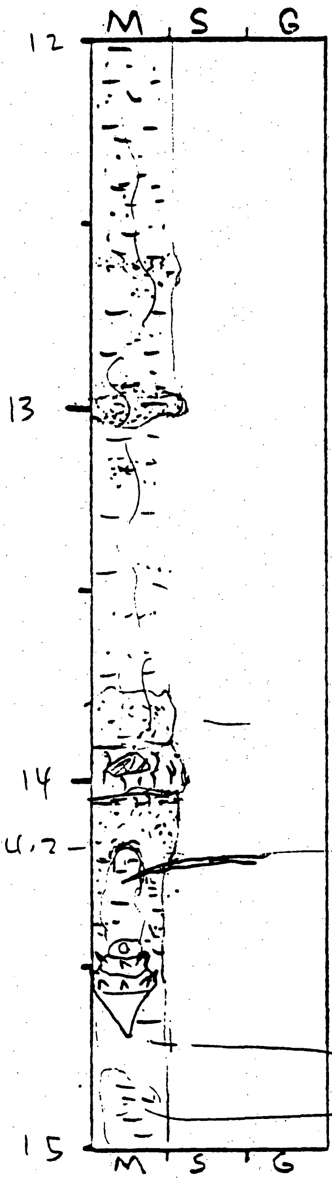

sandy mud
+ scattered shell frag.

burrowed

Olive gray

sand conc. in pockets & thin distorted layers

distorted
(thin sand layers interbedded with thin mud layers)

sandy mud

muddy sand

muddy shelly sand

muddy sand

Beaumont clay clast

clayey sand

Large Gastropod

void space from core catcher

Beaumont clay

Pale Olive with mottled dusky yellow in Beaumont clay surrounded by Olive gray muddy sd.

dusky yellow mottled in Pale Olive

General Comments:

CORE LOG

CORE # SBV-16 (F) TYPE_____ LOCATION_____
LATITUDE_____ LONGITUDE_____ SURFACE ELEVATION_____
DEPTH PENETRATED_____ LENGTH RECOVERED_____ %COMPACTION_____

OBTAINED BY_____ DATE_____
DESCRIBED BY_____ DATE_____

DEPTH (ft, m)	SKETCH	LITHOLOGY	STRUCTURE	REMARKS
15 – 15.3	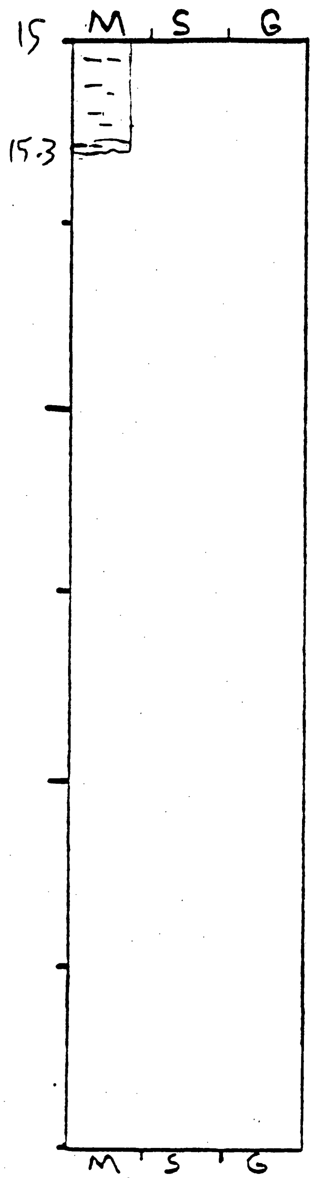	Beaumont clay		Pale Olive mottled with dusky yellow to Lt Olive brown.

General Comments:

CORE LOG

CORE # SBV-17(A) TYPE Vibracore LOCATION Sabine Bank
LATITUDE 29° 28.318 LONGITUDE 93° 45.257 SURFACE ELEVATION -23.5'
DEPTH PENETRATED ? LENGTH RECOVERED 14'7¼" % COMPACTION ?

OBTAINED BY Gibeaut - R/V Kit Jones DATE -
DESCRIBED BY White DATE 2-8-95

DEPTH (ft, m)	SKETCH	LITHOLOGY	STRUCTURE	REMARKS

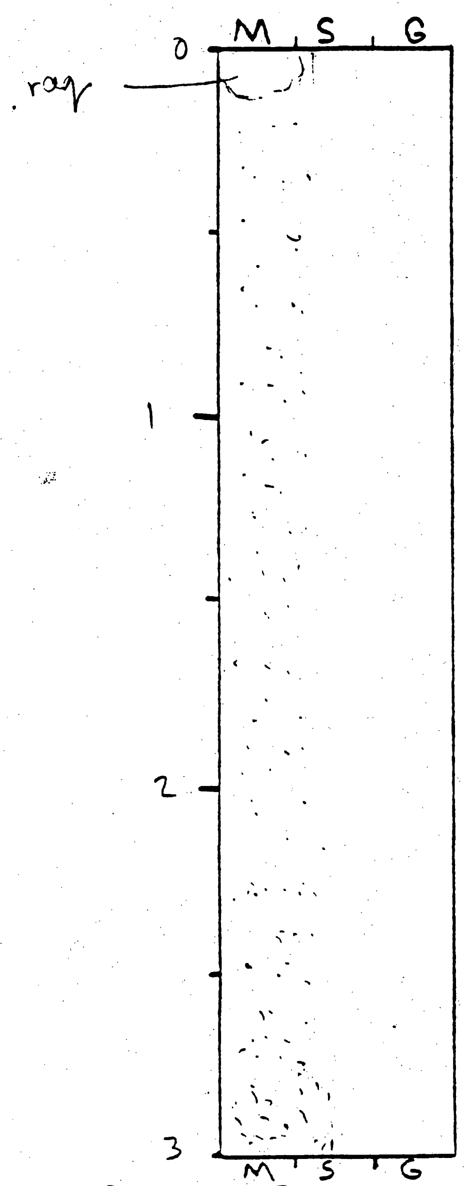

Fine quartz sand with v. coarse sand size shell frags. ≈ 10-20%. quartz sub-rounded, well sorted

Light Olive gray 5Y 5/2

Part of fining upward sequence

Lt Olive Gray 5Y 5/2

increase in shell frags near base to ≈ 20%-25%, v. coarse sd grain size bimodal with fine qtz sand

General Comments:

CORE LOG

CORE # SBV-17(B) TYPE ________ LOCATION ________________
LATITUDE ________ LONGITUDE ________ SURFACE ELEVATION ________
DEPTH PENETRATED ______ LENGTH RECOVERED ______ %COMPACTION ____

OBTAINED BY ______________________________ DATE ________
DESCRIBED BY ______________________________ DATE ________

DEPTH (ft, m)	SKETCH	LITHOLOGY	STRUCTURE	REMARKS

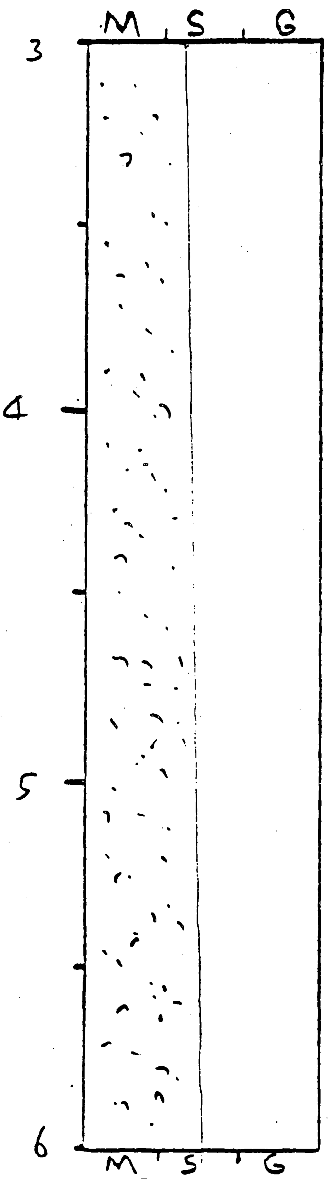

Fine (quartz) to v. coarse sand (shell)

Light Olive gray
5Y 5/2

shell fragments increase in quantity with depth
mostly v coarse sand to granule in size

Occasional pebble size shell frag.

Part of fining upward sequence

Lt Olive gray
5Y 5/2

Fine (quartz) to v. coarse sd
& granule in size (shell)
≈ 30% shells

General Comments:

CORE LOG

CORE # SBV-17(C) TYPE ______ LOCATION ______
LATITUDE ______ LONGITUDE ______ SURFACE ELEVATION ______
DEPTH PENETRATED ______ LENGTH RECOVERED ______ %COMPACTION ______

OBTAINED BY ______ DATE ______
DESCRIBED BY ______ DATE ______

DEPTH (ft, m)	SKETCH	LITHOLOGY	STRUCTURE	REMARKS

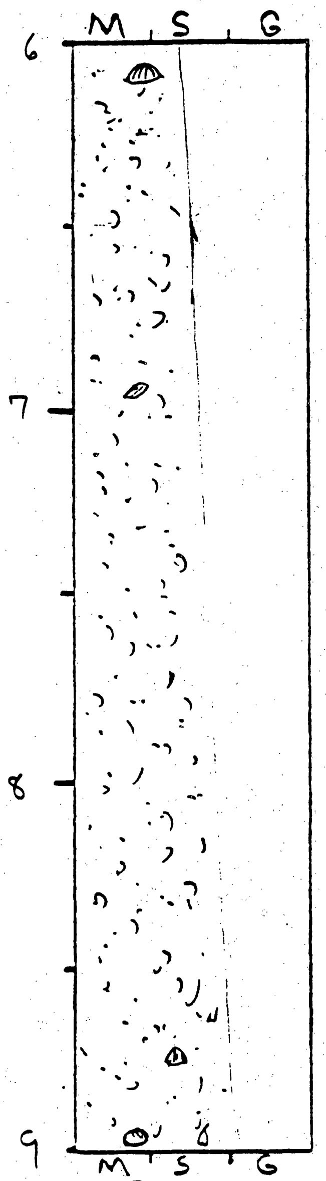

Fine quartz sand & shell frags
V coarse to granule in size
10cal pebble size shell,
Birrodal grain size

Lt Olive gray

part of
Fining upward
sequence

.. shell fragments become more abundant
& slight larger with depth

Shelly sand
≈ 40% shell fragments

Lt Olive gray

General Comments:

CORE LOG

CORE # SBV-17(D) TYPE________ LOCATION________________
LATITUDE__________ LONGITUDE__________ SURFACE ELEVATION__________
DEPTH PENETRATED______ LENGTH RECOVERED______ %COMPACTION____

OBTAINED BY______________________________ DATE__________
DESCRIBED BY______________________________ DATE__________

DEPTH (ft, m)	SKETCH	LITHOLOGY	STRUCTURE	REMARKS
9	M S G	shelly sand ≈ 50% shell		Lt olive gray to olive gray
		sand with 40% shell		
		sandy shell pocket		
10		Fine sand with ≈ 25% v. coarse to granule shell frags		Lt olive gray
		shell pocket		
11		fine quartz sand with 20-25% shells v. coarse sd to granule size.		Lt olive gray
12	M S G			

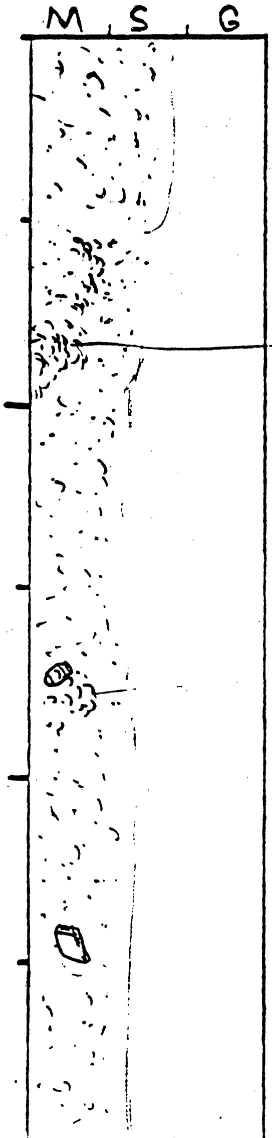

General Comments:

CORE LOG

CORE # SBV-17(E) TYPE______ LOCATION______
LATITUDE______ LONGITUDE______ SURFACE ELEVATION______
DEPTH PENETRATED______ LENGTH RECOVERED______ %COMPACTION______

OBTAINED BY______ DATE______
DESCRIBED BY______ DATE______

DEPTH (ft, m)	SKETCH	LITHOLOGY	STRUCTURE	REMARKS
12		fine sand w/ 20-75% shell frags		Lt Olive gray
		large gastropod (encrusted with worm tubes)		
		shell pocket		
13		Shelly sand zone (mixed not horizontal)		
		Fine sand (few shells)		
		Sandy shell (whole & fragments) fine sand to v coarse sd & granule size shell		
14		Fine sand scattered shells		Lt Olive gray
		core catcher		
15				

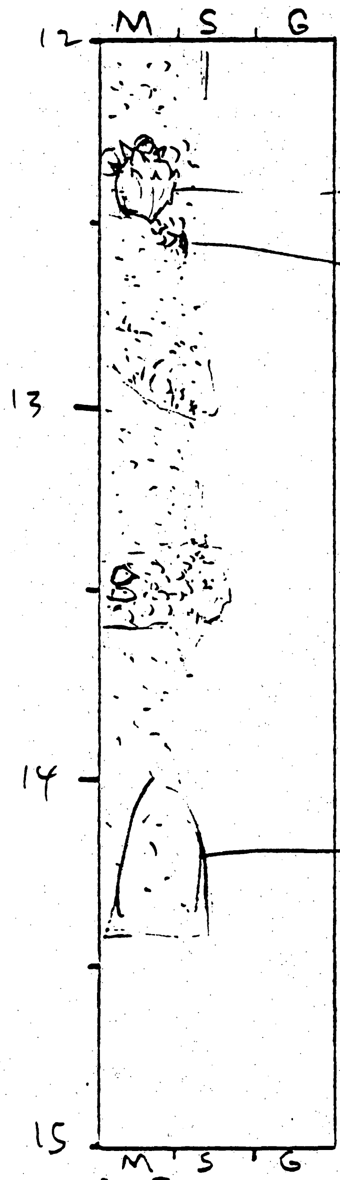

General Comments:

CORE LOG

CORE # SBV-18 (A) TYPE Vibracore LOCATION Sabine Bank
LATITUDE 29° 27.448' LONGITUDE 92° 48.413' SURFACE ELEVATION -30.5'
DEPTH PENETRATED ? LENGTH RECOVERED 10'4½' 14.4' %COMPACTION ?

OBTAINED BY Gibeaut - R/V Kit Jones DATE 10-14-94
DESCRIBED BY [illegible] DATE 2-9-95

DEPTH (ft, m)	SKETCH	LITHOLOGY	STRUCTURE	REMARKS

0 void from ragged or stuffed core

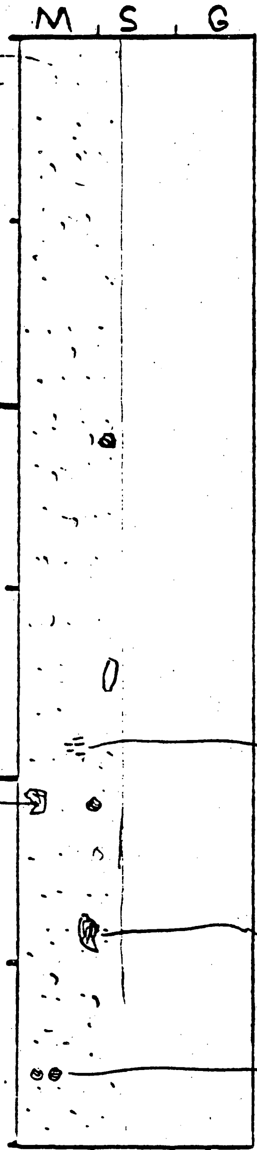

Fine sand, well sorted, sub rounded
Drk yellowish orange oxidation streaks in upper 0.4'.
scattered small shell frags (≈ 5%) very coarse sand size to granule

Lt Olive gray 5Y 5/- to Olive gray 5Y 4
yellowish gray on drying

— yellowish tint to sand in this area

1

v. scattered gravel size shell frags below 1.7'

mud clast

2 gastropod frag.

Fine sand

possibly whole Caro diana

Mulinia?

Lt Olive gray
yellowish gray on drying

3

General Comments:

CORE LOG

CORE # SBV-1? (B) TYPE ______ LOCATION ______
LATITUDE ______ LONGITUDE ______ SURFACE ELEVATION ______
DEPTH PENETRATED ______ LENGTH RECOVERED ______ %COMPACTION ______

OBTAINED BY ______ DATE ______
DESCRIBED BY ______ DATE ______

DEPTH (ft, m)	SKETCH	LITHOLOGY	STRUCTURE	REMARKS

M , S , G

3

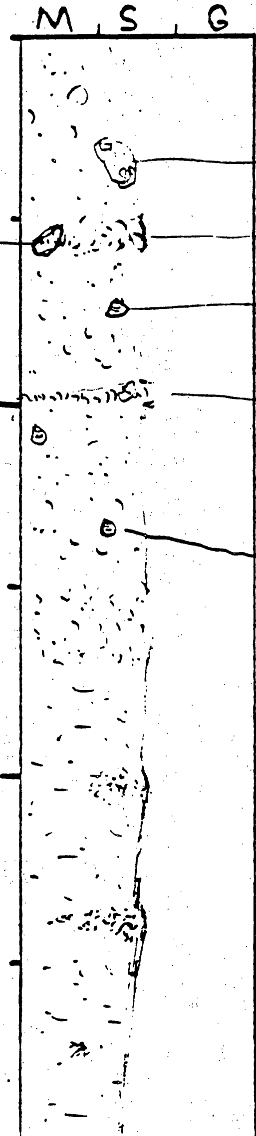

Fine sand
scattered shell frags.

lt olive gray 5Y 5/2
to olive gray 5Y 4/1

oyster shell frag (≈ 4cm)

3cm oyster shell frag

shell pocket (frags mostly v coarse sand size)

mulinia?

4

shelly sand layer (mostly v. coarse sand size one up to pebble size)

(coarsening upward
(becoming slightly muddy near base)

possibly mulinia

≈ 20% shell frag (v. coarse sand size in the area 4.5-4.7')

5

fine sand with local shell hash (coarse to v coarse sand size) pockets
slightly muddy below 4.7'

Olive gray
5Y 3/2

slightly muddy fine sand with scattered
shell frags local pockets
Mud increasing in abundance near base

6

M S G

General Comments:

CORE LOG

CORE # SBV-18(C) TYPE______ LOCATION______
LATITUDE______ LONGITUDE______ SURFACE ELEVATION______
DEPTH PENETRATED______ LENGTH RECOVERED______ % COMPACTION______

OBTAINED BY______ DATE______
DESCRIBED BY______ DATE______

DEPTH (ft, m)	SKETCH	LITHOLOGY	STRUCTURE	REMARKS
6		Fine sand, a few shells V. slightly muddy		Olive green 5Y 3/2 to 5Y 4/1
		Increase in shells 10-20%		
7		sand Mud increasing below 6.8'		
		slightly muddy sand scattered shell frags	burrows	mud increase with depth
8		very gradational contact	Intensely burrowed	
		muddy sand ... shell frags, and pockets of ... sand size shell frags discrete muddy sand zone Local granule size shell shell ≈ 10%.		& small whole shells Olive grey 5Y 3/2 (darker than near top)
9				

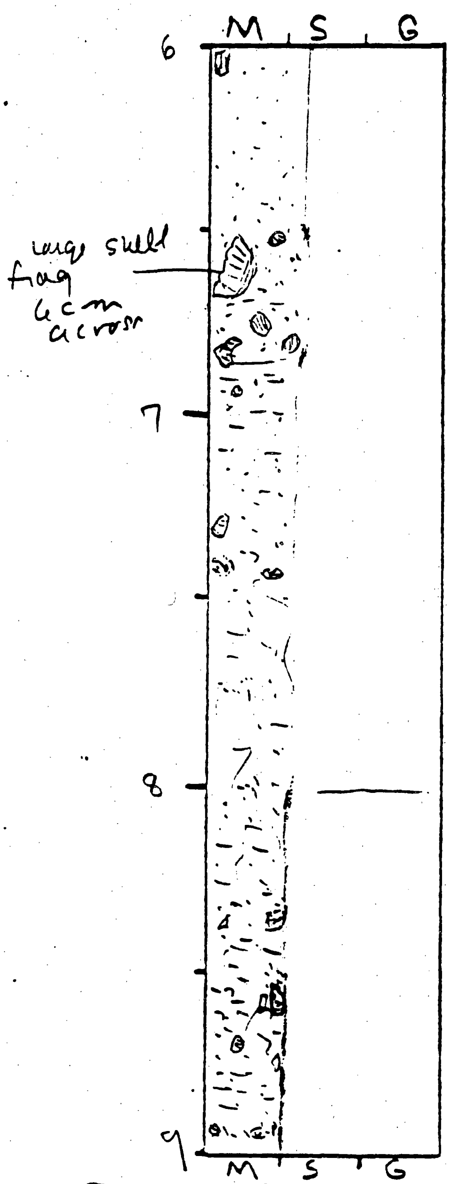

General Comments:

CORE LOG

CORE # SBV-18(D) TYPE____ LOCATION____
LATITUDE____ LONGITUDE____ SURFACE ELEVATION____
DEPTH PENETRATED____ LENGTH RECOVERED____ %COMPACTION____

OBTAINED BY____ DATE____
DESCRIBED BY____ DATE____

DEPTH (ft, m)	SKETCH	LITHOLOGY	STRUCTURE	REMARKS

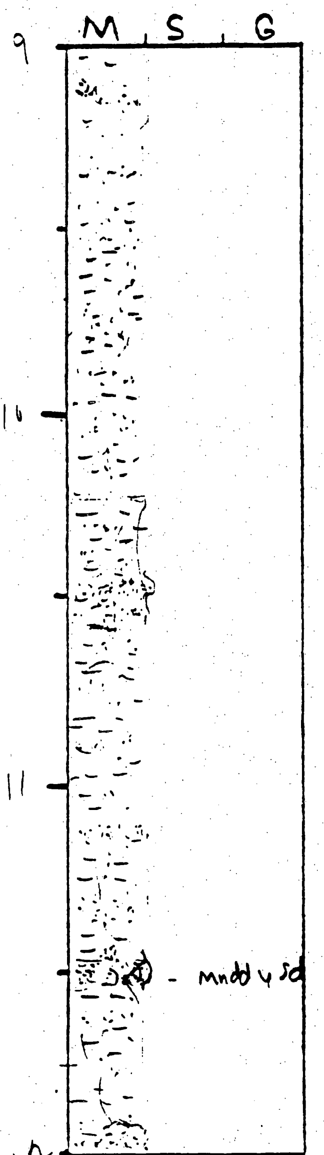

muddy sand
sand in pockets and irregular layers include v coarse sand size shell hash locally

Intensely burrowed

(5Y 3/2) Olive gray to dark gray

Distinct mud & sand zone

Color change in this core to darker gray

Mud increases with depth

sandy mud

muddy sand

Overall mud appears to become more abundant than sand below 10.2'

Intensely Burrowed

sandy mud to muddy sand
scattered small shell frags associated with sand pockets

Dark gray to Olive gray 5Y 3/2

muddy sand to sandy mud

General Comments:

CORE LOG

CORE # SBV-18 (E) TYPE ______ LOCATION ______
LATITUDE ______ LONGITUDE ______ SURFACE ELEVATION ______
DEPTH PENETRATED ______ LENGTH RECOVERED ______ %COMPACTION ______

OBTAINED BY ______ DATE ______
DESCRIBED BY ______ DATE ______

DEPTH (ft, m)	SKETCH	LITHOLOGY	STRUCTURE	REMARKS

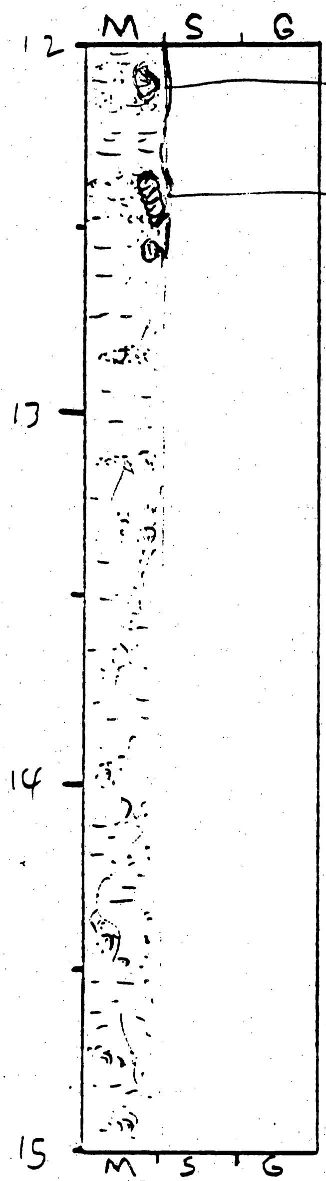

muddy sand
cardium 2.5cm

4cm (Large shell frag)

Drk gray to Olive gray 5Y 3/2

Intensely Burrowed

Sandy mud
scattered shell frags associated with sand pockets

Alternate mud & sand zones.

mud appear to be slightly more abundant than sd.

Drk gray to Olive gray 5Y 3/2

General Comments:

CORE LOG

CORE # SBV-18 F TYPE ______ LOCATION ______
LATITUDE ______ LONGITUDE ______ SURFACE ELEVATION ______
DEPTH PENETRATED ______ LENGTH RECOVERED ______ %COMPACTION ______

OBTAINED BY ______ DATE ______
DESCRIBED BY ______ DATE ______

DEPTH (ft. m)	SKETCH	LITHOLOGY	STRUCTURE	REMARKS

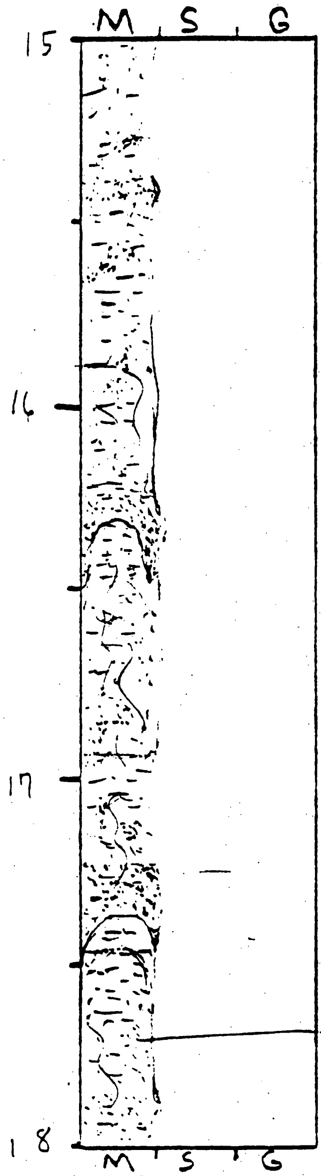

sandy mud

Dark gray to Olive gray 5Y 3/2

muddy sd — discrete sand & mud zone

scattered shell frags associated with sand pockets

sandy mud

muddy sand

disturbed sand layer (distorted by coring)

Intensely Burrowed

muddy sand to sandy mud

sandy mud — Indistinct contacts

sand to muddy sand (distorted by coring)

sandy mud

fluid (wet) sand mud to muddy sand zone

muddy sand

Olive gray 5Y 3/2

General Comments:

CORE LOG

CORE # SBV-18(G) TYPE Vibracore LOCATION Sabine Bank
LATITUDE 29° 27.642 LONGITUDE 93° 48.413 SURFACE ELEVATION -39.5'
DEPTH PENETRATED ? LENGTH RECOVERED 19'4½" %COMPACTION ?
19'4'

OBTAINED BY Gibeaut - R/V Kit Jones DATE 10-14-94
DESCRIBED BY White DATE

DEPTH (ft, m)	SKETCH	LITHOLOGY	STRUCTURE	REMARKS

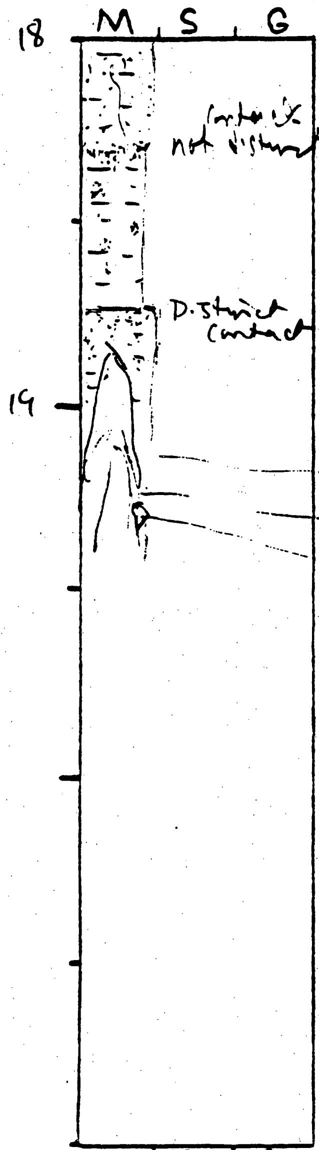

muddy sand to sandy mud (olive gray 5Y 3/2) to 5Y 4/1
w. scattered shell frags (<1%) Burrowed

Lt olive gray w shells
Clay traces of organics & silt pockets (olive gray)
Little disturbance except near top burrowed near top

muddy sand to sandy mud
Olive gray 5Y 4/1

chunks of stiffer clay in bottom core catcher

Possible organic fragments (wood) in sampling half of core

General Comments:

CORE LOG

CORE # SBV-19(A) **TYPE** Vibracore **LOCATION** Sabine Bank
LATITUDE 29° 26.411' **LONGITUDE** 93° 47.782 **SURFACE ELEVATION** -31.5'
DEPTH PENETRATED ? **LENGTH RECOVERED** 19' 4½" **% COMPACTION** ?

OBTAINED BY Gibeaut - R/V Kit Jones **DATE** 10-14-94
DESCRIBED BY White **DATE** 2-9-95

DEPTH (ft, m) | **SKETCH** | **LITHOLOGY** | **STRUCTURE** | **REMARKS**

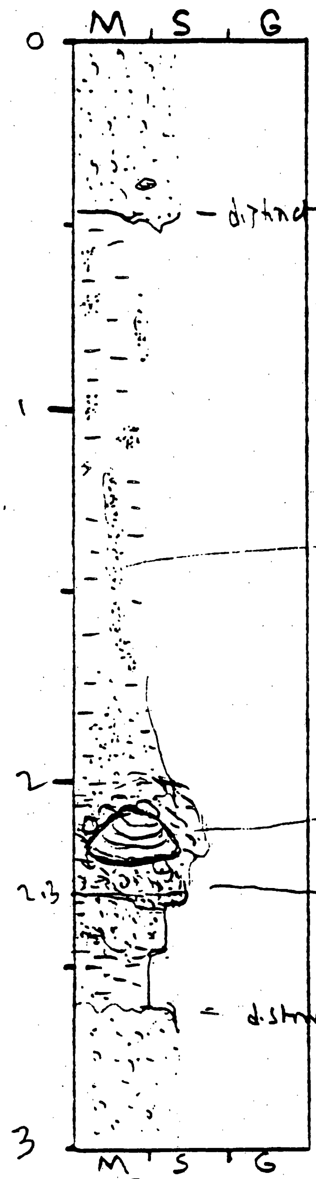

to v fine
Fine sand scattered shell shells & frags most granule to v-coarse sd size (5-10% shell frags)

Olive gray (5Y 4/1) More Brownish tint than below 2.3' which becomes grayer

- distinct contact

Sandy mud

sand filled burrow

Increase in sand possible due to burrow

Noticeable color change darker gray below shell zone

Large blk. Clam

Slightly muddy shelly sand to sandy shell very coarse sand size to granule size whole & shell frags.

muddy sand (no shell frags visible)

sandy mud (few to no shell frags)

Medium drk gray to Olive gray

= distinct but somewhat irregular contact

v fine Sand 5-10% shell frags v coarse + granule size

5Y 3/2

General Comments:

CORE LOG

CORE # SBV-19(B) TYPE ______ LOCATION ______
LATITUDE ______ LONGITUDE ______ SURFACE ELEVATION ______
DEPTH PENETRATED ______ LENGTH RECOVERED ______ %COMPACTION ______

OBTAINED BY ______ DATE ______
DESCRIBED BY ______ DATE ______

DEPTH (ft, m)	SKETCH	LITHOLOGY	STRUCTURE	REMARKS

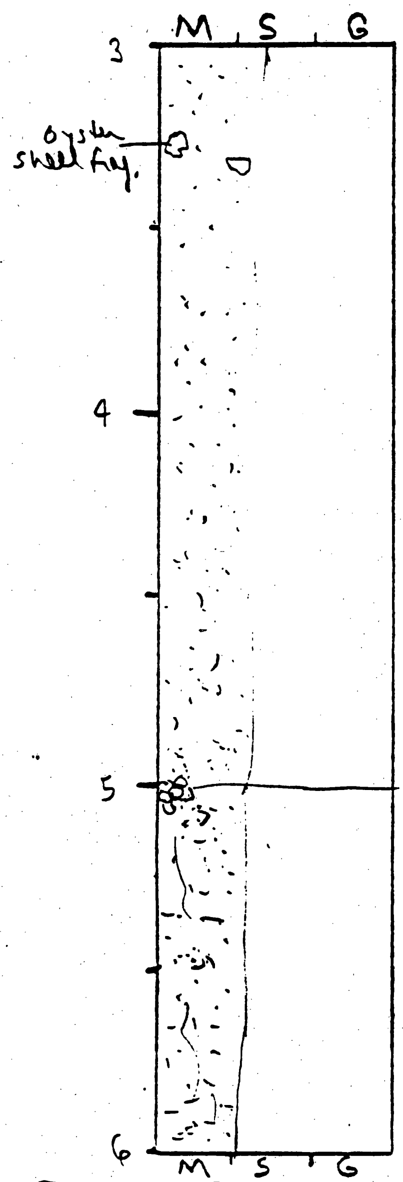

v. Fine sand slightly muddy scattered shell frags most very coarse to granule 10% mud increasing with depth

Olive gray (5Y 3/2) to med dark gray

coarsening upward in terms of decreasing mud content

shell pocket many whole shells granule to small pebbles in size
mud increase noticeable at about 5'

muddy sand
scattered shell frags
<5% shell frag
burrowed
mud increases near base

med. dark gray to Olive gray 5Y 3/2

General Comments:

CORE LOG

CORE # SBV-19 (C) TYPE____ LOCATION____
LATITUDE____ LONGITUDE____ SURFACE ELEVATION____
DEPTH PENETRATED____ LENGTH RECOVERED____ %COMPACTION____

OBTAINED BY____ DATE____
DESCRIBED BY____ DATE____

DEPTH (ft, m)	SKETCH	LITHOLOGY	STRUCTURE	REMARKS

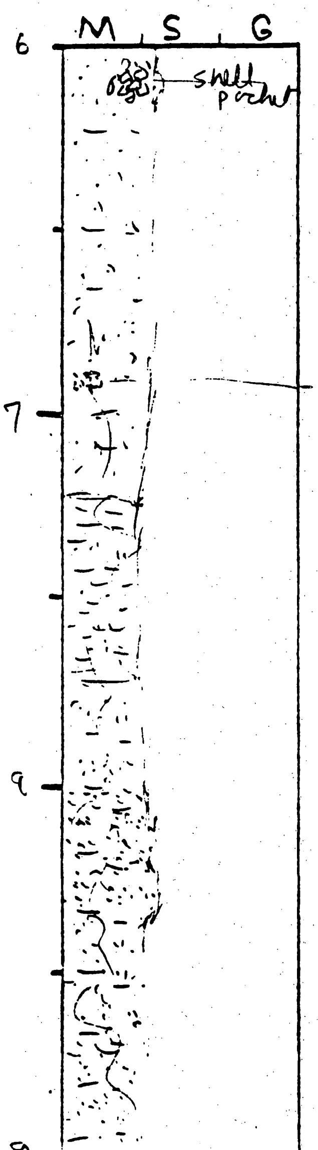

muddy sand
↓ scattered shell frags -- < 5% except in shell pockets

Olive gray 5Y 3/2 to med dark gray

shell frag pocket (v coarse sand size)

mud increase noticeable below 7.3'

wetter zone 7.3 – 7.8' Intensely burrowed
sandy mud to muddy sand

Discrete pockets of sand & mud

< 1% shell frags

Sand increase slightly below 8'
Muddy sand

Muddy sand → sandy mud

Intensely burrowed

Olive gray 5Y 3/2 to med dark gray

General Comments:

CORE LOG

CORE #SBV-19 (D) TYPE________ LOCATION________
LATITUDE________ LONGITUDE________ SURFACE ELEVATION________
DEPTH PENETRATED______ LENGTH RECOVERED______ %COMPACTION______

OBTAINED BY________________ DATE________
DESCRIBED BY________________ DATE________

DEPTH (ft, m)	SKETCH	LITHOLOGY	STRUCTURE	REMARKS
9	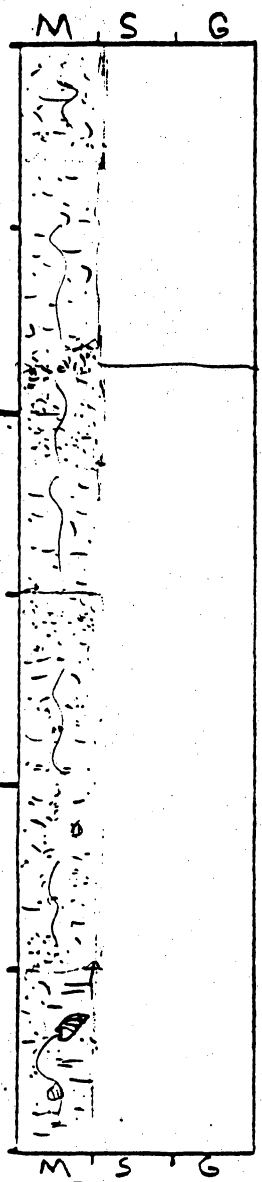	muddy sand to sandy mud ≈ 1% shell frag	Intensely burrowed	Olive gray (5Y 3/2) to med dark gray Intensely burrowed with almost equal portions of mud & sand difficult call about where sand is most abundant & mud is most abundant
		sandy mud to muddy sand		
		discrete sand & mud units churned by organisms		
		shell pocket		
10		Muddy sand to sandy mud		
		sandy mud to muddy sand		
		muddy sand to sandy mud		
11				
		sandy mud		
12				

General Comments:

CORE LOG

CORE # SBV-19 (E) TYPE________ LOCATION________________
LATITUDE__________ LONGITUDE__________ SURFACE ELEVATION________
DEPTH PENETRATED______ LENGTH RECOVERED______ %COMPACTION___

OBTAINED BY______________________________ DATE__________
DESCRIBED BY______________________________ DATE__________

DEPTH (ft, m) | SKETCH | LITHOLOGY | STRUCTURE | REMARKS

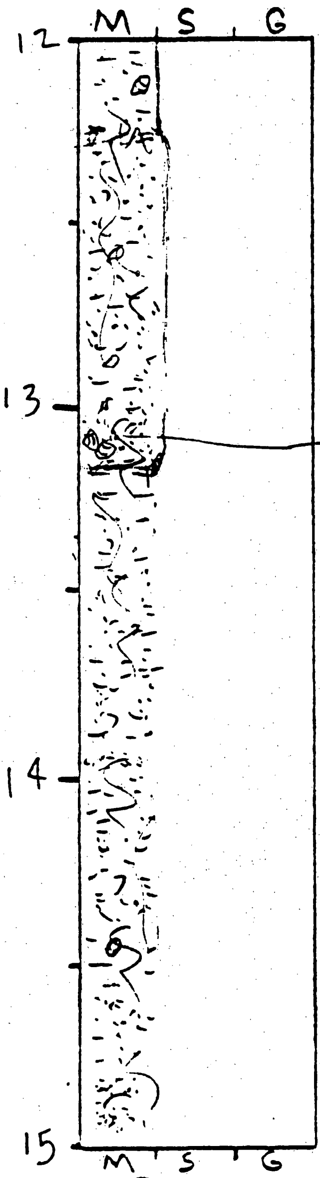

sandy mud
scattered shells - some whole and up to small pebble size

olive gray to med. dark gray

shell frags assorato with sand

≈ 1% shell frags

muddy sand to sandy mud

Intensely Burrowed

sand filled burrows

whole shells

sandy mud overall below ≈ 13.2' with local concentration of sand where it is more abundant than mud

Olive gray 5Y 3/2 to med dark gray

General Comments:

CORE LOG

CORE # SBV-19 (F) TYPE______ LOCATION______
LATITUDE______ LONGITUDE______ SURFACE ELEVATION______
DEPTH PENETRATED______ LENGTH RECOVERED______ % COMPACTION______

OBTAINED BY______ DATE______
DESCRIBED BY______ DATE______

DEPTH (ft, m)	SKETCH	LITHOLOGY	STRUCTURE	REMARKS
15		sandy mud	Intensely burrowed	Olive gray 5Y 3/2 to med dark
		muddy sand		
			shells ≈ 1% except in pockets	
	very large shell	shelly sandy mud? (shells scattered)		
16				
		sandy mud		complex intensely burrowed with sand filled burrows & pockets
		muddy sand		
	distinct contact	muddy shelly sand		
17		sandy mud	Intensely burrowed	
		muddy sand		
		muddy shelly sand		
		sandy mud		
	shell pocket	muddy sand (shells)		
		sandy mud		
18				

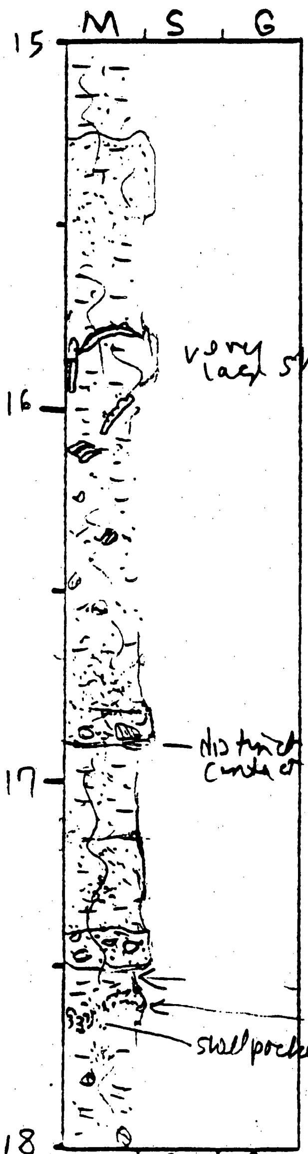

General Comments:

CORE LOG

CORE # SBV-19(G) TYPE_____ LOCATION_____
LATITUDE_____ LONGITUDE_____ SURFACE ELEVATION_____
DEPTH PENETRATED_____ LENGTH RECOVERED_____ %COMPACTION_____

OBTAINED BY_____ DATE_____
DESCRIBED BY_____ DATE_____

DEPTH (ft, m)	SKETCH	LITHOLOGY	STRUCTURE	REMARKS

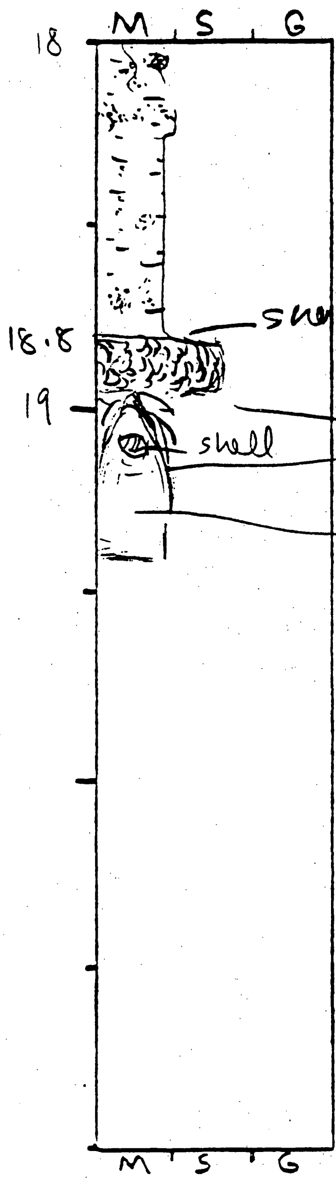

sandy mud scattered shell in sand pockets

mud or clay ; sand & silt scattered in burrows
Little burrowing compared to to above
some organics

sharp contact

Olive gray down to med-warm gray above shell zone,

muddy shell granule to small pebble size

bottom contact obscured by core catcher

core catcher

void

General Comments:

CORE LOG

CORE # SBV-201(A) **TYPE** Vibracore **LOCATION** Sabine Bank
LATITUDE 29° 25.035 **LONGITUDE** 93° 47.144 **SURFACE ELEVATION** -35.5'
DEPTH PENETRATED ? **LENGTH RECOVERED** 5'2" **%COMPACTION** ?

OBTAINED BY Gibeaut - R/V Kit Jones **DATE** 10-14-94
DESCRIBED BY White **DATE** 2-22-95

DEPTH (ft, m)	SKETCH	LITHOLOGY	STRUCTURE	REMARKS

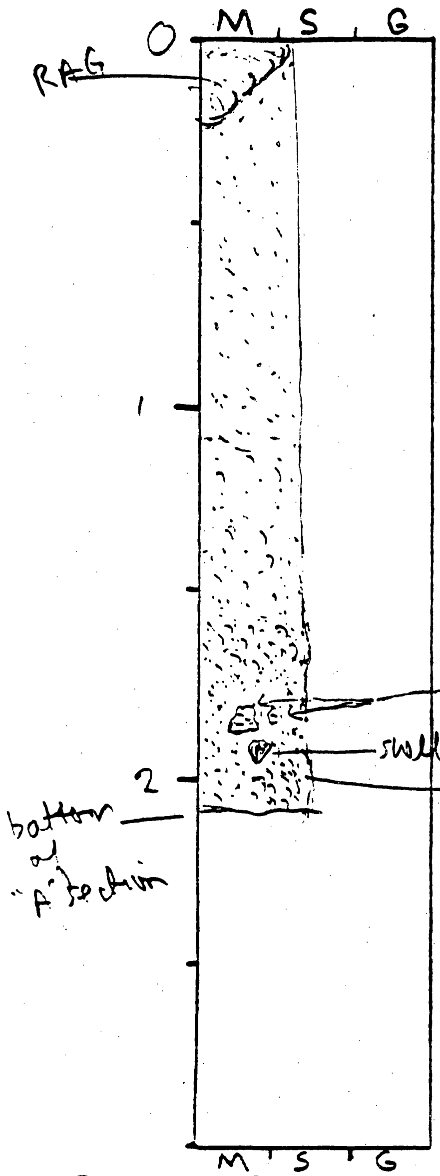

Fine quartz sand well sorted, sub rounded

Yellowish gray to Olive gray in center of core -- drys yellowish gray

Fining upward

Increase in shell frags (granule size) below about 1.1'

v. coarse to small granule size shells (30% shell frag)

fine sand with shell frags, locally concentrated in pockets

v coarse sand size to granule size

General Comments:

CORE LOG

CORE # SBV-20 (B) TYPE ________ LOCATION ____________________
LATITUDE ________ LONGITUDE ________ SURFACE ELEVATION ________
DEPTH PENETRATED ______ LENGTH RECOVERED ______ %COMPACTION ______

OBTAINED BY ______________________________ DATE ________
DESCRIBED BY ______________________________ DATE ________

DEPTH (ft, m)	SKETCH	LITHOLOGY	STRUCTURE	REMARKS

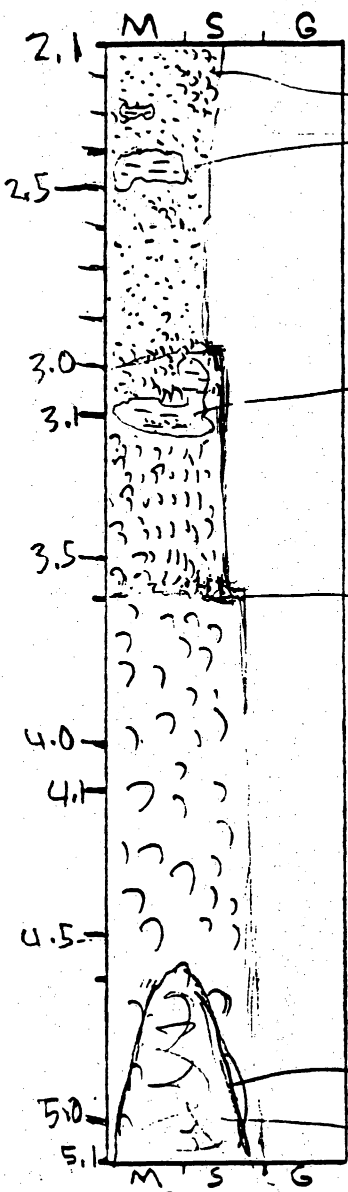

fine quartz sand with granule size shell shells concentrated in pocket
shell pocket
mud clasts (olive grey)

fine sand with increase of v. coarse to granule size shell hash near base
well sorted

yellowish gray to lt olive grey sand

mud or clay clast (Olive gray clasts)

shell hash granule size well sorted

distinct contact between granule size shell hash above & pebble size below

Relatively clean shell gravel pebble size well sorted

Drk gray to yellowish grey depending on shell colors

core catcher

Rag

General Comments:

CORE LOG

CORE # SBV-21(A) TYPE Vibrocore LOCATION Sabine Bank
LATITUDE 29° 23.800' LONGITUDE 93° 46.506' SURFACE ELEVATION -42.5'
DEPTH PENETRATED ? LENGTH RECOVERED 7'2½" %COMPACTION ?

OBTAINED BY Gibeaut - R/V Kit Jones DATE 10-14-94
DESCRIBED BY White DATE 2-22-95

DEPTH (ft, m)	SKETCH	LITHOLOGY	STRUCTURE	REMARKS
0		fine sand, scattered granule size shell frags increasing near base to 5%		Lt Olive gray (5Y 5/2)
		shelly sand, muddy near base		
		muddy sand with scattered shells		Olive gray (5Y 3/2)
		muddy shelly sand, some whole shells, small pebble size		
1		muddy shelly sand; slight decrease in shells relative to above		Olive grey
Bottom of "A" section		1.2 Large shell		

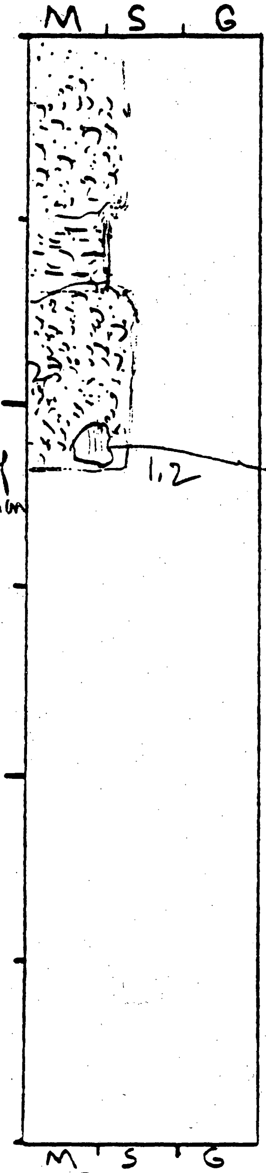

General Comments:

CORE LOG

CORE # SBV-21(B) TYPE ______ LOCATION ______
LATITUDE ______ LONGITUDE ______ SURFACE ELEVATION ______
DEPTH PENETRATED ______ LENGTH RECOVERED ______ %COMPACTION ______

OBTAINED BY ______ DATE ______
DESCRIBED BY ______ DATE ______

DEPTH (ft, m)	SKETCH	LITHOLOGY	STRUCTURE	REMARKS

M S G

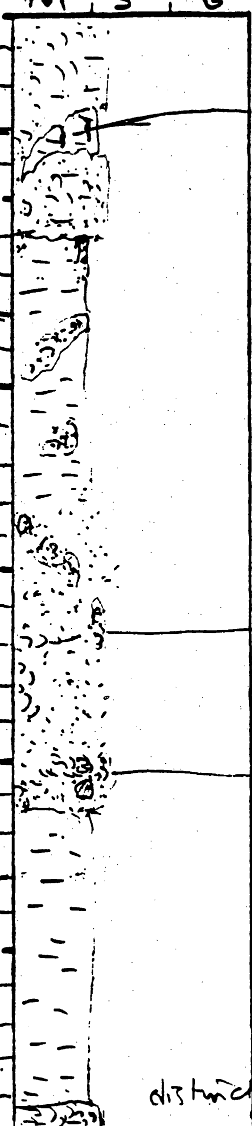

1.2' — muddy shelly sand — Olive gray 5Y 3/2

organic streaks in clay

1.5 — medium gray clay clast with organics

muddy shelly sand — Olive gray

clay, mottled color: medium gray mottled with Lt Olive gray and Dusky yellow (Dark gray organics, disseminated)

NO shells in clay except in clayey shelly sand pockets

Hint of oxidation 2.0 → possibly top of Basement

2.5

increase in sand

Clayey sand

some whole shells in pockets

Lt Olive gray (5Y 6/1) with dusky yellowish oxidation hue

3.0

shell pocket

3.5 — Lt Olive gray clay with dusky yellow layer at 3.5'

Lt Olive gray to pale Olive clay no shells (5Y 6/1 to 10Y 6/2)

4.0

distinct contact

4.2 — sdy clayey shell, granule size or sdy shelly clay

M S G

General Comments:

CORE LOG

CORE # SBV-21(C) TYPE______ LOCATION______
LATITUDE______ LONGITUDE______ SURFACE ELEVATION______
DEPTH PENETRATED______ LENGTH RECOVERED______ %COMPACTION______

OBTAINED BY______ DATE______
DESCRIBED BY______ DATE______

DEPTH (ft, m)	SKETCH	LITHOLOGY	STRUCTURE	REMARKS

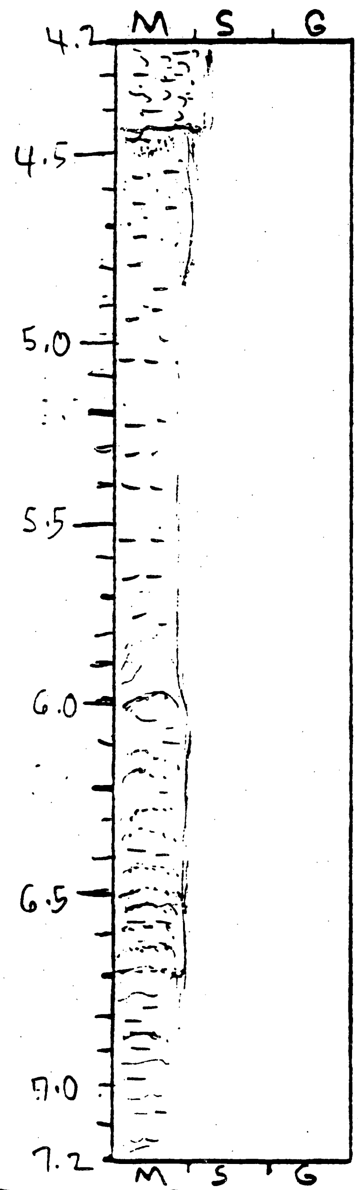

clayey sandy shell or sandy shelly clay
Lt Olive gray (5Y 6/1) to pale Olive
hint of yellowish gray, to Olive gray layers

slightly sandy or silty clay Lt Olive gray to pale Olive

mottled clay, yellowish gray with
dusky yellow mottling

Bioturbated

Lt Olive gray (Dusky yellow to dark yellowish orange)
Clay with thin Oxidized layers -- distorted by coring
horizontal sand layers (v. thin)

Lt Olive gray clay with Dusky yellow to dark yellowish orange
layers

General Comments:

CORE LOG

CORE # SBV-22 (A) **TYPE** Vibracore **LOCATION** Sabine Bank
LATITUDE 29° 25.163 **LONGITUDE** 93° 52.618 **SURFACE ELEVATION** -31.5'
DEPTH PENETRATED ? **LENGTH RECOVERED** 19' 3½" **% COMPACTION** ?

OBTAINED BY Gibeaut - R/V Kit Jones **DATE** 10-14-94
DESCRIBED BY White **DATE** 2-17-95

DEPTH (ft, m)	SKETCH	LITHOLOGY	STRUCTURE	REMARKS

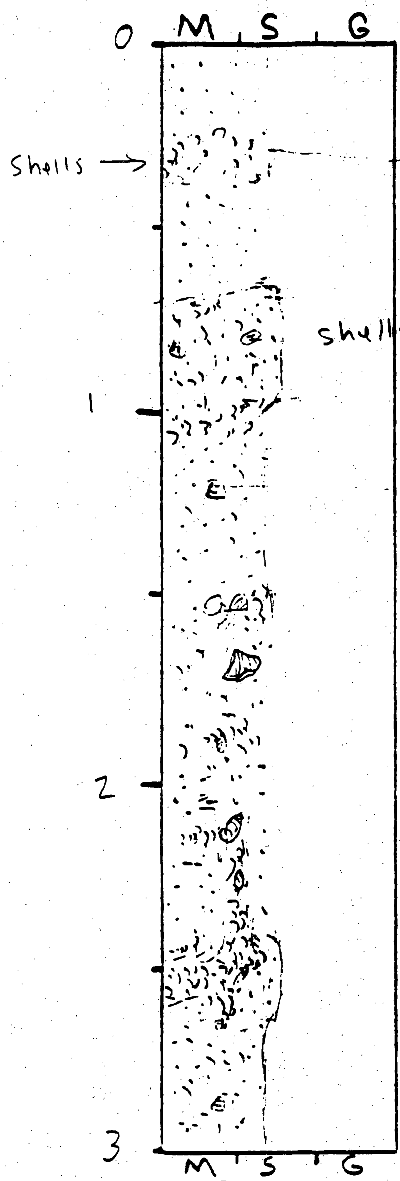

Fine quartz sand, scattered whole (granule) & shell & frags; concentrated shells locally in pockets — Olive gray 5Y 4/1

Dusky yellow in this zone (0.2 - 1') (≈ 25% granule size shells, whole & frags)

sand, shell frags ≈ 5%
— mud clast

sand, to locally shelly sand, increase in shells in pockets)

mud clasts, small, scattered

shelly sand (— shell filled burrow) to sandy shell — Olive gray 5Y 4/1 to local patch of LT olive gray

sand, scattered shell

General Comments:

CORE LOG

CORE # SBV-22(B) TYPE ______ LOCATION ______
LATITUDE ______ LONGITUDE ______ SURFACE ELEVATION ______
DEPTH PENETRATED ______ LENGTH RECOVERED ______ %COMPACTION ______

OBTAINED BY ______ DATE ______
DESCRIBED BY ______ DATE ______

DEPTH (ft, m)	SKETCH	LITHOLOGY	STRUCTURE	REMARKS

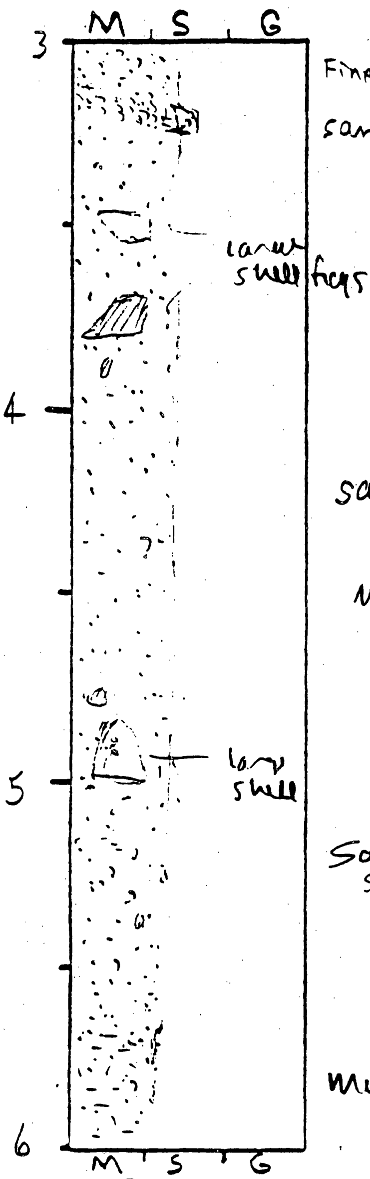

Fine quartz sand, slightly muddy, ≈ 1% shell frags, small, sandy shell, small granule size shell hash

Olive gray
5Y 3/2

sand, slightly muddy, scattered shell frag, (< 5%)

mud appears to increase with depth

Sand,
slightly muddy
scattered shell frags ≈ 5%

muddy sand, scattered shell frags
mud clasts

General Comments:

CORE LOG

CORE # SBV-22(C) TYPE________ LOCATION________
LATITUDE________ LONGITUDE________ SURFACE ELEVATION________
DEPTH PENETRATED______ LENGTH RECOVERED______ %COMPACTION____

OBTAINED BY________________ DATE________
DESCRIBED BY________________ DATE________

DEPTH (ft, m)	SKETCH	LITHOLOGY	STRUCTURE	REMARKS
6–9	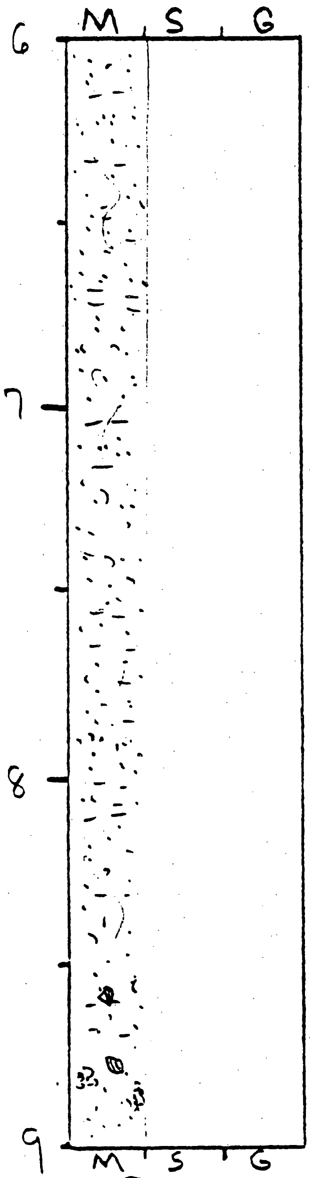	muddy sand mud clasts scattered shells, whole & frag. 5% locally 10% mostly granule in size	Burrowed	Olive gray 5Y 3/2

General Comments:

CORE LOG

CORE # SBV-22 (D) **TYPE**______ **LOCATION**______
LATITUDE______ **LONGITUDE**______ **SURFACE ELEVATION**______
DEPTH PENETRATED______ **LENGTH RECOVERED**______ **%COMPACTION**______

OBTAINED BY______ **DATE**______
DESCRIBED BY______ **DATE**______

DEPTH (ft, m)	SKETCH	LITHOLOGY	STRUCTURE	REMARKS

9

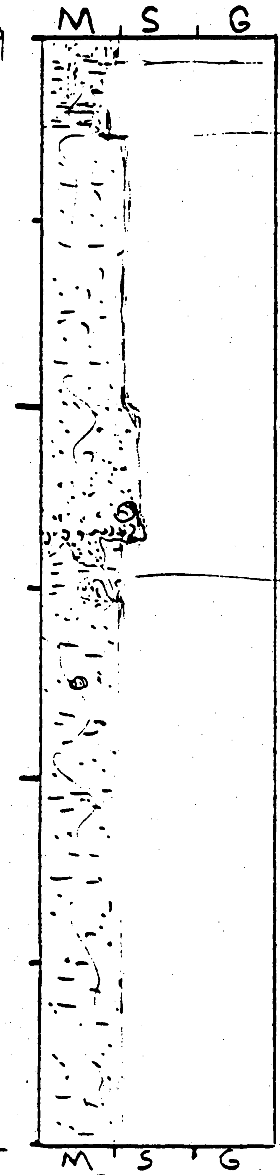

muddy sand — Burrowed

Sandy mud, shell frags associated with sd — Olive gray 5Y 3/2

muddy sand — scattered shell frags ≈ 5%

10

sand, only slightly muddy

Increase in shell frags at base of sand unit (≈ 20% shell)

mudclast — Olive gray to medium gray

very muddy sand
scattered shell frags ≈ 5%
mud clasts
burrowed

11

12

General Comments:

CORE LOG

CORE # SBV-22(E) TYPE______ LOCATION______
LATITUDE______ LONGITUDE______ SURFACE ELEVATION______
DEPTH PENETRATED______ LENGTH RECOVERED______ %COMPACTION______

OBTAINED BY______ DATE______
DESCRIBED BY______ DATE______

DEPTH (ft, m)	SKETCH	LITHOLOGY	STRUCTURE	REMARKS
12		v muddy sand		
		sandy mud	Intensely burrowed	Olive grey 5Y 3/2
12.4		sand, with thin shell hash lens (pocket)		
12.6		distinct but burrowed contact		
		Sandy mud to very muddy sand		
13		scattered small shell frags associated with sand		Intensely Burrowed
		Muddy sand to sandy mud		
14				
15		Sandy mud to muddy sand		

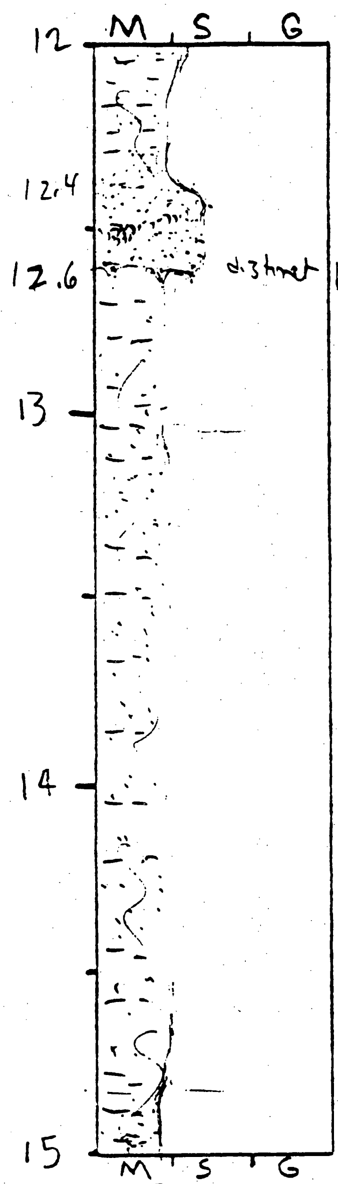

General Comments:

CORE LOG

CORE # SBV-22(F) TYPE ______ LOCATION ______
LATITUDE ______ LONGITUDE ______ SURFACE ELEVATION ______
DEPTH PENETRATED ______ LENGTH RECOVERED ______ %COMPACTION ______

OBTAINED BY ______ DATE ______
DESCRIBED BY ______ DATE ______

DEPTH (ft, m)	SKETCH	LITHOLOGY	STRUCTURE	REMARKS
15	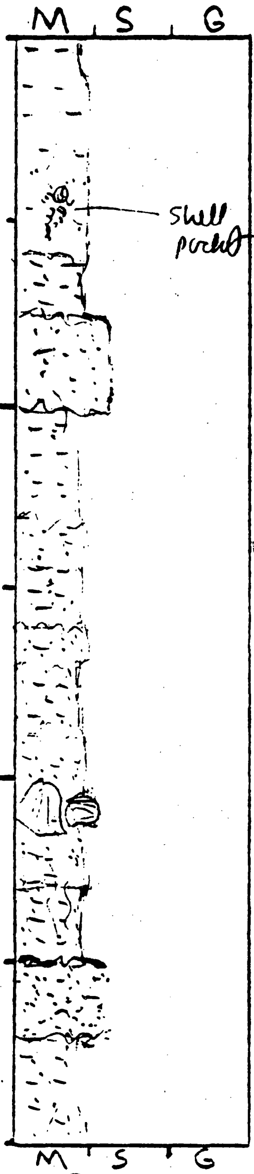	sandy mud to muddy sand		Olive gray 5Y 3/2 to Olive gray 5Y 4/1
		muddy sand	Intensely burrowed	
		sandy mud		
		sand, slightly muddy		
16		sandy mud	Discrete mud & sand	
		v. muddy sand		
		sandy mud		
		v. muddy sand		
		sandy mud		
17		2 large shells / muddy sand with shells		
		sandy mud		
		sand slightly muddy		
18		sandy mud		

General Comments:

CORE LOG

CORE # BBV-22(G) TYPE____ LOCATION____
LATITUDE____ LONGITUDE____ SURFACE ELEVATION____
DEPTH PENETRATED____ LENGTH RECOVERED____ %COMPACTION____

OBTAINED BY____ DATE____
DESCRIBED BY____ DATE____

DEPTH (ft, m)	SKETCH	LITHOLOGY	STRUCTURE	REMARKS
18		v. muddy sand scattered shells (3%)	Intensely burrowed	muddy Olive grey 5Y 3/2
		Sandy mud discrete sand & mud areas		
		muddy sand		
19		core catcher		
		void		

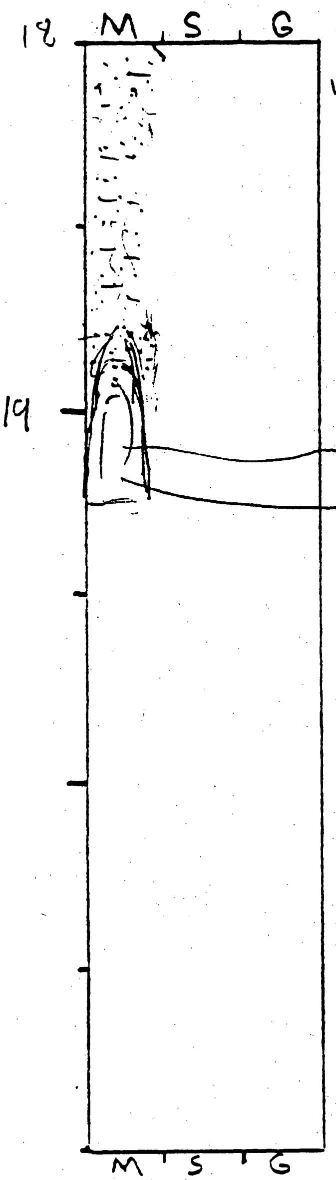

General Comments:

CORE LOG

CORE # SBV-23(A) **TYPE** Vibracore **LOCATION** Sabine Bank
LATITUDE 29° 24.610 **LONGITUDE** 93° 54.69 **SURFACE ELEVATION** -32'
DEPTH PENETRATED ? **LENGTH RECOVERED** 2' 11½" **%COMPACTION** ?

OBTAINED BY Gibeaut - R/V Kit Jones **DATE** 10-14-94
DESCRIBED BY JJ.. **DATE**

DEPTH (ft, m)	SKETCH	LITHOLOGY	STRUCTURE	REMARKS
0	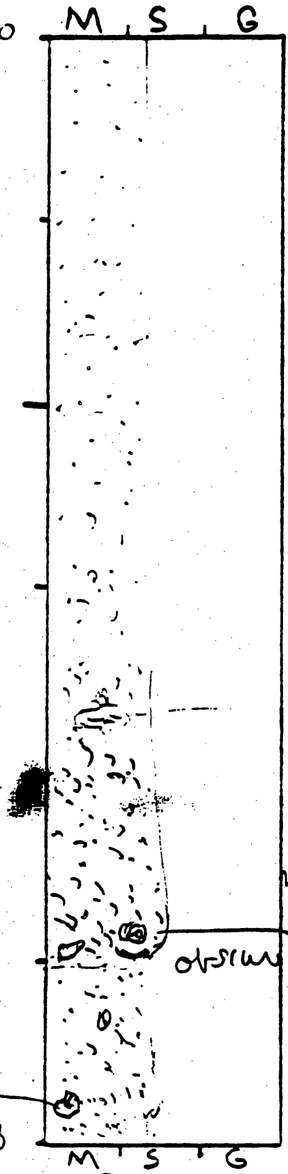	Fine Quartz sand, scattered small (v crse sd size) shell frags		yellowish gray
		Fining upward sequence		
1		shell frags increase with depth		Lt Olive gray to 5Y 5/2 to Olive gray 5Y4/1
		— mud clast (Olive gray)		
2		shelly sand, shell frags ≈ 30% to locally 50% most granule in size, some pebble size		
		whole gastropod > 0.1' long -- perfectly preserved; obscure contact		
		sand -- mixture of fine quartz to v crse shell frags. 20% shell frags		
3	larger shell			

General Comments:

CORE LOG

CORE # SBV-23 (B) TYPE ______ LOCATION ______
LATITUDE ______ LONGITUDE ______ SURFACE ELEVATION ______
DEPTH PENETRATED ______ LENGTH RECOVERED ______ %COMPACTION ______

OBTAINED BY ______ DATE ______
DESCRIBED BY ______ DATE ______

DEPTH (ft, m)	SKETCH	LITHOLOGY	STRUCTURE	REMARKS

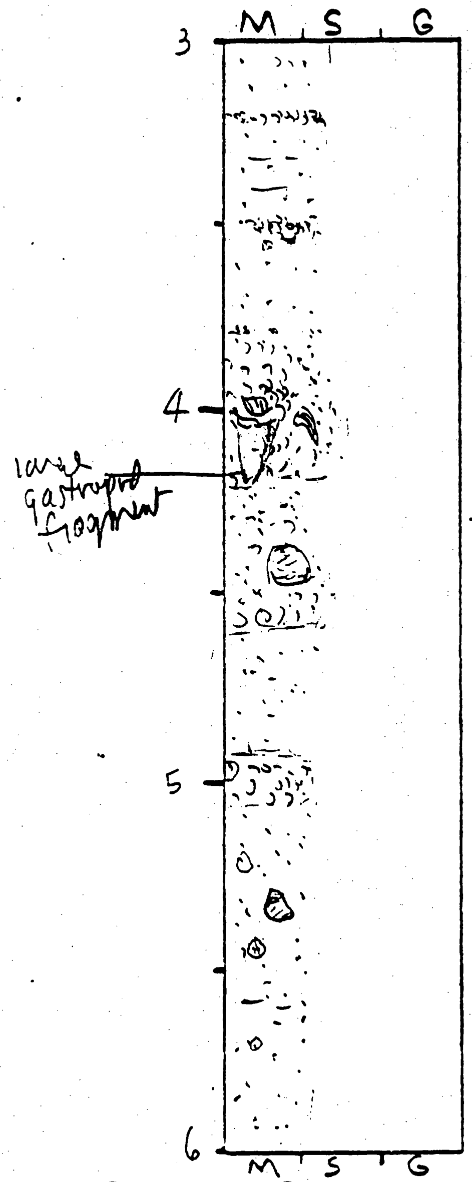

fine sand scattered v. crse & granule size shell frags -- concentrated locally

yellowish gray to Lt Olive gray sand

slightly muddy sand Olive gray 5Y 3/2

slightly muddy shelly sand

sand

shelly sd

slightly muddy sand

muddy shelly sd

mud v. coarse sig with depth

muddy sand
small mud clasts
scattered shells (< 5%)

Olive gray 5Y 3/2

General Comments:

CORE LOG

CORE # SRV-23(c) TYPE ______ LOCATION ______
LATITUDE ______ LONGITUDE ______ SURFACE ELEVATION ______
DEPTH PENETRATED ______ LENGTH RECOVERED ______ %COMPACTION ______

OBTAINED BY ______ DATE ______
DESCRIBED BY ______ DATE ______

DEPTH (ft, m)	SKETCH	LITHOLOGY	STRUCTURE	REMARKS
6		muddy sand scattered shells & frags ~10% shell frags		Olive gray 5Y 3/2
7	mud clast			
		discrete mud clasts mud appears to be increasing with depth		
8				
9				

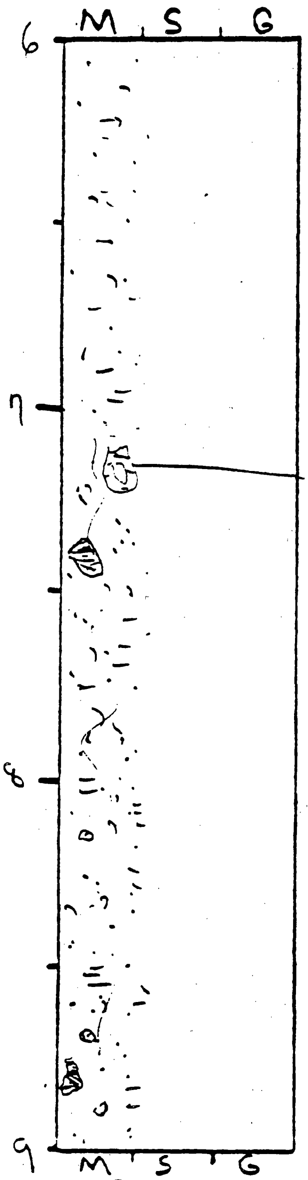

General Comments:

CORE LOG

CORE # SCV-23(D) TYPE ______ LOCATION ______
LATITUDE ______ LONGITUDE ______ SURFACE ELEVATION ______
DEPTH PENETRATED ______ LENGTH RECOVERED ______ %COMPACTION ______

OBTAINED BY ______ DATE ______
DESCRIBED BY ______ DATE ______

DEPTH (ft, m)	SKETCH	LITHOLOGY	STRUCTURE	REMARKS

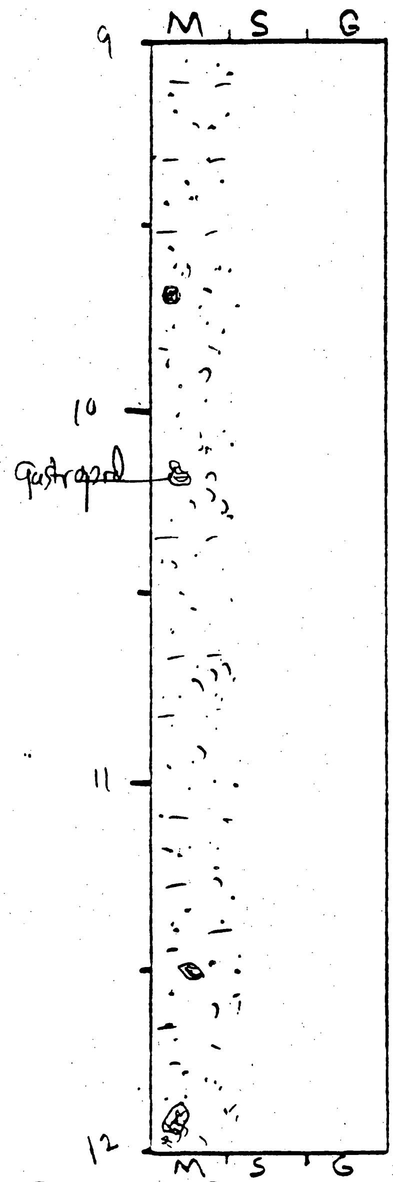

muddy sand
scattered small shell & frags
granule to small pebbles
≤ 10%

probably burrowed

discrete clay clasts

Olive gray
5Y 3/2

General Comments:

CORE LOG

CORE # SBV-23(E) TYPE______ LOCATION______
LATITUDE______ LONGITUDE______ SURFACE ELEVATION______
DEPTH PENETRATED______ LENGTH RECOVERED______ %COMPACTION______

OBTAINED BY______ DATE______
DESCRIBED BY______ DATE______

DEPTH (ft, m)	SKETCH	LITHOLOGY	STRUCTURE	REMARKS

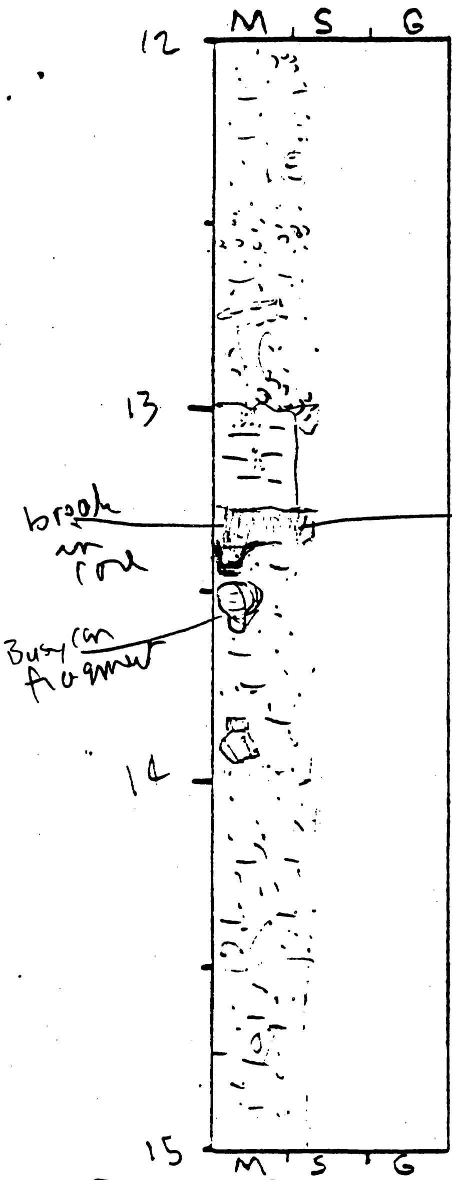

muddy sand — Olive grey 5Y 3/2

scattered shell frags
arenaceous forams
increase in pockets

[illegible] clay clasts

Burrowed

Clay, olive grey to med. gray (or mud, sand or silt locally)

void space (0.1' wide)

muddy sand

slightly muddy sand

Burrowed

muddy sand

General Comments:

CORE LOG

CORE # SBV-73(F) TYPE ______ LOCATION ______
LATITUDE ______ LONGITUDE ______ SURFACE ELEVATION ______
DEPTH PENETRATED ______ LENGTH RECOVERED ______ % COMPACTION ______

OBTAINED BY ______ DATE ______
DESCRIBED BY ______ DATE ______

DEPTH (ft, m)	SKETCH	LITHOLOGY	STRUCTURE	REMARKS

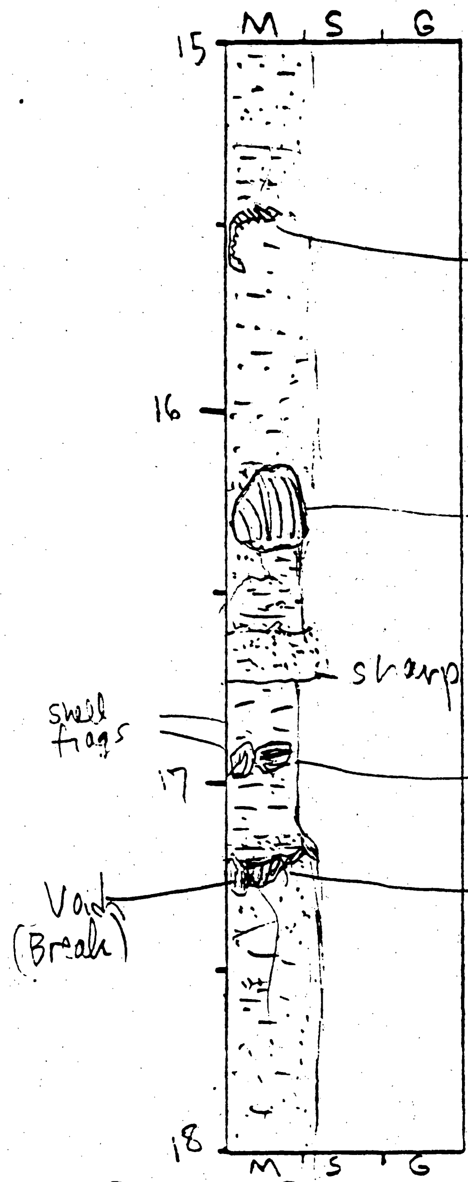

muddy sand (few v. small shell frags) — Olive gray 5Y 3/2

Burrowed

sandy mud

Large Dinocardium? shell frag

muddy sand

large Dinocardium shell frag — may have been displaced

sandy mud — burrowed

sharp contact

mud

shell frags in mud may have been moved during splitting

* This may be the area from which the shell fragments above at 16.25 & 16.9' came

muddy sand

General Comments:

CORE LOG

CORE # SBV-23(G) TYPE______ LOCATION______

LATITUDE______ LONGITUDE______ SURFACE ELEVATION______

DEPTH PENETRATED______ LENGTH RECOVERED______ %COMPACTION______

OBTAINED BY______ DATE______

DESCRIBED BY______ DATE______

DEPTH (ft, m)	SKETCH	LITHOLOGY	STRUCTURE	REMARKS
18		muddy sand	burrowed	Olive gray 5Y 3/2

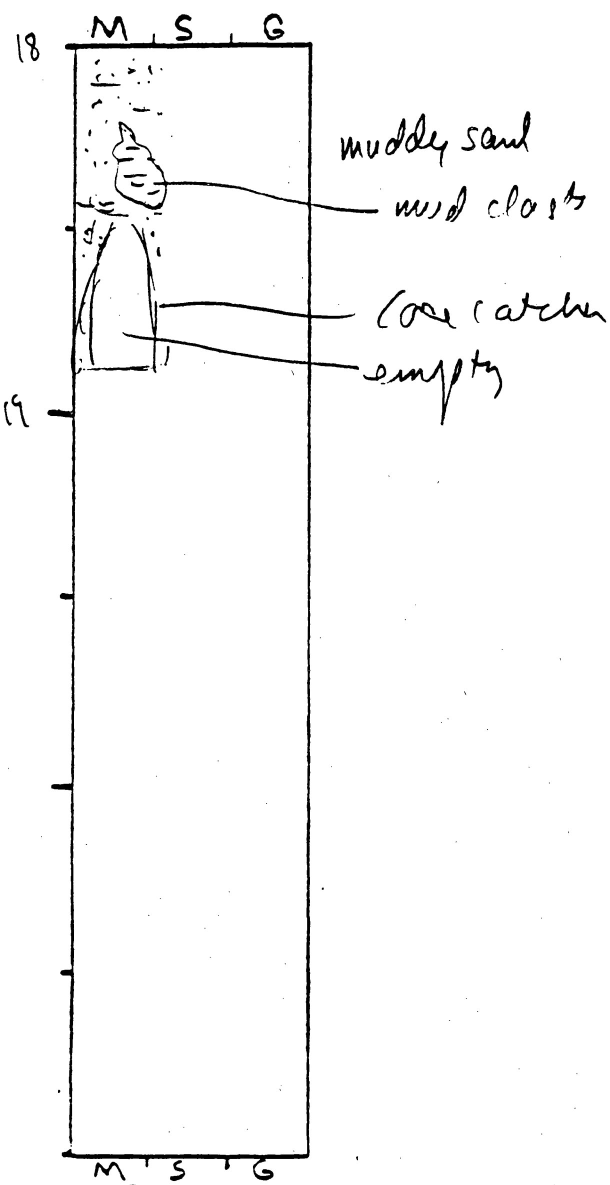

General Comments:

CORE LOG

CORE # SBV-24(A) **TYPE** Vibracore **LOCATION** Sabine Bank
LATITUDE 29° 23.378' **LONGITUDE** 93° 58.237' **SURFACE ELEVATION** -35'
DEPTH PENETRATED ? **LENGTH RECOVERED** 20' **%COMPACTION** ?

OBTAINED BY Gibeaut - R/V Kit Jones **DATE** 10-14-94
DESCRIBED BY White **DATE**

DEPTH (ft, m)	SKETCH	LITHOLOGY	STRUCTURE	REMARKS

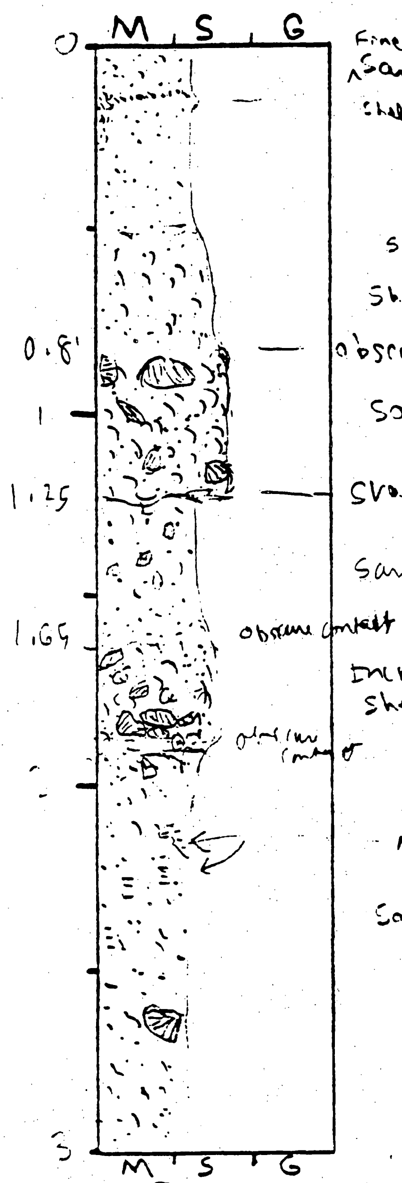

Fine to v fine Sand 95% quartz 5% shell frags (v coarse snd size) shell frags granule in size — Olive grey 5Y 4/1

Shells (whole & fragments increase below 0.5')
Shelly Sand

obscure contact

Sandy shell (granule to pebble size shell)

Sharp contact

Sand scattered shells (whole & frags) 5-10% shell

Increase in shells (whole & frags) granule to pebble size
Shelly Sand

mud clasts

Sand, slightly muddy ≈ 5% shell fragments (most small granule ...)

General Comments:

CORE LOG

CORE # 334-24(B) TYPE ______ LOCATION ______
LATITUDE ______ LONGITUDE ______ SURFACE ELEVATION ______
DEPTH PENETRATED ______ LENGTH RECOVERED ______ %COMPACTION ______

OBTAINED BY ______ DATE ______
DESCRIBED BY ______ DATE ______

DEPTH (ft, m)	SKETCH	LITHOLOGY	STRUCTURE	REMARKS

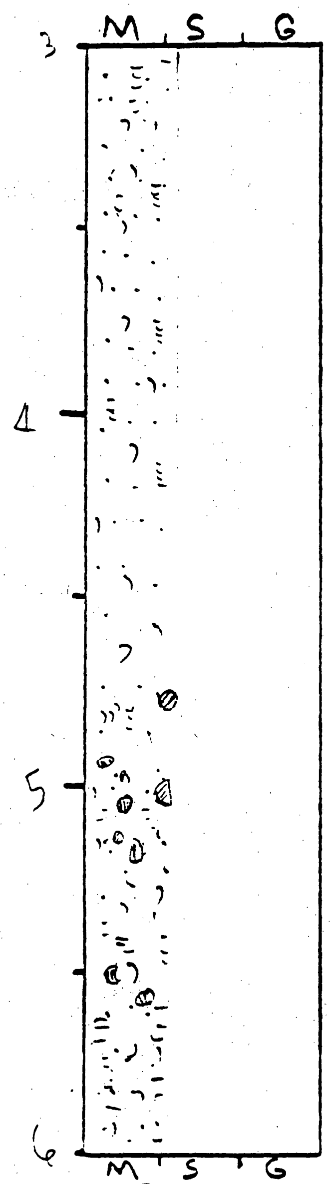

Sand, slightly muddy (scattered small mud clasts) Olive gray 5Y 4/1 to 5
scattered shell, whole & frags, mostly granule in size

≈ 10% shell fragments

Appears to be slight increase of mud with depth.

Much of this section could probably be called Muddy Sand

scattered mud clasts

shells more abundant in this section ≈ 20%

Mud more prominent than above

General Comments:

CORE LOG

CORE # SBY-2A(C) TYPE ______ LOCATION ______
LATITUDE ______ LONGITUDE ______ SURFACE ELEVATION ______
DEPTH PENETRATED ______ LENGTH RECOVERED ______ %COMPACTION ______

OBTAINED BY ______ DATE ______
DESCRIBED BY ______ DATE ______

DEPTH (ft, m)	SKETCH	LITHOLOGY	STRUCTURE	REMARKS

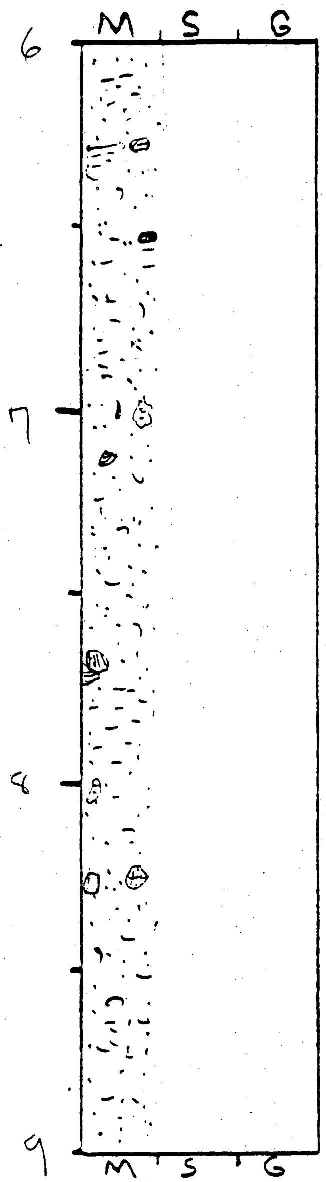

muddy sand (mud clasts larger than in above section)

Olive gray 5Y 3/2

scattered shell frags and whole shell, granule to small pebble in size ≈ 10-15%

larger mud clasts

General Comments:

CORE LOG

CORE # SBV-24(D) TYPE ______ LOCATION ______
LATITUDE ______ LONGITUDE ______ SURFACE ELEVATION ______
DEPTH PENETRATED ______ LENGTH RECOVERED ______ %COMPACTION ______

OBTAINED BY ______ DATE ______
DESCRIBED BY ______ DATE ______

DEPTH (ft, m)	SKETCH	LITHOLOGY	STRUCTURE	REMARKS

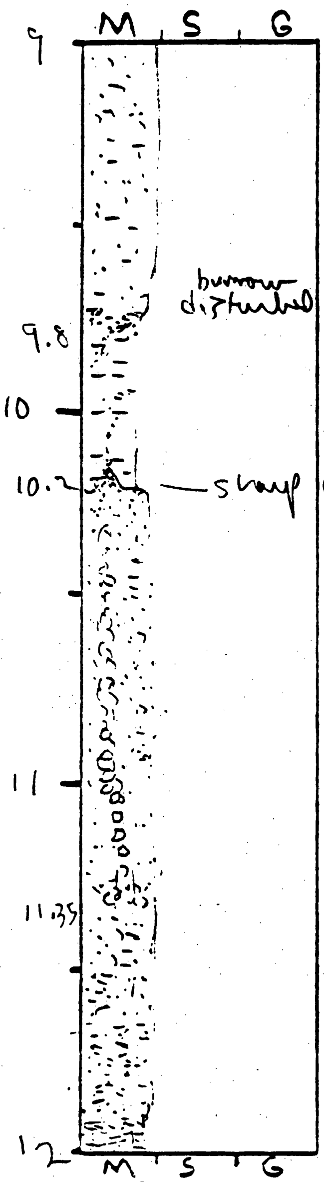

muddy sand, scattered small shell frags ~5%, discreet mud clasts — 5Y 3/2 Olive gray to med dark gray

contact

Clay or mud, sand in pockets, only one shell frag. — Clay medium gray to medium L gray

contact

muddy shelly sand, Numerous whole mulinia shells < 1cm in size apparently in burrow extending from about 10.3' to 11.35

shelly component ...

muddy sand
mud more abundant than above in this section, few shells frag
muddy sand to sandy mud — Olive Gray 5Y 3/2 to med dark gray

General Comments:

CORE LOG

CORE # SBV-24(E) TYPE ________ LOCATION ________
LATITUDE ________ LONGITUDE ________ SURFACE ELEVATION ________
DEPTH PENETRATED ______ LENGTH RECOVERED ______ %COMPACTION ____

OBTAINED BY ________________________ DATE ________
DESCRIBED BY ________________________ DATE ________

DEPTH (ft, m) | SKETCH | LITHOLOGY | STRUCTURE | REMARKS

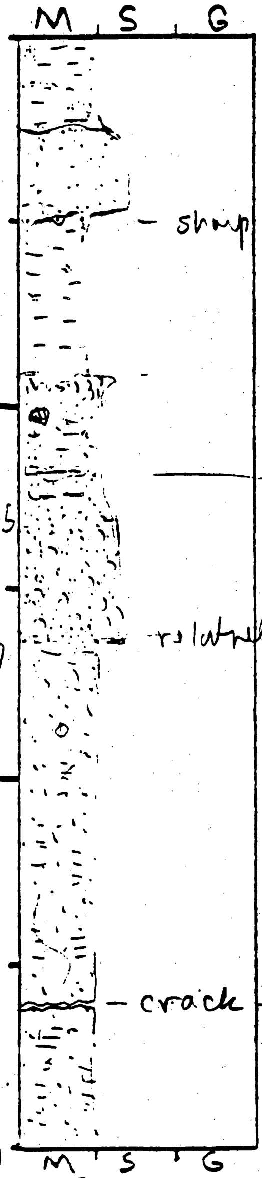

12 — sandy mud or clay, no shell, — mod gray to mod Lt gray

sand, few scattered shell frags. (≈1%) — Olive gray sd (5Y4/1)

— sharp lithologic contact although burrowed

clay or mud (less homogeneous), sand in small burrows only — mod to mod Lt gray clay

sandy shell horizon, small shell frags, granule

13 — muddy sand

— mud clasts, v. few shell frags (<1%)

13.35

sand, shell frags 10-20% — Olive gr sand (5Y 4/1)

13.7 — relatively sharp contact

14

Muddy sand, very scattered shell frags

abundant mud clasts — burrowed

— crack in core

Olive gray 5Y 3/2 to mod drk gray

15

General Comments:

CORE LOG

CORE # SBV-24F TYPE ________ LOCATION ____________
LATITUDE ________ LONGITUDE ________ SURFACE ELEVATION ________
DEPTH PENETRATED ______ LENGTH RECOVERED ______ %COMPACTION ____

OBTAINED BY ____________________ DATE ______
DESCRIBED BY ____________________ DATE ______

DEPTH (ft, m)	SKETCH	LITHOLOGY	STRUCTURE	REMARKS
15		v muddy sand		color mottly
		large shell frag (4 cm across)	burrowed	Olive gray
		sandy mud		5Y 4/1
		sand (distorted margins by coring)		
		sandy mud (mud becomes more pure near base)		
16	sharp contact	muddy, shelly sand or muddy sandy shell		
		primarily muddy sand, but sandy mud in places, & scattered shell frags; mud very abundant in places	Intensely burrowed	
17				
17.35		sandy mud		
		muddy sand		
		sandy mud (no shell frags)		
		muddy sand		
18		sandy mud (no shell frags) to mud at base		

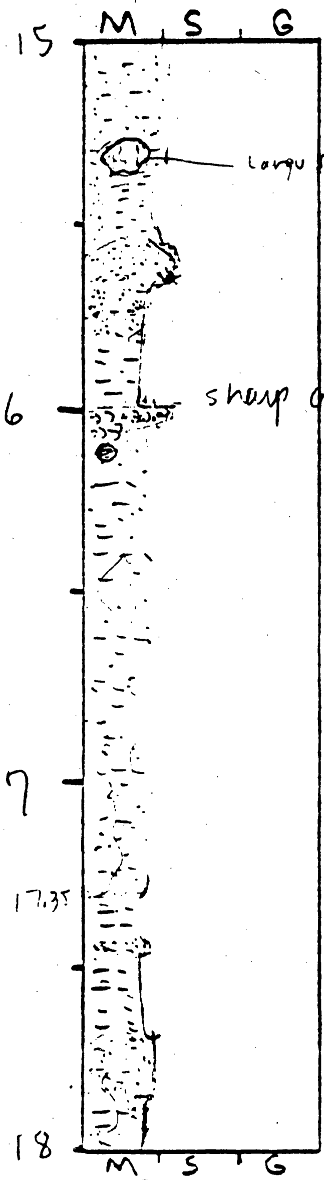

General Comments:

CORE LOG

CORE # SBV-24(G) TYPE ______ LOCATION ______
LATITUDE ______ LONGITUDE ______ SURFACE ELEVATION ______
DEPTH PENETRATED ______ LENGTH RECOVERED ______ %COMPACTION ______

OBTAINED BY ______ DATE ______
DESCRIBED BY ______ DATE ______

DEPTH (ft, m)	SKETCH	LITHOLOGY	STRUCTURE	REMARKS
18	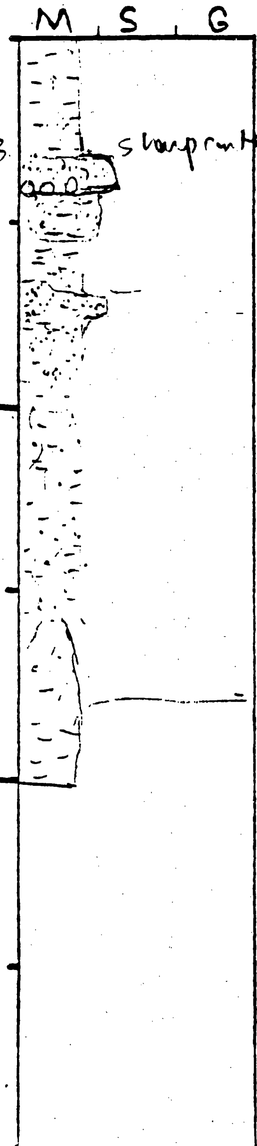	mud on clay small silted sand burrows		
18.3	sharp contact	slightly muddy sand, shells whole & frags	burrowed	Olive gray (5Y 4/1)
		muddy sand		
		sandy mud		
		sand, slightly muddy		Olive gray with some yellowish gray sd.
		sandy mud		
19		muddy sand to sandy mud, discrete mud & sand	Intensely burrows	Olive gray (5Y 4/1)
		core catcher		
		sandy mud		
20				

General Comments:

CORE LOG

CORE # SBV-29A) TYPE Vibrocore LOCATION Sabine Bank
LATITUDE 29° 20.815 LONGITUDE 94° 03.237 SURFACE ELEVATION -38.5'
DEPTH PENETRATED ? LENGTH RECOVERED 18' 11 3/4" % COMPACTION ?

OBTAINED BY Gibeaut - R/V Kit Jones DATE 10-14-94
DESCRIBED BY White DATE

DEPTH (ft, m)	SKETCH	LITHOLOGY	STRUCTURE	REMARKS

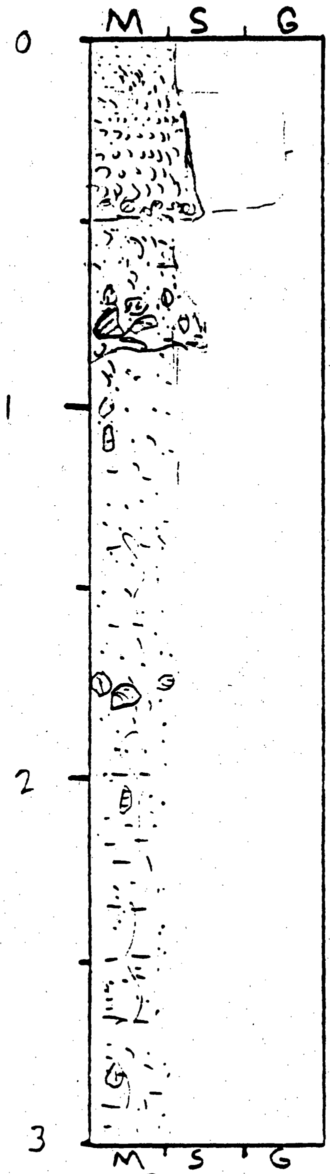

Fine quartz sand grading down into coarser shell hash — Olive gray sand (5Y 4/1)

Drk gray, include whole shells
Shell hash; fining upward, granule to v. coarse sand size

shelly sand Lt Olive gray (5Y 4/1)

sandy shell — Olive gray (5Y 4/1)

muddy sand, scattered small shell frags
occasional whole shell
mud increasing with depth

Burrowed

discrete small mud clasts
2-3 ft.

Olive gray (5Y 3/2)

General Comments:

CORE LOG

CORE # SBV-25(B) TYPE ______ LOCATION ______
LATITUDE ______ LONGITUDE ______ SURFACE ELEVATION ______
DEPTH PENETRATED ______ LENGTH RECOVERED ______ %COMPACTION ______

OBTAINED BY ______ DATE ______
DESCRIBED BY ______ DATE ______

DEPTH (ft, m)	SKETCH	LITHOLOGY	STRUCTURE	REMARKS
3–6	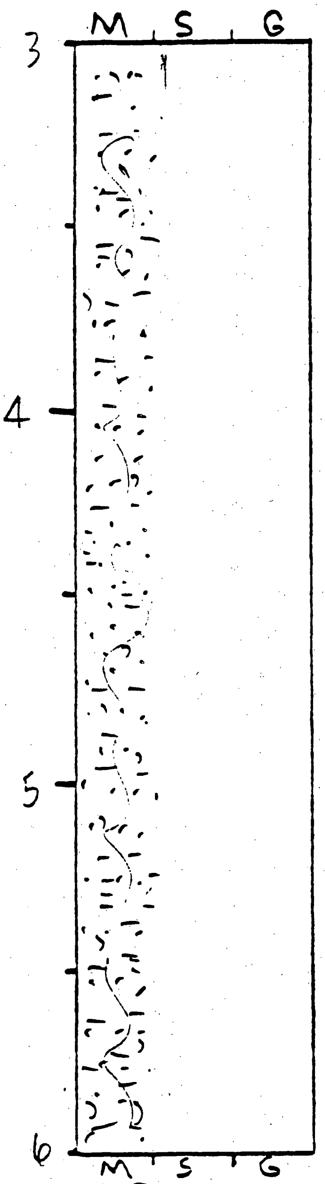	muddy sand scattered shells granule in size (5-10%) muddier than previous section (above) Discrete clay or mud	intensely burrowed	olive grey (5Y 3/2

General Comments:

CORE LOG

CORE # SBY-25 (C) TYPE________ LOCATION________
LATITUDE________ LONGITUDE________ SURFACE ELEVATION________
DEPTH PENETRATED______ LENGTH RECOVERED______ %COMPACTION____

OBTAINED BY________________ DATE________
DESCRIBED BY________________ DATE________

DEPTH (ft, m)	SKETCH	LITHOLOGY	STRUCTURE	REMARKS

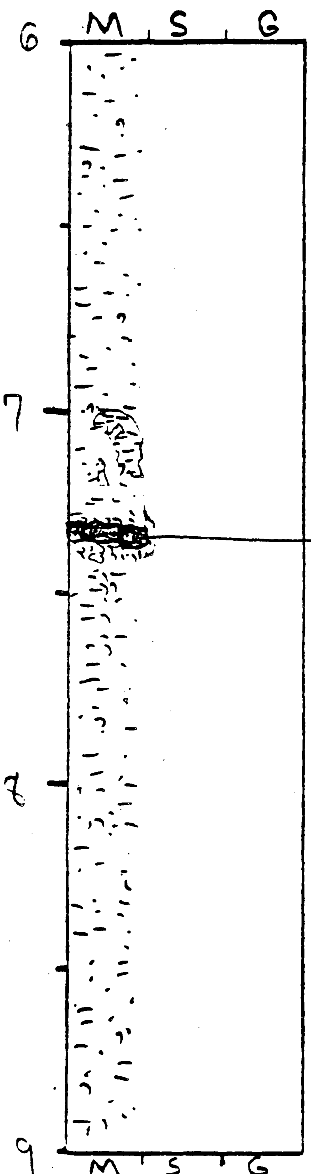

V. muddy sand
Scattered small shell frags < 5%
Discrete mud clast
Intensely burrowed

Olive grey (5Y 3/2)

break in core (void)
shelly muddy sand

General Comments:

CORE LOG

CORE # CPV-25 (D) TYPE______ LOCATION______
LATITUDE______ LONGITUDE______ SURFACE ELEVATION______
DEPTH PENETRATED______ LENGTH RECOVERED______ %COMPACTION______

OBTAINED BY______ DATE______
DESCRIBED BY______ DATE______

DEPTH (ft, m)	SKETCH	LITHOLOGY	STRUCTURE	REMARKS
9		V. muddy sand to locally sandy mud; scattered small shell frags <5%	intensely burrowed	Olive gray (5Y 3/2)
10		discrete mud clast		
11		mud clast; approaching sandy mud in composition		
12				

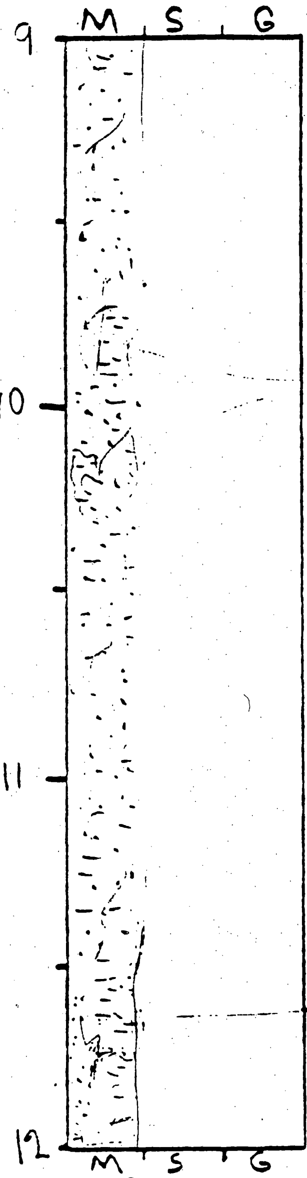

General Comments:

CORE LOG

CORE # SBV-25(E) TYPE ______ LOCATION ______
LATITUDE ______ LONGITUDE ______ SURFACE ELEVATION ______
DEPTH PENETRATED ______ LENGTH RECOVERED ______ %COMPACTION ______

OBTAINED BY ______ DATE ______
DESCRIBED BY ______ DATE ______

DEPTH (ft, m)	SKETCH	LITHOLOGY	STRUCTURE	REMARKS
12	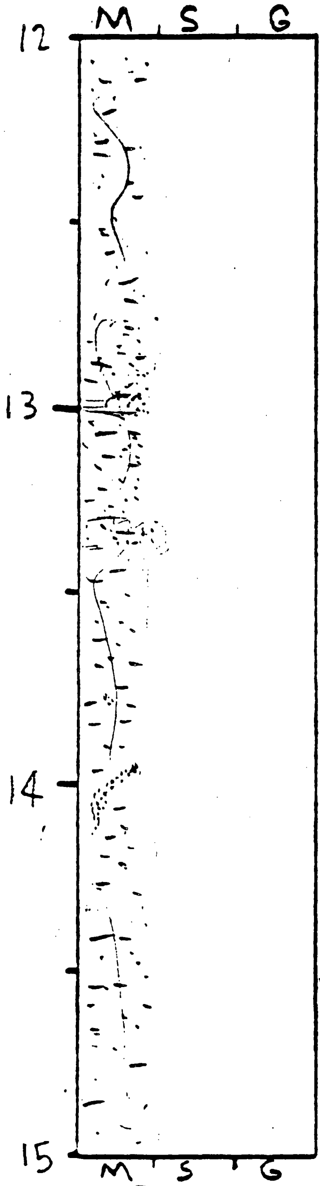	v muddy sand	Intensely burrowed	Olive gray (5Y 3/2)
13		sand mud		
		muddy sand	discrete mud & sand	
		sandy mud		
14				
		v muddy sand to sandy mud		Olive gray (5Y 3/2)
15				

General Comments:

CORE LOG

CORE # SBV-75(F) TYPE ________ LOCATION ____________________
LATITUDE ________ LONGITUDE ________ SURFACE ELEVATION ________
DEPTH PENETRATED ______ LENGTH RECOVERED ______ %COMPACTION ____

OBTAINED BY ______________________________ DATE ________
DESCRIBED BY ______________________________ DATE ________

DEPTH (ft, m)	SKETCH	LITHOLOGY	STRUCTURE	REMARKS

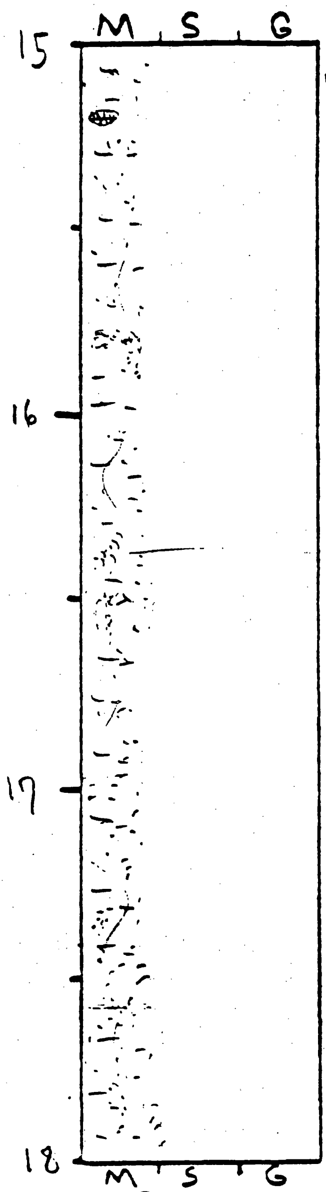

v muddy sand to sandy mud — Intensely burrowed — Olive gray (5Y 3/2)

scattered shell frags < 1% except for local pockets

shell pocket (small shell frags 10 to v coarse to granule)

Intensely burrowed

sandy mud
(mud appears dominant in this area)

muddy sand

General Comments:

CORE LOG

CORE # SBV-25(G) TYPE____ LOCATION____
LATITUDE____ LONGITUDE____ SURFACE ELEVATION____
DEPTH PENETRATED____ LENGTH RECOVERED____ %COMPACTION____

OBTAINED BY____ DATE____
DESCRIBED BY____ DATE____

DEPTH (ft, m)	SKETCH	LITHOLOGY	STRUCTURE	REMARKS

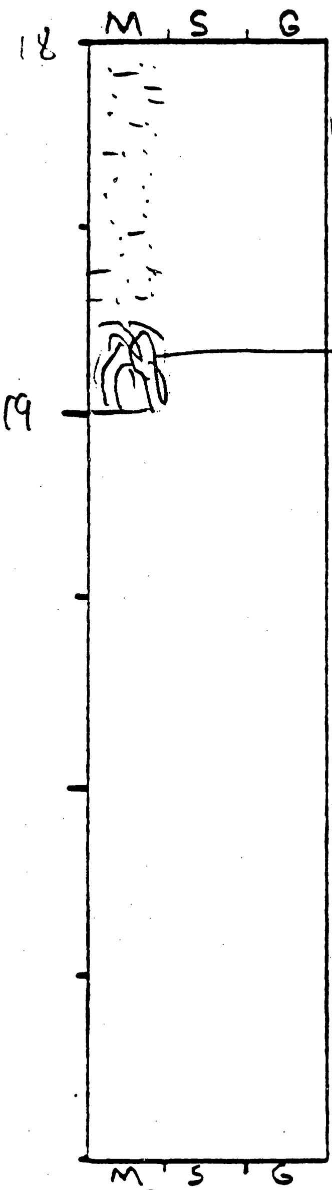

v. muddy sand

Olive Gray (5Y 3/2)

Core catcher

General Comments:

CORE LOG

CORE # HBV-1(A) TYPE Vibracore LOCATION Heald Bank
LATITUDE 29° 07.646' LONGITUDE 94° 11.265' SURFACE ELEVATION -28.5'
DEPTH PENETRATED ? LENGTH RECOVERED 9' 2" %COMPACTION ?

OBTAINED BY Gibeaut /R/V Kit Jones DATE 10-12-94
DESCRIBED BY White DATE

DEPTH (ft, m)	SKETCH	LITHOLOGY	STRUCTURE	REMARKS

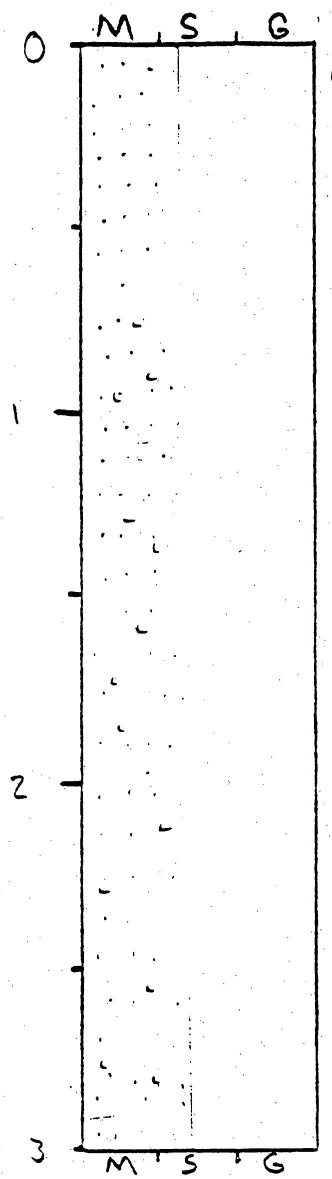

Fine quartz sand (99%)
Very well sorted
sub rounded to rounded

Light olive gray to yellowish gray

scattered (granule size & smaller) shell fragments (<2%)
more apparent below 0.6'

1.1 - 1.4' grayer in center of core

1.4 - 1.6 back to yellowish gray to light olive gray fine sand

1.6 - 2.8

fine sand -- medium dark gray
with hint of light olive gray
Light olive gray along margins next to core.

Scattered granule size & smaller shell fragments

fine, well to very well sorted, sand

Light olive gray fine sand

General Comments:

CORE LOG

CORE # HBV-1 (B) TYPE ______ LOCATION ______
LATITUDE ______ LONGITUDE ______ SURFACE ELEVATION ______
DEPTH PENETRATED ______ LENGTH RECOVERED ______ %COMPACTION ______

OBTAINED BY ______ DATE ______
DESCRIBED BY ______ DATE ______

DEPTH (ft, m)	SKETCH	LITHOLOGY	STRUCTURE	REMARKS

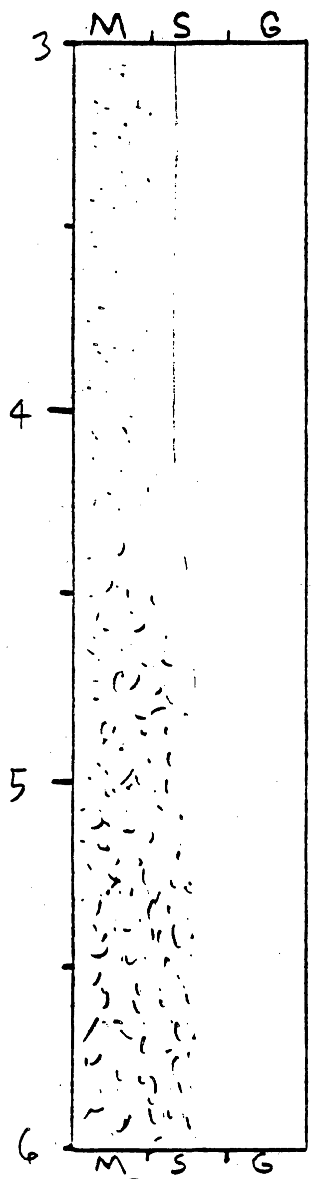

Fine, very well sorted rounded to sub rounded, sand 99% quartz sand — Light olive gray

Fine sand with increasing shell flakes (coarse to very coarse sand) below 3.5' ≈ 5% shell

Gradational increase in shell flake increasing to ≈ 30% below 4.4'

Fining upward

Fine sand mixed with coarse to very coarse sand-size shell fragments (& granule size) ≈ 50% shell frag. below 4.7'
shells increasing with depth

Light olive gray fine sand mixed with light & darker gray shell fragments speckled appearance

General Comments:

CORE LOG

CORE # HBV-1(C) TYPE________ LOCATION________________
LATITUDE________ LONGITUDE________ SURFACE ELEVATION________
DEPTH PENETRATED______ LENGTH RECOVERED______ %COMPACTION____

OBTAINED BY________________________ DATE________
DESCRIBED BY________________________ DATE________

DEPTH (ft, m)	SKETCH	LITHOLOGY	STRUCTURE	REMARKS

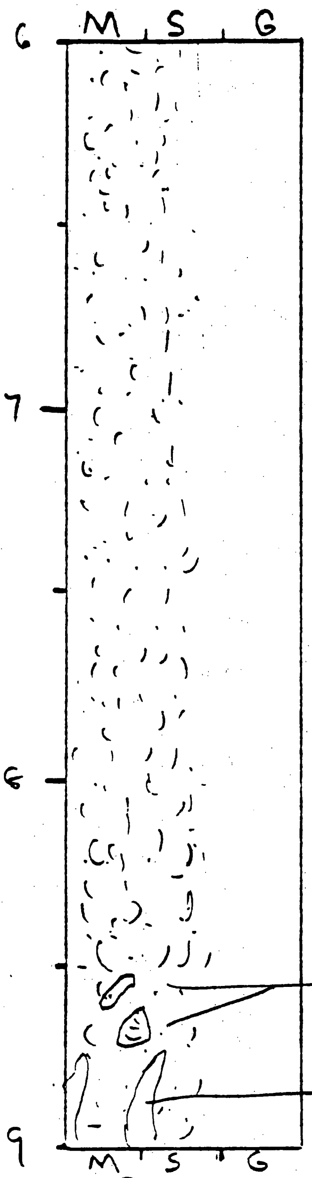

shelly sand or sandy shell
≈ 50% shell fragments
granule to pebble size
mixed with fine sand

Light olive gray sand peppered with darker & lighter shell fragments

fining upward
Shells becoming more abundant than sand at depth

shell fragments:
becomes coarser

Sandy shell

shell fragments 2-3 cm long.

core catcher

General Comments:

CORE LOG

CORE # HBV-1 (D) TYPE ______ LOCATION ______
LATITUDE ______ LONGITUDE ______ SURFACE ELEVATION ______
DEPTH PENETRATED ______ LENGTH RECOVERED ______ %COMPACTION ______

OBTAINED BY ______ DATE ______
DESCRIBED BY ______ DATE ______

DEPTH (ft, m)	SKETCH	LITHOLOGY	STRUCTURE	REMARKS
9	M, S, G	Predominantly fine quartz sand (95%) scattered shells		yellowish gray
Bottom				

General Comments:

CORE LOG

CORE # HBV-2(A) TYPE Vibracore LOCATION Heald Bank
LATITUDE 29°06.357' LONGITUDE 94°10.097' SURFACE ELEVATION -52.5'
DEPTH PENETRATED ? LENGTH RECOVERED 14' 7" (14.6') %COMPACTION ?

OBTAINED BY Gibeaut / R/V Kit Jones DATE 10-12-94
DESCRIBED BY White DATE

DEPTH (ft, m)	SKETCH	LITHOLOGY	STRUCTURE	REMARKS

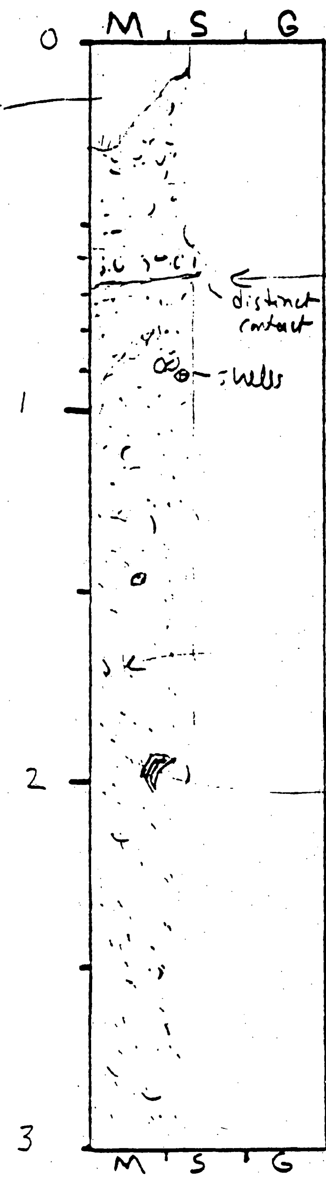

very fine quartz sand, well sorted, subangular, with scattered shell fragments (≈ 10%) — Light olive gray

very fine sand, few shells ≈ 1%

0.57-0.65' shelly sand — Yellowish gray to Lt olive gray

color change from yellowish gray to medium dark gray or Olive gray (5Y 3/2)

very fine sand, scattered shells — Olive gray to med. drk g.
shell frags ≈ 5%
most very coarse sand to granule in size
a few pebble size

color line - darker gray (Olive gray) on right
Light olive gray (appears slightly oxidized)
to Lt olive brown on left side
running down length of core

shell frag > 2 cm

silty very fine sand

General Comments:

CORE LOG

CORE # 4BV-2(B) TYPE________ LOCATION________________
LATITUDE__________ LONGITUDE__________ SURFACE ELEVATION__________
DEPTH PENETRATED______ LENGTH RECOVERED______ %COMPACTION____

OBTAINED BY______________________________ DATE________
DESCRIBED BY_____________________________ DATE________

DEPTH (ft, m)	SKETCH	LITHOLOGY	STRUCTURE	REMARKS
3		silty very fine sand scattered shell frag. local small shell pockets		mod. drk gray to olive gray
4		muddy sand (muddier sediment becomes apparent at about 4.2') "interbedded" with silty very fine sand		mod. dark gray Color along margins of left side light olive brown indicating slight oxidation
Light olive brown to lt olive gray 5		some-what mottled with medium dark gray mud & sand Indistinct mud layers scattered shell fragments mostly granule to very coarse sand size muddy very fine sand or sandy mud shells more abundant 5.3–5.7' 7–10%, shell fragments (granule to very coarse) shells decrease below 5.7' < 1% possible organic traces (specks)		med. drk gray color,
Oxidation boundary 6				

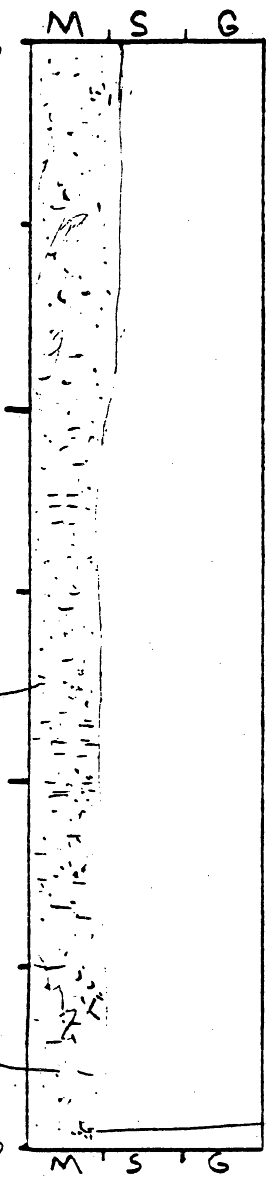

General Comments:

CORE LOG

CORE # HBV-2(C) TYPE ________ LOCATION ____________
LATITUDE ________ LONGITUDE ________ SURFACE ELEVATION ________
DEPTH PENETRATED ______ LENGTH RECOVERED ______ %COMPACTION ___

OBTAINED BY ______________________ DATE ________
DESCRIBED BY ______________________ DATE ________

DEPTH (ft, m)	SKETCH	LITHOLOGY	STRUCTURE	REMARKS

M S G

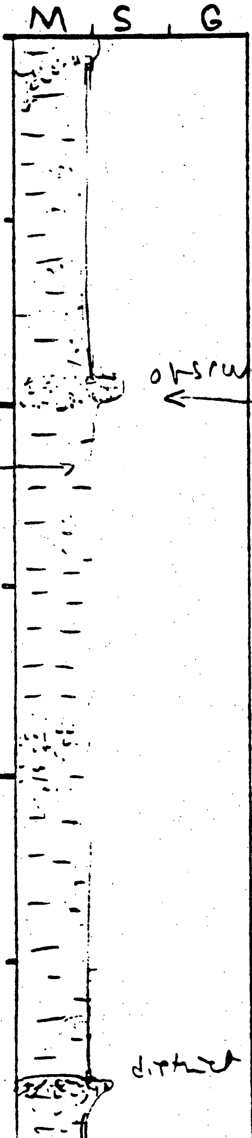

M S G

6

very fine sand muddy sand near top
shell fragments up to 75% in tilted layer at 6.2'.
shell fragments decrease to less than 20%

sandy mud

Mottled
Olive gray on right side of core

overall: Gradationally coarsening upward from shell layer at 8.75'

obscure contacts ← very fine sand, muddy

7

Color boundary →

brownish on left side

med. dark gray on right

Light olive gray on left side

mud with abund. silt
appears to be silty clay; few shell frags (<1%)

clay with shell fragments (15%)

Light Olive gray across most of core

8

mostly clay

rare shell frag <1% (v. coarse sand size)

distinct contact

8.75'

shelly mud (shell frags mostly granule size)
shells decrease to less than 5% toward bottom

9

General Comments:

CORE LOG

CORE # HBV-2(D) TYPE ________ LOCATION ________
LATITUDE ________ LONGITUDE ________ SURFACE ELEVATION ________
DEPTH PENETRATED ________ LENGTH RECOVERED ________ %COMPACTION ________

OBTAINED BY ________ DATE ________
DESCRIBED BY ________ DATE ________

DEPTH (ft, m)	SKETCH	LITHOLOGY	STRUCTURE	REMARKS

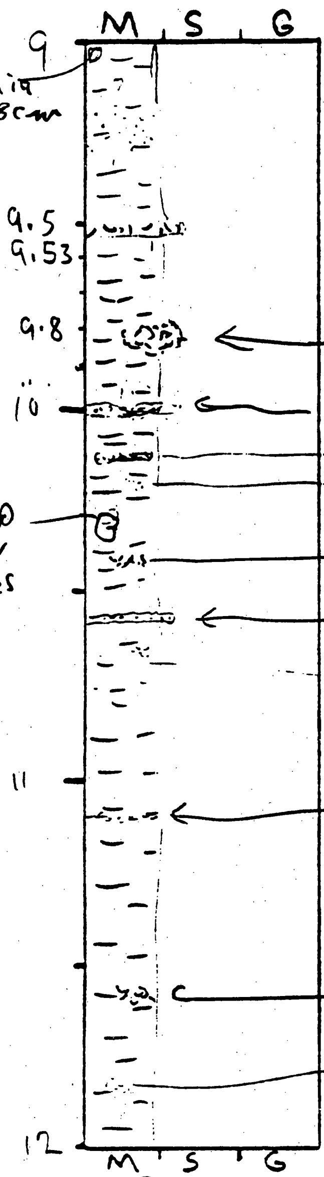

- mud with some slightly silty zones — Olive gray 5Y 4/2 to med drk gray
- rare shell *Mulinia lateralis*
- traces of organics
- muddy shell layer ≈ 1cm thick
- clay — Olive gray
- shell pocket granule to pebble size
- silty zone, broken or interrupted
- thin shelly mud (v. crse sand size)
- scattered organic carbon traces
- small shell fragments
- thin very fine sand layer — discrete, continuous
- organic carbon trace
- clay — Olive gray
- organic carbon trace
- shell fragments
- organic carbon traces

General Comments:

CORE LOG

CORE # HBV-2(E) TYPE ______ LOCATION ______
LATITUDE ______ LONGITUDE ______ SURFACE ELEVATION ______
DEPTH PENETRATED ______ LENGTH RECOVERED ______ %COMPACTION ______

OBTAINED BY ______ DATE ______
DESCRIBED BY ______ DATE ______

DEPTH (ft, m)	SKETCH	LITHOLOGY	STRUCTURE	REMARKS

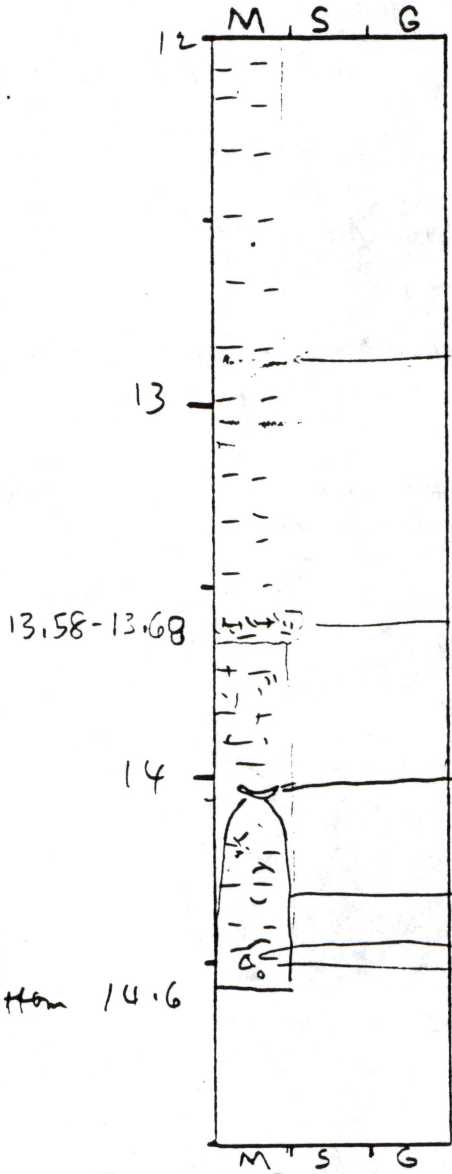

Clay

Med. dark gray clay to Olive gray

organic carbon specks

no shells

organic carbon traces

muddy shell (very coarse to granule)

Mud

scattered small shell fragments

medium dark gray to Olive gray

Large shell fragment

scattered shells

core catcher

shells

color brownish gray to brown

color possibly due to oxidation near core catcher

General Comments:

CORE LOG

CORE # HBV-3 (A) **TYPE** Vibracore **LOCATION** Heald Bank
LATITUDE 29° 07.373 **LONGITUDE** 94° 13.163 **SURFACE ELEVATION** -43.5'
DEPTH PENETRATED ? **LENGTH RECOVERED** 20' **%COMPACTION** ?

OBTAINED BY G. Gibeaut – R/V Kit Jones **DATE** 10-12-94
DESCRIBED BY White **DATE**

DEPTH (ft, m)	SKETCH	LITHOLOGY	STRUCTURE	REMARKS

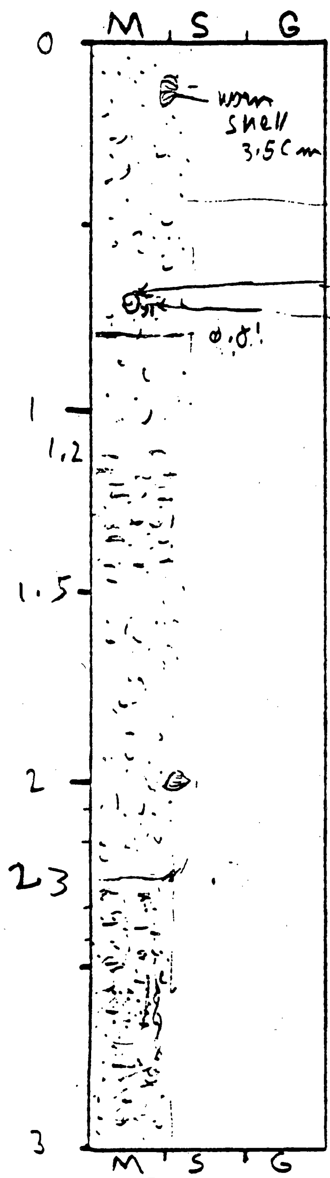

Fine quartz sand (90%)
well sorted, sub rounded
very coarse to occasional pebble size
and granule size shells & fragments
(shells 10-15%)
– color change gradational from
brownish above to grayer below
– very worn shell frag. (1.5 cm across)
– shell frag. pocket
color gray below 0.8' except along
margins of core where it is yellowish gray
fine sand with to v. fine
30%
small mud clasts ≥ 3mm to 5 mm in size
scattered small shells (very coarse sand)

fine to v. fine sand, scattered small shell frag.
less mud than above & below

muddy sand -- discrete clay or mud
clasts increasing in size & coalescing
with depth!
possibly from
burrowing
mud has vertical
component to it.

Light olive gray

olive gray ↓

General Comments:

CORE LOG

CORE # HBV-3(B) TYPE______ LOCATION______
LATITUDE______ LONGITUDE______ SURFACE ELEVATION______
DEPTH PENETRATED______ LENGTH RECOVERED______ %COMPACTION______

OBTAINED BY______ DATE______
DESCRIBED BY______ DATE______

DEPTH (ft, m)	SKETCH	LITHOLOGY	STRUCTURE	REMARKS
3 (void space)	M, S, G	Olive gray muddy sand; v. fine quartz sand; discrete mud clasts		Olive gray (5Y 3/2)
		v. fine sand, scattered mud clasts		
		shell fragments pockets (yellowish gray) very coarse sand size		
4				
4.3		v. fine sand to muddy sand with ≈ 25% mud clasts		
4.5		v. fine sand scattered mud clasts		
5		25% shell fragments (v. coarse sand size)		
		shell pocket		
		muddy sand (mud clasts more abundant than above)		
6	M, S, G			

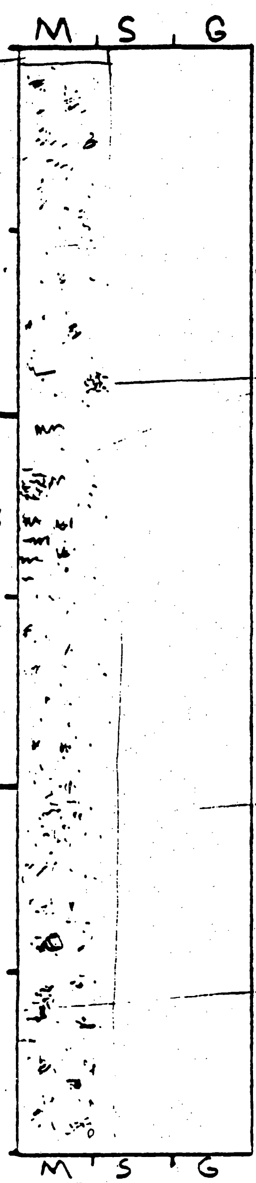

General Comments:

CORE LOG

CORE # HBV-3 (C) **TYPE** ______ **LOCATION** ______
LATITUDE ______ **LONGITUDE** ______ **SURFACE ELEVATION** ______
DEPTH PENETRATED ______ **LENGTH RECOVERED** ______ **%COMPACTION** ______

OBTAINED BY ______ **DATE** ______
DESCRIBED BY ______ **DATE** ______

DEPTH (ft, m)	SKETCH	LITHOLOGY	STRUCTURE	REMARKS
6 – 9	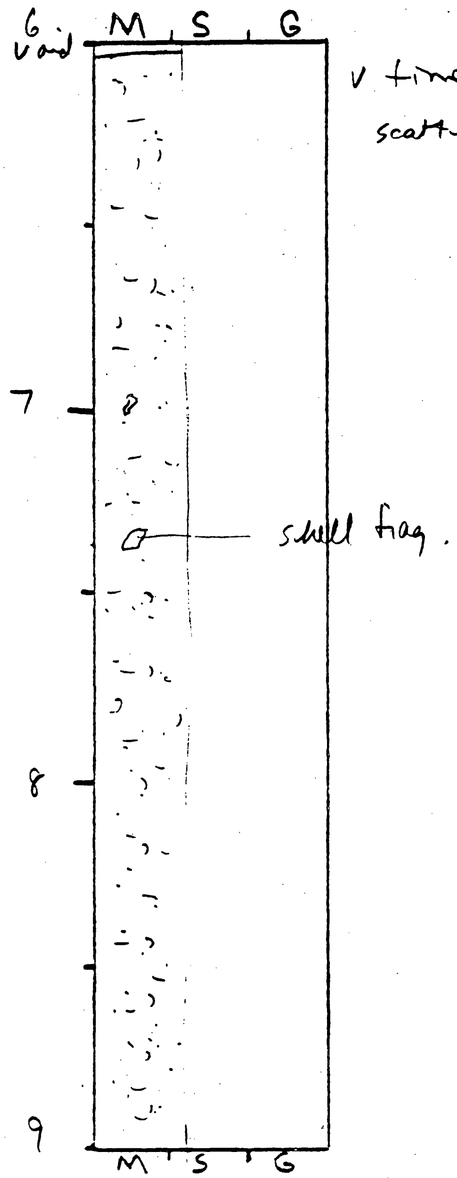	v fine sand slightly muddy scattered small (coarse to very coarse) shell fragments: ≈10% fragments rare larger fragments		olive gray

General Comments:

CORE LOG

CORE # HBV-31(D) TYPE_____ LOCATION_____
LATITUDE_____ LONGITUDE_____ SURFACE ELEVATION_____
DEPTH PENETRATED_____ LENGTH RECOVERED_____ %COMPACTION_____

OBTAINED BY_____ DATE_____
DESCRIBED BY_____ DATE_____

DEPTH (ft, m)	SKETCH	LITHOLOGY	STRUCTURE	REMARKS

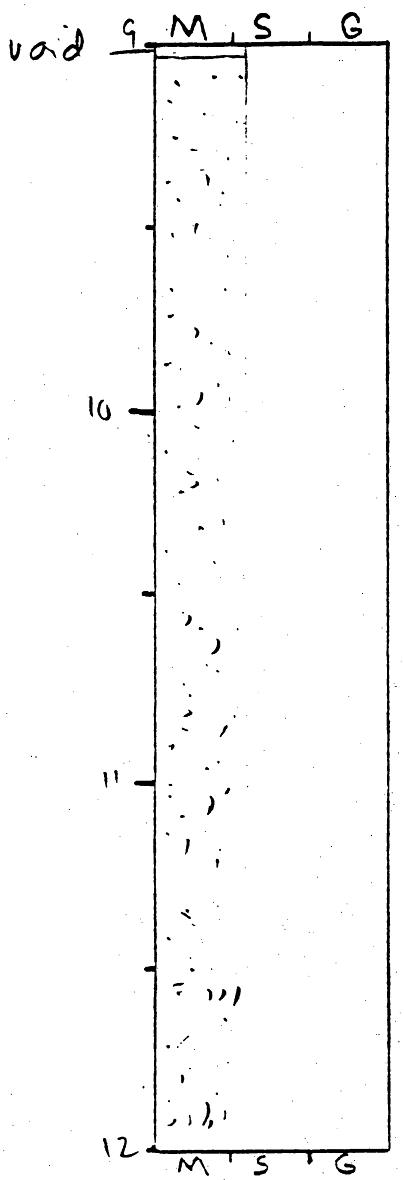

slightly muddy v. fine sand

scattered small shell fragments (< 5%)

Olive gray with light olive gray to light olive brown mottling from left side of core (and right side near bottom).

shell fragments increase in abundance and size below ≃ 10.5' (comprising ≃ 10%, locally concentrated ≃ 20%)

General Comments:

CORE LOG

CORE # HSV-3 (E) TYPE ______ LOCATION ______
LATITUDE ______ LONGITUDE ______ SURFACE ELEVATION ______
DEPTH PENETRATED ______ LENGTH RECOVERED ______ %COMPACTION ______

OBTAINED BY ______ DATE ______
DESCRIBED BY ______ DATE ______

DEPTH (ft, m)	SKETCH	LITHOLOGY	STRUCTURE	REMARKS

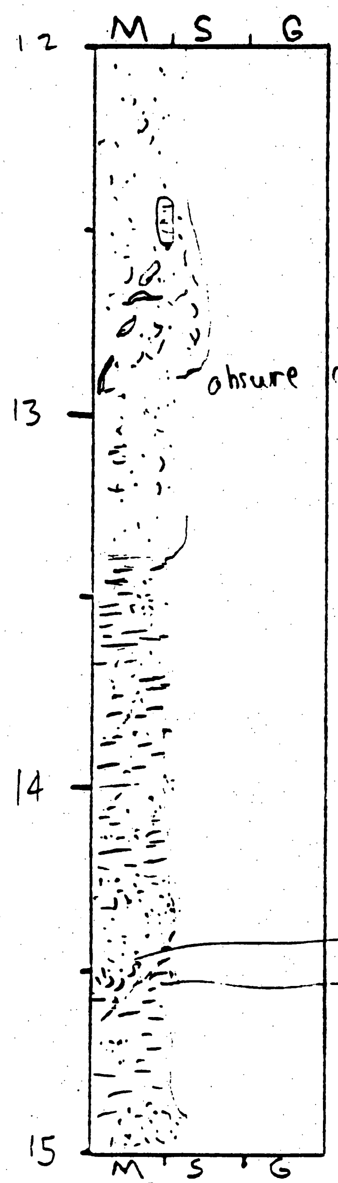

v. fine sand
slightly muddy
scattered shells
<10%

Olive
gray
(5Y 3/2)

Increase in shells (some gravel size)
>25% shelly sand

obscure contact

v. fine sand
Increase in mud with depth
scattered shells
muddy sand to sandy mud

(Mottling & irregular contact possibly due to burrowing)

13.7'–14'
mud becomes dominant
(sandy mud)

muddy sand

shell pocket muddy shelly sand
dipping contact
mud dominant (sandy mud)
sand dominant scattered shells

General Comments:

CORE LOG

CORE # HBV-3(F) TYPE_____ LOCATION_____
LATITUDE_____ LONGITUDE_____ SURFACE ELEVATION_____
DEPTH PENETRATED_____ LENGTH RECOVERED_____ %COMPACTION_____

OBTAINED BY_____ DATE_____
DESCRIBED BY_____ DATE_____

DEPTH (ft, m)	SKETCH	LITHOLOGY	STRUCTURE	REMARKS
15	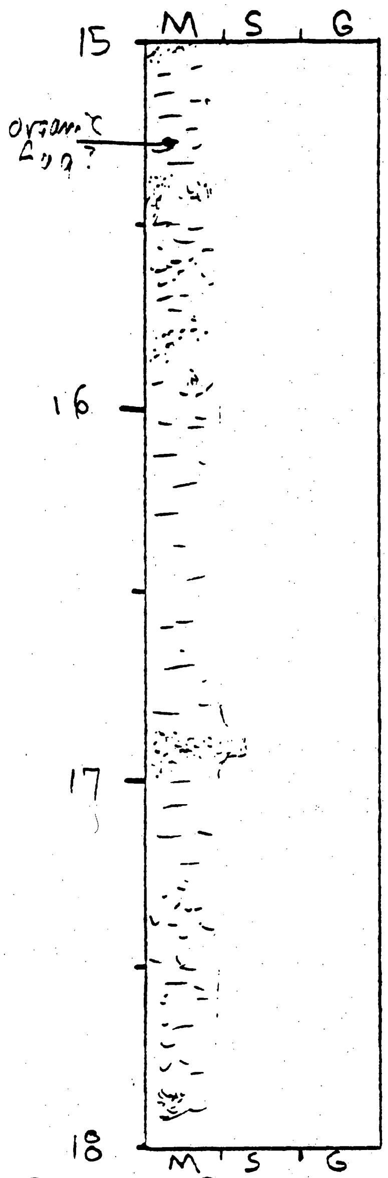	mottled clay with pockets of shell frag. & sand		mottled down length of core from light olive gray to olive gray
17		sand (very fine) stringer		

General Comments:

CORE LOG

CORE # NZV-3(G) TYPE______ LOCATION______
LATITUDE______ LONGITUDE______ SURFACE ELEVATION______
DEPTH PENETRATED______ LENGTH RECOVERED______ %COMPACTION______

OBTAINED BY______ DATE______
DESCRIBED BY______ DATE______

DEPTH (ft, m)	SKETCH	LITHOLOGY	STRUCTURE	REMARKS

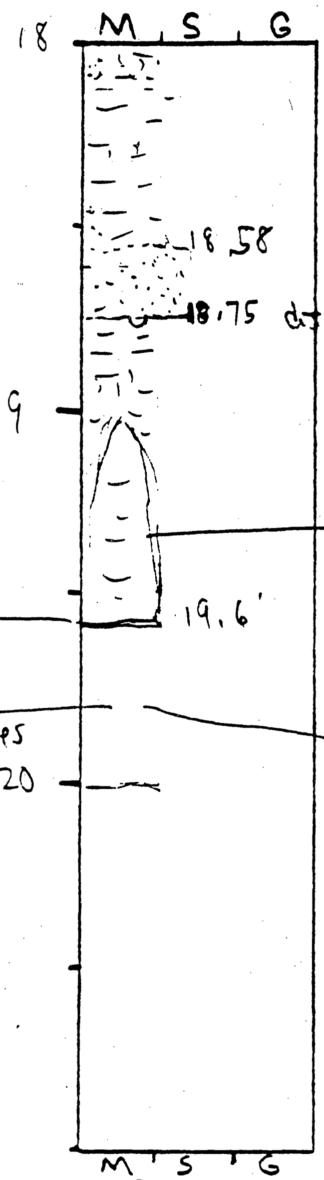

Bottom of core — 19.6'

This part in baggies

- olive gray mud — scattered small shells
- olive gray mud (clay)
- very fine sand — Light olive gray to dusky yellow
- 18.75 distinct sharp contact
- olive gray mud (clay) — very scattered shell fragments
- core catcher — oxidized mud (apparently due to core catcher) Light olive brown to moderate brown
- Soft olive gray mud in 2 baggies

General Comments:

Photographed 1-25-95

CORE LOG

CORE # HBV-4(A) **TYPE** Vibrocore **LOCATION** Heald Bank
LATITUDE 29° 08.443 **LONGITUDE** 94° 11.565' **SURFACE ELEVATION** -50.5'
DEPTH PENETRATED ? **LENGTH RECOVERED** 15' 2½" 15.7' **%COMPACTION** ?

OBTAINED BY Gibeaut - R/V Kit Jones **DATE** 10-12-94
DESCRIBED BY White **DATE**

DEPTH (ft, m)	SKETCH	LITHOLOGY	STRUCTURE	REMARKS

M S G

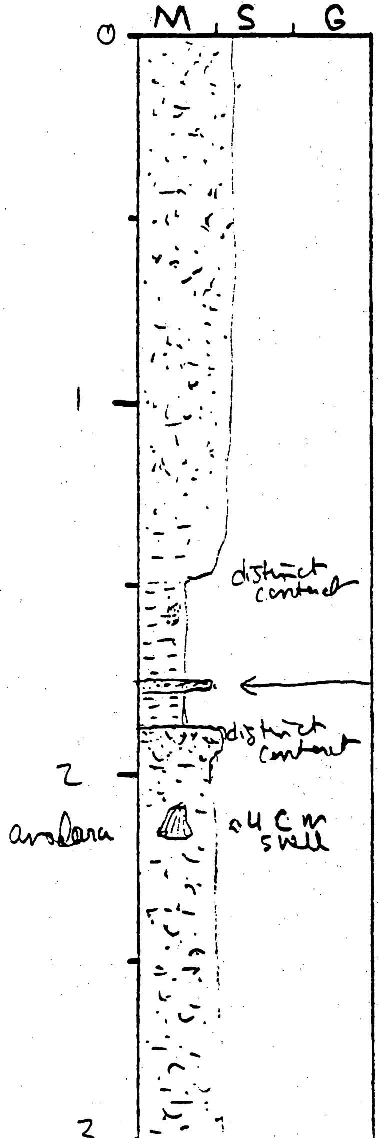

fine sand trace of mud
Shell fragments (10%) very coarse
well sorted sand
sub rounded

Olive gray color (5Y 3/2)

mud increasing slightly with depth

mud "clasts" appear at 1.4' in fine sand

Olive gray mud (clay)
fine sand pocket

olive gray (5Y 3/2) to dark greenish gray

thin fine sand stringer 1.76'

fine sand, shell fragments very coarse to granule size (25%) higher percentage in pocket
slightly muddy

fine sand
scattered shell very coarse to granule in size
(10% shell)
slightly muddy

Olive gray (5Y 3/2) to dark greenish gray

General Comments:

CORE LOG

CORE # HBV-4(B) TYPE_____ LOCATION_____
LATITUDE_____ LONGITUDE_____ SURFACE ELEVATION_____
DEPTH PENETRATED_____ LENGTH RECOVERED_____ %COMPACTION_____

OBTAINED BY_____ DATE_____
DESCRIBED BY_____ DATE_____

DEPTH (ft, m)	SKETCH	LITHOLOGY	STRUCTURE	REMARKS

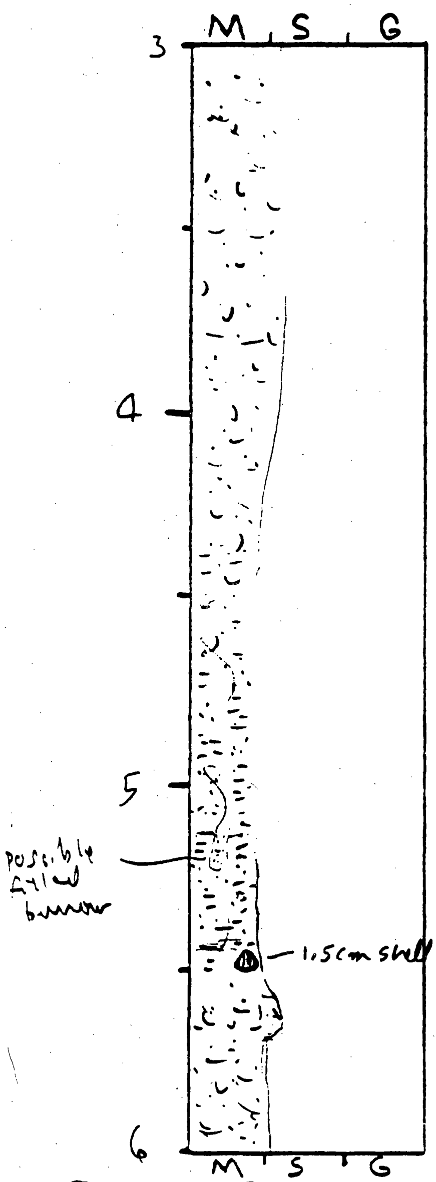

slightly muddy fine sand with scattered (10%) shell fragments up to granule in size and slightly larger

dark greenish gray to olive gray (5Y 3/2)

fine sand; mud becoming more apparent below 4.4'
scattered shells up to small pebble in size
15% shell

dark greenish gray to olive gray (5Y 3/1)

mud increasing with depth
muddy sand

obscure mud "clasty"
most abundant mud between 5.25' - 5.42'

concentration of shell material in fine sand ≈ 40%

fine sand, slightly muddy
scattered shell fragments.

General Comments:

CORE LOG

CORE # HBV-4(c) TYPE________ LOCATION________________
LATITUDE________ LONGITUDE________ SURFACE ELEVATION________
DEPTH PENETRATED______ LENGTH RECOVERED______ %COMPACTION____

OBTAINED BY________________________ DATE________
DESCRIBED BY________________________ DATE________

DEPTH (ft, m)	SKETCH	LITHOLOGY	STRUCTURE	REMARKS

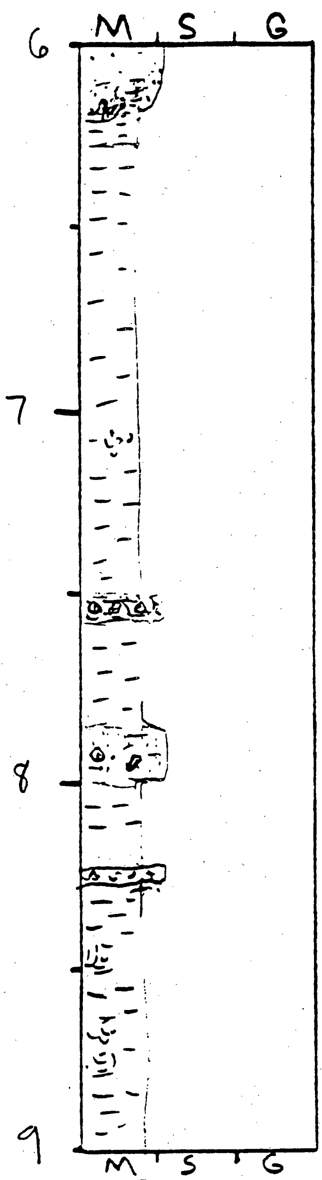

fine sand, slightly muddy, scattered shell
distinct contact at 6.25'
but irregular surface possibly from coring or burrowing.

Clay
few shell fragments

Local shell pockets

shelly muddy, sand stringer

fine sand scattered shells (up to small pebble in size)
muddy

shell stringer at 8.25'-8.30'
granule size

clay or mud, slightly sandy
shell pockets, granule in size.

Remarks: olive gray (5Y 3/2) to dark greenish gray

(5Y 3/2) Olive gray to dark greenish gray

General Comments:

CORE LOG

CORE # HBV-4(D) TYPE ______ LOCATION ______
LATITUDE ______ LONGITUDE ______ SURFACE ELEVATION ______
DEPTH PENETRATED ______ LENGTH RECOVERED ______ %COMPACTION ______

OBTAINED BY ______ DATE ______
DESCRIBED BY ______ DATE ______

DEPTH (ft, m)	SKETCH	LITHOLOGY	STRUCTURE	REMARKS

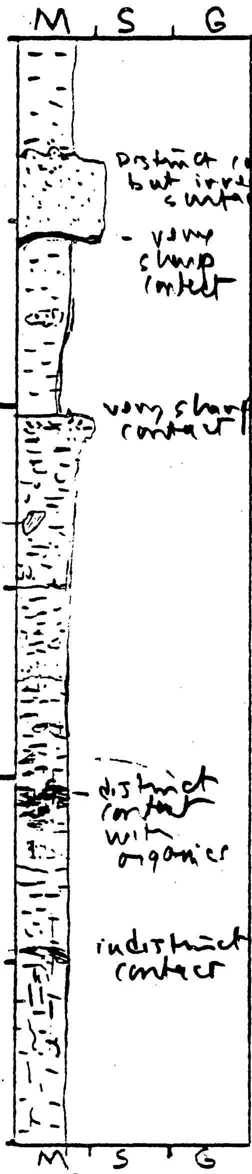

9 — clay — Medium dark gray clay to olive gray 5Y 3/2

9.32' — Distinct contact but irregular surface — very fine sand, well to very well sorted, subrounded — olive gray sand

9.55' — very sharp contact — slightly sandy mud down to 9.75' (medium dark gray clay)

Medium dark gray clay, disseminated organic traces, shells rare

10 — very sharp contact — shells & shell fragments (mostly) granule (mostly), locally small pebble size. This unit appears to be predominantly mud with shells more abundant at top, slightly sandy

broken shell 1.5cm

predominantly mud or clay w/ small pockets of very fine quartz sand.

lighter gray clay

medium dark gray clay with elliptical and irregular shapes of light gray clay; organic traces

11 — distinct contact with organics — organic layer from 11.07'-11.25 — grayish black at top grading downward into medium dark gray and medium light gray

Organic Clay
medium light gray clay, increasing organic traces.

indistinct contact — At about 11.45' vertical organic traces (roots?) (traces brownish black) in olive black (5Y 2/1) to olive gray clay — Olive black clay

12

General Comments:

CORE LOG

CORE # HBV-4(E) TYPE ______ LOCATION ______
LATITUDE ______ LONGITUDE ______ SURFACE ELEVATION ______
DEPTH PENETRATED ______ LENGTH RECOVERED ______ %COMPACTION ______

OBTAINED BY ______ DATE ______
DESCRIBED BY ______ DATE ______

DEPTH (ft, m)	SKETCH	LITHOLOGY	STRUCTURE	REMARKS

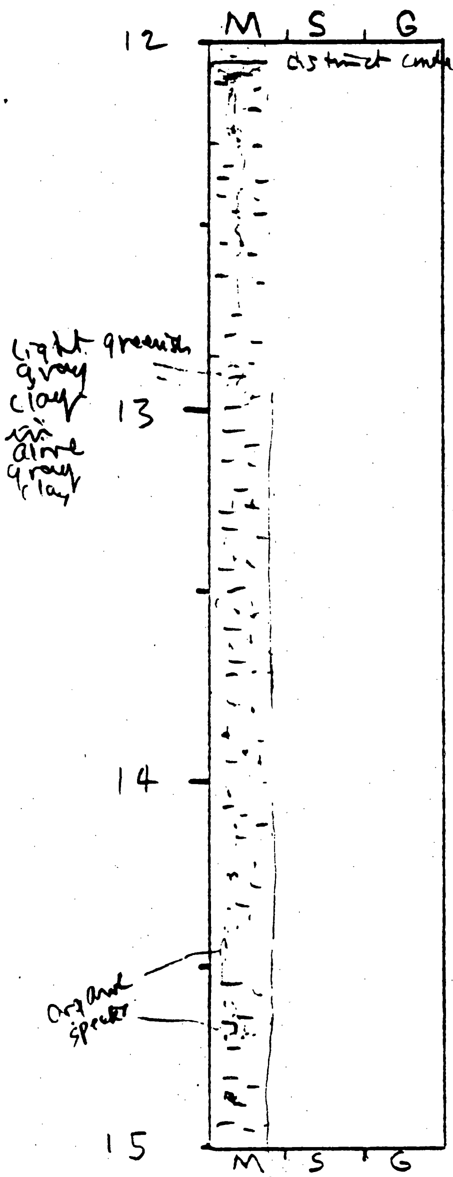

clay — olive gray to olive black

organic rich clay 12.05 – 12.3' — grayish black

clay with organic (grayish black) streak down center — olive gray to brownish gray

(No shells in this section)

traces of organics in clay — specks of organics

at about 13.5 sediments become lighter in color gradationally (olive gray to more brownish gray) (slightly silty) — brownish gray

traces of dark organics (disseminated in clay)

brownish gray

General Comments:

CORE LOG

CORE # HBV-4(F) TYPE ______ LOCATION ______
LATITUDE ______ LONGITUDE ______ SURFACE ELEVATION ______
DEPTH PENETRATED ______ LENGTH RECOVERED ______ %COMPACTION ______

OBTAINED BY ______ DATE ______
DESCRIBED BY ______ DATE ______

DEPTH (ft, m)	SKETCH	LITHOLOGY	STRUCTURE	REMARKS
15	M , S , G	relatively stiff clay mottled some oxidation organics disseminated in clay		
15.25'	— oxidation above			rusty color over medium gray above 15.25'
15.65- 15.70.	Bottom	oxidation traces at base (Core catcher was removed but may have caused some mot?) stiff clay probably prevented deeper penetration of sediment by core.		Light olive gray with patches of medium dark gray organics
16				

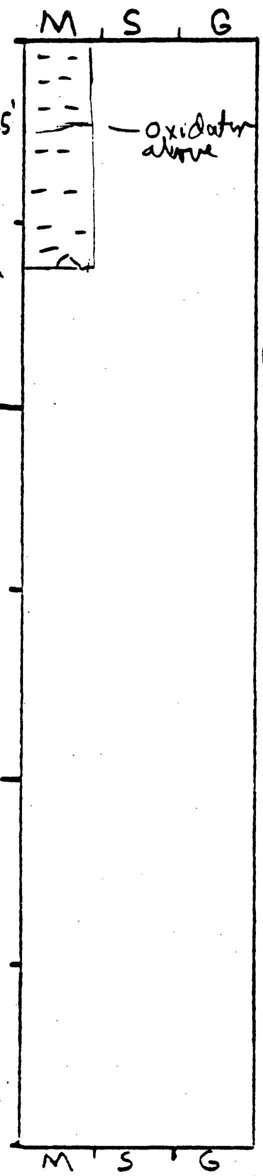

General Comments:

CORE LOG

CORE # HBY-5 (A) TYPE Vibracore LOCATION Heald Bank
LATITUDE 29° 08.131 LONGITUDE 94° 11.025 SURFACE ELEVATION -35'
DEPTH PENETRATED ? LENGTH RECOVERED 19'10" %COMPACTION ?

OBTAINED BY Gibeaut - R/V Kit Jones DATE 10-12-94
DESCRIBED BY White DATE

DEPTH (ft, m)	SKETCH	LITHOLOGY	STRUCTURE	REMARKS
		very well sorted subrounded fine sand, 99% quartz grains, shell fragments increasing with depth. Fining upward graded contact between 0.6-0.9 ft with coarse-sand size shell fragments bimodal (fine sand & coarse-sand fm shell fragments)		Greenish gray to light olive gray
1				
		10-25% shell (coarse sand) fragments		
2				
		5mm shell		

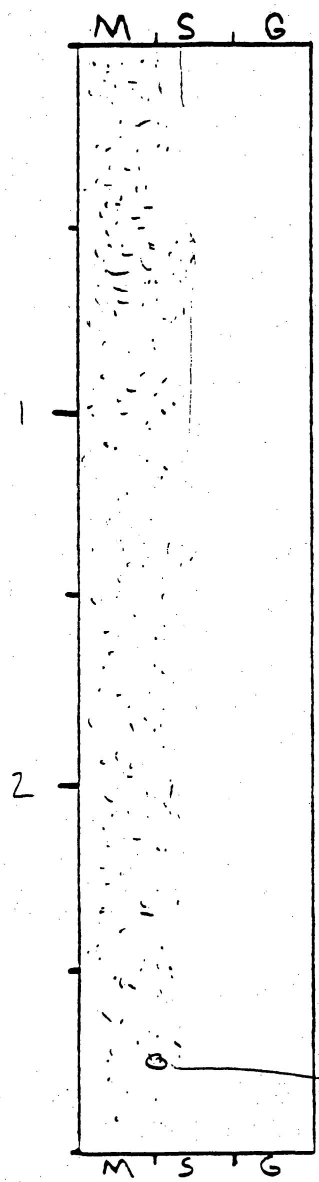

General Comments:

CORE LOG

CORE # HBV-5 (B) TYPE ________ LOCATION ________
LATITUDE ________ LONGITUDE ________ SURFACE ELEVATION ________
DEPTH PENETRATED ________ LENGTH RECOVERED ________ %COMPACTION ________

OBTAINED BY ________ DATE ________
DESCRIBED BY ________ DATE ________

DEPTH (ft, m)	SKETCH	LITHOLOGY	STRUCTURE	REMARKS
3	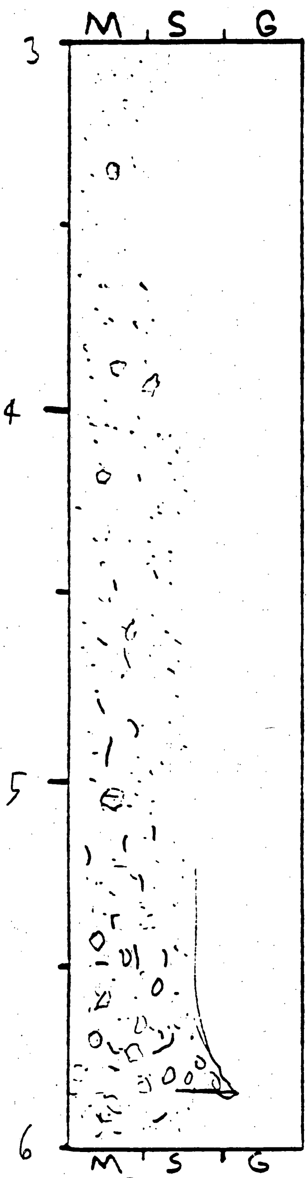	Fine, predominantly quartz sand (subrounded) (very well sorted) with scattered shells & shell fragments		Light olive gray
		Increase in shell with depth. Obscure contact at ≃ 3.8' (graded) fine well-sorted sand & increasing shell fragments very coarse		
5		fine quartz sand with coarse sand size shell fragments and scattered gravel size shell increasing to depth of 5.75'		
6		5.75' obscure contact with decrease in shell below. Fine sand with scattered shell		

General Comments:

CORE LOG

CORE # HBV-5(C) TYPE ________ LOCATION ________
LATITUDE ________ LONGITUDE ________ SURFACE ELEVATION ________
DEPTH PENETRATED ______ LENGTH RECOVERED ______ %COMPACTION ______

OBTAINED BY ________________________ DATE ________
DESCRIBED BY ________________________ DATE ________

DEPTH (ft, m)	SKETCH	LITHOLOGY	STRUCTURE	REMARKS
6		fine quartz sand, moderately well sorted, sub rounded, scattered to abundant shell fragments up to 25% or more increasing with depth; shelly sand		Light olive gray
7		shelly pocket; sandy shell or shelly sand		
possible sand filled burrow; 8; slightly darker gray in color		fine sand with scattered shells (coarse sand to granule)		
		Increase in shell (large shell fragments)	mostly sand but possibly shelly sand	
9		fine sand		

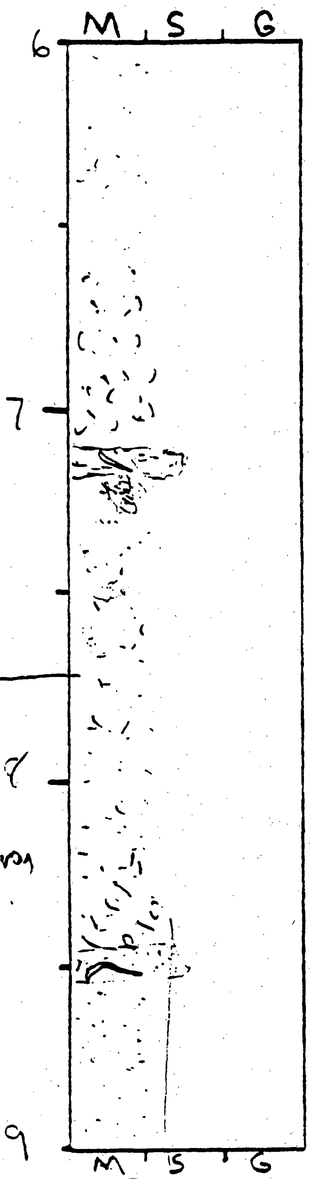

General Comments:

CORE LOG

CORE # HBV-5(D) TYPE________ LOCATION________
LATITUDE________ LONGITUDE________ SURFACE ELEVATION________
DEPTH PENETRATED______ LENGTH RECOVERED______ %COMPACTION____

OBTAINED BY________________ DATE________
DESCRIBED BY________________ DATE________

DEPTH (ft, m)	SKETCH	LITHOLOGY	STRUCTURE	REMARKS
9		fine quartz sand well sorted, subrounded		Light olive gray
10		Shell hash pockets and occassional large fragment (>1 cm)		
		Scattered gravel-size shell fragments in fine quartz sand		
11		Traces of mud below 11.3' (gradational contact) still predominantly fine sand but mud produces darker colored gray; scattered coarse-sand shell fragments		Dark greenish gray
12				

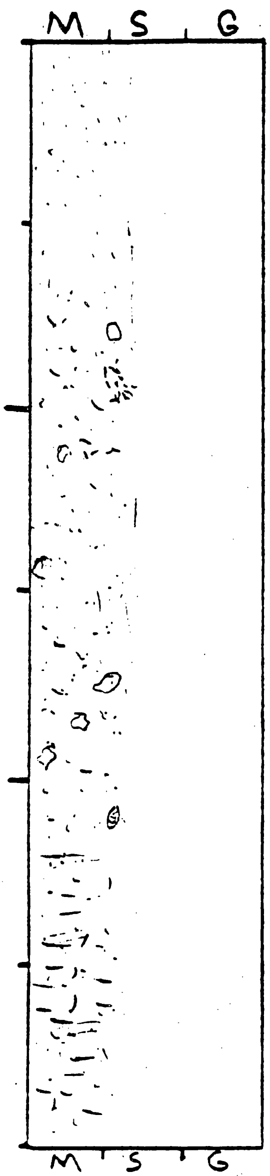

General Comments:

CORE LOG

CORE # μBV-5 (E) **TYPE** ______ **LOCATION** ______
LATITUDE ______ **LONGITUDE** ______ **SURFACE ELEVATION** ______
DEPTH PENETRATED ______ **LENGTH RECOVERED** ______ **%COMPACTION** ______

OBTAINED BY ______ **DATE** ______
DESCRIBED BY ______ **DATE** ______

DEPTH (ft, m)	SKETCH	LITHOLOGY	STRUCTURE	REMARKS

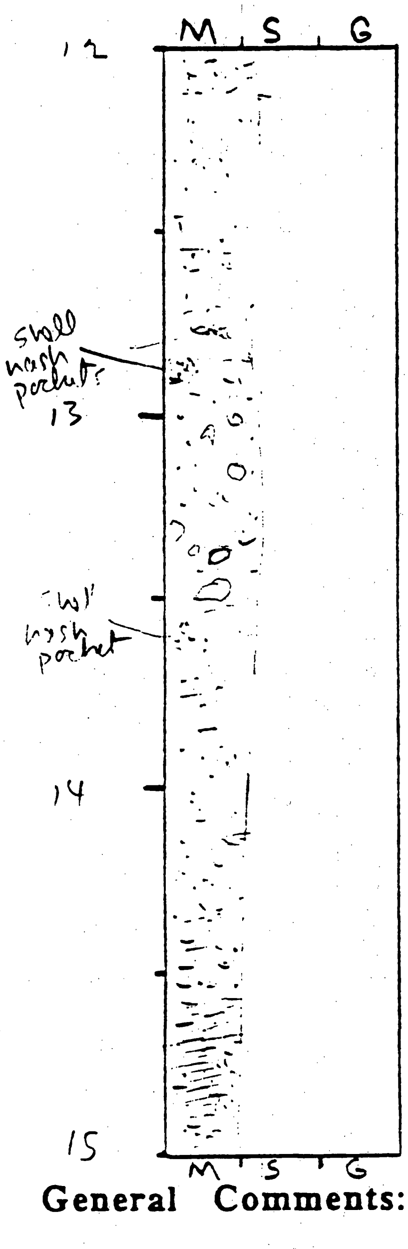

fine sand with coarse to (bimodal grain size) granule size shell fragments. Distinct contact with fine sand below; Quartz subrounded. Traces of mud below 12.5'

Olive gray to light olive gray in color

Predominantly fine quartz sand with scattered shells and shell hash pockets (very-coarse in grain size) & traces of mud

mud becoming more abundant with depth

Mottled color with lighter sand pockets in darker sand unit traces of mud. Shell fragments less abundant [illegible] 14.3' fine sand and possibly muddy sand mud more abundant near base of section

Dark gray to Light olive gray (Mottled)

Streaks of Dark yellowish brown on right margin

General Comments:

CORE LOG

CORE # HBV-5 (F) TYPE______ LOCATION______
LATITUDE______ LONGITUDE______ SURFACE ELEVATION______
DEPTH PENETRATED______ LENGTH RECOVERED______ %COMPACTION______

OBTAINED BY______ DATE______
DESCRIBED BY______ DATE______

DEPTH (ft, m)	SKETCH	LITHOLOGY	STRUCTURE	REMARKS
15	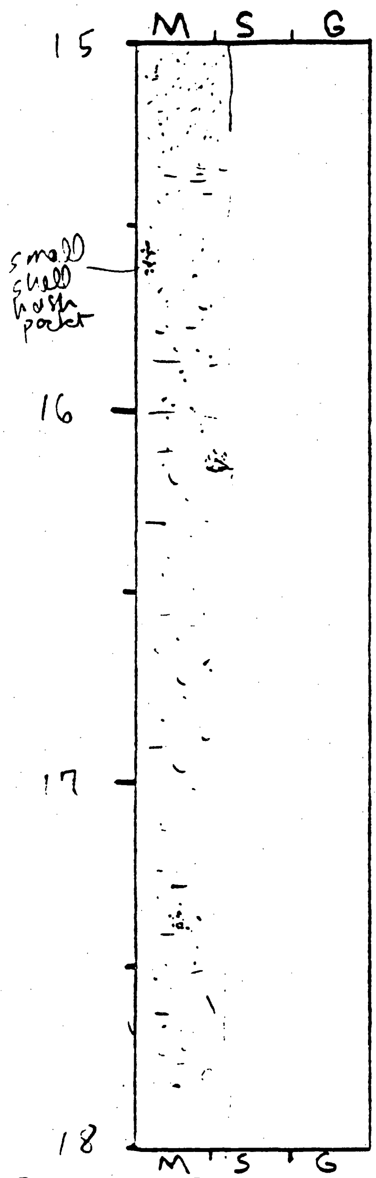	fine quartz sand well sorted		olive gray
		traces of mud more apparent below 15.4'.		becoming dark greenish gray to dark gray below 15.4'
16		fine quartz sand scattered shell fragments & occassional small (1-2 cm) shell hash pockets and more concentrated sand pockets slightly muddy		Dark greenish gray to Dark gray
17				
18				

General Comments:

CORE LOG

CORE # HBV-51(G) TYPE______ LOCATION______
LATITUDE______ LONGITUDE______ SURFACE ELEVATION______
DEPTH PENETRATED______ LENGTH RECOVERED______ %COMPACTION______

OBTAINED BY______ DATE______
DESCRIBED BY______ DATE______

DEPTH (ft, m)	SKETCH	LITHOLOGY	STRUCTURE	REMARKS
18		fine sand (quartz) slightly muddy		Dark gray color
	distinct contact	Large gastropod 8-9 cm long		Gastropod cut in half by saw (chambers showing)
19		color change below gastropod; fine sand with scattered shell frags. (less muddy)		Olive gray
		color change oxidation (possibly due to core catcher)		Moderate yellowish brown (core catcher) (5Y 5/4)
		19.8' Bottom		
20				

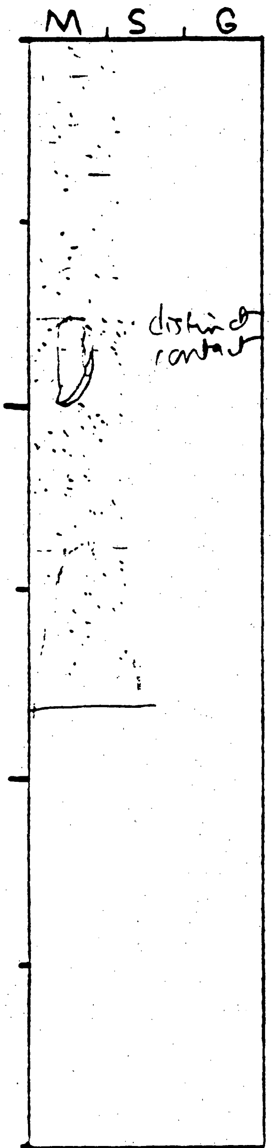

General Comments:

CORE LOG

CORE # HBV-6(A) TYPE Vibracore LOCATION Heald Bank
LATITUDE 29° 08.630' LONGITUDE 94° 09.949 SURFACE ELEVATION -34'
DEPTH PENETRATED ? LENGTH RECOVERED 10.6 %COMPACTION ?

OBTAINED BY Gibeaut - R/V Kit Jones DATE 10-12-94
DESCRIBED BY White DATE

DEPTH (ft, m)	SKETCH	LITHOLOGY	STRUCTURE	REMARKS
0–3	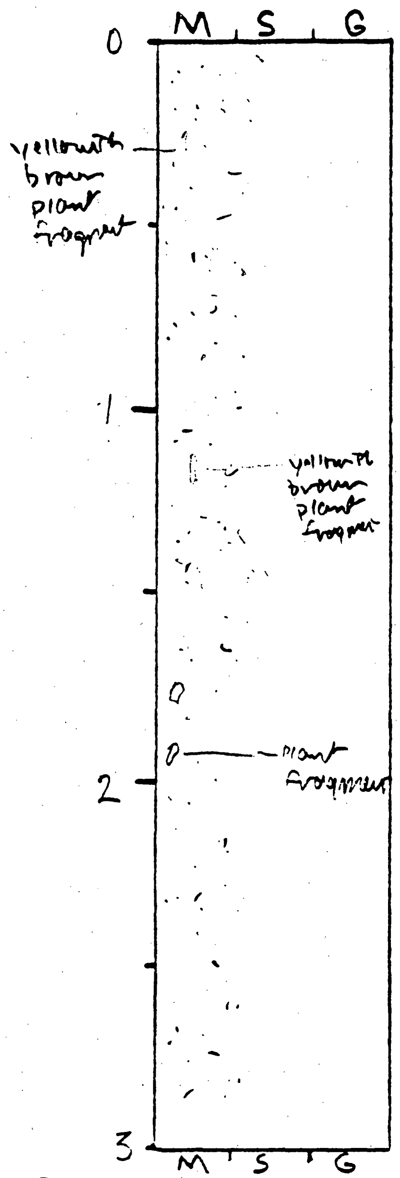	fine sand (quartz) with scattered shell fragments, possibly 20% shell granules & very coarse sand size. Locally, plant fragments		Light olive gray color

General Comments:

CORE LOG

CORE # HBV-G(B) TYPE ______ LOCATION ______
LATITUDE ______ LONGITUDE ______ SURFACE ELEVATION ______
DEPTH PENETRATED ______ LENGTH RECOVERED ______ %COMPACTION ______

OBTAINED BY ______ DATE ______
DESCRIBED BY ______ DATE ______

DEPTH (ft, m)	SKETCH	LITHOLOGY	STRUCTURE	REMARKS

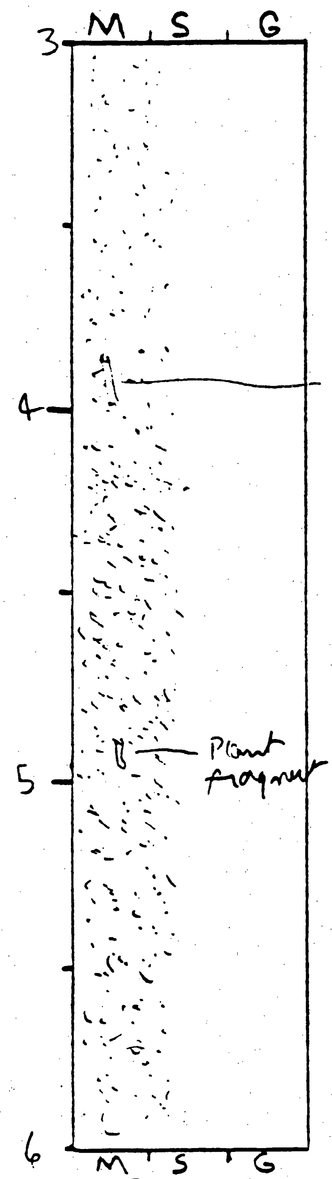

fine sand (quartz)
scattered shell fragments
granule to coarse grained.
quartz well sorted
sub-rounded

Light olive gray in color
with dark specks (=wood and some heavies frags)

5mm wide plant fragment

fine sand
Coarsening becomes more apparent below 4.3' but is Gradational.
Coarsening downward as shell material becomes more abundant ≈ 25%

General Comments:

CORE LOG

CORE # HBV-6(C) TYPE ________ LOCATION ________
LATITUDE ________ LONGITUDE ________ SURFACE ELEVATION ________
DEPTH PENETRATED ______ LENGTH RECOVERED ______ %COMPACTION ______

OBTAINED BY ________________________ DATE ________
DESCRIBED BY ________________________ DATE ________

DEPTH (ft, m)	SKETCH	LITHOLOGY	STRUCTURE	REMARKS
	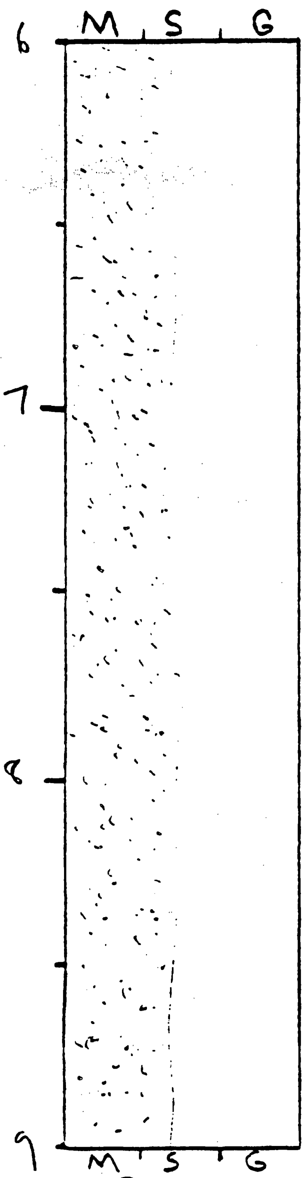	fine quartz sand with sand shell fragments coarse to granule in size; quartz well sorted, sub rounded. Appears to be slight coarsening with depth as shell fragments compose ~ 25% of sediment. Occasional shell fragment up to 6 mm in length		Light olive gray with black sprinkles from shell fragments & heavy mineral

General Comments:

CORE LOG

CORE # HBV-6 (D) TYPE ________ LOCATION ________
LATITUDE ________ LONGITUDE ________ SURFACE ELEVATION ________
DEPTH PENETRATED ______ LENGTH RECOVERED ______ %COMPACTION ____

OBTAINED BY ________________________ DATE ________
DESCRIBED BY ________________________ DATE ________

DEPTH (ft, m)	SKETCH	LITHOLOGY	STRUCTURE	REMARKS
9		fine sand (quartz) coarse to granule shell fragments ≈ 25% qtz sand sub-rounded well sorted		Light olive gray with darker speckles of shell fragments
10		Shelly sand to sandy shell most granule size or finer but some gravel size shells.		

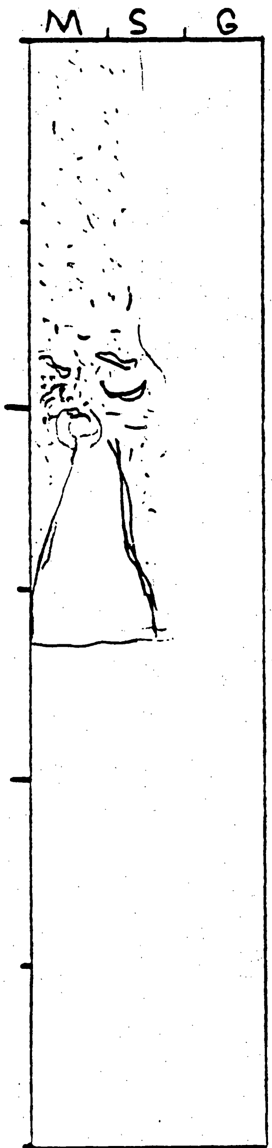

General Comments:

CORE LOG

CORE # HBV-7 (A) TYPE Vibracore LOCATION Heald Bank
LATITUDE 29° 08.672 LONGITUDE 94° 02.193 SURFACE ELEVATION -50'
DEPTH PENETRATED ? LENGTH RECOVERED 15' %COMPACTION ?

OBTAINED BY Gibeaut - R/V Kit Jones DATE 10-12-94
DESCRIBED BY White DATE

DEPTH (ft, m)	SKETCH	LITHOLOGY	STRUCTURE	REMARKS

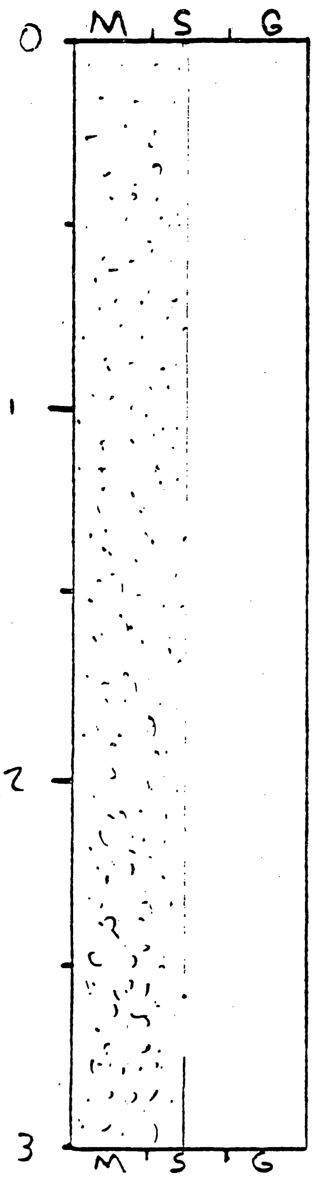

Lt olive gray to light olive brown Fine quartz sand with scattered shell fragments very coarse to granule in size becoming coarser toward bottom of core.

traces of clay in upper part of

Lt olive gray to Lt olive brown in color

becomes coarser at depth (increase in very coarse to granule size shell frags.

Gradational

shell ≈ 25% near bottom

General Comments:

CORE LOG

CORE # HBV-7 (B) TYPE ______ LOCATION ______
LATITUDE ______ LONGITUDE ______ SURFACE ELEVATION ______
DEPTH PENETRATED ______ LENGTH RECOVERED ______ %COMPACTION ______

OBTAINED BY ______ DATE ______
DESCRIBED BY ______ DATE ______

DEPTH (ft, m)	SKETCH	LITHOLOGY	STRUCTURE	REMARKS

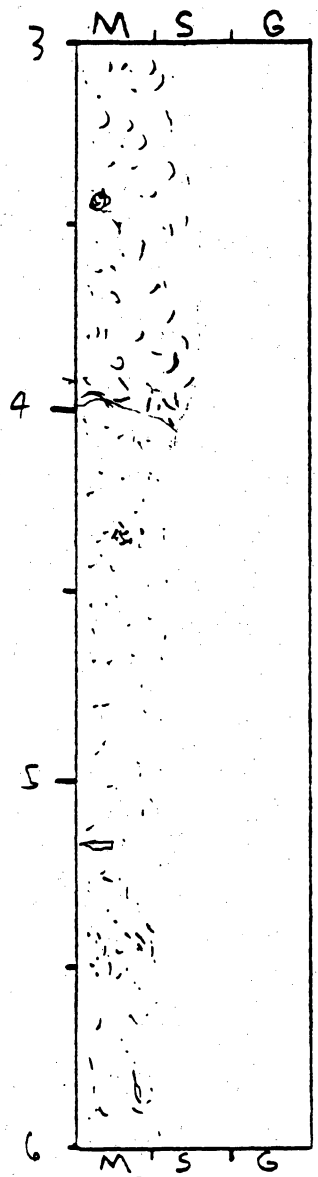

Lt Olive gray shelly fine sand to medium & coarse (from shell fragments)

Shell fragments & whole shells (7mm long)

sediments become grayer
< 10% shell fragments except for local pockets
v. fine sand with scattered shells

Lt Olive gray
to
Olive gray

Increase in shell: locally 10-15%

General Comments:

CORE LOG

CORE # HBV-7(C) TYPE_____ LOCATION_____
LATITUDE_____ LONGITUDE_____ SURFACE ELEVATION_____
DEPTH PENETRATED_____ LENGTH RECOVERED_____ %COMPACTION_____

OBTAINED BY_____ DATE_____
DESCRIBED BY_____ DATE_____

DEPTH (ft, m)	SKETCH	LITHOLOGY	STRUCTURE	REMARKS
6	M S G	v. fine muddy sand at top.		
		sandy clay or mud (few shells) Lt olive gray		mottly. Lt olive gray but some mottling (possible burrow) on right side Olive gray
		muddy sand		
		color change from Lt Olive gray (brownish) to Olive gray – dark gray. muddy sand		
7.				
		increase in mud in this area muddy sand a sandy mud		
		mud sand & shell very shelly		
8		fine sand, slightly muddy scattered shells		
		2 Large shells (2.5 cm long) in fine sand		
9 (mud)	M S G			

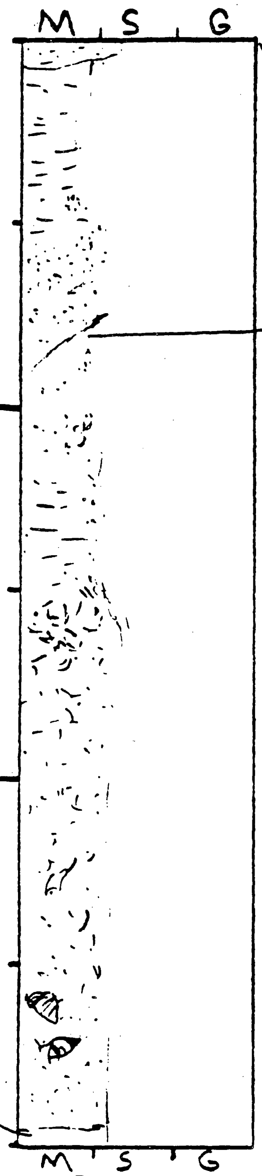

General Comments:

CORE LOG

CORE # 14BV-7 (D) TYPE_____ LOCATION_____
LATITUDE_____ LONGITUDE_____ SURFACE ELEVATION_____
DEPTH PENETRATED_____ LENGTH RECOVERED_____ %COMPACTION_____

OBTAINED BY_____ DATE_____
DESCRIBED BY_____ DATE_____

DEPTH (ft, m)	SKETCH	LITHOLOGY	STRUCTURE	REMARKS

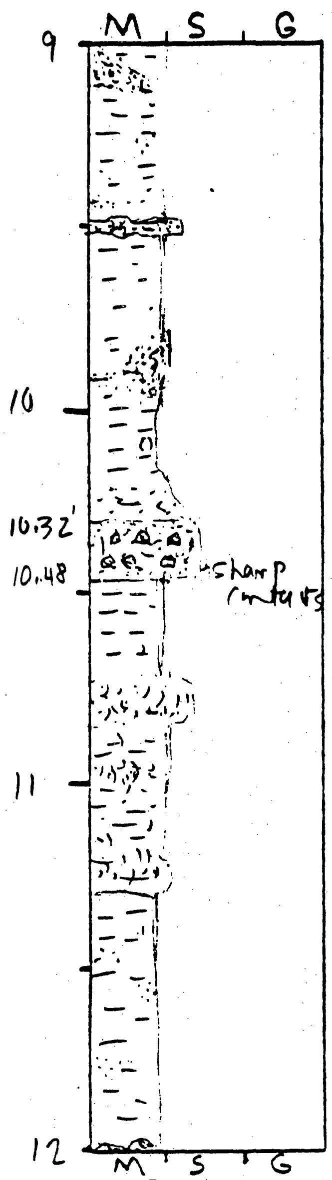

Olive gray mud with pockets of very fine sand (Olive Gray) 5Y 3/2
Some burrowing

thin sand layer

Sand pocket in mud

Some light olive gray mottling (brownish)

muddy sand zone above shell zone

shelly sand or sandy shell, shell fragments & whole shells up to 1 cm in

mud (rare shells)

Sandy shelly mud or muddy shell (fragments & whole shells 1 cm wide)

mixture of mud, sand & scattered shells

shelly mud or muddy shell, some sand

Mostly olive gray mud, some sand pockets
few shells

small pockets of brown sand in bottom, small whole shells

General Comments:

CORE LOG

CORE # HBV-7(E) TYPE ______ LOCATION ______
LATITUDE ______ LONGITUDE ______ SURFACE ELEVATION ______
DEPTH PENETRATED ______ LENGTH RECOVERED ______ %COMPACTION ______

OBTAINED BY ______ DATE ______
DESCRIBED BY ______ DATE ______

DEPTH (ft, m)	SKETCH	LITHOLOGY	STRUCTURE	REMARKS

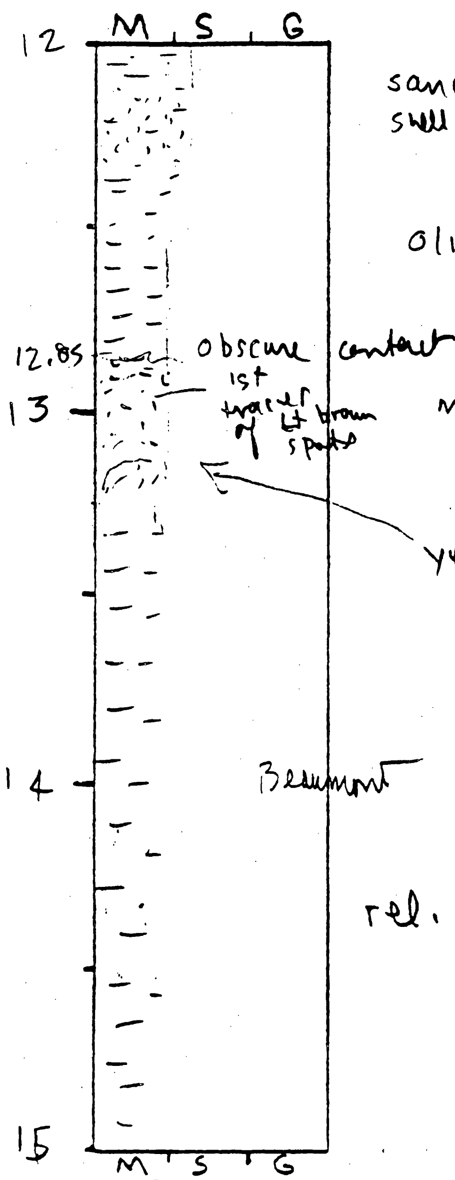

sandy, slightly shelly mud — mottled Lt olive gray and olive gray
shell frags v. coarse to granule
(≈ 20% shell frags)

olive gray mud

mottled color changing from Lt olive grey to yellowish gray & Dusky yellow mud
scattered shell frags (12.85' – 13.3)

yellowish gray color dominates below 13.1' (No shell fragments below 13.3)

yellowish gray with mottled areas of Lt olive gray & spots (< 5 mm dia) of Lt brown

rel. stiff yellowish gray clay

General Comments:

Addendum 12. Particle Size Analyses, Heald Bank and Sabine Bank Samples

Particle Size Analyses
Heald Bank and Sabine Bank samples

Lab #	Sample ID	Sand %	Silt %	Clay %
1	HBV-1-1.5	sieve		
2	HBV-1-5.5	sieve		
3	HBV-1-8.0	sieve		
4	HBV-2-1.5	81	8	11
5	HBV-2-4.5	34	40	26
6	HBV-2-7.5	12	60	27
7	HBV-2-10.2	6	28	66
8	HBV-3-1.8	sieve		
9	HBV-3-2.6	72	7	21
10	HBV-3-4.5	74	6	20
11	HBV-3-6.5	77	6	17
12	HBV-3-12.75	74	9	17
13	HBV-4-1.0	sieve		
14	HBV-4-5.0	sieve		
15	HBV-4-6.5	18	32	50
16	HBV-5-2.0	sieve		
17	HBV-5-5.75	sieve		
18	HBV-5-14.75	sieve		
19	HBV-5-19.1	sieve		
20	HBV-6-1.0	sieve		
21	HBV-6-4.5	sieve		
22	HBV-6-9.8	sieve		
23	HBV-7-2.5	sieve		
24	HBV-7-6.25	24	36	40
25	HBV-7-9.3	15	44	42
26	SBV-12-1.0	sieve		
27	SBV-12-4.5	sieve		
28	SBV-12-7.0	sieve		
29	SBV-12-11.0	76	12	12
30	SBV-11-0.25	67	16	16
31	SBV-11-4.5	44	29	27
32	SBV-10-0.7	68	16	16
33	SBV-10-3.2	54	26	20
34	SBV-10-7.0	25	42	34
35	SBV-10-11.2	6	28	66
36	SBV-13-0.4	sieve		

37	SBV-13-0.75	66	17	17
38	SBV-13-5.5	60	21	19
39	SBV-13-14	68	16	16
40	SBV-14-1.5	sieve		
41	SBV-14-4.2	sieve		
42	SBV-14-8.6	44	36	20
43	SBV-15-0.5	68	16	17
44	SBV-15-0.95	68	16	17
45	SBV-16-0.2	sieve		
46	SBV-16-2.5	sieve		
47	SBV-16-4.5	78	9	12
48	SBV-17-1.0	sieve		
49	SBV-17-5.8	sieve		
50	SBV-17-9.2	sieve		
51	SBV-17-14.0	sieve		
52	SBV-18-0.5	sieve		
53	SBV-18-5.7	sieve		
54	SBV-18-8.25	sieve		
55	SBV-19-0.8	20	42	38
56	SBV-19-2.8	sieve		
57	SBV-19-5.5	68	20	13
58	SBV-19-8.5	53	29	19
59	SBV-20-0.5	sieve		
60	SBV-20-2.7	sieve		
61	SBV-20-4.1	sieve		
62	SBV-21-1.0	sieve		
63	SBV-22-2.0	sieve		
64	SBV-22-5.75	sieve		
65	SBV-22-10.95	sieve		
66	SBV-22-13.5	sieve		
67	SBV-23-0.5	sieve		
68	SBV-23-5.5	sieve		
69	SBV-23-12.4	sieve		
70	SBV-23-17.8	49	34	17
71	SBV-24-2.2	sieve		
72	SBV-24-5.6	sieve		
73	SBV-24-7.0	sieve		
74	SBV-24-16.5	41	40	19
75	SBV-25-0.4	sieve		
76	SBV-25-1.5	sieve		
77	SBV-25-11.2	sieve		

Particle Size Analyses - Sieve

Heald Bank and Sabine Bank samples

		cumulative %'s													
Lab	Sample	-2.0ø	-1.5ø	-1.0ø	-0.5ø	0ø	0.5ø	1.0ø	1.5ø	2.0ø	2.5ø	3ø	3.5ø	4.0ø	pan
#	ID	%	%	%	%	%	%	%	%	%	%	%	%	%	%
1	HBV-1-1.5	0.0	0.0	0.1	0.4	0.6	1.0	1.7	2.9	7.7	43.9	93.0	99.7	99.9	100.0
2	HBV-1-5.5	0.0	0.8	4.0	10.5	20.3	31.3	38.9	43.4	48.7	69.4	94.9	99.5	99.8	100.0
3	HBV-1-8.0	5.2	10.7	18.5	28.7	38.6	46.4	51.2	54.3	58.3	73.8	95.1	99.5	99.7	100.0
4	HBV-2-1.5	0.3	0.4	0.7	0.9	1.2	1.6	2.0	2.3	2.9	7.0	41.9	87.0	97.4	100.0
5	HBV-2-4.5	hydrometer													
6	HBV-2-7.5	hydrometer													
7	HBV-2-10.2	hydrometer													
8	HBV-3-1.8	0.0	0.2	1.1	3.2	6.1	8.6	11.0	13.7	27.7	77.5	95.8	97.2	97.6	100.0
9	HBV-3-2.6	0.0	0.0	0.0	0.1	0.5	1.0	1.8	2.6	3.8	14.1	68.8	96.8	99.2	100.0
10	HBV-3-4.5	0.0	0.0	0.0	0.1	0.3	0.8	1.4	1.9	3.2	13.5	71.3	96.1	99.1	100.0
11	HBV-3-6.5	0.0	0.0	0.0	0.1	0.2	0.6	1.2	1.7	2.8	12.3	68.7	95.1	98.6	100.0
12	HBV-3-12.75	0.0	0.0	0.0	0.9	2.4	3.9	5.0	5.7	6.3	10.1	66.6	86.7	97.1	100.0
13	HBV-4-1.0	0.0	0.1	0.5	0.7	1.1	1.8	4.0	8.3	16.6	48.4	81.8	93.0	95.2	100.0
14	HBV-4-5.0	2.0	3.2	4.9	6.7	9.2	12.8	16.4	20.4	25.6	37.4	60.2	80.5	88.8	100.0
15	HBV-4-6.5	hydrometer													
16	HBV-5-2.0	0.0	0.1	0.2	1.0	2.6	5.8	9.8	13.8	22.6	55.0	93.1	99.5	99.8	100.0
17	HBV-5-5.75	2.3	2.8	4.0	6.2	9.7	14.8	19.5	23.4	30.1	58.7	93.2	99.3	99.7	100.0
18	HBV-5-14.75	0.3	0.5	1.0	2.4	5.0	8.5	11.8	15.2	19.3	38.4	79.5	93.3	94.9	100.0
19	HBV-5-19.1	0.0	0.0	0.2	1.2	3.4	6.5	9.4	12.5	16.4	28.5	69.9	91.0	94.4	100.0
20	HBV-6-1.0	0.0	0.1	0.4	1.2	3.2	6.9	11.0	15.2	24.9	64.2	95.3	99.3	99.6	100.0
21	HBV-6-4.5	0.0	0.1	0.6	2.3	6.1	12.3	18.4	23.7	33.8	70.3	96.0	99.4	99.7	100.0
22	HBV-6-9.8	8.6	9.6	11.2	14.3	19.4	25.9	31.9	36.5	45.3	76.4	97.2	99.5	99.7	100.0
23	HBV-7-2.5	1.3	2.4	4.8	10.6	20.5	34.1	47.8	54.7	68.2	84.8	97.2	99.7	99.8	100.0

24	HBV-7-6.25	hydrometer													
25	HBV-7-9.3	hydrometer													
26	SBV-12-1.0	0.1	0.2	0.6	1.3	2.4	4.7	9.7	14.7	29.4	73.5	98.3	99.8	99.9	100.0
27	SBV-12-4.5	20.2	23.8	28.1	32.5	36.7	40.2	43.5	46.6	55.4	81.0	98.7	99.8	99.9	100.0
28	SBV-12-7.0	0.4	0.5	0.8	1.1	1.7	2.7	4.5	7.1	17.2	62.4	95.6	99.0	99.4	100.0
29	SBV-12-11.0	0.0	0.0	0.0	0.0	0.0	0.5	1.2	2.3	7.2	35.8	86.3	92.5	95.6	100.0
30	SBV-11-0.25	hydrometer													
31	SBV-11-4.5	hydrometer													
32	SBV-10-0.7	hydrometer													
33	SBV-10-3.2	hydrometer													
34	SBV-10-7.0	hydrometer													
35	SBV-10-11.2	hydrometer													
36	SBV-13-0.4	2.7	4.9	7.7	11.5	16.1	20.6	25.2	29.0	35.8	54.7	84.1	93.2	95.9	100.0
37	SBV-13-0.75	hydrometer													
38	SBV-13-5.5	hydrometer													
39	SBV-13-14	hydrometer													
40	SBV-14-1.5	8.5	12.2	16.0	20.5	24.5	28.0	31.5	35.1	42.0	59.4	89.0	95.6	97.3	100.0
41	SBV-14-4.2	0.3	0.4	1.3	4.3	8.5	12.8	16.6	19.9	25.9	42.2	67.2	76.7	84.4	100.0
42	SBV-14-8.6	hydrometer													
43	SBV-15-0.5	hydrometer													
44	SBV-15-0.95	hydrometer													
45	SBV-16-0.2	0.0	0.0	0.4	1.4	3.3	5.7	9.3	13.1	21.0	37.0	80.8	97.5	98.7	100.0
46	SBV-16-2.5	24.6	35.5	48.6	60.5	69.2	75.5	79.5	82.8	87.5	91.6	97.6	99.5	99.6	100.0
47	SBV-16-4.5	0.0	0.0	0.0	0.5	1.1	2.0	3.9	4.7	7.5	19.4	58.8	93.6	98.8	100.0
48	SBV-17-1.0	0.1	0.5	1.5	2.9	4.9	7.4	10.3	13.7	25.3	60.6	95.4	99.6	99.8	100.0
49	SBV-17-5.8	2.1	3.9	6.6	10.5	15.4	20.1	24.2	27.8	38.2	66.3	95.7	99.6	99.8	100.0
50	SBV-17-9.2	2.8	5.0	9.1	14.9	21.5	27.6	32.5	36.9	46.9	70.8	96.3	99.6	99.8	100.0
51	SBV-17-14.0	0.9	1.7	3.1	4.4	5.7	7.4	9.6	11.9	23.4	58.4	94.7	99.4	99.8	100.0
52	SBV-18-0.5	0.0	0.1	1.2	2.6	4.2	5.7	8.0	10.5	21.4	51.7	93.4	99.2	99.6	100.0
53	SBV-18-5.7	2.4	3.7	5.7	8.9	12.5	16.3	20.3	24.3	30.7	50.8	84.4	92.7	95.0	100.0
54	SBV-18-8.25	4.9	7.3	9.9	14.0	18.5	23.3	27.9	32.5	39.2	53.5	80.6	90.8	93.4	100.0
55	SBV-19-0.8	hydrometer													
56	SBV-19-2.8	0.4	0.8	1.9	4.2	7.1	10.3	13.8	17.8	24.5	41.5	78.3	92.8	95.3	100.0

57	SBV-19-5.5	hydrometer													
58	SBV-19-8.5	hydrometer													
59	SBV-20-0.5	0.0	0.0	0.0	0.1	0.2	0.7	2.0	3.5	8.2	41.2	87.9	99.0	99.7	100.0
60	SBV-20-2.7	0.1	0.1	0.2	0.3	0.6	1.6	4.4	8.7	33.6	77.9	97.2	99.7	99.9	100.0
61	SBV-20-4.1	32.7	56.9	71.0	79.0	84.0	87.4	89.3	90.3	92.6	96.6	99.1	99.6	99.7	100.0
62	SBV-21-1.0	3.3	8.4	15.2	21.4	26.9	31.2	34.8	38.8	45.6	54.1	66.0	82.8	91.2	100.0
63	SBV-22-2.0	1.6	2.3	4.1	6.9	10.6	14.4	17.9	21.5	32.0	55.3	86.6	97.4	98.6	100.0
64	SBV-22-5.75	0.0	0.2	0.5	1.9	5.2	9.8	13.9	16.6	23.5	52.8	82.3	92.0	95.0	100.0
65	SBV-22-10.95	1.4	2.6	3.8	6.3	9.6	13.8	18.0	21.7	27.3	39.5	58.6	70.6	78.8	100.0
66	SBV-22-13.5	0.1	0.1	0.1	0.8	3.0	7.5	12.8	17.1	21.0	28.5	43.7	63.6	74.8	100.0
67	SBV-23-0.5	0.1	0.2	0.5	1.1	1.9	3.2	5.2	7.4	20.5	51.0	81.7	91.9	94.9	100.0
68	SBV-23-5.5	1.3	1.7	2.1	3.2	5.3	8.1	11.4	15.2	23.9	50.5	74.9	87.5	93.3	100.0
69	SBV-23-12.4	0.1	0.3	0.9	2.7	6.9	12.5	17.6	21.5	26.7	41.4	61.7	72.9	80.3	100.0
70	SBV-23-17.8	hydrometer													
71	SBV-24-2.2	0.4	0.4	0.8	1.5	3.0	5.6	8.8	12.1	17.8	41.2	80.3	91.8	94.5	100.0
72	SBV-24-5.6	0.4	0.6	1.2	2.5	5.3	9.4	13.4	16.7	21.2	35.7	65.8	80.7	88.0	100.0
73	SBV-24-7.0	0.0	0.9	1.4	3.1	6.5	11.1	15.2	18.4	22.8	37.0	65.1	80.7	87.1	100.0
74	SBV-24-16.5	hydrometer													
75	SBV-25-0.4	5.9	16.6	31.5	45.3	56.4	66.3	73.6	77.8	83.5	92.7	98.0	99.0	99.3	100.0
76	SBV-25-1.5	1.8	2.2	2.9	4.8	7.8	11.7	15.4	18.6	23.2	39.2	76.8	91.2	94.4	100.0
77	SBV-25-11.2	0.0	0.0	0.1	1.1	3.7	8.3	13.6	17.9	21.4	26.0	40.4	56.9	67.2	100.0